University of Nottingham
UK | CHINA | MALAYSIA

Obesity Mediated Dysregulation in the Expression and Action of Myostatin

Andrew Wilhelmsen, BSc. (Hons), MRes.

A thesis submitted to the University of Nottingham

for the degree of Doctor of Philosophy.

May 2022

Abstract

Background: Obesity is often associated with impaired sensitivity to the effects of insulin (insulin resistance) and dietary protein (anabolic resistance) and may exacerbate the age-related decline of skeletal muscle (sarcopenia). Myostatin is a protein that negatively regulates skeletal muscle growth but its inhibition in rodents also improves insulin sensitivity. In humans, myostatin appears to be upregulated by obesity and associated with insulin resistance, but observations are confounded by lifestyle factors and ageing. **Aims:** To delineate between the effects of obesity and ageing on myostatin expression in human skeletal muscle; to investigate the underlying causes of these effects; and to establish the functional significance and interconnectivity of modulating insulin sensitivity and myostatin expression in human skeletal muscle cells. **Methods:** In Chapter 3 a cross-sectional analysis of skeletal muscle gene expression was undertaken, in conjunction with correlation analyses between serum myostatin and descriptive characteristics, to isolate the effects of obesity and ageing *per se* on myostatin expression and abundance. In Chapters 4 and 5, *in vitro* and *ex vivo* techniques were employed using human primary myotubes to investigate the potential involvement of lipid-induced insulin and anabolic resistance and secretory cross-talk between subcutaneous adipose tissue and muscle, in the obesity-mediated upregulation of myostatin and the associated impairment of insulin and anabolic sensitivity. In Chapter 6, the novel polyphenol metabolite Urolithin A was applied to human myotubes and a model of adipocytes, to investigate its therapeutic potential to enhance insulin and anabolic sensitivity and to suppress myostatin expression. **Results:** In Chapter 3 it was revealed that muscle myostatin expression is uniquely upregulated by obesity with ageing, but not by ageing in the absence of obesity, and occurs concurrently with insulin resistance and abnormal regulation of pathways involved in the maintenance of skeletal muscle mass. This association was corroborated by positive correlations between serum myostatin and multiple indices of adiposity, but not age. In Chapters 4 and 5 it was demonstrated that neither acutely elevated fatty acid availability (which induced insulin and anabolic resistance), nor chronic exposure to obese subcutaneous adipose tissue conditioned medium (which did not induce insulin or anabolic resistance but altered the expression of genes involved in myogenesis and muscle protein breakdown) recapitulated the obesity-mediated upregulation of myostatin expression. In Chapter 6 it was demonstrated for the first time that Urolithin A suppresses myostatin expression and enhances glucose transport in human myotubes (and 3T3-L1 adipocytes), the latter of which was associated with an upregulation of GLUT4 expression. **Conclusions:** Skeletal muscle myostatin

expression is uniquely upregulated by obesity *per se*, but this does not appear to be mediated by lipid-induced insulin resistance, nor by the secretory milieux of obese subcutaneous adipose tissue. Nevertheless, both models perturbed factors involved in myogenesis and muscle protein breakdown, independent of an upregulation of myostatin. Thus, the factors responsible for the obesity-mediated upregulation of myostatin remain to be elucidated and future work to establish such causality is required. Furthermore, translational research to investigate the potential of Urolithin A to enhance glucose handling in peripheral tissues and to repress myostatin's inhibitory effects on muscle growth is warranted in humans and could be of particular benefit in conditions such as sarcopenic obesity.

Publications

Wilhelmsen, A., Davies, A., Mallinson, J., Pabla, P., Jones, R., Palmer, E., Dunn, W., Moran, G., Stephens, F. & Tsintzas, K. (2022). Acute effects of prior dietary fat ingestion on postprandial metabolic responses to protein and carbohydrate co-ingestion in overweight and obese men: A randomised crossover trial. *Clinical Nutrition*, *41*(8), 1623–1635 Doi:10.1016/j.clnu.2022.06.022.

Wilhelmsen, A., Tsintzas, K., & Jones, S. W. (2021). Recent advances and future avenues in understanding the role of adipose tissue cross talk in mediating skeletal muscle mass and function with ageing. *GeroScience*, *43*(1), 85–110. Doi:10.1007/s11357-021-00322-4

Templeman, I., Smith, H. A., Chowdhury, E., Chen, Y. C., Carroll, H., Johnson-Bonson, D., Hengist, A., Smith, R., Creighton, J., Clayton, D., Varley, I., Karagounis, L. G., **Wilhelmsen, A.**, Tsintzas, K., Reeves, S., Walhin, J. P., Gonzalez, J. T., Thompson, D., & Betts, J. A. (2021). A randomized controlled trial to isolate the effects of fasting and energy restriction on weight loss and metabolic health in lean adults. *Science Translational Medicine*, *13*(598), eabd8034. Doi:10.1126/scitranslmed.abd8034

Declarations

- Skeletal muscle biopsy samples used in Chapter 2 were sourced from a prior study of Dr Carolyn Chee.
- Skeletal muscle biopsies used for the generation of primary myogenic cultures in Chapters 3, 4, 5 and 6 were performed by Dr's Tariq Taylor, Natalie Shurr, Joseph Cullen and Ayushman Gupta.
- Measurement of donors' serum insulin presented in Chapter 4 were assayed by Dr Pardeep Pabla.
- Some cryopreserved myoblasts from older donors used in Chapters 5 and 6, as well as adipose-conditioned medium used in Chapter 5, was obtained from the laboratory of Dr Simon Jones.
- Urolithin A, for the experiments in Chapter 6, was provided by Dr Davide D'Amico

I hereby declare that apart from the aforementioned, all work undertaken and presented in this thesis is the product of my own efforts, during my time enrolled at the University of Nottingham. All sources of information, products and procedures, and visual artwork are duly referenced and acknowledged as accurately as possible. No part of this thesis has been submitted in any form for another higher degree.

Signed: _____

Date: _____13/05/22_____

Acknowledgements

First and foremost, I must acknowledge and thank my primary supervisor, Professor Kostas Tsintzas for all his support throughout the course of this doctoral programme. Kostas has never faltered in his generosity when offering his time, knowledge, and enthusiasm to support me and this project. Secondly, my sincerest thanks are due to Dr Simon Jones for his supervisory input and support. Dr Leonidas Karagounis for his supervisory support and for enabling industry collaboration. Dr Andrew Bennett of the FRAME alternatives laboratory must also be accredited for his knowledge and guidance in all matters of molecular biology.

To the laboratory technicians, Dr Scott Cooper and Monika Owen, I am grateful for your teaching and technical support at the lab bench. The body of *in vitro* work presented would not be possible without the generation of tissue samples from volunteers. I therefore must thank all the staff of the David Greenfield Human Physiology Unit for their efforts in enabling me to recruit and obtain samples from participants for these projects, particularly during the times of the COVID19 pandemic, where such matters became far more challenging. Dr Luisa Martinez-Pomares' kind words and generosity in a pastoral capacity never failed to uplift me, especially when I needed it most. To all my fellow doctoral students within the D83 office, I am grateful for the many laughs, rants, and pints at the Johnson Arms.

To my family and to Naomi, thank you. I hope I have made you proud.

To my dear nephew Henry, whose giggle lifts me up when I am low; aim high and work hard and you'll never go too far wrong.

COVID-19 Statement of Impact

Despite my best efforts, the full impact of the COVID-19 pandemic has not been fully mitigable. The University of Nottingham closed on March 15th, 2020 and did not reopen its doors to postgraduate researchers until August 24th, 2020. The impact of the pandemic, however, went beyond this lost time. I therefore applied my time and efforts in alternative ways and did my utmost to produce a thesis of sufficient quality and quantity to be proud of. A comprehensive overview of the various restrictions/challenges posed and my efforts to tackle them are described within Appendix 3. COVID-19 Impact Statement.

Brief overview of detriments to the completion of this thesis:

- Five consecutive months of laboratory time was lost to closure
- Unexpected caring responsibilities
- Non-essential human research was halted for 12 months
- *In vivo* interventional study had to be indefinitely suspended
- New clinical research fellow (essential for biopsies) not appointed until May 2021
- Restricted use of laboratory facilities until Autumn 2021
- Not able to undertake secondment (up to 12 months) with Nestlé in Switzerland
- Inability to complete a method development chapter (Appendix 2. An Inducible Model of Myostatin Overexpression)

Brief overview of mitigating action and alternative scholarly activities:

- Authored and published a review article on adipose-muscle cross talk in ageing
- Authored a manuscript based on data previously generated within our group
- Collaborated with another group on sample analysis and writing for a publication
- Undertook cross-sectional analysis of previously generated samples (Chapter 3)
- Obtained primary cells from a commercial source and collaborators to continue cell culture experiments when human participants could not be recruited
- Completed an *in vitro* study with an industry collaborator (Chapter 6)

I received confirmation on August 27th, 2021, of a 3-month funded extension (my funding period was due to end on September 31st, 2021). On November 16th, 2021, I was awarded a final funded extension of a further 3 months. Thus, this thesis and the associated publications represent my best efforts within the confines of a 6-month extension, to compensate for, among other things, 5 consecutive months of complete laboratory closure, 7 subsequent months of not being able to undertake non-essential human research, and a further 2 months of not having a full-time clinical research fellow to perform the necessary invasive procedures for primary cell culture generation.

Table of Contents

Table of Tables

Table of Figures

List of Abbreviations

[3H]2-DOG	Tritiated 2-Deoxy-D-Glucose
4E-BP1	Eukaryotic translation initiation factor 4E-Binding Protein 1
AA	Amino Acid
ACM	Adipose-Conditioned Medium
ACTRIIB	Activin Receptor Type II B (protein)
ACVR2B	Activin Receptor Type II B (gene)
Adipocyte-CM	Adipose-Conditioned Medium
Akt	Protein Kinase B
ALK	Activin-Like Kinase
AMPK	5' adenosine monophosphate-activated protein kinase
ANOVA	Analysis Of Variance
aPKC	Atypical Protein Kinase C
AS160	Protein Kinase B Substrate of 160 kDa
ATP	Adenosine Triphosphate
Att	Attachment Sites
BAT	Brown Adipose Tissue
BCA	Bicinchoninic Acid Assay
BCAA	Branched-Chain Amino Acid
BMI	Body Mass Index
BMP	Bone Morphogenetic Protein
BSA	Bovine Serum Albumin
CD36	Fatty Acid Translocase
cDNA	Complimentary DNA
CHO	Carbohydrate
Ct	Cycle Threshold
DAG	Diacylglycerol
DEXA	Dual X-Ray Absorptiometry
DMEM	Dulbecco’s Modified Eagle’s Medium
DMSO	Dimethyl Sulfoxide
DNA	Deoxyribose Nucleic Acid
dNTP	Deoxyribonucleotide Triphosphate
DOX	Doxycycline
E. Coli	Escherichia coli
EA	Ellagic Acid
EDTA	Ethylenediaminetetraacetic acid
EGTA	Ethylene Glycol-bis(β-aminoethyl ether)-N,N,N′,N′-Tetraacetic Acid
EIF-2 α	Eukaryotic Initiation Factor 2α
EMEM	Eagle’s Minimum Essential Medium
ERK	Extracellular Signal-Regulated Kinases
ET	Ellagitannins
EV	Extracellular Vesicle
FABP	Fatty Acid Binding Protein
FATP	Fatty Acid Transport Protein

FBS	Foetal Bovine Serum
FFA	Free Fatty Acid
FITC	Fluorescein isothiocyanate
FOXO	Forkhead Box Transcription Factors
FSTL	Follistatin-Like Protein
G3P	Glyceraldehyde 3-Phosphate
GASP	Growth Differentiation Factor-Associated Serum Protein
GDF	Growth Differentiation Factor
GFP	Green Fluorescent Protein
GLUT	Glucose Transporter
GSK3β	Glycogen Synthase Kinse 3-β
GTP	Guanosine 5'-Triphospate
HEK293-FT	Human Embryonic Kidney 293-FT Cells
HEPES	4-(2-HydroxyEthyl)-1-Piperazineethanesulfonic Acid
HRP	Horse Radish Peroxidase
HS	Horse Serum
IBMX	3-isobutyl-1-methylxanthine
IGF	Insulin-Like Growth Factor
IL	Interleukin
IPAQ	International Physical Activity Questionnaire
IRS	Insulin Receptor Substrate
KRPH	Krebs Ringer Phosphate HEPES Buffer
Lcn2	Lipocalin 2
LP	Lentiviral Particle
MAFbx	Muscle Atrophy F-Box/Atrogin-1
MD	Mean Difference
MGB	Major Groove Binder
MHC	Myosin Heavy Chain
MOI	Multiplicity of Infection
MRF	Myogenic Regulatory Factor
mRNA	Messenger Ribose Nucleic Acid
MSTN	Myostatin (Gene)
mTOR	Mammalian Target of Rapamycin
MUFA	Monounsaturated Fatty Acid
MuRF1	Muscle RING Finger-1
MyF	Myogenic Factor
MYOD	Myogenic Differentiation Factor
MYOG	Myogenin
ONW	Older Normal Weight
OOO	Older Overweight/Obese
PAGE	Polyacrylamide Gel Electrophoresis
Pax	Paired Box Transcription Factor
PBS	Phosphate Buffered Saline
PDC	Pyruvate Dehydrogenase Complex
PDK	Pyruvate Dehydrogenase Kinase
PDPK-1	Phosphoinositide-dependent kinase-1

PI3K	Phosphatidylinositol 3-Kinase
PIP_2/PIP_3	Phosphatidylinositol 4,5-biphosphate/triphosphate
PKC	Protein Kinase C
PLO	Palmitate, Linoleic and Oleic Acid Solution
PUFA	Polyunsaturated Fatty Acid
PVDF	Polyvinylidene Difluoride
qPCR	Real-Time Polymerase Chain Reaction
RER	Rough Endoplasmic Reticulum
RIPA	Radioimmunoprecipitation Assay Buffer
RNA	Ribose Nucleic Acid
ROS	Reactive Oxygen Species
RPM	Rotations Per Minute
RT	Reverse Transcription
SAT	Subcutaneous Adipose Tissue
SD	Standard Deviation
SDS	Sodium Dodecyl Sulphate
SEM	Standard Error of the Mean
SMAD	Small Mothers Against Decapentaplegic
SuNSET	Surface Sensing of Translation
T2D	Type II Diabetes Mellitus
TAG	Triacylglycerol
TBS-T	Tris Buffered Saline – Tween 20
TGF	Transforming Growth Factor
TNF	Tumour Necrosis Factor
TU	Transducing Units
UA	Urolithin A
UCP	Uncoupling Protein
VAT	Visceral Adipose Tissue
WAT	White Adipose Tissue
YNW	Young Normal Weight

Chapter 1. General Introduction

1.1 Skeletal Muscle

Skeletal muscle is a highly plastic, heterogeneous contractile tissue (Harridge, 2007) that typically accounts for 30-35% of total body mass in young females and 35-40% in young males, but tends to decline with age (Janssen, Heymsfield, Wang, & Ross, 2000). Mechanically, skeletal muscle principally serves to facilitate voluntary movement via the conversion of chemical energy into mechanical energy through the stimulation of motor neurons and the subsequent firing of the collection of motor units they innervate via a process of excitation-contraction coupling, involving the rapid communication between electrical events within the plasma membrane of skeletal muscle fibres and the release of Ca^{2+} from a membrane-bound structure called the sarcoplasmic reticulum, which ultimately activates the contractile machinery (Calderón, Bolaños, & Caputo, 2014). Beyond voluntary motion, skeletal muscle also has essential protective, insulating and endocrine functions (Frontera & Ochala, 2015). Crucially, in the context of this thesis, skeletal muscle plays an essential role in basal energy metabolism, including the storage of energy substrates; the production of heat; and serves as the body's greatest means for the insulin-stimulated disposal of circulating glucose (Koistinen & Zierath, 2002). Thus, the regulation of skeletal muscle mass and its metabolic functionality is vital for the preservation of the normoglycaemic physiological environment.

In turn, the regulation of skeletal muscle mass depends on the delicate balance of muscle protein synthesis and degradation, which is influenced by ageing, nutritional status, hormonal balance, physical in/activity, trauma, and disease states among many other factors (McCormick & Vasilaki, 2018; Russell, 2010). These processes include the generation of muscle via adult myogenesis (comprising the activation of muscle satellite cells; the proliferation of myoblasts; the withdrawal of myoblasts from the cell cycle; and their subsequent differentiation and fusion into multi-nucleated myofibres) (Le Grand & Rudnicki, 2007; Yamakawa, Kusumoto, Hashimoto, & Yuasa, 2020); the repair and remodelling of muscle tissue (Carosio, Berardinelli, Aucello, & Musarò, 2011) and its inter- and intra-cellular content (Addison et al., 2014); the interaction between skeletal muscle and the nervous system via motor neurones (Wilkinson, Piasecki, & Atherton, 2018); and the interplay between synthesis and breakdown of muscle protein (Breen & Phillips, 2011; Wall et al., 2015).

1.1.1 Architecture and Function

Skeletal muscle is comprised principally of highly structured myofibres (Figure 1.1), however other cell types are also incorporated, working together on various levels to maintain structure and function (Rubenstein et al., 2020). Briefly, these include neural and perineurial; endothelial and perithelial; immune; and fibroblast cells (M. A. Chapman, Meza, & Lieber, 2016).

Structurally, skeletal muscle is made up of many bundles of fibres termed fasciculi that are entirely enveloped in an irregular fibrous sheath extending from the tendons, known as the epimysium, which serves to protect the muscle from friction against surrounding tissues (Lieber, 2002). Each fasciculi comprises a bundled network of muscle fibres and blood vessels surrounded by a secondary sheath called the perimysium. A single muscle fibre is wrapped together with capillaries and nerves in a sheath of connective tissue termed the endomysium. Muscle fibres are each contacted by a motor nerve axon to form a neuromuscular junction; a synapse between the pre-synaptic nerve terminal and a mid-sarcolemmal region of the fibre which acts as the motor end plate. Beneath the endomysium is the muscle cell's plasma membrane (sarcolemma). Individual muscle cells comprise dense parallel arrangements of cylindrical elements called myofibrils which comprise repeating contractile units (sarcomeres) of thick and thin myofilaments, which produce their 'striated' appearance. Mature skeletal muscle cells are multinucleated striated fibres of between 10-100 μm diameter and up to 15 cm in length (Silbernagle, 2015).

A sarcomere is defined as the segment between adjacent Z-lines (or Z-discs), which can be subdivided into distinct bands. The Z-lines are produced by the cross-binding sites of α-actinin to the actin filaments, for which they serve as anchors (Burgoyne, Morris, & Luther, 2015). The Z-line and the actin-only containing domains together form the I-band, while the entire length of the thicker molecular-motor myosin filament within the sarcomere forms the boundaries of the A-band, within which is the myosin-only H-band, and the myomesin-rich middle region (M-band) which anchors the myosin filaments and supports the structure of the fibre. This architecture lends itself to the production of fast, powerful contractions with fine motor control, via the 'sliding' of these myofilaments over one another to shorten the effective fibre length. Together, these properties facilitate the tightly regulated yet plastic nature of skeletal muscle, which interplays with its endocrine and metabolic actions to regulate a plethora of systems that help to maintain system homeostasis.

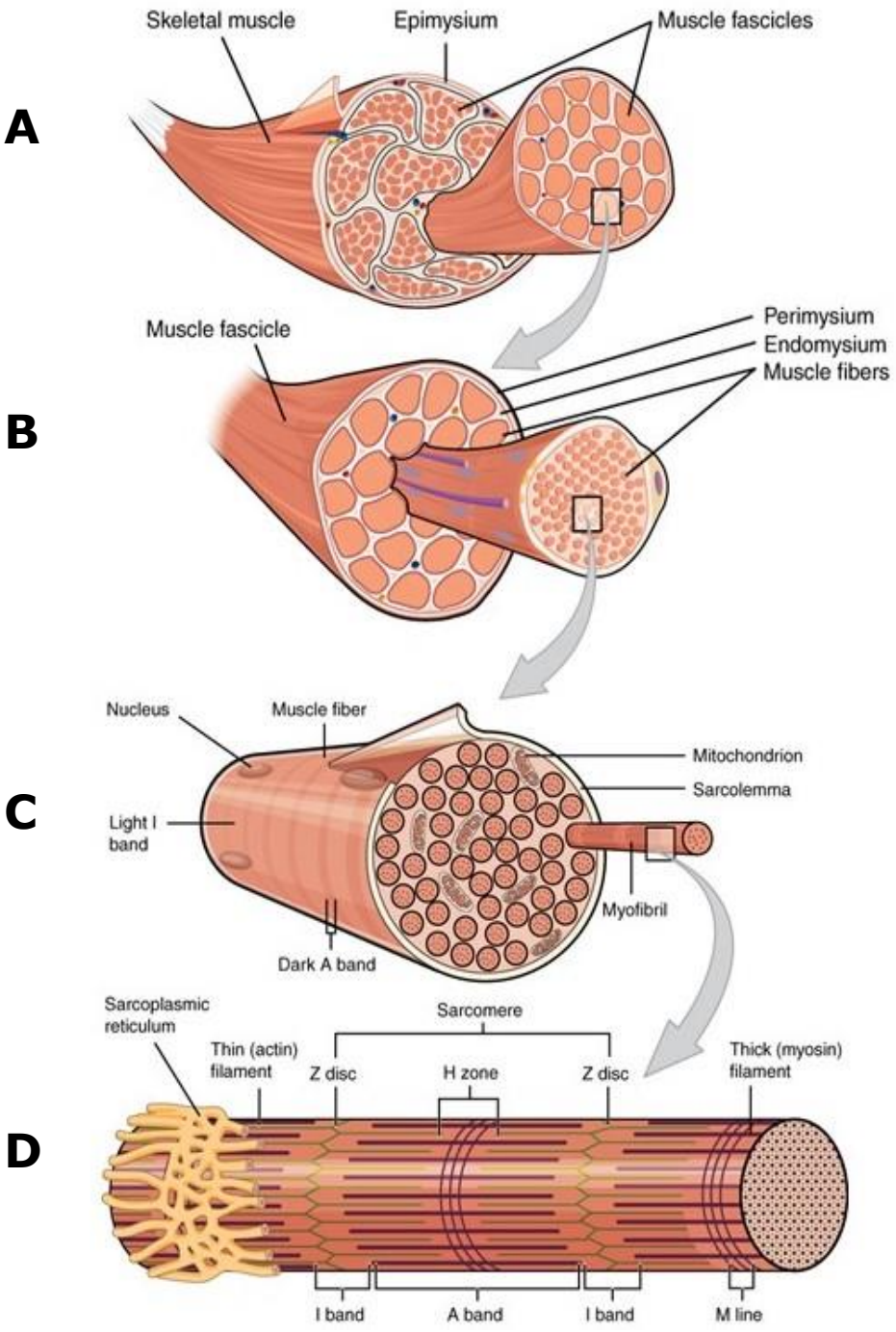

Figure 1.1. Macro- to microscopic architecture of human skeletal muscle. Skeletal muscles are comprised of many fascicles (**A**), each formed of many individual muscle fibres (**B**), which themselves contain many myofibrils (**C**) which are the contractile cylindrical organelles that facilitate mechanical motion via the adenosine triphosphate-mediated shortening of their sarcomeres (**D**). Adapted from Anatomy & Physiology, OpenStax College, provided by Rice University under CC BY 4.0.

1.1.2 Glucose Transport in Skeletal Muscle

Glucose is a ubiquitous cellular energy source within humans that is synthesised, released, transported into, and metabolised by a range of tissues. In a healthy 70 kg adult, a mere 4 g of glucose is typically circulating in the body (Wasserman, 2009). This circulating pool is tightly controlled by an integrated system of organs, hormones and cellular processes which fine tune their involvement according to the available supply, demand, and cellular environment. Insulin-independent glucose disposal accounts for the majority of glucose disposal in the fasted, resting state. Indeed, under such conditions brain and splanchnic organ glucose consumption accounts for 50-60% and ~25% of circulating glucose disposal, respectively, compared to the 20-30% attributable to skeletal muscle (R. A. DeFronzo, 1988, 2004; R. A. DeFronzo, Bonadonna, & Ferrannini, 1992; R. A. DeFronzo & Ferrannini, 1987; Zurlo, Larson, Bogardus, & Ravussin, 1990). Skeletal muscle, however, can vastly increase glucose disposal in response to stimuli such as insulin (by as much as 10-fold during hyperinsulinaemia) and contraction (by as much as 50-fold during exercise) (Holloszy & Hansen, 1996; Katz, Broberg, Sahlin, & Wahren, 1986). Skeletal muscle therefore constitutes the greatest mass of the insulin-sensitive tissues and as such is heavily implicated in glucose homeostasis, particularly in the postprandial state where insulin is elevated.

Glucose is a hydrophilic molecule, which severely hinders its ability to pass freely (passively) through the plasma membrane and into myocytes (Barnard & Youngren, 1992). While skeletal muscle glucose transport has long been defined as being chiefly carrier-mediated, identification and characterisation of these transport proteins and their involvement in skeletal muscle glucose uptake only occurred relatively recently (Birnbaum, 1989; Charron, Brosius, Alper, & Lodish, 1989; Mueckler et al., 1985). The glucose transporter/solute carrier family 2 (GLUT/SLC2) family of membrane proteins is now understood to comprise 14 proteins encoded within the human genome, divided into 3 classes (Joost et al., 2002). The first of these classes comprises the most extensively characterised glucose transporters (GLUTs 1,2, 3 and 4) which are distinguished by their distinct tissue distributions and hormonal regulation. (Joost et al., 2002). Of greatest significance to the transport of glucose in adult human skeletal muscle are GLUT1 and GLUT4.

The facilitative glucose transporter GLUT1 (encoded by the SLC2A1 gene) exhibits a relatively low Michaelis constant (an inverse measure of the affinity of an enzyme for its substrate) and is relatively lowly expressed in mature skeletal

muscle, where it almost exclusively abounds as a membrane bound protein (Chadt & Al-Hasani, 2020). Thus, GLUT1 is principally involved in regulating basal, constitutive glucose transport (Amira Klip, Volchuk, He, & Tsakiridis, 1996; Richter & Hargreaves, 2013). Glucose transporter protein 4 (GLUT4; encoded by the SLC2A4 gene) was first identified by James et al. (1988), who further revealed that its function was substantially mediated by the presence of insulin. It is now understood that while GLUT1 is principally involved in basal skeletal muscle glucose transport, it is GLUT4 that has the greatest influence on stimulated transport, which is chiefly mediated via its translocation from the intracellular compartments where it mainly resides under basal conditions, to the sarcolemma (J. Huang, Imamura, & Olefsky, 2001; Thorkil Ploug, van Deurs, Ai, Cushman, & Ralston, 1998).

In resting muscle, a recycling pathway ensures that GLUT4 is largely retained in the intracellular compartments within GLUT4 storage vesicles (GSV) (Foley, Boguslavsky, & Klip, 2011). In rat muscle it has been shown that a quarter of intracellular GLUT4 is associated with large structures, particularly within the trans-Golgi region, while three quarters resides within smaller tubulovesicular structures, close to the sarcolemma (T. Ploug & Ralston, 1998). Thus, in order for the skeletal muscle to effectively respond to the elevated circulating glucose of the postprandial period by rapidly increasing its transport into the myocyte for oxidative and non-oxidative disposal, GLUT4 must first be translocated to the sarcolemma; a process of GSV exocytosis that is stimulated both by insulin and contractile activity (Lauritzen, Galbo, Toyoda, & Goodyear, 2010; A. D. Lee, Hansen, & Holloszy, 1995).

While acute regulation of glucose uptake into skeletal muscle is therefore primarily dependent on the sensitivity of the GLUT4 pool to respond to translocation stimuli, the absolute abundance of GLUT4 within the muscle also dictates the maximal capacity for glucose uptake, with both of these factors being positively augmented by exercise training and repressed by physical inactivity (Jeffrey S. Greiwe, Holloszy, & Semenkovich, 2000; Host, Hansen, Nolte, Chen, & Holloszy, 1998; Richter & Hargreaves, 2013). To that effect, relationships between GLUT4 expression/protein content and lifestyle factors such as diet and exercise have been described (Dela et al., 1994; Ivy, 2004). The acute recruitment of GLUT4 to the sarcolemma in response to insulin and contractile activity, however, appear to be regulated differentially by the relative efficiencies of endocytosis and exocytosis of GLUT4-contatining vesicles (Foley et al., 2011; Karlsson et al., 2009).

1.2 Insulin and Skeletal Muscle

Insulin is an anabolic peptide hormone produced in the pancreas, which plays a vital role in normal metabolism by promoting the absorption of glucose from the blood into bodily tissues. In healthy individuals, insulin is precisely regulated within the circulation to match acute metabolic demands, whereby pancreatic β-cells detect changes in plasma glucose concentration and induce the production and release of insulin (Schmitz, Rungby, Edge, & Juhl, 2008). This regulation is tightly controlled at both the transcriptional and translational level, while the efficacy of the circulating hormone is a product of the sensitivity of target tissues to its presence, via receptor binding and subsequent signalling cascades.

1.2.1 Insulin Biosynthesis and Secretion

Banting and Macleod's 1923 Nobel Prize-winning discovery of insulin sparked a revolution in the treatment of diabetes and with it our understanding of glucose homeostasis (Banting, 1926; Banting, Best, Collip, Campbell, & Fletcher, 1991). Insulin has since been characterised as a peptide hormone consisting of two disulphide-linked polypeptide chains (A- and B-chains, comprising 21 and 30 amino acids, respectively), derived from the proteolysis of its precursor preproinsulin, which is synthesised within β-cells of the islets of Langerhans within the pancreas (Najjar, 2003). A 24-residue signal peptide promotes the relocation of the preproinsulin to the rough endoplasmic reticulum (RER) where the signal peptide is cleaved by a signal peptidase and the remaining polypeptide is translocated into the RER lumen, forming the prohormone precursor proinsulin (Weiss, Steiner, & Philipson, 2000). Within the RER, proinsulin undergoes folding; is transported into the trans-Golgi network where immature granules are formed; and undergoes proteolytic cleavage of the C-peptide fragment by a specialised set of endoproteases and carboxypeptidase activity, leaving just the disulphide-linked A- and B-chains (Davidson, Rhodes, & Hutton, 1988; Kemmler, Peterson, & Steiner, 1971). Two pairs of basic residues are removed by carboxypeptidase, resulting in the mature insulin form, which is packaged within mature granules to await exocytosis (Fu, Gilbert, & Liu, 2013). Mature secretory vesicles contain equimolar amounts of native insulin and C-peptide fragments, alongside far smaller amounts (making up 2-3% of vesicular content) of proinsulin and intermediate cleavage products.

Insulin secretion into the circulation in response to elevated glucose is characteristically biphasic (Bratanova-Tochkova et al., 2002). This is due to only 1-5% of insulin-containing vesicles being available for immediate exocytosis, termed the readily releasable pool, while the remaining 95-99% form a reserve

pool that must first be primed via modification and translocation towards the plasma membrane (Daniel, Noda, Straub, & Sharp, 1999; Hou, Min, & Pessin, 2009). Thus, even under maximal stimulation, only a small fraction of the total insulin pool is released, suggesting insulin secretion, rather than total pool content, is the limiting factor for glucose homeostasis in most healthy individuals.

The β-cells are grouped together in islets that are heavily connected to the local vasculature (Henderson & Moss, 1985; Jansson et al., 2016). GLUT2 traffics glucose into these cells, where it is first metabolised by glucokinase; ultimately generating adenosine triphosphate (ATP); increasing the ATP:ADP ratio; causing the closure of the ATP-sensitive K^+ channels; reducing K^+ permeability; thus depolarising the plasma membrane (resulting in a less negative charge inside the cell relative to the outside) (Fu et al., 2013; Suckale & Solimena, 2008; Weiss et al., 2000). This depolarisation occurs slowly across the membrane, followed by bursts of action potentials when the glucose concentration is 5-15 mM and continuous spiking when > 16 mM (Ashcroft, Harrison, & Ashcroft, 1984). Subsequent opening of the voltage-dependent Ca^{2+} channels leads to a Ca^{2+} influx and eventual exocytosis of the insulin-laden granules of the readily releasable pool via direct interactions between exocytotic proteins within the granule membrane and those of the plasma membrane which initiates fusion of the granules to the membrane (S.-N. Yang & Berggren, 2006; S. N. Yang & Berggren, 2005).

The action of insulin is antagonised by the peptide hormone glucagon, produced by pancreatic alpha cells, which stimulates hepatic glucose release via glycogenolysis (the breakdown of stored glycogen into glucose) and gluconeogenesis (the synthesis of glucose from non-carbohydrate substrates). Other hormones and neurotransmitters also play a role in regulating insulin production, secretion and signalling, including adrenaline, somatostatin and gut-derived hormones such as glucagon-like peptide and glucose-dependent insulinotropic peptide (Drucker, Philippe, Mojsov, Chick, & Habener, 1987; Mojsov, Weir, & Habener, 1987) and are reviewed elsewhere (Bratusch-Marrain, 1983; Lager, 1991; Pelle et al., 2022).

Insulin secretion predominantly occurs in discrete bursts approximately every 4 min, which correlates well with its half-life of just 4-6 min. Once exocytosis has occurred and insulin has entered into the portal vein, it first transits to the liver where >75% is bound and removed during first portal passage (Meier, Veldhuis, & Butler, 2005). The remaining fraction passes through the hepatic vein and into systemic circulation, where it is cleared and degraded by various tissues, principally via insulin-receptor tyrosine kinase binding and insulin degrading

enzyme activity, respectively (Duckworth, 1988). While receptor-mediated insulin binding occurs in all insulin-sensitive tissues, after first-transit hepatic binding, it is the skeletal muscle that binds to the lion-share of circulating insulin.

1.2.2 Insulin Receptor Binding in Skeletal Muscle

The cascade that actuates insulin-action in skeletal muscle can be broadly split into proximal and distal signalling events, reflecting receptor-level and post-receptor-level actions, respectively. Proximally, insulin first binds to the insulin receptor on the plasma membrane of muscle cells (Figure 1.2). The insulin receptor is a heterotetramer consisting of two extracellular (α) subunits, which bind the insulin ligand, that are disulphide-linked to two trans-membranous (β) subunits which once auto-phosphorylated, undergo conformational change, inducing function as receptor tyrosine kinases (Boucher, Kleinridders, & Kahn, 2014). The activated subunits allow the recruitment and phosphorylation of insulin receptor substrates (IRS), thus transmitting the signal across the plasma membrane.

1.2.3 Insulin Signalling in Skeletal Muscle

The IRS proteins are capable of binding and activating many downstream effector proteins, which form the distal portion of the insulin signalling pathway. IRS-1 contains several motifs that readily bind proteins with Src homology domain 2, which is involved in myriad downstream pathways, enabling a single phosphorylated IRS-1 protein to simultaneously activate a range of signalling pathways. Crucially for insulin-stimulated glucose uptake, the phosphorylation of IRS enables the binding and activation of phosphatidylinositol 3-kinase (PI3K), which in turn phosphorylates the membrane lipid phosphatidylinositol 4,5-biphosphate (PIP2), to form PIP3 (Myers et al., 1992; Shaw, 2011). PIP3 drives the activation of 3-phosphoinositide-dependent protein kinase 1 (PDPK1), which phosphorylates protein kinase B (Akt) and atypical protein kinase C (aPKC) (Farese, Sajan, & Standaert, 2005; Welsh et al., 2005).

Protein kinase B is able to phosphorylate the Rab-GTPase-activating proteins Akt substrate of 160kDa (AS160) and tre-2/BUB2/cdc 1 (TBC1D1; however TBC1D1 phosphorylation does not appear to be essential for the augmentation of glucose uptake in skeletal muscle (Cartee, 2015)), which promote the hydrolysis of guanosine-5'-triphosphate (GTP) to guanosine diphosphate on the vesicles containing GLUT4, releasing them from their translocation-inhibited state (Karlsson et al., 2005; Middelbeek et al., 2013). The GLUT4-containing vesicles are then able to translocate to the muscle cell surface for membrane binding, increasing the capacity for glucose transport into the muscle cell (Figure 1.2).

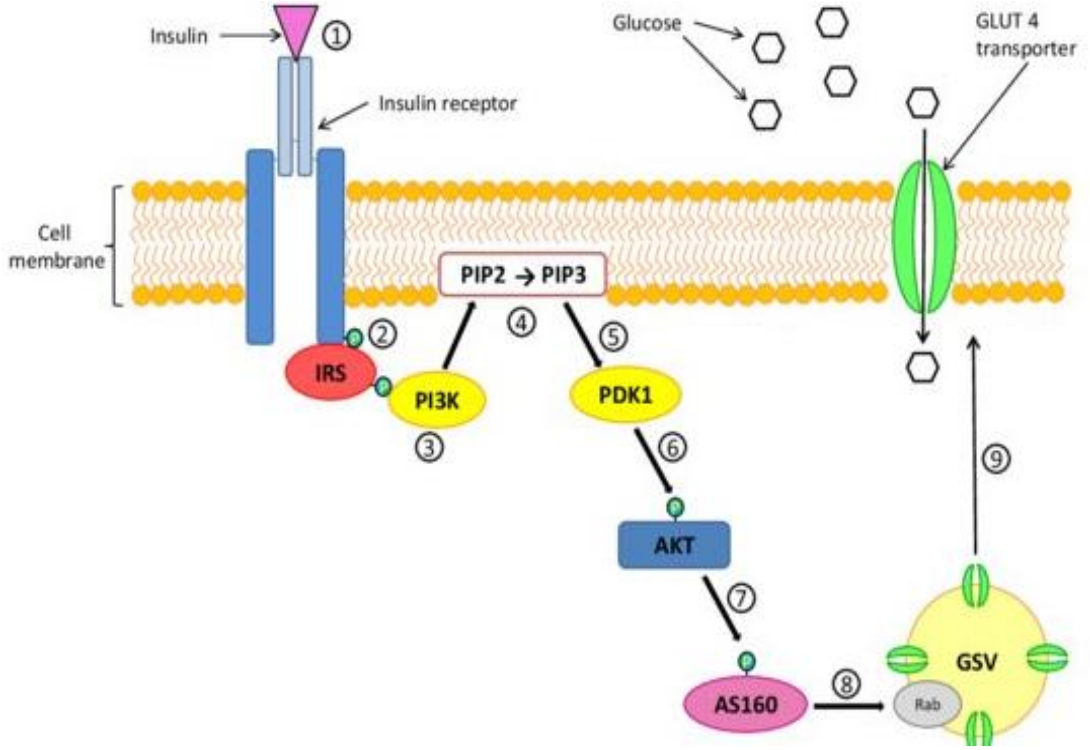

Figure 1.2. Insulin signalling in skeletal muscle that induces GLUT4 translocation.

Circulating insulin binds to its receptor on the cell membrane, phosphorylating and activating Shc and IRS substrate proteins. Activation of the IRS enables the binding and activation of PI3K, which in turn phosphorylates PIP2 to PIP3, activating PDPK1, which phosphorylates Akt and aPKC. Akt phosphorylates the Rab-GTPase-activating proteins AS160, which promotes GTP hydrolysis of the GLUT4 vesicles, allowing the translocation of GLUT4 to the membrane, where it facilitates glucose transport into the muscle. From Lankatillake, Huynh, and Dias (2019) under CC BY-NC 4.0.

1.3 Insulin Disturbances

Disturbance of the normal regulation of insulin production, secretion, receptor binding, signalling and subsequent action, independently or in communion with one another result in a systemic failure to adequately maintain normal glucose homeostasis (R. A. DeFronzo, 1997; Kahn, 1998). These disturbances can be the result of autoimmune disorders, which may be genetically influenced, such as in type I diabetes mellitus (Pociot & Lernmark, 2016), disease-associated such as may be the case with pancreatic cancer (Pannala, Basu, Petersen, & Chari, 2009), or the culmination of lifestyle associated factors that progressively diminish insulin sensitivity and/or secretion, such as is the case in Type 2 Diabetes Mellitus (T2D) (Guillausseau et al., 2008). Of principal interest here, is the decline in sensitivity to the normal effects of insulin within metabolically active tissues, particularly the skeletal muscle, which leads to a state termed insulin resistance.

1.3.1 Insulin Resistance

Insulin resistance is defined as a state in which a normal or elevated insulin level produces an attenuated biologic response (Cefalu, 2001), which in the context of skeletal muscle most notably presents as an impaired ability to stimulate glucose uptake (but also amino acid uptake and subsequent glucose and BCAA metabolism) in response to elevated insulin. Insulin resistance is also typically characterised by impaired insulin-stimulated glucose uptake in adipose tissue and the liver (Olefsky & Nolan, 1995), as well as a diminished sensitivity to the antilipolytic actions of insulin (Groop et al., 1989) and the insulin-mediated suppression of hepatic glucose production (Abdul-Ghani, Tripathy, & DeFronzo, 2006). In the long term, impaired sensitivity to insulin results in compensatory hyperinsulinaemia, which is maintained until this increased pancreatic demand can no longer be met and insulin secretory deficiencies occur (Reaven, 2005). Upon the occurrence of β-cell dysfunction, there becomes a functional imbalance between the glycaemic environment and the ability of tissues to take up circulating glucose, eventually resulting in a sustained hyperglycaemic state that is characteristic of T2D.

The occurrence of insulin resistance was first identified almost a century ago when it was observed that patients with diabetes could be divided into two sub-populations based on their relative sensitivity to the glycaemia-lowering effects of exogenous insulin, which approximately represented the types 1 and 2 diabetes mellitus, whereby T2D patients required markedly greater insulin dosage to elicit

reductions in circulating glucose concentration (Himsworth, 2011; Hunter & Garvey, 1998). Accordingly, impaired rates of glucose disposal and hyperinsulinaemia are proposed to precede β-cell dysfunction and are strong predictors of the development of T2D (Ormazabal et al., 2018; Warram, Martin, Krolewski, Soeldner, & Kahn, 1990). It has been proposed that diminished insulin-stimulated glucose uptake into peripheral tissues is often accompanied by perturbed sensitivity to the insulin-mediated suppression of hepatic glucose production, which further exacerbates the loss of glycaemic control (Abdul-Ghani et al., 2006). The twin cycle hypothesis described by R. Taylor (2008) proposes that chronic energy imbalance promotes the accumulation of fat within the liver, which is exacerbated due to hyperinsulinaemia in individuals with a degree of existing insulin resistance, leading to impaired sensitivity of the liver to suppress glucose production in response to insulin (the start of the first cycle). Plasma glucose thus rises and with it the secretion of insulin from the pancreas. The elevation of liver fat increases its triacylglycerol secretion, elevating its circulating abundance, which accumulates in the pancreatic islets and impairs their responsiveness to elevations in glucose concentration. Thus, the stimulation of insulin secretion is impaired and plasma glucose is further elevated, driving the second deleterious cycle. These cycles continue their adverse actions until eventually the inhibitory effects of fatty acids and glucose on the pancreatic islets ultimately reaches a threshold, at which point the onset of clinical diabetes can occur with relative haste (R. Taylor, 2008, 2013).

The terms insulin resistance and reduced insulin sensitivity are sometimes used interchangeable and thus considered as two sides of the same coin. This approach however lacks clarity. For the purpose of this thesis, insulin resistance within humans is broadly defined as an impaired ability for endogenous or exogenous insulin to increase glucose uptake and utilisation from the circulation, relative to the normal, healthy population (Lebovitz, 2001). Thus, insulin resistance can be clinically considered as a state of being whereby insulin-stimulated glucose disposal is fundamentally impaired. On the other hand, for the purpose of this thesis, insulin sensitivity is considered to be a measure of function of the body, or of an *in vitro* culture system, in response to insulin. Thus, insulin sensitivity may be better considered to provide an index to describe changes in the functional capacity of a system to respond to insulin stimulation. *Ergo*, one would measure insulin sensitivity in order to determine the presence of insulin resistance.

1.3.2 Aetiology of Insulin Resistance

Impaired insulin-stimulated glucose disposal is a key marker of insulin resistance in skeletal muscle, and glucose disposal is markedly diminished with T2D. The insulin resistant state is more often observed in individuals with obesity; however, obesity is not an essential prerequisite for insulin resistance, nor the development of T2D. In a five and a half year study of otherwise healthy participants, incident pre/type II diabetes rates were comparable between obese insulin resistant and non-obese insulin resistant individuals (Owei, Umekwe, Provo, Wan, & Dagogo-Jack, 2017).

Due to a range of genetic and lifestyle factors, the prevalence of the non-obese but metabolically dysfunctional and typically insulin resistant phenotype (so-called 'metabolically obese normal weight') varies greatly between population groups, ranging from 5-45% normal weight adults presenting with metabolic dysfunction, including insulin resistance, as indicated by an index of fasting glucose and insulin levels (Homeostatic Model Assessment of Insulin Resistance) (Conus, Rabasa-Lhoret, & Peronnet, 2007; Wildman, Muntner, Reynolds, & et al., 2008). Similarly, obesity without detectable insulin resistance, sometimes controversially termed metabolically benign obesity (although this term may also be applied more broadly to the presence of ≤2 components of the metabolic syndrome, which could potentially include insulin resistance), is reportedly observed in anywhere from 10-70% of obese individuals, depending on the criteria used and population assessed (Bluher, 2010; Blüher, 2012; E. Ferrannini et al., 1997; Rotar et al., 2017). Perhaps surprisingly, even in the morbidly obese, it has been shown that ~20% of males and ~30% of females present without the metabolic syndrome (Soverini et al., 2010) (a loosely defined cluster of metabolic and clinical conditions and risk factors, including impaired fasting glycaemia, glucose intolerance, insulin resistance, dyslipidaemia, hypertension and BMI >30, that drive a primary clinical outcome of cardiovascular disease (Grundy, Brewer, Cleeman, Smith, & Lenfant, 2004; Maison, Byrne, Hales, Day, & Wareham, 2001), which might reflect their typically lower waist circumference, blood pressure, and fasting metabolite concentrations than those seen in the obese insulin-resistant phenotype (Calori et al., 2011).

Mechanistically, the aetiology of insulin resistance, and ultimately T2D, is multifactorial and complex, with an element of genetic (Elgzyri et al., 2012; Meigs, Cupples, & Wilson, 2000) and epigenetic (Lehnen, Zechner, & Haaf, 2013; Rizzo et al., 2020) susceptibility. In this thesis, it is the role of lifestyle-associated factors that are of principal interest in the aetiology of insulin resistance,

specifically within the skeletal muscle. These factors include but are by no means limited to; overt hyperenergetic and high-fat habitual dietary intake; the ectopic accumulation of intramuscular lipid species and their fragments; mitochondrial dysfunction; and physical inactivity, which exacerbates all of these factors.

1.3.3 High Fat Diets and Lipid-Induced Insulin Resistance

High fat diets (HFD) are a common feature of obesity and may exacerbate the propensity for insulin resistance in the chronic hypercaloric environment (Bray & Popkin, 1998; Golay & Bobbioni, 1997). Over half a century ago, Randle and colleagues (1963) postulated a mechanism by which lipids may impair skeletal muscle glucose oxidation under insulin-stimulated conditions, through the inhibition of glycolysis. It is now a widely held belief that defective glucose transport and phosphorylation are principally implicated in the blunting of insulin-stimulated glucose metabolism, which may subsequently lead to impaired glycolysis and glycogen synthesis (Bonadonna et al., 1996; Garvey et al., 1998; Krebs & Roden, 2005; Roden et al., 1996; Samuel, Petersen, & Shulman, 2010). Ectopic fat accumulation, fatty-acid derived metabolites, mitochondrial fat overload and incomplete lipid oxidation are all proposed contributors to impaired insulin sensitivity in skeletal muscle in response to fat overload and HFD (Ciaraldi, Abrams, Nikoulina, Mudaliar, & Henry, 1995; Garvey et al., 1998; Koves et al., 2008).

A key feature of skeletal muscle insulin resistance in obesity is the accumulation of intramuscular lipid species (Kraegen, Cooney, & Turner, 2008). Four families of lipid species have been frequently associated with insulin resistance; diacylglycerols (DAG), ceramides, long-chain fatty acyl-CoAs, and acylcarnitines (Amati, 2012). Intramyocellular DAG accumulation may arise due to an inability to match the conversion rate of DAG to triacylglycerol (TAG), to that of fatty acid delivery (L. Liu et al., 2007; Schenk & Horowitz, 2007; Shulman, 2000). It is proposed that DAG activates PKC serine-threonine kinase family members, which promote phosphorylation of the insulin receptor and its substrate IRS-1, suppressing PI3K activity and impairing the insulin signalling cascade (Bollag, Roth, Beaudoin, Mochly-Rosen, & Koshland, 1986; Dresner et al., 1999; Samar I. Itani, Ruderman, Schmieder, & Boden, 2002; S I Itani, Zhou, Pories, MacDonald, & Dohm, 2000; Yu et al., 2002). However, not all studies demonstrate concurrent induction of insulin resistance and DAG accumulation in response to either acute (L. D. Høeg et al., 2011; Vistisen et al., 2008) or short-term lipid overload (Kostas Tsintzas et al., 2020). Furthermore, muscle DAG is not always elevated in insulin

resistant individuals (Anastasiou et al., 2009; L. Perreault, Bergman, Hunerdosse, & Eckel, 2010).

Ceramide is an important second signal molecule that links nutrient signals to inflammatory pathways (Ruvolo, 2001; Sokolowska & Blachnio-Zabielska, 2019; Summers, 2006; Timmers, Schrauwen, & de Vogel, 2008). The rate of de novo ceramide synthesis is governed by the availability of long-chain saturated fatty acids (Merrill, 2002; Merrill & Jones, 1990). Thus, in settings of elevated fatty acids, such as obesity and lipid infusion, intramuscular ceremide content is often elevated (J. M. Adams, 2nd et al., 2004; Straczkowski et al., 2004; Turinsky, O'Sullivan, & Bayly, 1990). Ceramides may impair insulin sensitivity via inhibiting PI3K signalling and Akt phosphorylation (Powell, Hajduch, Kular, & Hundal, 2003; Schmitz-Peiffer, Craig, & Biden, 1999; Stratford, Hoehn, Liu, & Summers, 2004).

Long-chain acyl-CoAs, which are elevated by increased lipid availability reflecting an imbalance between lipid-derived acetyl-CoA production and acetyl-CoA oxidation, have also been implicated in skeletal muscle insulin resistance (Cooney, Thompson, Furler, Ye, & Kraegen, 2002; Ellis et al., 2000; F. B. Stephens et al., 2015; K. Tsintzas et al., 2007). Long-chain acyl-CoAs are able to modulate skeletal muscle gene transcription (Hostetler, Kier, & Schroeder, 2006) and may induce insulin resistance through the attenuation of insulin-stimulated Pyruvate Dehydrogenase Kinase 4 (PDK4) suppression (K. Tsintzas et al., 2007). Upregulation of PDK4 is associated with inhibited pyruvate dehydrogenase complex (PDC) activity, which is a key limiting step in insulin-stimulated glucose oxidation (Chokkalingam et al., 2007; D. E. Kelley, Mokan, Simoneau, & Mandarino, 1993; Mandarino et al., 1987).

Acylcarnitines are intermediate oxidative metabolites that transport long-chain fatty acids across the mitochondrial membrane for β-oxidation (Kiens, 2006; McCoin, Knotts, & Adams, 2015). Both plasma and skeletal muscle long-chain acylcarnitines are elevated in individuals with insulin-resistant obesity and T2D (S. H. Adams et al., 2009; Ha et al., 2012; Hoppel & Genuth, 1980; Mihalik et al., 2010). It has been proposed that lipid-induced insulin resistance arises secondarily to mitochondrial overload, whereby excess lipid availability and/or incomplete fatty acid oxidation induces an imbalance between fatty acid availability and TCA cycle activity, leading to an accumulation of acylcarnitines (Koves et al., 2008; McCoin et al., 2015; Muoio & Neufer, 2012). Acylcarnitine treatment of C2C12 myotubes impairs insulin-stimulated Akt phosphorylation and glucose uptake (Aguer et al., 2015) and chain-shortened acylcarnitines activate pro-inflammatory pathways (S. H. Adams et al., 2009), although this pool is also

contributed to by the metabolism of branched-chain amino acids (Rousseau et al., 2019). The extent to which acylcarnitine accumulation impairs glucose uptake and metabolism in human skeletal muscle, however, is unclear (Schooneman, Vaz, Houten, & Soeters, 2012; F. B. Stephens et al., 2014). Together, these lipid-induced factors all appear to contribute to the development of insulin resistance in skeletal muscle, which is generally considered to be the initiating or primary defect that leads ultimately leads to the development of T2D (Ralph A. DeFronzo & Tripathy, 2009).

1.4 Anabolic Resistance

Often concurrent with insulin resistance is a phenomenon termed anabolic resistance (Breen et al., 2013; Morais, Jacob, & Chevalier, 2018; Morton, Traylor, Weijs, & Phillips, 2018; Murton et al., 2015). Taking a simplified view, anabolic resistance is a phenomenon whereby skeletal muscle becomes insensitive to anabolic signals such as protein provision, contractile activity, or hormonal stimulation, ultimately resulting in insufficient muscle protein synthesis to regulate skeletal muscle mass (Morton et al., 2018; Rennie & Wilkes, 2005). Although not universally agreed upon, some degree of anabolic resistance is often considered to be an inherent property of physical ageing and is postulated to be a central driver of sarcopenia (D. Cuthbertson et al., 2005; Katsanos, Kobayashi, Sheffield-Moore, Aarsland, & Wolfe, 2005). Furthermore, failure to adequately respond to anabolic signals has been reported following physical inactivity; in individuals with obesity; and is particularly problematic in critical care patients in whom inactivity is often confounded with reduced gastric and intestinal motility and nutrient uptake, which further limits responsiveness to the protein stimulus (M. J. Chapman et al., 2009; M. J. Chapman, Nguyen, & Fraser, 2007). While often concurrently present or induced (F. B. Stephens et al., 2015), there appears to be an uncoupling between insulin resistance and anabolic resistance, as demonstrated by the induction of anabolic, but not insulin resistance by a short-term HFD (Ato, Mori, Fujita, Mishima, & Ogasawara, 2021; Kostas Tsintzas et al., 2020) and the observation of impaired muscle protein synthetic response to protein feeding in young adults who are overweight or obese, despite presenting with normal insulin sensitivity (Beals et al., 2016).

Anabolic resistance appears to be a postprandial, but not post-absorptive phenomenon, with fasting muscle protein fractional synthesis rates not differing between the young, older, and older obese (Smeuninx, McKendry, Wilson, Martin, & Breen, 2017). Indeed, obesity appears to drive an intrinsic blunting of muscle protein synthesis in response to amino acid feeding, but not under post-absorptive

conditions (Murton et al., 2015). Furthermore, it is not only whole-body adiposity that is associated with anabolic resistance, but also lipid administration, HFD, and intramuscular lipid accumulation (S. R. Anderson, Gilge, Steiber, & Previs, 2008; F. B. Stephens et al., 2015; Tardif et al., 2014). Some researchers have described a caveat with regards to diabetic populations, as they may not present with impaired postprandial protein synthesis compared to normoglycaemic individuals, despite reduced lean mass, increased fat mass and lower mechanistic target of rapamycin (mTOR) signalling responses (D. J. Cuthbertson, Babraj, Leese, & Siervo, 2017; Kouw et al., 2015).

1.5 Sarcopenia

Ageing is a highly complex whole-system process. It remains unclear as to what extent physiological senescence is an inherent trajectory, or a product of converging lifestyle factors. What is clear, however, is that with increasing age, humans typically exhibit substantial functional declines in many organ systems, to the order of approximately 0-2% per year from the age of 30 (Sehl & Yates, 2001). Skeletal muscle tissue is the human body's principle protein bank, accounting for almost 60% of total body protein, which given the absence of a protein pool for storage, highlights the delicate and vital interplay between muscle protein synthesis and degradation for maintaining protein status (Guillet, Boirie, & Walrand, 2004; Poortmans, Carpentier, Pereira-Lancha, & Lancha, 2012).

The phenomenon of diminishing muscle mass with advancing age was first recognised almost a century ago (Critchley, 1931). By the mid-20th century, the general consensus was that no other decline in physical architecture or function was more pronounced than that of the loss of lean tissue mass with ageing. Despite the modern trend for ever-increasing body mass, a decline in skeletal muscle mass remains a prominent feature of advanced physical ageing. Rosenberg (1997) proposed the term *sarcopenia* (from the Greek *sarx*, meaning flesh, and *penia*, meaning loss) to describe the observed decrements in muscle mass and function, hoping that the use of a singular name would help unify and direct research from the scientific and medical community. Work by (2001) promoted adoption of the term, emphasising its association with geriatric frailty.

Despite the subsequent widespread adoption of Rosenberg's appellation, a universally accepted definition of sarcopenia remains elusive, with the term sarcopenia regularly being used to describe both an ageing process and a diagnosable syndrome. Indeed, the European Society of Clinical Nutrition and Metabolism have described sarcopenia as a disease of the elderly, but also stipulate that its development can be observed in other non-geriatric conditions

(Muscaritoli et al., 2010). The European Working Group on Sarcopenia in Older People suggested that the requisite criteria for the diagnosis of Sarcopenia should include low muscle strength and/or low physical performance in addition to low muscle mass, due to the non-linear relationships between the criteria (Goodpaster et al., 2006). In a revised consensus, the working group adjusted their stance to focus on low muscle strength as the primary parameter of sarcopenia, citing its superiority in predicting adverse outcomes (Lauretani et al., 2003).

Since skeletal muscle is responsible for a substantial proportion of insulin-stimulated glucose disposal via oxidation or conversion of glucose to muscle glycogen, diminishing skeletal muscle mass directly reduces whole body capacity for glucose disposal (R. A. DeFronzo, 2004). However, insulin resistance is not an unequivocal feature of sarcopenia in individuals with low overall bodyweight, although insulin resistance may promote sarcopenia (Abbatecola et al., 2011). Moreover, anabolic resistance and sarcopenia often go hand-in-hand (Haran, Rivas, & Fielding, 2012) and anabolic resistance to amino acids may precede the significant loss of muscle mass in ageing (Volpi, Mittendorfer, Rasmussen, & Wolfe, 2000)

1.5.1 Prevalence and Social Impact

Reported rates of muscle loss and the age of its onset varies greatly, however losses of around 1-2% per year in those over the age of 50 have been frequently described (von Haehling, Morley, & Anker, 2010). Determining the clinical prevalence of the sarcopenic condition is difficult, due to the greatly varying use of diagnostic criteria. It has been reported that prevalence ranges from 5-13% in those aged 60-70 years and affects as many as 50% of those over 80 years old (J. E. Morley, 2008). Myriad factors beyond chronological ageing can drive sarcopenia, but perhaps none more so than skeletal muscle disuse, which may arise from injury, immobility, and bed rest (Therakomen, Petchlorlian, & Lakananurak, 2020).

The implications of sarcopenia and frailty go beyond the physical consequences. It has been repeatedly shown that sarcopenic older adults report a lower quality of life (Rizzoli et al., 2013; Tsekoura, Kastrinis, Katsoulaki, Billis, & Gliatis, 2017) and greater depressive symptoms in patients with existing conditions (Nipp et al., 2018). The frailty associated with sarcopenia also affects social functioning (Hoogendijk, Suanet, Dent, Deeg, & Aartsen, 2016), which might reflect a reduced physical ability for social engagement and an increased fear of falls. Tragically, this relationship appears to be bi-directional, with high levels of loneliness being a predictive factor for frailty (Gale, Westbury, & Cooper, 2018; Shankar, McMunn,

Demakakos, Hamer, & Steptoe, 2017). Thus, the age-related decline in muscle mass, quality, and function, which can be exacerbated and perhaps driven by anabolic and insulin resistance, presents an area of research that is of the utmost importance in an ageing society.

1.6 Obesity and Metabolic Dysfunction

Obesity is broadly defined as an excess of body-fat mass, which for the purpose of public health assessment is recognised by a body mass index (BMI) >30kg·m^{-2}, though on an individual basis this may not always be a valid diagnostic tool due to a failure to account for lean tissue mass (NHS, 2019a). Obesity is caused by a chronic imbalance in energy provision and expenditure, largely reflecting a surplus of dietary intake and an insufficiency of physical activity (Schwartz et al., 2017). This sustained imbalance is believed to progressively drive a resetting of the body mass 'set point' at a new, greater mass, at which point energy balance is re-established, making long-term weight loss more challenging (Keesey & Hirvonen, 1997). Beyond the simple yet ineluctable role of energy balance in the development of obesity, the metabolic effects of, and possibly the susceptibility to, obesity may also be influenced by more subtle factors, such as dietary macronutrient composition, lipid composition of dietary fat intake, certain micronutrient deficiencies, microbiome composition, and habitual physical activity level (Canfora, Meex, Venema, & Blaak, 2019; Pramono, Jocken, & Blaak, 2019; San-Cristobal, Navas-Carretero, Martínez-González, Ordovas, & Martínez, 2020; Strasser, 2013).

The worldwide prevalence of obesity is increasing year on year, having nearly tripled since 1975. Approximately 2 billion people are overweight worldwide, one third of whom are obese (Seidell & Halberstadt, 2015). For the first time in human history, in 2004 for women and 2011 for men, more people on earth lived in countries with a greater proportion of obese than underweight individuals (NCD, 2016). Obesity is the principle characteristic of the metabolic syndrome and presents a growing global public health and economic burden, with NHS annual spending for over-weight and obesity in excess of £6 bn, while the cost to wider society may be seven fold that of the health service (Butland et al., 2007).

Of particular cause for concern, the increasing prevalence of obesity is reflected in a trend for increased abdominal adiposity, with prevalence having increased by ~50% in the United States since the 1980s (Ladabaum, Mannalithara, Myer, & Singh, 2014; Robinson, Utz, Keyes, Martin, & Yang, 2013). Current consensus suggests that for any given amount of body fat, individuals with focused central adiposity, exhibiting greater intra-abdominal and/or visceral adipose tissue, are

more likely to present with insulin resistance and associated markers of the metabolic syndrome (Despres, 2006; Despres et al., 1990). It has been suggested that visceral fat accumulation is causally related to insulin resistance; but it has equally been posited that excessive intra-abdominal fat accumulation is a symptom of dysfunctional subcutaneous adipose tissue, reflecting its insufficiency to function as an 'energy sink' during chronic energy surplus (Després & Lemieux, 2006).

Evidence suggests that in a positive energy balance state, preferentially routing surplus energy into subcutaneous tissue is positively associated with the preservation of insulin sensitivity, whereas preferential visceral fat deposition is associated with insulin resistance and ectopic fat accumulation within the liver, heart, and skeletal muscle (Hardy, Czech, & Corvera, 2012; McLaughlin, Lamendola, Liu, & Abbasi, 2011). Thus, visceral fat is often considered to be more pro-pathogenic than its subcutaneous counterpart (Elks & Francis, 2010). The capacity and propensity for adipose tissue to exert deleterious metabolic effects when in excessive abundance, reflects not only its own impaired ability to handle circulating substrates, but also its function as an endocrine body in its own right, capable of influencing other bodily tissues including skeletal muscle.

1.6.1 Sarcopenic Obesity: A Double-Edged Sword

Independently, obesity and sarcopenia pose significant health risks, however the global shift towards sedentariness and overconsumption may result in their concomitant development; so called sarcopenic obesity, or sarcobesity. Given the deleterious effects of obesity and sarcopenia on mobility, functional capacity and metabolic health, it stands to reason that their coexistence could exacerbate sarcopenia, however this is contested (Wannamethee & Atkins, 2015). As with sarcopenia, diagnosing a state of sarcopenic obesity is challenging due to a lack of consensus on both its definition and clinical characteristics (Batsis & Villareal, 2018). The sarcopenic-obese phenotype is posited to increase the risk of comorbidities such as osteoarthritis, type II diabetes, cardiovascular diseases and increase all-cause mortality (Atkins et al., 2014; S. Lee, Kim, & Kim, 2012; Sanada et al., 2018; Stephen & Janssen, 2009), however whether these effects are greater than that of sarcopenia alone is contested (Hamer & O'Donovan, 2017). Corroboratively, sarcopenic obesity has greater correlation strength with the degree of insulin resistance and hyperinsulinaemia in T2D patients, than sarcopenia or obesity alone (Son, Lee, Kim, & Yoo, 2012). Akin to insulin resistance, it has been proposed that effects of sarcopenic obesity are a product of the accumulation of lipids and their metabolites in skeletal muscle (Masgrau et

al., 2012), as well as cross-talk between adipose and muscle tissue (Paris, Bell, & Mourtzakis, 2020)

1.7 Skeletal Muscle as an Endocrine Organ

Skeletal muscle not only responds to external endocrine stimuli, but also acts as a secretory organ in its own right, capable of producing and secreting endogenous factors that elicit autocrine, paracrine and endocrine effects (Bente K. Pedersen & Febbraio, 2008). Since the identification of myostatin as the first known muscle-secreted cytokine (myokine) (McPherron et al., 1997), analysis of the secretome of human myocyte culture has identified over 600 myokines to date, though few have had their biological function well characterised (Gorgens, Eckardt, Jensen, Drevon, & Eckel, 2015). While functionally similar to hormones, and certainly the nomenclature is less than universally agreed upon, cytokines are generally accepted to differ from hormones in that hormones are secreted specifically from discrete endocrine tissues and act distally. Furthermore, at the molar level, cytokines display far greater potency and responsiveness than hormones, with normal concentrations that are in the pico-molar range that can increase up to 1000-fold with serious trauma and infection, compared to the typically nano-molar range of hormones that usually fluctuate only within an order of magnitude (Dinarello, 2007). For many of the described myokines, contractile activity is the principle regulator of expression, production and secretion. (Schnyder & Handschin, 2015). These contraction-mediated myokines are sometimes referred to as 'exerkines' or 'exercise factors'.

The most well characterised myokines are those secreted in response to contraction. These so-called 'exercise factors' were hypothesised to be responsible for the preventative, therapeutic and adaptive changes induced in various bodily tissues with exercise (Bente Klarlund Pedersen, Åkerström, Nielsen, & Fischer, 2007), and so began the search for the elusive exercise mimetic. It has since become apparent that no singular factor or factors are responsible for such changes. It is in fact the multiplicity and complexity of the highly versatile nature of factors such as peroxisome proliferator-activated receptor gamma coactivator 1-alpha, the so-called 'master regulator' of exercise adaptation, that facilitate the activation of complex and distinct biological programmes in multiple tissue via interactions with many different transcription factors (J. A. Hawley, Hargreaves, Joyner, & Zierath, 2014; John A. Hawley, Joyner, & Green, 2021). Indeed, with the rise of proteomic technologies in recent years, the secretome of cultured myotubes has since been comprehensively analysed, revealing over 600 secreted proteins (Gorgens et al., 2015; Hartwig et al., 2014; Ojima et al., 2014).

Most cytokines can act on multiple tissues, typically forming cascades whereby one cytokine triggers the production/secretion of others which may have synergistic or antagonistic effects. Myokines have been implicated in metabolic homeostasis, including the ability to modulate insulin action and cell-specific metabolism (Das, Graham, & Cardozo, 2020; Eckel, 2019). Myokines are involved in the anti-inflammatory effects of exercise with emerging involvement in cross-talk with adipose tissue (Bostrom et al., 2012), liver (Takahashi, Kotani, Tanaka, Egucih, & Anzai, 2018), bone (Hamrick, McNeil, & Patterson, 2010), β-cells (Bouzakri et al., 2011) and the brain (Bente Klarlund Pedersen, 2019), to name a few. Given the low-grade pro-inflammatory effects of chronic excess energy intake and the resulting hypertrophic adipose condition (Hui Wang & Ye, 2015), it follows that if muscle-derived factors communicate with other tissues, so too may other tissue-derived factors communicate with muscle.

1.8 Adipose Tissue as an Endocrine Organ

Once considered a passive energy reservoir, the discovery of the adipose-secreted factors adipsin and leptin revealed adipose tissue to be an endocrine organ (Cook et al., 1987; Siiteri, 1987; Y. Zhang et al., 1994). In an early study, it was observed that the adipose tissue of individuals with obesity demonstrated increased expression and secretion of tumour necrosis factor-alpha (TNF-α); it has since been shown that beyond the fundamental expansion of adipose tissue mass and adipocyte number, obesity promotes the accumulation of macrophages within adipose tissue and accelerates cellular senescence; leading to aberrant cytokine production and metabolic dysfunction (Hotamisligil, Shargill, & Spiegelman, 1993; Z. Liu, Wu, Jiang, Xu, & Cheng, 2020; Weisberg et al., 2003). Although many cytokines are secreted by adipose tissue, only a few including leptin and adiponectin are generally agreed to be 'true' adipokines that are abundantly secreted by adipocytes but not by other cells (Fantuzzi, 2005).

It is now understood that adipose tissue participates in a broad spectrum of inter-organ communication (Funcke & Scherer, 2019) and the presence of obesity conveys pleiotropic effects on endocrine and metabolic function (Frühbeck, Gómez-Ambrosi, Muruzábal, & Burrell, 2001; Mathus-Vliegen et al., 2012). In the presence of obesity, the secretion and processing of many of these adipose-derived factors have been implicated in the regulation of skeletal muscle insulin sensitivity, as well as mass and function, the latter of which is even more significant in the context of ageing (Bittel & Jaiswal, 2019; Nicholson, Church, Baker, & Jones, 2018; Haidong Wang & Wang, 2016; Wilhelmsen et al., 2021).

1.8.1 Adipose-Muscle Cross-Talk in the Presence of Obesity

Many tissues, including skeletal muscle and adipose, are able to interact and exert influence on one another (cross-talk). While cytokines can be secreted discretely, they are also transported by the secretion and transfer of extracellular vesicles (EVs) (Barnes & Somerville, 2020). EVs, principally divided into exosomes and microvesicles, are respectively released into the extracellular environment from endosomal and plasma membrane origins and are reviewed elsewhere (Raposo & Stoorvogel, 2013; Rome, Forterre, Mizgier, & Bouzakri, 2019). Alongside cytokines, EVs contain a broad array of cargo including proteins, lipids, organelle components and myriad non-coding RNAs, which have emerged as an important communication channel within and between different tissues, including skeletal muscle and adipose (Tkach & Théry, 2016). Pertinently, the discrete and EV-mediated secretion and processing of novel cytokines, long non-coding and micro RNAs, from adipose and skeletal muscle tissue, have been implicated in the regulation of skeletal muscle mass, function and pathologies, in the context of obesity and ageing (Bittel & Jaiswal, 2019; Haidong Wang & Wang, 2016).

The numerous ways in which the secretomes of skeletal muscle and adipose tissue communicate and interact to regulate metabolic function have only begun to be elucidated. What is emerging, however, is that these relationships are complex, multi-faceted, sometimes bi- and other times multi-directional (Indrakusuma, Sell, & Eckel, 2015). There is growing evidence that adipose-tissue abundance and depot type has an inherent effect on skeletal muscle tissue, which can be detrimental or beneficial. Indeed, transplantation of sub-cutaneous white adipose tissue (WAT) from exercise-trained mice into sedentary counterparts results in improved glucose tolerance and insulin sensitivity after just 9 days (Stanford et al., 2015). Inflammatory cytokines produced in adipose tissue, including interleukin- (IL)6 and TNF have been consistently shown to reduce the expression of the insulin-regulated glucose transporter GLUT-4 which abounds within adipose and striated muscle tissues (Rotter, Nagaev, & Smith, 2003; J. M. Stephens, Lee, & Pilch, 1997). Accordingly, when GLUT-4 expression is lacking, as frequently demonstrated in rodent knockout models, whole body insulin sensitivity is dramatically reduced (Carvalho, Kotani, Peroni, & Kahn, 2005).

Among the myriad factors that are differentially expressed and secreted in the presence of obesity and which may confer effects to the skeletal muscle, there are some which appear to have multifaceted implications for the regulation of metabolic function and the regulation of skeletal muscle mass (Piccirillo, 2019). Recent interest has been drawn towards the transforming growth factor-beta

(TGF-β) superfamily of cytokines, which are ubiquitous and essential, playing crucial roles in growth, inflammation and immunity (D. A. Clark & Coker, 1998). The TGF-β superfamily includes TGF1, 2 and 3, bone morphogenetic proteins (BMPs), growth differentiation factors (GDFs), activins and nodal-related proteins which are heavily involved in muscle, adipose and bone regulation (M. J. Lee, 2018).

These candidate proteins and their encoding genes have been identified in skeletal muscle and adipose tissue and implicated in many levels of the myocyte cell cycle, from cascades involved in cellular growth, differentiation and transformation, metabolic function and insulin sensitivity, through to cell death (Aihara, Ikeda, Yagi, Akaike, & Matsumoto, 2010; Iizuka, Machida, & Hirafuji, 2014; Tominaga & Suzuki, 2019). Within the TGF-β family, there is perhaps no factor which has drawn more interest in recent years for its possible therapeutic potential in the promotion of skeletal muscle metabolic function and mass, than that of myostatin.

1.9 Myostatin

In 1997, McPherron and colleagues identified a novel TGF-β superfamily member in mice named growth differentiation factor-8 (GDF-8) which was specifically expressed in developing and adult skeletal muscle tissue. Following disruption of the GDF-8 gene, they described hyper-muscularity in these mice compared to their wild-type counterparts, with GDF-8 null muscles weighing 2-3 times more (McPherron et al., 1997). Thus, it was suggested that GDF-8 functioned principally as a negative regulator of skeletal muscle growth and was thus named myostatin (gene name MSTN).

Since its discovery, the MSTN gene has been found to be highly conserved among a broad range of species, which includes humans, cattle, sheep, dog, rodents and zebrafish (Carnac, Vernus, & Bonnieu, 2007). The significance of myostatin is perhaps most well-known amongst the general public for its association with the Belgian Blue and Piedmontese cattle breeds, made famous for their hyper muscularity, or so-called double-muscling (Kambadur, Sharma, Smith, & Bass, 1997). While most prominently associated with skeletal muscle tissue and hence often referred to as a myokine, myostatin is also expressed to a lesser degree in cardiomyocytes and adipocytes, suggesting wide-spread effects throughout the body (McPherron et al., 1997; Sharma et al., 1999). Scientific interest in myostatin has continually grown since McPherron et al.'s early papers, as evidenced by trends in the relative abundance of published articles related to myostatin (Figure 1.3).

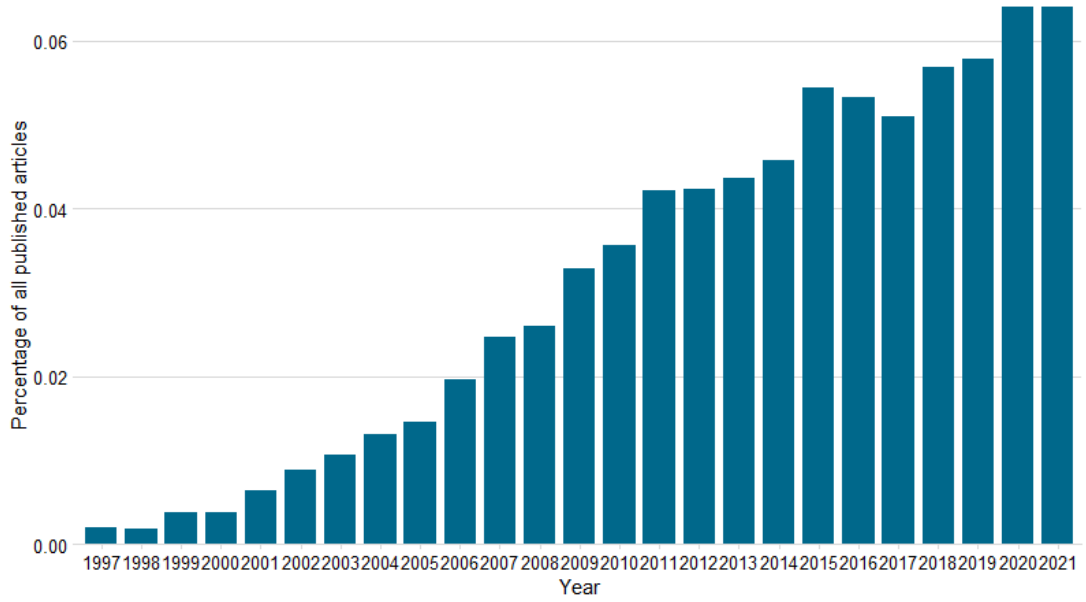

Figure 1.3. Historical interest in Myostatin research.

Data presented as the percentage of articles returned from a search query for 'Myostatin' relative to all available published articles from Europe PMC, since the publication of the landmark paper of McPherron, Lawler, and Lee (1997). Generated in RStudio using the R Stats 'europepmc' package.

1.9.1 Synthesis, Cleavage and Activation

Myostatin, akin to all TGF-β family members, comprises three distinct domains: an N-terminal signal domain, a propeptide domain and a C-terminal growth factor domain, but differs by having a shorter C-terminus nucleotide sequence (Deng et al., 2017). Myostatin is principally synthesised in skeletal muscle as a 375-amino acid (aa) precursor protein, termed pre-promyostatin (A. Breitbart, Auger-Messier, Molkentin, & Heineke, 2011). After synthesis and translocation to the endoplasmic reticulum, pre-promyostatin forms a disulphide-linked homodimer which is first cleaved to remove a 24aa signal peptide, producing promyostatin. Promyostatin is subsequently cleaved at an Arg-Ser-Arg-Arg site (occurring at aa 240-243) by furin-like protein convertases to generate a 243aa NH_2 [N] terminal fragment (pro-domain) and a 109aa COOH [C] terminal fragment, which are predicted to exist in the non-glycosylated state as 27.7 and 12.4 kDa proteins (Figure 1.4).

Myostatin has been abundantly detected both within muscle and serum. In skeletal muscle, the unprocessed pro-myostatin precursor is believed to most greatly abound, principally located in the muscle extracellular compartment, while in

serum it principally travels in a latent configuration bound to the pro-domain or in the mature homodimeric form (S. B. Anderson, Goldberg, & Whitman, 2008; Cotton et al., 2018; Hill et al., 2002; Zimmers et al., 2002). In both environments, the myostatin precursor configurations are more highly abundant than the biologically active homodimer (S. B. Anderson et al., 2008).

This biologically active C-terminal fragment remains in its disulphide-linked, open-armed homodimer conformation, tending to bind noncovalently to the pro-domain; inhibiting its activity by occluding receptor binding sites; forming the stable latent myostatin complex (Cotton et al., 2018; Jiang et al., 2004). The latent myostatin pro-domain-ligand complex may circulate in various conformational activity states, suggesting that myostatin regulation involves shifting activity states in response to the physiological environment (Walker et al., 2018). Within skeletal muscle fibres, pro- and latent myostatin resides in the extracellular space, proximal to the cell surface to which it binds (Pirruccello-Straub et al., 2018).

It was previously believed that the cleavage that gives rise to the latent complex occurred exclusively within the Golgi apparatus, meaning myostatin secreted from myocyctes was in the latent form, however it has since been demonstrated that the un-cleaved promyostatin may be more readily secreted (S. B. Anderson et al., 2008). Indeed, after secretion promyostatin can be sequestered in the skeletal muscle extracellular space by latent TGF-β binding protein 3, pro-domain mediated interactions with heparin sulphate proteoglycans and covalent binding to the surrounding matrix, where it can subsequently be cleaved by proprotein convertases (Sengle, Ono, Sasaki, & Sakai, 2011).

The mature (biologically active) myostatin homodimer can be activated by proteolytic cleavage from the pro-domain by the BMP-1/tolloid family of metalloproteinases (Figure 1.4), enabling binding of the active myostatin ligand to its receptors (Wolfman et al., 2003). These, perhaps along with other posttranslational modifications are believed to play significant roles in the physiological regulation of myostatin, which may be influenced by upstream regulatory factors such as growth hormones, anabolic agents, exercise and nutritional status (Nestor F Gonzalez-Cadavid & Bhasin, 2004). Furthermore, soluble antagonists such as follistatin, and follistatin-like proteins (FSTLs), GDF-associated serum proteins (GASPs) and decorin are also able to mediate myostatin inhibition through various mechanisms including inhibitory binding of the circulating protein (Cash et al., 2012; Y.-S. Lee & Lee, 2013; Miura et al., 2006).

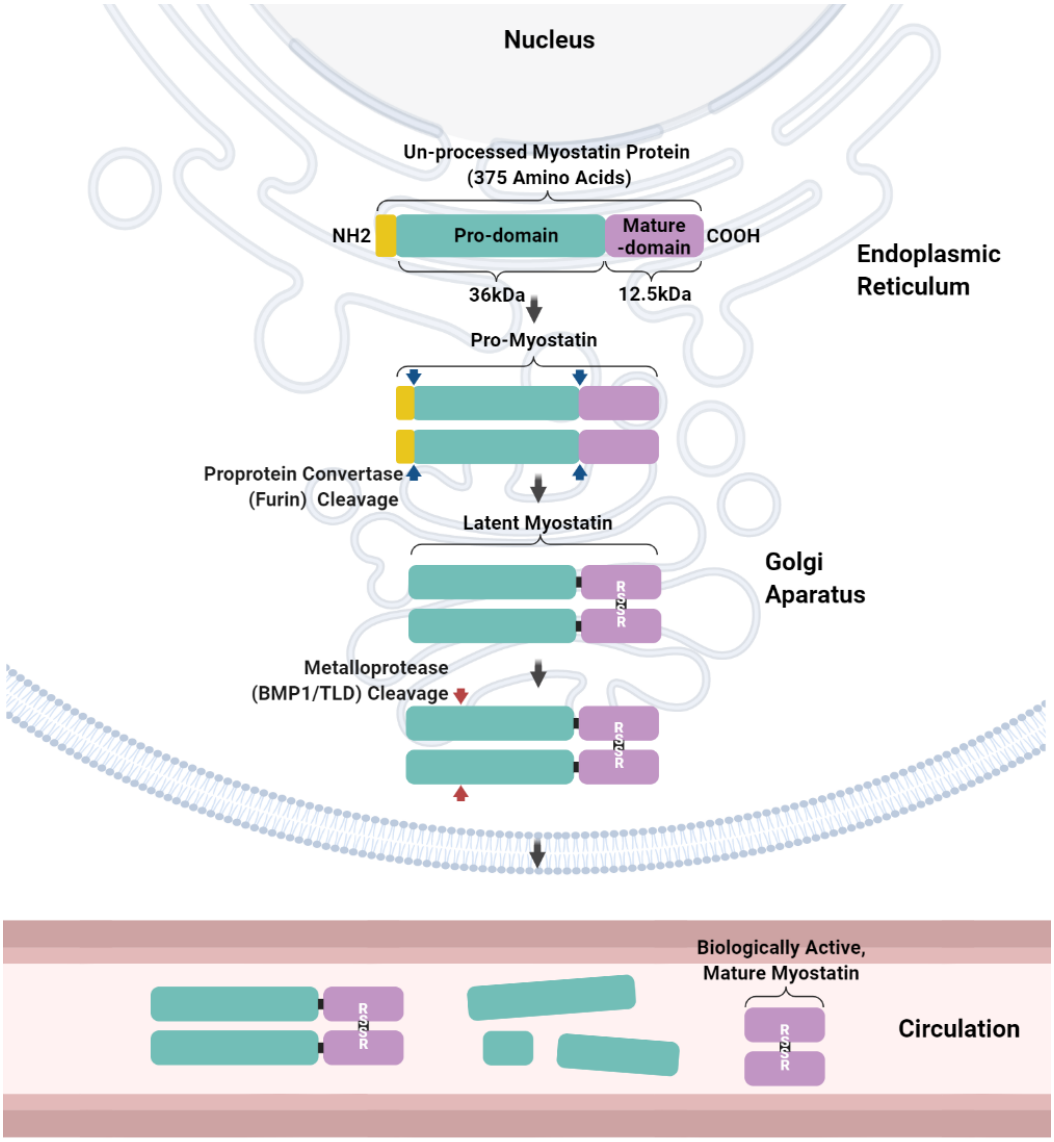

Figure 1.4. Overview of myostatin synthesis and processing.

Myostatin is synthesised as a 375 amino acid (aa) peptide (pre-promyostatin), comprising an N-terminal signal domain, a propeptide domain and a C-terminal growth factor domain. Following translocation to the endoplasmic reticulum, a 24aa signal peptide is first cleaved and a disulphide-linked (RSSR) homodimer (promyostatin) is formed. Promyostatin can be cleaved, predominantly in the Golgi apparatus by proprotein convertases (principally furin) to generate two 243aa NH_2-terminal and two 109aa COOH-terminal fragments that are bound non-covalently, holding myostatin in a latent state by inhibiting receptor binding. Proteolytic cleavage by metalloproteases such as BMP1/TLD within the intra or extracellular space convert the latent protein into its mature, biologically active homodimer, which is capable of binding to the ACTRIIB receptor. Myostatin can be secreted in the promyostatin state and processed extracellularly and has been found to circulate in both its latent and mature form. Created using BioRender.

1.9.2 Regulation of Myostatin Expression

Myostatin transcription is activated by numerous means (Grade, Mantovani, & Alvares, 2019), including changes in its promoter activity (Salerno et al., 2004), transcription factors (Grade et al., 2017), epigenetic regulators, post-transcriptional controllers (D. L. Allen & Loh, 2011) and auto-regulatory feedback (Craig McFarlane et al., 2014). While myostatin ligand binding induces suppression of the myogenic regulatory factors (MRFs) that promote the myogenic lineage and differentiation as will be discussed later, myostatin itself is a downstream target of MRFs as well as the myocyte enhancement factor-2 (MEF-2) family of transcription factors, which upregulate myostatin promoter activity (Grade et al., 2019; J. Li, Deng, Zhang, Cheng, & Wang, 2012; Spiller et al., 2002).

Perhaps the most well characterised of these relationships is between the MRFs and the myostatin promoter region (Grade et al., 2019). Gene promoters are sequences of DNA found at the 5' region of the gene, where RNA polymerase and transcription factors bind in order to drive (promote) gene expression (Wilt & Hake, 2004). Promoters are comprised of a core promoter, which is essential for basal transcription, and an upstream proximal promoter which contains other sequences that govern things such as tissue-specific transcriptional regulation (Heintzman & Ren, 2007).

The myostatin promoter region has several potential binding sites for muscle-specific transcription, including enhancer-box (E-box) motifs, which are known to be recognised and bound by the basic helix-loop-helix transcription (myogenic regulatory) factors (Grade et al., 2019; Hu, Chen, Zhang, & Lin, 2013; Zammit, 2017). By binding to these E-box motifs, MRFs can preferentially upregulate myostatin promoter activity and thus expression (Spiller et al., 2002). Myogenic differentiation factor (MYOD) is one such MRF that plays an important role in the regulation of myostatin transcription during myogenesis by binding to and preferentially upregulating the myostatin promoter (D. L. Allen & Unterman, 2007; Spiller et al., 2002).

It has also been demonstrated that the myostatin protein indirectly inhibits its own gene expression via an auto-regulatory negative feedback loop via the induction of expression of the inhibitory common partner (co-) Small Mothers Against Decapentaplegic (SMAD) SMAD7, which is activated by the downstream targets of myostatin, SMAD2/3 and SMAD4 (discussed in section 1.10.4) (Forbes et al., 2006; X. Zhu, Topouzis, Liang, & Stotish, 2004). It has been proposed that the regulation of myostatin gene expression may therefore be dependent upon the overall ratio of the regulatory SMADs (SMAD2 and 3) and inhibitory co-SMADs

(SMAD7) (D. L. Allen & Unterman, 2007). Furthermore, it has been shown that myostatin is also post-transcriptionally regulated by factors such as the microRNA miR-27b, which represses myostatin expression through a putative recognition sequence within the 3'-untranslated region of the gene, which is dependent upon the activity of SMAD3 (Craig McFarlane et al., 2014).

1.9.3 Myostatin in Circulation

Myostatin is considered a myokine; secreted predominantly from skeletal muscle however also to a lesser degree from adipose tissue, which can enter the circulation to act on other regions and tissues in a paracrine and endocrine fashion (Y.-S. Lee, Huynh, & Lee, 2016). Cleavage of the pro-domains by furin-like pro-protein convertases can occur during or after secretion (extracellularly). Thus, circulating myostatin is present as both an unprocessed precursor and a furin-cleaved complex. Several inhibitors of myostatin, including follistatin, follistatin-like protein 3 gene (FSTL3) and growth and differentiation factor-associated serum protein-1 (GASP-1) have also been found to be present in serum and can bind to circulatory myostatin (Hill et al., 2002; Hill, Qiu, Hewick, & Wolfman, 2003). The degree to which these inhibitors independently, and in combination with the inhibitory pro-domain, affect myostatin function, remains to be determined.

Past difficulty measuring circulating myostatin concentrations, due to its 90% sequence homology to GDF11, and the previously unknown nature of circulating myostatin being a predominantly latent complex bound to plasma proteins, have limited investigations into serum myostatin concentration in different populations and health statuses (Egerman et al., 2015). Reliable assay techniques have since been developed, however (Lakshman et al., 2009), and further investigation has been undertaken to determine the influence of circulating myostatin abundance (discussed in section 1.9.6). For myostatin protein to exert its effects, it must first bind to receptors to initiate a signalling cascade.

1.9.4 Receptor Binding and Signalling Cascades

Activation of the mature myostatin ligand enables initiation of a signalling cascade through the formation of a heterotetrameric complex with two activin-responsive type II receptors (ACTRIIA or ACTRIIB) at the cell membrane (Figure 1.5) and two type I receptor activin-like kinases (ALK4 or ALK5) (de Caestecker, 2004; S.-J. Lee & McPherron, 2001). The assembly of this heterotetramer triggers the phosphorylation and activation of the SMAD2 and SMAD3 transcription factors by the ALK receptors, which translocate to the nucleus to regulate gene expression alongside a co-SMAD; SMAD4 (A. Breitbart et al., 2011; Y. Chen et al., 2004;

Tsuchida et al., 2009). Myostatin-induced SMAD signalling broadly results in the inhibition of muscle growth and activation of atrophy signalling programmes (Braun & Gautel, 2011). Principally, this seems to occur by activation of the Forkhead box transcription factors (FOXO1, 2 and 3) and inhibition of the Akt/mTOR pathway (Trendelenburg et al., 2009) which will be discussed in more detail (sections 1.10.2 and 1.10.3)

1.9.5 Effects of Myostatin Signalling on Skeletal Muscle Growth

Myostatin's most fundamental effects are those which it exerts upon the restriction of skeletal muscle growth. Muscle growth is the product of an increased quantity of muscle fibres (hyperplasia) and/or increased fibre size (hypertrophy). Recombinant myostatin impairs myogenesis through suppression of satellite cell activation and myoblast proliferation and differentiation, while genetic inactivation impairs myotube formation *in vitro* (Artaza et al., 2005; Langley et al., 2002; McCroskery, Thomas, Maxwell, Sharma, & Kambadur, 2003; Thomas et al., 2000; Tsao et al., 2013). It has been shown *in vivo* that transgenic mice with a missense mutation to block myostatin activity, exhibit increased hyperplasia without a concomitant increase in hypertrophy, such as is naturally seen in Piedmonetese cattle (Nishi et al., 2002). Conversely, in transgenic mice that expressed a mutated myostatin cleavage site to create dominant negative myostatin (whereby the gene product of the mutation interferes with the wild-type gene product, thus impairing its function), muscle mass was 20-35% greater than in wild type animals, which was exclusively attributable to fibre hypertrophy (Xiaolei Zhu, Hadhazy, Wehling, Tidball, & McNally, 2000).

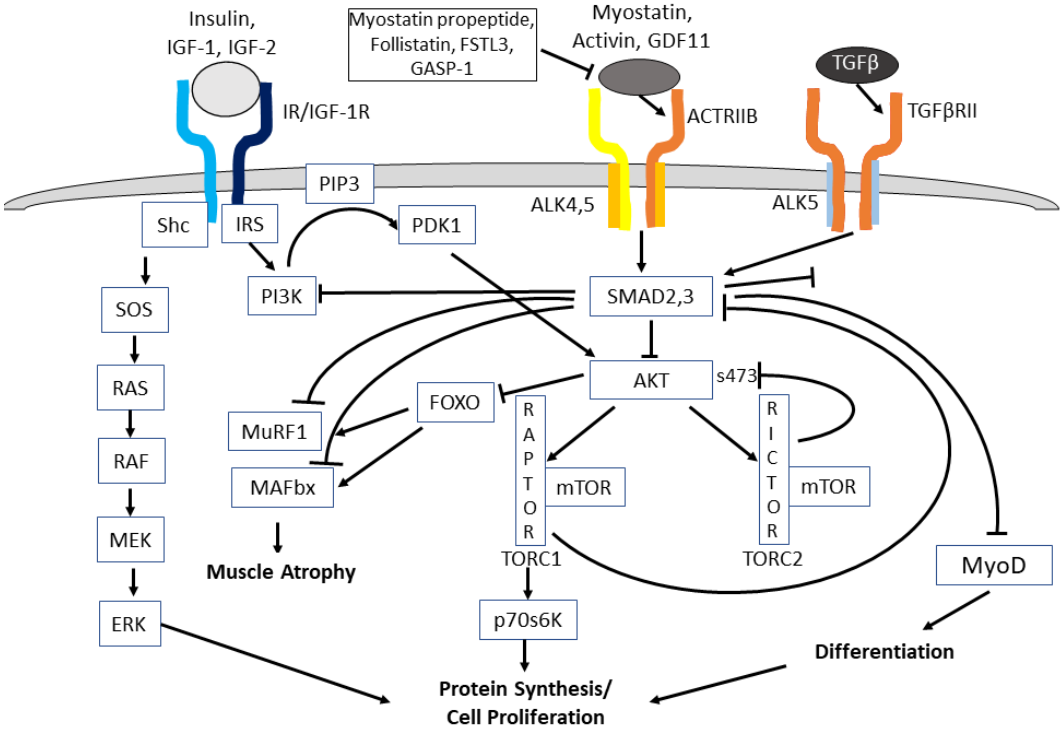

Figure 1.5. Myostatin signalling pathways involved in skeletal muscle remodelling and interactions with other anabolic signals.

The mature myostatin ligand, which is inhibited by the binding protein follistatin and the myostatin propeptide, binds to the ACTRIIB receptor, with recruitment of the ALK4 and ALK5 receptor kinases, phosphorylating both SMAD2 and SMAD3. SMAD2/3 activation promotes a cascade of anti-myogenic signals, including the impairment of muscle differentiation through MyoD inhibition. SMAD2/3 directly inhibit, but indirectly promote the activation of E3 ligases MuRF1 and MAFbx which are ordinarily upregulated by atrophy programs, distinguishing myostatin's effects from classical atrophy. SMAD2/3 interacts with the insulin/IGF signalling pathway through the inhibition of PI3K, which ordinarily leads to phosphorylation of Akt and subsequent promotion of protein synthetic pathways as well as the translocation of GLUT4 storage vesicles to the plasma membrane. Instead, the inhibition of Akt by the SMADs reduces mTOR signalling, which ordinarily drives protein synthetic and proliferative pathways.

1.9.6 Myostatin and Adipose Tissue

Myostatin is not only expressed and secreted by skeletal muscle tissue, but also to a lesser degree by adipose tissue. The Brüning group demonstrated that myostatin was secreted from brown adipose tissue (BAT), which subsequently acted in an autocrine fashion, reducing local insulin sensitivity (Steculorum et al., 2016). It appears that myostatin may play a significant role in the regulation of adipose tissue, with myostatin-deficient mice exhibiting 70% less adipose accumulation, which was attributed to increased fatty acid oxidation in WAT, skeletal muscle and liver, due to increased mitochondrial lipolytic enzyme activity and increased browning of WAT (C. Zhang et al., 2012). It has been speculated that the reduced fat mass seen in MSTN null mice may be an indirect effect of increased muscle mass, rather than a direct effect of stunted myostatin signalling within adipose tissue (T. Guo et al., 2009). To that effect, it has been postulated that this reduced adiposity may be the result of increased energy expenditure. In a murine model of myostatin deficiency where fat mass was reduced, despite a reduction in ambulatory activity and increased leptin sensitivity there was no corresponding reduction in energy intake (Sun Ju Choi et al., 2011). Concordantly, naturally occurring polymorphisms of the myostatin gene, which promote its expression, have been shown to be associated with generalised obesity, abdominal obesity and low lean body mass in humans (Bhatt et al., 2012).

1.9.7 Myostatin in Skeletal Muscle and Adipose Tissue Cross-Talk

Research has begun to uncover a role of myostatin in the interrelationship between muscle and adipose tissue (Dong et al., 2016). It has been shown that while adipose tissue-specific deletion of myostatin in HFD-fed mice did not increase muscle weight or body composition, nor tolerance of glucose and insulin (T. Guo et al., 2009), whole body myostatin knockout HFD-fed mice exhibited partial suppression of fat accumulation and abnormal glucose metabolism (McPherron & Lee, 2002). These studies suggest that skeletal muscle derived myostatin influences adipose regulation, but that this relationship may not function in the opposite direction, likely reflecting the order of magnitude lower expression of myostatin in adipose than muscle tissue (D. L. Allen et al., 2008).

In myostatin knockout mice, WAT develops characteristics associated with BAT, with substantial upregulation of signature BAT genes including uncoupling protein 1 (UCP1) and Peroxisome Proliferator-Activated Receptor Gamma Coactivator 1-alpha (PGC1-α) (Shan, Liang, Bi, & Kuang, 2013). Novely, the adipose browning phenotype was discovered not to be autonomously regulated within the adipocyte,

but rather was shown to be driven by the myokine irisin (FNDC5) which was secreted from the myostatin null skeletal muscle. Dong et al. (2016) subjected mice to 16 weeks of high fat diet feeding, during the final four weeks of which one group was treated with an anti-myostatin peptibody. The group receiving the peptibody displayed increased muscle growth, supressed macrophage infiltration and pro-inflammatory gene expression in both skeletal muscle and adipose tissue. Inhibition of myostatin was also shown to improve glucose homeostasis and increased browning of WAT, which the authors proposed was driven by an increased expression and abundance of irisin.

1.9.8 Myostatin and Sarcopenia

Myostatin expression and circulating abundance has been shown to be elevated in myriad conditions that induce significant muscle loss, including sarcopenia, cancer cachexia, and disease states that cause extended bed rest (Dasarathy, 2017; I. George et al., 2010; N. F. Gonzalez-Cadavid et al., 1998; Yarasheski, Bhasin, Sinha-Hikim, Pak-Loduca, & Gonzalez-Cadavid, 2002; Zhou et al., 2010). Muscle myostatin mRNA and protein expression was 2.0-fold and 1.4-fold higher, respectively, in older males with sarcopenia than younger males (Léger, Derave, De Bock, Hespel, & Russell, 2008). Similarly, myostatin mRNA expression was 56% greater in elderly women with reduced muscle cross-sectional area than young women (Raue, Slivka, Jemiolo, Hollon, & Trappe, 2006). Furthermore, several studies have demonstrated an association between elevated myostatin and reduced muscular strength (Han et al., 2011; Patel et al., 2014; Yasar et al., 2022).

It is worth considering, however, that patients suffering from these conditions are likely to have a reduced physical activity level and since myostatin expression is suppressed by exercise, these comparisons may be confounded. Indeed, while many studies show upregulation of myostatin in sarcopenia, it is not unequivocal, with several studies failing to find such an effect when participants are matched for BMI or fat mass (Ratkevicius et al., 2011). Conversely, another study demonstrated a tendency for higher basal muscle myostatin mRNA expression and significantly greater muscle myostatin protein content in older males, who were matched for total- and lean-body mass and body fat percentage with younger males (McKay, Ogborn, Bellamy, Tarnopolsky, & Parise, 2012).

In a recent study by Ryan and Li (2021) myostatin mRNA expression was found to be 50% greater in obese adults with sarcopenia than without, but was positively associated with several indices of adiposity. Indeed, while both groups were on average obese, the sarcopenic subpopulation had significantly greater body mass

and fat mass than their non-sarcopenic counterparts, confounding the effects of sarcopenia *per se* with that of sarcopenic obesity. Furthermore, in some elderly cohorts, it has been demonstrated that serum myostatin is positively associated with skeletal muscle mass index (Bergen et al., 2015; S. J. Choi et al., 2021). Evidently, the regulation of myostatin expression and abundance in sarcopenia is complex, and associations may be conflicted by the effects of adiposity and the aforementioned autoregulation of myostatin expression. Nevertheless, the therapeutic suppression of myostatin for the treatment of muscle wasting is greatly sought after (T. A. White & LeBrasseur, 2014).

1.9.9 Targeting Myostatin to Combat Muscle Wasting

Myostatin is considered a highly druggable target and various pharmacological means of inhibiting or disrupting myostatin expression, receptor binding, and signalling have been explored (T. A. White & LeBrasseur, 2014). These include the use of neutralising antibodies, inhibitory propeptides, soluble ACTRIIB receptors, administration of interacting proteins (T. A. White & LeBrasseur, 2014) and recently developments in the use of antibodies that block release from the pro-domain (Pirruccello-Straub et al., 2018). Pioneering work in rodent and non-human primate models has produced promising results with effects of increased muscle mass, regeneration, and metabolic function (LeBrasseur et al., 2009; Muramatsu et al., 2021; Siriett et al., 2007).

The first human trials of a myostatin inhibitor therapy for muscle wasting conditions commenced in 2004 (K. R. Wagner et al., 2008) and several drugs are now undergoing testing. Preliminary results of some Phase 2 trials have been promising (Smith & Lin, 2013), though only one has so far progressed on to a phase 3 trial (Saitoh et al., 2017). One such anti-myostatin antibody REGN-1033/ Trevogrumab, is involved in several ongoing and recently completed phase 2 clinical trials in healthy and sarcopenic volunteers. Similarly, in a phase 2 trial in elderly patients who had recently fallen, the humanised monoclonal antibody LY2495655 improved lean mass, and several parameters of muscle function (Becker et al., 2015). To date, however, such treatments have been hindered by side effects including urticaria, aseptic meningitis, epistaxis, diarrhoea, confusion and fatigue (Campbell et al., 2017; John E. Morley, 2016; K. R. Wagner et al., 2008). Clearly then, there is a significant bridge yet to be crossed before myostatin therapies could become widely implemented for muscle-wasting conditions.

1.9.10 Myostatin and Obesity: A Possible Link to Insulin Resistance

While the focus of research into the effects of myostatin in skeletal muscle has been on its anti-myogenic functions, another promising line of enquiry has emerged regarding the upregulation of myostatin in obesity and its potential involvement in insulin resistance. This interest was sparked by the early observations in myostatin null mice, whereby not only did they present with hyper muscularity, but they also exhibited enhanced glucose tolerance and reduced adiposity (McPherron & Lee, 2002). While it could be argued that this may have been an artefact of the increased muscle mass, subsequent studies have demonstrated that myostatin inhibition increases glucose disposal per body mass (Eilers, Chambers, Cleasby, & Foster, 2020) and upregulates GLUT4 expression in muscle (Dong et al., 2016).

Skeletal muscle myostatin mRNA expression, protein abundance and serum concentration are all reportedly increased with obesity (David L. Allen, Hittel, & McPherron, 2011; Amor et al., 2019; Hittel, Berggren, Shearer, Boyle, & Houmard, 2009; Léger et al., 2008). Corroboratively, it has been demonstrated that substantial weight-loss in morbidly and extremely obese women who underwent biliopancreatic diversion (Milan et al., 2004) or gastric bypass (J.-J. Park, Berggren, Hulver, Houmard, & Hoffman, 2006) was accompanied by ~1.7- and 2.4-fold reductions in muscle myostatin mRNA expression, respectively. A highly impactful paper by Hittel et al. (2009) demonstrated that myotubes derived from extremely obese women secreted 3-fold more myostatin than those from lean individuals, which was corroborated *in vivo* by findings of increased myostatin protein content within skeletal muscle and circulating concentration in plasma of obese individuals. Pertinently, muscle myostatin protein abundance was found to strongly correlate with the degree of fasting insulin resistance, as indicated by HOMA-IR score. Corroborating this association, both weight loss and exercise training, which improve indices of insulin sensitivity in individuals with obesity, have been demonstrated to reduce myostatin circulating abundance and skeletal muscle mRNA and protein expression in most (Hittel et al., 2010; Milan et al., 2004; Ryan, Ortmeyer, & Sorkin, 2012), but not all studies (Takao et al., 2021).

Supporting these observations, it was subsequently demonstrated that individuals with higher skeletal muscle myostatin expression require lower rates of glucose infusion during euglycaemic–hyperinsulinaemia to maintain normoglycaemia, evidence of reduced insulin sensitivity (Hjorth et al., 2016). Skeletal muscle myostatin expression, but not plasma concentration, was found to be significantly

higher in middle aged dysglycaemic than normoglycaemic participants, when measured in muscle biopsies obtained immediately- and 2 h-post aerobic exercise, but not at baseline; however baseline expression was moderately correlated with glucose infusion during a hyperinsulinaemic euglycaemic clamp, but not body fat percentage (Hjorth et al., 2016). Of note, while the two groups were matched for age, the dysglycaemic group had significantly higher BMI (28.9 ± 2.5 vs 23.5 ± 2.0), fat mass (44.0 ± 7.6 kg vs 31.5 ± 4.8 kg) and fat free mass (68.5 ± 5.7 kg vs 63.2 ± 6.2 kg), which may confound the effects of insulin resistance and excess adiposity.

Similarly, myostatin mRNA expression was found to be upregulated 1.6- and 1.8-fold in obese T2D patients and their first-degree non-obese relatives, respectively (Palsgaard et al., 2009). Conversely, in a cross-sectional study of T2D and non-T2D individuals, those with T2D were found to have lower serum myostatin concentrations, and myostatin concentration was found to decrease with increasing number of metabolic syndrome components (Han et al., 2014). This discrepancy possibly reflects the assay used to detect serum myostatin in Han's study. Unlike most commercially available kits, their assay was not specific to the mature myostatin protein, but rather detected the full-length protein, active peptide, and pro-peptide, which do not necessarily reflect its biological activity on account of the inhibitory nature of the pro-peptide.

It remains to be elucidated whether the association of insulin resistance and upregulated myostatin in obesity, as well as the observed insulin-sensitisation that is associated with myostatin suppression, reflect myostatin-mediated effects, or whether myostatin itself is altered by intrinsic effects of changes in insulin sensitivity and signalling in the face of obesity and subsequent weight loss.

1.10 Myogenic Culture as a Model of Skeletal Muscle

For over forty years, investigators have been utilising *in vitro* models of skeletal muscle, based on the pioneering works of Yaffe and Saxel (1977) and Blau and Webster (1981) by isolating and culturing muscle progenitor cells. The development of immortalised skeletal muscle cell lines such as the murine C2C12 and rat L6 developed by Blau, Chiu, and Webster (1983) and Yaffe (1968), which spontaneously differentiate in culture with serum withdrawal or continue to undergo mitotic division indefinitely under appropriate conditions, have enhanced the possibilities of the study of muscle physiology. One advantage of tissue culture models is the ability to mimic *in vivo* scenarios in isolation, via nutritional, pharmacological, or stimulatory modulation of culture conditions. Growth mediums typically contain physiological, or supra-physiological concentrations of

glucose, amino acids and minerals and vitamins, supplemented with animal sera to expose the cells to relevant growth factors, enzymes and metabolites.

Immortalised cell lines offer convenience and reduce the financial and temporal burdens of research, and have great merit for the study of some elements of muscle physiology, such as contraction, to which C2C12 myotubes demonstrate a robust response (Abdelmoez et al., 2020). Although more time and resource-intensive, the culture of myocytes from skeletal muscle tissue (primary myogenic culture) may provide a better model of many aspects of human muscle. Primary human myocytes better reflect the genetic profile of mature skeletal muscle and retain some degree of their donor's phenotype (Bell et al., 2010; Gaster, Rustan, Aas, & Beck-Nielsen, 2004; Thompson, Pratley, & Ossowski, 1996). For instance, myotubes derived from T2D donors have intrinsic defects in glucose transport and glycogen synthesis (Gaster, Petersen, Højlund, Poulsen, & Beck-Nielsen, 2002; McIntyre, Halse, Yeaman, & Walker, 2004), whereas myotubes derived from exercise-trained donors have greater capacity for lipid oxidation (Bourlier et al., 2013; Heden et al., 2017; Lund et al., 2018). This carry-over may be influenced by epigenetic regulation. Indeed, diet (Jacobsen et al., 2012), exercise (Barres et al., 2012) and a family history of T2D (Nitert et al., 2012) can alter skeletal muscle DNA methylation, which may influence satellite cells (Massenet, Gardner, Chazaud, & Dilworth, 2021; D. C. Turner et al., 2020). However, relative to mature muscle, primary human myotubes have reduced mitochondrial oxidative capacity and metabolic gene expression (Aas et al., 2013; Raymond et al., 2010); preferential utilisation of carbohydrate over lipid (Aas et al., 2011); diminished expression of GLUT4 and overabundance of GLUT1 (Al-Khalili et al., 2003; Sarabia, Lam, Burdett, Leiter, & Klip, 1992).

While many protocols have been developed, primary myogenic culture is fundamentally a three-step process. Briefly, the muscle precursor satellite cells are first extracted from whole muscle tissue using mechanical and enzymatic digestion. Secondly, the isolated cells are seeded and maintained in culture vessels with appropriate medium to support their activation and proliferation as myoblasts. Alternatively, explant culture can be established by placing muscle samples in culture vessels and utilising the myogenic outgrowth from this tissue (Harvey, Robertson, & Witkowski, 1979; Shahini et al., 2018). Finally, the mono-nucleated myoblasts can be differentiated into multi-nucleated myotubes through the prolonged reduction, species switching, or removal of animal sera from their culture medium.

1.10.1 Regulatory Factors and Processes Involved in Myogenesis

Differentiated muscle cells are not capable of mitotic division. Instead, the regulation and regeneration of adult skeletal muscle tissue is influenced by the abundance of muscle-specific progenitor satellite cells, which can commit to the myogenic lineage through the process of myogenesis (Bentzinger, Wang, & Rudnicki, 2012; Mauro, 1961). Satellite cells predominantly lie dormant in a quiescent state between the basal lamina and sarcolemma of muscle fibres. Activation, which can arise from local contractile activity, growth factors and myotrauma, can lead to proliferation of myoblasts, while some activated cells will return to their quiescent state to replenish the satellite cell pool (Snijders et al., 2015; Zammit et al., 2006). Myoblasts can cease to proliferate and fuse together to form multinucleated myotubes, aiding repair or forming new independent myofibres.

The process of myogenesis is co-ordinated by sequential expression of various transcription factors (Figure 1.6); chiefly, the myogenic regulatory factors (MRFs). These MRFs include myogenic factor 5 (Myf-5), MyoD, myogenin (MYOG) and MRF4, and are identified by their basic helix-loop-helix motif (Bentzinger et al., 2012). Quiescent satellite cells express the paired box transcription factor 7 (Pax7) and when activated co-express Pax7 with MyoD, which seems to instigate proliferation, until Pax7 is later downregulated and differentiation is stimulated (Zammit et al., 2004).

Myoblast fusion occurs when myoblasts exit the cell cycle and mitosis ceases to continue (Linkhart, Clegg, & Hauschika, 1981). This terminal differentiation is characterised by elongation, end-to-end alignment, and fusion of cells to form multinucleated myotubes (P. Clark, Dunn, Knibbs, & Peckham, 2002). In culture, myoblasts can be pushed towards differentiation by reducing the concentration of animal sera, typically from 10-20% foetal bovine serum (FBS) to 0-2% and/or the addition of/substitution with 2-6% horse serum (HS). This induces changes in the expression of myogenic promotors that drive differentiation, including increased myogenin and MRF4 and reduced CD34 and Pax7 (Deasy, Jankowski, & Huard, 2001). These differentiated myotubes demonstrate increased myosin heavy chain (MHC) content and creatine kinase activity, which is indicative of a shift towards a more specialised, contractile tissue, bearing resemblance to adult skeletal muscle (Berggren, Tanner, & Houmard, 2007).

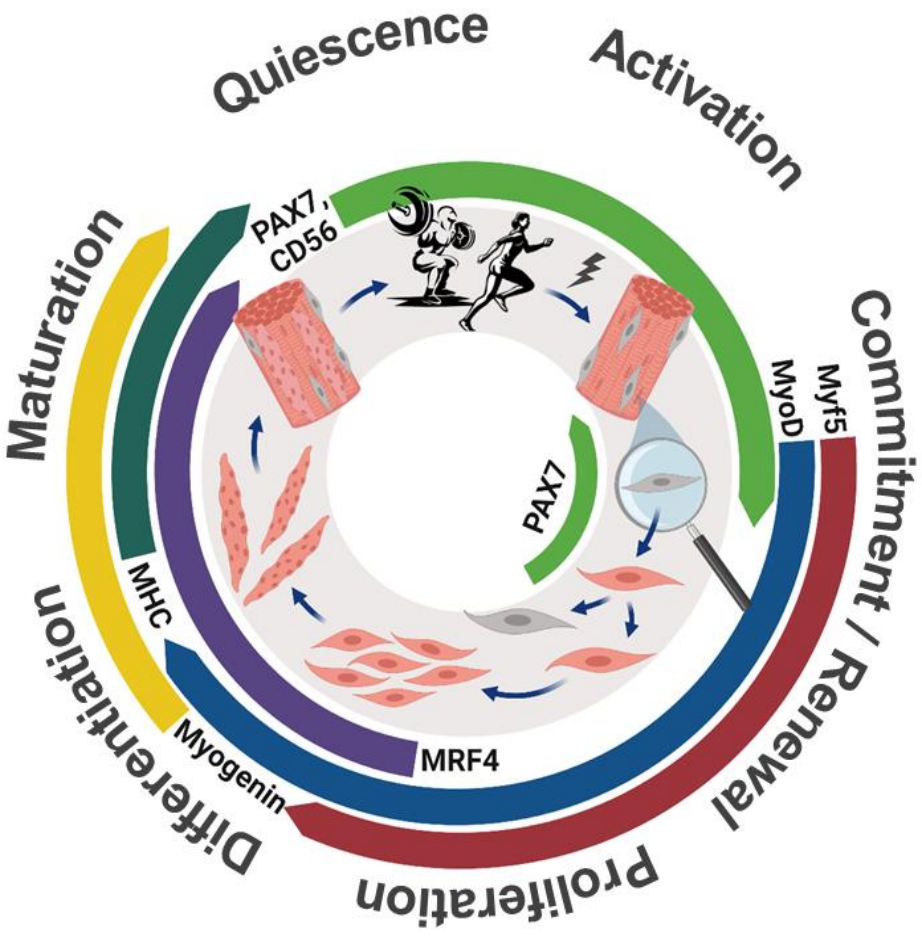

Figure 1.6. Schematic overview of key sequential expression patterns and morphological changes that give rise to the myogenic lineage.

Quiescent under resting conditions, satellite cells (grey mononucleated cells) are characterised and routinely identified by the expression of several fundamental genes including PAX7 and CD56. In response to mechanical stress or injury, and under sufficiently pro-anabolic conditions, satellite cells are activated from their dormant state and begin expressing the myogenic regulatory factors MyoD and Myf5. As they enter the cell cycle and migrate to affected sites, they undergo asymmetric division with most transforming into myogenic precursor cells (myoblasts) that will commit to the myogenic lineage (pink mononucleated cells), while some return to the quiescent state to replenish the satellite cell pool. Myoblasts undergo proliferation via mitosis, before expression of MRF4 and Myogenin promotes terminal differentiation, during which the expression of Myf5 and MyoD declines. Differentiation drives morphological changes from small, individual myoblasts to elongated cells, which fuse to form multi-nucleated myotubes. Increased expression of MHC promotes maturation into myofibres that may bind to existing fibres or form independent, contractile-competent fibres. Created using BioRender.

1.10.2 Effects of Myostatin Administration on Myogenic Cultures

It follows that myogenic culture can provide a useful tool to investigate, isolate, and modulate the effects of different physiological environments, conditions, and treatments on myostatin expression and function, and *vice versa*. Using primary human myoblasts Craig McFarlane et al. (2011) demonstrated that treatment with recombinant human myostatin inhibited both proliferation and differentiation. This was mediated by regulation of cell cycle progression through the upregulation of the cyclin-dependent kinase inhibitor p21 and impaired initiation of differentiation by suppression of MyoD, resulting in fewer and less fused myotubes. This effect has been demonstrated to be dose-responsive and functions through inactivation of the Akt/mTOR/p70S6 protein synthesis pathways (Lach-Trifilieff et al., 2014; Sartori et al., 2009; Trendelenburg et al., 2009), which mediates myoblast differentiation and myotube hypertrophy. Similarly, treatment of both primary bovine and C2C12 myoblasts with recombinant myostatin has been shown to impair differentiation by repressing MyoD, Myf5 and myogenin, though p21 was also suppressed (Langley et al., 2002; Thomas et al., 2000). Conversely, treatment of C2C12 myoblasts with recombinant myostatin generated in eukaryotes has been reported to stimulate, not inhibit, myoblast proliferation (Rodgers et al., 2014).

While myogenic pathways appear broadly perturbed by myostatin administration, atrophy pathways involving the upregulation of E3 ubiquitin ligases, appear not to be so greatly activated. Rather, myostatin signalling principally blocks the cascades responsible for growth and differentiation (Durieux et al., 2007; Trendelenburg et al., 2009). It has been argued, however, that reduced mTOR signalling is not solely attributable for myostatin-induced atrophy/growth suppression since isolated blockade of mTOR does not decrease muscle fibre diameter or protein synthesis below normal levels (S. L. Welle, 2009). It has been demonstrated that the myostatin-mediated impairment of myogenesis is also regulated non-canonically via the persistent activation of mitogen-activated protein kinase (MAPK) pathways, at the level of p38 (Philip, Lu, & Gao, 2005), extracellular signal-regulated kinases (ERK)1/2 (W. Yang et al., 2006) and c-Jun N-terminal kinase (JNK) (Z. Huang et al., 2007).

Effects of recombinant myostatin treatment on insulin sensitivity in C2C12 myoblasts and myotubes is conflicting. In one study, myostatin treatment of C2C12 myoblasts significantly reduced basal and insulin-stimulated IRS-1 tyrosine phosphorylation, expression, and activation of PI3K (X.-H. Liu, Bauman, &

Cardozo, 2018). Furthermore, GLUT4 mRNA and protein expression as well as its insulin-stimulated translocation was inhibited, resulting in suppressed glucose uptake. Conversely, in C2C12 myotubes, Y. Chen et al. (2010) demonstrated positive effects of myostatin treatment on glucose metabolism and several key regulatory genes, including GLUT1 and GLUT4. Similarly, Hjorth et al. (2016) found that 24h treatment of primary human myotubes with recombinant myostatin increased basal glucose uptake, which was additive to the effects of insulin, but did not affect Akt phosphorylation.

One recent study elegantly demonstrated diverging responses to recombinant myostatin treatment in C2C12 and human muscle cells before (in myoblasts) and after differentiation (in myotubes). Indeed, in C2C12 cells, but not human muscle cells, the effects of myostatin on canonical and noncanonical signalling was significantly reduced after differentiation (Lautaoja et al., 2020). Furthermore, basal myostatin expression tended to be ~3-fold greater in human myoblasts than myotubes, but 3-fold greater in C2C12 myotubes than myoblasts, which in the context of the aforementioned ability for myostatin to autoregulate its own expression, may explain some of the disparity seen between muscle cell species and differentiation status when treated with exogenous myostatin. Clearly, there is work yet to be done to establish the effects of physiological myostatin overabundance and upregulation on human skeletal muscle insulin sensitivity and myogenesis.

1.10.3 Effects of Myostatin Suppression on Myogenic Cultures

Similar effects to those reported from *in vivo* knockout or inhibition of myostatin on muscle growth, have been consistently demonstrated *in vitro*. Using myofibre explant culture, it was reported that myostatin-null explants demonstrated significantly greater outgrowth than wild type explants (McCroskery et al., 2003). Concordantly, in the same study, when myogenic cultures were established from isolated satellite cells of myostatin-null mice, myoblasts demonstrated accelerated proliferation. These effects were mirrored in differentiated primary myotubes cultured from myostatin knockout mice, which were found to have greater diameter and volume than control wild-type derived myotubes, which was associated with increased Akt/mTOR activation (Julie Rodriguez et al., 2011). Specifically, myostatin knockout appears to shift MHC expression in myoblasts towards faster isoforms and myostatin-null myoblasts formed myotubes that preferentially expressed faster MHC (M. Wang, Yu, Kim, Bidwell, & Kuang, 2012). Furthermore, these myotubes exhibited increased rates of polysome formation

(which occurs during polypeptide elongation) and protein synthesis, which was diminished by the addition of recombinant myostatin. Supportively, inhibition of myostatin action by impairing receptor binding with an anti-ACTRIIB antibody significantly reduces myostatin-induced SMAD2/3 phosphorylation and restores Akt/mTOR signalling through increased Akt phosphorylation (Lach-Trifilieff et al., 2014).

There is a dearth of research into the effects of myostatin inhibition or deletion on insulin sensitivity and signalling in myotubes. It was reported that myotubes derived from myostatin knockout mice exhibited greater total and phosphorylated:total protein ratios of Akt, mTOR and Ribosomal protein S6 in both the basal and insulin-stimulated state, relative to those derived from wild-type mice, however no direct indices of glucose handling were measured (Julie Rodriguez et al., 2011). While acute treatment (1-6 h) of C2C12 myotubes with recombinant myostatin increased glucose uptake, but decreased glycogen synthesis (increased glycolysis) which was associated with vastly increased IL-6 expression and secretion, co-incubation of myostatin and follistatin, or myostatin and myostatin propeptide (to inhibit myostatin function) both supressed glucose oxidation and lactate production (indicative of decreased glycolysis) relative to treatment with myostatin only (Y. Chen et al., 2010). The authors proposed that this demonstrated a novel mechanism by which myostatin may exacerbate muscle wasting in conditions such as cachexia through accelerated glycolysis and inflammatory activation, which may be combatted via inhibitory binding.

Longer term exposure (3 days) of differentiating C2C12 cells to recombinant myostatin impaired insulin-stimulated IRS-1 (Tyrosine895) and Akt phosphorylation, GLUT4 expression and both basal and insulin-stimulated glucose uptake (X.-H. Liu et al., 2018). The authors demonstrated, however, that inhibition of myostatin signalling via the use of SB431542, a specific inhibitor of ALK5 that blocks SMAD2/3 phosphorylation, in the presence of recombinant myostatin, restored and enhanced glucose handling, which was mediated by a restoration of basal and insulin-stimulated IRS-1 phosphorylation. Thus, *in vitro* inhibition of myostatin appears to confer changes in myotubes that may be indicative not only of improved muscle growth/regenerative capacity, but also of sensitivity to the normal metabolic actions of insulin, however this remains to be investigated at the level of functional outcomes such as glucose uptake and substrate metabolism in human primary cells.

1.11 Summary and Aims

Excessive adiposity, which is largely attributed to diet and lifestyle factors, is associated with declining metabolic health, particularly with regards to the regulation of glucose homeostasis through the action of insulin, but also of the regulation of muscle growth and regeneration, particularly in the presence of ageing. As the primary contributor to glucose disposal in the non-fasting state, skeletal muscle plays a vital role in this fine balancing act. Myostatin, a TGF-β family member that plays a significant role in negatively regulating skeletal muscle mass, has also been implicated in the development of insulin resistance, following initial observations of enhanced glucose-handling and resistance to high-fat-diet-induced obesity in myostatin-knockout mice. It has since been demonstrated in humans that myostatin appears to be upregulated by obesity and associated with insulin resistance, however the nature of this relationship remains to be elucidated and such associations are confounded by variables such as age and the use of non-human systems. Human primary myogenic culture offers a useful model of skeletal muscle, and it has been demonstrated that obese-derived muscle cells have greater expression of myostatin; are less sensitive to insulin; and can exhibit diminished growth. Thus, the main aims of this thesis were to distinguish between the effects of obesity and ageing on the (dys)regulation of myostatin; to elucidate the underlying causes of this dysregulation; and to establish the functional significance of physiologically altered myostatin expression and abundance in insulin resistant states in human muscle cells.

1.11.1 Chapter 3 Aims

In Chapter 3, a cross-sectional study of muscle samples from young normal weight, older normal weight and older overweight/obese adults was undertaken to delineate between the independent effects of obesity and ageing on the expression of skeletal muscle myostatin, its interacting proteins and its downstream signalling components. Additionally, serum myostatin concentration was assessed in a separate, well-characterised cohort who had wide-ranging age, adiposity and habitual physical activity level, in order to identify correlates of circulating myostatin abundance.

1.11.2 Chapter 4 Aims

Expanding upon the observed upregulation of myostatin expression in obese insulin resistant skeletal muscle, Chapter 4 sought to establish whether this upregulation could be recapitulated *in vitro* by the induction of lipid-induced insulin resistance in skeletal muscle cells from normal weight, insulin sensitive donors. Secondary aims were to investigate whether compositional modulation of the fatty

acid treatment would influence insulin/anabolic sensitivity and alter any such myostatin response.

1.11.3 Chapter 5 Aims

Chapter 5 employed *ex vivo* techniques to generate adipose-conditioned medium that reflects the adipose tissue secretome from adults with and without obesity. The primary aim of this study was to establish whether chronic exposure of human muscle cells to adipose conditioned medium from lean and obese adults exerted differential effects on the regulation of myostatin expression and function; insulin sensitivity; and myogenesis. The profile of a selection of adipokines was assessed in these adipose conditioned mediums to identify cytokines that are differentially secreted by obese adipose tissue.

1.11.4 Chapter 6 Aims

In Chapter 6, the novel polyphenolic metabolite, Urolithin A, which has been demonstrated to exert anti-obesogenic effects in rodents, was applied to human myotubes, to establish its capacity to influence insulin and anabolic sensitivity and myostatin expression. Additional experiments were undertaken using an *in vitro* model of adipose tissue, to establish whether such effects were specific to skeletal muscle or whether they could be recapitulated in other metabolic tissues.

Chapter 2. General Methods

2.1 *In Vivo* Methods

2.1.1 Ethical Approval and Volunteer Recruitment

Following approval from the University of Nottingham Medical School Ethics Committee (REC #143-1811), volunteers were recruited to undergo a skeletal muscle biopsy procedure for the generation of human primary myogenic cultures used in this thesis. Participants, comprising students and staff from the University of Nottingham as well as the general public were recruited through adverts on university notice boards; social media platforms; and the Call for Participants website (https://www.callforparticipants.com). Responders were invited to participate voluntarily. Upon first contact, volunteers who expressed an interest were provided with a participant information sheet providing full detail of the nature of the study and the commitments involved. Following a basic inclusion/exclusion-criteria screening email, participants were invited for an initial visit at the David greenfield Human Physiology Unit at the University of Nottingham Medical School, Queen's Medical Centre.

2.1.2 Consent and Participant Health Screening

At this first visit, the full inclusion/exclusion criteria, study protocol, and associated risks were discussed. Volunteers were excluded from participating if they met any of the following exclusion criteria:

- Aged < 18 or > 70 yrs.
- Body mass index (BMI) < 18.5 $kg \cdot m^{-2}$ or > 40.0 $kg \cdot m^{-2}$
- Regular smoking.
- Any metabolic (e.g., diabetes), endocrine (e.g., hyperthyroidism) or cardiovascular (e.g., coronary artery disease) diseases or abnormalities.
- Hypertension (blood pressure exceeding 140/90).
- Regular medication that is known to alter skeletal muscle regulation or cardiovascular function.
- High alcohol consumption (routinely > 4 units per day).
- Clinically significant abnormalities in full blood count, clotting factors, or urea and electrolyte screening.

Volunteers were informed that they were free to withdraw at any stage of their involvement of the study, without the need to provide justification and had the opportunity to ask any questions. If happy to proceed, written informed consent was obtained and a routine health screening was undertaken. This screening comprised standard anthropometric measures (height, body mass, waist, and hip

circumference), blood pressure, 12-lead electrocardiogram, venous blood samples for routine laboratory screening (including a full blood count, clotting factors, urea and electrolyte concentrations), and a short International Physical Activity Questionnaire (IPAQ). Medical screening results were reviewed by a clinician before participants were invited to undertake any further visits to the laboratory.

2.1.3 Collaborator Recruitment of Older Patients

For some experiments presented in this thesis, cryopreserved myoblasts and adipose-conditioned medium derived from adipose tissue samples, were obtained from collaborators at the Jones Laboratory at the University of Birmingham. These samples were obtained under the approval of the University of Birmingham Research Ethics and provided to us under a material transfer agreement between the two institutions. Skeletal muscle and adipose tissue samples were obtained from osteoarthritis patients undergoing total knee or hip joint replacement surgery. These patients provided informed consent prior to their surgeries. Patients with known secondary causes of osteoarthritis; those who had ever received intravenous or oral immunosuppressive medication; and those who had been given intra-articular steroid injections within 6 months of their surgery, were all excluded.

2.1.4 Participant Laboratory Visits

Participants were invited to attend the David Greenfield Human Physiology Unit one further time, following 48 h of exercise and alcohol abstinence, ending with an overnight water fast (≥ 12 h). Upon arrival to the laboratory in the morning (typically ~9:00 am) participants were asked to detail their physical activity within the last 48 h and to confirm if they had followed the fasting protocol. If satisfactory, body mass was measured before individuals rested semi-supine on a hospital bed, prior to blood and muscle sampling. Upon completion of the study visit, a light breakfast/lunch was provided, and participants were briefly monitored to ensure they were fit to leave the laboratory.

2.1.5 Collaborator Tissue Sampling and Culturing

Skeletal muscle and adipose tissue samples provided by collaborators at the University of Birmingham were obtained intra-operatively by the lead surgeon. Muscle samples were taken from quadriceps muscle close to the operative site and temporarily stored on ice in Dulbecco's modified eagle medium (DMEM/F12), while adipose samples were briefly stored in PBS. Samples were swiftly transported to the Jones laboratory for processing to isolate satellite cells for myogenic cultures (protocol described in section 2.2) and adipose-conditioned

medium for downstream experimental applications (section 2.4.2). Myogenic culture and adipose-conditioning techniques used at the University of Birmingham were identical to those derived from muscle and adipose samples in-house at the University of Nottingham.

2.1.6 Blood Sample Collection and Processing

A single blood sample (~7 mL) was obtained from a superficial vein within the antecubital fossa of one arm. A small aliquot (~1 mL) of whole blood was immediately transferred into a microtube for the measurement of blood glucose concentration (section 2.1.7). Of the remaining sample, ~3 mL was transferred to a vacutainer tube containing 7.5 $\mu L \cdot mL^{-1}$ EGTA-glutathione, and 3 mL into a spray-coated silica and polymer gel vacutainer tube, the latter being allowed to clot for at least 15 min at room temperature, before 10 min centrifugation at 4400 x G at 4°C to separate plasma and serum, respectively. Plasma and serum supernatant was transferred to Eppendorf tubes and stored at -80ºC until analysis.

2.1.7 Measurement of Whole Blood Glucose

Following collection, ~1 mL of whole blood was immediately transferred into a microtube containing sodium fluoride (to inhibit glycolysis) and heparin (to prevent clotting). This was placed on a roller for 3 min before being assayed using the glucose oxidase method (YSI 2300 STAT PLUS Glucose & Lactate Analyser, Yellow Springs Instruments, Ohio, USA). Briefly, membrane-bound glucose oxidase catalyses the conversion of glucose to gluconic acid and hydrogen peroxide (H_2O_2). The H_2O_2 is subsequently oxidised and releases electrons. When the reaction is in dynamic equilibrium, the electron flow (current) is proportional to the concentration of H_2O_2 produced. Thus, the difference between the sample-generated plateau current and the initial baseline current is proportional to the blood glucose concentration of the sample. The YSI analyser was calibrated each time before use using an internal glucose standard of 10 mM.

2.1.8 Measurement of Serum Insulin

An aliquot of serum (10 µL) was used for the determination of insulin concentrations by a commercially available enzyme-linked immunosorbent assay (EZHI-14K, Millipore Sigma), comprising pre-coated wells with monoclonal mouse anti-human insulin antibodies. Briefly, wells were incubated for 5 min in 300 µL wash buffer before the addition of 20 µL assay buffer and 10 µL serum samples. Next, 20 µL biotinylated detection antibody solution was added and the plate was sealed and incubated at room temperature with orbital shaking (500 RPM) for 1 h. Wells were washed three times prior to the addition of 100 µL streptavidin-

horseradish peroxidase solution, after which the plate was again sealed and incubated at room temperature with orbital shaking for 30 min. Wells were washed five more times, after which 100 µL substrate solution (3,3',5,5'-tetramethylbenzidine) was added to each well, which was sealed and incubated for 20 min with shaking, to induce colour development. Finally, 100 µL stop solution (0.3 M HCl) was added and absorbance was read at 450 nm. Both quality control and negative control samples, as well as a set of human insulin standards, were also ran on the same plate to enable the generation of a standard curve. Unknown values were interpolated from the fitting of a four-parameter logistic (4PL) curve to the standards of known concentrations.

2.1.9 Measurement of Fasting Insulin Sensitivity

Fasting concentrations of whole blood glucose (G_0 in $mmol \cdot L^{-1}$) and serum insulin (I_0 in $\mu IU \cdot mL^{-1}$) were used to calculate the Homeostasis Model Assessment of Insulin Resistance 2 (HOMA2-IR) as an index of insulin sensitivity, which is an updated approach to the original HOMA-IR method (Matthews et al., 1985). HOMA2-IR was calculated using the HOMA2 calculator software, which was downloaded from university of oxford. http://www.dtu.ox.ac.uk/.

2.1.10 Measurement of Serum Myostatin

The concentration of circulating myostatin was quantitatively assayed via a commercially available sandwich enzyme immunoassay (DGDF80, R&D Systems, MN, US). Serum obtained via serum separator tubes was processed to remove the pro-peptide from the GDF-8 complexes. To that effect, 100 µL samples were first activated by acid via the addition of 50 µL of 1 N HCl for 10 min at room temperature. Next, 50 µL of 1.2 N NaOH/0.5 M HEPES was added and mixed well to neutralise the solution, ensuring a resultant pH between 7.2-7.6. Finally, 200 µL of calibrator diluent was added to the neutralised samples (final dilution factor: 1:4)

A volume of 50 µL of Assay Diluent was then added to each well of a plate pre-coated with a monoclonal antibody specific for mature GDF-8 (biologically active, dimeric myostatin). Next, 50 µL of standards of known concentration, a negative control, or sample was added to each well such that any GDF-8 present within them was bound by the immobilized antibody. Wells were then sealed and incubated for 2 hours at room temperature on an orbital microplate shaker at 500 RPM. The content of the wells was aspirated and washed four times with a buffered wash solution to remove any unbound substances, and excess buffer removed by blotting the plate against clean paper towels. Following this, 200 µL of an enzyme-linked monoclonal antibody specific for mature GDF-8 conjugated to horseradish

peroxidase, was added to each well and the plate was resealed and incubated for 2 hours at room temperature with orbital shaking, before repeating the wash process.

After incubation and washing, 200 µL of Substrate Solution was added to each well and incubated for 30 minutes at room temperature in the dark. Following incubation, 50 µL of Stop Solution was added to each well, inducing a colour change that is proportional to the amount of GDF-8 initially bound from the sample, which was quantitatively assessed on a microplate reader via measuring optical densities at 450 nm and 570 nm (the latter being to correct for optical imperfections in the plate). A standard curve was generated by plotting the known concentrations of standards (2000 – 31.3 $pg \cdot mL^{-1}$) against the corrected optical density (OD) read out (OD 450 nm – OD 570 nm) and sample concentration was inferred via the standard curve using a 4-parameter logistical regression equation. These calculated values were corrected for the dilution factor of the sample in the reaction (1:4) to produce absolute serum concentrations in $pg \cdot mL^{-1}$. All diluted samples fell within the range of the standard curve.

2.1.11 Skeletal Muscle Tissue Sample Collection

Following a short period of semi-supine rest, a sample of vastus lateralis muscle tissue was obtained using the suction-modified percutaneous needle biopsy (Bergström) technique by a practicing clinician (Bergstrom, 1975; Shanely et al., 2014). Briefly, the incision site was cleaned with an iodine solution before the administration of 1 % lignocaine, first to the skin and then advancing into the muscle belly. A small incision was made with a scalpel, into which the Bergstrom needle was advanced into the muscle belly, while suction was applied to the inner trocar via a 50 mL syringe. The outer trocar was retracted to draw muscle into the opening, followed by rapid closure to cut a small sample of tissue, which was repeated several times while rotating the needle assembly, to ensure sufficient tissue for culturing was obtained. Muscle tissue was ejected into a petri dish on ice where any substantial connective tissue, adipose tissue and blood was dissected out before the clean muscle sample was transferred swiftly into a universal tube of ice cold 1 x PBS and kept on ice until processing later that morning.

Sustained pressure was applied to the incision before dressing the wound. Participants were advised to avoid vigorous physical activity for 72 h and to keep the site clean and dressed during this time. No adverse events relating to the biopsy procedure were reported.

2.2 *In Vitro* Methods: Myogenic Culture

2.2.1 Terminology

Variation in nature is handled by measuring a number (n) of independently sampled individuals, independently conducted experiments, or independent observations (Cumming, Fidler, & Vaux, 2007). There is inconsistency within cell biology regarding the terminology used to define n. This arises from discrepancies between what is considered a 'biological' replicate and is particularly troublesome when using primary cell cultures. Broadly, biological replicates refer to measurements of biologically distinct samples that demonstrate biological variation (Blainey, Krzywinski, & Altman, 2014). Difficulty arises when considering what constitutes a biologically distinct sample? It might be argued that each well of cells, when sustained in culture for a prolonged period, becomes somewhat biologically distinct, however reporting individual wells as biological replicates may be considered pseudo-replication (Pollard, Pollard, & Pollard, 2019). Alternatively, it may be argued that each flask/plate of cells, or cells of differing passage, represent biologically distinct replicates. This ambiguity leads to problems with the reporting of n values and error bars, which can be misleading (Cumming et al., 2007; Vaux, Fidler, & Cumming, 2012). Best practice is to consider biological replicates to be the most independent samples that can be generated within an experimental framework. In the context of this thesis, the following terminology will be applied in an effort to ensure maximum transparency:

Independent donor repeats: occur when an entire experimental procedure is replicated using primary cells derived from multiple human donors, such that cells from each donor, irrespective of the number of replicates or measurements, constitute n = 1. This is the highest order of biological distinction possible within the primary cell culture system and are preferable over treatment/technical replicates for inference about the mean and variance of a given biological population (Blainey et al., 2014); thus it is these data on which statistical analysis is undertaken (Lazic, Clarke-Williams, & Munafò, 2018). In this thesis, data from multiple independent donor repeats is handled as if the data were obtained *in vivo* from multiple participants and in accordance with recent guidelines these data points are presented as scatter plots in figures (Michel, Murphy, & Motulsky, 2020) and from these data statistical analysis is performed and effect sizes, confidence intervals and *P*-values are generated (Vaux et al., 2012).

Treatment replicates: are the number of replicate culture wells from a given *independent donor repeat* of a given experimental procedure, which all receive identical treatment/stimulation. Typically, 3-6 *treatment replicates* are performed

within each *independent donor repeat,* yielding 3-6 samples which will be experimentally measured. For any given experimental measure of interest, the mean of all treatment replicates will produce a value that reflects an estimation of that measure for one independent donor repeat. By contrast, treating these treatment replicates as biologically distinct replicates could constitute pseudo-replication in this context (Landis et al., 2012).

Technical replicates: are the number of times each sample (which may be a *treatment replicate* or a derivative thereof [e.g., RNA extracted from a treatment replicate]) is quantitatively measured. Technical replicates serve to minimise noise and error in the act of measurement. For instance, following reverse transcription of RNA extracted from 1 *treatment replicate*, qPCR is performed using 3 *technical replicates* (e.g., 3 identical wells in the 96-well plate). The mean of these 3 *technical replicates* provides a measure of that *treatment replicate* and the mean of all *treatment replicates* provide a measure of that treatment within that *independent donor repeat*.

2.2.2 Biological Variance within Primary Myogenic Cultures

The use of primary human myogenic culture as a model of skeletal muscle enables the recapitulation of donor heterogeneity (biological variance) within the culture system, that is not present when immortalised cell lines are studied instead. This can provide greater confidence in the physiological relevance of the models but potentially introduces additional confounding factors to the experiments. Thus, it is important to consider the characteristics of the donors from whom cultures are generated and to be transparent in the visual representation of the data arising from culture experiments using multiple independent donor repeats. To that effect, in all experimental chapters, substantial descriptive data on the donors from whom the cultures used were derived, is provided in a table, and individual data points representing each independent donor repeat are plotted for all relevant figures to allow the reader to view and interpret the biological variance within the experimental model for themselves.

2.2.3 Standard Myogenic Culture Conditions

Primary human myoblasts from skeletal muscle tissue samples obtained from participant muscle biopsies and intra-operative samples from the University of Birmingham's Jones laboratory, were isolated using a protocol derived from Dr Andrew Bennett of the University of Nottingham's FRAME laboratory. This protocol applies preferential plating (described below) to enhance the purity of the myogenic cell population through the removal of fibroblasts based on their greater adhesive tendency. It must be acknowledged, however, that no isolation method

of primary cells is perfect, and it must be recalled that muscle-derived fibroblasts proliferate vigorously in culture. Other techniques, such as magnetic-activated cell sorting, have been demonstrated to offer rigorous, but still not flawless, myogenic purification (Agley, Rowlerson, Velloso, Lazarus, & Harridge, 2015). To that effect, to further help preserve myogenic purity of the cultures and thus minimise the chance of fibroblasts outrunning the myogenic population, cultures were minimally passaged prior to experimental usage (see section 2.2.6). Using this protocol, our group has demonstrated the ability to consistently produce desmin-positive multi-nucleated myotubes that minimally express TE7 (Figure 2.1) (O'Leary et al., 2017), a fibroblast marker that is absent from pure myogenic cultures (Agley, Rowlerson, Velloso, Lazarus, & Harridge, 2013). For the aforementioned reasons, however, it cannot be definitively said that these cultures were 100% myogenic and will likely have contained modest populations of muscle-derived fibroblasts. All tissue culture work was performed within a class II biological safety cabinet and cultures were grown at 37ºC, 5% CO_2, using a growth medium mix comprising Ham's F-10 nutrient mix (Sigma, #N6013) with 2 mM L-glutamine and 1% penicillin/streptomycin, supplemented with either 20% foetal bovine serum (FBS; Gibco, #16140071) to facilitate proliferation of myoblasts, or 6% HS (Gibco, #26050088) to facilitate growth arrest and differentiation into multinucleated myotubes (Table 2.1).

Table 2.1. Standard mediums, sera and supplements for human myogenic cultures.

Media Function	Basal Medium	Sera	Additives
Myoblast Proliferation	Ham's F-10 (Sigma, #N6013)	20% Foetal Bovine Serum (Gibco, #16140071)	2 mM L-Glutamine (Sigma, #G7513) 1% Penicillin/Streptomycin (Sigma, #P4333)
Myotube Differentiation	Ham's F-10 (Sigma, #N6013)	6% Horse Serum (Gibco, #26050088)	2 mM L-Glutamine (Sigma, #G7513) 1% Penicillin/Streptomycin (Sigma, #P4333)
Myoblast Cryo-preservation	DMEM/F-12 (Gibco, #11320033)	25% Foetal Bovine Serum (Gibco, #16140071)	10% dimethyl sulfoxide 2 mM L-Glutamine (Sigma, #G7513)

2.2.4 Satellite Cell Isolation and Seeding

Fresh muscle tissue (typically ~100 mg) was finely minced using a scalpel and transferred to a universal tube containing 10 mL of 1x trypsin-EDTA and placed on a magnetic stirrer within an incubator for 15 min at 37ºC to facilitate digestion. The cell/tissue suspension was then passed several times through a 19G needle to aid mechanical separation of cells from any remaining connective tissue, before a further 15 min of digestion. Any undigested tissue (primarily collagenic) and debris was filtered out by passing the solution through a 100 µm cell strainer. The resultant cell suspension was transferred to a clean tube into which an equal volume of serum-containing growth medium was added to inactivate the trypsin.

Following centrifugation at 1700 RPM for 5min, the supernatant was aspirated, and cell pellet was re-suspended in 10 mL of medium supplemented with 20% FBS and transferred into an uncoated 175cm^2 (T175) flask for pre-plating. The flask was incubated at 37ºC for 20 min to purify the myogenic content of the suspension, via preferential adhesion and removal of fibroblast, which may otherwise outrun the myogenic population and dominate the culture (Agley et al., 2015). The non-adherent cell suspension was then carefully removed from the flask. This satellite cell-rich suspension was then transferred to either one or two T75 flasks, depending on the size of the observed cell pellet. These flasks were pre-coated with a 0.2% gelatine solution for ≥1 h, before excess gelatine was aspirated, and flasks were allowed to dry within the incubator for a further ≥1 h. Once in gelatine-coated flasks, satellite cells were left undisturbed for 72 h to enable adhesion and myogenic activation.

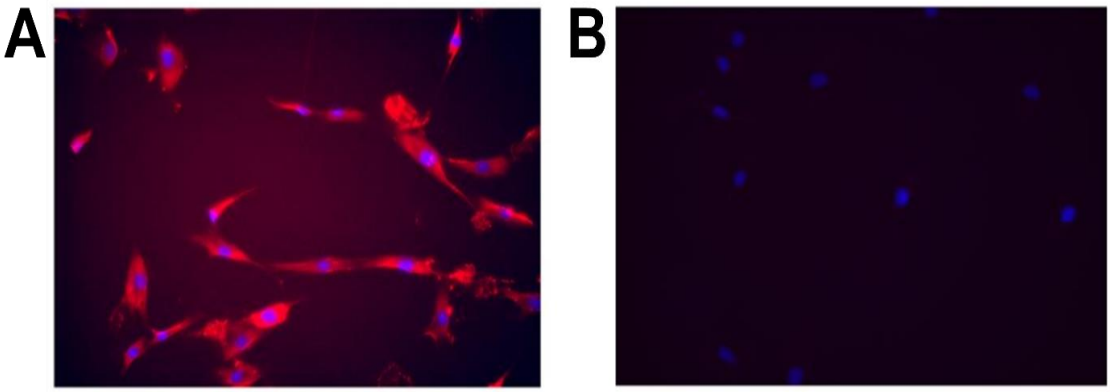

Figure 2.1. Primary human myoblasts do not express the fibroblast marker TE-7.

Primary human myoblasts (cultured in our group using the described methods) as well as synovial fibroblasts were fixed; immunofluorescence stained with the fibroblast marker TE-7 (red) and with DAPI (blue); and imaged on an epifluorescence microscope. Synovial fibroblasts, (**A**) and primary human myoblasts (**B**). Adapted from O'Leary et al. (2017).

2.2.5 Myoblast Cryopreservation, Thawing and Seeding

Of the myoblasts cultured at the University of Birmingham, one T75 flask of ~70% confluent myoblasts of minimal passage was cryopreserved from each participant by a member of the Jones Laboratory for future use. To cryopreserve cells, the growth media was first aspirated off and cells were washed with an equal volume of PBS. Cells were then incubated in 5 mL 0.05% Trypsin-EDTA at 37ºC for up to 5 min to dissociate myoblasts from the vessel surface. The flask was visualised under light microscopy to confirm detachment of the monolayer, at which point an equal volume of growth medium was added to neutralise the trypsin. The resultant cell suspension was transferred to a universal tube and centrifuged for 5 min at 460 x G to pellet the cells, which were subsequently re-suspended into fresh medium comprising 65% DMEM/F12, 25% FBS and 10% dimethyl sulfoxide (DMSO).

Myoblasts in preservation media were frozen down slowly in cryovials ($1x10^6$ cells·mL^{-1}) within a Mr Frosty freezing container (Thermo Scientific, MA, USA) held at -80ºC overnight, before being transferred to a liquid nitrogen Dewar for long-term storage. These cryopreserved myoblasts were transferred from the University of Birmingham to the University of Nottingham on dry ice, and promptly stored in liquid nitrogen without the occurrence of thawing. Cryopreserved primary human myoblasts were also obtained from a commercial source when

human recruitment could not be facilitated due to the COVID19 pandemic, which were isolated from a healthy Caucasian female (Thermo Fisher, cat. # A12555). To thaw cryopreserved myoblasts, cryovials were rapidly warmed in a water bath at 37ºC until nearly defrosted, at which point the suspension was added to 5 mL of pre-warmed 20% FBS-containing medium to minimise the cytotoxicity of the defrosted DMSO. The new solution was centrifuged at 1700 RPM for 5 min, media removed, and the resultant pellet was re-suspended into 10 mL of fresh proliferation medium and transferred to an uncoated flask for 20 min, for myogenic purification. Myoblasts were subsequently cultured identically to those obtained from fresh muscle biopsies.

2.2.6 Myoblast Proliferation, Sub-culturing, and Plating

Once healthy adherent cultures were established (72 h since satellite cell or cryopreserved myoblast seeding) growth medium was replaced every 48 h, until myoblasts reached ~70% confluence. To increase the cell population, myoblasts were sub-cultured at a ratio of either 1:2 or 1:3 depending on how fast they were proliferating. To this end, myoblasts were trypsin-dissociated from their vessel. Again, trypsin-EDTA was neutralised with growth medium, centrifuged for 5 min at 1700 RPM, and the pellet re-suspended in an appropriate volume of medium. Cell suspensions were again pre-plated into uncoated flasks for 20 min for myogenic purification. The remaining cell suspensions were diluted into an appropriate volume of medium for transfer either directly to plates for plating (myoblasts plated out at this stage are referred to as passage 0), or into an appropriate number of culture flasks to resume proliferation (thus becoming the 1st passage).

Serial passaging of primary human myoblasts can result in developmental and metabolic impairments (Nehlin, Just, Rustan, & Gaster, 2011) and a decline in donor phenotypic resemblance (Covington et al., 2015), on account of the fastest proliferating (typically least protein synthesising) cells being selectively retained. To establish an optimised maximal number of times that myoblasts were to be ordinarily passaged using these approaches, an experimental series was undertaken using primary human myoblasts from n = 1 young, lean donor. These cells were cultured as described above before commencing serial passaging such that 2/3 of the cells in the flask were plated out into 12-well plates for differentiation (as described below), while the remaining 1/3 were passaged into a new T75 flask until they again reached ~70% confluence. Using this approach, fully differentiated myotubes were generated at passages 0 (P0), P1, P2, P3 and P4.

Images were digitally captured using an inverted light microscope and 20x objective (Nikon Diaphot) with a phase contrast condenser (Nikon ELWD 0.3). As an index of myogenic capacity, mean myotube thickness was measured as described in Section 2.7, but without the use of fluorescent staining, due to using the same wells for both imaging and insulin-stimulated western blotting. Where possible, 10 myotubes were measured per field (but fewer if less than 10 discernible myotubes were visible), with 5 fields per well and 3 wells per passage. As an additional index, the mean number of myotubes per field that fully crossed each image from one border to its opposing parallel border was counted. After imaging, myotubes were either stimulated with or without 100 nM insulin for 15 min prior to harvesting and subsequent western blotting for pAkt and total Akt, as described in section 2.5.5. Additionally, wells were harvested using Trizol, with RNA extracted for the synthesis of cDNA, which was subsequently analysed using RT-qPCR to assess inflammatory gene expression, as described in sections 2.8.1 through 2.8.5.

The data from this experimental series revealed a clear progressive loss of myotube morphology and insulin sensitivity with serial passage (Figure 2.2). Indeed, by passage 4, cells had drastically altered morphology, presenting with a profoundly more fibroblastic appearance, and exhibited diminished Akt phosphorylation. The mRNA expression of TNF and IL-1β was not significantly altered by passage, but did vary between passages, however TNF tended to increase by small increments with each passage (data not shown). From this data, it was decided that so far as reasonably possible (depending on initial muscle biopsy yield) and in accordance with Covington et al. (2015), myoblasts would be plated out following only a single passage (to enable sufficient bulking of cell number). Under exceptional circumstances (where insufficient cell count was available for useful experimentation and providing cell morphology appeared normal within the proliferating culture) one additional passage was performed.

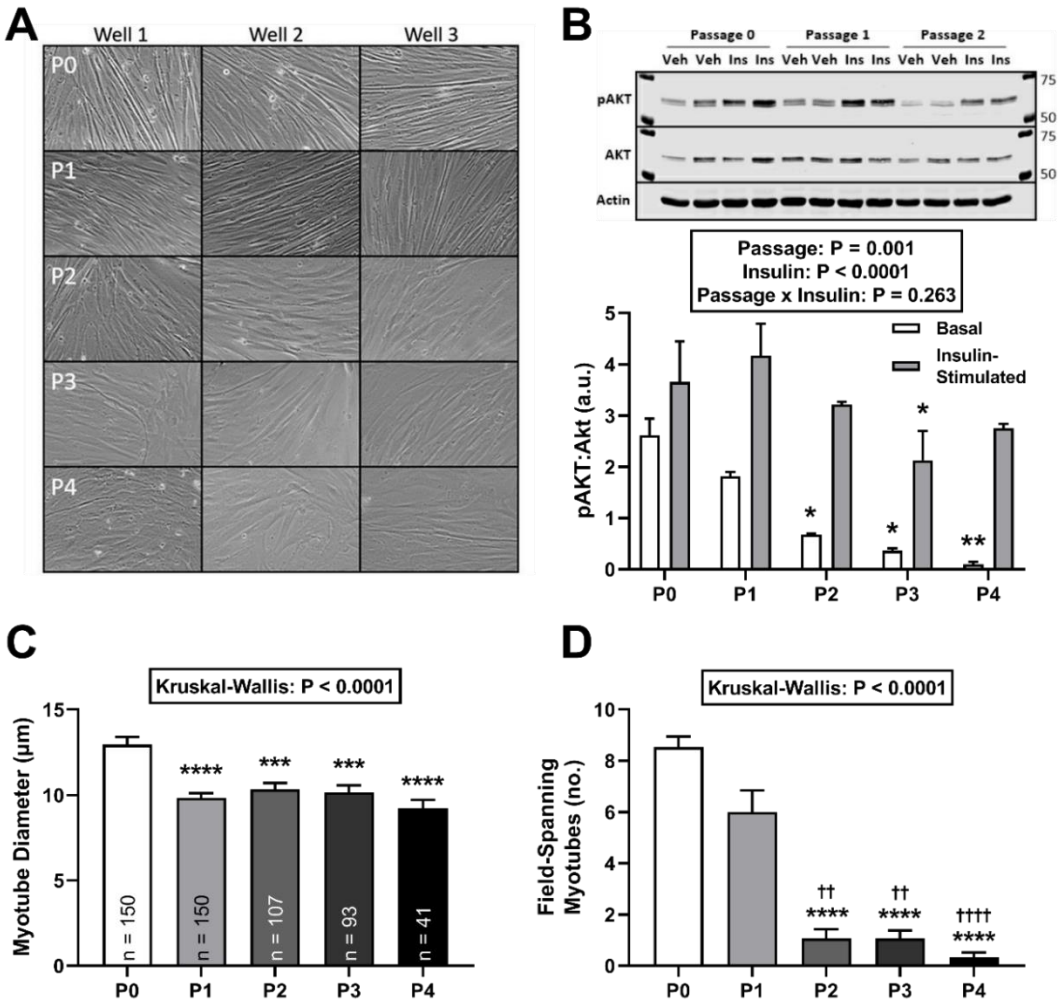

Figure 2.2. Effects of serial passage on myotube morphology and insulin sensitivity.

Primary human myoblasts (n = 1 independent donor repeat) were plated out (P0) or serially passaged four times (P1, P2, P3 and P4). Myoblasts were differentiated for 7 days before imaging on a light microscope prior to stimulation with or without insulin to assess Akt phosphorylation. Changes in myotube morphology with serial passage (**A**). Two-way ANOVA with post-hoc Tukey tests revealed that beyond P1, pAkt:Akt ratio declined with increasing passage (**B**). Myotube morphology data was not normally distributed, thus Kruskal-Wallis tests with Dunn's multiple comparison tests were employed. Myotube diameter declined with the first passage, however the number of discernible myotubes was not diminished (**C**). Subsequent passages exhibited diminishing numbers of discernible myotubes (total number counted per passage is displayed within each bar [max n = 150]). The mean number of field-spanning myotubes per field significantly declined after P1, with almost no field-spanning myotubes by P4. Significant difference from P0: $^{*}P < 0.05$; $^{**}P < 0.01$; $^{***}P < 0.001$; $^{****}P < 0.0001$. Significant difference from P1: $^{\dagger\dagger}P < 0.01$; $^{\dagger\dagger\dagger\dagger}P < 0.0001$. Data presented as Mean ± SEM.

2.2.7 Plating Out and Differentiation of Myoblasts to Myotubes

Once sufficient cells were obtained for their downstream experimental purpose, myoblasts were plated out at a fixed density of $5x10^3$ cells·cm^{-2} (to immediately produce >50% confluence). To estimate cell count and produce consistent cell seeding densities, a 10 µL aliquot of concentrated myoblast suspension was added to 10 µL of Trypan blue, and 10 µL of the mixed solution was pipetted under each side of a haemocytometer coverslip. Viable cells, as indicated by the absence of blue staining, within each of four 16-square quadrants were counted under a light microscope. Viable cell count (cells·mL^1) was estimated as the mean viable cell count per quadrant multiplied by $1x10^4$ (quadrant volume = 0.1 mm^3), multiplied by 2 (trypan dilution factor). Cells were then seeded onto 0.2% gelatine-coated plates or flasks according to their downstream experimental purpose, within an appropriate volume of medium to produce the standard seeding density in their respective wells (Table 2.2).

Upon reaching >90% confluence within their growth vessels, medium was switched to a differentiation mixture comprising Ham's F-10 with glutamine, 1% penicillin/streptomycin and 6% HS. In our hands, primary myogenic cultures demonstrate slightly differing rates of both proliferation and differentiation between donors. Thus, the decision of when to switch to differentiation medium and the duration of differentiation was not fixed. Typically, the time from muscle biopsy sampling to myoblast confluence in 8-10 culture plates was ~28 days and the time to achieve full differentiation was ~7 days.

Table 2.2. Culture vessel properties, media volumes and cell seeing densities required to achieve >80% confluence within 48 h of plating.

Culture Vessel	Surface Area (cm^2)	Approximate Cell Seeding count ($x10^4$)	Growth Medium Volume (mL)
6 well plate	9.0	5	2.0
12 well plate	4.0	2.5	1.0
24 well plate	2.0	1.2	0.5
48 well plate	1.0	0.6	0.3
96 well plate	0.3	0.3	0.2
T25 flask	25.0	12	5.0
T75 flask	75.0	36	15.0

2.3 Adipocyte Culture

The immortalised murine fibroblast cell line, 3T3-L1, was used as a model of human adipose tissue. Through multiple stages of media supplement manipulation (Table 2.3) this cell line can be pushed towards a highly differentiated, lipid-laden, adipocyte-like phenotype, that has consistently been demonstrated to provide a useful *in vitro* model of human white adipocytes (Green & Meuth, 1974; B. H. Jones, Standridge, & Moustaid, 1997; Morrison & McGee, 2015).

Cryopreserved 3T3-L1 cells were thawed and seeded into a T175 culture flask and were proliferated in DMEM high glucose (25 mM glucose) with 2 mM glutamine and 10% new-born calf serum (Sigma #N4637) and grown at 37ºC at 10% CO_2. Cells were passaged 1:8 before achieving 70% confluence, to avoid proliferative contact-inhibition. Cells were subsequently plated-out at a density of $1x10^4$ cells·cm^{-2}. Once tightly confluent after ~48 h, cells were washed and medium was replaced with DME high glucose with glutamine plus 10% FBS, 0.25 µM Dexamethasone, 0.5 mM 3-isobutyl-1-methylxanthine (IBMX) and 166 nM insulin for 48 h. Differentiation induction medium was then replaced with a differentiation continuation medium comprising DMEM high glucose with glutamine, 10% FBS and 166nM insulin for a further 48h. Finally, cells were maintained for 5-10 days in DMEM high glucose with glutamine and 10% FBS to allow maximal intracellular lipid accumulation. Cells were used experimentally once >80% of cells had adopted a distinct adipocyte-like phenotype (Figure 2.3).

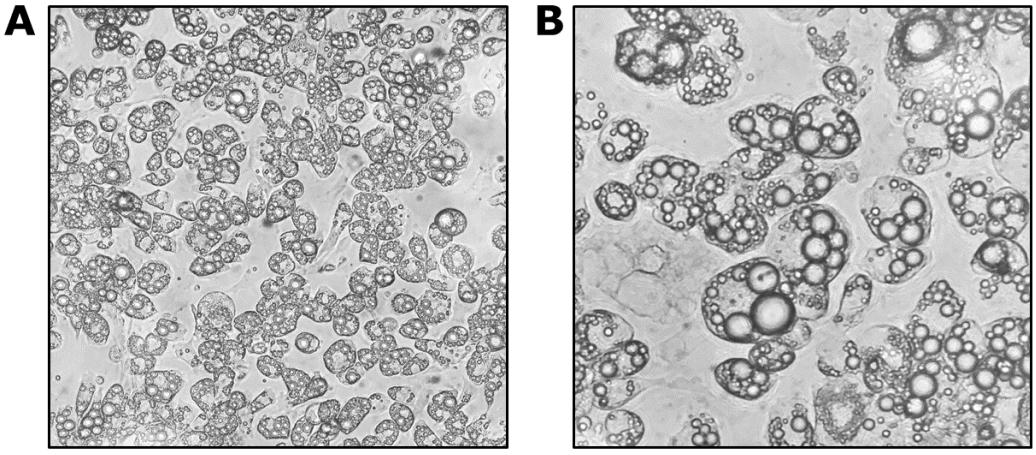

Figure 2.3. 3T3-L1 cells after adipogenic differentiation and maturation. Representative images obtained via light microscopy using a 20x (**A**) and 40x (**B**) objective show that large, distinct lipid droplets are visible in >80% of cells.

Table 2.3. Standard basal mediums, sera, and supplements for the culture and differentiation of 3T3-L1 fibroblasts into mature adipocytes.

Growth Phase/ Media Function	Basal Medium	Sera	Supplements
Proliferation	DMEM High Glucose + Glutamine (Sigma, #D5671)	10% New-born Calf serum (Sigma, #N4637)	1% Penicillin/Streptomycin (Sigma, #P4333)
Differentiation Induction	DMEM High Glucose + Glutamine (Sigma, #D5671)	10% Foetal Bovine Serum (Gibco, #16140071)	0.5 mM IBMX (Sigma, #I5879) 0.25 µM DMSO (Sigma, #D1756) 166 nM insulin (Sigma, #I9278) 1% Penicillin/Streptomycin Sigma, #P4333)
Differentiation Continuation	DMEM High Glucose + Glutamine (Sigma, #D5671)	10% Foetal Bovine Serum (Gibco, #16140071)	166 nM insulin (Sigma, #I9278) 1% Penicillin/Streptomycin (Sigma, #P4333)
Adipocyte Maintenance	DMEM High Glucose + Glutamine (Sigma, #D5671)	10% Foetal Bovine Serum (Gibco, #16140071)	1% Penicillin/Streptomycin (Sigma, #P4333)

2.4 Application of Cell Treatments

All experiments undertaken in this thesis were performed on myotubes, not myoblasts. To that effect, the treatments used in each experimental chapter were either applied for the entirety of the differentiation period (as in Chapter Five) or 6-8 days after the induction of differentiation (as in Chapters Three and Six), at which point cells were considered fully differentiated. In all experimental models, a Vehicle or Control condition was employed, whereby equivoluminous/equimolar amounts of the substance used as a carrier (vehicle) for the experimental treatment or by media devoid of conditioning (as in Chapter Five) was applied to the cells, under identical conditions to the active experimental treatments. In doing so, any observed effects were not mediated by the presence of the Vehicle or Control treatment itself.

2.4.1 Fatty Acid Treatments

To model lipid-induced insulin resistance *in vitro*, fully differentiated myotubes were incubated with fatty acid solutions (either palmitate alone, or in combination with linoleic and oleic acid; PLO) for 16 h. These three fatty acids represent the most abundant saturated, polyunsaturated, and mono-unsaturated FFAs, respectively, within human plasma. Fasting concentrations of palmitic, oleic and linoleic acid in the plasma of adults with obesity/T2D are typically reported to be between 190-250 μM, 80-160 μM and 150-250 μM, respectively (Denke & Grundy, 1992; Grapov, Adams, Pedersen, Garvey, & Newman, 2012; Grimsgaard, Bønaa, Jacobsen, & Bjerve, 1999; M. Perreault et al., 2014; Yi et al., 2007). Expanding upon unpublished work from our laboratory (R. Jones, 2019), concentrations of 250 μM, 50 μM and 150 μM (P, L and O respectively) were used for their demonstrable ability to impair insulin sensitivity, but not cell viability, over a 16 h time course, while retaining similarity to physiological abundances (discussed further in Section 4.1).

Because of their low solubility in aqueous solutions, fatty acids within the circulation are either incorporated into chylomicrons/lipoproteins or bound to albumin (van der Vusse, 2009). Although fatty acid transport into the skeletal muscle can occur via passive diffusion (J. A. Hamilton, Johnson, Corkey, & Kamp, 2001), it is principally governed by a number of transporters comprising fatty acid translocase (CD36), fatty acid transport proteins (FATPs) and fatty acid binding proteins (FABPs) (Bonen, Dyck, & Luiken, 1998). These proteins traffic fatty acids into the cytoplasm, where they are bound to cytoplasmic fatty acid binding proteins, which upon activation to acyl-CoA, the acyl-CoA esters can enter the

pathway for re-esterification into muscle lipid droplets or undergo further metabolism (Kiens, 2006).

Within the culture system, fatty acids must be coupled to carriers such as BSA to prevent the formation of toxic micelles. Thus, fatty acid solutions were formed by first conjugating individual fatty acids to fatty acid-free (< 0.2 $mg \cdot g^{-1}$ FA) BSA (Roche, cat #10775835001). A 2.5 mM solution of BSA was first prepared by slowly adding BSA to a 150 mM NaCl solution and heating at 50ºC. Next, a 20mM Palmitate stock was prepared by the progressive addition of palmitate to a solution of 150 mM NaCl and 100 mM NaOH, adjusted to pH 7.4, which was heated in a water bath to 80ºC with regular mixing until complete dissolution (the solution became almost transparent).

Physically hot (80ºC) palmitate was quickly added to the warm BSA at a molar ratio of 1:2.7 to ensure maximal binding (BSA can bind up to 7 FFA moieties if not already bound, hence the use of fatty acid-free BSA) and was incubated at 50ºC for 15 min, with regular vortex mixing, to enable complete coupling. Linoleic acid and Oleic acid solutions were similarly made up, as 10 mM stocks in 150 mM NaCl and 100 µM NaOH, adjusted to pH 7.4. These were added to an equal volume of 24% BSA, incubated at 50ºC and stirred until dissolution, to produce similar molar ratios. Fatty acid solutions were passed through a 0.45 µm sterile filter, aliquoted and stored at -20ºC for up to 3 months.

Fatty acid conjugates were thawed and heated to 50ºC in a water bath prior to experimental application. Sterile solutions of palmitate alone or mixtures of palmitate, linoleic and oleic acid were added to standard myoblast differentiation medium. Myotubes were incubated for 16 h with fatty acids or Vehicle (fatty acid-free BSA) to induce lipid-induced insulin resistance.

2.4.2 Adipose-Conditioned Medium

The majority of adipose-conditioned medium (ACM) used in this thesis was obtained from the University of Birmingham, however some was generated fresh in-house when substantial subcutaneous adipose tissue was concurrently extracted during muscle biopsies from donors with obesity. This in-house ACM was generated using identical conditions and combined with ACM from collaborators accordingly. Subcutaneous adipose tissue (SAT) was obtained intraoperatively from consenting patients undergoing total hip and knee replacement surgery at the Queen Elizabeth Hospital, Birmingham. Patients had broad-ranging BMI, body composition and age, allowing stratification of donor phenotype. To generate ACM, SAT samples were incubated in myotube differentiation medium (HAMS F-10 supplemented with 6% HS) at a ratio of 1 g

of tissue to 10 mL medium for 24 h. Larger samples were divided into segments of ~1 g to ensure that the surface area of adipose tissue exposed to medium remained approximately constant. It should be noted, that while these approaches were employed as a measure of quality control for the generation of ACM, adipose samples were whole tissue extractions and not purified adipocyte cell populations. Thus, samples from different donors may have demonstrated heterogeneity in the relative contributions of different cell populations as well as differences in adipocyte size and maturity. It must be considered, however, that this variation is also emblematic of the physiological heterogeneity of human obesity and reflects biological variability. Thus, for the experiments presented in Chapter Five, ACM was generated from many individuals to capture this variability, and multiple aliquots of ACM from different donors of matching phenotype (young lean, older lean and older obese) were pooled together prior to application to cells. Full details of this pooling are provided in Chapter Five. Upon reaching near-confluence, myoblasts were incubated in either unconditioned (Control) or adipose-conditioned media (Lean or Obese) for 6 days of differentiation, with media replenished every 48 h.

After 24 h of incubation, the medium was removed, sterile filtered and aliquoted into 5 mL samples and stored at -80°C. For experimental application, in accordance with prior work from our group (O'Leary et al., 2018), the pooled ACM was diluted 1:2 with fresh differentiation medium to ensure sufficient nutrient availability for cell survival and myogenic differentiation. Near-confluent myoblasts were incubated with either lean or obese ACM for a total of 6 days, with media being renewed from freshly-thawed aliquots every 48h

2.5 Live-Cell Assays

2.5.1 Assessment of Cell Viability

To assess the impact of experimental treatments on viability, cells grown in 24-well plates at appropriate densities were first exposed to experimental treatments before performing a Resazurin assay. Resazurin (7-Hydroxy-3H-phenoxazin-3-one 10-oxide) is a cell-permeable blue dye, itself weakly fluorescent, that is irreversibly reduced to the pink coloured and highly red fluorescent Resorufin by the mitochondrial respiratory chain in viable, metabolically active cells (Präbst, Engelhardt, Ringgeler, & Hübner, 2017). It is therefore used as an oxidation-reduction indicator, whereby Resorufin production is directly proportional to the number of living cells. Following experimental treatments, cells were washed once in Hanks Balanced Salt Solution (HBSS) before being incubated in 500 µL of Resazurin solution (10 $\mu g \cdot mL^{-1}$ in HBSS) for 60 min at 37ºC, 5% CO_2. The

resazurin/resorufin culture supernate was then transferred to cell-free plate (to avoid background fluorescence/interference arising from the cells themselves) and fluorescence intensity was measured on a fluorescence plate reader (CLARIOstar, BMG LABTECH, DE) at 545 nm excitation/ 600 nm emission, and a cell-free blank was used to adjust measured values. Data was expressed in fluorescence intensity units, with untreated cells considered to represent 100% relative viability.

2.5.2 Radio-labelled Glucose Uptake in Myotubes

It has previously been demonstrated that primary human myotubes derived from sedentary middle-aged adults exhibit diminished insulin-stimulated glucose uptake relative to habitually active age-matched controls, which may be attributable to reduced expression and translocation of GLUT4 (Bunprajun, Henriksen, Scheele, Pedersen, & Green, 2013). Indeed, these defects are consistent with those seen in vivo in the skeletal muscle of sedentary older adults (Gaster, Poulsen, Handberg, Schroder, & Beck-Nielsen, 2000; J. A. Houmard et al., 1991; J. A. Houmard et al., 1995). Thus, assessment of the capacity for insulin to stimulate glucose uptake in primary human myotubes provides a useful model of skeletal muscle that is broadly indicative of the insulin sensitivity of the donor's skeletal muscle *in vivo*.

Basal and insulin-stimulated glucose uptake was therefore assessed in myotubes using nominally radio-labelled (tritiated) 2-Deoxy-D-glucose (2-[1,2-^{3}H (N)]; PerkinElmer, MA, US). Tritiated 2-Deoxy-D-glucose ([^{3}H]2-DOG) is a glucose analogue in which the 2-hydroxyl group is replaced by hydrogen. The 2-DOG is readily unidirectionally transported into myotubes, principally via facilitated diffusion, where it is phosphorylated by hexokinases into glucose-6-phosphate (Zhao, Wieman, Jacobs, & Rathmell, 2008). Importantly, under the conditions employed within this assay, it has previously been confirmed that as in skeletal muscle tissue, hexose transport is the rate-limiting step (A. Klip, Logan, & Li, 1982). Once inside the cell, the absence of the 2-OH group prevents its isomerisation to fructose-6-phosphate, resulting in a failure to undergo further metabolism such that it accumulates within the cell (Pajak et al., 2019). The uptake of a given concentration of 2-DOG into both primary human and rat L6 myotubes in monolayer culture has been previously demonstrated to be linear over a 20 min period of incubation (A. Klip et al., 1982; Sarabia et al., 1992). Thus, [^{3}H]2-deoxy-d-glucose-6-phosphate accumulates linearly over time within the cell, allowing for lysed cells to be assayed for radioactivity as a function of net glucose uptake.

Following experimental treatments, growth medium was removed from fully differentiated myotubes grown in 6-well culture plates, and cell monolayers were washed twice in warm PBS before being incubated in serum-free Hams F-10 basal medium for 2 h at 37ºC. Myotubes were washed twice more and incubated in a reaction buffer (138 mM NaCl, 1.85 mM $CaCl_2$, 1.3 mM $MgSO_4$, 4.8 mM KCl, 50 mM HEPES pH7.4, + 0.2% w/v sterile-filtered BSA) to induce glucose starvation for 3 h at 37ºC. For the final 30 min of nutrient restriction, relevant wells were treated with 100 nM insulin (Actrapid, Novo Nordisk, Bagsværd, DK) at timed intervals and maintained at 37ºC. In each well at consistent timed intervals, 250 µL of 27.8 kBq [^{3}H]2-DOG and 10 µM of non-radio-labelled 2-DOG were added and incubated for 15 min on a plate warmer to facilitate the uptake of glucose (0.75 µCi·well^{-1}).

Myotubes were then washed 3 times in ice-cold PBS, containing 10 mM D-glucose to out-compete any unwashed radiolabel. Myotubes were lysed by manual well scraping for 60 s in 500 µL of 0.05 M NaOH 0.1% SDS lysis buffer, and the resultant suspension was pipetted up and down to ensure homogenisation. Lysates were transferred to scintillation vials and vortexed, before 50 µL of lysate was taken from each vial and transferred to individual Eppendorf tubes for later protein concentration determination by BCA assay. To each scintillation vial, 5 mL of scintillation fluid was added and vortexed for 10 s. Relative glucose uptake was obtained by the measurement of beta-particle emission, expressed as disintegrations per minute (DPM), using a liquid scintillation counter. Disintegration rates were normalised against the protein content of each well to account for variation in cell densities across wells and plates and converted to absolute glucose uptake rate (pmol·mg^{-1}·min^{-1}) (see below).

2.5.3 Radio-labelled Glucose Uptake in 3T3-L1 Adipocytes

Basal and insulin-stimulated glucose uptake was also measured in fully differentiated 3T3-L1 adipocytes using a very similar protocol to that employed for myotubes, which has been previously described in full detail (Lakshmanan, Elmendorf, & Ozcan, 2003). Briefly, cells were washed once with warm PBS, serum starved for 2 h, washed once more and incubated in 1 mL Kreb's Ringer phosphate HEPES (KRPH) buffer (136 mM NaCl, 20 mM HEPES pH 7.4, 5 mM sodium phosphate buffer pH 7.4 [4:1 NaH_2PO_4:Na_2HPO_4], 4.7 mM KCl, 1 mM $MGSO_4$, 1 mM $CaCl_2$) at 1 min intervals per well. After 5 min, cells were treated with either Vehicle (99:1 H_2O:acetone), or 100 nM insulin at 1 min intervals and incubated for 15 min, before the addition of 50 µL of KRPH-[^{3}H]2-deoxy-D-glucose ([^{3}H]2-DOG) to give a final activity of 0.75 µCi·well^{-1}.

After 15 min of incubation at 37ºC, cells were washed three times with 1 mL ice-cold PBS to stop the reaction and were air-dried for 15 min. Lastly, 1 mL of ice-cold 0.2 M NaOH solubilisation buffer was added, and cells were detached and solubilised by pipetting. 750 µL of solubilised cell solution was transferred to scintillation vials into which 5 mL of scintillation fluid was added, vortexed and activity measured via liquid scintillation. An aliquot of 50 µL was taken for determination of protein concentration via BCA assay. Relative glucose uptake (DPM) was measured using a liquid scintillation counter. Disintegration rates were normalised against the protein content of each well to account for variation in cell densities across wells and plates and converted to absolute glucose uptake rate (pmol·mg^{-1}·min^{-1}) (see below).

2.5.4 Conversion of DPMs into Absolute Glucose Uptake Rate

The DPM measurements for each sample were converted to absolute rates of glucose uptake (pmol·mg^{-1}·min^{-1}) using the following principles and equations:

- **Becquerel** (**Bq**) is a measure of radioactivity of a substance. 1 Bq = the quantity of material in which one nucleus decays per second.
- **Curie** (**Ci**) is another measure of radioactivity. 1 Ci = 3.7 x 10^{10} disintegrations per second (**DPS**), or (multiplied by 60) 2.22 x 10^{12} disintegrations per minute (**DPM**)
- Becquerels and Curies can be converted using the following equation:

$$1\ Ci\ =\ 3.7 \times 10^{10}\ Bq\ =\ 3.7 \times 10^{10}\ DPS\ =\ 2.22 \times 10^{12}\ DPM$$

- **Disintegrations per minute** (**DPM**) are the standard output unit of the liquid scintillation counter.
- **Specific Activity** (**SA**) is the relative activity of [^{3}H]2-DOG within the pool of labelled/unlabelled 2-DOG in the experimental well (Ci·mmol^{-1}). This is dependent on the activity of the stock labelled solution on the date of assay ('stock activity', calculated by IsoStock software), and the dilution of that solution into unlabelled 2-DOG solution for experimental application.

Specific activity (SA) of [^{3}H]2-DOG within the total pool of labelled/unlabelled 2-deoxy-D-glucose within the experimental well (Ci·mmol^{-1}) can be calculated with the formula:

Equation 1:

$$Specific\ Activity\ \ in\ well\ (SA;\ Ci \cdot mmol^{-1})\ =$$

$$Stock\ Activity\ (Ci \cdot mmol^{-1}) \times \frac{\left[\,^{3}H\,\right]2DOG\ Conc(mM) - \ Unlabelled\ 2DOG\ Conc(mM)}{\left[\,^{3}H\right]2DOG\ Conc(mM)}$$

The results obtained from the liquid scintillation counter (DPM) can be converted to radioactivity (Ci) with the formula:

Equation 2: $$Radioactivity\ (Ci) = \frac{DPM}{2.22\times10^{12}}$$

The radioactivity of a sample, calculated in *Equation 2*, can then be converted to absolute molar abundance within that sample (total glucose uptake) using the formula:

Equation 3: $$Total\ glucose\ uptake\ (mol) = Ci\ \times \frac{1\ mmol}{SA}$$

Using the total glucose uptake calculated in *Equation 3*, the rate of glucose uptake (over the 15 min [^{3}H]2-DOG incubation) per milligram of cell protein (obtained from BCA assay for each sample) per minute, can be calculated using the formula:

Equation 4:

$$Glucose\ uptake\ (pmol \cdot mg^{-1} \cdot min^{-1}) = \left(\frac{Total\ glucose\ uptake\ (mol)}{Total\ sample\ protein\ (\mu g) \times 15\ (min)}\right) \times 1 \times 10^{15}$$

Combining *Equations 2*, *3* and *4*, gives:

$$Glucose\ uptake\ (pmol \cdot mg^{-1} \cdot min^{-1}) = \left(\frac{DPM}{2.22\times10^{12} \times SA \times Total\ sample\ protein\ (\mu g) \times 15\ (min)}\right) \times 1 \times 10^{15}$$

Which can thus be shortened:

$$Glucose\ uptake\ (pmol \cdot mg^{-1} \cdot min^{-1}) = \left(\frac{450.45\ \times DPM}{SA\ \times\ Total\ sample\ protein\ (\mu g) \times 15\ (min)}\right)$$

2.5.5 Insulin-Stimulated Akt phosphorylation

As an additional marker of insulin-sensitivity with regards to signal transduction, sensitivity to the phosphorylative effects of insulin on Akt were measured via western blot. Following experimental treatments, fully differentiated myotubes cultured in 6-well plates were exposed to either Vehicle (equivoluminous PBS) or 100 nM insulin for 15 min, immediately prior to lysis in 150 µL RIPA buffer with added protease (Sigma-Aldrich, #P8340) and phosphatase (PhosStop, Roche) inhibitors. Equal quantities of cell protein were subsequently loaded onto 12% acrylamide gels, separated via SDS-PAGE and transferred overnight, as described in sections 2.8.6 and 2.8.7. Protein content of total Akt and phosphorylated

(Serine 473) Akt was assayed via western blot, using LI-COR fluorescent secondary antibodies (Table 2.6). Membranes were visualised on a LI-COR Odyssey CLx platform. Relative pAkt abundance was derived from the ratio of pAkt:Akt An index of insulin sensitivity with regards to signal transduction could therefore be produced by comparing the ratio of Akt:Akt from the basal to the insulin-stimulated state for each experimental condition.

2.5.6 SUnSET Protein Synthesis

Global rates of myotube protein synthesis were estimated using the Surface Sensing of Translation (SUnSET) technique (Goodman & Hornberger, 2013; Schmidt, Clavarino, Ceppi, & Pierre, 2009). This technique provides a non-radioactive means to estimate incorporation of amino acids into newly synthesised muscle proteins using the amino-nucleoside antibiotic puromycin. Puromycin is a structural analogue of the aminoacyl-transfer RNA; tyrosyl-tRNA, which at low concentrations is non-toxic and does not impair the overall rate of translation (Schmidt et al., 2009; Yarmolinsky & Haba, 1959). Puromycin is incorporated into elongating polypeptide chains through the formation of a peptide bond (Nathans, 1964). Due to the presence of a non-hydrolysable amide bond in place of a hydrolysable amide bond in aminoacyl-tRNAs, the addition of puromycin to a translating peptide chain prevents binding to the subsequent aminoacyl-tRNA, which therefore terminates peptide elongation and results in the ribosomal release of the truncated puromycin-labelled peptide (Goodman & Hornberger, 2013), which can be detected via western blot using an anti-puromycin antibody.

The acute addition of low concentrations of puromycin to live cells under favourable conditions and the subsequent detection and measurement of puromycin-labelled peptides in cell lysate therefore provides an index of the rate of global protein synthesis within cells. This has been demonstrated to be sufficiently sensitive to detect changes in myotube protein synthesis in response to activation of the ERK/Akt pathway (Yuan et al., 2017). Furthermore, changes in puromycin-labelled peptides have shown strong correlation with the incorporation of [^{3}H] phenylalanine into nascent peptides, demonstrating validity and sensitivity against standard procedures (Goodman et al., 2011).

Following experimental treatments, fully differentiated myotubes, cultured in 6-well plates, were washed once in warm PBS and serum starved in HAMS F-10 medium for 2 h. Medium was then replaced with a transport buffer (140 mM NaCl, 1.8 mM $CaCl_2$, 0.08 mM $MgSO_4$, 5.4 mM KCl, 25 mM HEPES pH 7.4) supplemented with 5 mM D-Glucose and 2 mM L-leucine for 3 h to stimulate protein synthesis. For the final 30 min of incubation, myotubes were treated with puromycin

dihydrochloride (Sigma-Aldrich, #P8833) at an end concentration of 1 μM. Transport buffer was then aspirated, and cells were washed 2x with ice-cold PBS, placed on ice and lysed in 120 μl of RIPA buffer (150 mM NaCl, 25 mM Tris-HCl pH 7.6, 1% Triton x-100. 1% Na-deoxycholate and 0.1% SDS) with added protease and phosphatase inhibitors. Cells were incubated on ice for 15 min, then scraped and repeatedly passed through narrow pipette tips and incubated for a further 15 min on ice. Samples were then centrifuged at 13,000 x G for 15 min at 4ºC and supernatants were transferred to new tubes.

Protein concentration of each sample was determined via Pierce BCA assay as described previously. Equal amounts of total protein were mixed with SDS loading buffer, ran on 12% SDS-PAGE gels and transferred overnight onto PVDF membranes which were probed with Anti-Puromycin antibody (clone 12D10; EMD Millipore, Burlington, MA, USA) at 1:10,000 and visualised using ECL-prime on X-ray film (Table 2.6). Following immunodetection, membranes were stained with 0.1% Coomassie R-250 in methanol:water 1:1 for 10 min and then de-stained with acetic acid:ethanol:water (1:5:4) for 10 min, before washing with water and air drying. The stained membrane was digitally imaged and total lane intensity, determined by densitometry (AIDA/ImageJ), was used as a loading control.

2.6 Immunofluorescent Staining of Myotubes

Following experimental treatments, fully differentiated myotubes, cultured in 24-well plates, were washed twice in PBS before fixing with 4% paraformaldehyde for 15 min at room temperature. Cells were washed twice more prior to permeabilisation with 0.3% Triton X-100 for 20 min at room temperature and subsequently washed twice. Wells were then blocked for 2 h in 5% (w/v) BSA with 0.1% Triton X-100. Rabbit anti-desmin antibody (Abcam, #ab8592) was diluted 1:500 in 1% BSA with 0.1% Triton X-100 and 300 μL of antibody solution was added to each well and incubated overnight at 4ºC on a rocking platform. The following day, wells were washed for 6 x 5 min with PBS and incubated in Alexa Fluor 488-conjugated donkey anti-rabbit secondary antibody (Invitrogen, #R37118) at 1:1000 in 1% BSA with 0.1% Triton X-100 for 1h in the dark at room temperature, before repeating the wash steps. Finally, 1 $\mu g \cdot mL^{-1}$ DAPI (Sigma, #32670) was added in the dark for 2 min without agitation, and wells were washed once more in PBS. Myotubes were imaged in-situ in the 24-well plate on a fluorescent microscope platform (Evos M7000, Thermo Fisher) using DAPI and GFP light cubes and a 10x objective (Olympus, UPLSAPO10X2).

2.6.1 Measurement of Myotube Thickness

Mean myotube thickness was measured 6 days post-induction of differentiation, as an index of myogenic capacity. Following immunofluorescent staining, 10 clear images were taken from pseudo-random locations (fields) across each well, with 3 replicate wells per experimental treatment (30 fields per treatment). Image analysis was performed in ImageJ. For each image, myotube thickness of the 5 largest discernible myotubes in each field (defined as desmin-positive tubular structures incorporating multiple nuclei) was measured. Thickness was measured as the diameter of the myotube (perpendicular to the direction of the longitudinal axis) in 3 places along their length at approximately 25%, 50% and 75% of the length of the visible structure within that field. From these three measurements of each myotube, a mean thickness was recorded. Mean myotube diameter (μm) data for each experimental treatment therefore reflects a total of 450 measurements of 150 different myotubes, across 3 replicate wells.

2.7 Molecular Biology Techniques

2.7.1 RNA Extraction

All work involving the use of ribonucleic acids (RNA) was undertaken using RNase-free microcentrifuge tubes, dedicated RNA-use-only pipettes with RNase and DNase free filter pipette tips. Extraction of RNA was performed on both cultured skeletal muscle cells and muscle tissue using the TRIzol™ (Thermo Fisher) method in accordance with the manufacturer's guidelines.

For cultured myotubes, after aspiration of the growth medium and washing in ice-cold PBS, cells were lysed in-situ with the addition of 80 μL TRIzol reagent·cm^{-2} of well surface area of the plate in which they were growing, followed by gentle pipetting up and down to homogenise the lysate. Whole muscle tissue was kept in liquid nitrogen until extraction, whereupon 1 mL TRIzol reagent was added per ~25 mg of wet tissue and immediately homogenised for 60 s with a polytron. Muscle or cell lysates were incubated in their TRIzol suspension for 5 min to allow complete dissociation and were then transferred to RNase free Eppendorf tubes into which 50 μg of glycogen was added to act as a co-precipitant to the RNA. For muscle tissue samples, 200 μL of chloroform:isoamyl alcohol (49:1) was added per 1 mL of TRIzol, whereas 100 μL of 1-Bromo-3-chloropropane (BCP) was added to cell lysates per 1 mL of TRIzol and incubated at room temperature for 2-3 min before being centrifuged at 12000 x G at 4^{0}C for 15 min to separate RNA from DNA and protein.

The colourless upper aqueous phase containing the RNA was transferred to a clean Eppendorf containing 400 µL ice-cold isopropanol and left overnight at -20ºC. Where insufficient cells were available to harvest separate plates for protein extraction, the lower protein-rich phenol-chloroform phase was kept for subsequent isolation of the protein fragment for immunoblotting experiments (section 2.8.6) and was stored at -20ºC until analysis. Samples were centrifuged again at 12,000 x G at 4ºC for 15 min, after which the supernatant was discarded, and the pellet allowed to air dry before being washed with 75% ethanol and centrifuged once more at 10,000 x G for 10 min. The ethanol supernatant was discarded, and the RNA pellet was air dried and re-suspended in 30 µL RNase-free water. The concentration and purity of the total RNA yield was determined via ultraviolet-visible spectrophotometry at 260 nm using a Nanodrop One (Fisher Scientific, Loughborough, UK). Samples were considered acceptably pure for downstream use if a 260/280 nm ratio >1.7 was obtained. Samples were stored at -80ºC.

2.7.2 First Strand cDNA Synthesis (Reverse Transcription)

Complimentary DNA (cDNA) was synthesised from the RNA template using the Invitrogen SuperScript™ system (all elements obtained from Thermo Fisher unless stated otherwise). Briefly, reverse transcriptase (RT) uses an RNA template and short primer sequence that compliments the 3' end of the RNA strand to synthesise first strand cDNA for use as a template during the polymerase chain reaction (PCR). Together, RT-PCR enables the subsequent detection of low-abundance RNAs within samples.

An aliquot of each total RNA sample was diluted to 0.05 $\mu g \cdot \mu L^{-1}$, 10 µL of which was added to an Eppendorf containing 0.0625 µL of random primers (hexamers) (Qiagen, #79236) 1µL of 10 mM deoxyribonucleotide triphosphates (dNTPs) (#R0191) and 1.375 µL of molecular biology grade water (HyClone, #10307052). Sample mixes were heated for 5 min at 65ºC in a thermal cycler and subsequently incubated on ice for 1 min. To the mix, 4 µL of 5 x First Strand Buffer, 1 µL Superscript III, 1 µL 0.1 M dithiothreitol (All # 18080093), and 1 µL RNaseOUT™ (#10777019) was added and gently homogenised by pipetting up and down. The resultant mix was incubated at 25ºC for 5 min, 50ºC for 60 min and finally inactivated by heating at 70ºC for 15 min.

2.7.3 Primer and Probe Design

Human DNA sequences were sourced through GenBank and primers and TaqMan probes were designed using PrimerExpress™ 2.0 software (Applied Biosystems), using standard acceptability criteria, ensuring primers spanned across exon-exon

boundaries (Table 2.4). Primers and probes were reconstituted to 100 μM according to the manufacturer's guidelines. Primer specificity was confirmed through BLAST nucleotide searching (www.ncbi.nlm.nih.gov/blast/Blast.cgi).

For certain genes of interest, PrimerExpress was unable to design acceptable primers/probe combinations using standard acceptability criteria. In these instances, pre-designed one-tube TaqMan gene expression assay kits were purchased from Thermo Fisher (Table 2.5) and used according to the manufacturer's protocol.

Table 2.4. Custom designed primer and TaqMan Probe sequences for real time PCR

Gene Name	Accession number	Primer/probe	Sequence (5' → 3')
Endogenous Reference Genes			
α-Actin	NM_001100	Forward primer	GAGCCGAGAGTAGCAGTTGTAGCT
		TaqMan probe	CCCGCCCAGAAACTAGACACAATGTGC
		Reverse primer	GCGGTGGTCTCGTCTTCGT
β-Actin	NM_001101.5	Forward primer	CCTGGCACCCAGCACAAT
		TaqMan probe	ATCAAGATCATTGCTCCTCCTGAGCGC
		Reverse primer	GCCGATCCACACGGAGTACT
RPLP0	NM_001002.4	Forward primer	TCGTGGAAGTGACATCGTCTTT
		TaqMan probe	CGTGGCAATCCCTGACGCACC
		Reverse primer	CTGTCTTCCCTGGGCATCA
HMBS	NM_000190.4	Forward primer	CCAGCTCCCTGCGAAGAG
		TaqMan probe	CCCAGCTGCAGAGAAAGTTCCCGC
		Reverse primer	TTCCCCGAATACTCCTGAACTC
Genes of Interest			
MSTN	NM_005259.2	Forward primer	GATGAGAATGGTCATGATCTTGCT
		TaqMan probe	TAACCTTCCCAGGACCAG
		Reverse primer	AAAAACGGATTCAGCCCATCT
IL-6	NM_000600.5	Forward primer	ACCTCTTCAGAACGAATTGACAAAC
		TaqMan probe	TACATCCTCGACGGCATCTCAGCCC
		Reverse primer	TGTTACTCTTGTTACATGTCTCCTTTCTC
IL-1β	NM_000576.3	Forward primer	CCCTAAACAGATGAAGTGCTCCTT
		TaqMan probe	CTGGACCTCTGCCCTCTGGATGGC
		Reverse primer	GGTGGTCGGAGATTCGTAGCT
TNF	NM_000594.4	Forward primer	CCCAGGGACCTCTCTCTAATCA
		Reverse primer	GGTTTGCTACAACATGGGCTACA
		TaqMan probe	CTCTGGCCCAGGCAGTCAGATCATCT
GLUT1	NM_006516.4	Forward primer	TGCCATTGCCGTTGCA
		TaqMan probe	CTCAAATTTCATTGTGGGCATGTGCTTCC
		Reverse primer	GACCACACAGTTGCTCCACATAC
GLUT4	NM_001042.3	Forward primer	CCCTGCAGTTTGGGTACAACA
		TaqMan probe	CCCCTCAGAAGGTGATT
		Reverse primer	GCCACGTCTCATTGTAGCTCTGT

Gene name abbreviations: Alpha Actin (α-Actin); Beta Actin (β-Actin); 60S Acidic Ribosomal Protein P0 (RPLP0); Hydroxymethylbilane Synthase (HMBS); Myostatin (MSTN); Interleukin-6 (IL-6); Interleukin-1 Beta (IL 1-β); Tumour Necrosis Factor (TNF); Glucose Transporter 1 (GLUT1); Glucose Transporter 4 (GLUT4).

Table 2.5. Pre-designed one-tube TaqMan assays for real time PCR.

Gene Name	Accession Number	Assay ID	Chromosome Location (on Build GRCh38)
ACVR2B	NM_001106.4	Hs00609603_m1	Chr.3: 38454299 - 38493142
FSTL3	NM_005860.3	Hs00610505_m1	Chr.19: 676389 - 683392
MyoD	NM_002478.5	Hs00159528_m1	Chr.11: 17719563 - 17722131
MyoG	NM_002479.6	Hs01072232_m1	Chr.1: 203083129 - 203086038
MuRF1	NM_032588.4	Hs00822397_m1	Chr.1: 26051304 - 26067634
MAFbx	NM_058229.3	Hs01041408_m1	Chr.8: 123497887 - 123541253

Gene name abbreviations: Activin Receptor Type-2B (ACVR2B); Follistatin-Like 3 (FSTL3); Myoblast determination Protein 1 (MyoD); Myogenin (MyoG); Muscle RING Finger 1 (MuRF1); Muscle Atrophy F-box (MAFbx).

2.7.4 Real Time PCR

Relative gene expression was performed in optically clear 96-well plates using real time PCR (qPCR) with fluorogenic probes comprising a 5' reporter (FAM dye) and a 3' nonfluorescent quencher. Reactions were performed in 96-well PCR plates (STARLAB, #E1403-6200) with a total reaction volume of 20 µL, measured in triplicate. For custom designed primers and probe sets, 15 µL of master mix solution was added, comprising 10 µL of 2x TaqMan Universal PCR MasterMix (PCR Biosystems, #PB20.22), 0.8 µL forward and 0.8 µL reverse primer, 0.4 µL probe, and 3 µL molecular biology grade water. For pre-designed one-tube TaqMan assays, 10 µL of 2x TaqMan Universal PCR MasterMix, 1 µL of primer/probe mix and 4 µL molecular biology grade water. For both custom and predesigned assays, 5 µL of cDNA was used. For each plate, 6 relative standards were employed in triplicate using 1 in 2 serial dilutions of a mixed pool of template DNA from each sample to be analysed, as well as a non-template control.

Real time PCR was performed using a StepOnePlus™ system (Applied Biosystems, CA, US) using a two-step thermal programme. Initially the plate was held for 50ºC for 2 min, after which polymerase was activated by heating at 95ºC for 10 min, followed by 40 cycles of the two-step denaturation (95ºC, 15 s), annealing and extension (60ºC, 60 s) phase.

2.7.5 Analysis of RT-qPCR Data

For quantification of relative gene expression, threshold fluorescence levels were first defined on a logarithmic view of the reaction curves, such that the threshold was above the range of background fluorescence and crossed all amplification curves in their linear phase (representing exponential amplification). Cycle threshold (Ct) values for each sample were therefore determined by the cycle number at which their amplification curve crossed this threshold. Using the regression equation derived from the standard curve of pooled samples, relative quantities of target and endogenous reference genes mRNA were calculated using the relative standard curve method as described by Larionov, Krause, and Miller (2005). The stability of candidate endogenous reference genes was assessed using NormFinder (Andersen, Jensen, & Ørntoft, 2004). Relative expression of genes of interest were normalised by dividing the relative quantity of target gene by the relative quantity of the most stable individual or combination of multiple (geometric mean) reference genes.

2.7.6 Protein Extraction and Quantification

Whole cell protein extraction was performed for determination of immunoreactive protein content of markers of interest. For direct extraction from cells grown in 12-well adherent culture plates, >90% confluent myotubes (~$5x10^4$ cells·$well^{-1}$) were lysed in RIPA lysis buffer (15 µL·cm^{-2}) with added protease (Sigma-Aldrich, #P8340) and phosphatase (PhosStop, Roche) inhibitors and mechanically dissociated by scraping. For skeletal muscle samples, ~30mg of wet tissue was first homogenised with a polytron in 300 µL HEPES buffer (50 mM HEPES, 10% glycerol, 1 mM EDTA, 150 mM NaCl, 1% Triton x-100, pH 7.5) with added protease and phosphatase inhibitors. Muscle/cell lysate was incubated on ice for 20min to allow for complete dissociation, whereafter the cell lysate/muscle homogenate was passed up and down multiple times through a gel-loading micropipette tip and subsequently centrifuged at 10,000 x G for 20 min at 4°C and the supernatant transferred to a clean Eppendorf.

Where an insufficient number of culture plates was available for dedicating to protein extraction, protein fractions were instead obtained from the lower protein-rich the phenol-chloroform phase following RNA precipitation. To that effect, DNA was first precipitated from the phenol-chloroform solution by adding 0.3 mL of 100% ethanol per 1 mL of TRIzol reagent: mixing and incubating at room temperature for 3 min and centrifuging at 2000 x G for 5 min at 4ºC to pellet DNA. The DNA-free phenol-ethanol supernatant was aspirated for subsequent protein precipitation. 1.5 mL of ice-cold isopropanol was added per 1 mL of TRIzol and

incubated at room temperature for 10 min, before centrifuging at 12000 x G for 10 min at 4ºC.

After removing the supernatant, the protein pellet was then washed in 0.3 M guanidine hydrochloride in 95% ethanol; incubated at room temperature for 20 min; centrifuged at 7500 x G for 5 min at 4ºC; and the supernatant was removed. This process was repeated twice more to purify the pellet. Next, 2 mL of 100% ethanol was added, vortexed and incubated at room temperature for 20 min, before centrifugation at 7500 x G for 5 min at 4ºC. The ethanol was then discarded, and pellets were briefly air-dried. Lastly, the protein pellet was re-suspended in 1% SDS and heated at 50ºC before a final centrifugation at 10,000 x G for 10 min at 4ºC to sediment any insoluble material. The resultant protein supernatant was stored at -20ºC until analysis.

For all protein extraction techniques, total protein concentration was determined using the Pierce bicinchoninic acid (BCA) assay (Thermo Fisher Scientific, #23225). Briefly, Samples were diluted to 1 in 10 in distilled water. A 10 µL aliquot of sample protein or Albumin protein standard, and 200 µL of working reagent were pipetted into a 96-well plate in duplicate and incubated at 37°C for 30 min. Following the addition of working reagent to the sample, peptides containing three or more amino acid residues form a coloured chelate complex with cupric ions in an alkaline environment containing sodium potassium tartrate (biuret reaction). Next, the BCA reacts with the newly reduced (cuprous) cations. The chelation of two molecules of BCA with one cuprous ion gives rise to purple colour formation, with linear absorbance at 562 nm that increases in proportion to sample protein concentration. Absorbance was read at 562 nm on a spectrophotometer (CLARIOstar, BMG Labtech). Protein concentration of each sample was subsequently calculated using the linear regression equation produced from plotting the known concentration of protein standards against the absorbance value for that standard minus the mean absorbance of protein-free blank wells.

2.7.7 SDS-PAGE and Western Blotting

Protein concentration of individual stocks were standardised with sodium dodecyl sulphate (SDS) loading buffer (containing bromophenol blue) and a diluent of matching buffer to that which the samples were harvested in (HEPES for muscle and RIPA or guanidine hydrochloride for cells) with added protease and phosphatase inhibitor cocktails, before boiling at 95°C for 5 min. Equal amounts of total muscle lysate proteins were loaded into the wells of a freshly made hand-cast SDS polyacrylamide gels (8-15% acrylamide, depending on molecular weights of target proteins) for separation via electrophoresis (SDS-PAGE) in a

vertical, dual plate tank filled with 1 x Tris-Glycine-SDS running buffer. Gels were run at a constant amplitude of either 40 or 80 mA (for 1 or 2 gels, respectively) for ~2 h.

Following electrophoresis, the gel-bound separated proteins were electroblotted overnight to either polyvinylidene difluoride (PVDF; used for all standard blotting using chemiluminescence), or nitrocellulose membranes (for phospho- and total-Akt using Alexa Fluor fluorescent antibodies), in an electrophoresis transfer cell (Bio-Rad, Hercules, CA, USA) filled with Tris-Glycine-Methanol transfer buffer for ≥ 16 h at a constant amplitude of 40 mA. Membranes were subsequently blocked in 5% (w/v) Marvel milk or bovine serum albumin (BSA) in tris buffered saline containing 0.1% (w/v) tween 20 (TBS-T) for 1 h at room temperature.

Blocked membranes were incubated overnight at 4°C with primary antibodies for the proteins of interest in 1-5% milk or BSA (w/v) (Table 2.6). The following day, after 5x5 min TBS-T washes, membranes were incubated for 1 h at room temperature with horse radish peroxidase-(HRP) linked secondary antibodies (Dako, Glostrup, DK) for the detection of primary antibodies. After 3 x 10 min washes, proteins were visualised by incubating membranes in an enhanced chemiluminescence detection reagent (Amersham ECL Prime, GE Healthcare Life Sciences) for 5 min before exposing them to X-ray film (Amersham Hyperfilm, GE Healthcare Life Sciences) in a dark room. Films were digitally scanned and the resulting immunoreactive bands were quantified using densitometry software (Aida Image Analyser v.4.27, Raytest Isotopenmessgeräte, DE and ImageJ, National Institutes of Health). Proteins of interest were normalised by dividing protein of interest band intensity against band intensity of an endogenous reference protein that demonstrated stable expression under those experimental conditions.

Table 2.6. Antibodies, concentrations, and conditions for the measurement of relative protein expression via western blotting.

	Species	Supplier	Product Code	Size (kDa)	Block	1^0 Antibody		2^0 Antibody	
						Dilution	Diluent	Dilution	Diluent
Endogenous Reference Proteins									
Actin	Rabbit	Sigma-Aldrich	A2066	42	5% Milk	1:5000	1% Milk	1:5000	1% Milk
Cyclophilin B	Mouse	Abcam	ab74173	20	5% Milk	1:4000	5% BSA	1:2000	5% BSA
Proteins of Interest									
Myostatin	Rabbit	Abcam	ab71808	43	5% Milk	1:1000	5% Milk	1:2000	5% Milk
pSMAD2 (Ser465/Ser467)	Rabbit	Cell Signalling Technology	18338	60	5% BSA	1:2000	5% BSA	1:2000	5% BSA
SMAD2	Rabbit	Cell Signalling Technology	5339	60	5% BSA	1:2000	5% BSA	1:2000	5% BSA
pAkt (Ser473)	Rabbit	Cell Signalling Technology	9271S	60	5% BSA	1:1000	5% BSA	1:5000	5% BSA
Total Akt	Mouse	Cell Signalling Technology	2920	60	5% BSA	1:1000	5% BSA	1:5000	5% BSA
Puromycin	Mouse	Sigma-Aldrich	MABE343	N/A	5% BSA	1:10,000	5% BSA	1:5000	5% BSA

2.7.8 Adipokine Screening of Adipose-Conditioned Medium

To assess differences between the adipose tissue secretomes of different donor phenotypes of ACM used in Chapter Five, the relative protein abundance of 58 well-characterised adipokines was assessed in each ACM pool using a commercially available human adipokine array kit (R&D Systems, #ARY204). This kit comprised capture and control antibodies spotted in duplicate on nitrocellulose membranes.

Prior to assaying, ACM pools were centrifuged at 10,000 x G for 10 min to remove any particulates. Membranes were first activated and then blocked for 1 h at room temperature in a BSA buffer on a rocking platform. After blocking, 400 µL of neat ACM stock was diluted with 500 µL of Array buffer and 600 µL of BSA buffer before 30 µL of biotinylated antibody cocktail solution was added and incubated at room temperature for 1 h. The BSA buffer was aspirated from the membranes and replaced with the antibody-conjugated ACM solution, which was incubated overnight on a rocking platform at 4ºC. After exactly 16 h incubation, ACM solutions were removed, and membranes were washed 3x with wash buffer for 10 min. Streptavidin-HRP solution was applied evenly over the surface of each membrane for 30 min before washing thrice more. A chemiluminescent detection solution was applied evenly to the surface of each membrane and incubated for 1 min before removing excess solution. Membranes were transferred to an autoradiography cassette and exposed to X-ray film in a dark room for 16 min.

Exposed films were digitally scanned and analysed in Aida Image analyser. A template was generated to consistently measure intensities across different membranes. Duplicate spot intensities for each adipokine were measured using densitometric analysis. Intensities of negative control spots, which did not contain any capture antibodies intensities and thus provided a measure of noise, were also measured, and subtracted from the intensity of proteins of interest, to account for background signal. Relative intensities were then able to be meaningfully and reliably compared between different membranes (different ACM pools).

2.8 Data Handling, Visualisation and Statistics

Data were ordinarily handled first in Excel (Microsoft, WA, US) before visualisation and statistical analysis was performed in GraphPad Prism 9 (GraphPad Software, CA, US). Specific data handling and statistical analyses employed in each chapter are detailed within the relevant chapters.

Chapter 3. The Effects of Obesity and Ageing on skeletal muscle Myostatin Expression and Abundance

3.1 Introduction

Skeletal muscle myostatin mRNA expression, protein abundance and serum concentration are all reportedly altered with obesity (David L. Allen et al., 2011; Hittel et al., 2009; Léger et al., 2008). Hittel et al. (2009) reported a ~20% greater abundance of myostatin protein in skeletal muscle from extremely obese middle-aged men than age-matched normal weight controls. Muscle myostatin protein content was found to correlate with BMI in Hittel's study, which is consistent with the positive association between muscle myostatin mRNA expression and BMI reported by Ryan and Li (2021). Indeed, muscle myostatin mRNA expression was found to be 1.4- to 1.9-fold higher in morbidly obese (BMI >40 $kg \cdot m^{-2}$) middle-aged individuals than age-matched lean (BMI <25 $kg \cdot m^{-2}$) individuals (J.-J. Park et al., 2006). Myostatin plasma concentration has also been reported to be 30-40% higher in extremely obese, middle-aged participants, than age-matched normal weight counterparts (Amor et al., 2019), which likely reflects the greater secretion of myostatin protein from obese skeletal muscle cells (Hittel et al., 2009). The association between obesity and measures of myostatin is further supported by weight-loss studies of morbidly and extremely obese women who underwent biliopancreatic diversion (Milan et al., 2004) or gastric bypass (J.-J. Park et al., 2006). Milan et al. (2004) and J.-J. Park et al. (2006) reported ~1.7- and 2.4-fold reductions in muscle myostatin mRNA expression, respectively, following weight loss equating to ~40 and 45% reductions in body mass over 12-18 months post-surgery.

Importantly, early research also demonstrated that myostatin knockout mice were more resistant to high-fat diet-induced impairment of glucose tolerance (McPherron & Lee, 2002) and exhibited improved glucose tolerance and insulin sensitivity (T. Guo et al., 2009). Ensuing studies revealed associations between elevated expression and abundance of myostatin and insulin resistance in humans (Amor et al., 2019; Hittel et al., 2009). Indeed, individuals with greater skeletal muscle myostatin expression required lower rates of glucose infusion during euglycaemic–hyperinsulinaemic clamps to maintain normoglycaemia (Hjorth et al., 2016). Potential causality of this relationship was demonstrated in murine and culture models, where treatment with recombinant myostatin decreased indices of insulin sensitivity, signalling, and glucose tolerance in some (Hittel et al., 2010; X.-H. Liu et al., 2018) but not all studies (Hjorth et al., 2016). Concordantly,

inhibition of myostatin has been demonstrated to be associated with improved insulin sensitivity (Camporez et al., 2016; Dong et al., 2016; Eilers et al., 2020; Eilers, Cleasby, & Foster, 2021). Mechanistically, however, it remains to be elucidated whether the insulin-sensitising effects of myostatin suppression, and indeed the association of upregulated myostatin and insulin resistance in obesity, are a function of myostatin-mediated changes in skeletal muscle mass, or of intrinsic changes in insulin sensitivity and signalling within the skeletal muscle tissue.

While the evidence that myostatin is upregulated in individuals with obesity is compelling, it must be recalled that adiposity and ageing often advance together (St-Onge, 2005). To date, cross-sectional studies predominantly investigate myostatin in obese and age-matched non-obese individuals, who are almost invariably middle-to-older-aged. Thus, it cannot be known from such studies whether myostatin expression and abundance are altered by ageing, independent of obesity.

In a cross-sectional study of both males and females, Yarasheski et al. (2002) reported that serum myostatin was higher in healthy older adults (60-75 yrs) than young adults (19-35 yrs); higher still in older frail individuals (76-92 yrs), and was inversely correlated with fat free mass (FFM). Concordantly, in community-dwelling older men (72.3 ± 2.4 yrs) myostatin expression was lower in a subset characterised by higher grip strength (Patel et al., 2014). In a study of young (21 ± 3 yrs) and older (70 ± 4 yrs) males matched for total, lean and fat mass, older males demonstrated significantly greater skeletal muscle myostatin protein content and a tendency (P = 0.07) for 1.7-fold higher mRNA expression (McKay et al., 2012). Comparable results were reported by Léger et al. (2008), who found myostatin expression at the mRNA and protein level was elevated in older (70 ± 0.3 yrs) than younger (20 ± 0.2, yrs) males by 2.0- and 1.4-fold, respectively. However, the downstream targets of myostatin; the E3 ligases, MAFbx and MuRF1, were not different between groups. In a similar comparison between normal weight, young and elderly women (23 ± 2 vs 85 ± 1 yrs), mRNA expression of myostatin was 56% greater in the older group and was accompanied by comparably greater expression of the MRFs; MYF5, MYOD, MYOG and MRF4 (Raue et al., 2006). Together, these studies suggest that changes in myostatin expression and abundance arising with ageing are accompanied by an uncoupling from, at least some of, its downstream effectors, possibly as means to try and preserve muscle mass.

Not all studies, however, have found differences in the expression and abundance of myostatin between young and older adults. S. Welle, Bhatt, Shah, and Thornton (2002) found skeletal muscle myostatin mRNA expression was not different between BMI- (but not skeletal muscle mass index-) matched, older (62-77 yrs) and younger (21-31 yrs) males. Dalbo et al. (2011) also found no difference in the mRNA expression of myostatin or the gene encoding its receptor, Activin receptor type 2B (ACVR2B), between young (21 ± 0.5 yrs) and older (66.4 ± 1.6 yrs) males. In Dalbo et al.'s study, however, older males had significantly greater body mass (94.2 ± 3.7 vs 82.3 ± 4.2 kg) and body fat percentage (27.4 ± 1.8 vs 15.4 ± 2.9%), confounding the relative effects of ageing and adiposity.

Conversely, Lakshman et al. (2009) found serum myostatin to be 14% higher in younger men (26.5 ± 4.6 yrs) than older men (66.4 ± 4.7 yrs) who were matched for lean mass but not body fat percentage (18.0 ± 6.4 vs 26.6 ± 5.4%, respectively), but observed no difference between young (19–21 yrs) and post-menopausal (67-87 yrs) women. It has been suggested that differential myostatin abundance between the sexes may be involved in the sexual dimorphism of skeletal muscle mass (McMahon et al., 2003; Peiris, Ponnampalam, Mitchell, & Green, 2010), with women typically exhibiting lower serum concentration, but not skeletal muscle expression or abundance (Dial et al., 2020; Maher et al., 2009). This suggests that elevated serum myostatin in males may be an artefact of their typically greater skeletal muscle mass, however interactions with ageing remain to be elucidated. In another study, muscle myostatin mRNA expression was found to be significantly lower in both ambulatory and non-ambulatory elderly women than young women (87 ± 3 and 85 ± 3 vs 24 ± 2 yrs, respectively) (Sandri et al., 2013). Conversely, myostatin protein content was greatest in the old ambulatory group and tended to be greater in the older non-ambulatory group, while plasma concentration was not different between groups, suggesting that circulating myostatin abundance may be synergistically regulated by compensatory changes in transcription and translation. This suggests that the measurement of myostatin at only one level of expression (transcription or translation) is insufficient to capture the full picture of its regulation in the context of ageing or metabolic dysfunction.

The lack of consistency within the literature might reflect failures to account for changes in body composition and muscle function with ageing, where concurrent declines in muscle mass and function and increases in adipose mass are common (Gallagher et al., 2000; Goodpaster et al., 2006; St-Onge, 2005). To date, the literature has focused on independent comparisons of either age or adiposity.

Given that the prevalence of overweight and obesity in England is >70% in those aged ≥ 45 yrs (NHS, 2019b), it is vital that these two factors are considered simultaneously in analyses that account for adiposity in both young and older individuals. Only then can targeted studies to better understand the physiological mechanisms of myostatin dysregulation be effectively pursued.

3.1 Aims

The primary aim of this study was to conduct 2 studies to determine how the expression of myostatin at the transcriptional (mRNA expression), translational (protein content) and circulatory (serum concentration) level are altered with obesity and ageing. To that effect, Study One sought to compare the expression of myostatin, its interacting proteins and downstream signalling components in a cross-sectional manner between young normal weight (YNW), older normal weight (ONW) and older overweight/obese (OOO) males, to delineate between the effects of ageing *per se* from that of ageing accompanied with obesity. As a novel measure, the direct effect of hyperinsulinaemia on myostatin expression and abundance was also assessed in the same three groups. Study Two assessed serum myostatin concentrations in a separate, well-characterised cohort who had wide-ranging age, adiposity, and habitual physical activity level, with the aim of identifying correlates of circulating myostatin abundance that might support the findings of Study One.

3.2 Methods

3.2.1 Study 1

To enable a cross-sectional analysis of skeletal muscle myostatin mRNA expression and protein abundance in human ageing and obesity, skeletal muscle tissue samples were obtained from a prior study undertaken within the Metabolic Physiology Research Group at the David Greenfield Human Physiology Unit, investigating the effects of 24 weeks of daily L-Carnitine supplementation and regular exercise on metabolic health (Chee, 2016; Chee et al., 2021). Healthy male volunteers were recruited who were either; young and non-obese (18-30 yrs, BMI ≤ 27), older and non-obese (≥65 yrs, BMI ≤ 27) or older and overweight/obese (≥65 yrs, BMI ≥27). Participants provided written informed consent and underwent a medical screening as described in Chapter 2 (section 2.1.1). Individuals were excluded if they had a history of diabetes, cardiovascular disease, or any other known metabolic or respiratory conditions. On a separate preliminary visit, participants underwent an incremental exercise test to exhaustion on an electronically braked cycle ergometer (Lode Excalibur,

Groningen, The Netherlands) to determine their rate of maximal oxygen consumption (VO_{2max}) using breath-by-breath online gas analysis (Quark CPET system, Cosmed, Italy).

For the main experimental visit, participants arrived at the laboratory at ~08:00 following an overnight fast and 48 h of abstinence from strenuous physical activity and alcohol consumption. A dual energy X-ray absorptiometry (DEXA) scan (Lunar Prodigy, GE Healthcare, US) was undertaken to determine body composition. Participants then rested semi-supine on a bed and a resting skeletal muscle biopsy was obtained. Following this, a retrograde cannula was inserted into a superficial hand vein, which was kept in a monitored hand-warming unit (55°C), to enable arterialised-venous blood samples to be obtained (Gallen & Macdonald, 1990). The cannula was kept patent via a saline drip. Whole body insulin sensitivity was then assessed using a 3 h hyperinsulinaemic-euglycaemic clamp as previously described (R. A. DeFronzo, Tobin, & Andres, 1979; J. K. Kim, 2009).

Briefly, insulin was continuously intravenously infused at 60 $mU \cdot m^{-2} \cdot min^{-1}$ to suppress endogenous glucose production (predominantly hepatic; reflecting the sum of hepatic gluconeogenesis and glycogenolysis) (Ralph A DeFronzo, Ferrannini, Hendler, Felig, & Wahren, 1983). A continuous infusion of 20% glucose was sustained at a variable rate to achieve euglycaemia (set at 4.5 $mmol \cdot L^{-1}$). It has previously been demonstrated under similar (50 $mU \cdot m^{-2} \cdot min^{-1}$ insulin) hyperinsulinaemic euglycaemic clamp conditions in healthy males, that hepatic glucose production (HGP) is completely suppressed (Chokkalingam et al., 2007). While insulin resistant adults do exhibit impaired insulin-mediated suppression of HGP under low rates of insulin infusion (Båvenholm, Pigon, Ostenson, & Efendic, 2001), this can be overcome with higher rates of insulin infusion. Indeed, in insulin resistant adults, HGP can be fully supressed to levels seen in insulin sensitive adults with an insulin infusion rate of 1.67 $mU \cdot kg^{-1} \cdot min^{-1}$ (Paolisso et al., 1991), which for the average ~85kg individual in the OOO group would equate to ~140 $mU \cdot min^{-1}$, which is similar to the ~120 $mU \cdot min^{-1}$ that would be used in the present study for such an individual (60 $mU \cdot m^{-2} \cdot min^{-1}$; with an estimated body surface area of ~2.0 m^2 based on a BMI of ~30 $kg \cdot m^{-2}$ (Du Bois & Du Bois, 1989)). Thus, the rate of glucose infused (GIR) was considered equal to the rate of glucose disposal, which under insulin-stimulated conditions is predominantly mediated by skeletal muscle uptake. A second skeletal muscle biopsy was obtained at the end of the 3 h clamp.

Skeletal Muscle Biopsies

Skeletal muscle biopsies of the vastus lateralis were obtained as described in Chapter 2 (2.1.11) using the suction-modified Bergström technique. Visible blood, adipose and connective tissue was removed, and muscle tissue was snap frozen and stored in liquid nitrogen until analysis.

RNA Extraction

Muscle tissue samples of 5-20 mg were cut under liquid nitrogen, transferred to RNase-free tubes and total RNA was extracted using the Trizol method as described in Chapter2 (2.8.1). Due to insufficient skeletal muscle tissue sample masses to reliably perform separate protein and RNA extraction on some samples (<10 mg), following extraction, protein-rich organic phases were stored at -20^{0}C for protein recovery. All protein extractions were therefore performed using the organic phases obtained from Trizol preparations.

Reverse Transcription and Real-Time PCR

Reverse transcription of RNA to cDNA was performed exactly as described in Chapter 2 (2.8.2). All samples were reverse transcribed on the same day using the same stock of reagents. A single set of pooled standards were used for the generation of relative standard curves for all qPCR target genes. Real-time PCR was performed as described in Chapter 2 (2.8.4) and quantified using the relative standard curve method.

Standardisation of RT-qPCR

A single batch of 'mastermix' was made for each gene of interest, and all samples/plates for each gene were ran on the same day. On the first plate for each gene, the 7 standards, a non-template control, and group-randomised paired participant samples (baseline and post-clamp) were loaded. A sample was chosen at random from the first plate and was loaded on each subsequent plate to serve as a control. Cycle threshold values of the control sample were compared across plates and the ΔCt of this sample was used as a reference to correct all other samples on the plate where necessary, to account for any minor changes in PCR efficiency between plates.

Normalisation of RT-qPCR Data

Reliably comparing gene expression between heterogeneous groups is particularly challenging in skeletal muscle, where there is also variability in muscle fibre compositions. Historically, single endogenous reference genes, believed to be constitutively expressed and thus termed 'housekeepers' were commonly

employed to serve as reference expression markers. It is now understood that many common reference genes are readily influenced by treatment/stimuli and crucially to this study; age (Touchberry, Wacker, Richmond, Whitman, & Godard, 2006). Indeed, aged skeletal muscle appears to have almost universally reduced expression of candidate reference genes, compared to that of young muscle (González-Bermúdez, Anglada, Genescà, Martín, & Terradas, 2019).

Accordingly, the expression of three candidate reference genes; α-Actin, HMBS and RPLP0 were measured to determine stability within participants before and after the hyperinsulinaemic-euglycaemic clamp and between groups. Two-way ANOVAs revealed no effect of hyperinsulinaemia on the expression of any candidate reference gene. NormFinder analysis (Andersen et al., 2004) was used on pooled pre- and post-clamp data, in combination with statistical and graphical assessment of variation within and between groups (Sundaram, Sampathkumar, Massaad, & Grenier, 2019), to determine the most stable combination of genes. NormFinder reported M-Values (a measure of stability, whereby decreasing values denote increasing stability) of 0.046, 0.058, and 0.069, for HMBS, α-Actin and RPLP0, respectively. The geometric mean of HMBS and RPLP0 demonstrated the best combination of within and between-group stability with no significant differences between, and the lowest variability within, donor groups (all $P > 0.05$). Thus, the relative expression of all genes of interest were normalised against the geometric mean of the relative expression of HMBS and RPLP0.

Protein Extraction and Quantification

Following Trizol RNA extraction, protein was recovered from the lower phase according to a modified version of the manufacturer's protocol (Simoes et al., 2013) in a similar fashion to that described in Chapter 2 (2.8.6) for the recovery of protein from the organic phases of cell Trizol extracts. Protein pellets were resuspended in 300–1000 µL (depending on pellet size) of deionised 8 M urea in 50 mM Tris Hydrochloride with 4% SDS, pH 8.0 and incubated at 55ºC for 30 min with regular mixing. Due to higher protein yields from muscle than cell extractions, protein solutions were sonicated for 3 cycles of 10 s at 30 Hz followed by 30 s on ice. Insoluble material was sedimented by centrifuging at 3200 x G for 10 min at 4ºC and the supernatants were stored at -20ºC.

Protein concentrations were determined using the BCA method, with standards prepared in diluted urea buffer to match that of the samples (end concentrations of 1.6 M urea, 10 mM Tric-HCl, 0.8% SDS). While these concentrations of urea, Tris and SDS are within the manufacturer's specified working range of the assay, they nevertheless interfere with its accuracy (Krieg, Dong, Schwamborn, &

Knuechel, 2005). For more accurate sample normalisation, following electroblotting membranes were stained with Revert 700 total protein stain (LI-COR Biotechnology, NEB, US), as described below.

Western Blotting and Normalisation

Western blotting was performed as in Chapter 2 (2.8.7), using the protein extracts recovered from Trizol preparations. Briefly, 40 µg of total protein per sample was loaded onto 15% acrylamide hand-cast gels and separated via SDS-PAGE. Paired samples from each participant (Baseline and post-clamp) were loaded sequentially, with participants from the three groups randomly distributed across multiple gels. Separated proteins were transferred to PVDF membranes overnight.

Due to the decreased accuracy of protein determination caused by the urea buffer, membranes were stained with Revert 700; a reversible, fluorescent protein stain that provides greater accuracy of normalisation than reference proteins alone (Kirshner & Gibbs, 2018). Membranes were first rinsed in water and incubated in stain solution for 5 min with gentle shaking, before rinsing twice in a wash solution of 6.7% (v/v) glacial acetic acid and 30% (v/v) methanol in deionised water. Membranes were imaged on an Odyssey Clx (LI-COR Biotechnology) at 700 nm, then rinsed twice more in water before proceeding downstream as usual. Membranes were then blocked, incubated with primary (Myostatin and pan Actin [to corroborate the sensitivity of the total protein stain, by visual comparison to a single reference protein]) and secondary antibodies and visualised using chemiluminescence and X-ray film. Relative expression of myostatin was determined by dividing the signal intensity of the target bands by the signal intensity of the total protein stain (25-150 kDa). A representative blot of actin abundance is also presented for reference.

3.2.2 Study 2

A separate analysis, using blood samples obtained from a separate cohort of participants, was undertaken to investigate potential correlates of circulating myostatin abundance in both males and females. Blood samples for the analysis of serum myostatin were obtained from 19 participants undergoing skeletal muscle biopsies from which myogenic cultures were established for *in vitro* studies within this thesis (Chapters 4, 5 and 6). In doing so, correlations could be made between serum myostatin abundance and various anthropometric and descriptive characteristics, including habitual physical activity (IPAQ), in donors of varying age and body composition.

Measurement of Serum Myostatin

In Study Two, venous blood samples were obtained from the antecubital fossa, in the rested, fasted state. Serum myostatin was measured using the R&D Systems GDF8 ELISA as described previously in Chapter 2 (2.1.10). All samples were thawed only once and assayed on the same plate to minimise variability. Samples were measured in duplicate and the mean coefficient of variation (%CV) for technical replicates was (Mean ± SD) 2.7 ± 1.8%.

Statistical Analysis

All statistical analyses were performed in GraphPad Prism 9. Descriptive data are presented as Mean ± SD (to provide a description of data distribution from the mean within the study participants), while experimental data are presented as Mean ± SEM (to provide a measure of the uncertainty in the estimate of the mean of the experimental outcome within the study population), with individual participant values represented by shapes in the presented figures, where relevant. Shapiro-Wilk tests were used to evaluate normality of data, since this test better retains power with small samples sizes (Razali & Wah, 2011). For normally distributed data, parametric tests were applied (ANOVA), while non-parametric tests (Kruskal-Wallis) we used for that which violated assumptions of normality (IL-1β mRNA expression). Differences between participant phenotype groupings (Young Normal Weight vs Older Normal Weight vs Older Overweight/Obese) were assessed using independent samples t-tests. Two-way ANOVA with repeated measures were used to assess the independent and interaction effects of group and hyperinsulinaemia on myostatin gene and protein expression. For all other analyses of gene expression, only samples obtained in the basal state were measured. Thus, one-way ANOVA/Kruskal-Wallis tests were used to assess the effect of group on gene expression. Post-hoc comparisons were performed using Tukey tests for parametric data, and Dunn's tests for non-parametric data. ANOVA results with $P < 0.10$ ANOVA are accompanied by their corresponding partial eta squared (n_p^2) values as a measure of effect size. Significant post-hoc comparisons are presented as mean difference [95% CI], where relevant.

Correlations were performed using Pearson's product moment correlations (r) and are accompanied by their corresponding P values. Broadly, r coefficients of ≤0.35 are considered weak, while 0.36 to 0.67 is considered moderate, and ≥0.68 is considered a strong correlation, however these must be interpreted in the context of both their biological and statistical significance (Schober, Boer, & Schwarte, 2018; Richard Taylor, 1990). Statistical test results are reported in boxes on each

figure, where relevant. Statistical significance was defined as $P < 0.05$. Post-hoc comparisons are indicated on each figure by lines connecting each comparator.

3.3 Results: Study 1

The three groups of participants were characteristically distinct (Table 3.1). The young normal weight (YNW) group had normal BMI and cardiopulmonary fitness that is within the normal range for their age (median for healthy 20 yrs males from prior studies: 48 $mL \cdot min^{-1} \cdot kg^{-1}$ (van der Steeg & Takken, 2021)) and were not insulin resistant, as indicated by the rate of glucose disposal during hyperinsulinaemic-euglycaemia (proposed cut off for insulin resistance during hyperinsulinaemic euglycaemic clamp [80 $mU \cdot kg^{-1}$ $FFM \cdot min^{-1}$]: 29.4 $\mu mol \cdot kg^{-1}$ $FFM \cdot min^{-1}$ (Tam et al., 2012)). Glucose disposal rates of this magnitude are consistent with prior studies of healthy young males under similar hyperinsulinaemic euglycaemia (Chokkalingam et al., 2007; F. B. Stephens et al., 2014). Participants in both the older normal weight (ONW) and older overweight/obese (OOO) groups were matched for age and were on average almost 50 years more senior than those in the young group. The OOO group had significantly higher body mass, BMI, total and trunk fat mass, body fat percentage and lower cardiopulmonary fitness than ONW. The YNW and ONW group did not significantly differ in their body mass, BMI or indices of adiposity, however ONW had significantly less (~15%) fat-free mass than YNW. Glucose disposal was not significantly different between YNW and ONW but was significantly lower in OOO than both ONW and YNW. Both advancing age and obesity were associated with significantly lower cardiopulmonary fitness, with OOO having significantly lower VO_{2max} than ONW.

Table 3.1. Grouped characteristic data of participants from whom skeletal muscle biopsies were obtained

	Group Mean (±SD)			One-way ANOVA
	Young Normal Weight	**Older Normal Weight**	**Older Overweight/ Obese**	***P***
n	6	6	8	
Age (yrs)	22.4 (±3.7)	70.6(±1.2)†	69.4 (±1.2)†	**<0.001**
Body Mass (kg)	77.8 (±15.0)	67.6 (±8.0)	84.9 (±6.4)‡	**0.015**
BMI ($kg \cdot m^{-2}$)	23.8 (±3.8)	23.1 (±2.4)	29.2 (±2.2)†‡	**0.002**
Total Fat Mass (kg)	13.36 (±7.98)	13.09 (±5.29)	26.53 (±3.27)†‡	**<0.001**
Trunk Fat Mass (kg)	6.10 (±3.95)	6.65 (±3.84)	16.39 (±2.32)†‡	**<0.001**
Total Fat-Free Mass (kg)	58.92 (±8.26)	50.29 (±3.79)†	53.11 (±4.52)	**0.050**
Body Fat Percentage (%)	16.3 (±7.2)	18.9 (±6.4)	31.2 (±2.5)†‡	**<0.001**
Bone Mineral Content (kg)	2.79 (±0.43)	2.43 (±0.23)	2.76 (±0.40)	0.193
Systolic Blood Pressure (mmHg)	133 (±12)	139 (±19)	145 (±15)	0.380
Diastolic Blood Pressure (mmHg)	67 (±5)	79 (±5)†	84 (±11)†	**0.006**
VO_2max ($mL \cdot min^{-1} \cdot kg^{-1}$)	44.5 (±6.1) (n=5)	31.8 (±3.1)† (n=5)	24.3 (±3.0)†‡ (n=3)	**<0.001**
Glucose Disposal Rate ($\mu mol \cdot kg^{-1}$ FFM$\cdot min^{-1}$)	74.2 (±16.0) (n=5)	57.2 (±6.5) (n=5)	41.9 (±12.9)†‡ (n=7)	**0.003**

Differences between group means for each descriptive parameter were assessed using ordinary one-way ANOVA with post-hoc unpaired t-tests: †Indicates significant difference from Young Normal Weight. ‡Indicates significant difference between Older Normal Weight and Older Overweight/Obese.

3.3.1 Ageing with obesity, but not ageing *per se*, is associated with increased skeletal muscle myostatin mRNA expression

Two-way ANOVA revealed a significant effect of group (P = 0.024; η_p^2 = 0.357) but not insulin on myostatin mRNA expression, and no interaction between the two. Post-hoc comparisons revealed OOO had 2-fold greater basal (Mean Difference [95% CI]: 1.32 [0.02, 2.63], $P < 0.05$) and 2.3-fold greater insulin-stimulated (Mean Difference [95% CI]: 1.59 [0.28, 2.89], $P < 0.05$) myostatin mRNA expression than ONW (Figure 3.1A). Neither basal nor insulin-stimulated myostatin mRNA expression was significantly different between YNW and ONW. Across all participants, basal myostatin mRNA expression tended to weakly correlate with BMI (r = 0.382, P = 0.097) (Figure 3.1B), but not any other anthropometric measure, nor was it associated with cardiopulmonary fitness or glucose disposal rate. The relative protein abundance of mature myostatin (~26 kDa immunoreactive band) was not affected by group or hyperinsulinaemia (Figure 3.1C). One-way ANOVA reported no effect of group on the mRNA expression of the myostatin receptor, ACVR2B (Figure 3.2A). However, Pearson's correlation revealed a moderate significant association between ACVR2B expression and trunk fat mass (r = 0.477, P = 0.033), when all participants were considered (Figure 3.2B). There was no effect of group on the mRNA expression of the myostatin binding protein, FSTL3 (Figure 3.2C) and its expression did not correlate with any other measure (data not shown).

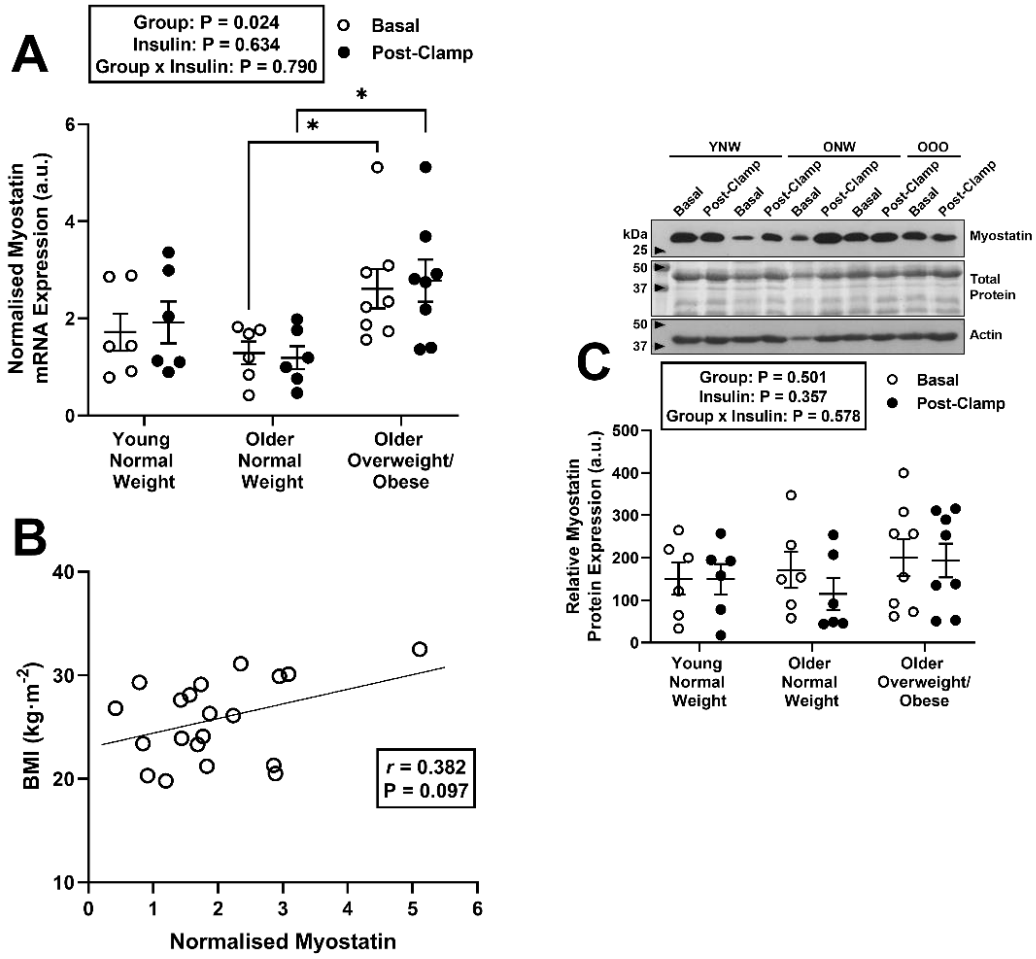

Figure 3.1. Effects of obesity and ageing on the mRNA and protein expression of myostatin in skeletal muscle.

Expression of myostatin mRNA and protein was measured via qPCR and western blot, respectively, in vastus lateralis muscle samples from Young Normal Weight (YNW; n = 6), Older Normal Weight (ONW; n = 6) and Older Overweight/Obese (OOO; n = 8) participants at baseline (Basal) and following a hyperinsulinaemic-euglycaemic clamp (Post-Clamp) (**A**). Correlation between basal myostatin mRNA expression and BMI (**B**). Protein expression of mature myostatin (~26 kDa immunoreactive band) was not different between groups and was unaffected by hyperinsulinaemia (**C**). Group data are presented as Mean ± SEM, with individual participant data plotted as open (basal) and closed (post-clamp) circles. Relative gene expression is normalised against the geometric mean of HMBS and RPLP0 (a.u.). Relative protein expression is normalised against the geometric mean of Actin intensity and the intensity of Revert total protein stain (from 150 – 25 kDa). Significant difference between groups: $*P < 0.05$.

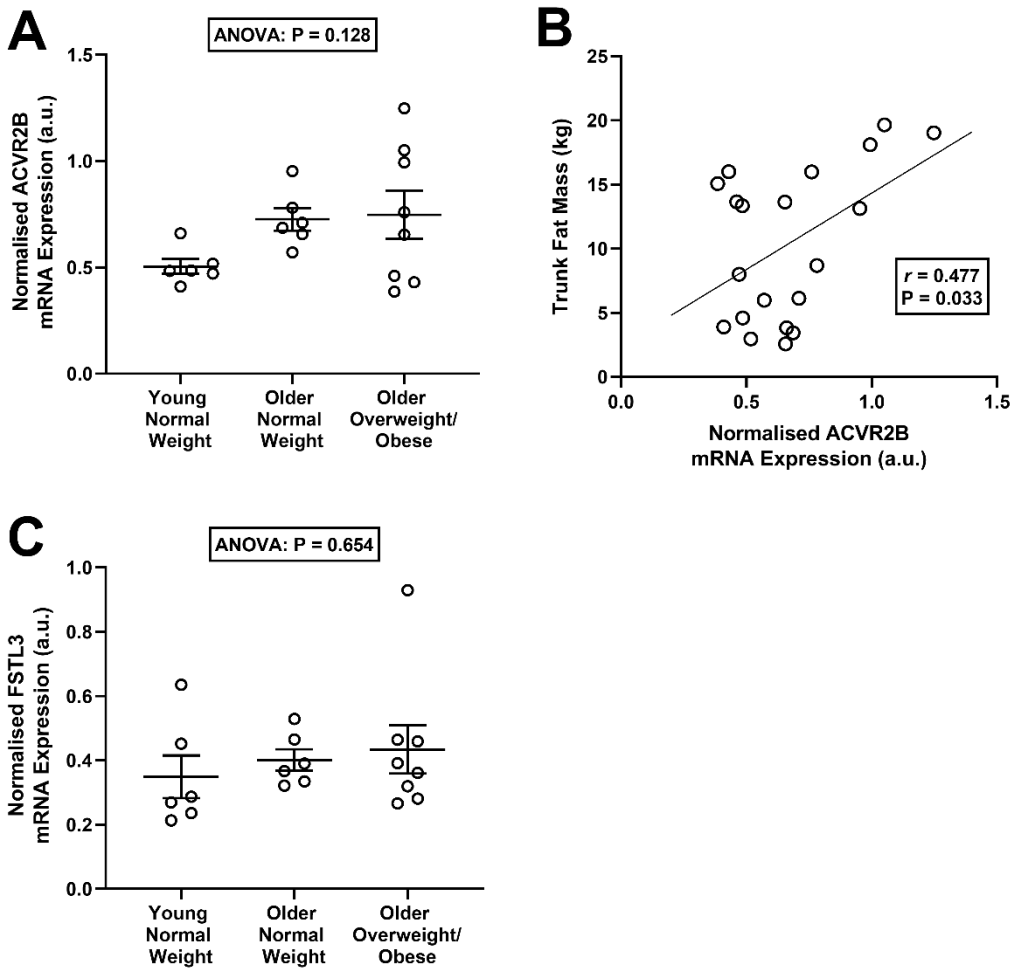

Figure 3.2. Effects of obesity and ageing on the mRNA expression of the Activin Receptor Type 2B and Follistatin-like 3 in skeletal muscle.

Expression of the myostatin receptor, Activin receptor type 2B (ACVR2B), and the myostatin binding protein, Follistatin-like 3 (FSTL3), was measured via qPCR in vastus lateralis muscle samples from Young Normal Weight (YNW; n = 6), Older Normal Weight (ONW; n = 6) and Older Overweight/Obese (OOO; n = 8) participants at baseline (**A**). Correlation between ACVR2B mRNA expression andh trunk fat mass (**B**). There was no effect of group on FSTL3 mRNA expression (**C**). Group data are presented as Mean ± SEM, with individual participant data plotted as open circles. Relative gene expression is normalised against the geometric mean of HMBS and RPLP0 (a.u.).

3.3.2 Ageing with obesity is associated with altered expression of myogenic and atrophic, but not inflammatory genes

One-way ANOVA revealed a significant effect of group on the mRNA expression of the myogenic regulatory factor MYOD (P = 0.048; η_p^2 = 0.303), with OOO demonstrating 2.3-fold greater expression than YNW (Mean Difference [95% CI]: 0.48 [0.01, 0.95] a.u.; $P < 0.05$) (Figure 3.3A). Pearson's correlation revealed significant moderate associations between the mRNA expression of MYOD and that of myostatin (r = 0.643, P = 0.003), as well as BMI and body fat percentage (r = 0.495, P = 0.027 and r = 0.451, P = 0.046, respectively; data not shown). Conversely, expression of MYOG was not significantly affected by group (Figure 3.3B) and did not correlate with myostatin expression or anthropometric measures.

Of the muscle-specific E3 ubiquitin ligases, MAFbx was reported by ANOVA to be significantly affected by group (P = 0.048; η_p^2 = 0.313), with post-hoc testing revealing 1.7-fold greater expression in OOO than YNW (Mean Difference [95% CI]: 3.48 [0.03, 6.92] a.u.; $P < 0.05$) and a tendency towards 1.6-fold greater expression in ONW than YNW (Mean Difference [95% CI]: 3.23 [0.45, 6.91] a.u.; P = 0.091) (Figure 3.3C). There was no effect of group on the expression of MuRF1 (Figure 3.3D). Neither MuRF1 nor MAFbx were significantly associated with myostatin expression nor any anthropometric measure, when all participants were considered.

Kruskal-Wallis test revealed no effect of group on the expression of IL-6 (Figure 3.4A), while one-way ANOVA revealed no significant effect of group on IL-1β (Figure 3.4B), or TNF (Figure 3.4C). Concordantly, their expression did not correlate with any other characteristic or gene expression.

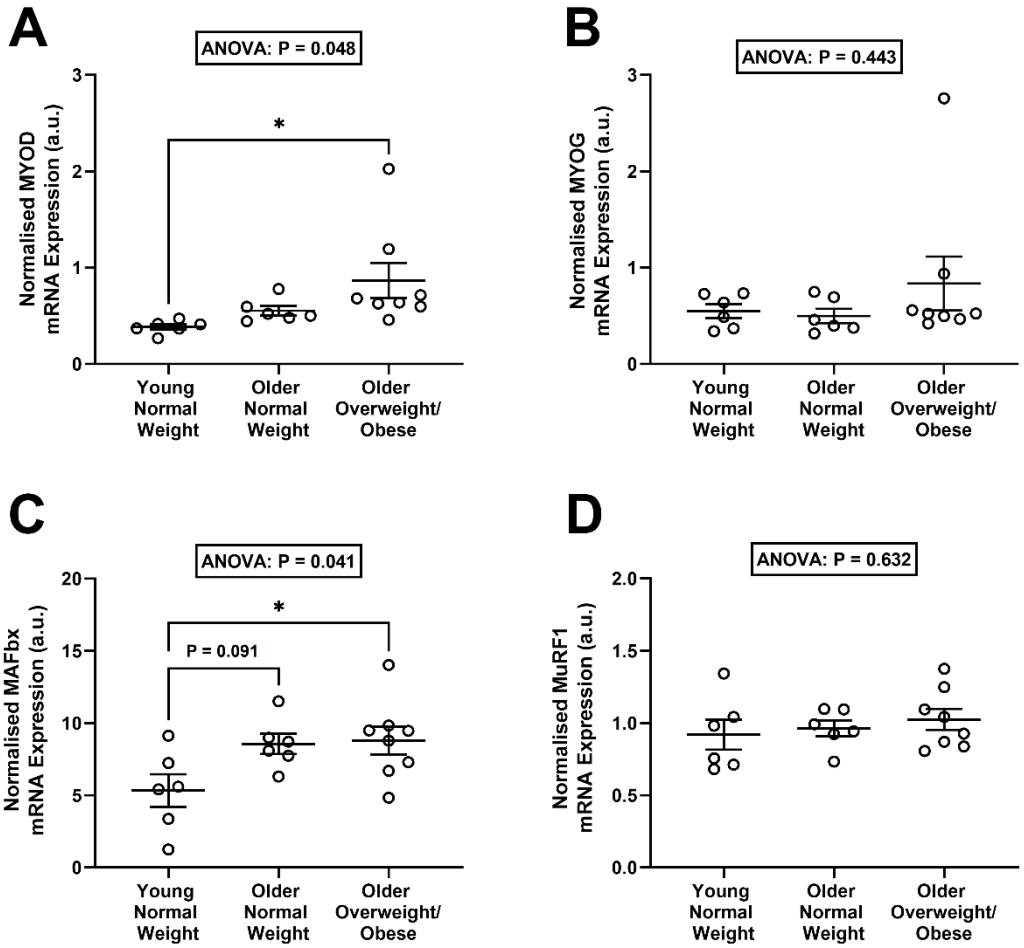

Figure 3.3. Effects of obesity and ageing on the mRNA expression of myogenic markers and E3 ligases in skeletal muscle.

Expression of the myogenic regulatory factors, MYOD (**A**) and MYOG (**B**) and the E3 ligases, MAFbx (**C**) and MuRF1 (**D**) were measured via qPCR in vastus lateralis muscle samples from Young Normal Weight (YNW; n = 6), Older Normal Weight (ONW; n = 6) and Older Overweight/Obese (OOO; n = 8) participants at baseline. One-way ANOVA revealed a significant effect of group on MYOD mRNA expression with OOO demonstrating significantly greater expression than YNW (**A**). There was no effect of group on the mRNA expression of MYOG (**B**). A significant effect of group was found on MAFbx expression, with OOO being significantly greater than YNW (**C**). MuRF1 expression was not different between groups (**D**). Group data are presented as Mean ± SEM, with individual participant data plotted as open circles. Relative gene expression is normalised against the geometric mean of HMBS and RPLP0 (a.u.). Significant difference between groups: $*P < 0.05$.

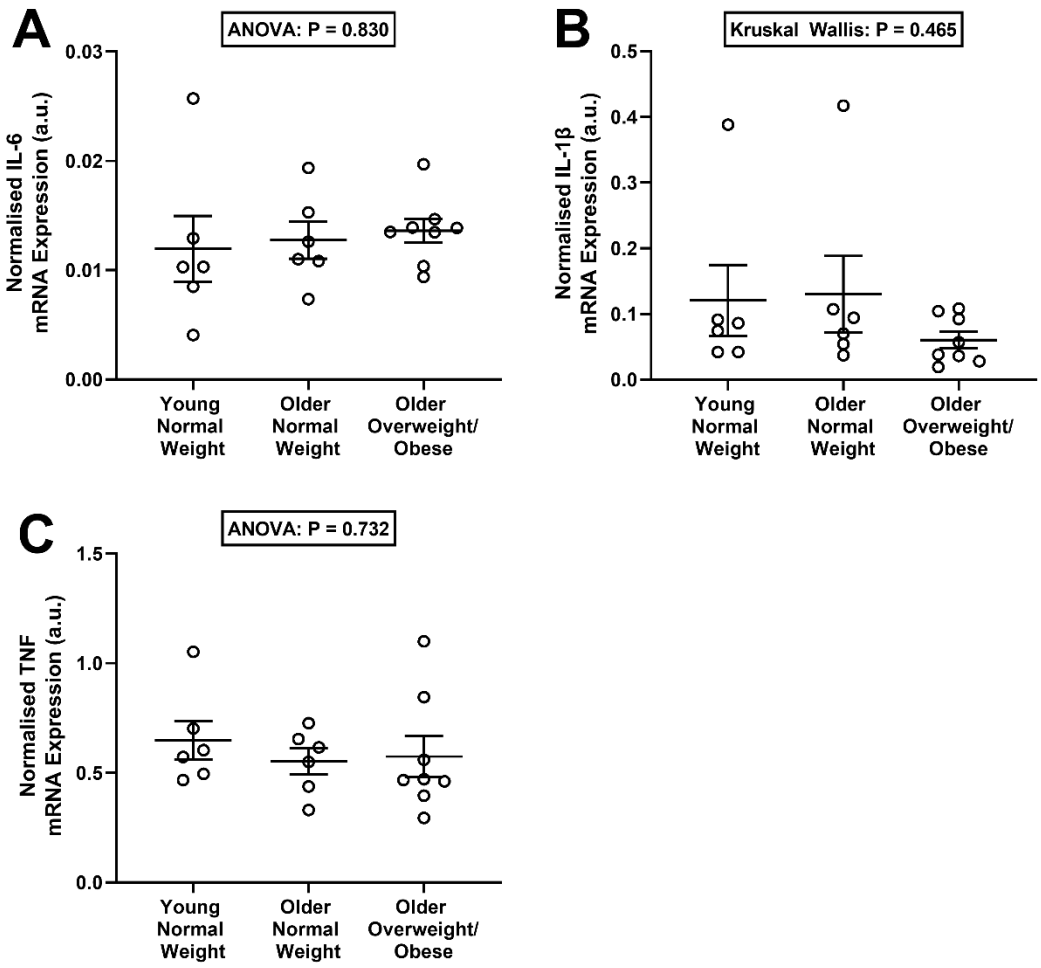

Figure 3.4. Effects of obesity and ageing on the mRNA expression of classical inflammatory genes in skeletal muscle.

Expression of the classical inflammatory markers, IL-6, IL-1β, and TNF, was measured via qPCR in vastus lateralis muscle samples from Young Normal Weight (YNW; n = 6), Older Normal Weight (ONW; n = 6) and Older Overweight/Obese (OOO; n = 8) participants at baseline. One-way ANOVA revealed no significant effect of group on IL-6 (**A**), IL-1β (**B**) or TNF (**C**) mRNA expression. Group data are presented as Mean ± SEM, with individual participant data plotted as open circles. Relative gene expression is normalised against the geometric mean of HMBS and RPLP0 (a.u.).

3.4 Results: Study 2

3.4.1 Obesity, but not ageing or fasting glycaemia, is associated with increased serum myostatin abundance.

Consistent with the association found in Study One between obesity and skeletal muscle myostatin mRNA expression, in a separate cohort of participants (Study Two), a similar pattern of association was revealed via correlation analyses between indices of obesity and the circulating concentration of the mature myostatin protein. Indeed, in serum samples obtained from participants (n = 19) of varying age (Range: 18 – 69 yrs) and BMI (Range: 19.8 - 38.5 $kg \cdot m^{-2}$) (Table 3.2), Pearson's correlations revealed significant moderate correlations between serum myostatin concentration and multiple indices of adiposity (Table 3.2) including BMI, body mass, waist circumference and hip circumference. Conversely, correlations between serum myostatin and age, fasting glucose concentration, and combined total weekly moderate and vigorous physical activity level, were weak and non-significant.

Table 3.2. Characteristic data of participants from whom serum myostatin was measured, and Pearson's correlations between serum myostatin concentration and participant characteristics.

			Pearson's Correlation Coefficient (Serum Myostatin vs Characteristic)	
	Group Mean (±SD)	**Range (Min–Max)**	***r***	***P***
n	19	-	-	-
Sex (M/F)	4/15	-	-	-
Age (yrs)	29.1 (±13.6)	18-69	-0.175	0.475
Body Mass (Kg)	71.3 (±17.5)	52-122	0.468	**0.043**
BMI ($kg \cdot m^{-2}$)	25.9 (±5.7)	19.8-38.5	0.466	**0.045**
Waist Circumference (cm)	83.0 (±14.9)	66.0-126.0	0.465	**0.045**
Hip Circumference (cm)	94.1 (±14.2)	76.5-129.0	0.529	**0.020**
Waist:Hip ratio	0.88 (±0.05)	0.80-0.98	0.022	0.93
Fasting Glucose ($mmol \cdot L^{-1}$)	4.13 (±0.42)	3.45-4.89	-0.242	0.319
Moderate/Vigorous Physical Activity (MET $min \cdot week^{-1}$)	1182 (±956)	0-2960	-0.123	0.626
Serum Myostatin ($ng \cdot mL^{-1}$)	3.85 (±1.30)	2.15-6.60	-	-

3.5 Discussion

The most significant finding of Study One was that of elevated skeletal muscle myostatin mRNA expression in older adults with overweight and obesity (who were insulin resistant), relative to age-matched normal weight older adults. Pertinently, in the absence of excessive adiposity, ageing alone was not associated with a change in myostatin gene expression in human skeletal muscle. The obesity-mediated upregulation of myostatin mRNA was not paralleled by changes in the protein abundance of the 26 kDA mature myostatin ligand. The mRNA expression of both the myogenic regulatory factor, MYOD, and the muscle-specific E3 ubiquitin ligase, MAFbx, were significantly increased in the old overweight/obese group relative to their younger normal weight counterparts, but were not significantly greater than in the older normal weight group. The observed association between myostatin expression and obesity *per se* in Study One was supported by the findings of Study Two, in which positive correlations between serum myostatin and multiple indices of adiposity, but not age, fasting glucose, or habitual physical activity level were found in a separate cohort of participants.

The finding of upregulated muscle myostatin expression in the presence of obesity is consistent with previous reports (Hittel et al., 2009; J.-J. Park et al., 2006) and the moderate correlation between myostatin expression with BMI is in line with the relationship reported by Ryan and Li (2021). Importantly, the addition of the young normal weight group in the present study enabled us to expand upon previous findings by confirming that this myostatin upregulation is unique to the aged overweight/obese population and is not influenced by ageing alone, when participants are matched for adiposity. It must be considered, however, that owing to the absence of a young group with obesity, it cannot be determined from this study whether obesity in the absence of ageing is also associated with an upregulation of myostatin mRNA expression. Conversely, in an earlier cross-sectional study, both myostatin and MAFbx mRNA expression in skeletal muscle were found to be significantly lower in elderly versus younger adults (72 ± 5 vs 32 ± 7 yrs, respectively) who were matched for BMI (26.4 ± 1.9 vs 26.4 ± 3.5 $kg \cdot m^{-2}$), although this alone is a rather crude index of adiposity, which the authors proposed to reflect a protective mechanism to preserve skeletal muscle mass with advancing age (Dennis et al., 2008).

The mechanism by which myostatin is upregulated in obesity, at the level of transcription, has not yet been fully established. However, myostatin transcription is known to be activated by numerous means (Carla Vermeulen Carvalho Grade et al., 2019), including changes in its promoter activity (Salerno et al., 2004),

transcription factors (C. V. C. Grade et al., 2017), epigenetic regulators, post-transcriptional controllers (D. L. Allen & Loh, 2011) and auto-regulatory feedback (Craig McFarlane et al., 2014). Perhaps most relevant to the present study, is the relationship between MYOD and myostatin. Canonical myostatin signalling activates SMAD2/3 which represses MRFs, including MYOD which activates genes involved in cell cycle progression, leading to myoblast proliferation but also early differentiation (Asfour, Allouh, & Said, 2018; M.-M. Chen, Zhao, Zhao, Deng, & Yu, 2021; Langley et al., 2002; R. Ríos, Carneiro, Arce, & Devesa, 2002; Thomas et al., 2000). However, MYOD itself is also able to upregulate myostatin transcription during myogenesis and is thus implicated in directing satellite cell function towards regenerating skeletal muscle (D. L. Allen & Unterman, 2007).

The myostatin promoter region has several potential binding sites for muscle-specific transcription, including enhancer-box (E-box) motifs, which are known to be recognised and bound by MRFs (Hu et al., 2013) (Grade et al., 2019; Zammit, 2017). MYOD binds to these E-box motifs, preferentially upregulating myostatin promoter activity and thus expression (Spiller et al., 2002). In the present study, the OOO group exhibited 2.3-fold greater MYOD expression than YNW, and MYOD demonstrated a positive correlation with the expression of myostatin. The capacity for MYOD to upregulate myostatin provides a potential mechanistic link between the observed concurrent upregulation in the OOO group, whereby the initial upregulation of MYOD in ageing with obesity may precede and promote the upregulation of myostatin. This finding, however, is at odds with reports of diminished MYOD in younger-to-middle-aged adults with obesity (Watts, McAinch, Dixon, O'Brien, & Cameron-Smith, 2013), which might suggest the perturbed regulation of MYOD is a feature only seen in advanced age, where age-related muscle loss is more likely to be present.

Conversely, MYOG, which functions as an antiproliferative factor that promotes withdrawal from the cell cycle and induces myoblast differentiation (Asfour et al., 2018; K. Singh & Dilworth, 2013; Zammit, 2017), was not significantly different between the three groups and did not correlate with any other measure. In a similar comparison between normal weight, young and elderly women (23 ± 2 vs 85 ± 1 yrs), where myostatin mRNA expression was 56% greater in the older group, the expression of the MRFs; MYF5, MYOD, MYOG and MRF4 were all comparably upregulated with ageing (Raue et al., 2006). In a study of age-matched lean (BMI: <25 $kg \cdot m^{-2}$) and morbidly obese (BMI: >40 $kg \cdot m^{-2}$) middle-aged individuals, despite an absence of difference in myostatin protein abundance, the mRNA expression of both MYOD and MYOG were ~50% lower in individuals

with obesity, which was likely attributable to increased phosphorylation of both SMAD2 and SMAD3 (Watts et al., 2013).

Together, these findings suggest that the stability, or even repression, of myostatin expression in skeletal muscle is a feature of healthy ageing that is perturbed in the presence of obesity. In the setting of advanced age and obesity, MYOD appears upregulated independent of the suppressive effects of canonical myostatin signalling, such that MYOD subsequently upregulated myostatin by targeting its promoter region. Conversely, in the absence of advanced age, the effects of obesity on the expression of MYOD and other MRFs is less clear, but it appears that the suppressive function of myostatin on MYOD may be maintained. The extent to which upregulated myostatin contributes to the perturbed myogenesis seen in obesity remains to be elucidated, and such findings warrant further investigation (Akhmedov & Berdeaux, 2013).

In contrast to the mRNA expression of myostatin, the skeletal muscle protein abundance of mature myostatin (~26 kDa immunoreactive protein) was found to be similar in all three donor groups and did not correlate with any indices of obesity or insulin sensitivity. The discrepancy between the difference between groups in the mRNA but not protein expression of myostatin is perhaps not surprising. It is not unusual for changes in the expression of a gene at the transcriptional level to not result in changes at the translational level in that encoded protein and indeed genome-wide correlation between mRNA and protein levels are notoriously poor (Koussounadis, Langdon, Um, Harrison, & Smith, 2015). These discrepancies are most commonly attributed to myriad post-transcriptional regulations such as 5'-end capping, RNA splicing and polyadenylation, which can all influence the fate of mRNAs (Corbett, 2018). Additionally, as discussed elsewhere in this thesis, only the ~26 kDa immunoreactive protein was measured in these studies, which reflects the biologically active mature myostatin homodimer. Thus, the measured form of myostatin protein reflects not the entirety of the pool of translated myostatin gene product, but only that which has undergone multiple steps of cleavage and processing. It remains to be established whether upregulation of myostatin mRNA may be better reflected at the protein level by changes in the total amount of myostatin protein, comprising all forms and fragments.

There is a paucity of cross-sectional studies assessing myostatin protein content to compare these findings to. In contrast to this study, Hittel et al. (2009) found myostatin protein content (26 kDa) to be elevated ~20% in obese middle-aged men relative to age-matched normal weight controls and was correlated with BMI. Unlike in this study, however, participants were extremely obese (48.9 ± 4.9

kg·m^{-2}) and middle-aged and thus not directly comparable to the OOO cohort in the present study. Roh, Hong, Chung, and Lee (2019) reported 2.6-fold greater abundance of skeletal muscle myostatin protein (43 kDa precursor form, which was not reliably detected with our antibody in the samples used in the present study) in sarcopenic older adults than age-matched non-sarcopenic controls (63.4 ± 8.1 vs 62.1 ± 7.9 yrs, respectively), however the absence of a young control group restricts comparisons with this study. McKay et al. (2012) reported that healthy older males (70 ± 4 yrs) exhibited 2-fold greater skeletal muscle myostatin protein abundance (~26 kDa) than younger males (21 ± 3 yrs), however both groups were, on average, overweight (mean BMI derived from available data: Young: 28.4 vs Old: 28.0 kg·m^{-2}), and thus cannot be entirely compared with the YNW group. These studies suggest that in the context of ageing, myostatin protein expression may be upregulated in the presence of extreme obesity or sarcopenia (plausibly reflecting the severity of metabolic dysregulation within the skeletal muscle) but not the more modest degree of obesity reported in the present study.

MuRF1 and MAFbx are muscle-specific E3 ubiquitin ligases that mediate muscle protein breakdown through the polyubiquitination of proteins, which targets them for proteolysis by the 26S proteasome, ultimately leading to muscle atrophy if not in balance with muscle protein synthesis (Gomes, Lecker, Jagoe, Navon, & Goldberg, 2001; Gumucio & Mendias, 2013; D. Liu et al., 2019). Ex-vivo incubation of rat skeletal muscle with full-length myostatin protein increases muscle proteolysis mediated by MuRF1 and MAFbx, which suggests that myostatin can increase skeletal muscle protein degradation (Manfredi, Paula-Gomes, Zanon, & Kettelhut, 2017). Research into the involvement of the ubiquitin-proteasome system in age-related muscle wasting is conflicting (Cai, Lee, Li, Tang, & Chan, 2004; Edström, Altun, Hägglund, & Ulfhake, 2006; Raue, Slivka, Jemiolo, Hollon, & Trappe, 2007; Rom & Reznick, 2016; Whitman, Wacker, Richmond, & Godard, 2005). In the present study, MAFbx but not MuRF1 mRNA expression was increased by ageing with obesity and tended to be similarly elevated in the presence of ageing alone, but did not correlate with indices of obesity. Mechanistically, there is an uncoupling of IGF/Akt signalling and perturbed Akt phosphorylation in older skeletal muscle, which might be indicative of perturbed downstream function of muscle protein-regulating pathways, since suppression of Akt phosphorylation activates the forkhead family of transcription factors (FKHR) which increase the transcription of MuRF1 and MAFbx (J. S. Greiwe, Cheng, Rubin, Yarasheski, & Semenkovich, 2001; Haddad & Adams, 2006).

In contrast to these findings, a study of young and older (20 ± 0.2 vs 70 ± 0.3 yrs) adults revealed that despite elevated myostatin mRNA and protein expression in older individuals, FKHR gene expression was suppressed, while the FKHR target genes MAFbx and MuRF1, were not different between groups (Léger et al., 2008). Extrapolation and comparison of Leger et al.'s findings to those of the present study is limited by the absence of participant phenotyping beyond age and body mass. It cannot be speculated, therefore, what other factors might provide possible explanations for differing results. With regards to the effects of obesity, it has been demonstrated that severely obese donor-derived myotubes innately differ in how they handle protein degradation. Indeed, under atrophic conditions, obese myotubes undergo a shift toward ubiquitin-proteasome system-mediated protein degradation, with higher specific activity of proteasomes, despite comparable mRNA expression of MuRF1 and MAFbx (Bollinger, Powell, Houmard, Witczak, & Brault, 2015). This alternative regulation of protein degradation may partially explain phenotypic differences and conflicting observations in obese, ageing muscle under catabolic stressors such as inactivity and systemic inflammation. Taken together, the findings of simultaneous significant upregulation of myostatin, MYOD and MAFbx in older obese muscle appears indicative of perturbed regulation of processes involved in both the breakdown and regeneration of skeletal muscle, while the regulatory profile of muscle in non-obese older donors more closely resembles that of healthy young muscle, but still tended to exhibit elevated MAFbx expression which may be indicative of elevated muscle protein degradation.

The mRNA expression of ACVR2B, the transmembrane receptor to which the mature myostatin ligand binds to commence signal transduction, was not significantly different between YNW, ONW and OOO. Similarly, Dalbo et al. (2011) found no difference in the mRNA expression of myostatin or ACVR2B, between young (21 ± 0.5 yrs) and older (66.4 ± 1.6 yrs) healthy males. This corroborates findings in a murine model of obesity, where leptin-deficient ob/ob mice demonstrated 2-fold greater muscle myostatin mRNA expression than wild type mice, but no difference in ACVR2B expression was found (D. L. Allen et al., 2008). Together, these data suggest that the upregulation of myostatin skeletal muscle mRNA expression and serum abundance in older adults with obesity, is not significantly offset by concurrent suppression of its receptor expression, which would perturb signal transduction from the mature myostatin ligand into the myocyte. Interestingly, however, when all participants were considered, ACVR2B expression demonstrated a weak but significant positive correlation with trunk fat

mass, suggesting a degree of adiposity-mediated suppression that is independent of age.

The mRNA expression of Follistatin-like 3 (FSTL3), which plays a potent antagonistic role in regulating myostatin's function by forming protein complexes with circulating myostatin that inhibit receptor activation by preventing the phosphorylation of Smad3 (Amthor et al., 2004; Cash et al., 2012; Hill et al., 2002), was not different between YNW, ONW and OOO. This contrasts the prior findings of Dalbo et al. (2011) who reported muscle FSTL3 mRNA expression, but not myostatin, to be >2-fold higher in older, heavier males (66.4 ± 1.6 yrs, 94.2 ± 3.7 kg) than younger males (21.0 ± 0.5 yrs, 82.3 ± 4.2 kg). The authors proposed that the upregulation of FSTL3 could be a protective mechanism in an attempt to preserve normal protein synthesis/catabolism rates with ageing, through the inhibition of myostatin. Similarly, McKay et al. (2012) found 1.5-fold greater FSTL3 mRNA expression in the skeletal muscle of healthy older males (70 ± 4 yrs) compared to younger males (21 ± 3 yrs), which was accompanied by upregulated myostatin mRNA. It is unclear what factors may be responsible for the absence of upregulated FSTL3 in the present study, however such observations and the relative importance of FSTL3 expression and circulating abundance in ageing and obesity warrants further investigation.

Neither the mRNA nor protein expression of myostatin correlated with glucose disposal rate during hyperinsulinaemic euglycaemia. In contrast, Hjorth et al. (2016) found a significant negative correlation between glucose infusion rate during hyperinsulinaemic-euglycaemic clamp and muscle mRNA expression, but not plasma concentration, of myostatin in sedentary, middle-aged (40-65 yrs) men with normoglycaemia or dysglycaemia. This discrepancy may reflect the fact that Hjorth and colleagues expressed glucose disposal per kg of whole-body mass, whereas in this study it is reported per kg of fat-free mass. In the absence of accounting for fat versus fat-free mass (indeed, the dysglycaemic group in the Hjorth study had 12.5 kg more fat mass on average, while only 4.5 kg greater fat-free mass), glucose disposal rate becomes a less specific measure of skeletal muscle insulin sensitivity (since it instead reflects the mass of the whole body). Therefore, glucose disposal per kg whole-body mass will be negatively skewed in the dysglycaemic group, on account of their greater overall body mass.

Nevertheless, in another study, Ryan, Li, Blumenthal, and Ortmeyer (2013) also found that basal myostatin mRNA expression was negatively associated with glucose disposal adjusted for fat-free mass during a similar clamp in sedentary, middle aged adults with obesity (61 ± 1 yrs, BMI: 31 ± 1 $kg \cdot m^{-2}$) who were

phenotypically similar to the OOO group in the present study, but had on average 9 kg more fat mass than OOO. Together, these findings suggest that a correlation between myostatin expression and glucose disposal may only be present in older adults with a greater degree of obesity than was present in OOO in this study. It must be recalled however, that while associative, neither causality nor the absence of causality can be determined from such correlation analyses. Thus, further research is essential in order to better understand the concurrent perturbation of myostatin expression and insulin sensitivity demonstrated here exclusively in older adults with obesity.

Our group has previously demonstrated that acute hyperinsulinaemia with euglycaemia invokes myriad transcriptional changes in skeletal muscle tissue (Kostas Tsintzas et al., 2013). The aforementioned study of Ryan et al. (2013) reported a statistical trend (P = 0.10) for a diverging effect of acute hyperinsulinaemia on myostatin mRNA expression before and after a 6 month aerobic exercise and weight loss intervention in sedentary, middle aged, obese adults, which improved mean glucose disposal by 18% and decreased myostatin expression by 19%. Prior to the intervention, hyperinsulinaemia tended to decrease myostatin expression, while post-intervention hyperinsulinaemia tended to increase its expression. While basal myostatin expression was negatively correlated with glucose disposal, the effect of hyperinsulinaemia on myostatin expression displayed a moderate positive correlation with the change in glucose disposal induced by the intervention. Thus, individuals who demonstrated the greatest improvement in insulin sensitivity in response to the intervention also exhibited the greatest hyperinsulinaemia-induced increase in myostatin expression, which the authors proposed was a novel link between changes in insulin sensitivity and myostatin expression. Thus, as an exploratory measure to expand upon the findings of Ryan et al., myostatin mRNA and protein expression following 3 h of hyperinsulinaemic euglycaemia was also assessed in the present study.

Neither the mRNA nor protein expression of myostatin was found to be altered by hyperinsulinaemia in any of the three groups. It should be recalled that unlike the present study, Ryan et al did observe a negative correlation between glucose disposal and basal myostatin expression and their study comprised both older males and females, the latter of whom demonstrate blunted repression of myostatin expression in response to exercise training (J. S. Kim, Cross, & Bamman, 2005). Nevertheless, in both the present study and that of Ryan and

colleagues, myostatin mRNA expression was not significantly altered by hyperinsulinaemia in the absence of exercise training.

Circulating levels of inflammatory cytokines are elevated with sarcopenia, obesity, and sarcopenic obesity (Cesari et al., 2005; J. S. Greiwe et al., 2001; Maachi et al., 2004; Reyna et al., 2008; Schrager et al., 2007), largely arising from the infiltration and accumulation of M1-like macrophages, from which inflammatory cytokines are abundantly secreted, into adipose tissues (Castoldi, Naffah de Souza, Câmara, & Moraes-Vieira, 2016; Hong et al., 2009; Khan et al., 2015; Koenen et al., 2011; Lumeng, Bodzin, & Saltiel, 2007; Huaizhu Wu & Ballantyne, 2017; H. Wu et al., 2010). Within skeletal muscle, however, the impact of ageing and obesity on inflammatory markers is less clear, with reports of both no difference (Léger et al., 2008; Przybyla et al., 2006; Thalacker-Mercer, Dell'Italia, Cui, Cross, & Bamman, 2010) and significantly increased (Hamada, Vannier, Sacheck, Witsell, & Roubenoff, 2005; Raue et al., 2007; Trenerry, Carey, Ward, Farnfield, & Cameron-Smith, 2008) expression of inflammatory cytokines and transcription factors in older adults. In the present study, the mRNA expression of IL-6, IL-1β and TNF was not different between the three groups. This contrasts the findings of Léger et al. (2008), where elevated myostatin expression in older muscle was accompanied by upregulated TNF and its target gene SOCS-3. Given that SOCS-3 is upregulated in sarcopenia (J. S. Greiwe et al., 2001; Haddad & Adams, 2006), it is plausible, that Leger's older cohort presented with significant sarcopenia. However, it must be noted that the ONW group in this study also had significantly lower fat-free mass than YNW (mean difference: 8.63 kg).

It has been proposed that the upregulation of inflammatory gene expression in skeletal muscle is a product of both local adipocyte and macrophage infiltration as well as the 'spill over' of inflammatory mediators from other organs (Peake, Gatta, & Cameron-Smith, 2010). Inflammatory signalling can upregulate myostatin, as demonstrated in principle by treatment of C2C12 myotubes with ammonium acetate, which increased the binding of the nuclear factor kappa B-subunit 65 (NF-κB-p65) to the myostatin promotor, upregulating its transcription (Qiu et al., 2013). This may be important, since NF-κB expression increases with obesity and ageing (Kauppinen, Suuronen, Ojala, Kaarniranta, & Salminen, 2013) and this pathway plays a key role in the induction and maintenance of inflammation (Tornatore, Thotakura, Bennett, Moretti, & Franzoso, 2012). Thus, the absence of differences in the expression of inflammatory cytokines in this study, despite the presence of advanced age and obesity, suggests that the ONW and OOO cohorts likely did not present with significant low-grade inflammation or substantial

muscular infiltration of macrophages. Therefore, in line with its obesity-associated mediation, it is plausible that the upregulation of myostatin in skeletal muscle is instead mediated by adipose-muscle cross talk.

The finding of upregulated myostatin mRNA in skeletal muscle from obese older adults in Study One was corroborated by the findings of Study Two, in which a separate cohort demonstrated correlations between serum myostatin concentration and multiple indices of adiposity, but not ageing, fasting glucose, or combined total weekly moderate and vigorous physical activity level. These findings are concordant with previous reports of 30-40% higher myostatin plasma concentration in extremely obese, insulin-resistant, middle-aged participants, relative to age-matched normal weight counterparts (Amor et al., 2019). Furthermore, these findings mirror those of Kern-Matschilles et al. (2021) who reported positive correlations of serum myostatin with BMI, body fat percentage and waist circumference, but not age, insulin sensitivity, muscle mass, or physical fitness in a study of premenopausal females. Myostatin expression and protein abundance is far greater in skeletal muscle than adipose tissue (D. L. Allen et al., 2008), and it is likely that skeletal muscle is the major source of circulating myostatin. To that effect, primary myotubes generated from extremely obese individuals have been demonstrated to secrete ~3-fold more myostatin than lean donor myotubes, (Hittel et al., 2009), suggesting that associations of increased serum myostatin with obesity, may be driven by increased muscle secretion.

Not all prior studies have reported the same pattern of upregulated circulating myostatin abundance with increasing adiposity (Hofmann et al., 2015; Ratkevicius et al., 2011) and one study even reported that serum myostatin concentration declined with increasing number of the metabolic syndrome components (Han et al., 2014). Schafer et al. (2016) found serum myostatin to peak in males in their 20's and declined over the subsequent decades, while in females it did not change as a function of age. Similarly, Lakshman et al. (2009) found serum myostatin to be higher in younger men (26.5 ± 4.6 yrs) than older men (66.4 ± 4.7 yrs) who were matched for lean mass but not body fat percentage (18.0 ± 6.4 vs 26.6 ± 5.4%, respectively) and observed no difference between young (19–21 yrs) and post-menopausal (67-87 yrs) females. In an older study using a radioimmunoassay technique, Yarasheski et al., (2002) reported that serum myostatin was higher in old healthy adults than younger adults; higher still in old frail individuals and was inversely correlated with fat free mass and muscle mass. Although ranging in age (18-69 yrs) and BMI (19.8-38.5 $kg \cdot m^{-2}$), none of the participants who provided blood samples for this secondary analysis in the present

study were elderly or morbidly obese and were rigorously screened and confirmed to be in good health. This plausibly puts them at odds from other studies of stratified young/old, normal weight/obese groups within the literature, where older participants often present with sarcopenia/sarcopenic obesity or frailty.

3.6 Limitations

This study provides an insightful cross-sectional analysis of changes in myostatin expression and associated factors in ageing and obesity, but several limitations must be considered. Firstly, the number of participants in Study One is smaller than would be ideal. As with all human research undertaken during this period, and as described elsewhere in this thesis, the restrictions imposed by the COVID19 pandemic prevented the active recruitment of participants. Thus, this study was undertaken using existing samples from prior studies and sample size was further restricted by the stringent matching of participants between groups, to better control for potential confounding factors compared to previous studies. Nevertheless, Study One demonstrated sufficient power to detect changes in myostatin expression with obese ageing and demonstrated this to be distinct from normal weight ageing. It is possible that further significant differences would have been teased out from the data if a higher n were possible. Indeed, based on the observed effect size (ES) from ANOVA on ACVR2B expression (ES = 0.60), which tended to be numerically higher in both older groups, post hoc power analysis suggested that a total samples size of n = 48 (i.e., n = 16 per group) would have been sufficient to detect a significant ($P < 0.05$) effect of group. The present data set therefore provides a useful basis for powering future investigations.

The design of the original *in vivo* study from which these samples were derived did not include a young group with obesity, and thus it was not possible to examine whether obesity in the absence of ageing is also associated with an upregulation of myostatin mRNA expression. The addition of such a group could have added valuable insight by further disentangling the effects of obesity *per se* from the confounding effects of ageing (i.e. is myostatin similarly upregulated in young adults with obesity as in older adults with obesity) as well as further insight into associations with insulin resistance. While this is a notable limitation of this study, it was nevertheless possible to identify the absence of change in myostatin expression in older adults in the absence of obesity. One further caveat to this, however, is the argument that in the absence of lifelong habitual physical activity, older adults may not reflect a true state of inherent biological ageing, but rather present with the comorbidity of physical decline (Harridge & Lazarus, 2017).

The three groups were generally well matched; however, it cannot be ignored that while YNW and ONW were matched for body mass, adiposity and BMI, ONW nevertheless had significantly lower fat free mass than YNW. This difference was unavoidable in the cohorts available for analysis, since muscle mass, and subsequent function, almost universally declines with advanced age at a rate of ~1% per year (Wilkinson et al., 2018), except in some cohorts of masters athletes (Harridge & Lazarus, 2017; Pearson et al., 2002; Wroblewski, Amati, Smiley, Goodpaster, & Wright, 2011). The modest loss of fat-free mass in the ONW versus YNW group, is therefore a feature of normal ageing that reflects the population as a whole.

The decision to report the protein content of 'mature' myostatin by quantifying immunoreactive bands of ~26 kDa (which corresponds to the predicted molecular weight of the biologically active mature myostatin ligand and has been reported as such in prior studies (Hittel et al., 2009; Ryan & Li, 2021; Watts et al., 2013)) was a pragmatic one. While some experiments undertaken during the completion of this thesis did demonstrate immunoreactive bands of higher molecular weight in primary myotube lysates (likely reflecting diminished furin cleavage of the precursor protein, which occurs both intra- and extra-cellularly *in vivo* (S. B. Anderson et al., 2008)), in the present study, the predicted ~43 kDa band was not consistently detected. Whether this is an effect of the Trizol extraction process cannot be confirmed. Anecdotally, in muscle samples used to optimise conditions for this antibody, which were extracted using HEPES buffer, bands at ~43, ~26 and ~12 kDa were detected, which correspond to the predicted weights of the myostatin precursor, mature homodimeric, and monomeric ligand, respectively.

In this study, an enzyme-linked immunosorbent assay was used, which is specific for the biologically active, mature circulating myostatin ligand (through a process of acid cleavage of the inhibitory latent complex and other inhibitory binding proteins) (Lakshman et al., 2009). Previous assays have failed to account for the inhibitory binding of myostatin to its latent complex/other circulatory proteins and had issues of cross reactivity with other TGF-β family members such as GDF-11 or GDF-15. The assay here employed overcomes these historical limitations but restricts confidence in the comparisons made to earlier studies. Furthermore, deriving absolute quantitation from this assay requires the assumption that all latent myostatin is fully and consistently cleaved by the acid processing step, which has not yet been verified (Astrid Breitbart et al., 2013). However, the range of concentrations reported in this study is very consistent with other studies using the same commercially available assay and indeed this assay has become a staple

of recent investigations (Dial et al., 2020; Du et al., 2021; Kortas et al., 2020; Kurose et al., 2021)

3.7 Conclusions

In summary, this study provides cross-sectional data that collectively suggest that both myostatin muscle expression and serum abundance is upregulated by obesity with ageing, but not by ageing in the absence of obesity. Indeed, the upregulation of myostatin consistently correlated with indices of adiposity, but not ageing. Upregulated muscle myostatin mRNA was not accompanied by changes in the expression of its receptor, ACVR2B, nor that of the inhibitory myostatin-binding protein, FSTL3, suggesting that the obesity-mediated upregulation is not offset by feedback mechanisms to inhibit its signal transduction. Downstream of myostatin, the expression of both the myogenic regulatory factor, MYOD (which may exacerbate myostatin's upregulation via targeting its promotor region), and the E3 ubiquitin ligase, MAFbx, were increased in older donors with obesity, suggesting a 'tug-of-war' between pathways that promote muscle cell proliferation and differentiation to preserve skeletal muscle regenerative capacity, and those that promote muscle atrophy under the induction of the myostatin signalling cascade. These differences between donor phenotypes occurred without changes in local muscle inflammatory markers, suggesting the possible influence of adipose-muscle cross-talk. The myostatin pathway is therefore uniquely upregulated in ageing with obesity and is associated with abnormal regulation of pathways involved in the maintenance of skeletal muscle mass.

Chapter 4. Effects of Lipid-Induced Insulin Resistance on the Regulation of Myostatin in Primary Human Myotubes

4.1 Introduction

High fat diets (HFD) are a common feature of obesity and may exacerbate the propensity for insulin resistance in the chronic hypercaloric environment (Bray & Popkin, 1998; Golay & Bobbioni, 1997). In western cultures, but increasingly globally, high dietary fat intake is a common feature not just of obesity, but of normal dietary habits (Golay & Bobbioni, 1997). Fat is the most energy dense macronutrient and is also highly palatable, yet only weakly suppresses satiety, which together promotes overconsumption and likely explains why high dietary fat intake is often accompanied by elevated body mass (Blundell, Burley, Cotton, & Lawton, 1993; Blundell & King, 1996). The products of HFD and fat overload; accumulation of ectopic fat and fatty-acid derived metabolites; mitochondrial fat overload; and incomplete lipid oxidation, are all proposed contributors to impaired insulin sensitivity in skeletal muscle (Ciaraldi et al., 1995; Garvey et al., 1998; Koves et al., 2008). Collectively, the sustained presence of a hyperenergetic, high fat diet, in communion with other lifestyle factors such as physical inactivity, and the contribution of genetic predisposition, all promote the development of insulin resistance in skeletal muscle tissue, which is discussed in more detail in Chapter 1 (section 1.31). Pertinently, these deleterious cascades can be recapitulated in the acute setting, both *in vivo* and *in vitro*, through various means of lipid overload, to enable exploration of the mechanisms involved (Mthembu et al., 2021).

Often concurrent with insulin resistance is an impairment of the amino acid stimulation of muscle protein synthesis, termed anabolic resistance (Morais et al., 2018; Morton et al., 2018), with individuals who are insulin resistant often demonstrating blunted amino acid-stimulated muscle protein synthesis (Breen et al., 2013; Murton et al., 2015). Akin to insulin resistance, anabolic resistance can be acutely induced via lipid overload (Smiles, Churchward-Venne, van Loon, Hawley, & Camera, 2019; F. B. Stephens et al., 2015). Interestingly, there appears to be an uncoupling between the short-term diet-induced accumulation of intramuscular lipids and anabolic resistance (Ato et al., 2021; Kostas Tsintzas et al., 2020).

Acute Lipid Overload and Insulin Resistance

Both short- and longer-term high fat diets impair skeletal muscle insulin sensitivity and glucose handling, however short-term dietary lipid overprovision does not always cause overt impairment of insulin-stimulated glucose transport in muscle (A. S. Anderson et al., 2015; Brøns et al., 2009; Cutler et al., 1995; Ehrlicher, Stierwalt, Newsom, & Robinson, 2021). Murine models have demonstrated diminished whole-body glucose tolerance after just 3 days of HFD, while skeletal muscle insulin resistance was present after 3 weeks (Y. S. Lee et al., 2011; N. Turner et al., 2013).

Acute lipid overload, by oral administration or intravenous infusion, provides a tool to study the mechanisms of lipid-induced insulin resistance (Nowotny et al., 2013). Infusion of lipid emulsions before or during hyperinsulinaemic-euglycaemia elevates free fatty acid (FFA) availability; reduces insulin-stimulated oxidative and non-oxidative glucose disposal; inhibits PDC activity; promotes accumulation of lipid intermediates (Griffin et al., 1999; Samar I. Itani et al., 2002; Kruszynska et al., 2002; F. B. Stephens et al., 2014; K. Tsintzas et al., 2007; Yki-Jarvinen, Puhakainen, & Koivisto, 1991). Such effects are consistent with those observed after longer term high-fat diets in human and animal models (Lackey et al., 2016; S.-Y. Park et al., 2005; von Frankenberg et al., 2017). Some (Dresner et al., 1999; Szendroedi et al., 2014), but not all (L. D. Høeg et al., 2011; Storgaard et al., 2004) studies report impaired PI3K activity and IRS-1 phosphorylation.

While diets chronically high in saturated fatty acids are broadly associated with insulin resistance, mono- and poly-unsaturated fatty acid-rich diets are typically associated with partial attenuation of this effect, relative to saturated fat-rich diets, though these effects may be diminished by high total dietary fat intake (Imamura et al., 2016; Riccardi, Giacco, & Rivellese, 2004; Vessby et al., 2001). Concordantly, modulating the fatty acid compositions of lipid boluses in the acute setting imparts divergent effects on insulin sensitivity and glucose handling (Xiao, Giacca, Carpentier, & Lewis, 2006). In healthy young men, but not middle-aged adults with T2D, the aberrant effects of omega-6 polyunsaturated fatty acid (n6-PUFA) infusion on insulin-stimulated glucose disposal was partially attenuated by the addition of n3-PUFA (Mostad et al., 2009; F. B. Stephens et al., 2014).

In Vitro Modelling of Acute Lipid-Induced Insulin Resistance

Akin to the effects seen *in vivo*, *in vitro* incubation of myotubes with saturated fatty acids, particularly palmitate, impairs insulin and anabolic sensitivity, with the accumulation of intramyocellular lipids and fragments considered a driving factor (J. A. Chavez & Summers, 2003; Hirabara, Curi, & Maechler, 2010; Perry et al., 2018). Acute treatment (1-24 h) of primary human myotubes with palmitic acid (125-500 μM) impairs insulin-stimulated glucose uptake, phosphorylation of Akt, AS160 and Glycogen synthase kinase 3 beta (GSK-3β), and increases intramyocellular ceramide content (Abildgaard et al., 2014; Bikman et al., 2010; Kausch et al., 2003; Mäkinen, Nguyen, Skrobuk, & Koistinen, 2017; Montell et al., 2001).

The exclusive application of palmitate does not reflect physiological lipaemia, and concentrations ≥500 μM impart lipotoxic effects (Bryner, Woodworth-Hobbs, Williamson, & Alway, 2012; M. Yang et al., 2013). Within human plasma, palmitic (16:0), linoleic (18:2 n-6) and oleic (18:1 n−9) acid are the most abundant saturated, polyunsaturated, and mono-unsaturated FFAs, respectively (Grimsgaard et al., 1999). Overnight fasting FFA concentration is typically ≤500 μM in healthy adults but can be elevated to ≥800 μM with obesity (Arner & Rydén, 2015; Boden, 2008; Opie & Walfish, 1963). Palmitic acid typically comprises 20-30% of plasma FFA (190-250 μM fasting concentration in obesity/T2D), while linoleic and oleic and acid contribute 15-30% (80-160 μM) and 10-20% (150-250 μM), respectively (Denke & Grundy, 1992; Grapov et al., 2012; Grimsgaard et al., 1999; M. Perreault et al., 2014; Yi et al., 2007).

Consistent with *in vivo* reports, certain species of unsaturated fatty acids, such as oleic acid, appear to be protective against palmitate-induced metabolic dysregulation (Gao, Griffiths, & Bailey, 2009), which may reflect the greater tendency for oleic acid to abound as intracellular FFA, whereas palmitic acid is more readily shuttled away from oxidation and towards incorporation into intramyocellular DAG (Gaster, Rustan, & Beck-Nielsen, 2005). Concordantly, co-incubation of myotubes with oleic and palmitic acid largely preserves the insulin-stimulated phosphorylation of Akt, AS160 and GSK-3β (Hirabara et al., 2010; Salvadó et al., 2013; Yuzefovych, Wilson, & Rachek, 2010); upregulates genes involved in β-oxidation (Coll et al., 2008; Mäkinen et al., 2017); and channels palmitic acid away from DAG/ceramide and towards TAG synthesis (Henique et al., 2010).

Effects of Lipid Overprovision on Myostatin

Obesity and insulin resistance have been consistently associated with upregulated myostatin in skeletal muscle (David L. Allen et al., 2011; Amor et al., 2019; Hittel et al., 2009; Hjorth et al., 2016). The potential involvement of upregulated myostatin in the development of muscle insulin resistance has been demonstrated in C2C12 myoblasts, whereby treatment with recombinant myostatin reduced insulin-stimulated phosphorylation of IRS-1 (Tyrosine^{495}), PI3k, and Akt, which was accompanied by reduced GLUT4 membrane translocation and expression (X.-H. Liu et al., 2018). Indeed, numerous studies have demonstrated that while myostatin administration impairs insulin-stimulated Akt phosphorylation (T. Guo et al., 2009; Hittel et al., 2010), genetic deletion or inhibition of myostatin enhances its stimulated phosphorylation, which may provide a mechanistic link between its roles in both insulin resistance and restricting protein synthesis, since both of these pathways converge on the activation of Akt (L. A. Consitt & Clark, 2018). Supportively, studies have recently demonstrated that myostatin inhibition increases skeletal muscle glucose disposal per unit body mass in HFD-fed mice, which may have been attributable to increased Akt phosphorylation and upregulated GLUT4 expression (Dong et al., 2016; Eilers et al., 2020).

Given the established propensity for upregulated myostatin expression in obesity, it must be considered whether this is mediated by metabolic features of obesity, such as lipid-induced insulin resistance. In C2C12 myotubes, acute palmitate incubation (350-500 μM for 24-30 h) increases myostatin, MAFbx and MuRF1 expression (T. J. Kim et al., 2021; H. Lee, Lim, & Choi, 2017), which may have been mediated by overproduction of reactive oxygen species and subsequent NFκB-mediated upregulation of TNF (D.-T. Wang, Yang, Huang, Zhang, & Lin, 2015). Pertinently, in Lee's study, co-incubation of palmitate with oleate restored normal myostatin expression. Concordant with the upregulation of myostatin, acute palmitate treatment of myotubes blunts protein synthesis, which may reflect impaired translation initiation via increased phosphorylation of eukaryotic initiation factor 2α (eIF2α) (Perry et al., 2018; Tardif et al., 2014).

While insulin sensitivity was not assessed in these studies, data from similar studies suggest that insulin resistance was likely induced (Capel et al., 2015; Rivera & Vaughan, 2021; M. Yang et al., 2013). Following the treatment of C2C12 myotubes with 500 μM palmitate for 24h, Liu et al. (2013) demonstrated both insulin resistance and upregulated myostatin protein content. However, it cannot be known from such studies whether insulin resistance mediated the upregulation of myostatin, or whether it was a by-product of lipotoxicity. Contrariwise,

treatment of proliferating C2C12 myoblasts with 100 μM palmitate for 48 h induced an almost global downregulation of gene expression, including myostatin (Grabiec et al., 2016). It is unclear whether this was an artefact of the significant loss of cell viability that was induced by the longer palmitate treatment, or a differential effect owing to the use of un-differentiated cells.

To date, the effects of the induction of lipid-induced insulin resistance on the expression of myostatin in primary human myotubes has not been investigated. Previous studies have been of limited physiological relevance, featuring non-physiological fatty acid treatments in non-human cells. Given the frequent concurrence of high-fat diets and obesity, and the association between obesity and myostatin upregulation, this warrants investigation.

4.2 Aims

The primary aim of this study was to establish whether the induction of lipid-induced insulin resistance in human skeletal muscle cells is concurrent with altered expression and abundance of myostatin. To that effect, human primary myotubes from well-characterised insulin-sensitive donors, were treated with physiologically relevant concentrations of fatty acids to induce insulin resistance with concurrent assessment of myostatin expression and anabolic sensitivity. Secondary aims were to investigate whether compositional modulation of the fatty acid treatment would influence insulin/anabolic sensitivity and alter any such myostatin response.

4.3 Methods

Participants

Healthy volunteers were recruited and screened as described in Chapter 2 (sections 2.1.1 and 2.1.2). Myogenic cultures from a total of n = 8 donors were used for the experiments detailed below. Participants were all young (age range: 19-29 yrs), normoglycaemic (fasting blood glucose < 5.0 $mmol \cdot L^{-1}$) and were, on average, of normal weight (BMI range: 20.3-26.9 $kg \cdot m^{-2}$) (Table 4.1). Participants were non-sedentary and reported (via IPAQ) spending (Mean ± SD) 204 (± 180) and 79 (± 92) $min \cdot week^{-1}$ performing vigorous- and moderate-intensity physical activity, respectively, as well as 811 (± 790) $min \cdot week^{-1}$ walking.

Culture and Incubation of Primary Myotubes with Fatty Acids

Primary myogenic cultures were established from skeletal muscle biopsy samples obtained via the suction-modified Bergstrom biopsy technique, as described previously (sections 2.1.11 through 2.2.6). Myogenic cells were isolated and cultured under standard conditions. Near-confluent myoblasts were differentiated for 6-8 days until fully formed myotubes were clearly visible, at which point myotubes were treated with either fatty acid/s or Vehicle (fatty acid-free BSA) for 16 h.

Fatty acid treatments comprised either Palmitate alone or the combination of Palmitate, Linoleic acid and Oleic acid (PLO). Fatty acids were conjugated with fatty acid-free BSA as detailed in Chapter 2, to give molar ratios of fatty acid to BSA of 2.7:1 (which is consistent with physiological molar ratios of FFA to albumin in healthy individuals (Oliveira et al., 2015)). Based on previous, unpublished work from our laboratory (R. Jones, 2019), 250 μM palmitate was used for its ability to produce adverse effects on insulin sensitivity/signalling without perturbing myotube morphology. For PLO treatment, Palmitate was combined with Linoleic and Oleic acids at a 5:1:3 molar ratio to produce treatment concentrations of 250 μM, 50 μM and 150 μM, respectively. These concentrations are within the physiological range seen circulating in obesity, however linoleic acid tends to be more abundant, as discussed in Section 4.1.3. This discrepancy reflects a compromise arising from preliminary experiments, whereby greater concentrations of linoleic acid accompanied by 250 μM palmitate caused a degree of visible cell loss and insulin resistance that was not mitigatable by the addition of oleic acid. Conjugated fatty acid solutions or equimolar fatty acid-free BSA (Vehicle) were mixed into standard myotube differentiation medium and sterile filtered immediately prior to application. Treatments were applied to fully differentiated myotubes in either 6-well plates for the measurement of glucose uptake or 12-well plates for the measurement of genes/proteins of interest and myotube diameter.

Radio-Labelled Glucose Uptake

Following 16 h treatments, glucose uptake was measured in the basal and insulin-stimulated state using the radio-labelled technique as described previously (section 2.5.2). Cells were washed once in 1 x PBS prior to commencing the assay. Fatty acid solutions were not added to the serum-free starvation media, nor the reaction buffer to which labelled glucose was added for assaying. Data are presented as the overall mean of independent donor repeats (n = 5-7). For each

independent donor repeat, each experimental treatment was replicated over 4-6 wells.

mRNA Expression

Following fatty acid or Vehicle treatment, cells were harvested using Tri-Reagent, prior to RNA extraction and cDNA synthesis using standard procedures as previously described (sections 2.7.1 through 2.7.5). For the analysis of relative mRNA expression, genes of interest were normalised against β-Actin expression, which NormFinder software revealed to demonstrate high stability within and between experiments and independent donor repeats, under these experimental conditions. Data are presented as the overall mean of independent donor repeats (n = 6-8). For each independent donor repeat, each experimental treatment was replicated over 3-4 wells.

Western Blotting

At the end of relevant treatments, myotubes were harvested in ice-cold RIPA buffer. Western blotting was undertaken as described in Chapter 2 (sections 2.7.6 and 2.7.7). Briefly, protein content was determined via BCA assay before equal amounts of total cell protein were separated via SDS-PAGE; transferred to PVDF overnight; blocked; incubated in primary (anti-myostatin, SMAD2 and pan-actin) and secondary antibodies; visualised using chemiluminescence and quantified via densitometry. Myostatin (~26 kDa immunoreactive protein) and SMAD2 (60 kDa) protein levels are expressed relative to pan-actin. Data are presented as the overall mean of independent donor repeats (n = 5-7). For each independent donor repeat, each experimental treatment was replicated over 3-4 wells.

Amino Acid-Stimulated Protein Synthesis

Leucine-stimulated protein synthesis was assessed using the SuNSET techniques, as described in Chapter 2 (section 2.5.6). Fully differentiated myotubes were treated with fatty acids or vehicle for 16 h. Fatty acid solutions and Vehicle were not added to the serum-free starvation media, nor transport buffer used for the addition of 2 mM leucine, 5 mM glucose and 1 μM puromycin. SDS-PAGE, immunoblotting (anti-puromycin), Coomassie staining, and densitometric quantification were performed as described previously (Chapter 2).

Measurement of Myotube Diameter

In an early, preliminary experiment to establish whether 16 h treatment with 250 μM palmitate induced myotube atrophy, mean myotube diameter was assessed in cells from n = 1 independent donor repeat treated with either Vehicle or Palmitate,

but not PLO, using the same principles of measurement as described in Chapter 2 (section 2.2.5). In this experiment, cells were not fluorescently stained, but rather were imaged under phase contrast light microscopy, to allow the same cells to subsequently be harvested for RNA extraction. Measurements were obtained from 5 replicate wells, with one image being captured from the centre of each well and the 10 most prominent myotubes were measured in triplicate as described previously. Thus, reported diameters are the mean of 150 measurements, comprising 50 myotubes per treatment.

Statistical Analysis

All statistical analysis was performed in GraphPad Prism 9. Descriptive data are presented as Mean ± SD, while experimental data are presented as Mean ± SEM of the mean of all independent donor repeats combined, with the mean of individual independent donor repeats represented by shapes in the presented figures, where relevant (correlation analyses). Where experimental restrictions (number of available cells and their proliferation rate) dictated incomplete comparisons of all 3 treatments, and thus differing numbers of independent donor repeats, the number of independent donor repeats is displayed within each bar of each figure, for transparency.

Assumptions of normality were tested via Shapiro-Wilks test and parametric tests (ANOVA) were applied where data were normally distributed. Owing to small discrepancies in the number of independent donor repeats of treatment conditions, a mixed-effects model (a combination of a between-groups and a within-groups ANOVA) was fitted instead of a repeated measures ANOVA to assess changes in glucose uptake in response to fatty acids or Vehicle treatment and the absence (Basal) or presence (Insulin-Stimulated) of insulin. Mixed-effects analyses or one-way repeated measures ANOVA were similarly used to assess changes in gene expression, protein content and protein synthesis in response to treatments. All ANOVA results with $P < 0.10$ are accompanied by their corresponding partial eta squared (n_p^2) values as a measure of effect size. Significant post-hoc differences (Tukey multiple comparisons when more than 3 comparisons are required; Fisher's LSD when only 3 comparisons are required) are presented as between-treatment mean difference [95% CI]. Correlations between measured outcomes, and between the measured outcomes and donor serum myostatin concentration were performed using Pearson's correlation and are accompanied by their corresponding *r* and *P* values. Shapiro-Wilk tests revealed that myotube diameter measurements were not normally distributed, and so were assessed via Mann Whitney test. Statistical test results are reported

in boxes on each figure, where relevant. Statistical significance was defined as $P < 0.05$. Statistically significant post-hoc comparisons are indicated on each figure by lines connecting each comparator.

4.4 Results

To elucidate whether lipid-induced insulin resistance is associated with changes in the expression and abundance of myostatin, primary myogenic cultures were established from healthy, normoglycaemic, donors with normal HOMA-2 insulin-sensitivity (Table 4.1). In doing so, lipid-induced insulin resistance, as a model of high fat obesogenic dietary habits, could be captured *in vitro,* without the risk of existing metabolic perturbations of the donors being carried forward into the myogenic culture model.

Myogenic cultures demonstrated fundamental sensitivity to insulin. Myotubes from every donor whose cells were assessed for glucose uptake (n = 7), when treated for 16 h with Vehicle, increased glucose uptake in response to stimulation with 100 nM insulin (Mean ± SEM fold-change from Basal to Insulin-Stimulated uptake: 1.4 ± 0.25). This fold-change of glucose uptake with insulin stimulation is highly consistent with prior studies of primary human myotubes (Chanon et al., 2017; Krützfeldt et al., 2000; Parikh et al., 2021). Absolute rates of 2-DOG uptake in primary human myotubes reported within the literature vary greatly, however the values presented here are consistent with results from independent laboratories using the same technique (Abdelmoez et al., 2020; Crawford et al., 2010).

Table 4.1. Characteristic data of participants who provided skeletal muscle tissue samples for the generation of myogenic cultures used in this chapter.

	Group Mean (±SD)	Range (Min - Max)
n	8	-
Sex (M/F (n))	3/5	-
Age (y)	23 (±3)	19 - 29
Mass (Kg)	66.8 (±12.2)	52.4 - 81.6
BMI ($Kg \cdot m^{-2}$)	23.1 (± 2.6)	20.3 - 26.9
Waist (cm)	77.8 (±7.3)	70.0 - 91.0
Hip (cm)	87.9 (±6.7)	76.5 - 96.5
Waist:Hip ratio	0.89 (±0.05)	0.80 - 0.95
Fasting Glucose ($mmol \cdot L^{-1}$)	4.15 (±0.47)	3.45 - 4.89
Fasting Serum Insulin ($mIU \cdot L^{-1}$)	9.17 (±3.02)	6.17 – 13.40
HOMA2-IR	1.12 (±0.38)	0.72 – 1.69
Fasting Serum Myostatin ($ng \cdot mL^{-1}$)	3.51 (± 1.25)	2.15 - 5.61

4.4.1 Acute fatty acid treatment induces insulin resistance in myotubes

Basal and insulin-stimulated glucose uptake was measured in fully differentiated myotubes following 16h treatment with either Vehicle (fatty acid-free BSA), Palmitate (250 μM), or a mixture of Palmitate, Linoleic and Oleic acids (PLO: 250:50:150 μM). Mixed-effects analysis revealed a significant interaction effect between Insulin and Treatment with fatty acids (P = 0.050, n_p^2 = 0.632), and a significant main effect of Insulin (P = 0.008, n_p^2 = 0.713) but not treatment (Figure 4.1). Post-hoc comparisons (Tukey's multiple comparisons) revealed no differences in basal glucose uptake between the three treatments, however a significant increase in insulin-stimulated glucose uptake was seen in Vehicle-treated (Mean difference [95% CI]: 9.5 [18.0, 1.1] pmol·mg^{-1}·min^{-1}; P < 0.05), but not Palmitate- or PLO-treated cells. While cells treated with PLO did not demonstrate a statistically significant increase in glucose uptake upon insulin stimulation, there was a modest numerical increase, compared to treatment with palmitate alone (Mean difference [95% CI]: 6.8 [15.8, -2.6] vs -0.9 [9.1, -10.8] pmol·mg^{-1}·min^{-1}, respectively). ANOVA reported no significant effect of fatty acid treatment on the mean total protein content of culture wells that were used for glucose uptake experiments, which were seeded at equal density, suggesting that the concentration and duration of treatments were not inducing a fundamental loss of cells relative to the Vehicle condition (Figure 4.1B).

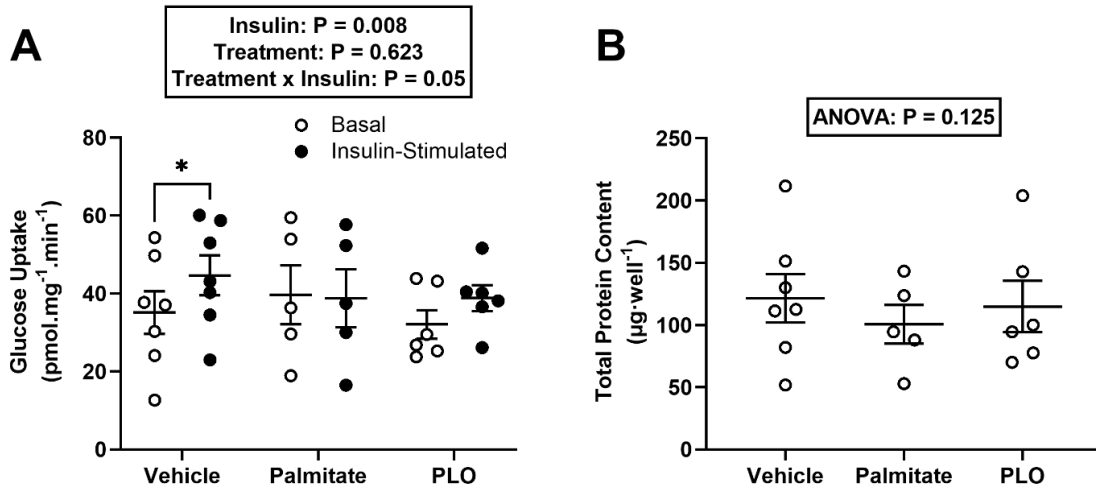

Figure 4.1. Effect of 16 h fatty acid treatments on glucose uptake in primary human myotubes.

Basal (open circles) and insulin-stimulated (100 nM; closed circles) glucose uptake was measured using [3H] 2-DOG. Insulin stimulation increased glucose uptake in Vehicle but not Palmitate or PLO-treated cells (**A**). No effect of 16 h fatty acid treatment on the total protein content of culture wells used for glucose uptake experiments (**B**). Data are presented as Mean ± SEM, with independent donor repeats plotted as circles. Each independent donor repeat comprised 3-6 replicate wells of each treatment condition, depending on the number of cells available. *Significant difference between treatments, as indicated: $P < 0.05$. Note: n = 5 independent donor repeats for comparisons of Vehicle vs Palmitate and n = 6 for comparisons of Vehicle vs PLO, due to differing numbers of primary cells available for some experiments.

4.4.2 Lipid-induced insulin resistance is not accompanied by an upregulation of myostatin in skeletal muscle cells

The induction of lipid-induced insulin resistance was not accompanied by changes in the expression or abundance of myostatin within human myotubes. Mixed-effects model analyses revealed no effect of fatty acid treatment on either myostatin mRNA expression or protein abundance (Figure 4.2A and B). Concordantly, the protein abundance of the myostatin-activated transcription factor, SMAD2, was similarly unaffected by fatty acid treatments (Figure 4.2C). Fasting serum myostatin concentration of the muscle tissue-donors displayed a moderate negative correlation (r = -0.631) with basal (Vehicle treatment) myostatin protein expression in myotubes from their respective donors, however this was not statistically significant (P = 0.128) (Figure 4.2D).

4.4.3 Acute palmitate treatment impairs myotube protein synthesis, but not diameter, and is restored by the addition of linoleic and oleic acids.

One-way ANOVA revealed a significant effect of fatty acid treatment on amino acid-stimulated myotube protein synthesis (P = 0.004, n_p^2 = 0.706), as indicated by the relative incorporation of puromycin into newly synthesised peptides (Figure 4.3C). Post-hoc comparisons (Fisher's LSD) identified significantly lower puromycin incorporation following Palmitate treatment, compared with Vehicle (0.2-fold lower, Mean difference [95% CI]: -0.233 [-0.078, -0.287] a.u.; P < 0.005). The addition of 50 μM linoleic and 150 μM oleic acid to the palmitate treatment (PLO) preserved myotube protein synthesis, such that PLO was not different from Vehicle. In a preliminary experiment to establish whether 16 h treatment with 250 μM palmitate induces myotube atrophy, Mann Whitney test revealed that exposure of myotubes to palmitate did not significantly alter mean myotube diameter (Vehicle: 12.73 ± 0.64 μm vs Palmitate: 12.14 ± 0.52 μm; P = 0.590) (Figure 4.3D), suggesting that the palmitate-induced reduction of protein synthesis did not translate to perturbed myotube morphology over this time scale.

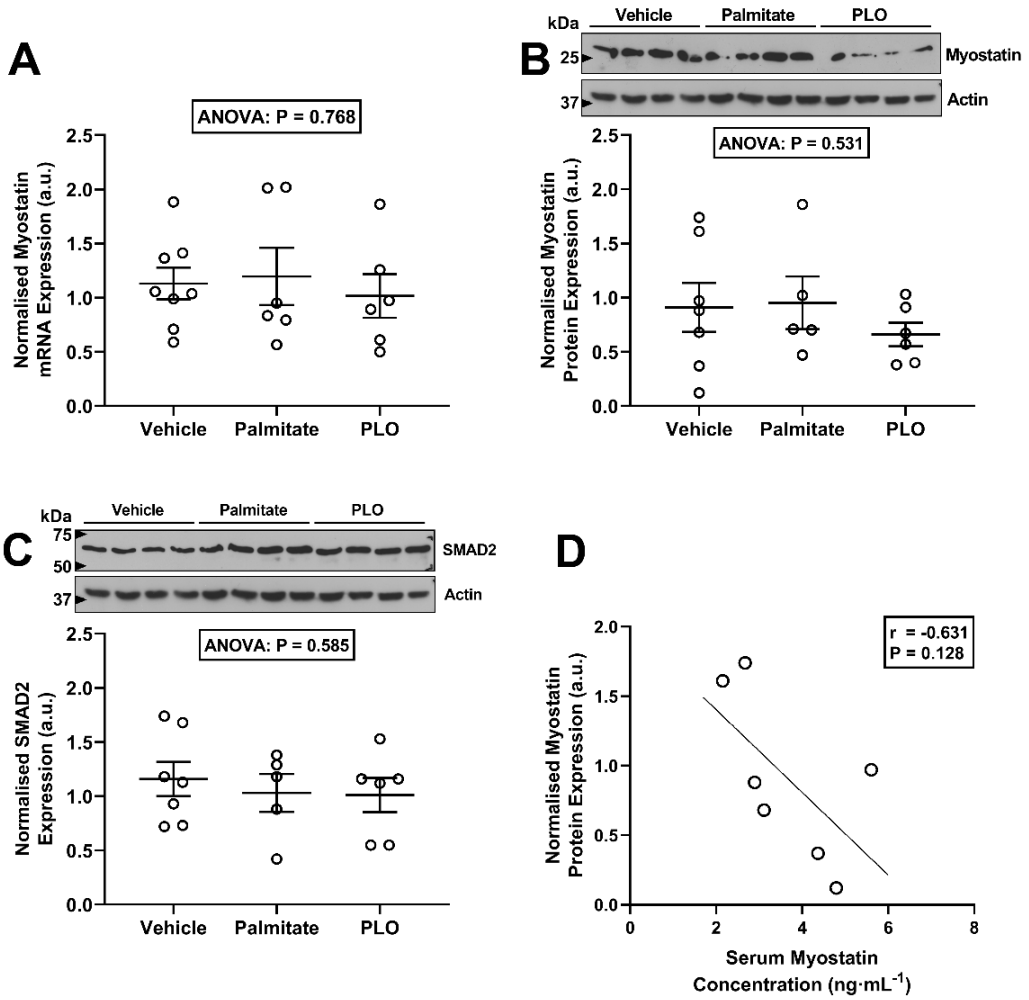

Figure 4.2. Effect of 16 h fatty acid treatments on the expression and abundance of myostatin and SMAD2 in primary human myotubes.

Neither myostatin mRNA expression (**A**) or protein abundance (**B**) were affected by palmitate or PLO treatment. Total SMAD2 protein expression was not affected by fatty acid treatments (**C**). Donor serum myostatin concentration and basal (Vehicle) myostatin protein expression in myotubes derived from those donors demonstrated a moderate, but not statistically significant, negative correlation (**D**). Data are presented as Mean ± SEM, with independent donor repeats plotted as circles. Each independent donor repeat comprised 4 replicate wells of each treatment condition. Note: different numbers of independent donor repeats were used for comparisons of Vehicle vs Palmitate and Vehicle vs PLO, within and between different outcomes due to differing numbers of primary cells available for some experiments.

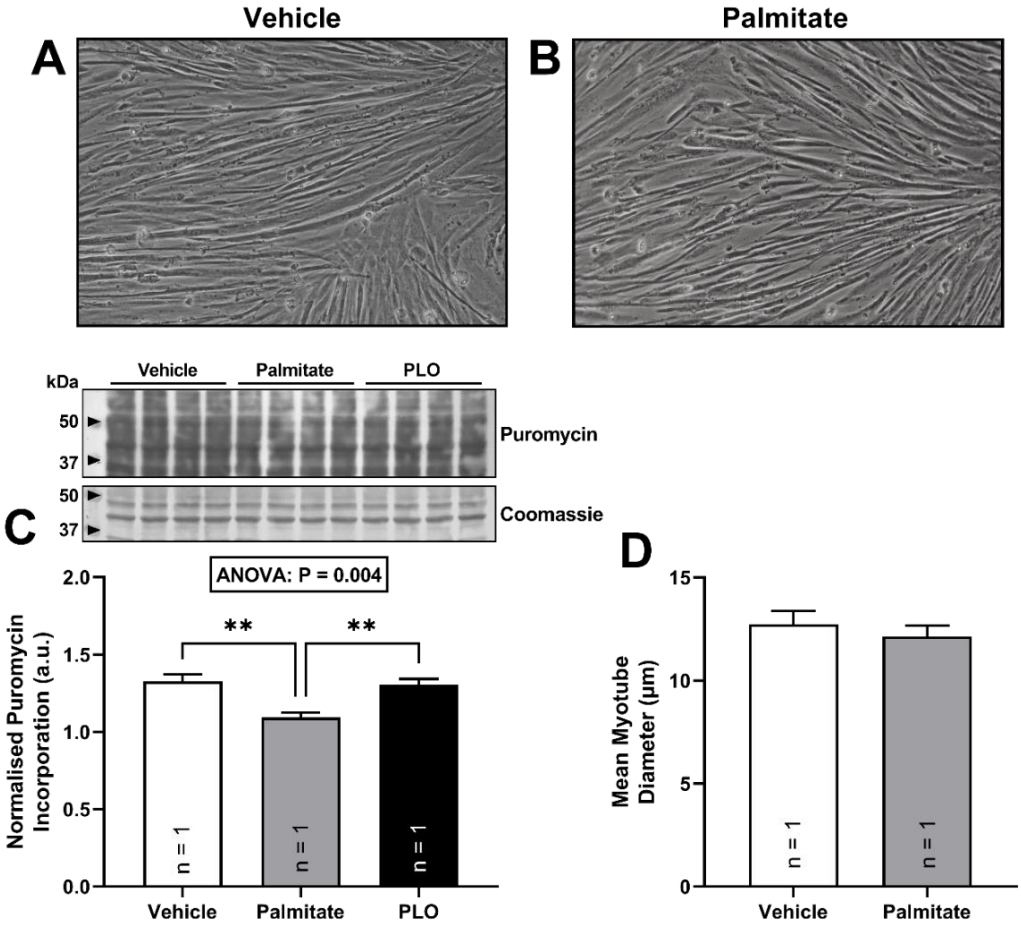

Figure 4.3. Effect of 16 h fatty acid treatments on protein synthesis and myotube diameter in primary human myotubes.

Representative brightfield micrographs of myotubes treated with Vehicle (**A**) or Palmitate (**B**). Palmitate, but not PLO, significantly reduced acid-stimulated myotube protein synthesis, relative to Vehicle (**C**). Palmitate treatment did not significantly alter mean myotube diameter (**D**). Data are presented as Mean ± SEM of values obtained from n = 1 independent donor repeat. For measurement of protein synthesis, data is the mean of 4 replicate wells of each treatment condition. For myotube diameter, data is the mean of triplicate measurements of a total of 50 myotubes, taken from 5 different replicate wells (of the 10 largest myotubes per well). Significant difference between treatments, as indicated: $^{**}P < 0.01$.

4.5 Discussion

Acute (16 h) incubation of primary human myotubes from normal-weight insulin sensitive donors with fatty acid solutions (250 μM palmitate alone, or with the addition of 50 μM linoleic and 150 μM oleic acid (PLO)) induced marked resistance to the insulin-stimulated elevation of glucose transport. The induction of lipid-induced insulin resistance was not accompanied by changes in the mRNA expression or protein abundance of myostatin within myotubes. Interestingly, there was a myostatin-independent suppression of global myotube protein synthesis with palmitate that was rescued in the PLO treatment, suggesting a dissociation between insulin and anabolic resistance in the latter treatment. Importantly, fatty acid treatment did not significantly reduce myotube diameter or the total protein content of culture wells, suggesting that this reduction was not a function of lipid-induced cell atrophy and/or apoptosis.

Mechanistic *in vivo* studies of lipid-induced insulin resistance in skeletal muscle are limited by the potential interference of organ cross-talk, particularly pertaining to the metabolic status of the adipose tissue and liver, which are heavily implicated in insulin resistance and obesity (da Silva Rosa, Nayak, Caymo, & Gordon, 2020). Therefore, the majority of mechanistic studies are *in vitro*, and have used murine C2C12 myotubes, which have profoundly different transcriptomic profiles and metabolic behaviours than human primary myotubes (Abdelmoez et al., 2020) and are standardly cultured in high glucose (25 mM) media. In the present study, primary human myotubes derived from insulin-sensitive donors were cultured in media with 6.1 mM glucose (which resembles the ~5.5 mM mean 24 h glucose concentrations reported in healthy adults using continuous glucose monitoring (Derosa et al., 2009; R. Jones et al., 2020)), to model the induction of insulin resistance, since they retain some elements of donor phenotype (Jacobs, Oosterhof, & Veerkamp, 1987; Kausch et al., 2003; Zuurveld, Oosterhof, Veerkamp, & van Moerkerk, 1985). The generation of myotubes from normal weight insulin-sensitive donors avoids the potentially confounding effects of dysfunctional metabolic programming (Joseph A. Houmard, Pories, & Dohm, 2011) that might be conferred if obese, insulin-resistant donors were used.

Palmitate-Induced Insulin Resistance is not Associated with Upregulation of Myostatin, but Confers Anabolic Resistance

Treatment of myotubes with 250 μM palmitate for 16 h did not alter basal glucose uptake but impaired its insulin-stimulated increase. Indeed, in Vehicle-treated cells, 100 nM insulin increased glucose uptake by 27% (mean difference [95% CI]) 9.5 (18.0, 1.1) $pmol \cdot mg^{-1} \cdot min^{-1}$, whereas palmitate treatment failed to evoke an insulin-stimulated increase (-0.9 [9.1,-10.9] $pmol \cdot mg^{-1} \cdot min^{-1}$), which is concordant with the complete impairment of insulin-mediated elevation of glucose uptake following exposure of primary human myotubes to 750 μM palmitate for 48 h (Mahfouz et al., 2014) and of C2C12 myotubes to 200 μM palmitate for 24 h (M. Yang et al., 2013). Thus, in relative terms, insulin-stimulated glucose uptake following palmitate treatment was 13.2% lower than vehicle in this study, which is broadly consistent with previously reported deleterious effects *in vivo*, albeit of smaller magnitude than the 25-28% reduction in glucose disposal rate reported after oral ingestion of 1.18 g·kg-1 body mass of palm oil (comprising ~44% palmitic acid), compared to vehicle (Hernández et al., 2017; Sarabhai et al., 2022).

It has previously been reported that insulin resistance is associated with increased expression of myostatin in humans (David L. Allen et al., 2011; Amor et al., 2019; Hittel et al., 2009; Hjorth et al., 2016) and that upregulation or administration of myostatin promotes insulin resistance in animal models, which may involve the repression of insulin-stimulated Akt phosphorylation by the activation of SMAD2/3 (Goodman, McNally, Hoffmann, & Hornberger, 2013), which subsequently impairs the distal insulin signalling cascade (T. Guo et al., 2009; Hittel et al., 2010; X.-H. Liu et al., 2018). Furthermore, based on studies where myostatin is knocked out, it has been proposed that myostatin represses AMP-activated protein kinase (AMPK) expression and activity (Dong et al., 2016; Shan, Liang, Bi, & Kuang, 2013; C. Zhang et al., 2011). AMPK functions as an energy-sensing metabolic switch that is activated in response to an elevated intracellular AMP:ATP ratio and subsequently activates ATP-generating pathways and systems, including the enhancement of glucose uptake via the stimulation of GLUT4 translocation (Rachek, Musiyenko, LeDoux, & Wilson, 2007). Therefore, it has been postulated that the upregulation of myostatin seen in obese adults could be detrimental to skeletal muscle insulin sensitivity and glucose handling via impaired insulin-stimulated Akt phosphorylation and insulin-independent AMPK activity (L. A. Consitt & Clark, 2018).

The present study demonstrates, for the first time in human skeletal muscle cells, that despite the induction of insulin resistance, neither the mRNA expression nor protein abundance of myostatin were altered by palmitate or PLO. This finding contrasts those of T. J. Kim et al. (2021) who reported a ~5-fold increase in the expression of myostatin protein (of ~43 kDa), with a concomitant and comparable upregulation of MuRF1 and MAFbx, when C2C12 myotubes were treated with 200 μM palmitate for 24 h. It must be recalled that in the present study, only the ~26 kDa immunoreactive protein, corresponding in size to the mature myostatin, was assessed. Thus, direct comparisons are restricted due to uncertainty as to the relative abundances and processing of the different myostatin forms in muscle cells. Kim and colleagues supported their observations in C2C12 cells by demonstrating changes of similar magnitude in myostatin, MuRF1 and MAFbx protein abundance in the skeletal muscle of C57BL/6 mice fed a high fat diet (60% energy contribution) for 8 weeks. It must be considered however, that in mice, 8 weeks of HFD represents a significant portion of the lifespan. While not reported within the results of Kim et al, based on prior findings of a 40% increase in adipose mass after 8 weeks HFD in the same strain of mice, relative to a low-fat diet (de Wilde et al., 2009), it is highly likely that Kim's mice developed obesity over this time frame, confounding the effects of lipid-induced insulin resistance *per se* and HFD-induced obesity.

A similar study also treated C2C12 myotubes with 500 μM palmitate for 24 h, which impaired insulin-stimulated glucose uptake and similarly induced a 3.3-fold increase in myostatin protein content (M. Liu et al., 2013). Importantly, Kim et al.'s study reported 60-70% reductions in both cell viability (assessed via MTT assay) and myotube diameter. While Liu et al. did not provide an assessment of cell viability, they applied a higher concentration of palmitate than Kim et al. (500 μM vs 200 μM, respectively) to C2C12 myotubes grown in the same medium composition, for the same 24 h duration. Thus, it is highly likely that similar or even greater diminutions of cell viability were observed in Liu's study, which raises questions as to the physiological relevance of their model. Indeed, concentrations of 0.5–2.0 mM palmitate have been consistently shown to drastically reduce myotube viability and induce apoptosis in C2C12 cells (Patková, Anděl, & Trnka, 2014; M. Yang et al., 2013). In contrast, in the present study, palmitate treatment did not affect myotube diameter, nor total well protein. While cell viability was not assayed in these experiments, under the myriad conditions employed within this thesis, primary human myotubes have demonstrated resilience to exogenous insults. Indeed, in Chapter 6, treatment of fully differentiated myotubes for 24 h with 10% DMSO (a highly cytotoxic concentration in most cell lines due to

perforation of lipid membranes (de Ménorval, Mir, Fernández, & Reigada, 2012; Notman, Noro, O'Malley, & Anwar, 2006)) induced a < 30% loss of cell viability.

In another study of C2C12 myotubes, H. Lee et al. (2017), reported that 30 h of exposure to 300 μM palmitate, but not 500 μM oleate or 500 μM palmitate + oleate, induced a 1.5-fold increase in the mRNA expression of myostatin and MAFbx. It must again be noted that palmitate treatment reduced myotube diameter by ~30% and induced 2-fold upregulation of TNF expression in the latter experiment, suggesting a degree of cellular stress that is not physiologically relevant in the setting of dietary lipid overprovision. This effect is more comparable to that observed in an additional experiment not presented in this Chapter, whereby sustained palmitate (250 μM) treatment of myoblasts during 6 days of differentiation induced visible cell loss. Indeed, myotubes chronically treated with palmitate yielded, on average, 30% less total protein and RNA , which was accompanied by significant downregulation of the reference gene, β-actin, which was otherwise stable in response to acute fatty acid insult. Together, these data suggest that contrary to results from murine skeletal muscle cells, acute fatty acid treatments (in the physiological micromolar range) do not significantly diminish primary human myotube viability or morphology. Thus, under this more physiological, non-cytotoxic model of lipid-induced insulin resistance, the induction of insulin resistance in human myotubes is not associated with changes in the expression or abundance of myostatin.

Concordant with the absence of change in myostatin, SMAD2 protein abundance was also not changed after 16 h of either palmitate or PLO. In contrast, equimolar (250 μM) palmitic acid and oleate treatment of C2C12 myotubes for 24, 48, and 72 h, decreased protein degradation rate relative to a fatty acid-free BSA vehicle, which was accompanied by diminished SMAD2 and SMAD3 mRNA expression after 48 h, but not 24 h (Bollinger, Campbell, & Brault, 2018). These findings, however, were accompanied by suppression of MuRF1, MAFbx and FoxO3, suggesting that in C2C12's, equimolar oleate can overcome the effects of palmitate, which has been previously shown to upregulate SMAD3 at the protein level (Q. Guo et al., 2019).

Despite an absence of change in myostatin or SMAD2 in the present study, amino-acid stimulated protein synthesis, as indicated by puromycin incorporation into myotubes, was reduced by 17% with palmitate treatment, relative to vehicle, demonstrating anabolic resistance, which may be driven by impaired translation initiation via increased phosphorylation of eIF2α (Perry et al., 2018). This corroborates findings of diminished puromycin incorporation after 48 h treatment

with 100 μM palmitate, which was accompanied by a reduction of C2C12 myotube diameter (da Paixão, Bolin, Silvestre, & Rodrigues, 2021). It should be noted that the data presented for puromycin incorporation in the current study is from n = 1 independent donor repeat, but should be considered in conjunction with prior (unpublished) data from our group that demonstrated a 15% reduction in puromycin incorporation after identical palmitate treatments of primary human myotubes from n = 3 independent donor repeats, and was accompanied by a ~25% reduction of system A transport of amino acids under basal conditions (R. Jones, 2019).

Broadly similar concentrations (100-750 μM) and durations (16-24 h) of palmitate treatment to that employed in the present study, have been demonstrated to impair insulin signalling and sensitivity (diminished glucose oxidation and glycogen synthesis) in C2C12 myotubes (J. A. Chavez & Summers, 2003; Hirabara et al., 2010; Perry et al., 2018), with concurrent elevations in inflammatory cytokine expression and secretion (Cruz & Beall, 2020). The authors of these studied proposed that the accumulation of intramyocellular lipid species and fragments, particularly ceramides, and the associated mitochondrial dysfunction that ensued, were the primary driving factors of this resistance. While not the focus of this study, it is likely that the observed functional impairment in insulin-stimulated glucose uptake was predominantly mediated by diminished sensitivity to/transduction of distal insulin signalling (Sarabhai et al., 2022), since palmitate has been shown to impair phosphorylation of Akt, AS160, and GSK-3β (Abildgaard et al., 2014; Bikman et al., 2010; Kausch et al., 2003; Mäkinen et al., 2017; Montell et al., 2001).

Mechanistically, the intramyocellular accumulation of lipid species, particularly DAG and ceramides, has been a particular focus of research interest, with some evidence of palmitate-mediated activation of the Atypical protein kinase C - Protein phosphatase 2A (aPKCζ-PP2A) pathway, whereby membrane-bound ceramide is known to inhibit ser473-phosphorylation of Akt (Blouin et al., 2010; Samar I. Itani et al., 2002; Sarabhai et al., 2022; Stratford et al., 2004). Palmitate, unlike unsaturated fatty acids, provides substrate for the biosynthesis of ceramides and activates Toll-like receptor 4 (TLR4) signalling, which transcriptionally upregulates ceramide synthesis enzymes (Bandet, Tan-Chen, Bourron, Le Stunff, & Hajduch, 2019; William L. Holland et al., 2011; Kelpe et al., 2003). Comparable with the present study, treatment of L6 myotubes with 200 μM palmitate for 16 h almost entirely blunted insulin-stimulated glucose uptake,

which was accompanied by a 5-fold increase in DAG accumulation, relative to vehicle (Hommelberg et al., 2011).

The degree to which this mechanism mediates lipid-induced insulin resistance in skeletal muscle is contested however (M. C. Petersen & Jurczak, 2016), since proximal insulin signalling (upstream of Akt) has not been found to be impaired in some studies of insulin resistant individuals (Louise D. Høeg et al., 2010; Storgaard et al., 2004), Furthermore, other studies have failed to demonstrate concurrent induction of insulin resistance and DAG accumulation in response to acute (L. D. Høeg et al., 2011; Vistisen et al., 2008) or short-term lipid overload (Kostas Tsintzas et al., 2020), nor a relationship between muscle DAG and insulin resistance in cross-sectional studies (Anastasiou et al., 2009; L. Perreault et al., 2010). Indeed, palmitate-induced endoplasmic reticulum (ER) stress persists in myotubes, despite TLR4 inhibition (Perry et al., 2018). Furthermore, some unsaturated fatty acids exert insulin-desensitising effects, without elevating myocyte ceramide content, suggesting ceramide accumulation is not an essential prerequisite of muscle insulin resistance (J. A. Chavez & Summers, 2003; W. L. Holland et al., 2007). Thus, it has been argued that the current understanding of ceramide signalling cannot fully explain the mechanisms responsible for lipid-induced insulin resistance in skeletal muscle (M. C. Petersen & Jurczak, 2016). It is important to recall that changes in insulin signalling do not necessarily equate to changes in metabolic function, since the addition of oleate to palmitate treatment of myotubes restores distal insulin signalling and prevents ER stress, but nevertheless impairs insulin-stimulated glucose uptake (Mäkinen et al., 2017), the latter being consistent with the effects seen in PLO treated cells in the present study.

Beyond glucose handling, the impairment of Akt phosphorylation by palmitate acts to impair protein synthesis and accelerate protein degradation via the Akt/ Forkhead box O3 (FoxO3) pathway. In C2C12 myotubes, 500 μM palmitate increased nuclear FoxO2 protein, with subsequent upregulation of the E3 ligase MAFbx and the autophagy mediator BCL2/adenovirus E1B 19 kDa protein-interacting protein 3 (Bnip3), resulting in increased myotube protein breakdown (M. E. Woodworth-Hobbs et al., 2014). In a follow-up study, palmitate also increased the phosphorylation eIF2α, which impairs the binding of the initiator transfer RNA to 40S ribosomal subunits, and thus impairs protein synthesis, which was also observed (Myra E. Woodworth-Hobbs et al., 2017). Similarly, treatment of C2C12 myotubes with 500 μM palmitate for 6h induced a 43% reduction in

protein synthesis (puromycin incorporation), with a concomitant 3.8-fold increase in the phosphorylation of eIF2α (Perry et al., 2018).

The increased phosphorylation of eIF2α, which is activated by protein kinase RNA-like endoplasmic reticulum kinase (PERK; which itself is activated in muscle cells by palmitic acid (Deldicque et al., 2010)), is consistent with the effects of high fat diet in aged mice (Tardif et al., 2014). *In vivo*, the contribution of saturated fatty acids, such as palmitic acid, to the deleterious effects of acute lipid overprovision are less clear. In healthy young and middle-aged overweight males, intralipid-infusion (comprising 44-62% linoleic acid, 19-30% oleic acid, and 7-14% palmitic acid), which elevated plasma FFA from 0.5 to 2 $mmol \cdot L^{-1}$, prevented the elevation of mixed-muscle fractional protein synthetic rate in response to an amino acid bolus (anabolic resistance) and was associated with increased phosphorylation of eIF2α at Ser51 (Smiles et al., 2019) and suppressed phosphorylation of eukaryotic translation initiation factor 4E-binding protein 1 (4E-BP1), which is an important repressor of protein translation within the mTOR pathway (Smiles et al., 2019; F. B. Stephens et al., 2015). Collectively, these findings suggest that acute lipid overload affects muscle protein turnover by multiple means; inducing the PERK-initiated branch of the unfolded protein response which impairs the initiation of protein translation; further inhibition of translation initiation via impaired mTOR signalling; and the upregulation of the ubiquitin proteasome system, which accelerates muscle protein degradation. In myogenic cultures, where confounding factors are minimised, palmitic acid appears to induce these effects most deleteriously. Thus, in the face of lipid overload *in vivo*, palmitic acid may contribute to and exacerbate anabolic resistance.

The Addition of Linoleic and Oleic Acid Prevents Palmitate-Induced Anabolic but Not Insulin Resistance

When linoleic and oleic acid was combined with palmitate (PLO), insulin-stimulated glucose uptake was still impaired, relative to vehicle. It is worth noting that because palmitate concentration was matched between treatments, PLO treatment did not expose cells to an equimolar total fatty acid load relative to palmitate (250 μM) but rather involved exposure to 450 μM total fatty acids. While the uptake of fatty acids as a function of unbound fatty acid concentration displays typical saturation kinetics in skeletal muscle tissue, the relationship between total fatty acid concentration and its uptake remains linear to ~1500 μM (Turcotte, Kiens, & Richter, 1991). Thus, under the conditions here employed with excessive albumin concentration to maximise binding, there is no reason to believe that the greater fatty acid load of PLO would have resulted in different uptake kinetics into

the myotubes. In skeletal muscle, it has been reported that protein abundance of the fatty acid transport proteins FABPpm, CD36 and FATP4, but not FATP1, are highly correlated with the capacities for oxidative metabolism, fatty acid oxidation and TAG esterification, with CD36 and FATP4 demonstrating the greatest efficacy to increase fatty acid transport, while FABPpm and CD36 have the greatest capacity to stimulate fatty acid oxidation (Nickerson et al., 2009).

Linoleic acid may have contributed to insulin resistance, since it has been previously shown to induce comparable impairments in insulin-stimulated glucose uptake and pAkt in some (Sinha, Perdomo, Brown, & O'Doherty, 2004) but not all studies (Nardi et al., 2014); however associations between dietary linoleic acid intake and metabolic health are conflicting (J. S. Lee et al., 2006; Matravadia, Herbst, Jain, Mutch, & Holloway, 2014). Conversely, physiological concentrations of oleic acid are not detrimental to insulin sensitivity and do not affect insulin-stimulated glucose uptake (Montell et al., 2001). Under similar experimental conditions to those employed here, the addition of oleic acid to palmitate largely restored the palmitate-induced decrease in insulin-stimulated glucose uptake in L6 myotubes (S. Y. Park et al., 2014; Sawada et al., 2012). The metabolic fate of intramyocellular glucose is similarly perturbed by palmitate, but not oleic acid, with palmitate, treated cells demonstrating reduced insulin-stimulated glycogen synthesis, glucose oxidation and lactate production (Hirabara et al., 2010).

In the present study, despite persisting impairment of insulin sensitivity and an absence of change in myostatin expression, PLO treated cells demonstrated preserved protein synthesis (puromycin incorporation), relative to palmitate treated cells. This novel finding in primary human myotubes expands upon the findings of H. Lee et al. (2017) in C2C12 myotubes, whereby treatment with as little as 300 μM palmitate for 30-36 h induced myotube atrophy, myonuclear fragmentation and mitochondrial superoxide production in a dose-dependent manner, while co-treatment of 300 μM palmitate and 500 μM oleate fully reversed these perturbations to the levels seen with vehicle treatment. Together, these findings demonstrate a potentially protective role of oleic acid in the preservation of anabolic sensitivity, with subsequent mitigation of palmitate-induced atrophy in cultured skeletal muscle cells that is not mediated by changes in the expression of myostatin. In the context of persisting insulin resistance with PLO treatment, these findings together demonstrate an uncoupling of lipid-induced insulin and anabolic resistance.

Mechanistically, the protective effects of oleic acid on muscle metabolic function appear to be mediated by multifaceted means, comprising the preservation of

predominantly distal insulin signal transduction (Alkhateeb & Qnais, 2017); the promotion of complete fatty acid oxidation (J.-H. Lim et al., 2013); the altered metabolic fate of fatty acids and glucose within the myocyte (Hirabara et al., 2010); and the prevention of mitochondrial dysfunction (Yuzefovych et al., 2010). At the signalling cascade level, unlike palmitate, incubation of human myotubes with oleic acid has been shown to significantly enhance insulin pathway sensitivity (Nardi et al., 2014). However, this increased sensitivity was not due to changes in proximal insulin signalling, but rather due to reduced dephosphorylation/ inactivation of Akt and extracellular signal-regulated kinases 1/2 (ERK1/2). Indeed, oleic acid did not affect the protein abundance of the insulin receptor β-subunit, IRS1 or PI3K-p85 subunit, which lie upstream of Akt and ERK1/2.

Additionally, the composition of fatty acid insult directs its metabolic fate within the myocyte. While palmitic and oleic acids are similarly incorporated into phospholipids, palmitic acid is more readily funnelled into DAG, the elevated intramyocellular accumulation of which is also associated with impaired anabolic sensitivity (Rivas et al., 2016), whereas oleic acid primarily contributes to TAG. Furthermore, the addition of oleate diverts palmitate towards TAG synthesis via PPARα activation which upregulates DAG acyltransferase 2, which is responsible for the synthesis of TAG from DAG (Coll et al., 2008), and in turn appears to abolish its negative effect on glucose uptake (Montell et al., 2001; Peng et al., 2011). The mechanisms by which the addition of linoleic and perhaps more pertinently, oleic acid, mediate the apparent uncoupling of palmitate-induced insulin and anabolic resistance, remains to be elucidated and warrants further investigation.

4.6 Limitations

In this study, efforts were taken to create a more physiologically relevant model of lipid-induced skeletal muscle insulin resistance. A combination of palmitic, linoleic and oleic acid (PLO) was therefore applied to primary human myotubes, reflecting the three most abundant fatty acids abounding within human plasma. A 5:1:3 molar ratio of P:L:O was employed, which is similar, but not entirely consistent with that reported within obese plasma (~5:4:3). This was the product of preliminary experiments revealing that in the presence of greater linoleic acid concentration, oleic acid was no longer at all able to mitigate the saturated fatty acid-induced deleterious effects on insulin-stimulated glucose uptake. Thus, 5:1:3 was a compromise aimed to enable such mitigation, such that if changes in myostatin were found with palmitate treatment, it might also be revealed whether the insulin-sensitising effects of oleic acid might prevent such changes. It must

also be noted that the total fatty acid concentration in PLO (450 μM) was almost twice that of palmitate alone (250 μM), however this reflects the approximate combined abundance of these three free fatty acids within the circulation and therefore allows comparisons to be made with the isolated effects of physiological palmitate.

While precise mechanisms of the insulin- and anabolic-desensitising effects of saturated fatty acids are not yet fully elucidated, proposed pathways have been reviewed elsewhere (Aas et al., 2005; Jose A. Chavez & Summers, 2012; Leslie A. Consitt, Bell, & Houmard, 2009; Kitessa & Abeywardena, 2016; Krebs & Roden, 2005; Martins et al., 2012). Therefore, reflecting the specific aims of this chapter, following the identification of an absence of change in either the mRNA or protein expression of myostatin, despite the induction of insulin resistance by palmitate, further assessment of mechanistic factors was not pursued. Instead, focus was turned to commencing the subsequent experimental series presented in Chapter 5, to continue searching for the source of the obesity-mediated perturbation of myostatin expression and function. Nevertheless, additional endpoints would doubtless have provided interesting data and it would be worthwhile in the future to further investigate the mechanisms by which addition of linoleic and oleic acids seems to prevent palmitate-induced anabolic resistance, independent of changes in myostatin and the induction of insulin resistance.

4.7 Conclusions

In summary, acute treatment (16 h) of primary human myotubes with 250 μM palmitate alone, or the combination of palmitate, linoleic and oleic acids (PLO; 250, 50, and 150 μM, respectively) impaired insulin-stimulated, but not basal, glucose uptake (*ergo*, induced insulin resistance). In the acute setting, the induction of lipid-induced insulin resistance is not accompanied by changes in the expression or abundance of myostatin or its downstream signalling component SMAD2. Nevertheless, palmitate treatment impaired amino-acid stimulated protein synthesis (*ergo*, induced anabolic resistance), which was preserved with PLO. Taken together, these findings suggest that the obesity-mediated upregulation of myostatin that is reported both in the literature and in Chapter 3 of this thesis, is not driven, at least acutely, by insulin resistance arising from excessive availability of dietary lipids.

Chapter 5. Obesity and Adipose-Muscle Cross Talk: Effects on Myostatin, Insulin Sensitivity and Myogenesis

5.1 Introduction

Once considered a passive energy reservoir, the discovery of the adipose-secreted factors adipsin and leptin revealed adipose tissue to be an endocrine organ (Cook et al., 1987; Siiteri, 1987; Y. Zhang et al., 1994). Following the observation that obese adipose tissue has increased expression and secretion of tumour necrosis factor-alpha (TNF-α), it has since been shown that adipose tissue participates in a broad spectrum of inter-organ communication (Funcke & Scherer, 2019) and obesity promotes the accumulation of immune cells within adipose tissue and accelerates cellular senescence (Hotamisligil et al., 1993; Z. Liu et al., 2020; Weisberg et al., 2003). Perhaps the most well documented effects of the excessive accrual of adipose tissue on its endocrine function, is the elevated production of classical pro-inflammatory cytokines, including TNF-α, IL-1β, IL-6, and interferon-gamma (Ellulu, Patimah, Khaza'ai, Rahmat, & Abed, 2017). Indeed, obesity is now characterised as a proinflammatory condition in which the increased abundance and hypertrophy of adipocytes and resident/infiltrating immune cells promote the elevated secretion and subsequently circulating abundance of inflammatory factors, most notably cytokines (Makki, Froguel, & Wolowczuk, 2013). Through this secretory function, excessive adiposity conveys pleiotropic effects on endocrine and metabolic function, contributing to pathophysiological consequences with ageing (Frühbeck et al., 2001; Mathus-Vliegen et al., 2012). Importantly, this must be considered in the context of evidence from studies that demonstrated a capacity for healthy adipose tissue to exert favourable effects on skeletal muscle, which emphasises the physiological significance of cross talk between the two tissues (Stanford et al., 2015).

Cross-Talk from Adipose to Skeletal Muscle Tissue is Mediated by the Adipose Tissue Secretome and Impacts Muscle Health

The proinflammatory nature of obesity can promote a chronic low-grade inflammatory state, which is a key feature of pathological muscle wasting and can also drive the development of insulin resistance, however many other factors are also involved (Costamagna, Costelli, Sampaolesi, & Penna, 2015; Shoelson, Lee, & Goldfine, 2006). Furthermore, beyond inflammatory cytokines, insulin resistance in human adipocytes induces marked changes to their secretome, including greater secretion of extracellular matrix proteins, factors involved in

angiogenesis and many enzymes and peptidases, which may confer effects on other tissues (J.-M. Lim, Wollaston-Hayden, Teo, Hausman, & Wells, 2014). Thus, cross-talk between adipose tissue and skeletal muscle is perturbed by the presence of obesity and may promote skeletal muscle dysfunction and insulin resistance.

To that effect, the regulation of skeletal muscle mass is complex and delicately balanced, involving many adipose-secreted molecules (including proteins and RNAs), which often display pleiotropic effects (Figure 5.1). Many of these factors appear perturbed by excessive adiposity, but effects are confounded by age, physical activity status, and comorbidities, frequently resulting in conflicting findings and limited reproducibility. Our group has recently discussed such factors and conflicts at length (Wilhelmsen et al., 2021). Similarly, the insulin-desensitising capacity of the obese adipose tissue secretome has also been demonstrated and implicates some of the same, but also many other, mediating factors, involving many interactions besides the activation of inflammatory pathways (Hotamisligil et al., 1993; Pogodziński, Ostrowska, Smarkusz-Zarzecka, & Zyśk, 2022). At present, there is a paucity of research seeking to isolate the effects of obesity on adipose-muscle crosstalk, specifically with regards to the concurrent modulation of skeletal muscle insulin and anabolic sensitivity, and the possible involvement of myostatin in these interactions.

Adipose Tissue and Myostatin

As demonstrated in Chapter 3, skeletal muscle myostatin expression and circulating abundance are elevated by the combination of obesity and advancing age (David L. Allen et al., 2011; Hittel et al., 2009; Milan et al., 2004). Myostatin is also expressed in adipose tissue, however data from ob/ob mice suggests mRNA expression is 50-100-fold lower than in skeletal muscle (D. L. Allen et al., 2008). Nevertheless, the mRNA expression of both myostatin and its receptor, ACVR2B, were found to be 50-100-fold higher in the adipose tissue of ob/ob than wild type mice. Conversely, despite elevated serum abundance, myostatin expression in SAT and VAT was not different between age-matched severely obese, overweight, and lean humans (Amor et al., 2019). These contradictory findings may reflect fundamental differences between human and murine adipose tissue expression profiles and brown adipocyte abundance, emphasising the need for more research using human models of obesity (Baboota et al., 2015; Zuriaga, Fuster, Gokce, & Walsh, 2017).

Adipose tissue-specific deletion of myostatin in HFD-fed mice did not affect muscle weight nor body composition, however whole-body knockout partially supressed

HFD-induced fat accumulation (T. Guo et al., 2009; McPherron & Lee, 2002). Conversely, muscle-specific inhibition of myostatin signalling increased lean mass and decreased fat mass in mice fed both chow and HFD (T. Guo et al., 2009). These studies suggest that secretion and signalling of myostatin in skeletal muscle influences the regulation of muscle and adipose mass, but adipose-derived myostatin does not, likely reflecting its vastly lower expression in adipose tissue. What remains to be established, however, is whether the upregulation of myostatin seen in obese skeletal muscle is mediated via adipose-muscle cross talk by other secretory factors that may be differentially secreted from adipose tissue in obesity and whether this upregulation is associated with changes in insulin and anabolic sensitivity.

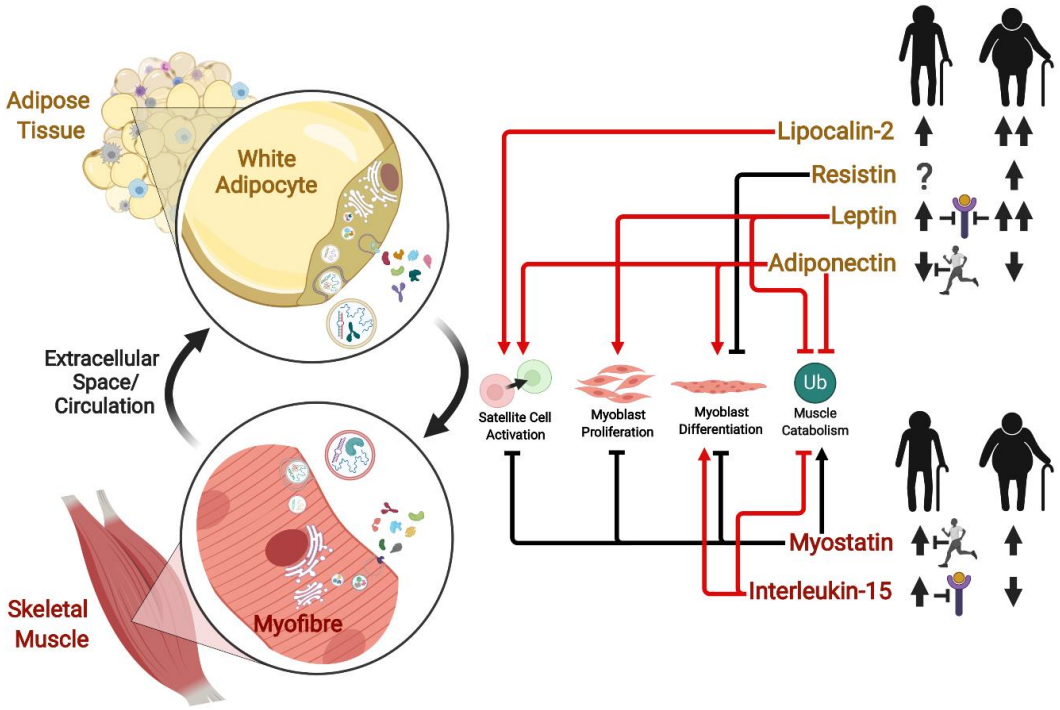

Figure 5.1. Cytokines secreted from skeletal muscle and adipose tissues involved in muscle-adipose cross talk and the regulation of skeletal muscle mass.

The expression, secretion and function of these cytokines may be perturbed by ageing and obesity, impairing muscle regulatory pathways. Processes regulating skeletal muscle mass have been condensed into four levels: activation of the muscle satellite cell pool; proliferation of myoblasts; differentiation into myotubes; and the catabolic processes (Ub) involved in the breakdown of muscle protein. Regardless of colour, arrows and block (inhibitory) lines indicate stimulatory and inhibitory effects, respectively. Red lines (whether arrows or block lines) indicate pro-myogenic effects, which may act to preserve muscle mass, while black lines (whether arrows or block lines) indicate anti-myogenic effects. The effects of ageing without obesity (silhouetted figure on the left) and ageing combined with obesity (silhouetted figure on the right) to increase or decrease the secretion and/or circulating abundance of these cytokines is indicated by thick black upward or downward-pointing arrows, respectively. Two upward arrows indicate a greater effect of obesity on the relevant cytokine with ageing. A question mark indicates an unknown effect. An inhibitory line extending from a running figure indicates that the proposed effect of ageing is offset when physical activity level is maintained with ageing. An inhibitory line extending to a cytokine receptor indicates that an increased abundance of that cytokine is associated with a reduction in expression of its receptor in skeletal muscle. *Created with BioRender.com and published in Wilhelmsen, Tsintzas, and Jones (2021).*

5.2 Aims

This study employed *ex vivo* techniques to generate adipose-conditioned medium that captures the adipose tissue secretome from middle-age and older adults with and without obesity. Firstly, adipose tissue secretome from lean and obese adults was applied to human primary myogenic cultures throughout their differentiation, in order to investigate its effects on the regulation of myostatin expression; insulin sensitivity; and indices of myogenesis, and whether these effects were altered by exposure to the obese secretome. Secondly, an assessment of the relative abundances of a selection of cytokines known to form part of the adipose tissue secretome was undertaken to identify the existence of any fundamental differences in the secretomes of lean and obese adipose tissue.

5.3 Methods

Participants

Due to the COVID-19 pandemic preventing the undertaking of human research when experiments for this chapter commenced, commercially sourced primary human myoblasts (Gibco: HSkM cells) from a young Caucasian donor were used for the first independent donor repeat. For the subsequent generation of primary myogenic cultures, n = 4 healthy young volunteers were recruited in house, while cryopreserved myoblasts from older donors, were obtained from the Jones Laboratory. Myogenic cultures from a total of n = 5 donors (3 young, 2 older) were used for the experiments detailed below (Table 5.2). All donors used in this experimental series were of normal weight.

Adipose tissue secretomes were captured through the exposure of differentiation medium to adipose tissue samples (adipose-conditioned medium; ACM) derived from volunteers recruited by collaborators from the Jones Laboratory, from lean and obese osteoarthritis (OA) patients undergoing total knee or hip joint replacement surgery, as described in Chapter 2.

Generation of Adipose-Conditioned Medium

The majority of the adipose-conditioned medium (ACM) used in this chapter was obtained intraoperatively from collaborators in the Jones Laboratory at the University of Birmingham, however some was generated fresh in-house when substantial subcutaneous adipose tissue (SAT) was concurrently extracted during muscle biopsies from donors with obesity for the generation of myogenic cultures used in other chapters of this thesis. Subcutaneous adipose tissue samples were obtained as previously described and adipose-conditioned differentiation medium was generated as detailed in Chapter 2 (section 2.4.2).

Previous work from our group (O'Leary et al., 2018) applied adipose tissue secretome (in the form of ACM) generated from individual donors to myoblasts from a different set of individual donors. This approach requires large volumes of ACM from each donor, limiting the number of independent donor repeats and treatment replicates that are possible. To mitigate the limited availability of ACM from some donors (owing to small adipose tissue samples), and the availability of samples at different times; samples from multiple donors were pooled together into either Lean or Obese pools according to donor phenotype (matching Lean and Obese for age, stature, and sex distribution, but not body mass or BMI).

Following the generation of the first Lean and Obese ACM pools, subsequent donor selections were made to match the donor characteristics of the new pools to those of the first pools. In this way, three pools of Lean and Obese ACM were generated, each comprising ACM from highly comparable sets of Lean or Obese donors. Thus, the mean characteristics of the donors used to generate all three pools of Lean ACM were matched for all measured descriptive characteristics, and all three pools of Obese ACM were similarly matched, such that no significant differences in any characteristic were present within the three pools of Lean or within the three pools of Obese ACM. Conversely, between the Lean and Obese pools, there were always significant differences in body mass and BMI, such that Obese always had consistently greater body mass and BMI than Lean (Table 5.1). This methodology was employed with the aim of better enabling identification of cytokines that are differentially secreted by SAT in obesity, by minimising the chances of Type 1 errors arising from the inter-individual variability of adipose tissue secretomes.

Table 5.1. Descriptive characteristics of donors of donors of subcutaneous adipose tissue used for the generation of multiple pools of Lean and Obese adipose-conditioned medium.

	First Pools		Second Pools		Third Pools		Two-way ANOVA		All Pools Combined	
	Group Mean (± SD)		Group Mean (± SD)		Group Mean (± SD)		Main Effect (*P*)		Group Mean (± SD)	
	Lean	Obese	Lean	Obese	Lean	Obese	Adiposity	Pool	Lean	Obese
Male/Female (n)	3/3	3/3	3/4	3/7	2/4	2/3	-	-	7/11	5/10
Age (yrs)	69 ± 8	73 ± 7	70 ± 13	70 ± 6	69 ± 9	64 ± 16	0.953	0.565	70 ± 10	68 ± 10
Height (m)	1.69 ± 0.06	1.68 ± 0.10	1.67 ± 0.12	1.65 ± 0.09	1.62 ± 0.07	1.67 ± 0.07	0.807	0.548	1.65 ± 0.09	1.66 ± 0.08
Body Mass (kg)	67.9 ± 7.6	88.3 ± 13.9****	69.6 ± 8.3	88.2 ± 11.5****	62.4 ± 7.9	95.1 ± 15.4****	**<0.0001**	0.995	66.3 ± 8.1	90.5 ± 12.8
BMI (kg·m^{-2})	23.9 ± 1.3	31.2 ± 3.4****	24.9 ± 0.9	32.3 ± 3.3****	23.8 ± 1.5	33.8 ± 3.1****	**<0.0001**	0.466	24.2 ± 1.4	32.8 ± 3.2
Waist (cm)	86.4 ± 2.5	106.5 ± 6.3***	88.2 ± 12.2	103.8 ± 6.8***	88.7 ± 8.3	104.2 ± 17.1***	**<0.0001**	0.976	88.0 ± 9.5	104.0 ± 10.9
Hip (cm)	102.0 ± 6.1	114.3 ± 6.0****	100.2 ± 9.4	117.4 ± 6.3****	97.7 ± 6.8	116.0 ± 11.2****	**<0.0001**	0.783	99.7 ± 7.9	116.9 ± 8.0

Main effects are two-way (pool x adiposity) ANOVA. Post-hoc comparisons are Tukey's multiple comparisons. Significantly different from Lean, within respective Pool: ***P < 0.001, ****P <0.0001. Note: A small volume of ACM, from a few donors used in the first pools, was also used in the second pools to generate a sufficient volume of ACM for the desired experimental plan. Hence, the number of donors (n) when all pools are combined is slightly lower than the sum of the number of donors used in each pool. The ACM which was common to both the first and second pools, only contributed 4% and 26% of the total pooled volume for Lean and Obese ACM in the second pools, respectively.

Assessment of Adipokines Within Adipose-Conditioned Medium

The relative protein abundance of 58 human cytokines known to be expressed by adipose tissue (adipokines) and related to obesity, were assessed in all pools of Lean and Obese ACM using a commercially available human adipokine array kit, as described in Chapter 2 (2.8.8). For each set of pools, the corresponding Lean and Obese ACM samples were assayed and visualised concurrently. To assess the relative contribution of the 6% HS within the media to the abundance of adipokines within the generated ACM, two samples of unconditioned (Control) medium, using two different batches of HS, were also assayed. All assays were performed identically, and a template was made for quantification to minimise sources of variation and allow comparisons within and between pools of ACM.

Culture and Differentiation of Primary Myoblasts with ACM

Myogenic cultures were established from cells derived from five unique individuals (independent donor repeats), in accordance with the methods described in Chapter 2 (2.2.2 through 2.2.6). Upon reaching near confluence, myoblasts were switched to either unconditioned (Control) or adipose-conditioned (Lean or Obese) differentiation medium. In accordance with prior work from our group (O'Leary et al., 2018) freshly thawed ACM (from either the first, second, or third pools) was diluted 1:2 with fresh differentiation medium to ensure sufficient nutrient availability. In all cases, media was renewed ever 48 h for a total of 6 days.

Radio-Labelled Glucose Uptake

Glucose uptake was measured in the basal and insulin-stimulated state using the radio-labelled technique as described previously in Chapter 2 (section 2.5.2). Adipose-conditioned media was not added to the serum-free starvation media, nor the reaction buffer to which labelled glucose was added for assaying. Each experimental treatment was replicated over 4-6 wells. Glucose uptake was only assayed in n = 3 independent donor repeats, owing to the volume of ACM required, since for this assay cells are cultured in 6-well plates. For one independent donor repeat (HSkM) Control treatments were not used, due to an insufficient number of available myoblasts when maintaining the maximum of 2 passages.

mRNA Expression

Cells were harvested using Tri-Reagent, prior to RNA extraction and cDNA synthesis using standard procedures as described in Chapter 2 (2.8.1 through 2.8.5). For each independent donor repeat, experimental treatments were

replicated over 3 wells. Genes of interest were quantified using the relative standard curve method, with the gene of interest normalised against the relative abundance of RPLP0, which NormFinder software revealed to demonstrate high stability within and between treatments and donors, under these experimental conditions. Due to substantial variability of the relative expression of several genes between independent donor repeats, data were converted to fold-changes from Control, to allow meaningful statistical comparisons to be made.

Western Blotting

Myotubes were harvested in ice-cold RIPA buffer. As an additional index of insulin sensitivity, myotubes in the first two independent donor repeats were also stimulated with or without 100 nM insulin for 15 min prior to lysis, for the assessment of pAkt:Akt. Western blotting was undertaken as described in Chapter 2 (2.8.6 through 2.8.7).

Amino-Acid Stimulated Protein Synthesis

Amino acid-stimulated protein synthesis was assessed using the SuNSET techniques, as described in Chapter 2 (2.5.6). ACM was not added to the serum-free starvation media, nor transport buffer used for the addition of leucine, glucose and puromycin. SDS-PAGE, immunoblotting (anti-puromycin), Coomassie staining, and densitometric quantification were performed as described previously.

Immunofluorescence Staining and Measurement of Myotube Diameter

For the assessment of myotube morphology, triplicate wells of myotubes were washed, fixed, permeabilised, stained with anti-Desmin and DAPI, and imaged, as detailed in Chapter 2 (2.6). Ten clear images were taken from randomised locations across each well and the diameters of the five largest discernible myotubes in each field were measured in triplicate using ImageJ, as described previously. Thus, myotube diameter data for each treatment condition (Control vs. Lean ACM vs. Obese ACM) of each independent donor repeat reflects 450 measurements of 150 unique myotubes.

Statistical Analysis

All statistical analysis was performed in GraphPad Prism 9. Descriptive data are presented as Mean ± SD, while experimental data are presented as Mean ± SEM of all independent donor repeats combined, or of all treatment repeats for each independent donor repeat. Shapiro-Wilk tests confirmed the normality of all data, thus only parametric analyses were employed. Comparisons of adipose tissue

donor characteristics for Lean vs. Obese and of differences between matched pools, presented in Table 5.1, were performed using two-way ANOVA (Adiposity x Pool) with post-hoc Tukey multiple comparisons. Specific differences in relative cytokine abundance of Lean vs. Obese ACM were assessed via unpaired t-tests.

For comparisons of glucose uptake and Akt phosphorylation status, when all independent donor repeats were combined, effects of ACM and insulin were assessed with two-way (mixed effects) ANOVA (ACM x Insulin). In order to consider glucose uptake responses in each independent donor repeat, separate two-way ANOVAs (main effects: ACM and Donor) were performed for basal and insulin-stimulated uptake. For all other outcomes (myotube diameter, gene and protein expression, and protein synthesis), combined data was handled with repeated measures one-way ANOVA, while considerations of separate independent donor repeats were handled with two-way ANOVA (ACM x Donor).

When considering combined data, significant ANOVA main effects were followed up with post-hoc Fisher's LSD, as only 3 comparisons were planned (Control vs. Lean ACM; Control vs. Obese ACM; and Lean ACM vs. Obese ACM). When considering independent donor repeats data separately, significant main effects were also followed up with Fisher's LSD as each repeat was considered an independent experiment, such that, only the same 3 comparisons were considered within each independent donor repeat. ANOVA results are accompanied in text, where relevant, by their corresponding partial eta squared (n_p^2) values as a measure of effect size. Significant post-hoc differences are presented as fold-changes or percent differences, where relevant (Mean Difference [95% CI] are not presented in this chapter due to the low n of all comparisons making the reporting of such data of limited value). Statistical test results are reported in boxes on each figure, where relevant. Statistical significance was defined as $P < 0.05$. Post-hoc comparisons are indicated on each figure by lines connecting each comparator.

5.4 Results

5.4.1 Adipokine profiling of Lean and Obese subcutaneous adipose tissue secretomes

The relative abundance of 58 cytokines known to be secreted from adipose tissue (adipokines) was determined in all three donor-matched pools of Lean or Obese adipose-conditioned medium. All 58 cytokines were detected within all ACM pools, with a ~40-fold difference in relative abundance between the least (TGF-β1) and most (IL-6) abundant proteins (Figure 5.2). Control media containing 6% HS from two different batches (Figure 5.3; Control; 'Serum 1' and 'Serum 2' columns) demonstrated extremely consistent profiles and far lower abundances of most measured cytokines, confirming that adipose tissue secretome was the source of differences in cytokine abundance between Lean and Obese. Four out of the 58 cytokines assessed demonstrated significant overall differences between the Lean and Obese secretome, while a further 5 demonstrated tendencies ($P < 0.10$) for differences. Obese secretome was found to have significantly greater abundance of Complement Factor D than Lean secretome (6 % greater; $P < 0.05$), and a tendency ($P < 0.10$) for consistently greater abundances of Oncostatin-M (37 % greater). Conversely, Lean secretome had a significantly greater abundance of Endocan (70 % greater; $P < 0.01$), Myeloperoxidase (96 % greater; $P < 0.05$) and Lipocalin 2 (36 % greater; $P < 0.01$), relative to Obese, and a tendency ($P < 0.10$) for consistently greater abundances of Adiponectin, Macrophage Colony Stimulating Factor, Cathespin D and C-Reactive Protein (7, 36, 15 and 25 % greater, respectively). Many other cytokines displayed numerical, but not statistically significant, differences between Lean and Obese secretome, reflecting a degree of variability within and between Lean and Obese secretomes. For ease of visualisation, a heat map of the relative cytokine abundance within all pools is presented in Figure 5.2.

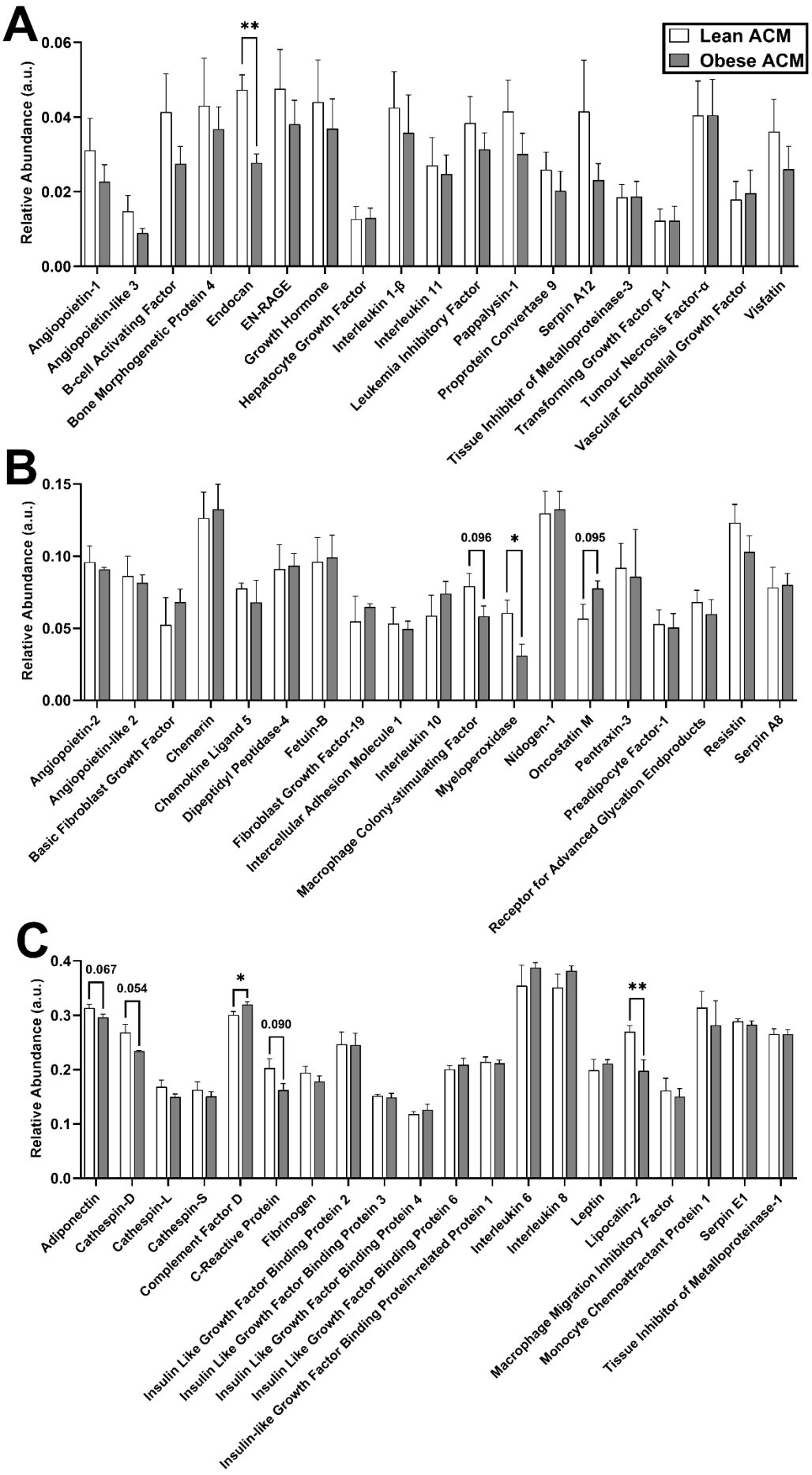
A
Lean ACM
Obese ACM
Relative Abundance (a.u.)
0.00
0.02
0.04
0.06
**
Angiopoietin-1
Angiopoietin-like 3
B-cell Activating Factor
Bone Morphogenetic Protein 4
Endocan
EN-RAGE
Growth Hormone
Hepatocyte Growth Factor
Interleukin 1-β
Interleukin 11
Leukemia Inhibitory Factor
Pappalysin-1
Proprotein Convertase 9
Serpin A12
Tissue Inhibitor of Metalloproteinase-3
Transforming Growth Factor β-1
Tumour Necrosis Factor-α
Vascular Endothelial Growth Factor
Visfatin
B
Relative Abundance (a.u.)
0.00
0.05
0.10
0.15
0.096
*
0.095
Angiopoietin-2
Angiopoietin-like 2
Basic Fibroblast Growth Factor
Chemerin
Chemokine Ligand 5
Dipeptidyl Peptidase-4
Fetuin-B
Fibroblast Growth Factor-19
Intercellular Adhesion Molecule 1
Interleukin 10
Macrophage Colony-stimulating Factor
Myeloperoxidase
Nidogen-1
Oncostatin M
Pentraxin-3
Preadipocyte Factor-1
Receptor for Advanced Glycation Endproducts
Resistin
Serpin A8
C
Relative Abundance (a.u.)
0.0
0.1
0.2
0.3
0.4
0.067
0.054
*
0.090
**
Adiponectin
Cathespin-D
Cathespin-L
Cathespin-S
Complement Factor D
C-Reactive Protein
Fibrinogen
Insulin Like Growth Factor Binding Protein 2
Insulin Like Growth Factor Binding Protein 3
Insulin Like Growth Factor Binding Protein 4
Insulin Like Growth Factor Binding Protein 6
Insulin-like Growth Factor Binding Protein-related Protein 1
Interleukin 6
Interleukin 8
Leptin
Lipocalin-2
Macrophage Migration Inhibitory Factor
Monocyte Chemoattractant Protein 1
Serpin E1
Tissue Inhibitor of Metalloproteinase-1

Figure 5.2. Average relative abundances of adipokines within all three pools of adipose conditioned medium, derived from either Lean or Obese subcutaneous adipose tissue.

The relative abundance of 58 cytokines known to be secreted from adipose tissue (adipokines) was determined using membrane-bound capture antibodies. Adipokines are split into tertiles based on their relative abundance, presented as those with a mean relative abundance of < 0.05 (**A**), 0.05-0.15 (**B**), and >0.15 (**C**) arbitrary unis (a.u). Data are presented as combined Mean ± SEM of duplicate measurements of each adipokine from all three pools of Lean and Obese ACM. Differences in cytokine abundances between Lean and Obese ACM were determined using unpaired t-tests. Significant differences between Lean and Obese: $*P < 0.05$; $**P < 0.01$; or trends for a difference ($P < 0.10$), are indicated where relevant.

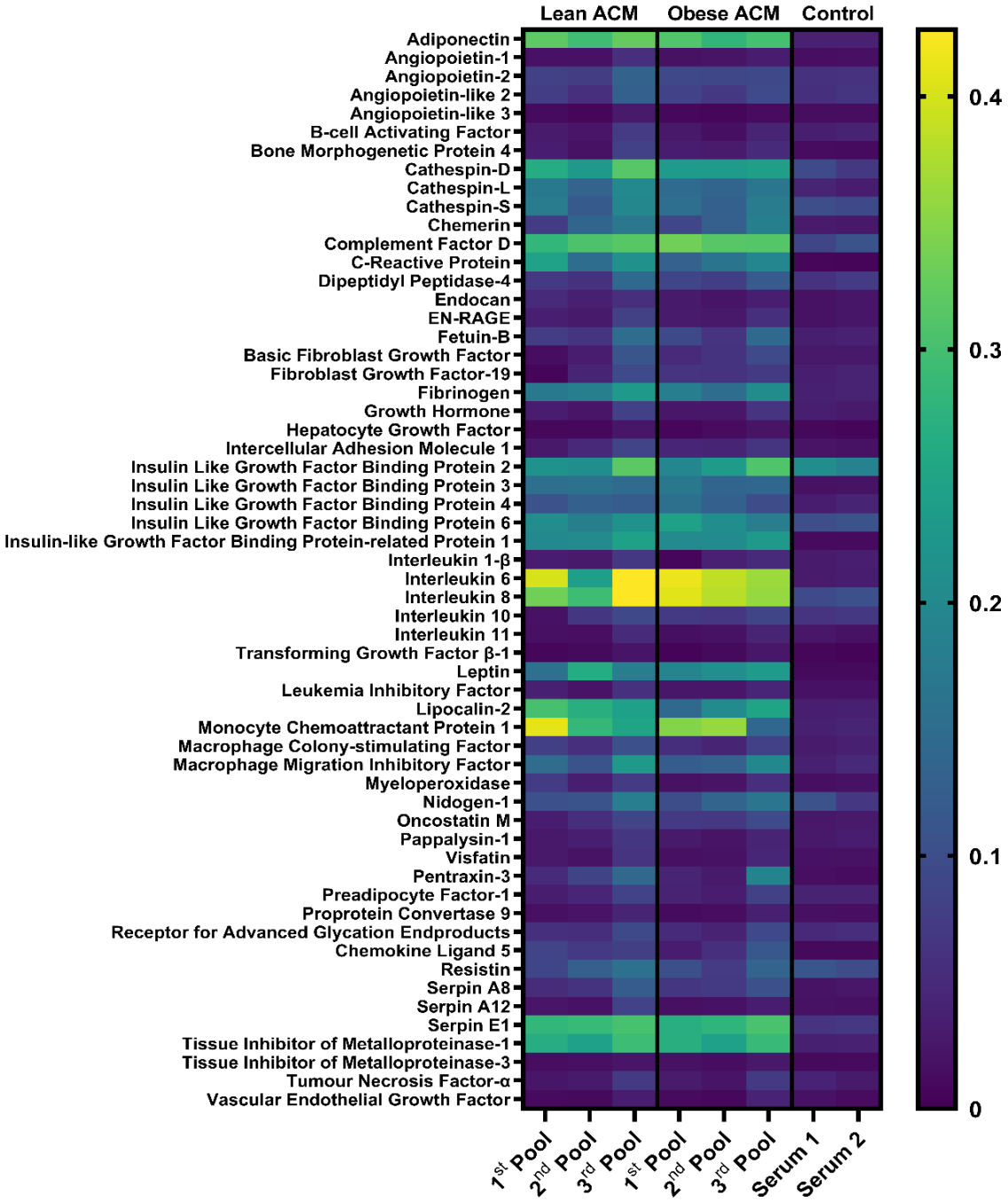

Figure 5.3. Heat map demonstrating the relative abundances of adipokines within each individual pool of ACM, reflecting the subcutaneous adipose tissue secretomes of Lean and Obese donors.

The relative abundance of 58 cytokines known to be secreted from adipose tissue (adipokines) was determined in adipose-conditioned medium and two samples of unconditioned medium containing a different batch of 6% horse serum. Data for each individual pool are presented as individual quadrilaterals on the heat map. Lower relative abundance is indicated by darker, bluer shades, while higher abundance is indicated by brighter, yellower shades.

Table 5.2. Descriptive characteristics of donors of skeletal muscle tissue used for the generation of myogenic cultures, and the pools of adipose conditioned medium that were applied to each respective donor's cells

	Adipose-Conditioned Medium Pools Applied					
	First	Second		Third		
Donor ID	HSkM	MSTN12	MSTN13	MFX182	RHH173	**Mean ± SD**
Sex (M/F)	F	F	F	F	M	1/4
Age (yrs)	'Young'	20	28	63	83	48 ± 30
Height (m)	-	1.69	1.54	1.63	1.75	1.65 ± 0.09
Weight (kg)	-	56.9	54.0	60.9	75	61.7 ± 9.4
BMI ($kg \cdot m^{-2}$)	'Healthy'	19.8	22.8	22.9	24.5	22.5 ± 2.0
Waist (cm)	-	66	71	76	97	78 ± 14
Hip (cm)	-	79	82	97	104	91 ± 12

Note: The cells used in the first set of experiments (HSkM) were commercially sourced and thus, limited characteristic data is available for that donor.

5.4.2 Effects of Lean and Obese subcutaneous adipose tissue secretome on myotube diameter

One-way ANOVA revealed no effect of ACM treatment on mean myotube diameter when all independent donor repeats were combined (n = 4). Thus, the overall mean myotube diameter, was not significantly different between cells exposed to Control, Lean or Obese secretome (13.53 ± 0.64 vs. 13.46 ± 0.53 vs. 13.27 ± 0.73 μm, respectively; Figure 5.4B). When independent donor responses were considered (Figure 5.4C), two-way ANOVA did not reveal an effect of ACM, but a significant effect of donor was found ($P < 0.0001$). Specifically, myotubes derived from the one elderly donor (RHH173) demonstrated tendencies ($P = 0.089$ and $P = 0.084$) for a 6% reduction in diameter following exposure to Obese adipose secretome, relative to both Control and Lean (11.86 ± 0.28 vs. 12.62 ± 0.29 vs. 12.64 ± 0.32 μm, respectively).

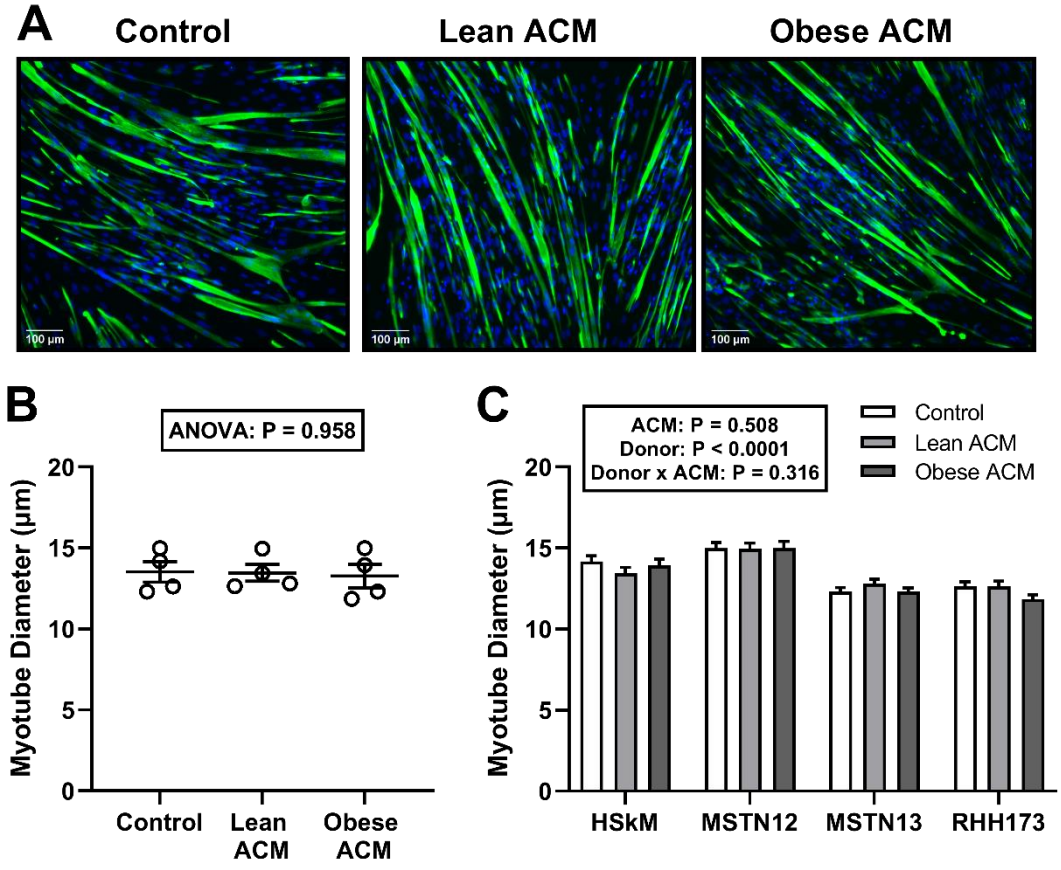

Figure 5.4. Effects of Lean and Obese subcutaneous adipose tissue secretome (ACM) on myotube diameter.

Primary human myotubes from n = 4 independent donors were differentiated in either standard differentiation medium (Control), Lean ACM, or Obese ACM for 6 days, prior to immunofluorescence staining (Desmin [green] and DAPI [blue]) and assessment of mean myotube diameter. Representative micrographs (10x objective; scale bar = 100 µm) of desmin-positive multinucleated myotubes (**A**). No effect of treatment was found when all independent donor repeats were combined (**B**) or considered separately (**C**). Data are presented as Mean ± SEM, with open circles representing independent donor repeats. Each treatment condition for each independent donor repeat comprises 450 measurements of 150 myotubes, from a total of 15 images obtained from 3 replicate wells.

5.4.3 Effects of Lean and Obese subcutaneous adipose tissue secretome on indices of insulin sensitivity

When all independent donor repeats (n = 3) were combined, mixed effects analysis did not reach statistical significance for effects of insulin or ACM treatment, nor an interaction between the two (Figure 5.5A). When considering independent donor repeats, two-way ANOVA revealed significant main effects of ACM treatment ($P < 0.0001$; $n_p^2 = 0.647$) and Donor ($P < 0.0001$; $n_p^2 = 0.756$) on basal glucose uptake. Post-hoc comparisons revealed significantly greater basal glucose uptake following exposure to both Lean and Obese adipose secretome, relative to Control (~1.2- to 1.5-fold; all $P < 0.0001$) in two independent donor repeats (MFX182 and RHH173; both older donors), however no differences between exposure to Lean and Obese secretome were detected in any independent donor repeat (Figure 5.5B). Similarly, two-way ANOVA revealed significant main effects of ACM treatment ($P = 0.001$; $n_p^2 = 0.343$) and Donor ($P < 0.0001$; $n_p^2 = 0.511$) on insulin-stimulated glucose uptake, with significantly greater uptake following Lean secretome treatment relative to Control in RHH173 (1.4-fold greater; $P < 0.05$), and greater uptake with Obese secretome relative to Control in both MFX182 and RHH173 (1.1-fold and 1.5-fold greater, respectively; both $P < 0.05$). No differences were detected between the effects of Lean and Obese secretomes in any independent donor repeat (Figure 5.5C).

When all independent donor repeats (n = 2) were combined, mixed effects analysis revealed significant effects of both insulin ($P < 0.001$; $n_p^2 = 0.978$) and ACM ($P = 0.011$; $n_p^2 = 0.895$) treatment on Akt phosphorylation (pAkt:Akt ratio) but not an interaction between the two (Figure 5.5D). Post hoc tests revealed a tendency for greater basal pAkt:Akt ratio after exposure to both Lean and Obese secretome relative to Control ($P = 0.072$ and $P = 0.074$, respectively) as well as significantly greater insulin-stimulated pAkt:Akt ratio after both Lean and Obese secretome, relative to Control (both $P < 0.001$). However, no differences were revealed between the effects of Lean and Obese secretome on either basal or insulin-stimulated pAkt:Akt ratio.

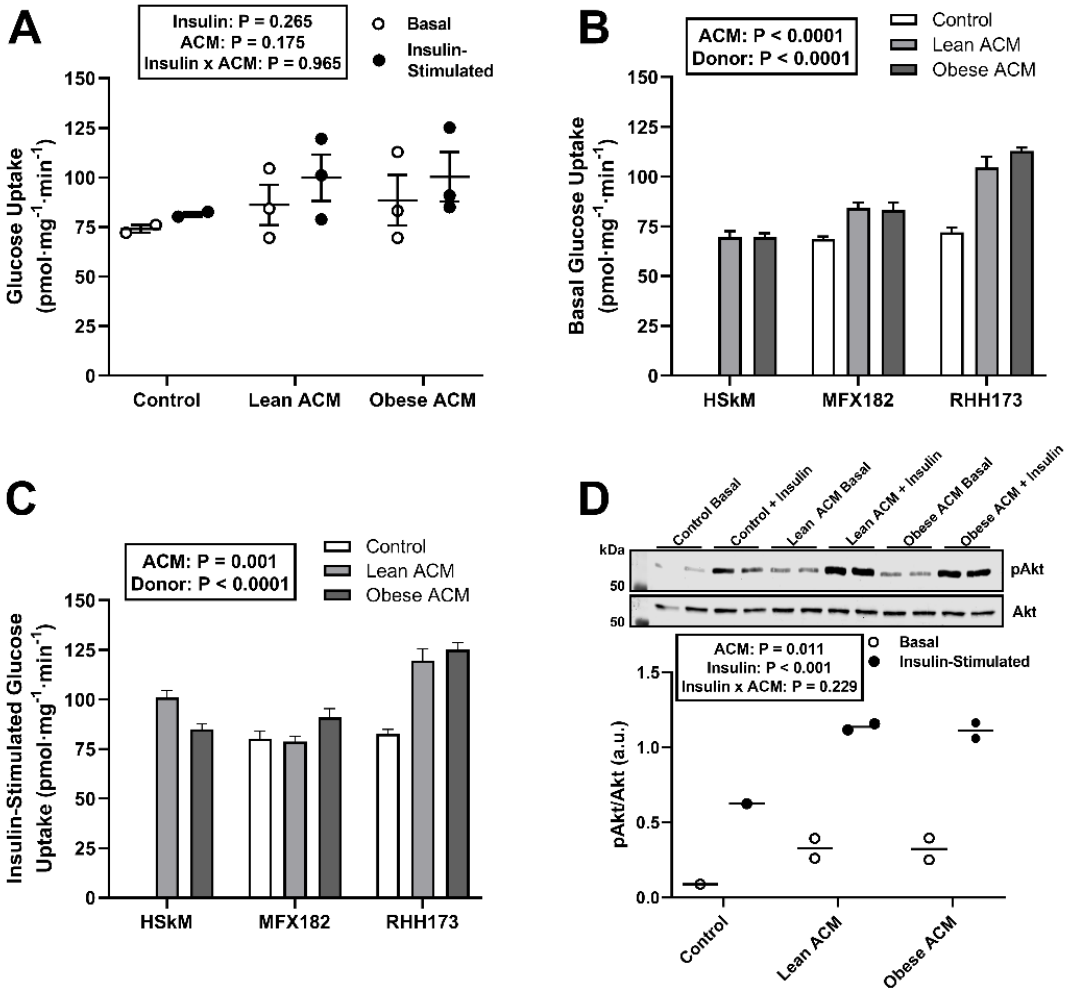

Figure 5.5. Effects of Lean and Obese subcutaneous adipose tissue secretome (ACM) on indices of insulin sensitivity in myotubes.

When all independent donor repeats were considered (n = 3), no effects of ACM or insulin, nor an interaction between the two, were found for glucose uptake (**A**). When considering independent donor responses, significant effects of ACM Treatment and Donor on Basal (**B**) and insulin-stimulated (**C**) glucose uptake were revealed. A consistent pattern in the activation status of Akt (pAkt:Akt ratio) (n = 2) was detected via western blot (representative blot shown) (**D**). Data are presented as Mean ± SEM, with open circles representing independent donor repeats. Post-hoc comparisons of Control vs. Lean/Obese ACM are not displayed. Note: one experimental repeat did not include Control treatment, thus not all comparisons are of equal n.

5.4.4 Effects of Lean and Obese Subcutaneous adipose tissue secretome on the mRNA and protein expression of myostatin and associated factors

When all independent donor repeats were combined (n = 4), one-way ANOVA revealed a significant effect of treatment on myostatin mRNA expression (P < 0.0001; n_p^2 = 0.927) (Figure 5.6A), with lower expression following exposure to both Lean and Obese SAT secretome, relative to Control (0.4- and 0.5-fold lower, respectively; P < 0.001 for both comparisons) and a tendency for a difference between the effects of Lean and Obese secretome (P = 0.084). When considering independent donor responses; two-way ANOVA revealed significant effects of treatment (P < 0.0001; n_p^2 = 0.879) and donor (P = 0.002; n_p^2 = 0.327), and an interaction between the two (P = 0.009; n_p^2 = 0.364) (Figure 5.6B). Relative to Control, Obese secretome suppressed myostatin expression significantly more than Lean secretome in 3 out of 4 independent donor repeats.

When combined (n = 4), one-way ANOVA did not reveal a significant treatment effect on the myostatin receptor, ACVR2B (Figure 5.6C). When considering independent donor responses; two-way ANOVA revealed significant effects of treatment (P < 0.001; n_p^2 = 0.392) and donor (P < 0.001; n_p^2 = 0.414), and an interaction between the two (P < 0.001; n_p^2 = 0.169) (Figure 5.6D). Relative to Control, Lean adipose secretome significantly increased the expression of ACVR2B in two independent donor repeats (MFX182 and RHH173; both older donors), while Obese secretome increased ACVR2B expression relative to Lean secretome in RHH173 (the eldest donor) (Figure 5.6D).

When combined (n = 4), ANOVA revealed no effect of treatment on the abundance of the mature myostatin protein (~26 kDa), nor the signal transducer SMAD2, either when all independent donor repeats were combined or considered individually (Figure 5.7A, B, C and D).

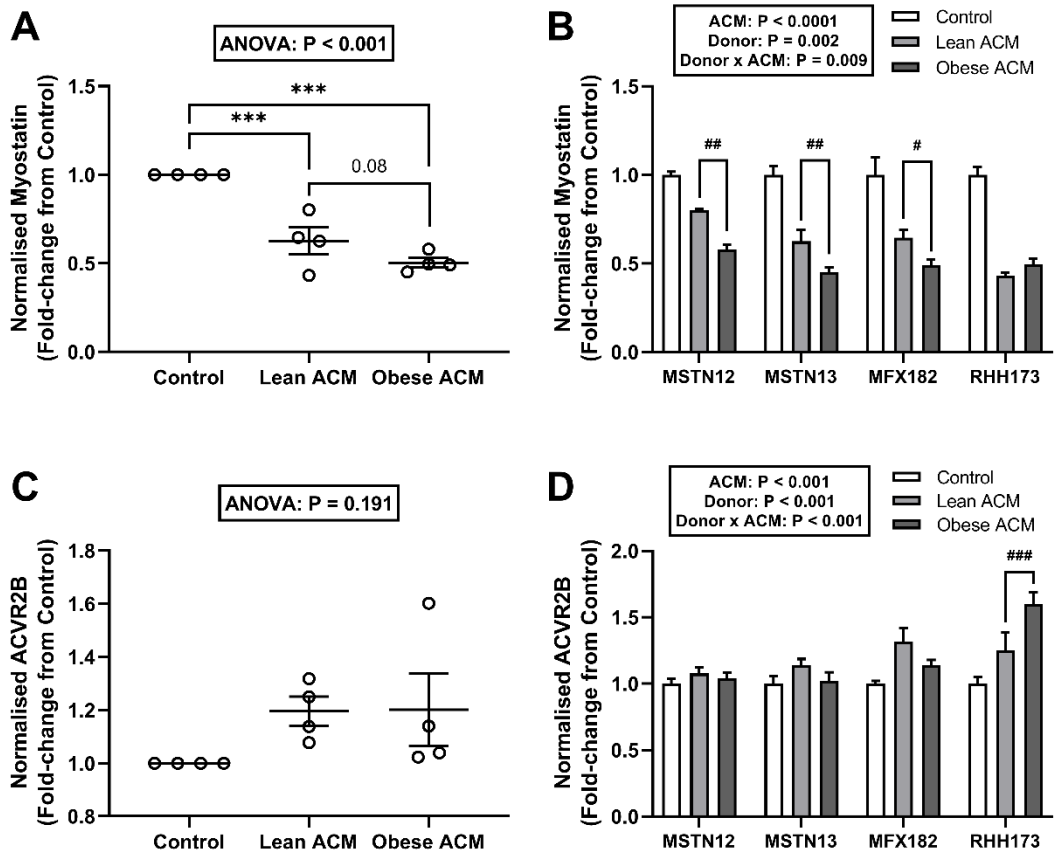

Figure 5.6. Effects of Lean and Obese subcutaneous adipose tissue secretome (ACM) on the mRNA expression of myostatin and its receptor in myotubes.

When all independent donor repeats were combined (n = 4), a significant effect of treatment on myostatin mRNA expression was found (**A**). When considering independent donor responses; significant effects of treatment, donor, and an interaction between the two were revealed (**B**). Expression ACVR2B was not affected by treatment when all independent donor repeats (n = 4) were combined (**C**), however when considering independent donor responses; significant effects of treatment, donor, and an interaction between the two were detected (**D**). Data are normalised against RPLP0 expression and presented as Mean ± SEM fold-change from Control, with open circles representing independent donor repeats. Post-hoc comparisons are Fisher's LSD. Significantly different from Control: ***P < 0.001. For independent donor responses, only significant differences between Lean and Obese ACM are presented: $^{\#}P$ < 0.05; $^{\#\#}P$ < 0.01, $^{\#\#\#}P$ < 0.001.

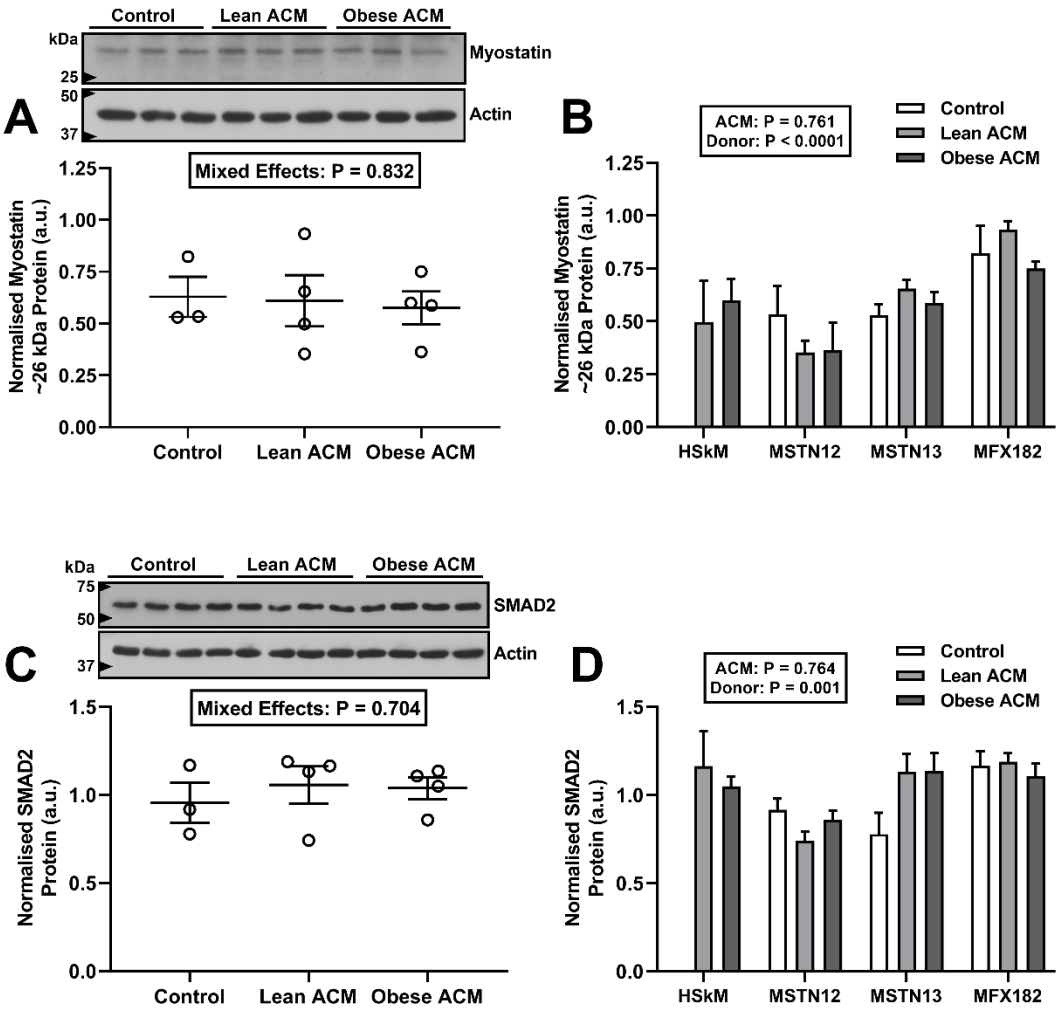

Figure 5.7. Effects of Lean and Obese subcutaneous adipose tissue secretome (ACM) on myostatin and SMAD2 protein expression in myotubes.

When all independent donor repeats were combined (n = 4), no effect of treatment on myostatin protein abundance was found (representative blot is shown above) (**A**). When considering independent donor responses; an effect of donor but not treatment was found (**B**). Protein abundance of SMAD2 was not affected by treatment when all independent donor repeats were combined (n = 4) (representative blot is shown above) (**C**) or considered individually (**D**). Data are presented as Mean ± SEM of normalised protein of interest abundance, with open circles representing independent donor repeats. Note: one experimental repeat did not include Control treatment, thus not all comparisons are of equal n.

5.4.5 Effects of Lean and Obese subcutaneous adipose tissue secretome on amino acid-stimulated protein synthesis

When all independent donor repeats were combined (n = 3), ANOVA revealed no effect of ACM treatment on amino acid-stimulated (2 mM L-leucine) myotube protein synthesis, as indicated by the relative incorporation of puromycin into newly synthesised peptides (Figure 5.8A). Similarly, when considering independent donor responses; two-way ANOVA revealed no effect of ACM treatment. While an effect of donor was found (P < 0.0001; n_p^2 = 0.645), no significant difference between Control, Lean, and Obese secretome treatment was revealed in any independent donor repeat (Figure 5.8B).

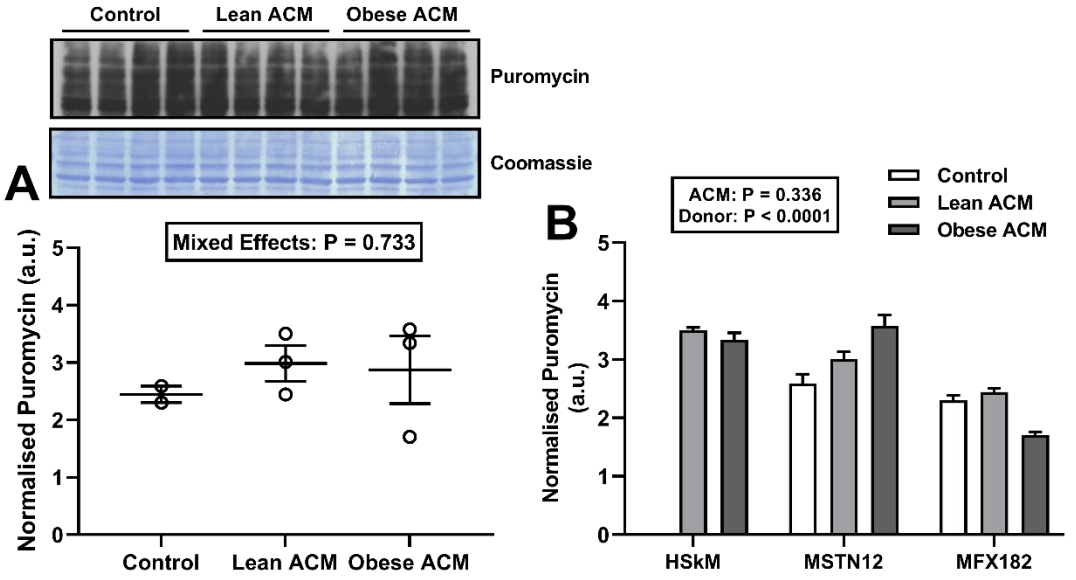

Figure 5.8. Effects of Lean and Obese subcutaneous adipose tissue secretome (ACM) on amino acid-stimulated protein synthesis in myotubes.

When all independent donor repeats were combined (**A**; n = 3) or considered separately (**B**) no overall effect of ACM treatment on amino acid-stimulated protein synthesis was detected (**A**). Data are presented as Mean ± SEM of puromycin normalised against Coomassie, with open circles representing independent donor repeats. A representative blot is shown above A. Note: one experimental repeat did not include Control treatment, thus not all comparisons are of equal n, and such discrepancies are labelled within each respective bar of the figure.

5.4.6 Effects of Lean and Obese subcutaneous adipose tissue secretome on the mRNA expression of myogenic regulatory factors and E3 ubiquitin ligases

When all independent donor repeats were combined (n = 4), one-way ANOVA revealed no effect of treatment on MYOD mRNA expression (Figure 5.9A). When considering independent donor responses; two-way ANOVA revealed significant effects of treatment ($P < 0.0001$; $n_p^2 = 0.651$) and donor ($P < 0.0001$; $n_p^2 = 0.724$), and an interaction between the two ($P < 0.0001$; $n_p^2 = 0.820$) (Figure 5.9B). MYOD expression was greater after Lean secretome exposure than both Control and Obese secretome in two independent donor repeats (MSTN12 and MSTN13; both younger donors), while one repeat (RHH173; elderly donor) exhibited greater MYOD expression after Obese secretome exposure, compared to Lean.

When combined (n = 4) no effect of treatment was found on MYOG mRNA expression (Figure 5.9C). When considering independent donor responses; significant effects of treatment ($P < 0.001$; $n_p^2 = 0.399$) and donor ($P = 0.016$; $n_p^2 = 0.259$) were revealed (Figure 5.9D). MYOG expression was greater after Lean secretome exposure than Obese secretome exposure in two repeats (MSTN12 and MSTN13; both younger donors), while akin to MYOD, one repeat (RHH173; elderly donor) exhibited greater expression after Obese secretome, compared to Lean. Comparisons between Lean and Obese secretome on MYOG in one repeat (MFX182) could not be made on account of unsuccessful amplification of the Obese ACM-treated samples and insufficient primer/probe mix to repeat the qPCR assay.

No effect of treatment on combined (n = 4) MuRF1 mRNA expression (Figure 5.9E) was identified. When considering independent donor responses; significant effects of treatment ($P < 0.001$; $n_p^2 = 0.351$) but not donor, and an interaction between the two ($P = 0.002$; $n_p^2 = 0.417$) were revealed (Figure 5.9F). MuRF1 expression was greater after Lean secretome than both Control and Obese secretome in three out of four independent donor repeats, while one repeat (RHH173; elderly donor) exhibited greater MuRF1 expression after Obese secretome, compared to Lean.

No effect of treatment was found on combined (n = 4) MAFbx mRNA expression (Figure 5.9G), however when considering independent donor responses, significant effects of treatment ($P = 0.018$; $n_p^2 = 0.200$) and donor ($P = 0.001$; $n_p^2 = 0.357$) and an interaction between the two ($P < 0.001$; $n_p^2 = 0.510$) were found (Figure 5.9H). MAFbx expression was significantly increased by Obese secretome relative to Lean in one repeat (MFX182; older donor) and was numerically greater than Lean (and significantly greater than Control) in the elderly repeat (RHH173).

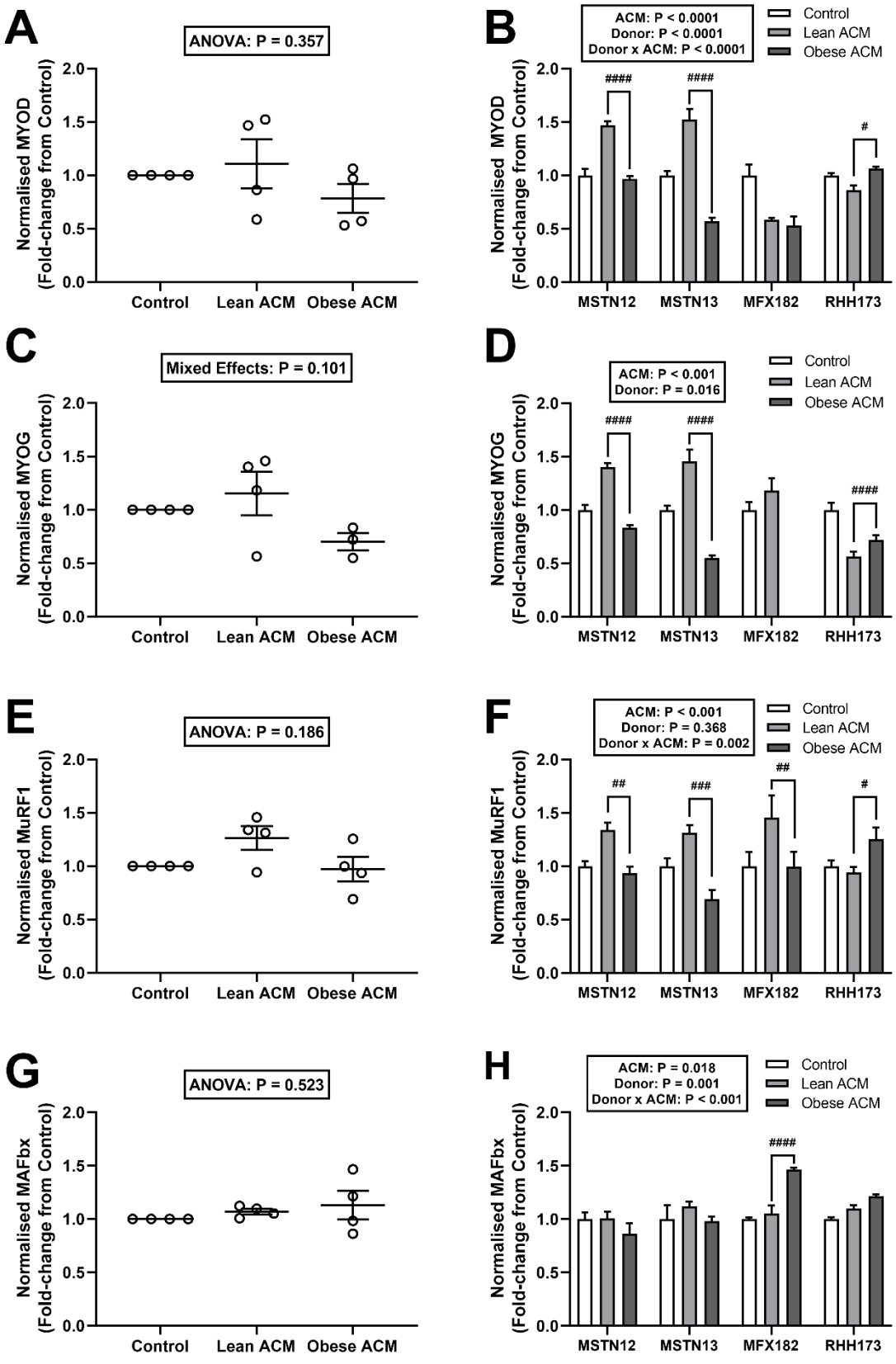
A
ANOVA: P = 0.357
Normalised MYOD (Fold-change from Control)
Control
Lean ACM
Obese ACM
B
ACM: P < 0.0001
Donor: P < 0.0001
Donor x ACM: P < 0.0001
Control
Lean ACM
Obese ACM
Normalised MYOD (Fold-change from Control)
MSTN12
MSTN13
MFX182
RHH173
C
Mixed Effects: P = 0.101
Normalised MYOG (Fold-change from Control)
D
ACM: P < 0.001
Donor: P = 0.016
E
ANOVA: P = 0.186
Normalised MuRF1 (Fold-change from Control)
F
ACM: P < 0.001
Donor: P = 0.368
Donor x ACM: P = 0.002
G
ANOVA: P = 0.523
Normalised MAFbx (Fold-change from Control)
H
ACM: P = 0.018
Donor: P = 0.001
Donor x ACM: P < 0.001

Figure 5.9. Effects of Lean and Obese subcutaneous adipose tissue secretome (ACM) on the mRNA expression of myogenic regulatory factors and E3 ubiquitin ligases in myotubes.

When all independent donor repeats were combined (n = 4), no effect of treatment was revealed on the expression of the myogenic regulatory factors, MYOD (**A**) and MYOG (**C**), nor the E3 ubiquitin ligases, MuRF1 (**E**) and MAFbx (**G**). However, when independent donor responses were considered, significant treatment effects and treatment x donor interactions were revealed for MYOD, MuRF1 and MAFbx (**B**, **F**, and **H**, respectively), while main effects of treatment and donor were revealed for MYOG (**D**). Data are normalised against RPLP0 expression and presented as Mean ± SEM fold-change from Control treated cells, with open circles representing independent donor repeats. Post-hoc comparisons are Fisher's LSD. For independent donor responses, only significant differences between Lean and Obese ACM are presented: $^{\#\#}P < 0.01$; $^{\#\#\#}P < 0.001$; $^{\#\#\#\#}P < 0.0001$.

5.4.7 Effects of Lean and Obese subcutaneous adipose tissue secretome on inflammatory marker mRNA expression

When all independent donor repeats were combined (n = 4), one-way ANOVA revealed no effect of treatment on IL-6 mRNA expression (Figure 5.10A). When considering independent donor responses; two-way ANOVA revealed significant effects of treatment ($P < 0.0001$; $n_p^2 = 0.698$), donor ($P < 0.0001$; $n_p^2 = 0.705$) and their interaction ($P < 0.0001$; $n_p^2 = 0.831$) (Figure 5.10B). Post-hoc comparisons demonstrated that IL-6 expression was significantly greater after exposure to Obese adipose secretome than Lean secretome in the two younger independent donor repeats (MSTN12 and MSTN13), while the opposite was true in the two older independent donor repeats (MFX182 and RHH173), such that IL-6 was upregulated by the Obese secretome relative to Lean.

When combined (n = 4), no effect of treatment on IL-1β mRNA expression was found (Figure 5.10C), however when assessing independent donor responses significant effects of treatment ($P < 0.0001$; $n_p^2 = 0.746$), donor ($P = 0.0017$; $n_p^2 = 0.244$) and an interaction ($P < 0.0001$; $n_p^2 = 0.773$) were revealed (Figure 5.10D). Responses in IL-1β expression were similar to those of IL-6. Expression was significantly greater after Obese secretome than Lean secretome in the two younger independent donor repeats (MSTN12 and MSTN13), while the inverse was true in the two older independent donor repeats (MFX182 and RHH173).

When combined (n = 4), no effect of treatment was revealed on TNF mRNA expression (Figure 5.10E). When assessing independent donor responses; no effect of treatment but an effect of donor ($P < 0.0001$; $n_p^2 = 0.476$) and an interaction between the two was found ($P < 0.001$; $n_p^2 = 0.462$) (Figure 5.10F). Effects of adipose tissue secretome on TNF expression were varied, with two independent donor repeats demonstrating significantly greater TNF expression following exposure to Obese secretome relative to Lean (MSTN13 and RHH173), while one independent donor repeat exhibited significantly lower expression after Obese secretome, relative to Lean (MFX182).

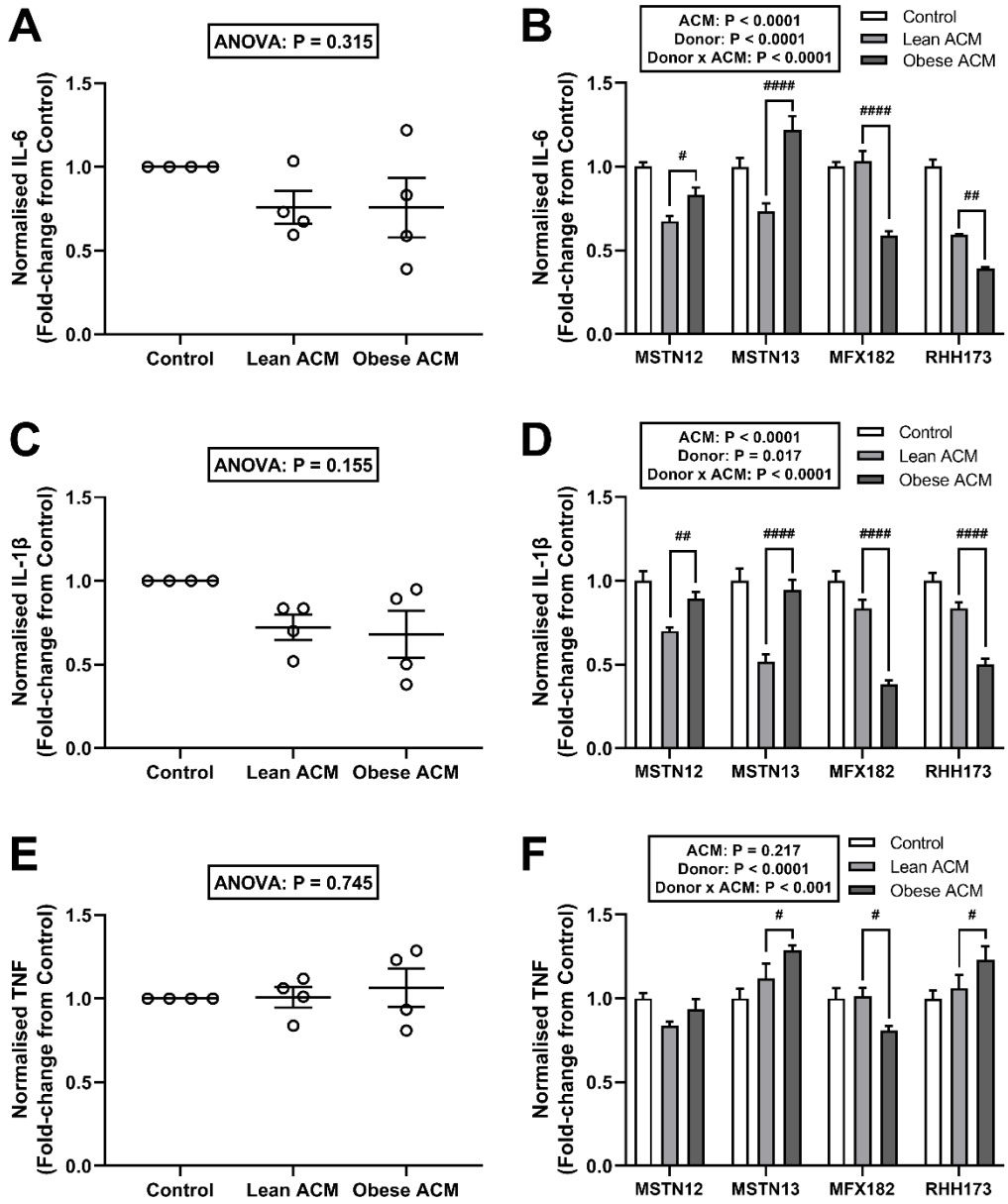

Figure 5.10. Effects of Lean and Obese subcutaneous adipose tissue secretome (ACM) on the mRNA expression of inflammatory markers in myotubes.

When all independent donor repeats were combined (n = 4), no effect of treatment on the expression of IL6 (**A**), IL-1β (**C**), or TNF (**E**) were found. When independent donor repeat responses were considered, significant effects of treatment and donor, and treatment x donor interactions were revealed for IL-6 and IL-1β (**B** and **D**), while no effect of treatment, but donor and interaction effects were revealed (**F**). Data are normalised against RPLP0 expression and presented as Mean ± SEM fold-change from Control treated cells, with open circles representing independent donor repeats. Post-hoc comparisons are Fisher's LSD. For independent donor responses, only significant differences between Lean and Obese ACM are presented: $^{\#}P < 0.05$; $^{\#\#}P < 0.01$; $^{\#\#\#\#}P < 0.0001$.

5.5 Discussion

The most notable finding of this study was the overall suppression of myostatin mRNA, but not protein, expression when primary human myotubes were differentiated for 6 days in SAT secretome derived from both Lean and Obese adults, relative to unconditioned medium (Control). This suppression tended to be greatest when myotubes were exposed to the Obese secretome relative to the Lean secretome and was not accompanied by significant changes in basal or insulin-stimulated glucose uptake when all independent donor repeats were considered, although both Lean and Obese adipose secretome enhanced basal and insulin-stimulated phosphorylation of Akt, relative to Control. For all measured outcomes, independent donor repeats displayed substantial variability, possibly reflecting the age of the donors from which myogenic cultures were established. Indeed, myotubes derived from the two younger donors, but not the 2 older donors, demonstrated robust and statistically significant increased expression of promyogenic genes (MYOD and MYOG) in response to Lean adipose secretome, relative to Obese secretome.

Effects of Lean and Obese Subcutaneous Adipose Tissue Secretome on the Expression of Myostatin and Genes Involved in Myogenic Regulation

Relative to unconditioned medium, the SAT secretome from both Lean and Obese donors suppressed the mRNA expression of myostatin by 40% and 50%, respectively. The suppressive effect of Obese adipose secretome tended to be greater than that of the Lean secretome. Neither the Lean nor Obese adipose secretome-mediated suppression of myostatin mRNA was accompanied by changes in mature myostatin protein expression, myotube protein synthesis or mean myotube diameter. Given the role of myostatin in blocking myoblast differentiation and protein synthesis via the down-regulation of muscle regulatory factors (Langley et al., 2002; Craig McFarlane et al., 2011); the promotion of muscle protein degradation via the up-regulation of E3 ligases (C. McFarlane et al., 2006); and the observation of obesity-mediated upregulation of myostatin in skeletal muscle in Chapter 3, it is surprising that under these experimental conditions, the obese SAT secretome conferred the opposite effect. It is interesting to recall, however, that concurrent with the reduction in myostatin expression in the present study, neither the Lean nor Obese adipose tissue secretome induced insulin resistance, but rather enhanced glucose handling and insulin-stimulated Akt phosphorylation in some independent donor repeats. Thus, the association between changes in myostatin expression and insulin sensitivity was still

demonstrated but was not influenced by the donor phenotype of the adipose tissue secretome.

Despite inducing greater suppression of myostatin mRNA expression, the Obese SAT secretome downregulated MYOD and MYOG expression, relative to the Lean adipose secretome, significantly in two independent donor repeats and numerically in another. One possible cause for these seemingly dichotomous findings might be that all the donors from whom myogenic cultures were established in this study, were of normal weight, rather than obese. It is plausible that chronic exposure of normal weight donor myotubes to the obese adipose secretome could elicit a protective feedback loop, since myostatin auto-regulates its promoter through negative feedback inhibition (Forbes et al., 2006). Furthermore, while myostatin ligand binding induces suppression of MRFs, myostatin itself is a downstream target of MYOD, which preferentially upregulates myostatin promoter activity (Spiller et al., 2002). Thus, upregulation of MYOD can promote myostatin expression. Indeed, the three independent donor repeats that demonstrated lower expression of MYOD following Obese ACM, were also the three that exhibited lower expression of myostatin. Therefore, by day 6 of ACM exposure, myostatin may have been suppressed in an attempt to counteract the anti-myogenic insult of the obese secretome. It is also worth considering that relative to Control, the Lean adipose tissue secretome significantly increased MYOD and MYOG expression in myotubes derived from the two younger, but not the two older donors, which may reflect diminished resilience to cytokine insult in muscle cells derived from older donors. This notion is consistent with the finding of O'Leary et al. (2018) who demonstrated that obese ACM impaired myogenesis in myotubes derived from older but not younger donors.

Within the present literature, no comparable studies of the effects of ACM on the regulation of myostatin in primary human myotubes could be found. However, some evidence is available from co-culture studies of adipogenic and myogenic cell lines. Seo, Suzuki, Kobayashi, and Nishimura (2019) co-cultured C2C12 myotubes with mature 3T3-L1 adipocytes for up to 5 days and reported fluctuating perturbations of myogenic gene expression, upregulated E3 ligase expression and increased myostatin protein abundance, relative to an adipocyte-free control after 1, 3 and 5 days of co-culture (~2-, 1.3- and 1.4-fold greater, respectively). After 1 day of co-culture, the differences between Control and co-cultured cells were most pronounced, with suppression of MYOD, MYOG and myosin heavy chain (MHC) at both the mRNA and protein level, with simultaneous upregulation of the protein content of MuRF1 and MAFbx. Interestingly, the change in expression of

most of these markers reversed over the course of the 5 days, such that their levels either nearly returned to, or surpassed, their baseline values (for instance, by day 5, MYOG protein abundance was no longer suppressed, but rather, was upregulated). Unlike the present study, myotube diameter was reduced by almost half in the presence of co-cultured adipocytes. It is important to note that adipocytes were seeded at an equal density to myoblasts and were co-cultured on inserts within the myotube wells, such that approximately twice as many cells were sharing the same static nutrient pool.

Sell et al. (2008), exposed primary human myotubes to adipocyte-conditioned mean (CM) derived from mammary fat of normal weight and moderately overweight donors (Mean ± SD BMI: 24.5 ± 0.9 $kg \cdot m^{-2}$) for 48 h and reported downregulated MYOD, MYOG and MHC, relative to unconditioned medium. Similarly, Pellegrinelli et al. (2015) demonstrated that co-culture of myotubes with obese donor visceral adipocytes for 24 h reduced the mRNA expression of MYOD and MYOG, relative to untreated myotubes. In the latter study, this was accompanied by reduced basal phosphorylation of P70-S6 Kinase 1 and Eukaryotic translation initiation factor 4E-binding protein 1 (4E-BP1), and impaired insulin-like growth factor (IGF)-2/IGF binding protein (BP)-5 stimulated Akt phosphorylation, which is indicative of impaired muscle protein synthetic signalling. The authors also reported that obese visceral adipocyte co-culture did not affect the gene expression of MuRF1 or MAFbx. In the present study, Lean, but not Obese SAT secretome, upregulated MuRF1 expression in three out of four independent donor repeats, demonstrating that while the Lean SAT secretome promoted myogenic gene expression in some independent donor repeats, it induced concurrent upregulation of E3 ligase expression, which may in part explain why there was no net change in myotube protein synthesis and diameter.

The potentially beneficial, promyogenic and insulin-sensitising effects demonstrated in the present study when human myotubes were exposed to Lean SAT secretome, relative to Control, has not been reported in co-culture or adipocyte-CM studies. This discrepancy in findings emphasises the different secretory profiles of isolated adipocytes compared to whole human adipose tissue. This supports prior evidence that in normal weight individuals with metabolically healthy adipose tissue, the adipose secretome plays an important role in supporting myogenesis and promoting muscle metabolic health (Gunawardana, 2014). This concept is further exemplified in murine studies, whereby the transplantation of adipose tissue from exercise-trained mice into sedentary mice

exerts beneficial effects on metabolic parameters such as insulin sensitivity (Stanford et al., 2015).

In the absence of an upregulation of myostatin in the present study, which ordinarily suppresses MRF expression via canonical signalling and may promote E3 ligase expression via non-canonical signalling, there are other plausible mechanisms by which the divergent changes in MRF and E3 ligase expression seen following exposure to the Obese adipose secretome, relative to that of Lean, might have been mediated. One such plausible mechanism is the IGF-1/Akt signalling pathway, which stimulates mammalian target of rapamycin (mTOR)-dependent protein synthesis and inhibits the FOXO-dependent transcription of E3 ligases (Bodine et al., 2001; Sartorelli & Fulco, 2004). MRFs are ordinarily induced via the sustained (>24 h) binding and signalling of IGFs, which is concentration dependent (Florini, Ewton, & Roof, 1991), however this regulation is severely perturbed in the face of elevated inflammatory cytokines (Akhmedov & Berdeaux, 2013; Broussard et al., 2004; Broussard et al., 2003). The relative abundance of IGF-BPs, which serve as transport proteins for IGFs and regulate their bioavailability (H. Ding & Wu, 2018), was not significantly different between Lean and Obese ACM, however the abundance of the IGFs themselves was not assessed. IGF-1 is prolifically secreted from human adipocytes and the stromal vascular fraction of adipose tissue and suppresses myostatin expression during myogenic differentiation (Retamales et al., 2015). Free IGF-1, but not IGF-BPs, is reportedly upregulated by obesity (D'Esposito et al., 2012; Frystyk, Skjaerbaek, Vestbo, Fisker, & Orskov, 1999; Nam et al., 1997). This imbalance between IGF-1 and IGFBPs may unfavourably alter the biological activity of IGF-1 since the sequestration of IGFs by different species of IGFBPs can cause both inhibition and potentiation of IGFs actions, however this relationship is complex and remains to be fully elucidated (Bach, 2018).

Effects of Lean and Obese Subcutaneous Adipose Tissue Secretome on Myotube Morphology

Myotube diameter was not significantly affected by either Lean or Obese adipose secretome, however it is interesting to note that the most elderly donor (83 yrs) did exhibit a tendency towards a modest reduction in myotube diameter following exposure to Obese secretome, relative to both Control and Lean secretome. Owing to the novelty of the design of this study, there is little existing data to draw comparisons against. However, O'Leary et al. (2018) similarly reported no effect of 8 days of exposure to Lean or Obese ACM during differentiation on myotube thickness in cells from young donors, but found a significant reduction in the

diameter of myotubes derived from older donors. Together, this suggests that myotubes derived from elderly donors may be more susceptible to deleterious effects of obese SAT secretome on myogenic differentiation. Pellegrinelli et al. (2015) found no effect of 48 h exposure to lean subcutaneous adipocyte-CM on myotube diameter or fusion index, but a detrimental effect of obese visceral adipocyte-CM on diameter, in primary myotubes derived from a new-born infant. This is concordant with the broadly more metabolically deleterious and pro-inflammatory nature of visceral adipose tissue, relative to that of the subcutaneous depot. Indeed, for any given amount of total body fat, relatively greater visceral adiposity significantly increased the risk of the metabolic syndrome (Després & Lemieux, 2006).

Effects of Lean and Obese Subcutaneous Adipose Tissue Secretome on Insulin Sensitivity

In this study, it is shown for the first time that differentiation of primary human myogenic cultures within the presence of SAT secretome from lean or obese donors, does not impair basal or insulin stimulated glucose uptake, but rather when considering independent donor repeats, it was evident that both the Lean and Obese secretome elevated basal, and to a lesser extent, insulin-stimulated glucose uptake relative to Control. However, no differences were found between the effects of the Lean and Obese adipose secretomes. Furthermore, both Lean and Obese secretome enhanced the insulin-stimulated phosphorylation of Akt, but there was no difference between the two types of secretome.

To date, only two studies could be found within the literature that have directly assessed the effects of the whole SAT secretome, via the application of ACM, on myotube glucose uptake (Lam, Hatzinikolas, et al., 2011; Lam, Janovská, et al., 2011). In both studies, Lam et al. treated fully differentiated L6 myotubes with subcutaneous ACM from extremely obese adults. Unlike the present study, however, myotubes were exposed to ACM for only 6 h. Obese ACM treatment at a wide range of dilutions (including 1:2, as employed in the present study), did not alter basal or insulin-stimulated glucose uptake (Lam, Janovská, et al., 2011). Conversely, visceral ACM significantly impaired insulin-stimulated, but not basal, glucose uptake in both studies. Consistently, Sachs et al. (2019) found that treatment of primary myotubes from obese donors, with intramuscular- and visceral- but not subcutaneous ACM generated from obese donors, impaired insulin-stimulated glycogen synthesis. In contrast to the present study, Zoso et al. (2019) reported diminished insulin-stimulated Akt phosphorylation when fully differentiated human myotubes were exposed to obese visceral ACM for 24h,

relative to un-conditioned medium. The ACM used in Zoso's study was derived from a single donor with obesity and applied to myotubes from only two donors, limiting extrapolation of their findings.

More studies have employed either isolated adipocyte-CM or co-culture of adipocytes and skeletal muscle cells (Kuppusamy, Kim, Soundharrajan, Hwang, & Choi, 2021), than treatment of muscle cells with subcutaneous ACM. Such studies are not entirely comparable with the present study, and this must be kept in mind when considering differences in findings. In contrast to the present study, Dietze et al. (2002) demonstrated that co-culture of primary human myotubes and adipocytes for 48 h impaired insulin-stimulated phosphorylation of Akt and IRS-1. In a subsequent study, utilising human adipocyte-CM, the same authors demonstrated impaired insulin-stimulated GLUT4 translocation after adipocyte-CM exposure (Dietze-Schroeder, Sell, Uhlig, Koenen, & Eckel, 2005). Similarly, treatment of primary human myotubes with human adipocyte-CM from multiple donors for 24 h also impaired insulin-stimulated Akt phosphorylation, but did not affect GLUT4 abundance (Sell et al., 2008). In another study, co-culture of primary human myotubes with human adipocytes for 24 h upregulated GLUT1 mRNA expression in myotubes from lean but not obese donors, and GLUT4 expression in myotubes derived from both lean and obese donors, but did not affect insulin-stimulated glucose uptake (Kovalik et al., 2011). More akin to the findings of the present study, co-culture of L6 myoblasts with either primary rat adipocytes or adipocyte-CM elevated basal glucose uptake, which increased with longer incubation and was associated with increased GLUT4 translocation and GLUT1 expression (Vu et al., 2011). It has been proposed that the discrepancy in the effects of adipocyte-CM on insulin sensitivity between Dietze et al. and Vu et al. may be related to the chronic presence of insulin throughout co-culture versus the addition of insulin only prior to metabolic assays (Kudoh, Satoh, Hirai, Watanabe, & Shimabukuro, 2018).

The contrasts of the present study with the limited literature on this topic, and the variability of findings within that literature, may be attributed to several factors. Principally, in the present study, the exposure of primary human myotubes to human ACM, which directly captures the whole SAT secretome, rather than adipocyte-CM or co-culture which only serve to model it, invariably presents a more physiological model of adipose-muscle cross talk, since whole SAT includes the stromal vascular fraction, which is a more prolific secretor of inflammatory cytokines than mature adipocytes (Blaber et al., 2012). Furthermore, myotube co-culture with adipocytes versus adipocyte-CM appears to differentially alter

myotube insulin sensitivity, with reports of co-culture inducing a more deleterious blunting of Akt phosphorylation, suggesting paracrine activity that may not be conferred in conditioned medium (Seyoum, Fite, & Abou-Samra, 2011). Another potential source of variation is muscle tissue donor phenotype when primary human myotubes are used. Indeed, Kovalik and colleagues (2011) demonstrated that co-culture of human adipocytes with primary myotubes from lean, but not obese, donors increased insulin-stimulated pAKT:Akt and glycogen synthesis. While co-culture experiments provide an excellent model of paracrine interactions between muscle and adipose tissue, such as might be seen in the setting of inter/intramuscular adipose accumulation, the methods employed in the present study provide a valuable tool to assess the endocrine impact of excessive whole-body subcutaneous adiposity, by modelling the exposure of human muscle cells to circulating secreted factors.

Effects of Lean and Obese Subcutaneous Adipose Tissue Secretome on Inflammatory Markers and Association With Deleterious Outcomes

While no overall effects of either the Lean or Obese SAT secretome were found on the expression of the classical inflammatory markers IL-6, IL-1β and TNF, akin to the effects seen on the MRFs, a distinct pattern of diverging response was observed between myotubes derived from younger donors and those derived from older donors. To that effect, both IL-6 and IL-1β demonstrated extremely similar patterns of response, with upregulated expression with exposure to the Obese secretome, relative to Lean, in myotubes derived from younger donors, but suppressed expression with exposure to the Obese secretome in myotubes derived from older donors. This pattern was not present in TNF expression. These differential changes may in part explain the differential effects seen in MRF expression, since the independent donor repeats that exhibited a pro-inflammatory response to the Obese SAT secretome, relative to Lean, were the same that exhibited suppression of MRF expression. This finding mimics that of Seo et al. (2019), who demonstrated simultaneous upregulation of IL-6 and TNF expression with downregulation of MYOD, MYOG and MHC after 1 day of co-culturing of differentiating C2C12 myotubes with 3T3-L1 adipocytes. Indeed, while acute local inflammation can stimulate myogenesis *in vivo*, chronic and excessively elevated inflammation diminishes muscle regenerative capacity (Howard, Pasiakos, Blesso, Fussell, & Rodriguez, 2020). Furthermore, low-level systemic inflammation is sometimes observed with obesity and is broadly associated with both insulin resistance and sarcopenia (Beyer, Mets, & Bautmans, 2012; Ellulu et al., 2017; Shoelson et al., 2006).

It is surprising that the pro-inflammatory effects of the Obese SAT secretome were not observed in older donor myotubes and this discrepancy warrants further investigation. Speculatively, it could be postulated that since neither the Lean nor Obese SAT secretome stimulated a robust pro-inflammatory response (or induced insulin resistance) above Control, that there may be a donor-age-related blunting of responsiveness to pro-inflammatory insults. This may be implicated in the predominantly oppositional responses seen in these cells in response to the Obese secretome throughout this chapter, relative to their younger donor counterparts. To that effect, as a visual tool, the effects of Lean and Obese SAT secretome on myotubes was stratified by muscle tissue donor age (Appendix 1. Supplement to Chapter 5; Fig. 1). While the limited nature of this comparison restricts the use of statistical analyses, it nevertheless provides a useful summation of the differential observed effects on gene expression.

Differences Between the Captured Cytokine Profiles of The Lean and Obese Subcutaneous Adipose Secretomes

While statistical comparisons were restricted by the use of n = 3 pools for each adiposity state, the phenotypic differences imprinted by lean and obese adipose tissue were nevertheless evidenced by statistical differences and trends in several cytokines. Causal relationships between individual cytokines within the Lean and Obese ACM, and the effects observed in response to ACM exposure, cannot be determined by the data presented in this chapter. Indeed, there are many more features of the SAT secretome that were not measured, including myriad other cytokines, enzymes, growth factors, and non-coding RNAs (Wilhelmsen et al., 2021). It is still worthwhile, however, to briefly explore which of the cytokines that were measured displayed robust differences between the Lean and Obese SAT secretomes and their potential implications in skeletal muscle metabolic health.

There was a tendency for decreased abundance of adiponectin in Obese ACM, relative to Lean ACM, which is consistent with its expression within adipose tissue and its abundance within the circulation, in obese populations (Arita et al., 1999; Kern, Di Gregorio, Lu, Rassouli, & Ranganathan, 2003; Matsubara, Maruoka, & Katayose, 2002; Ryan et al., 2003). Indeed, adiponectin biosynthesis is perturbed in obese adipose tissue, which appears to be mediated by a negative feedback loop between adiponectin and adipose tissue, whereby the up-regulation of adiponectin abundance induced by the elevated mass of adipose tissue, induces a subsequent reduction in its own expression as well as the AdipoR2 receptor to which it binds, via receptor-mediated repression of the transcriptional activity of peroxisome proliferator-activated receptor gamma (Bauche et al., 2006; Lin & Li,

2012), impairing its ability to exert its insulin-sensitising effects via the upregulation of fatty acid oxidation and the suppression of hepatic glucose production (Lihn, Pedersen, & Richelsen, 2005; Yamauchi et al., 2001).

The proteoglycan Endocan, which is highly expressed by adipocytes and inhibits leukocyte adhesion and migration through the endothelium (Janke et al., 2006; Sarrazin et al., 2006), was also found to abound in significantly lower amounts in Obese ACM, relative to Lean ACM. At the circulatory level, Endocan has previously been reported to be both up- (Bicer et al., 2017; Gungor et al., 2016; Klisić, Kavarić, Spasojević-Kalimanovska, Kotur-Stevuljević, & Ninić, 2021) and down-regulated with increasing indices of adiposity (Delibas, Yapca, & Laloglu, 2018; Janke et al., 2006; Musialowska, Zbroch, Koc-Zorawska, Musialowski, & Malyszko, 2018; Rodrigues et al., 2015; Yilmaz et al., 2014).

Complement Factor D (Adipsin) is a serine protease that is predominantly produced by adipocytes and is involved in innate immunity (Barratt & Weitz, 2021; Cook et al., 1987; Volanakis & Narayana, 1996; R. T. White et al., 1992), but also stimulates adipocyte TAG storage (Song et al., 2016; Van Harmelen et al., 1999). Adipsin was, on average, ~7% higher in Obese ACM than Lean ACM. Complement Factor D has similarly been reported to be both elevated (Milek et al., 2022; Napolitano et al., 1994; Pomeroy et al., 2003), and reduced (Flier, Cook, Usher, & Spiegelman, 1987; Lowell et al., 1990; Rosen et al., 1989) in the presence of obesity

Lipocalin 2 (Lcn2) is a secretory glycoprotein that is abundantly expressed in adipocytes, which binds and transports small hydrophobic molecules such as fatty acids, steroids and retinol (Kjeldsen, Johnsen, Sengeløv, & Borregaard, 1993; Yan et al., 2007; J. Zhang et al., 2008). On average, Lcn2 was 37% more abundant in Lean than Obese ACM This is perhaps surprising given that both the circulating abundance (Auguet et al., 2011; X. Liu et al., 2011; Y. Wang et al., 2007; Yan et al., 2007) and adipose mRNA expression (Catalán et al., 2009; Yan et al., 2007; J. Zhang et al., 2008) of Lcn2 have previously been found to be elevated with obesity and inflammation, however the significance of this relationship is contested on account of ligand-ligand binding, post-translational modifications and protein-protein interactions resulting in multiple circulating forms of Lcn2 which elicit distinct functions (D. Li, Yan Sun, Fu, Xu, & Wang, 2020). Further demonstrating the complex association and involvement of Lcn2 in metabolic health, Lcn2 knockout impairs muscle regeneration (Rebalka et al., 2018) and has been found to confer both protection from, and exacerbation of, diet- and ageing-

induced metabolic dysregulation (H. Guo et al., 2010; Ishii et al., 2017; Law et al., 2010).

Not all adipose-secreted cytokines exhibited the differences one might expect between lean and obese donors. Indeed, C-reactive protein – an inflammatory marker that is a significant predictor of incident cardiovascular diseases (Paul M. Ridker, 2001; Paul M Ridker, 2003), and is elevated in the circulation of adults with obesity (Aronson et al., 2004; Visser, Bouter, McQuillan, Wener, & Harris, 1999) – tended to be elevated in Lean ACM. Similarly, myeloperoxidase, an enzyme secreted primarily by activated neutrophils that catalyses the formation of reactive oxygen species (Podrez, Abu-Soud, & Hazen, 2000; R. Zhang et al., 2002) and is elevated in the circulation of obese individuals(Correia-Costa et al., 2016; Qaddoumi et al., 2020; Zaki et al., 2018), was approximately two-fold more abundant in Lean ACM than Obese ACM. However, it must be recalled that ACM was derived from OA patients undergoing joint replacement surgery, and thus individual donors (whether lean or obese) may have substantially elevated and variable levels of circulating inflammatory markers.

Several other cytokines also tended to display mean differences between Lean and Obese ACM (Macrophage Colony-Stimulating Factor, Oncostatin M and Cathespin-D), which have all been suggested to be altered with obesity (L. Ding et al., 2020; Komori & Morikawa, 2018; Levine, Jensen, Eberhardt, & O'Brien, 1998; Masson et al., 2011; Sanchez-Infantes et al., 2014; Sugita, Kamei, Oka, Suganami, & Ogawa, 2007; Xu, Mariman, Goossens, Blaak, & Jocken, 2020). The function of these cytokines in health and disease has been reviewed elsewhere (Benes, Vetvicka, & Fusek, 2008; Chitu & Stanley, 2006; Elks & Stephens, 2015; John A Hamilton, 2008; Richards, 2013; Tsukuba et al., 2000)

5.6 Limitations

This study provides novel observations regarding the effects of sustained exposure to both the lean and obese human SAT secretome on primary human muscle cells. However, several limitations must be addressed. Firstly, it must be recognised that adipose-conditioning was performed on myotube differentiation medium that contained 6% Horse serum. Thus, when profiling the cytokine constituents of Lean and Obese ACM, a small portion of these relative abundances were attributable to the presence of serum. Importantly, this approach was applied to all adipose tissue explants, such that overall differences between Lean and Obese ACM, are likely to reflect differences in cytokine abundance secreted from the adipose tissue. Furthermore, two samples of Control medium containing two different batches of HS were also screened for the 58 measured cytokines (Figure 5.3) and

demonstrated substantially lower relative abundances of the vast majority of measured cytokines and minimal inter-batch variation (far lower than the differences seen between ACM groups). It must also be acknowledged that despite consistent matching of donor phenotype, there was still a degree of variability between pools of ACM, which was most evident in the third pool of Lean ACM, which exhibited greater relative abundance of the interleukin family of cytokines than the other two pools of Lean ACM. This strengthens the justification for the use of multiple pools of ACM versus applying ACM from a single donor to myotubes, since it better captures human variability and minimises the risk of individual outlier donors skewing results.

Secondly, this study harvested myotubes after 6-days of exposure to the SAT secretome during myogenic differentiation. This method provides a more physiological model of myogenesis than the short term (ie. 24-28 h) models mostly reported in the literature but restricts comparisons between studies. It would have been valuable to have also harvested cells following the induction of differentiation, to examine whether myostatin was acutely upregulated. In doing so, confidence could be gained in the hypothesis that the suppression observed in myostatin after 6 days is the product of a negative regulatory feedback loop. Due to the use of low-passage primary human myotubes and the limited availability of SAT/ACM, it was not possible to perform both short- and long-term treatments within the available timeframe.

Finally, the ACM used in these experiments was generated from lean and obese donors who were undergoing total joint replacement due to OA. Thus, both groups likely presented with a more inflammatory secretory phenotype than non-OA donors (Thijssen, van Caam, & van der Kraan, 2014). However, given that in England each year >80,000 hip and >90,000 knee replacement surgeries are undertaken (NHS, 2022), and >50% of adults over the age of 65 present with radiographic evidence of osteoarthritis (Miller, Rejeski, Messier, & Loeser, 2001), the use of this patient group does not represent an insignificant niche of society, but rather reflects a relatively common feature of ageing.

5.7 Conclusions

Relative to unconditioned medium, chronic (6 days) exposure of human primary myotubes to the subcutaneous adipose tissue secretome suppressed the mRNA expression of myostatin and this effect tended to be greater when myotubes were exposed to the Obese secretome relative to the Lean secretome, which may have been mediated by alternative regulation of myostatin expression via a MYOD-mediated or self-inhibitory feedback loop. The reduction in myostatin expression

was accompanied by a pattern of improved glucose transport and insulin-sensitivity following exposure to the adipose tissue secretome, but this effect was not influenced by the donor phenotype of the adipose tissue secretome. However, diverging effects of Lean and Obese secretome emerged between myotubes derived from younger and older donors. Younger donor myotubes exhibited broadly beneficial effects of Lean secretome on the expression of genes involved in myogenesis and muscle protein breakdown, while the effects of Obese secretome on these indices were broadly deleterious and triggered pro-inflammatory gene expression. Conversely, relative to their younger counterparts, myotubes derived from older donors exhibited blunted responses of pro-inflammatory markers and genes involved in myogenesis upon exposure to both Lean and Obese secretome. In the context of this thesis, the obese subcutaneous adipose tissue secretome does not appear to explain the upregulation of myostatin expression previously observed in obese skeletal muscle *in vivo*.

Chapter 6. The Polyphenol Metabolite Urolithin A Suppresses Myostatin Expression and Improves Glucose Handling in Skeletal Muscle Cells.

6.1 Introduction

In recent years, multiple nutritional products have emerged onto the market with claims of anti-myostatin, pro-anabolic effects (Evans et al., 2021; S. J. Lee, Gharbi, Shin, Jung, & Park, 2021; Sharp et al., 2014; Willoughby, 2004). To date, however, there is little robust evidence of their effectiveness in well-controlled human trials. Naturally occurring polyphenolic plant extracts, such as the flavanol epicatechin, have demonstrated the ability to suppress skeletal muscle myostatin abundance in mice (Gutierrez-Salmean et al., 2014). Indeed, while myriad polyphenols have demonstrated *in vitro* and *in vivo* benefits to skeletal muscle in rodent models, including anti-inflammatory and anti-catabolic effects (Francaux & Deldicque, 2018; Meador et al., 2015; J. Rodriguez, Caille, Ferreira, & Francaux, 2017; Salucci & Falcieri, 2020), to date the significant translation of these effects into ageing humans remains elusive (Nikawa, Ulla, & Sakakibara, 2021).

A promising body of research is developing investigating the influences of polyphenolic compounds such as ellagitannins (ETs) and ellagic acid (EAs). While ETs and EAs, such as punicalagin, are nearly ubiquitous in nature and can be obtained through the diet via consumption of pomegranate, walnuts, and certain berries, they themselves are poorly absorbed and demonstrate limited direct biological activity (Raimundo, Ferreira, Tomás-Barberán, Santos, & Menezes, 2021; S. Zhang et al., 2019). Indeed, EA has a poor pharmacokinetic profile, with low water solubility and intestinal permeability and a short plasma half-life due to rapid elimination by first-pass metabolism, such that <1% of an orally ingested EA load is detected within the circulation (Bala, Bhardwaj, Hariharan, & Kumar, 2006; Ceci, Graziani, Faraoni, & Cacciotti, 2020; González-Sarrías et al., 2015; Kang, Buckner, Shay, Gu, & Chung, 2016; Seeram et al., 2006). Furthermore, human responsiveness to polyphenol administration is highly variable, which may reflect differential processing in the gut (Scalbert, Morand, Manach, & Rémésy, 2002). Thus, emerging research has sought to investigate the functional biological role of ET and EA downstream circulating metabolites.

Urolithins: Gut Microbiota-Derived Ellagitannin Metabolites

Ellagitannins and Ellagic acid are metabolised by the microbiota of the gut, with ETs first being hydrolysed into EAs in the upper gastrointestinal tract by gut bacterial enzymes known as tannases (Tomás-Barberán et al., 2017). Ellagic acid is further metabolised by gut microflora of the large intestine, through the loss of one of its two lactones and the removal of hydroxyl groups, to form a group of biologically active compounds termed urolithins (Espín, Larrosa, García-Conesa, & Tomás-Barberán, 2013). Urolithins abound as A, B, C and D forms, which are characterised by the presence of an α-benzo-coumarin scaffold (D'Amico et al., 2021), and are more readily absorbed than the polyphenols from which they are derived (Espín et al., 2013). The bacterium or bacteria responsible for the conversion of EAs to urolithins in humans remains to be elucidated (Cortés-Martín, Selma, Tomás-Barberán, González-Sarrías, & Espín, 2020).

The most intensively investigated of the urolithins is Urolithin A (UA). First identified as an EA metabolite in rats (Doyle & Griffiths, 1980), it was subsequently shown to be similarly present in the digestive tracts of humans and confirmed to be of microbial metabolic origin (Cerdá, Periago, Espín, & Tomás-Barberán, 2005). Once absorbed, Urolithins undergo phase II metabolism in the liver, to form conjugates; principally UA-glucorinide and UA-sulfate (Figure 6.1) (García-Villalba, Beltrán, Espín, Selma, & Tomás-Barberán, 2013; García-Villalba et al., 2017). Glucorinide and sulfate conjugates of UA are the predominant forms found within human circulation (0.2 - 20 μM)(Espín et al., 2013), however the physiological significance of conjugated versus unconjugated UA (termed 'parent UA') is unclear (Bobowska et al., 2021).

In studies of bioavailability, UA was detected in the plasma within 6-8 h of pomegranate juice ingestion (a rich source of ET and EA), suggesting colonic production, and persisted in urine and plasma for 48-72 h, suggesting enterohepatic recirculation (Cerdá et al., 2005; Seeram et al., 2006). Following acute ingestion of ET and EA, plasma abundance of UA glucuronide and UA sulfate have been reported to peak at 14-25 μM (Cerdá, Espín, Parra, Martínez, & Tomás-Barberán, 2004; Tomás-Barberan, Espín, & García-Conesa). Importantly, however, in a study of 100 human participants, only 12 were found to present with detectable levels (≥ 22 nM) of UA glucoronide in the basal state, while following the provision of pomegranate juice, only ~40% of participants demonstrated significant conversion into UA (A. Singh et al., 2022). The ability to convert ET and EA into UA appears to be influenced by age and health status (Cortés-Martín et al., 2020).

The common inability for endogenous conversion of ETs and EAs into UA, highlights the potential for direct supplementation with UA itself. Indeed, acute supplementation with 500 mg of UA increased plasma UA, providing >6-fold exposure to circulating UA than pomegranate juice (A. Singh et al., 2022). Furthermore, UA can be subsequently detected in multiple tissues, including skeletal muscle and adipose (Andreux et al., 2019; Heilman, Andreux, Tran, Rinsch, & Blanco-Bose, 2017), suggesting that it may accumulate with chronic supplementation, which could increase its physiological effectiveness beyond its circulating half-life of ~24 h (Andreux et al., 2019).

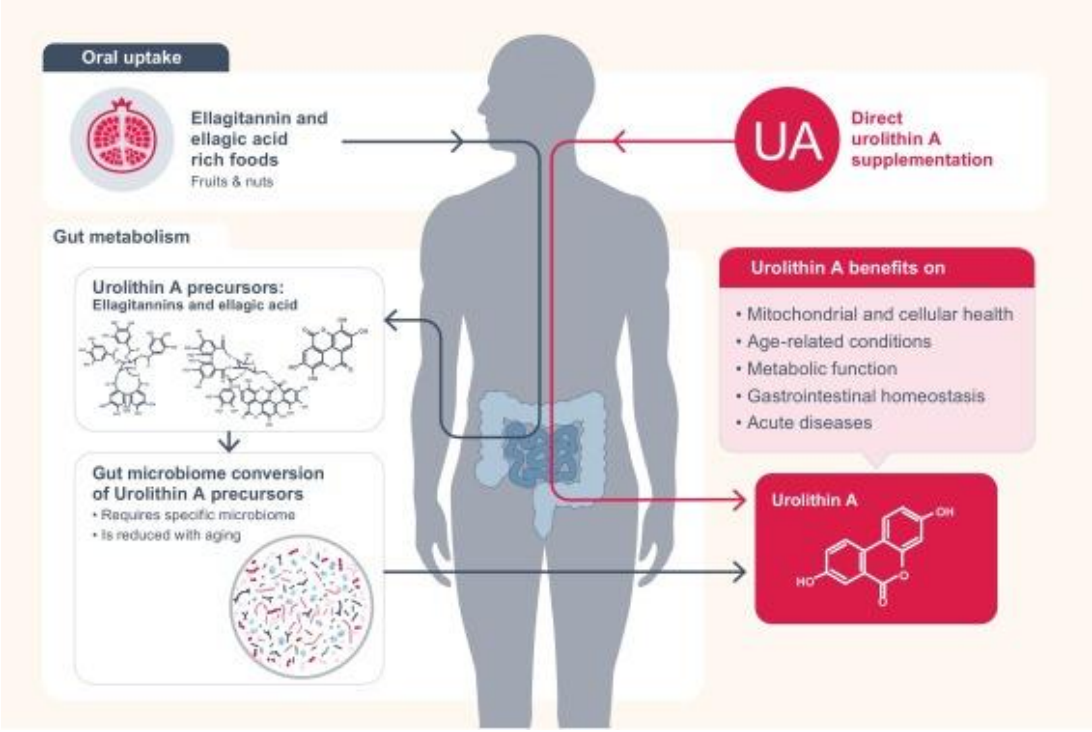

Figure 6.1. Overview of the processes involved in achieving circulating bioavailability of the gut-microbiome-derived metabolite Urolithin A.
Taken from D'Amico et al. (2021).

Potential of Urolithin A as a Nutraceutical to Improve Skeletal Muscle Health

Research investigating UA has focused on its positive effects on mitophagy - the effective recycling (autophagy) of defective mitochondria. *In vivo* evidence consistently demonstrates an impaired capacity for mitophagy in ageing and dystrophic human skeletal muscle (Drake & Yan, 2017; Leduc-Gaudet, Hussain, Barreiro, & Gouspillou, 2021; Luan et al., 2021) as well as models of disuse atrophy (Ji & Yeo, 2019). This impairment has been associated with functional decline in older adults (Drummond et al., 2014), which is a common feature of frailty (Fried et al., 2001). In a murine model of Duchenne's Muscular Dystrophy, UA improved muscle function by preserving mitophagy, respiratory capacity and the regenerative capacity of muscle stem cells (Luan et al., 2021) and increased angiogenesis within the skeletal muscle of C57/BL mice (Ghosh et al., 2020).

UA has also demonstrated promising early results for preserving skeletal muscle function in ageing models. UA preserved mobility and pharyngeal pumping in C. elegans worms, which was associated with the preservation of mitochondrial respiratory capacity (Ryu et al., 2016). Translated into rodents, Ryu et al. (2016) and Luan et al. (2021), demonstrated improved exercise capacity after UA treatment in models of age-related muscular decline.

In a first-in-human clinical trial, Andreux et al. (2019) acutely and chronically administered UA to healthy, sedentary, elderly adults. UA demonstrated a favourable safety profile and significant biological availability. The authors reported upregulation of mitochondrial genes and a tendency for increased mitochondrial to nuclear DNA ratio in the skeletal muscle, as well as a concomitant reduction in many species of plasma acylcarnitines (the form in which fatty acids enter the mitochondria to undergo oxidation, and the abundance of which negatively correlates with mitochondrial function) over 28 days, when either 500 or 1000 $mg \cdot day^{-1}$ was provided. Furthermore, free carnitine levels were unchanged following treatment, suggesting this reduction was not secondary to changes in total free carnitine availability. While the degree to which the reduction in plasma acylcarnitines was mediated by skeletal muscle is unclear, the concurrent upregulation of gene sets associated with mitochondrial function suggest its implication.

In a follow-up to the aforementioned trial, S. Liu et al. (2022) undertook a four-month-long double-blind, placebo-controlled randomised clinical trial in adults aged 65-90 years. Participants received a daily dose of either 1000 mg UA or placebo, and muscle fatigue tests and plasma biomarkers were assessed at

baseline, two and four months of supplementation. While UA did not improve 6-minute walk distance, it did increase muscle fatigue resistance (measured as the number of contractions at 70% maximal force until volitional failure) and plasma acylcarnitines declined in a similar fashion to that reported by Andreux et al. (2019), however change in total free carnitine was not assessed.

Recent studies have also shown promising effects of UA on glucose tolerance and insulin sensitivity in obesity and ageing. In a murine model of HFD-induced obesity, daily intraperitoneal administration of UA improved systemic insulin sensitivity, reduced adipocyte hypertrophy and liver TAG accumulation and increased adiponectin plasma abundance (Toney et al., 2019). Consistently, UA was found to improve glucose tolerance and plasma insulin concentration in models of obesity and T2D (Xia et al., 2020; J. Yang et al., 2020). Promisingly, in the adipose tissue and liver of HFD-fed mice who received UA treatment, acute hyperinsulinaemia induced greater activation of the proximal insulin signalling proteins pAkt and pIRS-1 (Toney et al., 2019). Additionally, Toney et al. reported a trend towards, while Xia et al. (2020) demonstrated a significant reduction in, white adipose tissue mass. Xia et al. (2020) found evidence of browning of white adipose tissue and subsequently enhanced thermogenesis; a process of contested physiological significance in humans (Herz & Kiefer, 2019; Kiefer, 2017).

UA appears to stimulate several metabolic changes that might support skeletal muscle health and function, however this has not been explored in human muscle cells and its effects on myostatin and anabolic sensitivity have not been investigated, leaving important questions unanswered regarding the potential to extrapolate findings from animal models to the human body (Ávila-Gálvez, González-Sarrías, & Espín, 2018; García-Villalba et al., 2022; Mena & Del Rio, 2018). This deficit is important to assess, since mitochondrial dysfunction in skeletal muscle, which UA appears to mitigate, significantly contributes to the aetiology of sarcopenia (Coen, Musci, Hinkley, & Miller, 2019); while in the context of insulin sensitivity, skeletal muscle accounts for a substantial portion of whole body glucose disposal under insulin stimulated conditions (Eleuterio Ferrannini et al., 1988; Thiebaud et al., 1982).

6.2 Aims

The primary aim of this investigation was to establish whether acute treatment of primary human myotubes with UA confers changes in insulin and anabolic sensitivity and myostatin expression, and whether such changes are correlated. Secondly, as an exploratory measure, responsiveness to UA was compared between donor phenotypes (Normal Weight vs Obese and Young vs Older), to identify possible avenues of interest for future investigations. Lastly, additional experiments were undertaken using an *in vitro* model of adipose tissue, to establish whether such effects are specific to skeletal muscle or whether they may be recapitulated in other metabolic tissues.

6.3 Methods

Primary Cell Culture

Primary human myogenic cultures were established from skeletal muscle biopsy samples obtained as described previously (Chapter 2, section 2.2). Some of the myoblasts from older adults with or without obesity used in this chapter were obtained from collaborators at the University of Birmingham.

Adipocyte Cell Culture

Cultures of 3T3-L1 murine fibroblasts were cultured and differentiated into adipocytes as previously described in Chapter Two (section 2.3).

Urolithin A Treatments

After 6-8 days of differentiation, myotubes were incubated for 24 h in standard differentiation medium (HAM's F10 + 6% HS) supplemented with varying concentrations of UA or a matched vehicle treatment (0.1% DMSO). Lyophilised UA was provided by collaborators (Amazentis SA, Lausanne, CH) and was first dissolved in 100% DMSO and aliquots were stored at -20°C. Treatment concentrations ranged from 0.002-50 μM, with the former approximately representing the minimum basal abundance of parent UA in the fasted state, 24 h after ingestion of the final bolus of 28 days of UA supplementation in humans (Figure 6.2) and the latter having been demonstrated to most substantially induce mitophagy and to phosphorylate AMPK-α in C2C12 myoblasts when treated with UA for 20-24 h (Andreux et al., 2019; Ryu et al., 2016).

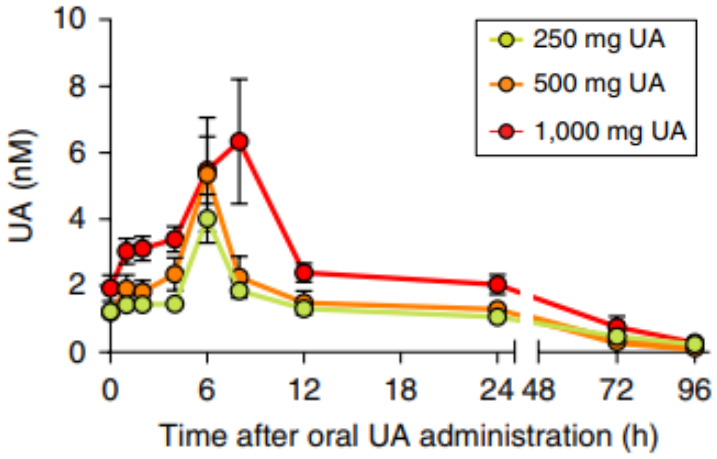

Figure 6.2. Dose-dependent increase in plasma concentration of parent UA following supplementation in adults.

Plasma parent UA concentration was measured during the 96 h sampling period following UA administration on the last day of 28 days of treatment with 250, 500 and 1,000 mg doses. Data presented as Mean ± SEM (n = 9 participants). *Adapted from Andreux et al. (2019).*

Cell Viability

Human myotubes from n = 1 older donor, and 3T3-L1 adipocytes of low passage, cultured in 24-well plates, were exposed to varying concentrations of UA for 24 h. Older donor myotubes were used on account of their greater susceptibility to a loss of myogenic capacity, relative to those from younger donors (O'Leary et al., 2018). Therefore, the concentrations tolerated by older donor cells would be tolerated by younger donor cells. Changes in cell viability were assessed via resazurin assay, as previously described (section 2.5.1). 10% DMSO was used as a positive control to induce cell death and confirm assay sensitivity.

Glucose Uptake

Basal and insulin-stimulated glucose uptake was determined in myotubes and adipocytes cultured in 6-well plates as previously described (sections 2.5.2 and 2.5.3, respectively). Urolithin A was not added to the serum-free starvation media, or reaction buffer used for the addition of insulin and labelled glucose.

mRNA Expression

Following UA or Vehicle treatment, cells grown in 12-well plates were harvested using Tri-Reagent, prior to RNA extraction and cDNA synthesis using standard procedures as previously described (sections 2.8.1 through 2.8.5). For the

analysis of relative mRNA expression, genes of interest were normalised against the geometric mean of Hydroxymethylbilane Synthase (HMBS) and Ribosomal Protein Lateral Stalk Subunit P0 (RPLP0) expression, which geNorm revealed to demonstrate high stability within and between experiments and donors, under these experimental conditions. Data are presented as the mean relative expression of gene of interest divided by the geometric mean of the relative expression of the 2 endogenous reference genes.

Amino Acid-Stimulated Protein Synthesis

Amino acid-stimulated protein synthesis was assessed using the SuNSET techniques, as described in Chapter 2 (section 2.5.6). Fully differentiated myotubes were treated with UA at varying concentrations for 24 h. After 24 h, cells were washed twice before starvation and puromycin treatment. UA was not added to the serum-free starvation media, nor transport buffer used for the addition of 2 mM leucine, 5 mM glucose and 1 μM puromycin.

Statistical Analysis

Statistical analysis was performed in GraphPad Prism 9. Descriptive data are presented as Mean ± SD, while experimental data are presented as Mean ± SEM of independent donor repeats. Where experimental restrictions (number of available primary cells and changes to experimental conditions) resulted in differing numbers of independent donor repeats, the number of independent donor repeats is displayed within each bar of each figure and mentioned in the results, for clarity and transparency.

Assumptions of normality were tested via Shapiro-Wilks test. Due to the absence of glucose uptake data for intermediate concentrations of UA from some independent donor repeats, a Mixed Effects ANOVA was fitted rather than a two-way repeated measures ANOVA, to assess changes in glucose uptake in response to treatments in the presence and absence of insulin. Due to the variability and limited numbers of donor replicates (with high inter-donor variability), post-hoc comparisons for glucose uptake are Fisher's LSD, to reduce the chance of Type II errors (false negatives) due to possible underpowering. One-way repeated measures ANOVA were used to assess changes in cell viability, gene expression, and protein synthesis, with post-hoc Tukey multiple comparisons. ANOVA results with $P < 0.10$ are accompanied by their corresponding partial eta squared (n_p^2) values as a measure of effect size. Significant ($P < 0.05$) post-hoc comparisons are presented as mean difference [95% CI], where relevant. Correlations were performed using Pearson's correlation coefficient (r) and are accompanied by their

corresponding *P* values. Statistical test results (ANOVAs and correlations) are reported in boxes on each figure, while statistically significant ($P < 0.05$), or those with $P < 0.10$, post-hoc comparisons are indicated by lines connecting each comparator. Statistical significance was defined as $P < 0.05$.

As additional exploratory outcomes, the effects of donor phenotype (Obesity and Ageing) on responsiveness to UA was considered by stratifying data from independent donor repeats into Normal Weight or Obese (effects of obesity) and Young or Older (effects of ageing). Descriptive characteristic differences for donor phenotype groupings (Normal Weight vs Obese and Young vs Older) were assessed via independent samples t-tests. Only data from Vehicle vs 50 µM UA is presented in these additional analyses, since this concentration induced the most profound effects when all independent donor repeats were considered, and where the number of independent donor repeats was greatest. Due to the relatively small and uneven sample sizes in these comparisons, statistical analysis has not been undertaken. Instead, data are presented as Mean ± SEM fold-change from Vehicle for each stratification, to compare responsiveness to UA between stratifications that may help inform and power future investigations.

6.4 Results

6.4.1 Myogenic cultures and their donors

Myogenic cultures were established from a total of n = 8 individuals, comprising n = 3 Young and Normal Weight, n = 3 Older and Normal Weight and n = 2 Older and Obese, healthy adults. Descriptive donor data is presented in Table 6.1. Due to variable muscle biopsy yields and differing rates of proliferation and differentiation, the data presented in this chapter has variable numbers of independent donor repeats. The experiments performed in each independent donor repeat was determined principally by the number of myoblasts yielded from each myogenic culture prior to plating-out, since cultures were restricted to no more than two passages to best preserve any effects of donor phenotype.

Table 6.1. Characteristic data for all skeletal muscle biopsy donors, from whom myogenic cultures were derived.

All Donors		
Donor Characteristic	**Mean (± SD)**	**Range (Min – Max)**
Sex (M/F (n))	4/4	-
Age (y)	47 (± 26)	20-81
BMI ($kg \cdot m^{-2}$)	27.1 (± 5.8)	21.1-38.5
Mass (kg)	82.3 (± 21.4)	60.5-122.0
Waist (cm)	97(± 20)	76-126
Hip (cm)	104 (± 14)	87-129
Waist:Hip ratio	0.92 (± 0.09)	0.81-1.03

6.4.2 Effects of 24 h Urolithin A treatments on myotube viability

Exposure to 10% DMSO for 24 h induced significant cell death and served as a positive control for the assay. One-way ANOVA revealed a significant effect of treatment on cell viability (P = 0.002; η_P^2 = 0.782) (Figure 6.3). Post-hoc comparisons indicated that significant toxicity (~30% loss of cell viability, relative to vehicle) only occurred when myotubes were exposed to 100 µM UA for 24 h (Mean Difference [95% CI]: -69162 [-15838, -122486] a.u.; P < 0.01). Based on these observations, in conjunction with previously reported findings, 24 h treatments were subsequently employed, with an upper concentration limit of 50 µM UA.

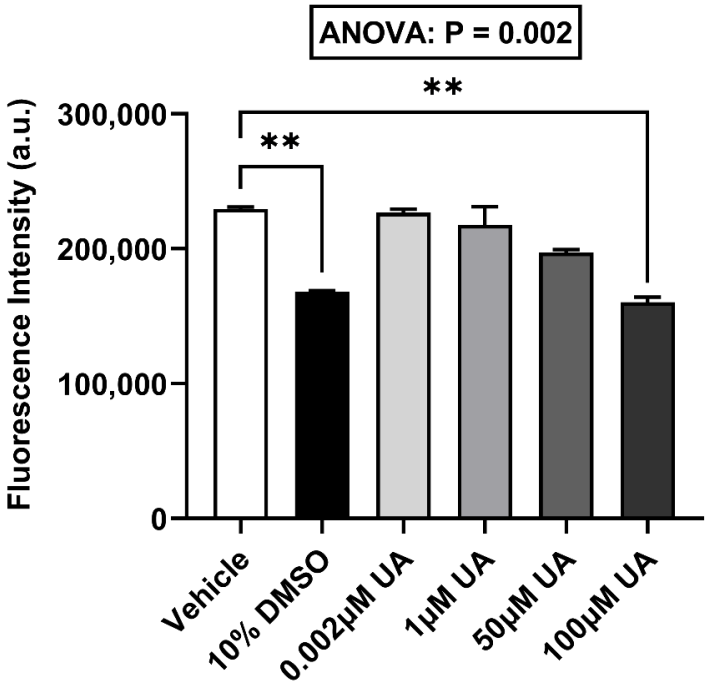

Figure 6.3. Effect of 24 h UA exposure on primary human myotube viability.

Viability was assessed in myotubes from n = 1 independent donor repeat (older male donor) via Resazurin assay. Data presented as Mean ± SEM of fluorescence intensity – background (n =3 replicate wells per treatment). **Significant difference (P < 0.01) from Vehicle, indicating a loss of cell viability.

6.4.3 Effects of Urolithin A on basal and insulin-stimulated glucose uptake in myotubes

When glucose uptake data from all independent donor repeats (n = 6) was combined, Mixed Effects ANOVA revealed significant treatment effects of both UA (P = 0.043; η_P^2 = 0.410) and insulin (P = 0.008; η_P^2 = 0.781), but not an interaction between the two (Figure 6.4). Post-hoc comparisons (Fisher's LSD) revealed greater basal (Mean Difference [95% CI]: 0.21 [0.01, 0.41]-fold greater; P < 0.05) and insulin-stimulated (Mean Difference: 0.24 [0.04, 0.43]-fold greater; P < 0.05) glucose uptake with 50 μM UA, compared to Vehicle. While greater in absolute terms, the relative effect of insulin-stimulation to increase glucose uptake beyond the 50 μM UA-treated basal level was similar to that of vehicle treated cells (17% vs 18%, respectively). No significant effects of 0.002 μM or 1 μM UA were seen on basal or insulin-stimulated glucose uptake.

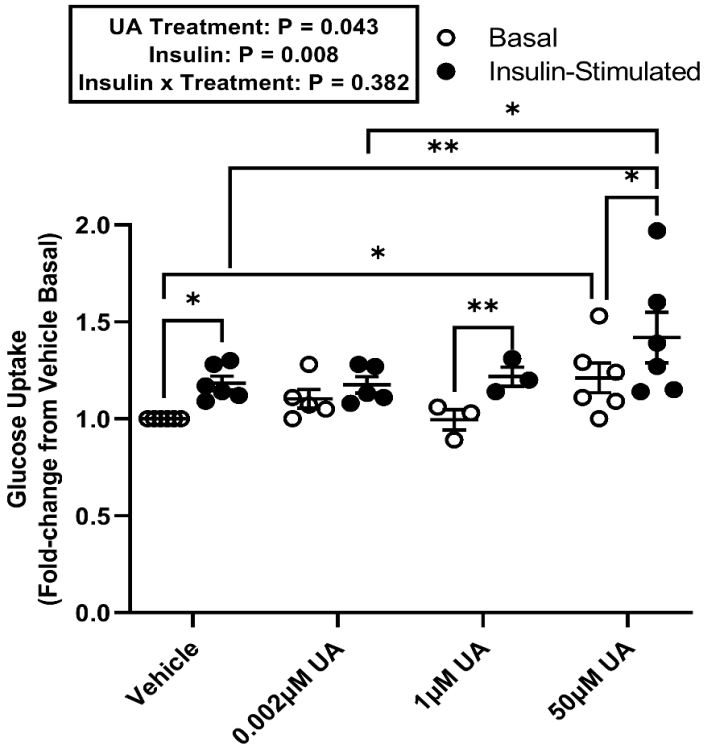

Figure 6.4. Effect of 24 h UA exposure on glucose uptake in primary human myotubes.

Basal (open circles) and insulin-stimulated (100 nM; closed circles) glucose uptake was measured using [3H] 2-DOG. Data are presented as Mean ± SEM of fold-change from Vehicle Basal for each repeat. Data points are the mean of 4-6 replicate wells for each treatment. Significant differences between treatments: *P < 0.05, **P < 0.01. Note: n = 6 independent donor repeats for experiments using Vehicle vs 50 μM UA, while 0.002 μM and 1 μM n = 5 and n = 3, respectively.

6.4.4 Effects of Urolithin A on the mRNA expression of myostatin and glucose transporters in myotubes

The relative mRNA expression of myostatin, GLUT1 and GLUT4 was assessed in n = 7 independent donor repeats. Repeated measures one-way ANOVA found a significant effect of UA treatments on the relative mRNA expression of myostatin (P = 0.031; η_P^2 = 0.382) (Figure 6.5A). Post-hoc comparisons revealed a significant suppression of myostatin (14%) after treatment with 50 µM UA compared to Vehicle (Mean Difference [95% CI]: -0.210 [-0.031, -0.390] a.u.; P < 0.01). Pearson's correlation coefficient found no association between fold-change in myostatin expression from Vehicle to 50 µM UA and either basal (r = 0.020, P = 0.970; Figure 6.5B) or insulin-stimulated (r = -0.133, P = 0.802; Figure 6.5C) glucose uptake fold-change from Vehicle to 50 µM UA.

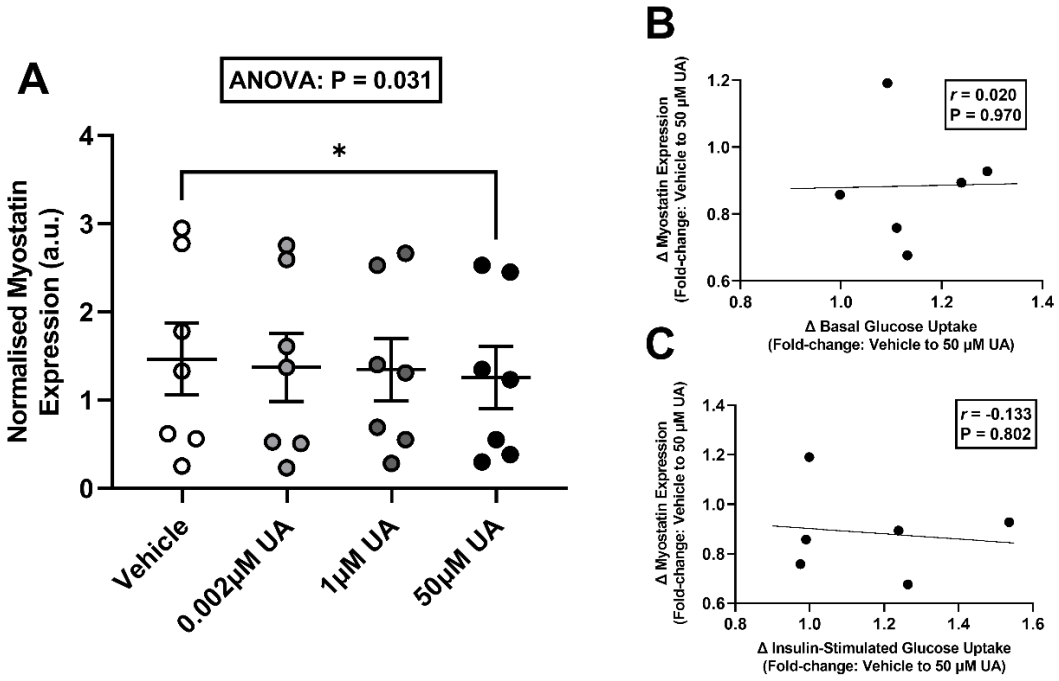

Figure 6.5. Effect of 24 h UA exposure on myostatin mRNA expression in primary human myotubes.

The effects of 24 h UA exposure on the mRNA expression of myostatin was assessed via RT-qPCR (n =7) (**A**). Associations between fold-change in myostatin expression from Vehicle to 50 µM UA with basal (n = 6) (**B**) and insulin-stimulated (n = 6) (**C**) fold-change in glucose uptake from Vehicle to 50 µM UA. Data is presented as Mean ± SEM of Myostatin expression relative to the geometric mean of HMBS and RPLP0, with circles representing independent donor repeats. Significant difference from Vehicle: *P < 0.05.

Repeated measures one-way ANOVA revealed no overall effect of UA treatment on the relative mRNA expression of GLUT1 (Figure 6.6A), but a significant effect of UA treatment on the relative mRNA expression of GLUT4 was identified (P = 0.016; η_P^2 = 0.427). Post-hoc comparisons identified 1.8-fold greater GLUT4 expression after treatment with 50 μM UA compared to Vehicle (Mean Difference [95% CI]: 0.788 [0.080, 1.496] a.u.; $P < 0.01$) (Figure 6.6B).

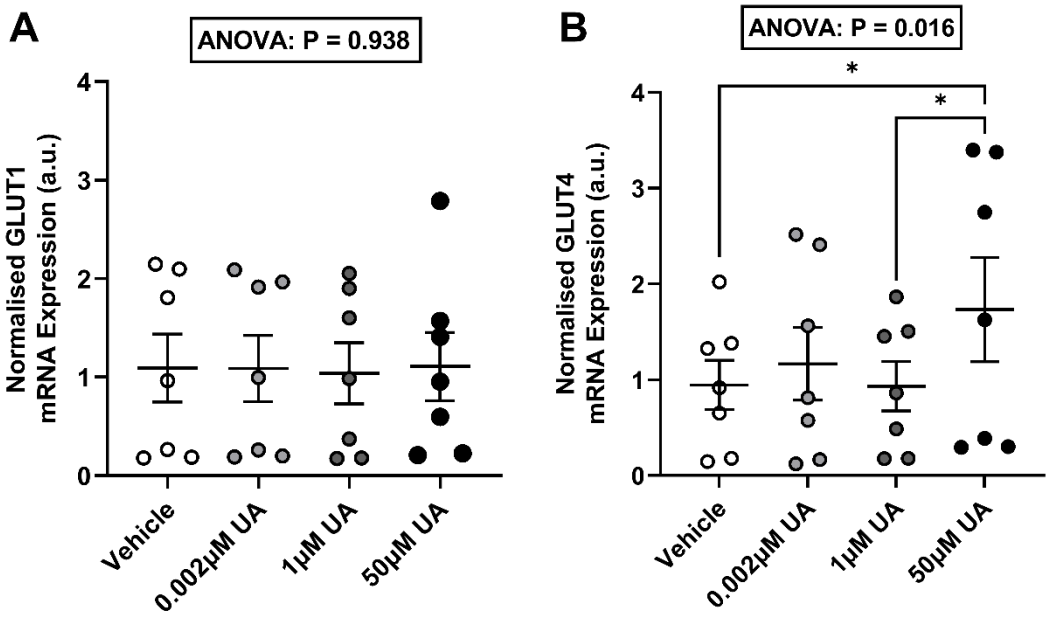

Figure 6.6. Effect of 24 h UA exposure on GLUT1 and GLUT4 mRNA expression in primary human myotubes.

The effects of 24 h UA exposure on the mRNA expression of GLUT1 (**A**) and GLUT4 (**B**) was assessed via RT-qPCR (n = 7). Data are presented as Mean ± SEM of GLUT1 and GLUT4 expression, relative to the geometric mean of HMBS and RPLP0, with circles representing independent donor repeats. Significant differences between treatments, as indicated: *$P < 0.05$.

6.4.5 Effects of Urolithin A on amino acid-stimulated protein synthesis

Amino acid-stimulated protein synthesis, as indicated by the ratio of puromycin: Coomassie lane intensity from a Western blot (representing relative abundance of newly synthesised puromycin-labelled peptides, relative to total protein), was assessed in n = 4 independent donor repeats. Repeated measures one-way ANOVA revealed no effect of UA treatment on global protein translation (Figure 6.7).

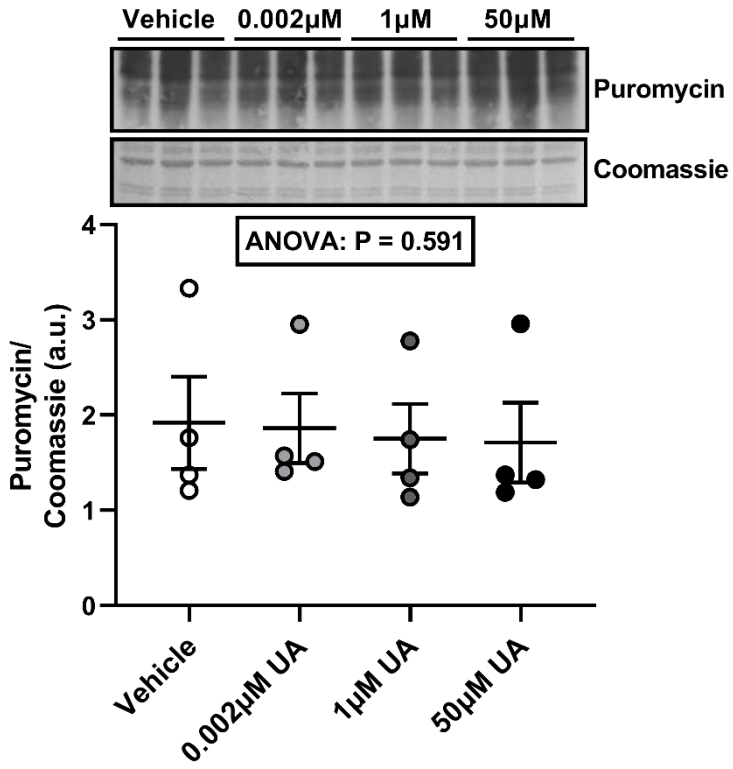

Figure 6.7. Effect of 24 h UA exposure on amino-acid-stimulated protein synthesis in primary human myotubes.

Protein synthesis, as indicated by puromycin incorporation, was assessed via western blot (n = 4). Data is presented as Mean ± SEM of normalised whole-lane puromycin intensity, with circles representing independent donor repeats.

6.4.6 Exploratory comparison between the effects of 24 h exposure to 50 μM UA in primary human myotubes from normal weight and obese donors

As an exploratory outcome, the effects of donor obesity on responsiveness to UA was considered by stratifying data from independent donor repeats into Normal Weight (BMI range: 21-26; total n = 6) or Obese (BMI range: 30-39; total n = 2) donor phenotypes. Donor characteristic data demonstrated that the two groups did not differ in mean age, but the Obese group had significantly higher BMI (Mean ± SD: 34.4 ± 5.8 vs 24.1 ± 2.2 $kg \cdot m^{-2}$; $P = 0.013$), as well as body mass, waist, and hip circumferences than their Normal Weight counterparts (Table 6.2). Of note, the Obese group comprised only male donors.

When glucose uptake data was stratified by BMI (Normal Weight (n = 4) vs Obese (n = 2)), on average 50 μM UA treatment increased basal glucose uptake (expressed as fold-change from Vehicle basal) more in Normal Weight than Obese independent donor repeats (Mean ± SEM: 1.27 ± 0.11-fold vs 1.10 ± 0.01-fold, respectively) (Figure 6.8A). Glucose uptake was similarly increased by insulin stimulation in Vehicle treated cells in both Normal Weight and Obese independent donor repeats, however only in Normal Weight independent donor repeats did 50 μM UA treatment further increase glucose uptake relative to Vehicle with insulin stimulation (Normal Weight: 1.53 ± 0.17-fold vs 1.17 ± 0.04-fold; Obese: 1.21 ± 0.07-fold vs 1.22 ± 0.08-fold, respectively). Changes in the mRNA expression of myostatin, GLUT1 and GLUT4 after 50 μM UA treatment (expressed as fold-change from Vehicle) were reasonably comparable between Normal Weight (n = 5) and Obese (n = 2) independent donor repeats (Figure 6.8B).

Table 6.2. Characteristic data for Normal Weight and Obese skeletal muscle biopsy donors, from whom myogenic cultures were derived.

	Mean (± SD)		*P*
Donor Characteristic	**Normal Weight Donors**	**Obese Donors**	**Normal Weight vs. Obese**
Sex (M/F (n))	2/4	2/0	-
Age (y)	43 (± 30)	57 (± 11)	0.558
BMI ($kg \cdot m^{-2}$)	24.1 (± 2.2)	34.4 (± 5.8)	**0.013**
Mass (kg)	71.4 (± 9.5)	109.6 (± 17.6)	**0.011**
Waist (cm)	86 (± 11)	123 (± 5)	**0.009**
Hip (cm)	97 (± 7)	122 (± 10)	**0.013**
Waist:Hip ratio	0.89 (± 0.07)	1.01 (± 0.04)	0.086

Comparisons between Normal Weight and Obese donor characteristics were performed using unpaired t-tests.

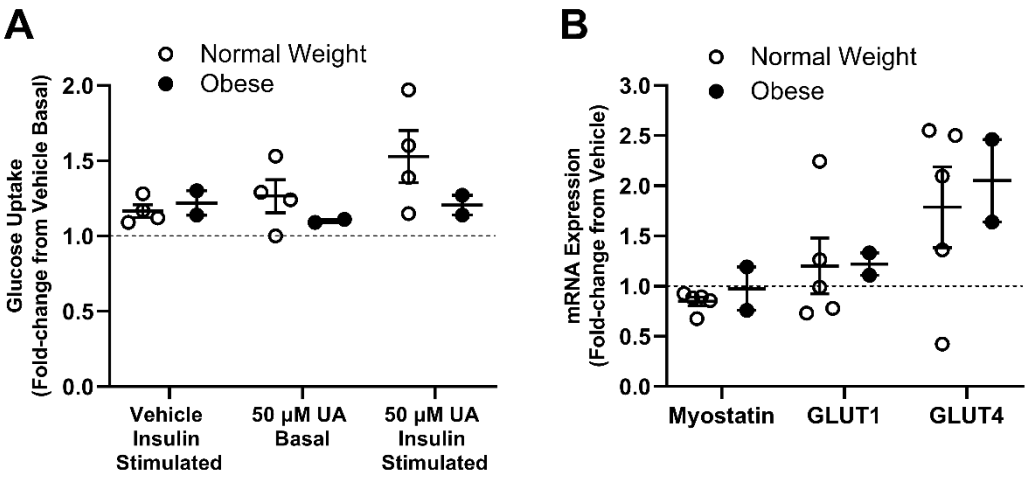

Figure 6.8. Exploratory comparison between the effects of 24 h exposure to 50 µM UA in primary myotubes from normal weight and obese donors. Basal (open circles) and insulin-stimulated (100 nM; closed circles) glucose uptake was measured using [3H] 2-DOG. Data from Normal Weight (n = 4) and Obese (n = 2) independent donor repeats are presented as Mean ± SEM of fold-change from Vehicle Basal (**A**). The relative mRNA expression of myostatin, GLUT1 and GLUT4 was measured via RT-qPCR; data from Normal Weight (n = 5) and Obese (n = 2) independent donor repeats are presented as Mean ± SEM of fold-change from Vehicle (**B**). Dashed line denotes the Basal Vehicle level (normalised to = 1), thus values above the dashed line reflect relative increases and values below reflect relative decreases from Basal Vehicle.

6.4.7 Exploratory comparison between the effects of 24 h exposure to 50 μM UA in primary human myotubes from young and older donors

As an exploratory outcome, the effects of donor age on responsiveness to UA was considered by stratifying data from independent donor repeats into Young (age range: 20–22 yrs; total n = 3) and Older (age range: 49–81 yrs; total n = 5) donor groups. Donor characteristic data demonstrated that the two groups did not significantly differ except for mean age (Mean ± SD: 21 ± 1 vs 66 ± 13 yrs; *P* = 0.002) (Table 6.3).

When glucose uptake data was stratified by age (Young (n = 3) vs Older (n = 3)), on average 50 μM UA treatment increased basal glucose uptake (expressed as fold change from Vehicle basal) more in Young than Older independent donor repeats (Mean ± SEM: 1.27 ± 0.15-fold vs 1.15 ± 0.05-fold, respectively) (Figure 6.9A). Glucose uptake was similarly increased by insulin stimulation in Vehicle treated cells in Young and Older independent donor repeats, however in Young independent donor repeats 50 μM UA treatment further increased insulin stimulated glucose uptake relative to Vehicle more than in Older independent donor repeats (Young: 1.57 ± 0.24-fold vs 1.18 ± 0.06-fold; Older: 1.27 ± 0.07-fold vs 1.19 ± 0.06-fold, respectively). Changes in the mRNA expression of myostatin and GLUT4 after 50 μM UA treatment (expressed as fold-change from Vehicle) were similar between Young (n = 2) and Older (n = 5) independent donor repeats (Figure 6.9B). Conversely, following treatment with 50 μM UA, on average GLUT1 expression was reduced in Young, but increased in Older independent donor repeats, relative to Vehicle (0.88 ± 0.11-fold vs 1.34 ± 0.25-fold, respectively) (Figure 6.9B).

Table 6.3. Characteristic data for Young and Older skeletal muscle biopsy donors, from whom myogenic cultures were derived.

	Mean (± SD)		*P*
Donor Characteristic	**Young Donors**	**Older Donors**	**Young vs. Older**
Sex (M/F (n))	1/2	3/2	-
Age (y)	21 (± 1)	66 (± 13)	**0.002**
BMI ($kg \cdot m^{-2}$)	24.4 (± 3.0)	29.0 (± 7.1)	0.347
Mass (kg)	72.8 (± 10.9)	89.5 (± 26.0)	0.351
Waist (cm)	83 (± 8)	107 (± 21)	0.117
Hip (cm)	94 (± 6)	112 (± 14)	0.089
Waist:Hip ratio	0.88 (± 0.07)	0.95 (± 0.09)	0.327

Comparisons between Young and Older donor characteristics were performed using unpaired t-tests.

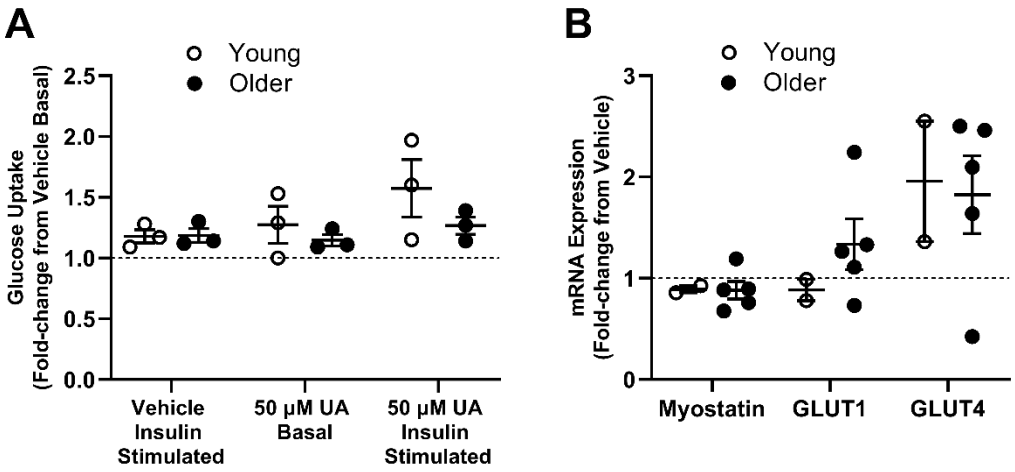

Figure 6.9. Exploratory comparison between the effects of 24 h exposure to 50 µM UA in primary myotubes from young and older donors.

Basal (open circles) and insulin-stimulated (100 nM; closed circles) glucose uptake was measured using [3H] 2-DOG. Data from Young (n = 3) and Older (n = 3) independent donor repeats are presented as Mean ± SEM of fold-change from Vehicle Basal (**A**). The relative mRNA expression of myostatin, GLUT1 and GLUT4 was measured via RT-qPCR; data from Young (n = 2) and Older (n = 5) independent donor repeats are presented as Mean ± SEM of fold-change from Vehicle (**B**). Dashed line denotes the Basal Vehicle level (normalised to = 1), thus values above the dashed line reflect relative increases and values below reflect relative decreases from Basal Vehicle.

6.4.8 Effects of 24 h Urolithin A treatments on 3T3-L1 adipocyte viability

Exposure of 3T3-L1 adipocytes to 10% DMSO induced significant cell death and served as a positive control for the viability assay. One-way ANOVA revealed a significant effect of treatment on cell viability ($P < 0.0001$; $\eta_P^2 = 0.949$) (Figure 6.10). Consistent with our observations in primary human myotubes, post-hoc comparisons indicated that significant toxicity only occurred when adipocytes were exposed to 100 µM UA (Mean Difference [95% CI]: -16945 [-3402, -30488] a.u.; $P < 0.01$). Treatment with 100 µM UA for 24 h resulted in an ~8% loss of cell viability, relative to Vehicle (considered to represent 100% viability). Thus, equal concentrations of UA as used for myotube experiments, were used to assess the effects of UA on adipocyte glucose uptake.

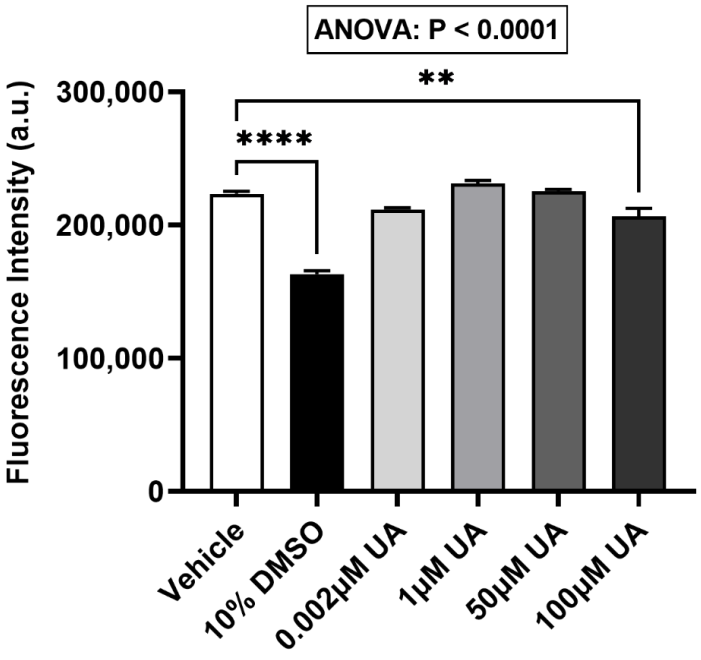

Figure 6.10. Effect of 24 h UA exposure on 3T3-L1 adipocyte viability.
Viability was assessed in differentiated 3T3-L1 adipocytes via Resazurin assay. Data presented as Mean ± SEM of fluorescence intensity – background (n = 4 replicate wells per treatment). $^{**}P < 0.01$ and $^{****}P < 0.0001$ indicate significant differences from Vehicle.

6.4.9 Effects of 24 h Urolithin A treatments on basal and insulin-stimulated glucose uptake in adipocytes

Two-way ANOVA revealed an interaction effect between UA and insulin treatment ($P < 0.0001$; $\eta_P^2 = 0.718$), as well as main effects of UA treatment ($P < 0.0001$; $\eta_P^2 = 0.777$) and insulin ($P < 0.0001$; $\eta_P^2 = 0.997$) on glucose uptake. Subsequent one-way ANOVAs revealed that UA increased both basal ($P = 0.017$; $\eta_P^2 = 0.508$, Figure 6.11A) and insulin-stimulated ($P < 0.0001$; $\eta_P^2 = 0.861$, Figure 6.11B) glucose uptake. While in the basal state, only 50 μM UA significantly increased glucose uptake from Vehicle (Mean Difference [95% CI]: 8.08 [1.62, 14.54] pmol·mg^{-1}·min^{-1}; $P < 0.05$), in the insulin-stimulated state, increasing UA concentration increased glucose uptake. Indeed, treatment with 0.002 μM UA increased insulin-stimulated glucose uptake 1.09-fold relative to Vehicle (Mean Difference: 39.74 [1.19, 78.29] pmol·mg^{-1}·min^{-1}; $P < 0.05$), while treatment with 1 μM and 50 μM (a 500- and 25,000-fold increase in UA concentration, respectively) induced 1.15-fold (Mean Difference: 69.40 [33.99, 104.80] pmol·mg^{-1}·min^{-1}; $P < 0.001$) and 1.21-fold (Mean Difference: 98.85 [65.46, 132.20] pmol·mg^{-1}·min^{-1}; $P < 0.0001$) respective increases.

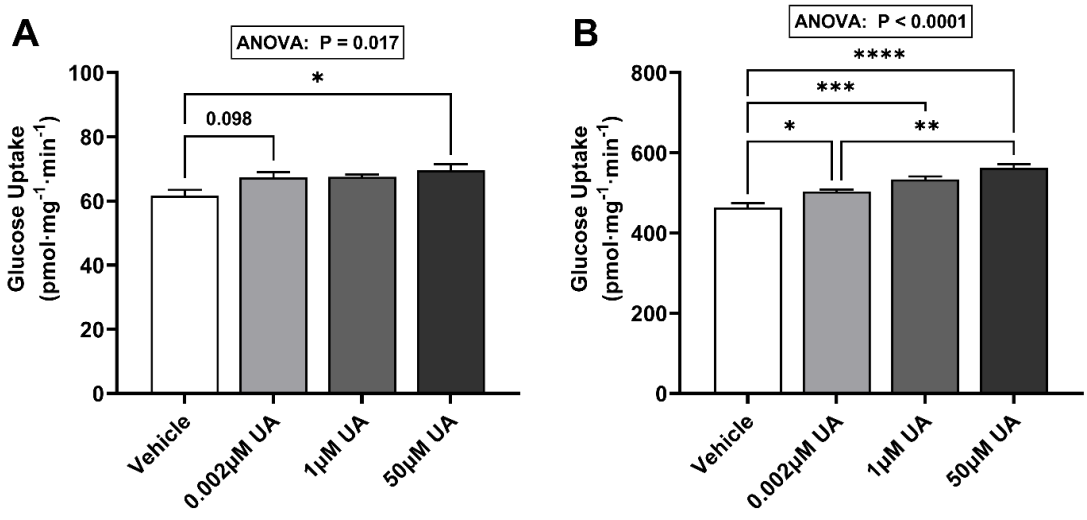

Figure 6.11. Effect of 24 h UA exposure on basal and insulin-stimulated glucose uptake in 3T3-L1 adipocytes.

Basal (**A**) and insulin-stimulated (**B**; 100 nM) glucose uptake was measured using [3H] 2-DOG. Data are Mean ± SEM of n = 5 replicate wells per treatment. *$P < 0.05$; **$P < 0.01$; ***$P < 0.001$ and ****$P < 0.0001$ denote significant differences between treatments as indicated.

6.5 Discussion

The present study is the first of its kind, so far as can be found within the literature, to assess the potential for Urolithin A to improve indices of metabolic health in primary human myotubes. This body of work expands upon the effects of UA previously reported in non-human myogenic cultures and animal models, by demonstrating that acute (24 h) treatment of primary human myotubes with 50 μM UA improves both basal and insulin-stimulated glucose uptake, which was associated with upregulation of GLUT4 expression. UA also suppressed the expression of myostatin but did not alter anabolic sensitivity to amino acids. Pertinently, the beneficial effects of UA largely persisted in cells derived from donors with obesity and of advanced age. Furthermore, it was demonstrated that the propensity for UA to promote cellular glucose uptake under basal and insulin-stimulated conditions was not a unique feature of myotubes and was similarly recapitulated in 3T3-L1 adipocytes, even at the lowest concentration tested (0.002 μM). This work endeavoured to answer the recent call for improved physiological relevance in Urolithin research (García-Villalba et al., 2022). Thus, this study provides the first data to explore the effects of a broad spectrum of UA concentrations, including minimum circulating abundances reported an *in vivo* study, while also demonstrating non-toxic effects at the highest concentration applied.

A significant loss of myotube viability occurred when myotubes were exposed to 100 μM UA (but not 0.002, 1 or 50 μM) for 24 h. This corroborates previous data from murine C2C12 myotubes, which reported beneficial effects of 1-50 μM UA on C2C12 myotube viability when challenged with 0.75 mM palmitate (Chan, 2018). Therefore, in conjunction with previous results in C2C12 cells, a maximal treatment concentration of 50 μM was used moving forward.

In the present study, treatment of myotubes with 50 μM UA elicited a 21% increase in basal glucose uptake, which was preserved but not further enhanced in the insulin-stimulated state. This suggests that UA has comparable potential to confer beneficial effects in skeletal muscle glucose uptake in both the post-absorptive and post-prandial state. It must be considered that in cultured human myotubes, GLUT1 (a non-insulin-dependent glucose transporter (Gaster, Franch, et al., 2000)) is overexpressed relative to GLUT4 (an insulin-dependent glucose transporter; myotube GLUT1:GLUT4 is ~7:1), when compared to skeletal muscle *in vivo* where GLUT1 expression is lower than GLUT4 (Gaster, Handberg, Beck-Nielsen, & Schroder, 2000; Sarabia et al., 1992). These findings are consistent with a prior study demonstrating positive effects of EA on C2C12 basal glucose

uptake, at concentrations ranging from 1 nM to 0.5 μM (Poulose, Prasad, Haridas, & Gopalakrishnapillai, 2011).

Mechanistically, the increased glucose uptake observed with high-dose UA may be attributable to upregulation of GLUT4. While GLUT4 abundance in primary human myotubes is low, it is still significantly recruited to the plasma membrane upon insulin stimulation (Al-Khalili et al., 2003) and is translocated in C2C12s upon stimulation with low doses of EA (Poulose et al., 2011). Indeed, while lowly expressed overall, treatment with 50 μM UA induced an almost 2-fold increase in GLUT4 mRNA expression. While GLUT1, the predominant glucose transporter in primary human myotubes, did not appear to be affected by UA at the mRNA level, it is worth noting that upon closer inspection of independent donor repeats it was evident that GLUT1 was upregulated by 50 μM UA in 4 out of 7 independent donor repeats. In this subset of donor repeats (all of whom were older), responsiveness to GLUT1 upregulation (ΔGLUT1 expression) was strongly and significantly correlated with the change in basal (r = 0.982, P = 0.018) but not insulin-stimulated (r = 0.530, P = 0.466) glucose uptake (data not shown). While the ability to extrapolate this observation is severely restricted by its sample size, it warrants further investigation since it appears to have favourably affected only older donor cells.

In the context of the well-established propensity for UA to promote mitochondrial function and biogenesis in skeletal muscle (Andreux et al., 2019; Luan et al., 2021), the increased capacity for myotubes to uptake glucose in the present study, may contribute towards an increased capacity for oxidative phosphorylation, which is perturbed in insulin resistant individuals (K. F. Petersen, Dufour, Befroy, Garcia, & Shulman, 2004; Sergi et al., 2019). Supporting this hypothesis, it has previously been demonstrated that chronic UA administration upregulates the activity of mitochondrial respiratory complexes I and II in the skeletal muscle of muscular dystrophic or HFD-fed mice (Luan et al., 2021; Ryu et al., 2016). In the postprandial state, as much as 50% of the glucose that is taken up by skeletal muscle undergoes oxidation, demonstrating the importance of this mechanism in glucose homeostasis (D. Kelley et al., 1988). To that effect, glucose is first metabolised to pyruvate via glycolysis and can subsequently enter the mitochondria for further metabolism within the TCA cycle. Thus, it is plausible that the observed enhancement of glucose uptake functions to serve the UA-mediated increased capacity of the mitochondria, which expands upon the previously demonstrated UA-induced upregulation of basal oxygen consumption

in C2C12 myotubes (Ryu et al., 2016) and whole-body oxygen consumption in mice (Xia et al., 2020).

Another novel finding of this study was that myostatin mRNA expression declined with increasing UA concentration, such that although treatment with 0.002 μM UA did not significantly suppress its expression, a tendency for modest suppression was seen with 1 μM UA (~8% reduction, $P = 0.076$) and significant suppression was observed following 50 μM UA (~14% reduction, $P < 0.01$). Importantly, the ability for UA to suppress myostatin expression was not dependent upon donor phenotype, with all but one donor demonstrating at least an 8% reduction in expression with 50 μM UA, relative to Vehicle. While this finding presents only a modest effect size (Cohen's $d = 0.21$), given myostatin's involvement in the repression of muscle growth and regeneration (Langley et al., 2002; W. E. Taylor et al., 2001; Kathryn R. Wagner, Liu, Chang, & Allen, 2005) and the elevated myostatin mRNA expression seen in older adults with obesity presented in Chapter 2, even modest suppression of myostatin, if chronically sustained, may present a promising avenue for nutraceutical mitigation of sarcopenic obesity. Importantly, in the present study, the suppression of myostatin expression was accompanied by increased basal and insulin-stimulated glucose uptake, although the magnitudes of change of myostatin and glucose uptake were not significantly correlated. Given that the dysregulation of both of these factors is a common feature of obesity in older adults, these findings emphasise the potential value of further research within this area.

The present study provides the first report of the effects of UA on protein synthesis in primary human myotubes. Despite suppressing myostatin expression after 24 h of Urolithin A treatment, no effect was found on amino acid-stimulated myotube protein synthesis, as indicated by the incorporation of the tyrosyl-tRNA analogue Puromycin into newly synthesised peptides. It would be valuable for future research to explore whether chronic UA treatment would maintain or enhance the suppression of myostatin, and whether this would ultimately translate to changes in muscle protein synthesis and/or breakdown. This is consistent with a study of C2C12 myotubes by Julie Rodriguez et al. (2017) who found that 24 h treatment with 15 μM UA did not affect myotube protein synthesis, although equimolar treatment with Urolithin B induced a ~2-fold increase, when similarly assessed using the SuNSET technique. The authors noted that despite Urolithin A and B differing only by a single hydroxyl group, they appear to mediate significantly different effects on skeletal muscle cells, with Urolithin B improving growth and differentiation via increased protein synthetic rate and repression of the ubiquitin-

proteasome catabolic pathway (as evidenced by reduced FoxO1, FoxO3, MAFbx and MuRF1 expression and less protein ubiquitination).

Together, these data suggest that the impact of urolithins on the relationship between myostatin and its downstream mediators of myogenic repression and atrophy is complex. Indeed, when Julie Rodriguez et al. (2017) studied denervation-induced atrophy in mice, Urolithin B treatment did not significantly alter the denervation-induced upregulation of myostatin expression relative to Vehicle (DMSO), but did significantly reduce expression of MuRF1 and MAFbx. This uncoupling of myostatin and E3 ligase expression is consistent with our findings in Chapter 5, where we observed differential changes in the expression of myostatin, E3 ubiquitin ligases, and myotube protein synthesis following exposure to the obese adipose tissue secretome. It is important to consider, however, that *in vivo* it is not the acute, but the chronic elevation of muscle protein synthesis that must be achieved to preserve muscle mass with ageing, and it is plausible that sustained UA-mediated myostatin suppression (through chronic treatment/supplementation) could succeed, where acute suppression did not.

In accordance with the secondary aims of this investigation, responses to 50 μM UA treatment were stratified by donor phenotype as an exploratory comparison. The observed increase in glucose uptake from Vehicle Basal was present, albeit partially blunted, in myotubes derived from both Obese and Older donors, relative to their younger, Normal Weight counterparts. In young, Normal Weight donor myotubes, 50 μM UA increased both basal and insulin-stimulated glucose uptake beyond that of the respective vehicle treatments. Myotubes derived from Obese and Older donors both demonstrated ~10% increased basal glucose uptake in response to 50 μM UA, however the additive effect of 50 μM UA with insulin-stimulation was not present in Obese and was reduced in Older independent donor repeats, relative to Normal Weight and Younger. Nevertheless, a 10% increase in basal glucose disposal could be of physiological significance *in vivo*, particularly for the maintenance of post-absorptive glycaemia, if sustained chronically. This is an important finding for the implications of UA as a novel nutraceutical, since impaired glucose handling disproportionately affects the aged, obese population. This finding expands on the recent work of both J. Yang et al. (2020) and Toney et al. (2019) who reported that in mice with high fat/high sucrose diet-induced insulin resistance, chronic administration of UA or UA and EA (8 and 12 weeks, respectively) decreased fasting glucose concentration and improved insulin-mediated glucose disposal during glucose and insulin tolerance tests.

Adipocyte Viability and Glucose Uptake

Previous work from independent groups has suggested that polyphenols are capable of exerting insulin-sensitising effects on adipocytes via upregulation of GLUT4 expression and enhanced activation of PI3K and AMPK pathways (Cao, Polansky, & Anderson, 2007; G. Li et al., 2018; Nagai et al., 2014; Torabi & DiMarco, 2016). Pertinently, EA, the precursor from which Urolithins are derived, has been demonstrated to stimulate glucose transport in 3T3-L1 adipocytes, via AMPK-mediated pathways (Poulose et al., 2011). In support of this proposed mechanism, UA treatment improves whole-body insulin sensitivity and promotes adipocyte browning in rodents (Abdulrahman et al., 2020; Xia et al., 2020), and suppresses lipid accumulation while promoting fatty acid oxidation via AMPK activation in human adipogenic stem cells and 3T3-L1 adipocytes, suggesting UA favourably modifies energy sensing pathways in adipocytes (Kang, Kim, Tomás-Barberán, Espín, & Chung, 2016; Les, Arbonés-Mainar, Valero, & López, 2018).

Following on from the results obtained from primary myotubes, the potential effects of UA in adipose tissue was investigated, using the immortalised murine fibroblast cell line, 3T3-L1. This cell line can be pushed towards a highly differentiated, lipid-laden, adipocyte-like phenotype, that has consistently been demonstrated to provide a useful *in vitro* model of human white adipocytes (Green & Meuth, 1974; B. H. Jones et al., 1997; Morrison & McGee, 2015). Consistent with myotubes, only when cells were treated with 100 μM UA, did a significant loss of cell viability occur, at a rate of ~8% reduction after 24 h. Therefore, identical UA treatments were applied to 3T3-L1 adipocytes, as was applied to primary myotubes, to elucidate whether the observed glucose disposal-stimulating effects of UA were a unique response of skeletal muscle cells or functionally conserved in cells from other metabolically active tissues.

Consistent with the observations in myotubes, UA treatment demonstrated a significant and positive effect on glucose uptake in 3T3-L1 adipocytes. Notably, even at the lowest tested UA concentration (0.002 μM) there was a tendency for increased basal and significantly increased insulin-stimulated glucose uptake. Importantly, since this concentration reflects the chronically-sustained fasted circulating concentration of UA reported after repeat supplementation (Andreux et al., 2019), this suggests that even modest, sustained dosing of UA *in vivo* could plausibly exert metabolically significant effects on adipose tissue. Cisneros-Zevallos et al. (2020) demonstrated that treatment of 3T3-L1 adipocytes with 25 μM UA to for 8 days during differentiation, resulted in a ~50% reduction in TAG accumulation, which was associated with a ~50% reduction in GLUT4 expression,

but a preserved capacity for insulin-stimulated Akt phosphorylation (Cisneros-Zevallos et al., 2020). Combining these findings with the present observations, suggests that adipocyte maturity influences the nature of response to UA exposure, which is consistent with observations of the effect of UA's precursor; EA (Okla et al., 2015). Indeed, while exposure of mature adipocytes to UA increases basal and insulin-stimulated glucose uptake via changes in energy sensing pathways, exposure of immature adipocytes to UA, as observed by Cisneros-Zevallos et al. (2020), appears to induce alternative metabolic programming that reduces substrate uptake in the immature cells, subsequently impairing lipid accumulation/adipogenesis.

6.6 Limitations and Future Directions

This study demonstrated the potential of Urolithin A as a nutraceutical for the preservation and promotion of skeletal muscle metabolic health. Robust efforts were made to create *in vitro* models with significant physiological relevance, however there are several limitations which must be acknowledged. Firstly, owing to restrictions of time and the enduring challenges of human volunteer research during the COVID-19 pandemic, the number of donor replicates employed were not optimal for the phenotypic stratification analyses performed. Efforts were made to make clear in the results the restricted ability to draw statistical comparisons and extrapolate findings from these analyses, however they proved sufficiently robust to suggest differential effects that are worth pursuing further.

Secondly, in these experiments, culture systems were treated with UA itself, so-called 'parent UA'. It must be considered that parent UA is not the dominant form within the circulation. Rather, its phase II metabolites (predominantly UA-glucorinide and UA-sulfate) abound in far greater concentrations (Andreux et al., 2019). It is worth noting, however, that following oral ingestion of UA in humans, the combined plasma concentration of parent, glucorinide and sulfate forms of UA can reach ~3 μM. Furthermore, consideration must be given to the fact that static culture systems lack the circulatory flow of an *in vivo* system. Indeed, absolute exposure of muscle cells to circulating factors is a function of both their concentration and the rate of flow through the tissue. It stands to reason, therefore, that greater concentrations of any given treatment would likely be required within a static *in vitro* system to recapitulate the effects seen in the dynamic *in vivo* environment. It is yet unclear what the functional differences between exposure to UA and its metabolites are and future research must seek to better understand their respective significance.

Finally, while upregulated GLUT4, and to a lesser extent GLUT1, were successfully identified as mechanistic candidates for the UA-mediated effects on glucose uptake, further exploration to elucidate UA's mechanism of action on myostatin expression or its downstream pathway was not undertaken. This was a limitation imposed by temporal restrictions, requiring strict prioritisation of laboratory analyses, but highlights an important avenue for future investigation. To that effect, additional cDNA samples from all independent donor repeats treated with all UA concentrations were generated, as well as snap-frozen pellets of cells treated with Vehicle or 50 μM UA, which were sent to our external collaborators for more comprehensive profiling of gene expression, particularly pertaining to key mitochondrial genes, and exploratory untargeted metabolomics, respectively.

Myostatin is considered a highly druggable target, and various pharmacological means of inhibiting or disrupting myostatin have been explored, including neutralising antibodies, inhibitory propeptides, soluble ACTRIIB receptors, interacting proteins, and antibodies that block release from the pro-domain (Pirruccello-Straub et al., 2018; T. A. White & LeBrasseur, 2014). The present study demonstrates a potential novel nutraceutical approach for the modulation of myostatin expression that negates prior issues of poor ET/EA bioavailability and pharmacokinetics. Nevertheless, it is also worth considering the possibility for pharmaceutical recapitulation of these effects, such as has been previously demonstrated for other polyphenolic compounds via the production of synthetic analogues, some of which show similar pre-clinical and clinical benefits to their naturally-occurring counterparts (Colomer, Sarrats, Lupu, & Puig, 2017). Indeed, recent work has successfully generated synthetic Urolithins and urolithin derivatives, which have been recognised as lead compounds for novel drug development (Djedjibegovic, Marjanovic, Panieri, & Saso, 2020; Noshadi et al., 2020). These advances, in tandem with novel approaches for commercially viable up-scaling-of the production of synthetic polyphenols and their metabolites, while maintaining quality and consistency, are opening the door to further exploration of targeted novel therapies and should continue to be explored under conditions of maximal physiological relevance (Kallscheuer, Vogt, & Marienhagen, 2017; Rainha, Gomes, Rodrigues, & Rodrigues, 2020).

6.7 Conclusions

This study provides the first direct evidence of metabolically beneficial effects of Urolithin A in primary human skeletal muscle cells. It was demonstrated that acute UA treatment improves both basal and insulin-stimulated glucose uptake in both skeletal muscle and adipose cells, and that these effects in skeletal muscle cells may be mediated by the upregulation of GLUT4 expression. Importantly, these effects persisted, albeit to a lesser extent, in the presence of donor obesity and advanced age, although the limited number of independent donor repeats employed precluded firm conclusions being made. Additionally, it was revealed that UA exerts a dose-responsive suppressive effect on the expression of myostatin in human skeletal muscle cells. Although this did not translate to enhanced muscle protein synthesis in the acute setting (24 h treatment), it could be beneficial in the context of chronic supplementation and future research should also seek to assess effects on muscle protein breakdown. Importantly, the present study demonstrated the suppression of myostatin in muscle cells and increased glucose uptake into adipocytes, even at a concentration of UA that reflects circulating abundance *in vivo* after dietary supplementation, suggesting plausible translation into human studies of obesity and ageing, where these effects should be investigated further.

Chapter 7. General Discussion

7.1 Background

Obesity is typically associated with declining metabolic health, including impaired regulation of glucose homeostasis and metabolism through the action of insulin (insulin resistance). Often concurrent with insulin resistance is an impairment of the amino acid stimulation of muscle protein synthesis, termed anabolic resistance (Morais et al., 2018; Morton et al., 2018). Together, the obesity-associated impairment of insulin and anabolic sensitivity contribute to pathophysiological consequences with ageing, including the decline of skeletal muscle mass and function, termed sarcopenia, which is of growing prevalence (Mathus-Vliegen et al., 2012; J. E. Morley, 2008). Since skeletal muscle is responsible for a significant part of postprandial glucose disposal, the concurrent diminution of skeletal muscle mass and insulin sensitivity directly reduces whole body glucose disposal and jeopardises glucose homeostasis (R. A. DeFronzo, 2004). It is vital to understand factors that are dysregulated in obesity and ageing to develop novel therapeutic strategies.

Myostatin is a TGF-β family member that negatively regulates skeletal muscle growth (McPherron et al., 1997). Myostatin has also been implicated in the regulation of insulin sensitivity, with myostatin knockout mice exhibiting resistance to HFD-induced obesity and glucose intolerance (T. Guo et al., 2009; McPherron & Lee, 2002). More recently, it has been demonstrated in humans that myostatin appears to be upregulated by obesity and associated with insulin resistance (David L. Allen et al., 2011; Hittel et al., 2009). However, adiposity, insulin resistance and ageing often advance together in humans and thus observational studies are confounded by these commonalities (St-Onge, 2005).

Myostatin administration impairs insulin-stimulated Akt phosphorylation (T. Guo et al., 2009; Hittel et al., 2010; X.-H. Liu et al., 2018), while the genetic deletion or inhibition of myostatin enhances it, which may provide a mechanistic link between its roles in insulin and anabolic signalling, since both of these pathways converge on the activation of Akt (L. A. Consitt & Clark, 2018). Pertinently, myostatin inhibition increases skeletal muscle glucose disposal in HFD-fed mice, with increased Akt phosphorylation and upregulated GLUT4 expression (Dong et al., 2016; Eilers et al., 2020). To date, studies of myostatin manipulation have predominantly utilised rodents or cell lines, which restricts the extrapolation of their findings into humans. Exactly what drives the upregulation of myostatin in obesity is unclear and it remains to be established whether this observed

upregulation is a contributor to, or a product of, the development of skeletal muscle insulin resistance.

There is growing interest in myostatin as a therapeutic target, particularly for muscle wasting conditions. Various pharmacological means of inhibiting or disrupting myostatin expression, receptor binding, and signalling have been explored (T. A. White & LeBrasseur, 2014). Thus far, only a handful of these therapeutics have been trialled in humans, and there is little robust evidence of their effectiveness for promoting muscle mass and function. The potential application of candidate myostatin-suppressing compounds as insulin-sensitising factors has yet to be substantially explored in humans or human primary muscle cells, which provide a relevant model of human skeletal muscle (Aas et al., 2013). Indeed, it has been demonstrated that obese-derived muscle cells have greater expression of myostatin; impaired insulin sensitivity; and exhibit perturbed regulation of anabolic and catabolic pathways (Hittel et al., 2009). Thus, human primary myogenic culture offers a valuable tool that can be exploited to investigate the underlying causes and physiological significance of the modulation of myostatin expression and function.

7.2 Main Aims of This Thesis

The main aims of this thesis were to distinguish between the effects of obesity and ageing on the regulation of myostatin; to investigate potential underlying causes of this (dys)regulation; and to establish the functional significance and interconnectivity of modulating insulin and anabolic sensitivity and myostatin expression in human muscle cells. Specific primary aims of each experimental chapter were as follows:

In Chapter 3, a cross-sectional analysis was undertaken to delineate between the independent effects of obesity and ageing on the skeletal muscle expression of myostatin, its interacting proteins and its downstream signalling components.

Chapter 4 sought to establish whether the obesity-mediated upregulation of myostatin was driven by the induction of lipid-induced insulin resistance, through the recapitulation of this process in human skeletal muscle cells.

Chapter 5 investigated whether expression of myostatin and its downstream targets, as well as insulin and anabolic sensitivity, are influenced by cross-talk with subcutaneous adipose tissue. To that effect, *ex vivo* and *in vitro* techniques were combined to model secretory cross-talk between SAT from lean and obese individuals, and human skeletal muscle cells.

In Chapter 6, the novel polyphenol metabolite, Urolithin A, which has been demonstrated to exert metabolically beneficial effects in non-human models, was applied to human muscle cells as well as a model of adipocytes, to investigate its therapeutic potential to influence insulin and anabolic sensitivity and myostatin expression.

7.3 Summary and Implications of Main Findings

In Chapter 3, gene and protein expression analysis of skeletal muscle samples revealed that myostatin mRNA expression was elevated ~2-fold in older adults with overweight and obesity who were insulin resistant, relative to age-matched normal weight older adults. Pertinently, in the absence of excessive adiposity, ageing alone was not associated with a change in myostatin gene expression, relative to younger normal weight adults. The obesity-mediated upregulation of myostatin mRNA was not paralleled by changes in the protein abundance of the 26 kDA mature myostatin ligand. Downstream of myostatin, the expression of both the myogenic regulatory factor, MYOD (which may exacerbate myostatin's upregulation via targeting its promotor region), and the E3 ubiquitin ligase, MAFbx, were respectively increased 2.3- and 1.7-fold in older donors with obesity relative to young normal weight adults but were not significantly greater than their age-matched normal weight counterparts. These findings suggest a 'tug-of-war' between pathways that promote skeletal muscle regenerative capacity, and those that promote muscle atrophy under the induction of the myostatin signalling cascade.

There was no difference in the expression of muscle inflammatory markers between older normal weight and obese individuals, suggesting the upregulation of myostatin is not driven by local inflammation. Furthermore, upregulated myostatin mRNA was not accompanied by changes in the expression of its receptor, ACVR2B, nor that of the inhibitory myostatin-binding protein, FSTL3, suggesting that its obesity-mediated upregulation is not offset by feedback mechanisms to inhibit its receptor binding and signal transduction. The observed association between myostatin expression and obesity *per se* was supported by findings in a separate cohort of participants, in which positive correlations between serum myostatin and multiple indices of adiposity, but not age or habitual physical activity level were observed. Taken together, Chapter 3 provides evidence that myostatin skeletal muscle mRNA expression and serum abundance are uniquely upregulated by obesity with ageing, but not by ageing in the absence of obesity, which is associated with abnormal regulation of pathways involved in the maintenance of skeletal muscle mass.

Having identified in Chapter 3 that myostatin expression is upregulated in older adults with obesity and insulin resistance, but not by ageing *per se*, Chapter 4 investigated whether lipid-induced insulin resistance could upregulate myostatin. To that effect, primary human myotubes from normal-weight insulin sensitive donors were incubated with fatty acid solutions at physiologically relevant concentrations that reflect levels seen in obese plasma and are known to induce insulin resistance in human myotubes (250 μM palmitate alone, or with the addition of 50 μM linoleic and 150 μM oleic acid (PLO)) for 16 h.

Acute palmitate and PLO treatment induced marked resistance to the stimulating effects of insulin on glucose uptake. These lipid-induced perturbations, however, were not accompanied by changes in the mRNA expression or protein abundance of myostatin. There was a myostatin-independent suppression of global myotube protein synthesis by 20% with palmitate but not PLO treatment, likely reflecting a protective effect of oleic acid and demonstrating a dissociation between insulin and anabolic resistance. Thus, acutely elevated free fatty acid availability can induce insulin and anabolic resistance in skeletal muscle cells but does not alter the expression or abundance of myostatin. These findings suggest that the obesity-mediated upregulation of myostatin observed in Chapter 3 may not be driven, at least acutely, by insulin resistance arising from excessive availability of dietary lipids.

Efforts were made in Chapter 5 to recapitulate the effects of adipose-muscle cross talk *in vitro* to elucidate whether the obesity-associated upregulation of myostatin might be mediated by an altered adipose tissue secretome in obesity. *Ex vivo* and *in vitro* techniques were combined to culture primary myotubes in the presence of the subcutaneous adipose tissue secretomes of normal weight and obese older adults. Relative quantitation of cytokines known to be secreted by human adipose tissue confirmed the substantial secretion of factors from adipose tissue explants into the culture medium and revealed different secretory phenotypes between the SAT of lean and obese older adults.

Relative to unconditioned medium, chronic (6 days) exposure of human primary myotubes to SAT secretome suppressed the mRNA expression of myostatin and this effect tended to be greater when myotubes were exposed to the Obese secretome than the Lean secretome, which may have been mediated by alternative regulation of myostatin expression via a MYOD-mediated or self-inhibitory feedback loop. The reduction in myostatin expression was accompanied by a pattern of improved glucose transport and insulin-sensitivity following exposure to the adipose tissue secretome. Thus, the obese SAT secretome does

not appear to explain the upregulation of myostatin expression previously observed in obese skeletal muscle *in vivo*. Nevertheless, findings of concurrent suppression of myostatin expression and a pattern of improved indices of insulin sensitivity in response to both Lean and Obese SAT secretome exposure, relative to unconditioned medium, supports the association between reciprocal changes in myostatin expression and insulin sensitivity.

In Chapter 6, experiments were undertaken to assess the effects of a novel nutraceutical compound on myostatin expression and whether any such changes are associated with changes in indices of insulin and anabolic sensitivity. Urolithin A is a recently identified polyphenol metabolite that has demonstrated promising effects on the preservation of insulin sensitivity and muscle metabolic health, principally via the promotion of mitophagy, in non-human models of ageing skeletal muscle (Luan et al., 2021; Ryu et al., 2016; Toney et al., 2019).

This study provided the first evidence of metabolically beneficial effects of Urolithin A in human primary myotubes. Acute (24 h) treatment with 50 μM UA improved both basal and insulin-stimulated glucose uptake by ~20%, which may have been mediated by a 2-fold upregulation in GLUT4 expression. UA suppressed the mRNA expression of myostatin by 14%, which did not translate to enhanced amino acid stimulated protein synthesis in the acute setting but could be beneficial in the context of chronic supplementation. Pertinently, in an exploratory sub-analysis it was demonstrated that the beneficial effects of UA appear to largely persist in cells derived from donors with obesity and of advanced age. Furthermore, it was demonstrated that UA also increased glucose uptake in 3T3-L1 adipocytes. Together these findings suggest plausible translation into human studies of obesity and ageing, where these effects, as well as implications for muscle protein breakdown, should be investigated further.

Synthesising the findings of this thesis with the existing field of literature, it is becoming increasingly apparent that the dysregulated expression and abundance of myostatin previously reported in some studies of older adults (McKay et al., 2012; Yarasheski et al., 2002), is likely driven by the presence of obesity and/or insulin resistance, which has become a common feature of ageing. What remains less clear, however, is the nature of the reported association between myostatin and insulin resistance, that was first demonstrated in myostatin knockout mice who exhibited enhanced insulin sensitivity and other favourable metabolic changes (McPherron & Lee, 2002). Indeed, the obese cohort in Chapter 3 also exhibited impaired insulin sensitivity relative to their leaner age-matched counterparts, and thus the independent effect of insulin resistance could not be separated. Thus, the

subsequent experimental chapters sought to disentangle this association by isolating factors involved in the development of insulin resistance in obesity.

While neither acute lipid-induced insulin resistance nor the obese SAT secretome upregulated myostatin mRNA or protein expression in human muscle cells, it must be recalled that the insulin resistant state in obesity is a chronic, not acute, syndrome (Hardy et al., 2012). Furthermore, contrary to expectations, both Lean and Obese SAT secretome suppressed myostatin mRNA expression and was accompanied by improved indices of insulin sensitivity, relative to unconditioned medium, although the obese secretome was broadly more pro-inflammatory. As such, a causal relationship between myostatin and insulin resistance cannot be verified by these findings, but they do suggest that the upregulation of myostatin expression observed in obesity may not be driven by the SAT secretome.

The findings of Chapter 5 differ from some existing studies that modelled the effects of adipose-muscle cross talk using co-cultured adipocyte cell lines or adipocyte-conditioned media. Indeed, several studies demonstrated adipocyte secretome-mediated upregulation of myostatin and impaired insulin sensitivity (Dietze et al., 2002; Seo et al., 2019). Chapter 5, however, used a more novel approach to capture and apply the whole subcutaneous adipose tissue secretome which doubtless better reflects physiological adipose-muscle cross talk and challenges the relevance of using cell lines for such investigations. It remains to be established, however, whether other adipose tissue compartments that are expanded in obesity, such as visceral and intramuscular adipose tissue, might mediate upregulation of muscle myostatin. Visceral adipose tissue provides a prime candidate for the continuation of such an investigation, since its secretome confers more deleterious effects on muscle cell insulin sensitivity and myogenesis than the subcutaneous depot (Pellegrinelli et al., 2015; Zoso et al., 2019), while intramuscular adipose tissue could confer paracrine effects, which may explain the contrasts with findings of co-culture studies. Finally, the Urolithin-A mediated suppression of myostatin and concurrent improvement in glucose handling in both myotubes and adipocytes, provided further evidence supporting the association between changes in muscle myostatin and insulin sensitivity at the tissue level, but was not able to confirm causality or directionality of this association.

Thus, this thesis challenges the purported association of chronological ageing with upregulated myostatin, and instead proposes that such a trajectory is not biologically inherent, but an artefact of obesity-mediated metabolic dysregulation. Instead, the findings of this body of work further supports the broad association between changes in myostatin expression/abundance and changes in insulin

sensitivity. Furthermore, it is demonstrated that muscle myostatin expression can be therapeutically targeted and suppressed, which may also confer favourable effects on glucose handling, and could prove most valuable for conditions such as sarcopenic obesity. There remain unanswered and newly arising questions as to the source of the obesity-mediated upregulation of myostatin; whether the actions of myostatin actively exacerbates insulin resistance, or indeed *vice versa*; and whether therapeutic suppression of myostatin *in vivo* will reap the same rewards demonstrated *in vitro*. Such quandaries should form the basis of future investigations, and should build upon the findings of this thesis, in conjunction with the existing literature, with a focus on mechanistic studies.

7.4 Strengths and Limitations

Having detailed within each chapter the specific limitations of the approaches and models applied, protracted repetition will be avoided. Instead, the relative merit and novelty, but also the practical limitations, of the work detailed within this thesis will be considered.

A consistent priority and strength of the *in vitro* work undertaken was the creation of models of skeletal muscle that were of greater physiological relevance than the immortalised cell lines that are commonly used. Thus, participants were first screened and phenotypically characterised before skeletal muscle biopsies were taken for the generation of primary myogenic cultures. Following preliminary work to establish guidelines for their culture, cells were ordinarily passaged a maximum of two times to best preserve myogenic capacity and any phenotypic traits that were conferred to the culture. These cultures were maintained in a glucose concentration (6.1 mM) that broadly reflects the mean 24 h glycaemic level of healthy free-living humans. In Chapter 4, the concentrations of palmitate, linoleic and oleic acids used were similar to those seen in the circulation of obese individuals, while in Chapter 5 whole SAT explants from many patients were used to model the adipose tissue secretomes of lean and obese older adults. In that study, however, the effects of the visceral adipose tissue secretome were not investigated, which certainly warrants further investigation on account of its more pro-inflammatory nature and greater association with the metabolic syndrome (Despres, 2006). Indeed, previous studies have reported more deleterious effects of obese human visceral adipose secretome on insulin sensitivity in muscle cells than the subcutaneous secretome (Lam, Janovská, et al., 2011). Furthermore, in Chapter 6 a range of concentrations of UA were applied to cells, including, for the first time in published experiments, the minimum circulating abundance reported in humans after supplementation.

Such considerations enable greater confidence in the physiological relevance of the models employed, but come with significant burdens and practical limitations. The recruitment, screening, biopsy sampling, myogenic isolation, proliferation and differentiation of these cultures is far more time and resource intensive than the use of alternatives such as C2C12 cells. Thus, it was not feasible, particularly under the constraints detailed in Appendix 3. COVID-19 Impact Statement, to perform as many independent donor repeats of experiments, nor to have as many treatment replicates, as would be preferable. Nevertheless, statistical power was still achieved for many of the main effects assessed within these chapters, which is a credit to the stringency of the approaches applied. Where exploratory analyses may have been underpowered to detect statistically significant effects, they nevertheless provide valuable data to build upon and provide estimations of power for future investigations.

A staple for the proliferation of myogenic cultures is the addition of animal sera to the culture medium to provide the necessary growth factors, hormones, enzymes and cytokines. The most commonly used serum for proliferating myogenic cultures is foetal bovine serum, which typically constitutes a minimum of 10% the media volume (in this thesis, 20% FBS was always used). Such animal sera remain relatively poorly characterised and inevitably exhibit a degree of variation between batches (Yao & Asayama, 2017). While serum-free alternatives are available and have been successfully applied to some cell lines, to date their functionality in myogenic cultures is significantly impaired relative to serum supplementation (Kolkmann, Post, Rutjens, van Essen, & Moutsatsou, 2020). Myogenic cultures can also be sustained in human sera (George, Velloso, Alsharidah, Lazarus, & Harridge, 2010), which might be of greater physiological relevance, but may also introduce another element of variability between experiments. An exploration of the use of human sera for primary myogenic culture was beyond the scope of this thesis but would doubtless be an interesting and useful avenue for future investigation to refine these models.

Throughout the chapters of this thesis, the various treatments that were applied to cells were all grounded in a reflection of physiological abundances and interactions. It must be considered however that the culture systems employed were static and two-dimensional, which is to say that cultures were grown in adherent monolayers and did not involve an element of 'flow'. *In vivo*, healthy muscle tissue is highly capillarised and supplied with a constant flow of blood and thus circulating factors. It is not possible to model this flow and flux in the employed static monolayer system. Instead, any treatment applied will

immediately abound at its maximal concentration and progressively decline as it is actively taken up into the cells or degrades. This may in part explain the generally reduced sensitivity of cultured cells to a given treatment, relative to that seen *in vivo*. The advances being made in microfluidics, 3-D organoid culture and electrical pulse stimulation models of skeletal muscle will lend themselves to more accurate recapitulation of human skeletal muscle *in vitro*.

7.5 Future Directions

This thesis identified that obesity *per se* is associated with the upregulation of myostatin, which is independent of the effects of ageing, and subsequently explored the effects of features of obesity on the regulation of myostatin expression and abundance in the context of perturbed insulin and anabolic sensitivity. Obesity, however, is a condition of the whole human system and it is not possible within the confines of a single thesis to fully explore its integrated effects on the skeletal muscle. The findings presented here, however, provide a springboard from which further research can be propelled.

The observation in Chapter 4 that acute palmitate exposure does not promote altered myostatin expression, despite the induction of insulin and anabolic resistance is an interesting one, but it must be considered that insulin resistance is often a process that develops over the lifetime. Of course, the lifetime of a primary myocyte is far shorter than a human being, but it would nevertheless be interesting to establish, proliferate and differentiate human myogenic cultures in the sustained presence of elevated FFAs as a model of the obese circulatory environment. Sustained treatment would likely cause significant intramyocellular lipid deposition (Abildgaard et al., 2014), which is a common feature of muscle insulin resistance *in vivo* but may be abrogated when myostatin is inhibited (LeBrasseur et al., 2009). Such experiments would likely require a reduced abundance of FFAs, however, as preliminary work to that effect (not shown) demonstrated that differentiating myoblasts for 7 days in 250 μM palmitate caused a marked reduction in protein content, RNA yield and myotube formation.

Having identified differential effects and adipokine profiles of lean and obese SAT secretome on myostatin expression and genes involved in muscle protein synthesis and breakdown in Chapter 5, it follows that further analysis of the secretory constituents of adipose tissue, and subsequent application of recombinant forms of differentially abundant factors might reveal further insight into the mechanisms responsible for the observed upregulation of myostatin in obesity. To that effect, comprehensive proteomic and lipidomic analysis of ACM would enable the identification of many more differentially secreted factors.

Furthermore, while the subcutaneous adipose compartment is typically the most abundant in obesity, visceral adipose tissue shows a markedly greater pro-inflammatory profile, while the proximity of inter/intramuscular adipose tissue grants it the greatest opportunity to exert paracrine effects on skeletal muscle tissue. Therefore, the secretomes of all three of these adipose tissue compartments are worthy of further investigation with regards to their involvement in human skeletal muscle health and metabolism. The exploration of inter/intramuscular adipose tissue will doubtless prove challenging, however, due to its physical location and relative scarcity making its extraction from human participants difficult. Cadaveric samples or rodent models are perhaps more practical for the expansion of these experiments using inter/intramuscular ACM.

The effects of Urolithin A on indices on both myostatin expression and glucose handling in myotubes was a novel finding that should be explored further. In line with the enhanced uptake of glucose into the myotubes, UA induced a 2-fold upregulation of GLUT4 expression. It was hypothesised that, consistent with the findings of small animal models of ageing skeletal muscle, this might reflect the induction of mitophagy and subsequently improved mitochondrial capacity. While time restricted further analysis from being undertaken, cDNA samples were sent to our industry collaborators to undertake comprehensive profiling of genes involved in mitophagy and mitochondrial function, as well as snap-frozen cells for untargeted metabolomic analysis. Additional qPCR analysis will bolster the observations made in Chapter 6, while the latter will facilitate an unbiased, top-down approach that could support the generation of new hypotheses regarding the mechanisms responsible for mediating UA's anti-myostatin, insulin sensitising effects in skeletal muscle cells. Finally, having recently demonstrated a favourable safety profile and robust bioavailability in humans (Andreux et al., 2019), the logical goal is translation into clinical trials to ascertain the real-world application of UA, or synthetic analogues as discussed in Chapter 6, as a treatment for the preservation of skeletal muscle health in obesity and ageing.

In this thesis, the expression of myostatin was suppressed by both the SAT secretome and by Urolithin A, with concurrent positive effects on indices of insulin sensitivity. The expression of myostatin was not, however, successfully upregulated experimentally. Isolated overexpression of myostatin in primary human myotubes could provide mechanistic insight. To that effect, as detailed in Appendix 3. COVID-19 Impact Statement, an additional experimental chapter was commenced, but not completed (as a consequence of the COVID-19 pandemic). The developmental process of generating a model of myostatin overexpression

using a doxycycline-inducible lentiviral toolkit, with the aim of translation into primary human myotubes is described fully in Appendix 2. An Inducible Model of Myostatin Overexpression. While beyond the scope of feasibility to complete this work and present its findings within this thesis, future research to generate a highly relevant model of human muscle, in which myostatin overexpression can effectively be 'switched on', would allow for far more specific examination of its effects on muscle insulin sensitivity, since the upregulation of myostatin would be the start of the cascade of intracellular events in such an experimental model, rather than a result of other factors.

7.6 Concluding Remarks

The work embodied within this thesis demonstrates that muscle myostatin expression is uniquely upregulated in older adults with obesity and insulin resistance, but not by ageing *per se*. Indeed, the mRNA expression and serum abundance of myostatin were found to correlate with indices of adiposity but not age or physical activity status. Experiments were therefore undertaken to discern the potential involvement of key features of obesity on the upregulation of muscle myostatin and its purported association with insulin and anabolic resistance. It was revealed that neither the acute induction of insulin and anabolic resistance by elevated fatty acid availability, nor the secretory milieux of obese subcutaneous adipose tissue induced the upregulation of myostatin expression in human primary muscle cells, despite perturbing the expression of some factors involved in both muscle protein synthesis and breakdown. The underlying factors responsible for the obesity-mediated upregulation of myostatin remain to be elucidated and future work to establish such causality is warranted. On the other hand, it was demonstrated for the first time that the novel nutraceutical compound Urolithin A suppresses myostatin expression and enhances glucose transport in human myotubes, the latter of which may have been attributed to the upregulation of GLUT4 expression, which together reinforce the purported association of changes in myostatin expression with changes in insulin sensitivity. Urolithin A also enhanced glucose uptake in 3T3-L1 adipocytes in a dose-dependent manner, suggesting potentially widespread effects on glucose handling. Having recently demonstrated a favourable safety profile, translational research to investigate the potential for concurrent improvement of glucose handling and repression of myostatin's inhibitory effects on muscle growth is warranted and could be of benefit in conditions such as sarcopenic obesity.

References

Aas, V., Bakke, S. S., Feng, Y. Z., Kase, E. T., Jensen, J., Bajpeyi, S., . . . Rustan, A. C. (2013). Are cultured human myotubes far from home? *Cell and Tissue Research, 354*(3), 671-682. doi:10.1007/s00441-013-1655-1

Aas, V., Hessvik, N. P., Wettergreen, M., Hvammen, A. W., Hallen, S., Thoresen, G. H., & Rustan, A. C. (2011). Chronic hyperglycemia reduces substrate oxidation and impairs metabolic switching of human myotubes. *Biochimica et Biophysica Acta, 1812*(1), 94-105. doi:10.1016/j.bbadis.2010.09.014

Aas, V., Rokling-Andersen, M., Wensaas, A. J., Thoresen, G. H., Kase, E. T., & Rustan, A. C. (2005). Lipid metabolism in human skeletal muscle cells: effects of palmitate and chronic hyperglycaemia. *Acta Physiologica Scandinavica, 183*(1), 31-41. doi:https://doi.org/10.1111/j.1365-201X.2004.01381.x

Abbatecola, A. M., Paolisso, G., Fattoretti, P., Evans, W. J., Fiore, V., Dicioccio, L., & Lattanzio, F. (2011). Discovering pathways of sarcopenia in older adults: A role for insulin resistance on mitochondria dysfunction. *The Journal of Nutrition, Health & Aging, 15*(10), 890-895. doi:10.1007/s12603-011-0366-0

Abdelmoez, A. M., Puig, L. S., Smith, J. A. B., Gabriel, B. M., Savikj, M., Dollet, L., . . . Pillon, N. J. (2020). Comparative profiling of skeletal muscle models reveals heterogeneity of transcriptome and metabolism. *American Journal of Physiology-Cell Physiology, 318*(3), C615-C626. doi:10.1152/ajpcell.00540.2019

Abdul-Ghani, M. A., Tripathy, D., & DeFronzo, R. A. (2006). Contribution of beta-cell dysfunction and insulin resistance to the pathogenesis of impaired glucose tolerance and impaired fasting glucose. *Diabetes Care, 29*. doi:10.2337/dc05-2179

Abdulrahman, A. O., Kuerban, A., Alshehri, Z. A., Abdulaal, W. H., Khan, J. A., & Khan, M. I. (2020). Urolithins Attenuate Multiple Symptoms of Obesity in Rats Fed on a High-Fat Diet. *Diabetes, Metabolic Syndrome and Obesity, 13*, 3337-3348. doi:10.2147/dmso.S268146

Abildgaard, J., Henstridge, D. C., Pedersen, A. T., Langley, K. G., Scheele, C., Pedersen, B. K., & Lindegaard, B. (2014). In Vitro Palmitate Treatment of Myotubes from Postmenopausal Women Leads to Ceramide Accumulation, Inflammation and Affected Insulin Signaling. *PloS One, 9*(7), e101555. doi:10.1371/journal.pone.0101555

Adams, J. M., 2nd, Pratipanawatr, T., Berria, R., Wang, E., DeFronzo, R. A., Sullards, M. C., & Mandarino, L. J. (2004). Ceramide content is increased in skeletal muscle from obese insulin-resistant humans. *Diabetes, 53*(1), 25-31. doi:10.2337/diabetes.53.1.25

Adams, S. H., Hoppel, C. L., Lok, K. H., Zhao, L., Wong, S. W., Minkler, P. E., . . . Garvey, W. T. (2009). Plasma acylcarnitine profiles suggest incomplete long-chain fatty acid beta-oxidation and altered tricarboxylic acid cycle activity in type 2 diabetic African-American women. *Journal of Nutrition, 139*(6), 1073-1081. doi:10.3945/jn.108.103754

Addison, O., Drummond, M. J., LaStayo, P. C., Dibble, L. E., Wende, A. R., McClain, D. A., & Marcus, R. L. (2014). Intramuscular fat and inflammation differ in older adults: the impact of frailty and inactivity. *The Journal of Nutrition, Health & Aging, 18*(5), 532-538. doi:10.1007/s12603-014-0019-1

Agley, C. C., Rowlerson, A. M., Velloso, C. P., Lazarus, N. L., & Harridge, S. D. R. (2015). Isolation and Quantitative Immunocytochemical Characterization of Primary Myogenic Cells and Fibroblasts from Human Skeletal Muscle. *JoVE*(95), e52049. doi:doi:10.3791/52049

Agley, C. C., Rowlerson, A. M., Velloso, C. P., Lazarus, N. R., & Harridge, S. D. R. (2013). Human skeletal muscle fibroblasts, but not myogenic cells, readily

undergo adipogenic differentiation. *Journal of Cell Science, 126*(24), 5610-5625. doi:10.1242/jcs.132563

Aguer, C., McCoin, C. S., Knotts, T. A., Thrush, A. B., Ono-Moore, K., McPherson, R., . . . Harper, M.-E. (2015). Acylcarnitines: potential implications for skeletal muscle insulin resistance. *FASEB journal: official publication of the Federation of American Societies for Experimental Biology, 29*(1), 336-345. doi:10.1096/fj.14-255901

Aihara, K., Ikeda, Y., Yagi, S., Akaike, M., & Matsumoto, T. (2010). Transforming Growth Factor-β1 as a Common Target Molecule for Development of Cardiovascular Diseases, Renal Insufficiency and Metabolic Syndrome. *Cardiology Research and Practice, 2011*, 175381. doi:10.4061/2011/175381

Akhmedov, D., & Berdeaux, R. (2013). The effects of obesity on skeletal muscle regeneration. *Frontiers in Physiology, 4*. doi:10.3389/fphys.2013.00371

Al-Khalili, L., Chibalin, A. V., Kannisto, K., Zhang, B. B., Permert, J., Holman, G. D., . . . Krook, A. (2003). Insulin action in cultured human skeletal muscle cells during differentiation: assessment of cell surface GLUT4 and GLUT1 content. *Cellular and Molecular Life Sciences, 60*(5), 991-998. doi:10.1007/s00018-003-3001-3

Alkhateeb, H., & Qnais, E. (2017). Preventive effect of oleate on palmitate-induced insulin resistance in skeletal muscle and its mechanism of action. *Journal of Physiology and Biochemistry, 73*(4), 605-612. doi:10.1007/s13105-017-0594-9

Allen, D. L., Cleary, A. S., Speaker, K. J., Lindsay, S. F., Uyenishi, J., Reed, J. M., . . . Mehan, R. S. (2008). Myostatin, activin receptor IIb, and follistatin-like-3 gene expression are altered in adipose tissue and skeletal muscle of obese mice. *American Journal of Physiology: Endocrinology and Metabolism, 294*(5), E918-927. doi:10.1152/ajpendo.00798.2007

Allen, D. L., Hittel, D. S., & McPherron, A. C. (2011). Expression and function of myostatin in obesity, diabetes, and exercise adaptation. *Medicine and Science in Sports and Exercise, 43*(10), 1828-1835. doi:10.1249/MSS.0b013e3182178bb4

Allen, D. L., & Loh, A. S. (2011). Posttranscriptional mechanisms involving microRNA-27a and b contribute to fast-specific and glucocorticoid-mediated myostatin expression in skeletal muscle. *American Journal of Physiology: Cell Physiology, 300*(1), C124-137. doi:10.1152/ajpcell.00142.2010

Allen, D. L., & Unterman, T. G. (2007). Regulation of myostatin expression and myoblast differentiation by FoxO and SMAD transcription factors. *American Journal of Physiology: Cell Physiology, 292*(1), C188-199. doi:10.1152/ajpcell.00542.2005

Amati, F. (2012). Revisiting the diacylglycerol-induced insulin resistance hypothesis. *Obesity Reviews, 13*(S2), 40-50. doi:https://doi.org/10.1111/j.1467-789X.2012.01036.x

Amirouche, A., Durieux, A.-C. c., Banzet, S. b., Koulmann, N., Bonnefoy, R. g., Mouret, C., . . . Freyssenet, D. (2009). Down-Regulation of Akt/Mammalian Target of Rapamycin Signaling Pathway in Response to Myostatin Overexpression in Skeletal Muscle. *Endocrinology, 150*(1), 286-294. doi:10.1210/en.2008-0959

Amor, M., Itariu, B. K., Moreno-Viedma, V., Keindl, M., Jurets, A., Prager, G., . . . Stulnig, T. M. (2019). Serum Myostatin is Upregulated in Obesity and Correlates with Insulin Resistance in Humans. *Experimental and Clinical Endocrinology and Diabetes, 127*(8), 550-556. doi:10.1055/a-0641-5546

Amthor, H., Nicholas, G., McKinnell, I., Kemp, C. F., Sharma, M., Kambadur, R., & Patel, K. (2004). Follistatin complexes Myostatin and antagonises Myostatin-mediated inhibition of myogenesis. *Developmental Biology, 270*(1), 19-30. doi:https://doi.org/10.1016/j.ydbio.2004.01.046

Anastasiou, C. A., Kavouras, S. A., Lentzas, Y., Gova, A., Sidossis, L. S., & Melidonis, A. (2009). Diabetes mellitus is associated with increased

intramyocellular triglyceride, but not diglyceride, content in obese humans. *Metabolism: Clinical and Experimental, 58*(11), 1636-1642. doi:10.1016/j.metabol.2009.05.019

Andersen, C. L., Jensen, J. L., & Ørntoft, T. F. (2004). Normalization of real-time quantitative reverse transcription-PCR data: a model-based variance estimation approach to identify genes suited for normalization, applied to bladder and colon cancer data sets. *Cancer Research, 64*(15), 5245-5250. doi:10.1158/0008-5472.Can-04-0496

Anderson, A. S., Haynie, K. R., McMillan, R. P., Osterberg, K. L., Boutagy, N. E., Frisard, M. I., . . . Hulver, M. W. (2015). Early skeletal muscle adaptations to short-term high-fat diet in humans before changes in insulin sensitivity. *Obesity (Silver Spring), 23*(4), 720-724. doi:10.1002/oby.21031

Anderson, S. B., Goldberg, A. L., & Whitman, M. (2008). Identification of a novel pool of extracellular pro-myostatin in skeletal muscle. *Journal of Biological Chemistry, 283*(11), 7027-7035. doi:10.1074/jbc.M706678200

Anderson, S. R., Gilge, D. A., Steiber, A. L., & Previs, S. F. (2008). Diet-induced obesity alters protein synthesis: tissue-specific effects in fasted versus fed mice. *Metabolism: Clinical and Experimental, 57*(3), 347-354. doi:10.1016/j.metabol.2007.10.009

Andreux, P. A., Blanco-Bose, W., Ryu, D., Burdet, F., Ibberson, M., Aebischer, P., . . . Rinsch, C. (2019). The mitophagy activator urolithin A is safe and induces a molecular signature of improved mitochondrial and cellular health in humans. *Nature Metabolism, 1*(6), 595-603. doi:10.1038/s42255-019-0073-4

Arita, Y., Kihara, S., Ouchi, N., Takahashi, M., Maeda, K., Miyagawa, J., . . . Matsuzawa, Y. (1999). Paradoxical decrease of an adipose-specific protein, adiponectin, in obesity. *Biochemical and Biophysical Research Communications, 257*(1), 79-83. doi:10.1006/bbrc.1999.0255

Arner, P., & Rydén, M. (2015). Fatty Acids, Obesity and Insulin Resistance. *Obesity Facts, 8*(2), 147-155. doi:10.1159/000381224

Aronson, D., Bartha, P., Zinder, O., Kerner, A., Markiewicz, W., Avizohar, O., . . . Levy, Y. (2004). Obesity is the major determinant of elevated C-reactive protein in subjects with the metabolic syndrome. *International Journal of Obesity, 28*(5), 674-679. doi:10.1038/sj.ijo.0802609

Artaza, J. N., Bhasin, S., Magee, T. R., Reisz-Porszasz, S., Shen, R., Groome, N. P., . . . Gonzalez-Cadavid, N. F. (2005). Myostatin inhibits myogenesis and promotes adipogenesis in C3H 10T(1/2) mesenchymal multipotent cells. *Endocrinology, 146*(8), 3547-3557. doi:10.1210/en.2005-0362

Asfour, H. A., Allouh, M. Z., & Said, R. S. (2018). Myogenic regulatory factors: The orchestrators of myogenesis after 30 years of discovery. *Experimental Biology and Medicine (Maywood, N.J.), 243*(2), 118-128. doi:10.1177/1535370217749494

Ashcroft, F. M., Harrison, D. E., & Ashcroft, S. J. H. (1984). Glucose induces closure of single potassium channels in isolated rat pancreatic β-cells. *Nature, 312*(5993), 446-448. doi:10.1038/312446a0

Atkins, J. L., Whincup, P. H., Morris, R. W., Lennon, L. T., Papacosta, O., & Wannamethee, S. G. (2014). Sarcopenic obesity and risk of cardiovascular disease and mortality: a population-based cohort study of older men. *Journal of the American Geriatrics Society, 62*(2), 253-260. doi:10.1111/jgs.12652

Ato, S., Mori, T., Fujita, Y., Mishima, T., & Ogasawara, R. (2021). Short-term high-fat diet induces muscle fiber type-selective anabolic resistance to resistance exercise. *J Appl Physiol (1985), 131*(2), 442-453. doi:10.1152/japplphysiol.00889.2020

Auguet, T., Quintero, Y., Terra, X., Martínez, S., Lucas, A., Pellitero, S., . . . Richart, C. (2011). Upregulation of lipocalin 2 in adipose tissues of severely obese women: positive relationship with proinflammatory cytokines. *Obesity (Silver Spring), 19*(12), 2295-2300. doi:10.1038/oby.2011.61

Ávila-Gálvez, M., González-Sarrías, A., & Espín, J. C. (2018). In Vitro Research on Dietary Polyphenols and Health: A Call of Caution and a Guide on How To Proceed. *Journal of Agricultural and Food Chemistry, 66*(30), 7857-7858. doi:10.1021/acs.jafc.8b03377

Baboota, R. K., Sarma, S. M., Boparai, R. K., Kondepudi, K. K., Mantri, S., & Bishnoi, M. (2015). Microarray Based Gene Expression Analysis of Murine Brown and Subcutaneous Adipose Tissue: Significance with Human. *PloS One, 10*(5), e0127701. doi:10.1371/journal.pone.0127701

Bach, L. A. (2018). 40 YEARS OF IGF1: IGF-binding proteins. *Journal of Molecular Endocrinology, 61*(1), T11-T28. doi:10.1530/jme-17-0254

Bala, I., Bhardwaj, V., Hariharan, S., & Kumar, M. N. V. R. (2006). Analytical methods for assay of ellagic acid and its solubility studies. *Journal of Pharmaceutical and Biomedical Analysis, 40*(1), 206-210. doi:https://doi.org/10.1016/j.jpba.2005.07.006

Bandet, C. L., Tan-Chen, S., Bourron, O., Le Stunff, H., & Hajduch, E. (2019). Sphingolipid Metabolism: New Insight into Ceramide-Induced Lipotoxicity in Muscle Cells. *International Journal of Molecular Sciences, 20*(3), 479. Retrieved from https://www.mdpi.com/1422-0067/20/3/479

Banting, F. G. (1926). An Address on Diabetes and Insulin: Being The Nobel Lecture Delivered at Stockholm on September 15th, 1925. *Canadian Medical Association Journal, 16*(3), 221-232.

Banting, F. G., Best, C. H., Collip, J. B., Campbell, W. R., & Fletcher, A. A. (1991). Pancreatic extracts in the treatment of diabetes mellitus: preliminary report. 1922. *CMAJ : Canadian Medical Association journal = journal de l'Association medicale canadienne, 145*(10), 1281-1286.

Barnard, R. J., & Youngren, J. F. (1992). Regulation of glucose transport in skeletal muscle. *FASEB Journal, 6*(14), 3238-3244.

Barnes, B. J., & Somerville, C. C. (2020). Modulating Cytokine Production via Select Packaging and Secretion From Extracellular Vesicles. *Frontiers in Immunology, 11*(1040). doi:10.3389/fimmu.2020.01040

Barratt, J., & Weitz, I. (2021). Complement Factor D as a Strategic Target for Regulating the Alternative Complement Pathway. *Frontiers in Immunology, 12*. doi:10.3389/fimmu.2021.712572

Barres, R., Yan, J., Egan, B., Treebak, J. T., Rasmussen, M., Fritz, T., . . . Zierath, J. R. (2012). Acute exercise remodels promoter methylation in human skeletal muscle. *Cell Metabolism, 15*(3), 405-411. doi:10.1016/j.cmet.2012.01.001

Batsis, J. A., & Villareal, D. T. (2018). Sarcopenic obesity in older adults: aetiology, epidemiology and treatment strategies. *Nature reviews. Endocrinology, 14*(9), 513-537. doi:10.1038/s41574-018-0062-9

Bauche, I. B., Ait El Mkadem, S., Rezsohazy, R., Funahashi, T., Maeda, N., Miranda, L. M., & Brichard, S. M. (2006). Adiponectin downregulates its own production and the expression of its AdipoR2 receptor in transgenic mice. *Biochemical and Biophysical Research Communications, 345*(4), 1414-1424. doi:10.1016/j.bbrc.2006.05.033

Båvenholm, P. N., Pigon, J., Ostenson, C. G., & Efendic, S. (2001). Insulin sensitivity of suppression of endogenous glucose production is the single most important determinant of glucose tolerance. *Diabetes, 50*(6), 1449-1454. doi:10.2337/diabetes.50.6.1449

Beals, J. W., Sukiennik, R. A., Nallabelli, J., Emmons, R. S., van Vliet, S., Young, J. R., . . . Burd, N. A. (2016). Anabolic sensitivity of postprandial muscle protein synthesis to the ingestion of a protein-dense food is reduced in overweight and obese young adults. *The American Journal of Clinical Nutrition, 104*(4), 1014-1022. doi:10.3945/ajcn.116.130385

Becker, C., Lord, S. R., Studenski, S. A., Warden, S. J., Fielding, R. A., Recknor, C. P., . . . Benichou, O. (2015). Myostatin antibody (LY2495655) in older

weak fallers: a proof-of-concept, randomised, phase 2 trial. *Lancet Diabetes Endocrinol, 3*(12), 948-957. doi:10.1016/s2213-8587(15)00298-3

Bell, J. A., Reed, M. A., Consitt, L. A., Martin, O. J., Haynie, K. R., Hulver, M. W., . . . Dohm, G. L. (2010). Lipid partitioning, incomplete fatty acid oxidation, and insulin signal transduction in primary human muscle cells: effects of severe obesity, fatty acid incubation, and fatty acid translocase/CD36 overexpression. *Journal of Clinical Endocrinology and Metabolism, 95*(7), 3400-3410. doi:10.1210/jc.2009-1596

Benes, P., Vetvicka, V., & Fusek, M. (2008). Cathepsin D—many functions of one aspartic protease. *Critical Reviews in Oncology/Hematology, 68*(1), 12-28.

Bentzinger, C. F., Wang, Y. X., & Rudnicki, M. A. (2012). Building muscle: molecular regulation of myogenesis. *Cold Spring Harbor Perspectives in Biology, 4*(2). doi:10.1101/cshperspect.a008342

Bergen, H. R., Farr, J. N., Vanderboom, P. M., Atkinson, E. J., White, T. A., Singh, R. J., . . . LeBrasseur, N. K. (2015). Myostatin as a mediator of sarcopenia versus homeostatic regulator of muscle mass: insights using a new mass spectrometry-based assay. *Skeletal Muscle, 5*(1), 21. doi:10.1186/s13395-015-0047-5

Berggren, J. R., Tanner, C. J., & Houmard, J. A. (2007). Primary cell cultures in the study of human muscle metabolism. *Exercise and Sport Sciences Reviews, 35*(2), 56-61. doi:10.1249/JES.0b013e31803eae63

Bergstrom, J. (1975). Percutaneous needle biopsy of skeletal muscle in physiological and clinical research. *Scandinavian Journal of Clinical and Laboratory Investigation, 35*(7), 609-616.

Beyer, I., Mets, T., & Bautmans, I. (2012). Chronic low-grade inflammation and age-related sarcopenia. *Current Opinion in Clinical Nutrition and Metabolic Care, 15*(1), 12-22. doi:10.1097/MCO.0b013e32834dd297

Bhatt, S. P., Nigam, P., Misra, A., Guleria, R., Luthra, K., Jain, S. K., & Qadar Pasha, M. A. (2012). Association of the Myostatin Gene with Obesity, Abdominal Obesity and Low Lean Body Mass and in Non-Diabetic Asian Indians in North India. *PloS One, 7*(8), e40977. doi:10.1371/journal.pone.0040977

Bicer, M., Guler, A., Unal Kocabas, G., Imamoglu, C., Baloglu, A., Bilgir, O., . . . Calan, M. (2017). Endocan is a predictor of increased cardiovascular risk in women with polycystic ovary syndrome. *Endocrine Research, 42*(2), 145-153. doi:10.1080/07435800.2016.1255896

Bikman, B. T., Zheng, D., Reed, M. A., Hickner, R. C., Houmard, J. A., & Dohm, G. L. (2010). Lipid-induced insulin resistance is prevented in lean and obese myotubes by AICAR treatment. *American Journal of Physiology: Regulatory, Integrative and Comparative Physiology, 298*(6), R1692-1699. doi:10.1152/ajpregu.00190.2009

Birnbaum, M. J. (1989). Identification of a novel gene encoding an insulin-responsive glucose transporter protein. *Cell, 57*(2), 305-315.

Bittel, D. C., & Jaiswal, J. K. (2019). Contribution of Extracellular Vesicles in Rebuilding Injured Muscles. *Frontiers in Physiology, 10*, 828-828. doi:10.3389/fphys.2019.00828

Blaber, S. P., Webster, R. A., Hill, C. J., Breen, E. J., Kuah, D., Vesey, G., & Herbert, B. R. (2012). Analysis of in vitro secretion profiles from adipose-derived cell populations. *Journal of Translational Medicine, 10*, 172. doi:10.1186/1479-5876-10-172

Blainey, P., Krzywinski, M., & Altman, N. (2014). Replication. *Nature methods, 11*(9), 879-880. doi:10.1038/nmeth.3091

Blau, H. M., Chiu, C. P., & Webster, C. (1983). Cytoplasmic activation of human nuclear genes in stable heterocaryons. *Cell, 32*(4), 1171-1180.

Blau, H. M., & Webster, C. (1981). Isolation and characterization of human muscle cells. *Proceedings of the National Academy of Sciences, 78*(9), 5623-5627. doi:10.1073/pnas.78.9.5623

Blouin, C. M., Prado, C., Takane, K. K., Lasnier, F., Garcia-Ocana, A., Ferré, P., . . . Hajduch, E. (2010). Plasma membrane subdomain compartmentalization contributes to distinct mechanisms of ceramide action on insulin signaling. *Diabetes, 59*(3), 600-610. doi:10.2337/db09-0897

Bluher, M. (2010). The distinction of metabolically 'healthy' from 'unhealthy' obese individuals. *Current Opinion in Lipidology, 21*(1), 38-43. doi:10.1097/MOL.0b013e3283346ccc

Blüher, M. (2012). Are there still healthy obese patients? *Current Opinion in Endocrinology, Diabetes, and Obesity, 19*(5), 341-346. doi:10.1097/MED.0b013e328357f0a3

Blundell, J. E., Burley, V. J., Cotton, J. R., & Lawton, C. L. (1993). Dietary fat and the control of energy intake: evaluating the effects of fat on meal size and postmeal satiety. *American Journal of Clinical Nutrition, 57*(5 Suppl), 772S-777S; discussion 777S-778S. doi:10.1093/ajcn/57.5.772S

Blundell, J. E., & King, N. A. (1996). Overconsumption as a cause of weight gain: behavioural-physiological interactions in the control of food intake (appetite). *Ciba Foundation Symposium, 201*, 138-154; discussion 154-158, 188-193. Retrieved from http://www.ncbi.nlm.nih.gov/pubmed/9017279

Bobowska, A., Granica, S., Filipek, A., Melzig, M. F., Moeslinger, T., Zentek, J., . . . Piwowarski, J. P. (2021). Comparative studies of urolithins and their phase II metabolites on macrophage and neutrophil functions. *European Journal of Nutrition, 60*(4), 1957-1972. doi:10.1007/s00394-020-02386-y

Boden, G. (2008). Obesity and free fatty acids. *Endocrinology and Metabolism Clinics of North America, 37*(3), 635-646, viii-ix. doi:10.1016/j.ecl.2008.06.007

Bodine, S. C., Stitt, T. N., Gonzalez, M., Kline, W. O., Stover, G. L., Bauerlein, R., . . . Yancopoulos, G. D. (2001). Akt/mTOR pathway is a crucial regulator of skeletal muscle hypertrophy and can prevent muscle atrophy in vivo. *Nature Cell Biology, 3*(11), 1014-1019. doi:10.1038/ncb1101-1014

Bollag, G. E., Roth, R. A., Beaudoin, J., Mochly-Rosen, D., & Koshland, D. E. (1986). Protein kinase C directly phosphorylates the insulin receptor in vitro and reduces its protein-tyrosine kinase activity. *Proceedings of the National Academy of Sciences, 83*(16), 5822-5824. doi:10.1073/pnas.83.16.5822

Bollinger, L. M., Campbell, M. S., & Brault, J. J. (2018). Palmitate and oleate co-treatment increases myocellular protein content via impaired protein degradation. *Nutrition, 46*, 41-43. doi:https://doi.org/10.1016/j.nut.2017.07.017

Bollinger, L. M., Powell, J. J. S., Houmard, J. A., Witczak, C. A., & Brault, J. J. (2015). Skeletal muscle myotubes in severe obesity exhibit altered ubiquitin-proteasome and autophagic/lysosomal proteolytic flux. *Obesity (Silver Spring, Md.), 23*(6), 1185-1193. doi:10.1002/oby.21081

Bonadonna, R. C., Bonora, E., Prato, S. D., Saccomani, M. P., Cobelli, C., Natali, A., . . . Gulli, G. (1996). Roles of Glucose Transport and Glucose Phosphorylation in Muscle Insulin Resistance of NIDDM. *Diabetes, 45*(7), 915-925. doi:10.2337/diab.45.7.915

Bonen, A., Dyck, D. J., & Luiken, J. J. (1998). Skeletal muscle fatty acid transport and transporters. *Advances in Experimental Medicine and Biology, 441*, 193-205. doi:10.1007/978-1-4899-1928-1_18

Bostrom, P., Wu, J., Jedrychowski, M. P., Korde, A., Ye, L., Lo, J. C., . . . Spiegelman, B. M. (2012). A PGC1-alpha-dependent myokine that drives brown-fat-like development of white fat and thermogenesis. *Nature, 481*(7382), 463-468. doi:10.1038/nature10777

Boucher, J., Kleinridders, A., & Kahn, C. R. (2014). Insulin receptor signaling in normal and insulin-resistant states. *Cold Spring Harbor Perspectives in Biology, 6*(1). doi:10.1101/cshperspect.a009191

Bourlier, V., Saint-Laurent, C., Louche, K., Badin, P.-M., Thalamas, C., de Glisezinski, I., . . . Moro, C. (2013). Enhanced Glucose Metabolism Is

Preserved in Cultured Primary Myotubes From Obese Donors in Response to Exercise Training. *The Journal of Clinical Endocrinology & Metabolism, 98*(9), 3739-3747. doi:10.1210/jc.2013-1727

Bouzakri, K., Plomgaard, P., Berney, T., Donath, M. Y., Pedersen, B. K., & Halban, P. A. (2011). Bimodal effect on pancreatic beta-cells of secretory products from normal or insulin-resistant human skeletal muscle. *Diabetes, 60*(4), 1111-1121. doi:10.2337/db10-1178

Bratanova-Tochkova, T. K., Cheng, H., Daniel, S., Gunawardana, S., Liu, Y. J., Mulvaney-Musa, J., . . . Sharp, G. W. (2002). Triggering and augmentation mechanisms, granule pools, and biphasic insulin secretion. *Diabetes, 51 Suppl 1*, S83-90.

Bratusch-Marrain, P. R. (1983). Insulin-counteracting hormones: Their impact on glucose metabolism. *Diabetologia, 24*(2), 74-79. doi:10.1007/BF00297384

Braun, T., & Gautel, M. (2011). Transcriptional mechanisms regulating skeletal muscle differentiation, growth and homeostasis. *Nature Reviews: Molecular Cell Biology, 12*(6), 349-361. doi:10.1038/nrm3118

Bray, G. A., & Popkin, B. M. (1998). Dietary fat intake does affect obesity! *The American Journal of Clinical Nutrition, 68*(6), 1157-1173. doi:10.1093/ajcn/68.6.1157

Breen, L., & Phillips, S. M. (2011). Skeletal muscle protein metabolism in the elderly: Interventions to counteract the 'anabolic resistance' of ageing. *Nutrition & Metabolism, 8*(1), 68. doi:10.1186/1743-7075-8-68

Breen, L., Stokes, K. A., Churchward-Venne, T. A., Moore, D. R., Baker, S. K., Smith, K., . . . Phillips, S. M. (2013). Two weeks of reduced activity decreases leg lean mass and induces "anabolic resistance" of myofibrillar protein synthesis in healthy elderly. *The Journal of Clinical Endocrinology and Metabolism, 98*(6), 2604-2612. doi:10.1210/jc.2013-1502

Breitbart, A., Auger-Messier, M., Molkentin, J. D., & Heineke, J. (2011). Myostatin from the heart: local and systemic actions in cardiac failure and muscle wasting. *American Journal of Physiology: Heart and Circulatory Physiology, 300*(6), H1973-1982. doi:10.1152/ajpheart.00200.2011

Breitbart, A., Scharf, G. M., Duncker, D., Widera, C., Gottlieb, J., Vogel, A., . . . Heineke, J. (2013). Highly specific detection of myostatin prodomain by an immunoradiometric sandwich assay in serum of healthy individuals and patients. *PloS One, 8*(11), e80454-e80454. doi:10.1371/journal.pone.0080454

Brøns, C., Jensen, C. B., Storgaard, H., Hiscock, N. J., White, A., Appel, J. S., . . . Vaag, A. (2009). Impact of short-term high-fat feeding on glucose and insulin metabolism in young healthy men. *Journal of Physiology, 587*(Pt 10), 2387-2397. doi:10.1113/jphysiol.2009.169078

Broussard, S. R., McCusker, R. H., Novakofski, J. E., Strle, K., Shen, W. H., Johnson, R. W., . . . Kelley, K. W. (2004). IL-1beta impairs insulin-like growth factor i-induced differentiation and downstream activation signals of the insulin-like growth factor i receptor in myoblasts. *Journal of Immunology, 172*(12), 7713-7720. doi:10.4049/jimmunol.172.12.7713

Broussard, S. R., McCusker, R. H., Novakofski, J. E., Strle, K., Shen, W. H., Johnson, R. W., . . . Kelley, K. W. (2003). Cytokine-hormone interactions: tumor necrosis factor alpha impairs biologic activity and downstream activation signals of the insulin-like growth factor I receptor in myoblasts. *Endocrinology, 144*(7), 2988-2996. doi:10.1210/en.2003-0087

Bryner, R. W., Woodworth-Hobbs, M. E., Williamson, D. L., & Alway, S. E. (2012). Docosahexaenoic Acid protects muscle cells from palmitate-induced atrophy. *ISRN obesity, 2012*, 647348-647348. doi:10.5402/2012/647348

Bunprajun, T., Henriksen, T. I., Scheele, C., Pedersen, B. K., & Green, C. J. (2013). Lifelong Physical Activity Prevents Aging-Associated Insulin Resistance in Human Skeletal Muscle Myotubes via Increased Glucose Transporter Expression. *PloS One, 8*(6), e66628. doi:10.1371/journal.pone.0066628

Burgoyne, T., Morris, E. P., & Luther, P. K. (2015). Three-Dimensional Structure of Vertebrate Muscle Z-Band: The Small-Square Lattice Z-Band in Rat Cardiac Muscle. *Journal of Molecular Biology, 427*(22), 3527-3537. doi:10.1016/j.jmb.2015.08.018

Butland, B., Jebb, S., Kopelman, P., McPherson, K., Thomas, S., Mardell, J., & Parry, V. (2007). Foresight - Tackling obesities: Future choices - project report.

Cai, D., Lee, K. K. H., Li, M., Tang, M. K., & Chan, K. M. (2004). Ubiquitin expression is up-regulated in human and rat skeletal muscles during aging. *Archives of Biochemistry and Biophysics, 425*(1), 42-50. doi:https://doi.org/10.1016/j.abb.2004.02.027

Calderón, J. C., Bolaños, P., & Caputo, C. (2014). The excitation-contraction coupling mechanism in skeletal muscle. *Biophysical reviews, 6*(1), 133-160. doi:10.1007/s12551-013-0135-x

Calori, G., Lattuada, G., Piemonti, L., Garancini, M. P., Ragogna, F., Villa, M., . . . Perseghin, G. (2011). Prevalence, metabolic features, and prognosis of metabolically healthy obese Italian individuals: the Cremona Study. *Diabetes Care, 34*(1), 210-215. doi:10.2337/dc10-0665

Campbell, C., McMillan, H. J., Mah, J. K., Tarnopolsky, M., Selby, K., McClure, T., . . . Attie, K. M. (2017). Myostatin inhibitor ACE-031 treatment of ambulatory boys with Duchenne muscular dystrophy: Results of a randomized, placebo-controlled clinical trial. *Muscle and Nerve, 55*(4), 458-464. doi:10.1002/mus.25268

Camporez, J.-P. G., Petersen, M. C., Abudukadier, A., Moreira, G. V., Jurczak, M. J., Friedman, G., . . . Shulman, G. I. (2016). Anti-myostatin antibody increases muscle mass and strength and improves insulin sensitivity in old mice. *Proceedings of the National Academy of Sciences, 113*(8), 2212-2217. doi:doi:10.1073/pnas.1525795113

Canfora, E. E., Meex, R. C. R., Venema, K., & Blaak, E. E. (2019). Gut microbial metabolites in obesity, NAFLD and T2DM. *Nature Reviews Endocrinology, 15*(5), 261-273. doi:10.1038/s41574-019-0156-z

Cao, H., Polansky, M. M., & Anderson, R. A. (2007). Cinnamon extract and polyphenols affect the expression of tristetraprolin, insulin receptor, and glucose transporter 4 in mouse 3T3-L1 adipocytes. *Archives of Biochemistry and Biophysics, 459*(2), 214-222. doi:10.1016/j.abb.2006.12.034

Capel, F., Acquaviva, C., Pitois, E., Laillet, B., Rigaudière, J.-P., Jouve, C., . . . Morio, B. (2015). DHA at nutritional doses restores insulin sensitivity in skeletal muscle by preventing lipotoxicity and inflammation. *The Journal of Nutritional Biochemistry, 26*(9), 949-959. doi:10.1016/j.jnutbio.2015.04.003

Carnac, G., Vernus, B., & Bonnieu, A. (2007). Myostatin in the Pathophysiology of Skeletal Muscle. *Current Genomics, 8*(7), 415-422. doi:10.2174/138920207783591672

Carosio, S., Berardinelli, M. G., Aucello, M., & Musarò, A. (2011). Impact of ageing on muscle cell regeneration. *Ageing Res Rev, 10*(1), 35-42. doi:https://doi.org/10.1016/j.arr.2009.08.001

Cartee, G. D. (2015). Roles of TBC1D1 and TBC1D4 in insulin- and exercise-stimulated glucose transport of skeletal muscle. *Diabetologia, 58*(1), 19-30. doi:10.1007/s00125-014-3395-5

Carvalho, E., Kotani, K., Peroni, O. D., & Kahn, B. B. (2005). Adipose-specific overexpression of GLUT4 reverses insulin resistance and diabetes in mice lacking GLUT4 selectively in muscle. *American Journal of Physiology: Endocrinology and Metabolism, 289*(4), E551-561. doi:10.1152/ajpendo.00116.2005

Cash, J. N., Angerman, E. B., Kattamuri, C., Nolan, K., Zhao, H., Sidis, Y., . . . Thompson, T. B. (2012). Structure of myostatin.follistatin-like 3: N-terminal domains of follistatin-type molecules exhibit alternate modes of binding. *Journal of Biological Chemistry, 287*(2), 1043-1053. doi:10.1074/jbc.M111.270801

Castoldi, A., Naffah de Souza, C., Câmara, N. O. S., & Moraes-Vieira, P. M. (2016). The Macrophage Switch in Obesity Development. *Frontiers in Immunology, 6*. doi:10.3389/fimmu.2015.00637

Catalán, V., Gómez-Ambrosi, J., Rodríguez, A., Ramírez, B., Silva, C., Rotellar, F., . . . Frühbeck, G. (2009). Increased adipose tissue expression of lipocalin-2 in obesity is related to inflammation and matrix metalloproteinase-2 and metalloproteinase-9 activities in humans. *Journal of Molecular Medicine, 87*(8), 803. doi:10.1007/s00109-009-0486-8

Ceci, C., Graziani, G., Faraoni, I., & Cacciotti, I. (2020). Strategies to improve ellagic acid bioavailability: from natural or semisynthetic derivatives to nanotechnological approaches based on innovative carriers. *Nanotechnology, 31*(38), 382001. doi:10.1088/1361-6528/ab912c

Cefalu, W. T. (2001). Insulin resistance: cellular and clinical concepts. *Experimental Biology and Medicine (Maywood, N.J.), 226*(1), 13-26.

Cerdá, B., Espín, J. C., Parra, S., Martínez, P., & Tomás-Barberán, F. A. (2004). The potent in vitro antioxidant ellagitannins from pomegranate juice are metabolised into bioavailable but poor antioxidant hydroxy-6H-dibenzopyran-6-one derivatives by the colonic microflora of healthy humans. *European Journal of Nutrition, 43*(4), 205-220. doi:10.1007/s00394-004-0461-7

Cerdá, B., Periago, P., Espín, J. C., & Tomás-Barberán, F. A. (2005). Identification of urolithin a as a metabolite produced by human colon microflora from ellagic acid and related compounds. *Journal of Agricultural and Food Chemistry, 53*(14), 5571-5576. doi:10.1021/jf050384i

Cesari, M., Kritchevsky, S. B., Baumgartner, R. N., Atkinson, H. H., Penninx, B. W., Lenchik, L., . . . Pahor, M. (2005). Sarcopenia, obesity, and inflammation--results from the Trial of Angiotensin Converting Enzyme Inhibition and Novel Cardiovascular Risk Factors study. *American Journal of Clinical Nutrition, 82*(2), 428-434. doi:10.1093/ajcn.82.2.428

Chadt, A., & Al-Hasani, H. (2020). Glucose transporters in adipose tissue, liver, and skeletal muscle in metabolic health and disease. *Pflügers Archiv - European Journal of Physiology, 472*(9), 1273-1298. doi:10.1007/s00424-020-02417-x

Chan, B. (2018). *Ellagic Acid and Urolithin A Improve Insulin Sensitivity in Diet-Induced Insulin Resistant Mice and Reduce Detrimental Effects of Palmitate Administration in Differentiated C2C12 Myotubes*.

Chanon, S., Durand, C., Vieille-Marchiset, A., Robert, M., Dibner, C., Simon, C., & Lefai, E. (2017). Glucose Uptake Measurement and Response to Insulin Stimulation in In Vitro Cultured Human Primary Myotubes. *J Vis Exp*(124). doi:10.3791/55743

Chapman, M. A., Meza, R., & Lieber, R. L. (2016). Skeletal muscle fibroblasts in health and disease. *Differentiation, 92*(3), 108-115. doi:10.1016/j.diff.2016.05.007

Chapman, M. J., Fraser, R. J., Matthews, G., Russo, A., Bellon, M., Besanko, L. K., . . . Horowitz, M. (2009). Glucose absorption and gastric emptying in critical illness. *Critical Care (London, England), 13*(4), R140. doi:10.1186/cc8021

Chapman, M. J., Nguyen, N. Q., & Fraser, R. J. (2007). Gastrointestinal motility and prokinetics in the critically ill. *Current Opinion in Critical Care, 13*(2), 187-194. doi:10.1097/MCC.0b013e3280523a88

Charron, M. J., Brosius, F. C., 3rd, Alper, S. L., & Lodish, H. F. (1989). A glucose transport protein expressed predominately in insulin-responsive tissues. *Proceedings of the National Academy of Sciences of the United States of America, 86*(8), 2535-2539.

Chavez, J. A., & Summers, S. A. (2003). Characterizing the effects of saturated fatty acids on insulin signaling and ceramide and diacylglycerol accumulation in 3T3-L1 adipocytes and C2C12 myotubes. *Archives of Biochemistry and Biophysics, 419*(2), 101-109. doi:https://doi.org/10.1016/j.abb.2003.08.020

Chavez, Jose A., & Summers, Scott A. (2012). A Ceramide-Centric View of Insulin Resistance. *Cell Metabolism, 15*(5), 585-594. doi:https://doi.org/10.1016/j.cmet.2012.04.002

Chee, C. (2016). *The influence of age and nutrients on insulin sensitivity.* (PhD). University of Nottingham, Retrieved from http://eprints.nottingham.ac.uk/32935/

Chee, C., Shannon, C. E., Burns, A., Selby, A. L., Wilkinson, D., Smith, K., . . . Stephens, F. B. (2021). Increasing skeletal muscle carnitine content in older individuals increases whole-body fat oxidation during moderate-intensity exercise. *Aging Cell, 20*(2), e13303. doi:10.1111/acel.13303

Chen, M.-M., Zhao, Y.-P., Zhao, Y., Deng, S.-L., & Yu, K. (2021). Regulation of Myostatin on the Growth and Development of Skeletal Muscle. *Frontiers in Cell and Developmental Biology, 9*. doi:10.3389/fcell.2021.785712

Chen, Y., Mironova, E., Whitaker, L. L., Edwards, L., Yost, H. J., & Ramsdell, A. F. (2004). ALK4 functions as a receptor for multiple TGF beta-related ligands to regulate left-right axis determination and mesoderm induction in Xenopus. *Developmental Biology, 268*(2), 280-294. doi:10.1016/j.ydbio.2003.12.035

Chen, Y., Ye, J., Cao, L., Zhang, Y., Xia, W., & Zhu, D. (2010). Myostatin regulates glucose metabolism via the AMP-activated protein kinase pathway in skeletal muscle cells. *International Journal of Biochemistry and Cell Biology, 42*(12), 2072-2081. doi:10.1016/j.biocel.2010.09.017

Chitu, V., & Stanley, E. R. (2006). Colony-stimulating factor-1 in immunity and inflammation. *Current Opinion in Immunology, 18*(1), 39-48. doi:https://doi.org/10.1016/j.coi.2005.11.006

Choi, S. J., Lee, M. S., Kang, D. H., Ko, G. J., Lim, H. S., Yu, B. C., . . . An, W. S. (2021). Myostatin/Appendicular Skeletal Muscle Mass (ASM) Ratio, Not Myostatin, Is Associated with Low Handgrip Strength in Community-Dwelling Older Women. *International Journal of Environmental Research and Public Health, 18*(14). doi:10.3390/ijerph18147344

Choi, S. J., Yablonka-Reuveni, Z., Kaiyala, K. J., Ogimoto, K., Schwartz, M. W., & Wisse, B. E. (2011). Increased energy expenditure and leptin sensitivity account for low fat mass in myostatin-deficient mice. *American Journal of Physiology-Endocrinology and Metabolism, 300*(6), E1031-E1037. doi:10.1152/ajpendo.00656.2010

Chokkalingam, K., Jewell, K., Norton, L., Littlewood, J., van Loon, L. J. C., Mansell, P., . . . Tsintzas, K. (2007). High-Fat/Low-Carbohydrate Diet Reduces Insulin-Stimulated Carbohydrate Oxidation but Stimulates Nonoxidative Glucose Disposal in Humans: An Important Role for Skeletal Muscle Pyruvate Dehydrogenase Kinase 4. *The Journal of Clinical Endocrinology & Metabolism, 92*(1), 284-292. doi:10.1210/jc.2006-1592

Ciaraldi, T. P., Abrams, L., Nikoulina, S., Mudaliar, S., & Henry, R. R. (1995). Glucose transport in cultured human skeletal muscle cells. Regulation by insulin and glucose in nondiabetic and non-insulin-dependent diabetes mellitus subjects. *Journal of Clinical Investigation, 96*(6), 2820-2827. doi:10.1172/jci118352

Cisneros-Zevallos, L., Bang, W. Y., & Delgadillo-Puga, C. (2020). Ellagic Acid and Urolithins A and B Differentially Regulate Fat Accumulation and Inflammation in 3T3-L1 Adipocytes While Not Affecting Adipogenesis and Insulin Sensitivity. *International Journal of Molecular Sciences, 21*(6), 2086. Retrieved from https://www.mdpi.com/1422-0067/21/6/2086

Clark, D. A., & Coker, R. (1998). Transforming growth factor-beta (TGF-beta). *International Journal of Biochemistry and Cell Biology, 30*(3), 293-298.

Clark, P., Dunn, G. A., Knibbs, A., & Peckham, M. (2002). Alignment of myoblasts on ultrafine gratings inhibits fusion in vitro. *International Journal of Biochemistry and Cell Biology, 34*(7), 816-825.

Cleasby, M. E., Jarmin, S., Eilers, W., Elashry, M., Andersen, D. K., Dickson, G., & Foster, K. (2014). Local overexpression of the myostatin propeptide increases glucose transporter expression and enhances skeletal muscle glucose disposal. *American journal of physiology. Endocrinology and metabolism, 306*(7), E814-E823. doi:10.1152/ajpendo.00586.2013

Coen, P. M., Musci, R. V., Hinkley, J. M., & Miller, B. F. (2019). Mitochondria as a Target for Mitigating Sarcopenia. *Frontiers in Physiology, 9*. doi:10.3389/fphys.2018.01883

Coll, T., Eyre, E., Rodríguez-Calvo, R., Palomer, X., Sánchez, R. M., Merlos, M., . . . Vázquez-Carrera, M. (2008). Oleate Reverses Palmitate-induced Insulin Resistance and Inflammation in Skeletal Muscle Cells. *Journal of Biological Chemistry, 283*(17), 11107-11116. doi:10.1074/jbc.M708700200

Colomer, R., Sarrats, A., Lupu, R., & Puig, T. (2017). Natural Polyphenols and their Synthetic Analogs as Emerging Anticancer Agents. *Current Drug Targets, 18*(2), 147-159. doi:10.2174/1389450117666160112113930

Consitt, L. A., Bell, J. A., & Houmard, J. A. (2009). Intramuscular Lipid Metabolism, Insulin Action and Obesity. *IUBMB Life, 61*(1), 47-55. doi:10.1002/iub.142

Consitt, L. A., & Clark, B. C. (2018). The Vicious Cycle of Myostatin Signaling in Sarcopenic Obesity: Myostatin Role in Skeletal Muscle Growth, Insulin

Signaling and Implications for Clinical Trials. *The Journal of frailty & aging, 7*(1), 21-27. doi:10.14283/jfa.2017.33

Conus, F., Rabasa-Lhoret, R., & Peronnet, F. (2007). Characteristics of metabolically obese normal-weight (MONW) subjects. *Applied Physiology, Nutrition, and Metabolism. Physiologie Appliquée, Nutrition et Métabolisme, 32*(1), 4-12. doi:10.1139/h07-926

Cook, K. S., Min, H. Y., Johnson, D., Chaplinsky, R. J., Flier, J. S., Hunt, C. R., & Spiegelman, B. M. (1987). Adipsin: a circulating serine protease homolog secreted by adipose tissue and sciatic nerve. *Science, 237*(4813), 402-405. doi:10.1126/science.3299705

Cooney, G. J., Thompson, A. L., Furler, S. M., Ye, J., & Kraegen, E. W. (2002). Muscle long-chain acyl CoA esters and insulin resistance. *Annals of the New York Academy of Sciences, 967*, 196-207. doi:10.1111/j.1749-6632.2002.tb04276.x

Corbett, A. H. (2018). Post-transcriptional regulation of gene expression and human disease. *Current Opinion in Cell Biology, 52*, 96-104. doi:https://doi.org/10.1016/j.ceb.2018.02.011

Correia-Costa, L., Sousa, T., Morato, M., Cosme, D., Afonso, J., Moura, C., . . . Azevedo, A. (2016). Association of myeloperoxidase levels with cardiometabolic factors and renal function in prepubertal children. *European Journal of Clinical Investigation, 46*(1), 50-59. doi:https://doi.org/10.1111/eci.12564

Cortés-Martín, A., Selma, M. V., Tomás-Barberán, F. A., González-Sarrías, A., & Espín, J. C. (2020). Where to Look into the Puzzle of Polyphenols and Health? The Postbiotics and Gut Microbiota Associated with Human Metabotypes. *Molecular Nutrition & Food Research, 64*(9), 1900952. doi:https://doi.org/10.1002/mnfr.201900952

Costamagna, D., Costelli, P., Sampaolesi, M., & Penna, F. (2015). Role of Inflammation in Muscle Homeostasis and Myogenesis. *Mediators of Inflammation, 2015*, 805172. doi:10.1155/2015/805172

Cotton, T. R., Fischer, G., Wang, X., McCoy, J. C., Czepnik, M., Thompson, T. B., & Hyvönen, M. (2018). Structure of the human myostatin precursor and determinants of growth factor latency. *The EMBO Journal, 37*(3), 367-383. doi:10.15252/embj.201797883

Covington, J. D., Myland, C. K., Rustan, A. C., Ravussin, E., Smith, S. R., & Bajpeyi, S. (2015). Effect of serial cell passaging in the retention of fiber type and mitochondrial content in primary human myotubes. *Obesity (Silver Spring), 23*(12), 2414-2420. doi:10.1002/oby.21192

Crawford, S. A., Costford, S. R., Aguer, C., Thomas, S. C., deKemp, R. A., DaSilva, J. N., . . . Harper, M. E. (2010). Naturally occurring R225W mutation of the gene encoding AMP-activated protein kinase (AMPK)γ3 results in increased oxidative capacity and glucose uptake in human primary myotubes. *Diabetologia, 53*(9), 1986-1997. doi:10.1007/s00125-010-1788-7

Critchley, M. (1931). THE NEUROLOGY OF OLD AGE. *The Lancet, 217*(5621), 1119-1127. doi:10.1016/S0140-6736(00)90705-0

Cruz, A. M., & Beall, C. (2020). Extracellular ATP Increases Glucose Metabolism in Skeletal Muscle Cells in a P2 Receptor Dependent Manner but Does Not Contribute to Palmitate-Induced Insulin Resistance. *Frontiers in Physiology, 11*, 567378-567378. doi:10.3389/fphys.2020.567378

Cumming, G., Fidler, F., & Vaux, D. L. (2007). Error bars in experimental biology. *Journal of Cell Biology, 177*(1), 7-11. doi:10.1083/jcb.200611141

Cuthbertson, D., Smith, K., Babraj, J., Leese, G., Waddell, T., Atherton, P., . . . Rennie, M. J. (2005). Anabolic signaling deficits underlie amino acid resistance of wasting, aging muscle. *FASEB Journal, 19*(3), 422-424. doi:10.1096/fj.04-2640fje

Cuthbertson, D. J., Babraj, J., Leese, G., & Siervo, M. (2017). Anabolic resistance does not explain sarcopenia in patients with type 2 diabetes mellitus, compared with healthy controls, despite reduced mTOR pathway activity. *Clinical Nutrition, 36*(6), 1716-1719. doi:10.1016/j.clnu.2016.11.012

Cutler, D. L., Gray, C. G., Park, S. W., Hickman, M. G., Bell, J. M., & Kolterman, O. G. (1995). Low-carbohydrate diet alters intracellular glucose metabolism but not overall glucose disposal in exercise-trained subjects. *Metabolism: Clinical and Experimental, 44*(10), 1264-1270. doi:https://doi.org/10.1016/0026-0495(95)90027-6

D'Esposito, V., Passaretti, F., Hammarstedt, A., Liguoro, D., Terracciano, D., Molea, G., . . . Formisano, P. (2012). Adipocyte-released insulin-like growth factor-1 is regulated by glucose and fatty acids and controls breast cancer cell growth in vitro. *Diabetologia, 55*(10), 2811-2822. doi:10.1007/s00125-012-2629-7

D'Amico, D., Andreux, P. A., Valdés, P., Singh, A., Rinsch, C., & Auwerx, J. (2021). Impact of the Natural Compound Urolithin A on Health, Disease, and Aging. *Trends in Molecular Medicine, 27*(7), 687-699. doi:10.1016/j.molmed.2021.04.009

da Paixão, A. O., Bolin, A. P., Silvestre, J. G., & Rodrigues, A. C. (2021). Palmitic Acid Impairs Myogenesis and Alters Temporal Expression of miR-133a and miR-206 in C2C12 Myoblasts. *International Journal of Molecular Sciences, 22*(5), 2748. doi:10.3390/ijms22052748

da Silva Rosa, S. C., Nayak, N., Caymo, A. M., & Gordon, J. W. (2020). Mechanisms of muscle insulin resistance and the cross-talk with liver and adipose tissue. *Physiol Rep, 8*(19), e14607. doi:https://doi.org/10.14814/phy2.14607

Dalbo, V. J., Roberts, M. D., Sunderland, K. L., Poole, C. N., Stout, J. R., Beck, T. W., . . . Kerksick, C. M. (2011). Acute loading and aging effects on myostatin pathway biomarkers in human skeletal muscle after three sequential bouts of resistance exercise. *Journals of Gerontology. Series A: Biological Sciences and Medical Sciences, 66*(8), 855-865. doi:10.1093/gerona/glr091

Daniel, S., Noda, M., Straub, S. G., & Sharp, G. W. (1999). Identification of the docked granule pool responsible for the first phase of glucose-stimulated insulin secretion. *Diabetes, 48*(9), 1686-1690.

Das, D. K., Graham, Z. A., & Cardozo, C. P. (2020). Myokines in skeletal muscle physiology and metabolism: Recent advances and future perspectives. *Acta Physiologica, 228*(2), e13367. doi:10.1111/apha.13367

Dasarathy, S. (2017). Myostatin and beyond in cirrhosis: all roads lead to sarcopenia. *J Cachexia Sarcopenia Muscle, 8*(6), 864-869. doi:10.1002/jcsm.12262

Davidson, H. W., Rhodes, C. J., & Hutton, J. C. (1988). Intraorganellar calcium and pH control proinsulin cleavage in the pancreatic beta cell via two distinct site-specific endopeptidases. *Nature, 333*(6168), 93-96. doi:10.1038/333093a0

de Caestecker, M. (2004). The transforming growth factor-beta superfamily of receptors. *Cytokine and Growth Factor Reviews, 15*(1), 1-11.

de Ménorval, M.-A., Mir, L. M., Fernández, M. L., & Reigada, R. (2012). Effects of Dimethyl Sulfoxide in Cholesterol-Containing Lipid Membranes: A Comparative Study of Experiments In Silico and with Cells. *PloS One, 7*(7), e41733. doi:10.1371/journal.pone.0041733

de Wilde, J., Smit, E., Mohren, R., Boekschoten, M. V., de Groot, P., van den Berg, S. A., . . . Mariman, E. C. (2009). An 8-week high-fat diet induces obesity and insulin resistance with small changes in the muscle transcriptome of C57BL/6J mice. *J Nutrigenet Nutrigenomics, 2*(6), 280-291. doi:10.1159/000308466

Deasy, B. M., Jankowski, R. J., & Huard, J. (2001). Muscle-derived stem cells: characterization and potential for cell-mediated therapy. *Blood Cells, Molecules, and Diseases, 27*(5), 924-933. doi:10.1006/bcmd.2001.0463

DeFronzo, R. A. (1988). The Triumvirate: β-Cell, Muscle, Liver: A Collusion Responsible for NIDDM. *Diabetes, 37*(6), 667-687. doi:10.2337/diab.37.6.667

DeFronzo, R. A. (1997). Insulin resistance: a multifaceted syndrome responsible for NIDDM, obesity, hypertension, dyslipidaemia and atherosclerosis. *Netherlands Journal of Medicine, 50*(5), 191-197. doi:10.1016/s0300-2977(97)00012-0

DeFronzo, R. A. (2004). Pathogenesis of type 2 diabetes mellitus. *Medical Clinics of North America, 88*(4), 787-835, ix. doi:10.1016/j.mcna.2004.04.013

DeFronzo, R. A., Bonadonna, R. C., & Ferrannini, E. (1992). Pathogenesis of NIDDM. A balanced overview. *Diabetes Care, 15*(3), 318-368.

DeFronzo, R. A., & Ferrannini, E. (1987). Regulation of hepatic glucose metabolism in humans. *Diabetes/Metabolism Reviews, 3*(2), 415-459.

DeFronzo, R. A., Ferrannini, E., Hendler, R., Felig, P., & Wahren, J. (1983). Regulation of Splanchnic and Peripheral Glucose Uptake by Insulin and Hyperglycemia in Man. *Diabetes, 32*(1), 35-45. doi:10.2337/diab.32.1.35

DeFronzo, R. A., Tobin, J. D., & Andres, R. (1979). Glucose clamp technique: a method for quantifying insulin secretion and resistance. *American Journal of Physiology, 237*(3), E214-223. doi:10.1152/ajpendo.1979.237.3.E214

DeFronzo, R. A., & Tripathy, D. (2009). Skeletal Muscle Insulin Resistance Is the Primary Defect in Type 2 Diabetes. *Diabetes Care, 32*(Suppl 2), S157-S163. doi:10.2337/dc09-S302

Dela, F., Ploug, T., Handberg, A., Petersen, L. N., Larsen, J. J., Mikines, K. J., & Galbo, H. (1994). Physical Training Increases Muscle GLUT4 Protein and mRNA in Patients With NIDDM. *Diabetes, 43*(7), 862-865. doi:10.2337/diab.43.7.862

Deldicque, L., Cani, P. D., Philp, A., Raymackers, J.-M., Meakin, P. J., Ashford, M. L. J., . . . Baar, K. (2010). The unfolded protein response is activated in skeletal muscle by high-fat feeding: potential role in the downregulation of protein synthesis. *American Journal of Physiology-Endocrinology and Metabolism, 299*(5), E695-E705. doi:10.1152/ajpendo.00038.2010

Delibas, I. B., Yapca, O. E., & Laloglu, E. (2018). Does endocan level increase in women with polycystic ovary syndrome? A case - control study. *Ginekologia Polska, 89*(9), 500-505. doi:10.5603/GP.a2018.0085

Deng, B., Zhang, F., Wen, J., Ye, S., Wang, L., Yang, Y., . . . Jiang, S. (2017). The function of myostatin in the regulation of fat mass in mammals. *Nutrition & Metabolism, 14*(1), 29. doi:10.1186/s12986-017-0179-1

Denke, M. A., & Grundy, S. M. (1992). Comparison of effects of lauric acid and palmitic acid on plasma lipids and lipoproteins. *The American Journal of Clinical Nutrition, 56*(5), 895-898. doi:10.1093/ajcn/56.5.895

Dennis, R. A., Przybyla, B., Gurley, C., Kortebein, P. M., Simpson, P., Sullivan, D. H., & Peterson, C. A. (2008). Aging alters gene expression of growth and remodeling factors in human skeletal muscle both at rest and in response to acute resistance exercise. *Physiological Genomics, 32*(3), 393-400. doi:10.1152/physiolgenomics.00191.2007

Derosa, G., Salvadeo, S. A., Mereu, R., D'Angelo, A., Ciccarelli, L., Piccinni, M. N., . . . Tinelli, C. (2009). Continuous glucose monitoring system in free-living healthy subjects: results from a pilot study. *Diabetes Technology & Therapeutics, 11*(3), 159-169. doi:10.1089/dia.2008.0101

Després, J.-P., & Lemieux, I. (2006). Abdominal obesity and metabolic syndrome. *Nature, 444*, 881. doi:10.1038/nature05488

Despres, J. P. (2006). Is visceral obesity the cause of the metabolic syndrome? *Annals of Medicine, 38*(1), 52-63. doi:10.1080/07853890500383895

Despres, J. P., Moorjani, S., Lupien, P. J., Tremblay, A., Nadeau, A., & Bouchard, C. (1990). Regional distribution of body fat, plasma lipoproteins, and cardiovascular disease. *Arteriosclerosis, 10*(4), 497-511.

Dial, A. G., Monaco, C. M. F., Grafham, G. K., Romanova, N., Simpson, J. A., Tarnopolsky, M. A., . . . Hawke, T. J. (2020). Muscle and serum myostatin expression in type 1 diabetes. *Physiol Rep, 8*(13), e14500-e14500. doi:10.14814/phy2.14500

Dietze-Schroeder, D., Sell, H., Uhlig, M., Koenen, M., & Eckel, J. r. (2005). Autocrine Action of Adiponectin on Human Fat Cells Prevents the Release of Insulin Resistance-Inducing Factors. *Diabetes, 54*(7), 2003-2011. doi:10.2337/diabetes.54.7.2003

Dietze, D., Koenen, M., Röhrig, K., Horikoshi, H., Hauner, H., & Eckel, J. (2002). Impairment of insulin signaling in human skeletal muscle cells by co-culture with human adipocytes. *Diabetes, 51*(8), 2369-2376. doi:10.2337/diabetes.51.8.2369

Dinarello, C. A. (2007). Historical insights into cytokines. *European Journal of Immunology, 37 Suppl 1*(Suppl 1), S34-S45. doi:10.1002/eji.200737772

Ding, H., & Wu, T. (2018). Insulin-Like Growth Factor Binding Proteins in Autoimmune Diseases. *Frontiers in Endocrinology, 9*. doi:10.3389/fendo.2018.00499

Ding, L., Goossens, G. H., Oligschlaeger, Y., Houben, T., Blaak, E. E., & Shiri-Sverdlov, R. (2020). Plasma cathepsin D activity is negatively associated with hepatic insulin sensitivity in overweight and obese humans. *Diabetologia, 63*(2), 374-384. doi:10.1007/s00125-019-05025-2

Djedjibegovic, J., Marjanovic, A., Panieri, E., & Saso, L. (2020). Ellagic Acid-Derived Urolithins as Modulators of Oxidative Stress. *Oxidative Medicine and Cellular Longevity, 2020*, 5194508. doi:10.1155/2020/5194508

Dong, J., Dong, Y., Dong, Y., Chen, F., Mitch, W. E., & Zhang, L. (2016). Inhibition of myostatin in mice improves insulin sensitivity via irisin-mediated cross talk between muscle and adipose tissues. *International Journal of Obesity (2005), 40*(3), 434-442. doi:10.1038/ijo.2015.200

Doyle, B., & Griffiths, L. A. (1980). The metabolism of ellagic acid in the rat. *Xenobiotica, 10*(4), 247-256. doi:10.3109/00498258009033752

Drake, J. C., & Yan, Z. (2017). Mitophagy in maintaining skeletal muscle mitochondrial proteostasis and metabolic health with ageing. *Journal of Physiology, 595*(20), 6391-6399. doi:10.1113/jp274337

Dresner, A., Laurent, D., Marcucci, M., Griffin, M. E., Dufour, S., Cline, G. W., . . . Shulman, G. I. (1999). Effects of free fatty acids on glucose transport and IRS-1-associated phosphatidylinositol 3-kinase activity. *Journal of Clinical Investigation, 103*(2), 253-259. doi:10.1172/jci5001

Drucker, D. J., Philippe, J., Mojsov, S., Chick, W. L., & Habener, J. F. (1987). Glucagon-like peptide I stimulates insulin gene expression and increases cyclic AMP levels in a rat islet cell line. *Proceedings of the National Academy of Sciences of the United States of America, 84*(10), 3434-3438. doi:10.1073/pnas.84.10.3434

Drummond, M. J., Addison, O., Brunker, L., Hopkins, P. N., McClain, D. A., LaStayo, P. C., & Marcus, R. L. (2014). Downregulation of E3 ubiquitin ligases and mitophagy-related genes in skeletal muscle of physically inactive, frail older women: a cross-sectional comparison. *Journals of Gerontology. Series A: Biological Sciences and Medical Sciences, 69*(8), 1040-1048. doi:10.1093/gerona/glu004

Du Bois, D., & Du Bois, E. F. (1989). A formula to estimate the approximate surface area if height and weight be known. 1916. *Nutrition, 5*(5), 303-311; discussion 312-303.

Du, Y., Xu, C., Shi, H., Jiang, X., Tang, W., Wu, X., . . . Cheng, Q. (2021). Serum concentrations of oxytocin, DHEA and follistatin are associated with osteoporosis or sarcopenia in community-dwelling postmenopausal women. *BMC Geriatrics, 21*(1), 542-542. doi:10.1186/s12877-021-02481-7

Duckworth, W. C. (1988). Insulin degradation: mechanisms, products, and significance. *Endocrine Reviews, 9*(3), 319-345. doi:10.1210/edrv-9-3-319

Durieux, A. C., Amirouche, A., Banzet, S., Koulmann, N., Bonnefoy, R., Pasdeloup, M., . . . Freyssenet, D. (2007). Ectopic expression of myostatin induces atrophy of adult skeletal muscle by decreasing muscle gene expression. *Endocrinology, 148*(7), 3140-3147. doi:10.1210/en.2006-1500

Eckel, J. (2019). Myokines in metabolic homeostasis and diabetes. *Diabetologia, 62*(9), 1523-1528. doi:10.1007/s00125-019-4927-9

Edström, E., Altun, M., Hägglund, M., & Ulfhake, B. (2006). Atrogin-1/MAFbx and MuRF1 Are Downregulated in Aging-Related Loss of Skeletal Muscle. *The Journals of Gerontology: Series A, 61*(7), 663-674. doi:10.1093/gerona/61.7.663

Egerman, M. A., Cadena, S. M., Gilbert, J. A., Meyer, A., Nelson, H. N., Swalley, S. E., . . . Glass, D. J. (2015). GDF11 Increases with Age and Inhibits Skeletal Muscle Regeneration. *Cell Metabolism, 22*(1), 164-174. doi:10.1016/j.cmet.2015.05.010

Ehrlicher, S. E., Stierwalt, H. D., Newsom, S. A., & Robinson, M. M. (2021). Short-Term High-Fat Feeding Does Not Alter Mitochondrial Lipid Respiratory Capacity but Triggers Mitophagy Response in Skeletal Muscle of Mice. *Frontiers in Endocrinology, 12*. doi:10.3389/fendo.2021.651211

Eilers, W., Chambers, D., Cleasby, M., & Foster, K. (2020). Local myostatin inhibition improves skeletal muscle glucose uptake in insulin-resistant high-fat diet-fed mice. *American Journal of Physiology-Endocrinology and Metabolism, 319*(1), E163-E174. doi:10.1152/ajpendo.00185.2019

Eilers, W., Cleasby, M., & Foster, K. (2021). Development of antisense-mediated myostatin knockdown for the treatment of insulin resistance. *Scientific Reports, 11*(1), 1604. doi:10.1038/s41598-021-81222-7

Elgzyri, T., Parikh, H., Zhou, Y., Dekker Nitert, M., Rönn, T., Segerström, Å. B., . . . Hansson, O. (2012). First-degree relatives of type 2 diabetic patients have reduced expression of genes involved in fatty acid metabolism in skeletal muscle. *The Journal of Clinical Endocrinology and Metabolism, 97*(7), E1332-1337. doi:10.1210/jc.2011-3037

Elks, C. M., & Francis, J. (2010). Central Adiposity, Systemic Inflammation, and the Metabolic Syndrome. *Current Hypertension Reports, 12*(2), 99-104. doi:10.1007/s11906-010-0096-4

Elks, C. M., & Stephens, J. M. (2015). Oncostatin M Modulation of Lipid Storage. *Biology, 4*(1), 151-160. Retrieved from https://www.mdpi.com/2079-7737/4/1/151

Ellis, B. A., Poynten, A., Lowy, A. J., Furler, S. M., Chisholm, D. J., Kraegen, E. W., & Cooney, G. J. (2000). Long-chain acyl-CoA esters as indicators of lipid metabolism and insulin sensitivity in rat and human muscle. *American Journal of Physiology. Endocrinology and Metabolism, 279*(3), E554-560. doi:10.1152/ajpendo.2000.279.3.E554

Ellulu, M. S., Patimah, I., Khaza'ai, H., Rahmat, A., & Abed, Y. (2017). Obesity and inflammation: the linking mechanism and the complications. *Archives of medical science : AMS, 13*(4), 851-863. doi:10.5114/aoms.2016.58928

Espín, J. C., Larrosa, M., García-Conesa, M. T., & Tomás-Barberán, F. (2013). Biological significance of urolithins, the gut microbial ellagic Acid-derived metabolites: the evidence so far. *Evidence-Based Complementary and Alternative Medicine, 2013*, 270418. doi:10.1155/2013/270418

Evans, W., Shankaran, M., Nyangau, E., Field, T., Mohammed, H., Wolfe, R., . . . Hellerstein, M. (2021). Effects of Fortetropin on the Rate of Muscle Protein Synthesis in Older Men and Women: A Randomized, Double-Blinded, Placebo-Controlled Study. *The journals of gerontology. Series A, Biological sciences and medical sciences, 76*(1), 108-114. doi:10.1093/gerona/glaa162

Fantuzzi, G. (2005). Adipose tissue, adipokines, and inflammation. *Journal of Allergy and Clinical Immunology, 115*(5), 911-919; quiz 920. doi:10.1016/j.jaci.2005.02.023

Farese, R. V., Sajan, M. P., & Standaert, M. L. (2005). Atypical protein kinase C in insulin action and insulin resistance. *Biochemical Society Transactions, 33*(Pt 2), 350-353. doi:10.1042/bst0330350

Ferrannini, E., Natali, A., Bell, P., Cavallo-Perin, P., Lalic, N., & Mingrone, G. (1997). Insulin resistance and hypersecretion in obesity. European Group for the Study of Insulin Resistance (EGIR). *Journal of Clinical Investigation, 100*(5), 1166-1173. doi:10.1172/jci119628

Ferrannini, E., Simonson, D. C., Katz, L. D., Reichard, G., Jr., Bevilacqua, S., Barrett, E. J., . . . DeFronzo, R. A. (1988). The disposal of an oral glucose load in patients with non-insulin-dependent diabetes. *Metabolism - Clinical and Experimental, 37*(1), 79-85. doi:10.1016/0026-0495(88)90033-9

Flier, J. S., Cook, K. S., Usher, P., & Spiegelman, B. M. (1987). Severely impaired adipsin expression in genetic and acquired obesity. *Science, 237*(4813), 405-408. doi:10.1126/science.3299706

Florini, J. R., Ewton, D. Z., & Roof, S. L. (1991). Insulin-like growth factor-I stimulates terminal myogenic differentiation by induction of myogenin gene

expression. *Molecular Endocrinology, 5*(5), 718-724. doi:10.1210/mend-5-5-718

Foley, K., Boguslavsky, S., & Klip, A. (2011). Endocytosis, recycling, and regulated exocytosis of glucose transporter 4. *Biochemistry, 50*(15), 3048-3061. doi:10.1021/bi2000356

Forbes, D., Jackman, M., Bishop, A., Thomas, M., Kambadur, R., & Sharma, M. (2006). Myostatin auto-regulates its expression by feedback loop through Smad7 dependent mechanism. *Journal of Cellular Physiology, 206*(1), 264-272. doi:https://doi.org/10.1002/jcp.20477

Francaux, M., & Deldicque, L. (2018). Using polyphenol derivatives to prevent muscle wasting. *Current Opinion in Clinical Nutrition and Metabolic Care, 21*(3), 159-163. doi:10.1097/mco.0000000000000455

Fried, L. P., Tangen, C. M., Walston, J., Newman, A. B., Hirsch, C., Gottdiener, J., . . . McBurnie, M. A. (2001). Frailty in older adults: evidence for a phenotype. *Journals of Gerontology. Series A: Biological Sciences and Medical Sciences, 56*(3), M146-156. doi:10.1093/gerona/56.3.m146

Frontera, W. R., & Ochala, J. (2015). Skeletal Muscle: A Brief Review of Structure and Function. *Calcified Tissue International, 96*(3), 183-195. doi:10.1007/s00223-014-9915-y

Frühbeck, G., Gómez-Ambrosi, J., Muruzábal, F. J., & Burrell, M. A. (2001). The adipocyte: a model for integration of endocrine and metabolic signaling in energy metabolism regulation. *American Journal of Physiology-Endocrinology and Metabolism, 280*(6), E827-E847. doi:10.1152/ajpendo.2001.280.6.E827

Frystyk, J., Skjaerbaek, C., Vestbo, E., Fisker, S., & Orskov, H. (1999). Circulating levels of free insulin-like growth factors in obese subjects: the impact of type 2 diabetes. *Diabetes/Metabolism Research and Reviews, 15*(5), 314-322. doi:10.1002/(sici)1520-7560(199909/10)15:5<314::aid-dmrr56>3.0.co;2-e

Fu, Z., Gilbert, E. R., & Liu, D. (2013). Regulation of insulin synthesis and secretion and pancreatic Beta-cell dysfunction in diabetes. *Current Diabetes Reviews, 9*(1), 25-53.

Funcke, J. B., & Scherer, P. E. (2019). Beyond adiponectin and leptin: adipose tissue-derived mediators of inter-organ communication. *Journal of Lipid Research, 60*(10), 1648-1684. doi:10.1194/jlr.R094060

Gale, C. R., Westbury, L., & Cooper, C. (2018). Social isolation and loneliness as risk factors for the progression of frailty: the English Longitudinal Study of Ageing. *Age and Ageing, 47*(3), 392-397. doi:10.1093/ageing/afx188

Gallagher, D., Ruts, E., Visser, M., Heshka, S., Baumgartner, R. N., Wang, J., . . . Heymsfield, S. B. (2000). Weight stability masks sarcopenia in elderly men and women. *American Journal of Physiology-Endocrinology and Metabolism, 279*(2), E366-E375. doi:10.1152/ajpendo.2000.279.2.E366

Gallen, I. W., & Macdonald, I. A. (1990). Effects of blood glucose concentration on thermogenesis and glucose disposal during hyperinsulinaemia. *Clinical Science (London, England: 1979), 79*(3), 279-285.

Gao, D., Griffiths, H. R., & Bailey, C. J. (2009). Oleate protects against palmitate-induced insulin resistance in L6 myotubes. *British Journal of Nutrition, 102*(11), 1557-1563. doi:10.1017/S0007114509990948

García-Villalba, R., Beltrán, D., Espín, J. C., Selma, M. V., & Tomás-Barberán, F. A. (2013). Time Course Production of Urolithins from Ellagic Acid by Human

Gut Microbiota. *Journal of Agricultural and Food Chemistry, 61*(37), 8797-8806. doi:10.1021/jf402498b

García-Villalba, R., Giménez-Bastida, J. A., Cortés-Martín, A., Ávila-Gálvez, M. Á., Tomás-Barberán, F. A., Selma, M. V., . . . González-Sarrías, A. (2022). Urolithins: a Comprehensive Update on their Metabolism, Bioactivity, and Associated Gut Microbiota. *Molecular Nutrition & Food Research, n/a*(n/a), 2101019. doi:https://doi.org/10.1002/mnfr.202101019

García-Villalba, R., Vissenaekens, H., Pitart, J., Romo-Vaquero, M., Espín, J. C., Grootaert, C., . . . Tomas-Barberan, F. A. (2017). Gastrointestinal Simulation Model TWIN-SHIME Shows Differences between Human Urolithin-Metabotypes in Gut Microbiota Composition, Pomegranate Polyphenol Metabolism, and Transport along the Intestinal Tract. *Journal of Agricultural and Food Chemistry, 65*(27), 5480-5493. doi:10.1021/acs.jafc.7b02049

Garvey, W. T., Maianu, L., Zhu, J. H., Brechtel-Hook, G., Wallace, P., & Baron, A. D. (1998). Evidence for defects in the trafficking and translocation of GLUT4 glucose transporters in skeletal muscle as a cause of human insulin resistance. *Journal of Clinical Investigation, 101*(11), 2377-2386. doi:10.1172/jci1557

Gaster, M., Franch, J., Staehr, P., Beck-Nielsen, H., Smith, T., & Schrøder, H. D. (2000). Induction of GLUT-1 protein in adult human skeletal muscle fibers. *American Journal of Physiology: Endocrinology and Metabolism, 279*(5), E1191-1195. doi:10.1152/ajpendo.2000.279.5.E1191

Gaster, M., Handberg, A., Beck-Nielsen, H., & Schroder, H. D. (2000). Glucose transporter expression in human skeletal muscle fibers. *American Journal of Physiology: Endocrinology and Metabolism, 279*(3), E529-538. doi:10.1152/ajpendo.2000.279.3.E529

Gaster, M., Petersen, I., Højlund, K., Poulsen, P., & Beck-Nielsen, H. (2002). The Diabetic Phenotype Is Conserved in Myotubes Established From Diabetic Subjects. *Evidence for Primary Defects in Glucose Transport and Glycogen Synthase Activity, 51*(4), 921-927. doi:10.2337/diabetes.51.4.921

Gaster, M., Poulsen, P., Handberg, A., Schroder, H. D., & Beck-Nielsen, H. (2000). Direct evidence of fiber type-dependent GLUT-4 expression in human skeletal muscle. *American Journal of Physiology: Endocrinology and Metabolism, 278*(5), E910-916. doi:10.1152/ajpendo.2000.278.5.E910

Gaster, M., Rustan, A. C., Aas, V., & Beck-Nielsen, H. (2004). Reduced lipid oxidation in skeletal muscle from type 2 diabetic subjects may be of genetic origin: evidence from cultured myotubes. *Diabetes, 53*(3), 542-548.

Gaster, M., Rustan, A. C., & Beck-Nielsen, H. (2005). Differential Utilization of Saturated Palmitate and Unsaturated Oleate. *Evidence From Cultured Myotubes, 54*(3), 648-656. doi:10.2337/diabetes.54.3.648

George, I., Bish, L. T., Kamalakkannan, G., Petrilli, C. M., Oz, M. C., Naka, Y., . . . Maybaum, S. (2010). Myostatin activation in patients with advanced heart failure and after mechanical unloading. *European Journal of Heart Failure, 12*(5), 444-453. doi:10.1093/eurjhf/hfq039

George, T., Velloso, C. P., Alsharidah, M., Lazarus, N. R., & Harridge, S. D. (2010). Sera from young and older humans equally sustain proliferation and differentiation of human myoblasts. *Experimental Gerontology, 45*(11), 875-881. doi:10.1016/j.exger.2010.07.006

Ghosh, N., Das, A., Biswas, N., Gnyawali, S., Singh, K., Gorain, M., . . . Sen, C. K. (2020). Urolithin A augments angiogenic pathways in skeletal muscle by

bolstering NAD(+) and SIRT1. *Scientific Reports, 10*(1), 20184. doi:10.1038/s41598-020-76564-7

Golay, A., & Bobbioni, E. (1997). The role of dietary fat in obesity. *International Journal of Obesity and Related Metabolic Disorders, 21 Suppl 3*, S2-11.

Gomes, M. D., Lecker, S. H., Jagoe, R. T., Navon, A., & Goldberg, A. L. (2001). Atrogin-1, a muscle-specific F-box protein highly expressed during muscle atrophy. *Proceedings of the National Academy of Sciences of the United States of America, 98*(25), 14440-14445. doi:10.1073/pnas.251541198

González-Bermúdez, L., Anglada, T., Genescà, A., Martín, M., & Terradas, M. (2019). Identification of reference genes for RT-qPCR data normalisation in aging studies. *Scientific Reports, 9*(1), 13970-13970. doi:10.1038/s41598-019-50035-0

Gonzalez-Cadavid, N. F., & Bhasin, S. (2004). Role of myostatin in metabolism. *Current Opinion in Clinical Nutrition and Metabolic Care, 7*(4), 451-457. doi:10.1097/01.mco.0000134365.99523.7f

Gonzalez-Cadavid, N. F., Taylor, W. E., Yarasheski, K., Sinha-Hikim, I., Ma, K., Ezzat, S., . . . Bhasin, S. (1998). Organization of the human myostatin gene and expression in healthy men and HIV-infected men with muscle wasting. *Proceedings of the National Academy of Sciences of the United States of America, 95*(25), 14938-14943.

González-Sarrías, A., García-Villalba, R., Núñez-Sánchez, M. Á., Tomé-Carneiro, J., Zafrilla, P., Mulero, J., . . . Espín, J. C. (2015). Identifying the limits for ellagic acid bioavailability: A crossover pharmacokinetic study in healthy volunteers after consumption of pomegranate extracts. *Journal of Functional Foods, 19*, 225-235. doi:https://doi.org/10.1016/j.jff.2015.09.019

Goodman, C. A., & Hornberger, T. A. (2013). Measuring protein synthesis with SUnSET: a valid alternative to traditional techniques? *Exercise and Sport Sciences Reviews, 41*(2), 107-115. doi:10.1097/JES.0b013e3182798a95

Goodman, C. A., Mabrey, D. M., Frey, J. W., Miu, M. H., Schmidt, E. K., Pierre, P., & Hornberger, T. A. (2011). Novel insights into the regulation of skeletal muscle protein synthesis as revealed by a new nonradioactive in vivo technique. *FASEB journal : official publication of the Federation of American Societies for Experimental Biology, 25*(3), 1028-1039. doi:10.1096/fj.10-168799

Goodman, C. A., McNally, R. M., Hoffmann, F. M., & Hornberger, T. A. (2013). Smad3 induces atrogin-1, inhibits mTOR and protein synthesis, and promotes muscle atrophy in vivo. *Molecular endocrinology (Baltimore, Md.), 27*(11), 1946-1957. doi:10.1210/me.2013-1194

Goodpaster, B. H., Park, S. W., Harris, T. B., Kritchevsky, S. B., Nevitt, M., Schwartz, A. V., . . . Newman, A. B. (2006). The loss of skeletal muscle strength, mass, and quality in older adults: the health, aging and body composition study. *Journals of Gerontology. Series A: Biological Sciences and Medical Sciences, 61*(10), 1059-1064.

Gorgens, S. W., Eckardt, K., Jensen, J., Drevon, C. A., & Eckel, J. (2015). Exercise and Regulation of Adipokine and Myokine Production. *Progress in Molecular Biology and Translational Science, 135*, 313-336. doi:10.1016/bs.pmbts.2015.07.002

Grabiec, K., Majewska, A., Wicik, Z., Milewska, M., Błaszczyk, M., & Grzelkowska-Kowalczyk, K. (2016). The effect of palmitate supplementation on gene expression profile in proliferating myoblasts. *Cell Biology and Toxicology, 32*(3), 185-198. doi:10.1007/s10565-016-9324-2

Grade, C. V. C., Mantovani, C. S., & Alvares, L. E. (2019). Myostatin gene promoter: structure, conservation and importance as a target for muscle modulation. *Journal of Animal Science and Biotechnology, 10*(1), 32. doi:10.1186/s40104-019-0338-5

Grade, C. V. C., Mantovani, C. S., Fontoura, M. A., Yusuf, F., Brand-Saberi, B., & Alvares, L. E. (2017). CREB, NF-Y and MEIS1 conserved binding sites are essential to balance Myostatin promoter/enhancer activity during early myogenesis. *Molecular Biology Reports, 44*(5), 419-427. doi:10.1007/s11033-017-4126-z

Grapov, D., Adams, S. H., Pedersen, T. L., Garvey, W. T., & Newman, J. W. (2012). Type 2 Diabetes Associated Changes in the Plasma Non-Esterified Fatty Acids, Oxylipins and Endocannabinoids. *PloS One, 7*(11), e48852. doi:10.1371/journal.pone.0048852

Green, H., & Meuth, M. (1974). An established pre-adipose cell line and its differentiation in culture. *Cell, 3*(2), 127-133. doi:10.1016/0092-8674(74)90116-0

Greiwe, J. S., Cheng, B., Rubin, D. C., Yarasheski, K. E., & Semenkovich, C. F. (2001). Resistance exercise decreases skeletal muscle tumor necrosis factor alpha in frail elderly humans. *FASEB Journal, 15*(2), 475-482. doi:10.1096/fj.00-0274com

Greiwe, J. S., Holloszy, J. O., & Semenkovich, C. F. (2000). Exercise induces lipoprotein lipase and GLUT-4 protein in muscle independent of adrenergic-receptor signaling. *Journal of Applied Physiology, 89*(1), 176-181. doi:10.1152/jappl.2000.89.1.176

Griffin, M. E., Marcucci, M. J., Cline, G. W., Bell, K., Barucci, N., Lee, D., . . . Shulman, G. I. (1999). Free fatty acid-induced insulin resistance is associated with activation of protein kinase C theta and alterations in the insulin signaling cascade. *Diabetes, 48*(6), 1270-1274. doi:10.2337/diabetes.48.6.1270

Grimsgaard, S., Bønaa, K. H., Jacobsen, B. K., & Bjerve, K. S. (1999). Plasma Saturated and Linoleic Fatty Acids Are Independently Associated With Blood Pressure. *Hypertension, 34*(3), 478-483. doi:doi:10.1161/01.HYP.34.3.478

Groop, L. C., Bonadonna, R. C., DelPrato, S., Ratheiser, K., Zyck, K., Ferrannini, E., & DeFronzo, R. A. (1989). Glucose and free fatty acid metabolism in non-insulin-dependent diabetes mellitus. Evidence for multiple sites of insulin resistance. *Journal of Clinical Investigation, 84*(1), 205-213. doi:10.1172/jci114142

Grundy, S. M., Brewer, H. B., Jr., Cleeman, J. I., Smith, S. C., Jr., & Lenfant, C. (2004). Definition of metabolic syndrome: Report of the National Heart, Lung, and Blood Institute/American Heart Association conference on scientific issues related to definition. *Circulation, 109*(3), 433-438. doi:10.1161/01.Cir.0000111245.75752.C6

Guillausseau, P. J., Meas, T., Virally, M., Laloi-Michelin, M., Medeau, V., & Kevorkian, J. P. (2008). Abnormalities in insulin secretion in type 2 diabetes mellitus. *Diabetes and Metabolism, 34 Suppl 2*, S43-48. doi:10.1016/s1262-3636(08)73394-9

Guillet, C., Boirie, Y., & Walrand, S. (2004). An integrative approach to in-vivo protein synthesis measurement: from whole tissue to specific proteins. *Current Opinion in Clinical Nutrition and Metabolic Care, 7*(5), 531-538.

Gumucio, J. P., & Mendias, C. L. (2013). Atrogin-1, MuRF-1, and sarcopenia. *Endocrine, 43*(1), 12-21. doi:10.1007/s12020-012-9751-7

Gunawardana, S. C. (2014). Benefits of healthy adipose tissue in the treatment of diabetes. *World Journal of Diabetes, 5*(4), 420-430. doi:10.4239/wjd.v5.i4.420

Gungor, A., Palabiyik, S. S., Bayraktutan, Z., Dursun, H., Gokkaya, N., Bilen, A., & Bilen, H. (2016). Levels of endothelial cell-specific molecule-1 (ESM-1) in overt hypothyroidisim. *Endocrine Research, 41*(4), 275-280. doi:10.3109/07435800.2015.1135443

Guo, H., Jin, D., Zhang, Y., Wright, W., Bazuine, M., Brockman, D. A., . . . Chen, X. (2010). Lipocalin-2 deficiency impairs thermogenesis and potentiates diet-induced insulin resistance in mice. *Diabetes, 59*(6), 1376-1385. doi:10.2337/db09-1735

Guo, Q., Wei, X., Hu, H., Yang, D., Zhang, B., Fan, X., . . . Gu, N. (2019). The saturated fatty acid palmitate induces insulin resistance through Smad3-mediated down-regulation of FNDC5 in myotubes. *Biochemical and Biophysical Research Communications, 520*(3), 619-626. doi:https://doi.org/10.1016/j.bbrc.2019.10.077

Guo, T., Jou, W., Chanturiya, T., Portas, J., Gavrilova, O., & McPherron, A. C. (2009). Myostatin Inhibition in Muscle, but Not Adipose Tissue, Decreases Fat Mass and Improves Insulin Sensitivity. *PloS One, 4*(3), e4937. doi:10.1371/journal.pone.0004937

Gutierrez-Salmean, G., Ciaraldi, T. P., Nogueira, L., Barboza, J., Taub, P. R., Hogan, M. C., . . . Ramirez-Sanchez, I. (2014). Effects of (-)-epicatechin on molecular modulators of skeletal muscle growth and differentiation. *The Journal of Nutritional Biochemistry, 25*(1), 91-94. doi:10.1016/j.jnutbio.2013.09.007

Ha, C. Y., Kim, J. Y., Paik, J. K., Kim, O. Y., Paik, Y. H., Lee, E. J., & Lee, J. H. (2012). The association of specific metabolites of lipid metabolism with markers of oxidative stress, inflammation and arterial stiffness in men with newly diagnosed type 2 diabetes. *Clinical Endocrinology, 76*(5), 674-682. doi:10.1111/j.1365-2265.2011.04244.x

Haddad, F., & Adams, G. R. (2006). Aging-sensitive cellular and molecular mechanisms associated with skeletal muscle hypertrophy. *J Appl Physiol (1985), 100*(4), 1188-1203. doi:10.1152/japplphysiol.01227.2005

Hamada, K., Vannier, E., Sacheck, J. M., Witsell, A. L., & Roubenoff, R. (2005). Senescence of human skeletal muscle impairs the local inflammatory cytokine response to acute eccentric exercise. *FASEB Journal, 19*(2), 264-266. doi:10.1096/fj.03-1286fje

Hamer, M., & O'Donovan, G. (2017). Sarcopenic obesity, weight loss, and mortality: the English Longitudinal Study of Ageing. *American Journal of Clinical Nutrition, 106*(1), 125-129. doi:10.3945/ajcn.117.152488

Hamilton, J. A. (2008). Colony-stimulating factors in inflammation and autoimmunity. *Nature Reviews Immunology, 8*(7), 533-544.

Hamilton, J. A., Johnson, R. A., Corkey, B., & Kamp, F. (2001). Fatty acid transport: the diffusion mechanism in model and biological membranes. *Journal of Molecular Neuroscience, 16*(2-3), 99-108; discussion 151-107. doi:10.1385/jmn:16:2-3:99

Hamrick, M. W., McNeil, P. L., & Patterson, S. L. (2010). Role of muscle-derived growth factors in bone formation. *Journal of Musculoskeletal & Neuronal Interactions, 10*(1), 64-70.

Han, D. S., Chen, Y. M., Lin, S. Y., Chang, H. H., Huang, T. M., Chi, Y. C., & Yang, W. S. (2011). Serum myostatin levels and grip strength in normal subjects

and patients on maintenance haemodialysis. *Clinical Endocrinology, 75*(6), 857-863. doi:10.1111/j.1365-2265.2011.04120.x

Han, D. S., Chu-Su, Y., Chiang, C. K., Tseng, F. Y., Tseng, P. H., Chen, C. L., . . . Yang, W. S. (2014). Serum myostatin is reduced in individuals with metabolic syndrome. *PloS One, 9*(9), e108230. doi:10.1371/journal.pone.0108230

Haran, P. H., Rivas, D. A., & Fielding, R. A. (2012). Role and potential mechanisms of anabolic resistance in sarcopenia. *Journal of Cachexia, Sarcopenia and Muscle, 3*(3), 157-162. doi:10.1007/s13539-012-0068-4

Hardy, O. T., Czech, M. P., & Corvera, S. (2012). What causes the insulin resistance underlying obesity? *Current Opinion in Endocrinology, Diabetes, and Obesity, 19*(2), 81-87. doi:10.1097/MED.0b013e3283514e13

Harridge, S. D. R. (2007). Plasticity of human skeletal muscle: gene expression to in vivo function. *Experimental Physiology, 92*(5), 783-797. doi:https://doi.org/10.1113/expphysiol.2006.036525

Harridge, S. D. R., & Lazarus, N. R. (2017). Physical Activity, Aging, and Physiological Function. *Physiology, 32*(2), 152-161. doi:10.1152/physiol.00029.2016

Hartwig, S., Raschke, S., Knebel, B., Scheler, M., Irmler, M., Passlack, W., . . . Lehr, S. (2014). Secretome profiling of primary human skeletal muscle cells. *Biochimica et Biophysica Acta, 1844*(5), 1011-1017. doi:10.1016/j.bbapap.2013.08.004

Harvey, A. L., Robertson, J. G., & Witkowski, J. A. (1979). Maturation of human skeletal muscle fibres in explant tissue culture. *Journal of the Neurological Sciences, 41*(1), 115-122. doi:https://doi.org/10.1016/0022-510X(79)90145-X

Hawley, J. A., Hargreaves, M., Joyner, M. J., & Zierath, J. R. (2014). Integrative biology of exercise. *Cell, 159*(4), 738-749. doi:10.1016/j.cell.2014.10.029

Hawley, J. A., Joyner, M. J., & Green, D. J. (2021). Mimicking exercise: what matters most and where to next? *The Journal of Physiology, 599*(3), 791-802. doi:https://doi.org/10.1113/JP278761

Heden, T. D., Ryan, T. E., Ferrara, P. J., Hickner, R. C., Brophy, P. M., Neufer, P. D., . . . Funai, K. (2017). Greater Oxidative Capacity in Primary Myotubes from Endurance-trained Women. *Medicine and Science in Sports and Exercise, 49*(11), 2151-2157. doi:10.1249/MSS.0000000000001352

Heilman, J., Andreux, P., Tran, N., Rinsch, C., & Blanco-Bose, W. (2017). Safety assessment of Urolithin A, a metabolite produced by the human gut microbiota upon dietary intake of plant derived ellagitannins and ellagic acid. *Food and Chemical Toxicology, 108*(Pt A), 289-297. doi:10.1016/j.fct.2017.07.050

Heintzman, N. D., & Ren, B. (2007). The gateway to transcription: identifying, characterizing and understanding promoters in the eukaryotic genome. *Cellular and Molecular Life Sciences, 64*(4), 386-400. doi:10.1007/s00018-006-6295-0

Henderson, J. R., & Moss, M. C. (1985). A MORPHOMETRIC STUDY OF THE ENDOCRINE AND EXOCRINE CAPILLARIES OF THE PANCREAS. *Quarterly Journal of Experimental Physiology, 70*(3), 347-356. doi:10.1113/expphysiol.1985.sp002920

Henique, C., Mansouri, A., Fumey, G., Lenoir, V., Girard, J., Bouillaud, F., . . . Cohen, I. (2010). Increased mitochondrial fatty acid oxidation is sufficient

to protect skeletal muscle cells from palmitate-induced apoptosis. *The Journal of biological chemistry, 285*(47), 36818-36827. doi:10.1074/jbc.M110.170431

Hernández, E. Á., Kahl, S., Seelig, A., Begovatz, P., Irmler, M., Kupriyanova, Y., . . . Roden, M. (2017). Acute dietary fat intake initiates alterations in energy metabolism and insulin resistance. *The Journal of clinical investigation, 127*(2), 695-708. doi:10.1172/JCI89444

Herz, C. T., & Kiefer, F. W. (2019). Adipose tissue browning in mice and humans. *Journal of Endocrinology, 241*(3), R97-R109. doi:10.1530/JOE-18-0598

Hill, J. J., Davies, M. V., Pearson, A. A., Wang, J. H., Hewick, R. M., Wolfman, N. M., & Qiu, Y. (2002). The myostatin propeptide and the follistatin-related gene are inhibitory binding proteins of myostatin in normal serum. *Journal of Biological Chemistry, 277*(43), 40735-40741. doi:10.1074/jbc.M206379200

Hill, J. J., Qiu, Y., Hewick, R. M., & Wolfman, N. M. (2003). Regulation of myostatin in vivo by growth and differentiation factor-associated serum protein-1: a novel protein with protease inhibitor and follistatin domains. *Molecular Endocrinology, 17*(6), 1144-1154. doi:10.1210/me.2002-0366

Himsworth, H. P. (2011). Diabetes mellitus: its differentiation into insulin-sensitive and insulin-insensitive types. *Diabetic Medicine, 28*(12), 1440-1444. doi:10.1111/j.1464-5491.2011.3508.x

Hirabara, S. M., Curi, R., & Maechler, P. (2010). Saturated fatty acid-induced insulin resistance is associated with mitochondrial dysfunction in skeletal muscle cells. *Journal of Cellular Physiology, 222*(1), 187-194. doi:10.1002/jcp.21936

Hittel, D. S., Axelson, M., Sarna, N., Shearer, J., Huffman, K. M., & Kraus, W. E. (2010). Myostatin decreases with aerobic exercise and associates with insulin resistance. *Medicine and Science in Sports and Exercise, 42*(11), 2023-2029. doi:10.1249/MSS.0b013e3181e0b9a8

Hittel, D. S., Berggren, J. R., Shearer, J., Boyle, K., & Houmard, J. A. (2009). Increased secretion and expression of myostatin in skeletal muscle from extremely obese women. *Diabetes, 58*(1), 30-38. doi:10.2337/db08-0943

Hjorth, M., Pourteymour, S., Görgens, S. W., Langleite, T. M., Lee, S., Holen, T., . . . Norheim, F. (2016). Myostatin in relation to physical activity and dysglycaemia and its effect on energy metabolism in human skeletal muscle cells. *Acta Physiologica, 217*(1), 45-60. doi:doi:10.1111/apha.12631

Høeg, L. D., Sjøberg, K. A., Jeppesen, J., Jensen, T. E., Frøsig, C., Birk, J. B., . . . Kiens, B. (2011). Lipid-induced insulin resistance affects women less than men and is not accompanied by inflammation or impaired proximal insulin signaling. *Diabetes, 60*(1), 64-73. doi:10.2337/db10-0698

Høeg, L. D., Sjøberg, K. A., Jeppesen, J., Jensen, T. E., Frøsig, C., Birk, J. B., . . . Kiens, B. (2010). Lipid-Induced Insulin Resistance Affects Women Less Than Men and Is Not Accompanied by Inflammation or Impaired Proximal Insulin Signaling. *Diabetes, 60*(1), 64-73. doi:10.2337/db10-0698

Hofmann, M., Halper, B., Oesen, S., Franzke, B., Stuparits, P., Tschan, H., . . . Wessner, B. (2015). Serum concentrations of insulin-like growth factor-1, members of the TGF-beta superfamily and follistatin do not reflect different stages of dynapenia and sarcopenia in elderly women. *Experimental Gerontology, 64*, 35-45. doi:10.1016/j.exger.2015.02.008

Holland, W. L., Bikman, B. T., Wang, L.-P., Yuguang, G., Sargent, K. M., Bulchand, S., . . . Summers, S. A. (2011). Lipid-induced insulin resistance mediated by

the proinflammatory receptor TLR4 requires saturated fatty acid-induced ceramide biosynthesis in mice. *The Journal of clinical investigation, 121*(5), 1858-1870. doi:10.1172/JCI43378

Holland, W. L., Brozinick, J. T., Wang, L. P., Hawkins, E. D., Sargent, K. M., Liu, Y., . . . Summers, S. A. (2007). Inhibition of ceramide synthesis ameliorates glucocorticoid-, saturated-fat-, and obesity-induced insulin resistance. *Cell Metabolism, 5*(3), 167-179. doi:10.1016/j.cmet.2007.01.002

Holloszy, J. O., & Hansen, P. A. (1996). Regulation of glucose transport into skeletal muscle. In *Reviews of Physiology Biochemistry and Pharmacology, Volume 128: Volume: 128* (pp. 99-193). Berlin, Heidelberg: Springer Berlin Heidelberg.

Hommelberg, P. P. H., Plat, J., Sparks, L. M., Schols, A. M. W. J., van Essen, A. L. M., Kelders, M. C. J. M., . . . Langen, R. C. J. (2011). Palmitate-induced skeletal muscle insulin resistance does not require NF-κB activation. *Cellular and molecular life sciences : CMLS, 68*(7), 1215-1225. doi:10.1007/s00018-010-0515-3

Hong, E. G., Ko, H. J., Cho, Y. R., Kim, H. J., Ma, Z., Yu, T. Y., . . . Kim, J. K. (2009). Interleukin-10 prevents diet-induced insulin resistance by attenuating macrophage and cytokine response in skeletal muscle. *Diabetes, 58*(11), 2525-2535. doi:10.2337/db08-1261

Hoogendijk, E. O., Suanet, B., Dent, E., Deeg, D. J., & Aartsen, M. J. (2016). Adverse effects of frailty on social functioning in older adults: Results from the Longitudinal Aging Study Amsterdam. *Maturitas, 83*, 45-50. doi:10.1016/j.maturitas.2015.09.002

Hoppel, C. L., & Genuth, S. M. (1980). Carnitine metabolism in normal-weight and obese human subjects during fasting. *American Journal of Physiology, 238*(5), E409-415. doi:10.1152/ajpendo.1980.238.5.E409

Host, H. H., Hansen, P. A., Nolte, L. A., Chen, M. M., & Holloszy, J. O. (1998). Rapid reversal of adaptive increases in muscle GLUT-4 and glucose transport capacity after training cessation. *Journal of Applied Physiology, 84*(3), 798-802. doi:10.1152/jappl.1998.84.3.798

Hostetler, H. A., Kier, A. B., & Schroeder, F. (2006). Very-long-chain and branched-chain fatty acyl-CoAs are high affinity ligands for the peroxisome proliferator-activated receptor alpha (PPARalpha). *Biochemistry, 45*(24), 7669-7681. doi:10.1021/bi060198l

Hotamisligil, G. S., Shargill, N. S., & Spiegelman, B. M. (1993). Adipose expression of tumor necrosis factor-α: Direct role in obesity-linked insulin resistance. *Science, 259*(5091), 87-91. doi:10.1126/science.7678183

Hou, J. C., Min, L., & Pessin, J. E. (2009). Insulin granule biogenesis, trafficking and exocytosis. *Vitamins and Hormones, 80*, 473-506. doi:10.1016/S0083-6729(08)00616-X

Houmard, J. A., Egan, P. C., Neufer, P. D., Friedman, J. E., Wheeler, W. S., Israel, R. G., & Dohm, G. L. (1991). Elevated skeletal muscle glucose transporter levels in exercise-trained middle-aged men. *American Journal of Physiology-Endocrinology and Metabolism, 261*(4), E437-E443. doi:10.1152/ajpendo.1991.261.4.E437

Houmard, J. A., Pories, W. J., & Dohm, G. L. (2011). Is There a Metabolic Program in the Skeletal Muscle of Obese Individuals? *Journal of Obesity, 2011*, 250496. doi:10.1155/2011/250496

Houmard, J. A., Weidner, M. D., Dolan, P. L., Leggett-Frazier, N., Gavigan, K. E., Hickey, M. S., . . . Dohm, G. L. (1995). Skeletal muscle GLUT4 protein

concentration and aging in humans. *Diabetes, 44*(5), 555-560. doi:10.2337/diab.44.5.555

Howard, E. E., Pasiakos, S. M., Blesso, C. N., Fussell, M. A., & Rodriguez, N. R. (2020). Divergent Roles of Inflammation in Skeletal Muscle Recovery From Injury. *Frontiers in Physiology, 11*. doi:10.3389/fphys.2020.00087

Hu, W., Chen, S., Zhang, R., & Lin, Y. (2013). Single nucleotide polymorphisms in the upstream regulatory region alter the expression of myostatin. *In Vitro Cellular and Developmental Biology: Animal, 49*(6), 417-423. doi:10.1007/s11626-013-9621-5

Huang, J., Imamura, T., & Olefsky, J. M. (2001). Insulin can regulate GLUT4 internalization by signaling to Rab5 and the motor protein dynein. *Proceedings of the National Academy of Sciences, 98*(23), 13084-13089. doi:10.1073/pnas.241368698

Huang, Z., Chen, D., Zhang, K., Yu, B., Chen, X., & Meng, J. (2007). Regulation of myostatin signaling by c-Jun N-terminal kinase in C2C12 cells. *Cellular Signalling, 19*(11), 2286-2295. doi:10.1016/j.cellsig.2007.07.002

Hunter, S. J., & Garvey, W. T. (1998). Insulin action and insulin resistance: diseases involving defects in insulin receptors, signal transduction, and the glucose transport effector system 11In collaboration with The American Physiological Society, Thomas E. Andreoli, MD, Editor. *The American Journal of Medicine, 105*(4), 331-345. doi:https://doi.org/10.1016/S0002-9343(98)00300-3

Iizuka, K., Machida, T., & Hirafuji, M. (2014). Skeletal Muscle Is an Endocrine Organ. *Journal of Pharmacological Sciences, 125*(2), 125-131. doi:https://doi.org/10.1254/jphs.14R02CP

Imamura, F., Micha, R., Wu, J. H. Y., de Oliveira Otto, M. C., Otite, F. O., Abioye, A. I., & Mozaffarian, D. (2016). Effects of Saturated Fat, Polyunsaturated Fat, Monounsaturated Fat, and Carbohydrate on Glucose-Insulin Homeostasis: A Systematic Review and Meta-analysis of Randomised Controlled Feeding Trials. *PLoS Medicine, 13*(7), e1002087. doi:10.1371/journal.pmed.1002087

Indrakusuma, I., Sell, H., & Eckel, J. (2015). Novel Mediators of Adipose Tissue and Muscle Crosstalk. *Current Obesity Reports, 4*(4), 411-417. doi:10.1007/s13679-015-0174-7

Ishii, A., Katsuura, G., Imamaki, H., Kimura, H., Mori, K. P., Kuwabara, T., . . . Mori, K. (2017). Obesity-promoting and anti-thermogenic effects of neutrophil gelatinase-associated lipocalin in mice. *Scientific Reports, 7*(1), 15501. doi:10.1038/s41598-017-15825-4

Itani, S. I., Ruderman, N. B., Schmieder, F., & Boden, G. (2002). Lipid-Induced Insulin Resistance in Human Muscle Is Associated With Changes in Diacylglycerol, Protein Kinase C, and IκB-α. *Diabetes, 51*(7), 2005-2011. doi:10.2337/diabetes.51.7.2005

Itani, S. I., Zhou, Q., Pories, W. J., MacDonald, K. G., & Dohm, G. L. (2000). Involvement of protein kinase C in human skeletal muscle insulin resistance and obesity. *Diabetes, 49*(8), 1353-1358. doi:10.2337/diabetes.49.8.1353

Ivy, J. L. (2004). Muscle insulin resistance amended with exercise training: role of GLUT4 expression. *Medicine and Science in Sports and Exercise, 36*(7), 1207-1211.

Jacobs, A. E., Oosterhof, A., & Veerkamp, J. H. (1987). Palmitate oxidation and some enzymes of energy metabolism in human muscles and cultured muscle

cells. *International Journal of Biochemistry, 19*(11), 1049-1054. doi:10.1016/0020-711x(87)90305-3

Jacobsen, S. C., Brons, C., Bork-Jensen, J., Ribel-Madsen, R., Yang, B., Lara, E., . . . Vaag, A. (2012). Effects of short-term high-fat overfeeding on genome-wide DNA methylation in the skeletal muscle of healthy young men. *Diabetologia, 55*(12), 3341-3349. doi:10.1007/s00125-012-2717-8

James, D. E., Brown, R., Navarro, J., & Pilch, P. F. (1988). Insulin-regulatable tissues express a unique insulin-sensitive glucose transport protein. *Nature, 333*(6169), 183-185. doi:10.1038/333183a0

Janke, J., Engeli, S., Gorzelniak, K., Feldpausch, M., Heintze, U., Böhnke, J., . . . Sharma, A. M. (2006). Adipose tissue and circulating endothelial cell specific molecule-1 in human obesity. *Hormone and Metabolic Research, 38*(1), 28-33. doi:10.1055/s-2006-924973

Janssen, I., Heymsfield, S. B., Wang, Z. M., & Ross, R. (2000). Skeletal muscle mass and distribution in 468 men and women aged 18-88 yr. *J Appl Physiol (1985), 89*(1), 81-88. doi:10.1152/jappl.2000.89.1.81

Jansson, L., Barbu, A., Bodin, B., Drott, C. J., Espes, D., Gao, X., . . . Carlsson, P.-O. (2016). Pancreatic islet blood flow and its measurement. *Upsala Journal of Medical Sciences, 121*(2), 81-95. doi:10.3109/03009734.2016.1164769

Ji, L. L., & Yeo, D. (2019). Mitochondrial dysregulation and muscle disuse atrophy. *F1000Research, 8*, F1000 Faculty Rev-1621. doi:10.12688/f1000research.19139.1

Jiang, M. S., Liang, L. F., Wang, S., Ratovitski, T., Holmstrom, J., Barker, C., & Stotish, R. (2004). Characterization and identification of the inhibitory domain of GDF-8 propeptide. *Biochemical and Biophysical Research Communications, 315*(3), 525-531. doi:10.1016/j.bbrc.2004.01.085

Jones, B. H., Standridge, M. K., & Moustaid, N. (1997). Angiotensin II Increases Lipogenesis in 3T3-L1 and Human Adipose Cells*. *Endocrinology, 138*(4), 1512-1519. doi:10.1210/endo.138.4.5038

Jones, R. (2019). *FAT AND PROTEIN METABOLISM: INTERACTIONS IN HUMAN SKELETAL MUSCLE.* (PhD.). University of Nottingham,

Jones, R., Pabla, P., Mallinson, J., Nixon, A., Taylor, T., Bennett, A., & Tsintzas, K. (2020). Two weeks of early time-restricted feeding (eTRF) improves skeletal muscle insulin and anabolic sensitivity in healthy men. *The American Journal of Clinical Nutrition, 112*(4), 1015-1028. doi:10.1093/ajcn/nqaa192

Joost, H.-G., Bell, G. I., Best, J. D., Birnbaum, M. J., Charron, M. J., Chen, Y. T., . . . Thorens, B. (2002). Nomenclature of the GLUT/SLC2A family of sugar/polyol transport facilitators. *American Journal of Physiology-Endocrinology and Metabolism, 282*(4), E974-E976. doi:10.1152/ajpendo.00407.2001

Joulia, D., Bernardi, H., Garandel, V., Rabenoelina, F., Vernus, B., & Cabello, G. (2003). Mechanisms involved in the inhibition of myoblast proliferation and differentiation by myostatin. *Experimental Cell Research, 286*(2), 263-275. doi:https://doi.org/10.1016/S0014-4827(03)00074-0

Kahn, B. B. (1998). Type 2 Diabetes: When Insulin Secretion Fails to Compensate for Insulin Resistance. *Cell, 92*(5), 593-596. doi:10.1016/S0092-8674(00)81125-3

Kallscheuer, N., Vogt, M., & Marienhagen, J. (2017). A Novel Synthetic Pathway Enables Microbial Production of Polyphenols Independent from the

Endogenous Aromatic Amino Acid Metabolism. *ACS Synth Biol, 6*(3), 410-415. doi:10.1021/acssynbio.6b00291

Kambadur, R., Sharma, M., Smith, T. P., & Bass, J. J. (1997). Mutations in myostatin (GDF8) in double-muscled Belgian Blue and Piedmontese cattle. *Genome Research, 7*(9), 910-916.

Kang, I., Buckner, T., Shay, N. F., Gu, L., & Chung, S. (2016). Improvements in Metabolic Health with Consumption of Ellagic Acid and Subsequent Conversion into Urolithins: Evidence and Mechanisms. *Advances in Nutrition, 7*(5), 961-972. doi:10.3945/an.116.012575

Kang, I., Kim, Y., Tomás-Barberán, F. A., Espín, J. C., & Chung, S. (2016). Urolithin A, C, and D, but not iso-urolithin A and urolithin B, attenuate triglyceride accumulation in human cultures of adipocytes and hepatocytes. *Molecular Nutrition & Food Research, 60*(5), 1129-1138. doi:https://doi.org/10.1002/mnfr.201500796

Karlsson, H. K., Chibalin, A. V., Koistinen, H. A., Yang, J., Koumanov, F., Wallberg-Henriksson, H., . . . Holman, G. D. (2009). Kinetics of GLUT4 trafficking in rat and human skeletal muscle. *Diabetes, 58*(4), 847-854. doi:10.2337/db08-1539

Karlsson, H. K., Zierath, J. R., Kane, S., Krook, A., Lienhard, G. E., & Wallberg-Henriksson, H. (2005). Insulin-stimulated phosphorylation of the Akt substrate AS160 is impaired in skeletal muscle of type 2 diabetic subjects. *Diabetes, 54*(6), 1692-1697. doi:10.2337/diabetes.54.6.1692

Katsanos, C. S., Kobayashi, H., Sheffield-Moore, M., Aarsland, A., & Wolfe, R. R. (2005). Aging is associated with diminished accretion of muscle proteins after the ingestion of a small bolus of essential amino acids. *American Journal of Clinical Nutrition, 82*(5), 1065-1073. doi:10.1093/ajcn/82.5.1065

Katz, A., Broberg, S., Sahlin, K., & Wahren, J. (1986). Leg glucose uptake during maximal dynamic exercise in humans. *American Journal of Physiology, 251*(1 Pt 1), E65-70. doi:10.1152/ajpendo.1986.251.1.E65

Kauppinen, A., Suuronen, T., Ojala, J., Kaarniranta, K., & Salminen, A. (2013). Antagonistic crosstalk between NF-κB and SIRT1 in the regulation of inflammation and metabolic disorders. *Cellular Signalling, 25*(10), 1939-1948. doi:10.1016/j.cellsig.2013.06.007

Kausch, C., Staiger, H., Staiger, K., Krützfeldt, J., Matthaei, S., Häring, H. U., & Stumvoll, M. (2003). Skeletal muscle cells from insulin-resistant (non-diabetic) individuals are susceptible to insulin desensitization by palmitate. *Hormone and Metabolic Research, 35*(10), 570-576. doi:10.1055/s-2003-43501

Keesey, R. E., & Hirvonen, M. D. (1997). Body Weight Set-Points: Determination and Adjustment. *The Journal of Nutrition, 127*(9), 1875S-1883S. doi:10.1093/jn/127.9.1875S

Kelley, D., Mitrakou, A., Marsh, H., Schwenk, F., Benn, J., Sonnenberg, G., . . . et al. (1988). Skeletal muscle glycolysis, oxidation, and storage of an oral glucose load. *The Journal of clinical investigation, 81*(5), 1563-1571. doi:10.1172/JCI113489

Kelley, D. E., Mokan, M., Simoneau, J. A., & Mandarino, L. J. (1993). Interaction between glucose and free fatty acid metabolism in human skeletal muscle. *Journal of Clinical Investigation, 92*(1), 91-98. doi:10.1172/jci116603

Kelpe, C. L., Moore, P. C., Parazzoli, S. D., Wicksteed, B., Rhodes, C. J., & Poitout, V. (2003). Palmitate inhibition of insulin gene expression is mediated at the

transcriptional level via ceramide synthesis. *Journal of Biological Chemistry, 278*(32), 30015-30021. doi:10.1074/jbc.M302548200

Kemmler, W., Peterson, J. D., & Steiner, D. F. (1971). Studies on the conversion of proinsulin to insulin. I. Conversion in vitro with trypsin and carboxypeptidase B. *Journal of Biological Chemistry, 246*(22), 6786-6791.

Kern-Matschilles, S., Gar, C., Wanger, L., Haschka, S. J., Potzel, A. L., Hesse, N., . . . Lechner, A. (2021). Association of Serum Myostatin with Body Weight, Visceral Fat Volume, and High Sensitivity C-Reactive Protein But Not With Muscle Mass and Physical Fitness in Premenopausal Women. *Experimental and Clinical Endocrinology and Diabetes*(EFirst).

Kern, P. A., Di Gregorio, G. B., Lu, T., Rassouli, N., & Ranganathan, G. (2003). Adiponectin expression from human adipose tissue: relation to obesity, insulin resistance, and tumor necrosis factor-alpha expression. *Diabetes, 52*(7), 1779-1785. doi:10.2337/diabetes.52.7.1779

Khan, I. M., Perrard, X. Y., Brunner, G., Lui, H., Sparks, L. M., Smith, S. R., . . . Ballantyne, C. M. (2015). Intermuscular and perimuscular fat expansion in obesity correlates with skeletal muscle T cell and macrophage infiltration and insulin resistance. *International Journal of Obesity (2005), 39*(11), 1607-1618. doi:10.1038/ijo.2015.104

Kiefer, F. W. (2017). The significance of beige and brown fat in humans. *Endocrine connections, 6*(5), R70-R79. doi:10.1530/EC-17-0037

Kiens, B. (2006). Skeletal muscle lipid metabolism in exercise and insulin resistance. *Physiological Reviews, 86*(1), 205-243. doi:10.1152/physrev.00023.2004

Kim, J. K. (2009). Hyperinsulinemic-euglycemic clamp to assess insulin sensitivity in vivo. *Methods in Molecular Biology, 560*, 221-238. doi:10.1007/978-1-59745-448-3_15

Kim, J. S., Cross, J. M., & Bamman, M. M. (2005). Impact of resistance loading on myostatin expression and cell cycle regulation in young and older men and women. *American Journal of Physiology: Endocrinology and Metabolism, 288*(6), E1110-1119. doi:10.1152/ajpendo.00464.2004

Kim, T. J., Pyun, D. H., Kim, M. J., Jeong, J. H., Abd El-Aty, A. M., & Jung, T. W. (2021). Ginsenoside compound K ameliorates palmitate-induced atrophy in C2C12 myotubes via promyogenic effects and AMPK/autophagy-mediated suppression of endoplasmic reticulum stress. *Journal of Ginseng Research*. doi:https://doi.org/10.1016/j.jgr.2021.09.002

Kirshner, Z. Z., & Gibbs, R. B. (2018). Use of the REVERT((R)) total protein stain as a loading control demonstrates significant benefits over the use of housekeeping proteins when analyzing brain homogenates by Western blot: An analysis of samples representing different gonadal hormone states. *Molecular and Cellular Endocrinology, 473*, 156-165. doi:10.1016/j.mce.2018.01.015

Kitessa, S. M., & Abeywardena, M. Y. (2016). Lipid-Induced Insulin Resistance in Skeletal Muscle: The Chase for the Culprit Goes from Total Intramuscular Fat to Lipid Intermediates, and Finally to Species of Lipid Intermediates. *Nutrients, 8*(8), 466. Retrieved from https://www.mdpi.com/2072-6643/8/8/466

Kjeldsen, L., Johnsen, A. H., Sengeløv, H., & Borregaard, N. (1993). Isolation and primary structure of NGAL, a novel protein associated with human neutrophil gelatinase. *Journal of Biological Chemistry, 268*(14), 10425-10432. Retrieved from http://www.jbc.org/content/268/14/10425.abstract

Klip, A., Logan, W. J., & Li, G. (1982). Hexose transport in L6 muscle cells. Kinetic properties and the number of [3H]cytochalasin B binding sites. *Biochimica et Biophysica Acta, 687*(2), 265-280. doi:10.1016/0005-2736(82)90555-7

Klip, A., Volchuk, A., He, L., & Tsakiridis, T. (1996). The glucose transporters of skeletal muscle. *Seminars in Cell and Developmental Biology, 7*(2), 229-237. doi:https://doi.org/10.1006/scdb.1996.0031

Klisić, A., Kavarić, N., Spasojević-Kalimanovska, V., Kotur-Stevuljević, J., & Ninić, A. (2021). Serum endocan levels in relation to traditional and non-traditional anthropometric indices in adult population. *Journal of medical biochemistry, 40*(1), 41-48. doi:10.5937/jomb0-25170

Koenen, T. B., Stienstra, R., van Tits, L. J., Joosten, L. A., van Velzen, J. F., Hijmans, A., . . . de Graaf, J. (2011). The inflammasome and caspase-1 activation: a new mechanism underlying increased inflammatory activity in human visceral adipose tissue. *Endocrinology, 152*(10), 3769-3778. doi:10.1210/en.2010-1480

Koistinen, H. A., & Zierath, J. R. (2002). Regulation of glucose transport in human skeletal muscle. *Annals of Medicine, 34*(6), 410-418.

Kolkmann, A. M., Post, M. J., Rutjens, M. A. M., van Essen, A. L. M., & Moutsatsou, P. (2020). Serum-free media for the growth of primary bovine myoblasts. *Cytotechnology, 72*(1), 111-120. doi:10.1007/s10616-019-00361-y

Komori, T., & Morikawa, Y. (2018). Oncostatin M in the development of metabolic syndrome and its potential as a novel therapeutic target. *Anatomical Science International, 93*(2), 169-176. doi:10.1007/s12565-017-0421-y

Kortas, J., Ziemann, E., Juszczak, D., Micielska, K., Kozłowska, M., Prusik, K., . . . Antosiewicz, J. (2020). Iron Status in Elderly Women Impacts Myostatin, Adiponectin and Osteocalcin Levels Induced by Nordic Walking Training. *Nutrients, 12*(4). doi:10.3390/nu12041129

Koussounadis, A., Langdon, S. P., Um, I. H., Harrison, D. J., & Smith, V. A. (2015). Relationship between differentially expressed mRNA and mRNA-protein correlations in a xenograft model system. *Scientific Reports, 5*(1), 10775. doi:10.1038/srep10775

Kouw, I. W., Gorissen, S. H., Burd, N. A., Cermak, N. M., Gijsen, A. P., van Kranenburg, J., & van Loon, L. J. (2015). Postprandial Protein Handling Is Not Impaired in Type 2 Diabetes Patients When Compared With Normoglycemic Controls. *Journal of Clinical Endocrinology and Metabolism, 100*(8), 3103-3111. doi:10.1210/jc.2015-1234

Kovalik, J.-P., Slentz, D., Stevens, R. D., Kraus, W. E., Houmard, J. A., Nicoll, J. B., . . . Muoio, D. M. (2011). Metabolic remodeling of human skeletal myocytes by cocultured adipocytes depends on the lipolytic state of the system. *Diabetes, 60*(7), 1882-1893. doi:10.2337/db10-0427

Koves, T. R., Ussher, J. R., Noland, R. C., Slentz, D., Mosedale, M., Ilkayeva, O., . . . Muoio, D. M. (2008). Mitochondrial overload and incomplete fatty acid oxidation contribute to skeletal muscle insulin resistance. *Cell Metabolism, 7*(1), 45-56. doi:10.1016/j.cmet.2007.10.013

Kraegen, E. W., Cooney, G. J., & Turner, N. (2008). Muscle insulin resistance: A case of fat overconsumption, not mitochondrial dysfunction. *Proceedings of the National Academy of Sciences, 105*(22), 7627-7628. doi:10.1073/pnas.0803901105

Krebs, M., & Roden, M. (2005). Molecular mechanisms of lipid-induced insulin resistance in muscle, liver and vasculature. *Diabetes, Obesity and*

Metabolism, 7(6), 621-632. doi:https://doi.org/10.1111/j.1463-1326.2004.00439.x

Krieg, R. C., Dong, Y., Schwamborn, K., & Knuechel, R. (2005). Protein quantification and its tolerance for different interfering reagents using the BCA-method with regard to 2D SDS PAGE. *Journal of Biochemical and Biophysical Methods, 65*(1), 13-19. doi:10.1016/j.jbbm.2005.08.005

Kruszynska, Y. T., Worrall, D. S., Ofrecio, J., Frias, J. P., Macaraeg, G., & Olefsky, J. M. (2002). Fatty acid-induced insulin resistance: decreased muscle PI3K activation but unchanged Akt phosphorylation. *Journal of Clinical Endocrinology and Metabolism, 87*(1), 226-234. doi:10.1210/jcem.87.1.8187

Krützfeldt, J., Kausch, C., Volk, A., Klein, H. H., Rett, K., Häring, H. U., & Stumvoll, M. (2000). Insulin signaling and action in cultured skeletal muscle cells from lean healthy humans with high and low insulin sensitivity. *Diabetes, 49*(6), 992-998. doi:10.2337/diabetes.49.6.992

Kudoh, A., Satoh, H., Hirai, H., Watanabe, T., & Shimabukuro, M. (2018). Preliminary Evidence for Adipocytokine Signals in Skeletal Muscle Glucose Uptake. *Frontiers in Endocrinology, 9*. doi:10.3389/fendo.2018.00295

Kuppusamy, P., Kim, D., Soundharrajan, I., Hwang, I., & Choi, K. C. (2021). Adipose and Muscle Cell Co-Culture System: A Novel In Vitro Tool to Mimic the In Vivo Cellular Environment. *Biology, 10*(1), 6. Retrieved from https://www.mdpi.com/2079-7737/10/1/6

Kurose, S., Onishi, K., Takao, N., Miyauchi, T., Takahashi, K., & Kimura, Y. (2021). Association of serum adiponectin and myostatin levels with skeletal muscle in patients with obesity: A cross-sectional study. *PloS One, 16*(1), e0245678. doi:10.1371/journal.pone.0245678

Lach-Trifilieff, E., Minetti, G. C., Sheppard, K., Ibebunjo, C., Feige, J. N., Hartmann, S., . . . Glass, D. J. (2014). An antibody blocking activin type II receptors induces strong skeletal muscle hypertrophy and protects from atrophy. *Molecular and Cellular Biology, 34*(4), 606-618. doi:10.1128/MCB.01307-13

Lackey, D. E., Lazaro, R. G., Li, P., Johnson, A., Hernandez-Carretero, A., Weber, N., . . . Osborn, O. (2016). The role of dietary fat in obesity-induced insulin resistance. *American journal of physiology. Endocrinology and metabolism, 311*(6), E989-E997. doi:10.1152/ajpendo.00323.2016

Ladabaum, U., Mannalithara, A., Myer, P. A., & Singh, G. (2014). Obesity, abdominal obesity, physical activity, and caloric intake in US adults: 1988 to 2010. *American Journal of Medicine, 127*(8), 717-727.e712. doi:10.1016/j.amjmed.2014.02.026

Lager, I. (1991). The insulin-antagonistic effect of the counterregulatory hormones. *Journal of Internal Medicine. Supplement, 735*, 41-47. Retrieved from http://europepmc.org/abstract/MED/2043222

Lakshman, K. M., Bhasin, S., Corcoran, C., Collins-Racie, L. A., Tchistiakova, L., Forlow, S. B., . . . Lavallie, E. R. (2009). Measurement of myostatin concentrations in human serum: Circulating concentrations in young and older men and effects of testosterone administration. *Molecular and Cellular Endocrinology, 302*(1), 26-32. doi:10.1016/j.mce.2008.12.019

Lakshmanan, J., Elmendorf, J. S., & Ozcan, S. (2003). Analysis of insulin-stimulated glucose uptake in differentiated 3T3-L1 adipocytes. *Methods in Molecular Medicine, 83*, 97-103. doi:10.1385/1-59259-377-1:097

Lam, Y. Y., Hatzinikolas, G., Weir, J. M., Janovská, A., McAinch, A. J., Game, P., . . . Wittert, G. A. (2011). Insulin-stimulated glucose uptake and pathways regulating energy metabolism in skeletal muscle cells: the effects of subcutaneous and visceral fat, and long-chain saturated, n-3 and n-6 polyunsaturated fatty acids. *Biochimica et Biophysica Acta, 1811*(7-8), 468-475. doi:10.1016/j.bbalip.2011.04.011

Lam, Y. Y., Janovská, A., McAinch, A. J., Belobrajdic, D. P., Hatzinikolas, G., Game, P., & Wittert, G. A. (2011). The use of adipose tissue-conditioned media to demonstrate the differential effects of fat depots on insulin-stimulated glucose uptake in a skeletal muscle cell line. *Obesity Research & Clinical Practice, 5*(1), e43-e54. doi:https://doi.org/10.1016/j.orcp.2010.12.002

Landis, S. C., Amara, S. G., Asadullah, K., Austin, C. P., Blumenstein, R., Bradley, E. W., . . . Silberberg, S. D. (2012). A call for transparent reporting to optimize the predictive value of preclinical research. *Nature, 490*(7419), 187-191. doi:10.1038/nature11556

Langley, B., Thomas, M., Bishop, A., Sharma, M., Gilmour, S., & Kambadur, R. (2002). Myostatin Inhibits Myoblast Differentiation by Down-regulating MyoD Expression. *Journal of Biological Chemistry, 277*(51), 49831-49840. doi:10.1074/jbc.M204291200

Lankatillake, C., Huynh, T., & Dias, D. (2019). Understanding glycaemic control and current approaches for screening antidiabetic natural products from evidence-based medicinal plants. *Plant Methods*. doi:10.1186/s13007-019-0487-8

Larionov, A., Krause, A., & Miller, W. (2005). A standard curve based method for relative real time PCR data processing. *BMC Bioinformatics, 6*, 62-62. doi:10.1186/1471-2105-6-62

Lauretani, F., Russo, C. R., Bandinelli, S., Bartali, B., Cavazzini, C., Di Iorio, A., . . . Ferrucci, L. (2003). Age-associated changes in skeletal muscles and their effect on mobility: an operational diagnosis of sarcopenia. *J Appl Physiol (1985), 95*(5), 1851-1860. doi:10.1152/japplphysiol.00246.2003

Lauritzen, H. P., Galbo, H., Toyoda, T., & Goodyear, L. J. (2010). Kinetics of contraction-induced GLUT4 translocation in skeletal muscle fibers from living mice. *Diabetes, 59*(9), 2134-2144. doi:10.2337/db10-0233

Lautaoja, J. H., Pekkala, S., Pasternack, A., Laitinen, M., Ritvos, O., & Hulmi, J. J. (2020). Differentiation of Murine C2C12 Myoblasts Strongly Reduces the Effects of Myostatin on Intracellular Signaling. *Biomolecules, 10*(5), 695. Retrieved from https://www.mdpi.com/2218-273X/10/5/695

Law, I. K., Xu, A., Lam, K. S., Berger, T., Mak, T. W., Vanhoutte, P. M., . . . Wang, Y. (2010). Lipocalin-2 deficiency attenuates insulin resistance associated with aging and obesity. *Diabetes, 59*(4), 872-882. doi:10.2337/db09-1541

Lazic, S. E., Clarke-Williams, C. J., & Munafò, M. R. (2018). What exactly is 'N' in cell culture and animal experiments? *PLoS Biology, 16*(4), e2005282. doi:10.1371/journal.pbio.2005282

Le Grand, F., & Rudnicki, M. A. (2007). Skeletal muscle satellite cells and adult myogenesis. *Current Opinion in Cell Biology, 19*(6), 628-633. doi:https://doi.org/10.1016/j.ceb.2007.09.012

Lebovitz, H. E. (2001). Insulin resistance: definition and consequences. *Experimental and Clinical Endocrinology and Diabetes, 109 Suppl 2*, S135-148. doi:10.1055/s-2001-18576

LeBrasseur, N. K., Schelhorn, T. M., Bernardo, B. L., Cosgrove, P. G., Loria, P. M., & Brown, T. A. (2009). Myostatin inhibition enhances the effects of exercise

on performance and metabolic outcomes in aged mice. *Journals of Gerontology. Series A: Biological Sciences and Medical Sciences, 64*(9), 940-948. doi:10.1093/gerona/glp068

Leduc-Gaudet, J.-P., Hussain, S. N. A., Barreiro, E., & Gouspillou, G. (2021). Mitochondrial Dynamics and Mitophagy in Skeletal Muscle Health and Aging. *International Journal of Molecular Sciences, 22*(15), 8179. doi:10.3390/ijms22158179

Lee, A. D., Hansen, P. A., & Holloszy, J. O. (1995). Wortmannin inhibits insulin-stimulated but not contraction-stimulated glucose transport activity in skeletal muscle. *FEBS Letters, 361*(1), 51-54.

Lee, H., Lim, J.-Y., & Choi, S.-J. (2017). Oleate Prevents Palmitate-Induced Atrophy via Modulation of Mitochondrial ROS Production in Skeletal Myotubes. *Oxidative Medicine and Cellular Longevity, 2017*, 2739721-2739721. doi:10.1155/2017/2739721

Lee, J. S., Pinnamaneni, S. K., Eo, S. J., Cho, I. H., Pyo, J. H., Kim, C. K., . . . Watt, M. J. (2006). Saturated, but not n-6 polyunsaturated, fatty acids induce insulin resistance: role of intramuscular accumulation of lipid metabolites. *Journal of Applied Physiology (Bethesda, Md.: 1985), 100*(5), 1467-1474. doi:10.1152/japplphysiol.01438.2005

Lee, M. J. (2018). Transforming growth factor beta superfamily regulation of adipose tissue biology in obesity. *Biochim Biophys Acta Mol Basis Dis, 1864*(4 Pt A), 1160-1171. doi:10.1016/j.bbadis.2018.01.025

Lee, S.-J., & McPherron, A. C. (2001). Regulation of myostatin activity and muscle growth. *Proceedings of the National Academy of Sciences, 98*(16), 9306-9311. doi:10.1073/pnas.151270098

Lee, S., Kim, T. N., & Kim, S. H. (2012). Sarcopenic obesity is more closely associated with knee osteoarthritis than is nonsarcopenic obesity: a cross-sectional study. *Arthritis and Rheumatism, 64*(12), 3947-3954. doi:10.1002/art.37696

Lee, S. J., Gharbi, A., Shin, J. E., Jung, I. D., & Park, Y. M. (2021). Myostatin inhibitor YK11 as a preventative health supplement for bacterial sepsis. *Biochemical and Biophysical Research Communications, 543*, 1-7. doi:https://doi.org/10.1016/j.bbrc.2021.01.030

Lee, Y.-S., Huynh, T. V., & Lee, S.-J. (2016). Paracrine and endocrine modes of myostatin action. *J Appl Physiol (1985), 120*(6), 592-598. doi:10.1152/japplphysiol.00874.2015

Lee, Y.-S., & Lee, S.-J. (2013). Regulation of GDF-11 and myostatin activity by GASP-1 and GASP-2. *Proceedings of the National Academy of Sciences, 110*(39), E3713-E3722. doi:10.1073/pnas.1309907110

Lee, Y. S., Li, P., Huh, J. Y., Hwang, I. J., Lu, M., Kim, J. I., . . . Kim, J. B. (2011). Inflammation is necessary for long-term but not short-term high-fat diet-induced insulin resistance. *Diabetes, 60*(10), 2474-2483. doi:10.2337/db11-0194

Léger, B., Derave, W., De Bock, K., Hespel, P., & Russell, A. P. (2008). Human sarcopenia reveals an increase in SOCS-3 and myostatin and a reduced efficiency of Akt phosphorylation. *Rejuvenation Res, 11*(1), 163-175b. doi:10.1089/rej.2007.0588

Lehnen, H., Zechner, U., & Haaf, T. (2013). Epigenetics of gestational diabetes mellitus and offspring health: the time for action is in early stages of life. *Molecular Human Reproduction, 19*(7), 415-422. doi:10.1093/molehr/gat020

Les, F., Arbonés-Mainar, J. M., Valero, M. S., & López, V. (2018). Pomegranate polyphenols and urolithin A inhibit α-glucosidase, dipeptidyl peptidase-4, lipase, triglyceride accumulation and adipogenesis related genes in 3T3-L1 adipocyte-like cells. *Journal of Ethnopharmacology, 220*, 67-74. doi:https://doi.org/10.1016/j.jep.2018.03.029

Levine, J. A., Jensen, M. D., Eberhardt, N. L., & O'Brien, T. (1998). Adipocyte macrophage colony-stimulating factor is a mediator of adipose tissue growth. *The Journal of clinical investigation, 101*(8), 1557-1564. doi:10.1172/JCI2293

Li, D., Yan Sun, W., Fu, B., Xu, A., & Wang, Y. (2020). Lipocalin-2-The myth of its expression and function. *Basic & Clinical Pharmacology & Toxicology, 127*(2), 142-151. doi:10.1111/bcpt.13332

Li, G., Luan, G., He, Y., Tie, F., Wang, Z., Suo, Y., . . . Wang, H. (2018). Polyphenol Stilbenes from Fenugreek (Trigonella foenum-graecum L.) Seeds Improve Insulin Sensitivity and Mitochondrial Function in 3T3-L1 Adipocytes. *Oxidative Medicine and Cellular Longevity, 2018*, 7634362. doi:10.1155/2018/7634362

Li, J., Deng, J., Zhang, J., Cheng, D., & Wang, H. (2012). [Regulation of myostatin promoter activity by myocyte enhancer factor 2]. *Sheng Wu Gong Cheng Xue Bao, 28*(8), 918-926.

Lieber, R. L. (2002). *Skeletal muscle structure, function, and plasticity*: Lippincott Williams & Wilkins.

Lihn, A. S., Pedersen, S. B., & Richelsen, B. (2005). Adiponectin: action, regulation and association to insulin sensitivity. *Obesity Reviews, 6*(1), 13-21. doi:10.1111/j.1467-789X.2005.00159.x

Lim, J.-H., Gerhart-Hines, Z., Dominy, J. E., Lee, Y., Kim, S., Tabata, M., . . . Puigserver, P. (2013). Oleic Acid Stimulates Complete Oxidation of Fatty Acids through Protein Kinase A-dependent Activation of SIRT1-PGC1α Complex *. *Journal of Biological Chemistry, 288*(10), 7117-7126. doi:10.1074/jbc.M112.415729

Lim, J.-M., Wollaston-Hayden, E. E., Teo, C. F., Hausman, D., & Wells, L. (2014). Quantitative secretome and glycome of primary human adipocytes during insulin resistance. *Clinical Proteomics, 11*(1), 20-20. doi:10.1186/1559-0275-11-20

Lin, H., & Li, Z. (2012). Adiponectin self-regulates its expression and multimerization in adipose tissue: an autocrine/paracrine mechanism? *Medical Hypotheses, 78*(1), 75-78. doi:10.1016/j.mehy.2011.07.063

Linkhart, T. A., Clegg, C. H., & Hauschika, S. D. (1981). Myogenic differentiation in permanent clonal mouse myoblast cell lines: regulation by macromolecular growth factors in the culture medium. *Developmental Biology, 86*(1), 19-30.

Liu, D., Qiao, X., Ge, Z., Shang, Y., Li, Y., Wang, W., . . . Chen, S. Z. (2019). IMB0901 inhibits muscle atrophy induced by cancer cachexia through MSTN signaling pathway. *Skelet Muscle, 9*(1), 8. doi:10.1186/s13395-019-0193-2

Liu, L., Zhang, Y., Chen, N., Shi, X., Tsang, B., & Yu, Y. H. (2007). Upregulation of myocellular DGAT1 augments triglyceride synthesis in skeletal muscle and protects against fat-induced insulin resistance. *Journal of Clinical Investigation, 117*(6), 1679-1689. doi:10.1172/jci30565

Liu, M., Qin, J., Hao, Y., Liu, M., Luo, J., Luo, T., & Wei, L. (2013). Astragalus polysaccharide suppresses skeletal muscle myostatin expression in diabetes:

involvement of ROS-ERK and NF-kappaB pathways. *Oxidative Medicine and Cellular Longevity, 2013*, 782497. doi:10.1155/2013/782497

Liu, S., D'Amico, D., Shankland, E., Bhayana, S., Garcia, J. M., Aebischer, P., . . . Marcinek, D. J. (2022). Effect of Urolithin A Supplementation on Muscle Endurance and Mitochondrial Health in Older Adults: A Randomized Clinical Trial. *JAMA Network Open, 5*(1), e2144279-e2144279. doi:10.1001/jamanetworkopen.2021.44279

Liu, X.-H., Bauman, W. A., & Cardozo, C. P. (2018). Myostatin inhibits glucose uptake via suppression of insulin-dependent and -independent signaling pathways in myoblasts. *Physiol Rep, 6*(17), e13837-e13837. doi:10.14814/phy2.13837

Liu, X., Hamnvik, O. P., Petrou, M., Gong, H., Chamberland, J. P., Christophi, C. A., . . . Mantzoros, C. S. (2011). Circulating lipocalin 2 is associated with body fat distribution at baseline but is not an independent predictor of insulin resistance: the prospective Cyprus Metabolism Study. *European Journal of Endocrinology of the European Federation of Endocrine Societies, 165*(5), 805-812. doi:10.1530/eje-11-0660

Liu, Z., Wu, K. K. L., Jiang, X., Xu, A., & Cheng, K. K. Y. (2020). The role of adipose tissue senescence in obesity- and ageing-related metabolic disorders. *Clinical Science, 134*(2), 315-330. doi:10.1042/cs20190966

Lowell, B. B., Napolitano, A., Usher, P., Dulloo, A. G., Rosen, B. S., Spiegelman, B. M., & Flier, J. S. (1990). Reduced adipsin expression in murine obesity: effect of age and treatment with the sympathomimetic-thermogenic drug mixture ephedrine and caffeine. *Endocrinology, 126*(3), 1514-1520. doi:10.1210/endo-126-3-1514

Luan, P., D'Amico, D., Andreux, P. A., Laurila, P.-P., Wohlwend, M., Li, H., . . . Auwerx, J. (2021). Urolithin A improves muscle function by inducing mitophagy in muscular dystrophy. *Science Translational Medicine, 13*(588), eabb0319. doi:doi:10.1126/scitranslmed.abb0319

Lumeng, C. N., Bodzin, J. L., & Saltiel, A. R. (2007). Obesity induces a phenotypic switch in adipose tissue macrophage polarization. *Journal of Clinical Investigation, 117*(1), 175-184. doi:10.1172/jci29881

Lund, J., Helle, S. A., Li, Y., Løvsletten, N. G., Stadheim, H. K., Jensen, J., . . . Rustan, A. C. (2018). Higher lipid turnover and oxidation in cultured human myotubes from athletic versus sedentary young male subjects. *Scientific Reports, 8*(1), 17549. doi:10.1038/s41598-018-35715-7

Maachi, M., Piéroni, L., Bruckert, E., Jardel, C., Fellahi, S., Hainque, B., . . . Bastard, J. P. (2004). Systemic low-grade inflammation is related to both circulating and adipose tissue TNFα, leptin and IL-6 levels in obese women. *International Journal of Obesity, 28*(8), 993-997. doi:10.1038/sj.ijo.0802718

Maher, A. C., Fu, M. H., Isfort, R. J., Varbanov, A. R., Qu, X. A., & Tarnopolsky, M. A. (2009). Sex Differences in Global mRNA Content of Human Skeletal Muscle. *PloS One, 4*(7), e6335. doi:10.1371/journal.pone.0006335

Mahfouz, R., Khoury, R., Blachnio-Zabielska, A., Turban, S., Loiseau, N., Lipina, C., . . . Hajduch, E. (2014). Characterising the inhibitory actions of ceramide upon insulin signaling in different skeletal muscle cell models: a mechanistic insight. *PloS One, 9*(7), e101865-e101865. doi:10.1371/journal.pone.0101865

Maison, P., Byrne, C. D., Hales, C. N., Day, N. E., & Wareham, N. J. (2001). Do different dimensions of the metabolic syndrome change together over time?

Evidence supporting obesity as the central feature. *Diabetes Care, 24*(10), 1758-1763.

Mäkinen, S., Nguyen, Y. H., Skrobuk, P., & Koistinen, H. A. (2017). Palmitate and oleate exert differential effects on insulin signalling and glucose uptake in human skeletal muscle cells. *Endocrine connections, 6*(5), 331-339. doi:10.1530/EC-17-0039

Makki, K., Froguel, P., & Wolowczuk, I. (2013). Adipose tissue in obesity-related inflammation and insulin resistance: cells, cytokines, and chemokines. *ISRN inflammation, 2013*, 139239-139239. doi:10.1155/2013/139239

Mandarino, L. J., Wright, K. S., Verity, L. S., Nichols, J., Bell, J. M., Kolterman, O. G., & Beck-Nielsen, H. (1987). Effects of insulin infusion on human skeletal muscle pyruvate dehydrogenase, phosphofructokinase, and glycogen synthase. Evidence for their role in oxidative and nonoxidative glucose metabolism. *The Journal of clinical investigation, 80*(3), 655-663. doi:10.1172/JCI113118

Manfredi, L. H., Paula-Gomes, S., Zanon, N. M., & Kettelhut, I. C. (2017). Myostatin promotes distinct responses on protein metabolism of skeletal and cardiac muscle fibers of rodents. *Brazilian Journal of Medical and Biological Research, 50*(12), e6733. doi:10.1590/1414-431x20176733

Martins, A. R., Nachbar, R. T., Gorjao, R., Vinolo, M. A., Festuccia, W. T., Lambertucci, R. H., . . . Hirabara, S. M. (2012). Mechanisms underlying skeletal muscle insulin resistance induced by fatty acids: importance of the mitochondrial function. *Lipids in Health and Disease, 11*(1), 30. doi:10.1186/1476-511X-11-30

Masgrau, A., Mishellany-Dutour, A., Murakami, H., Beaufrere, A. M., Walrand, S., Giraudet, C., . . . Boirie, Y. (2012). Time-course changes of muscle protein synthesis associated with obesity-induced lipotoxicity. *Journal of Physiology, 590*(20), 5199-5210. doi:10.1113/jphysiol.2012.238576

Massenet, J., Gardner, E., Chazaud, B., & Dilworth, F. J. (2021). Epigenetic regulation of satellite cell fate during skeletal muscle regeneration. *Skeletal Muscle, 11*(1), 4. doi:10.1186/s13395-020-00259-w

Masson, O., Prébois, C., Derocq, D., Meulle, A., Dray, C., Daviaud, D., . . . Liaudet-Coopman, E. (2011). Cathepsin-D, a Key Protease in Breast Cancer, Is Up-Regulated in Obese Mouse and Human Adipose Tissue, and Controls Adipogenesis. *PloS One, 6*(2), e16452. doi:10.1371/journal.pone.0016452

Mathus-Vliegen, E. M. H., Basdevant, A., Finer, N., Hainer, V., Hauner, H., Micic, D., . . . Zahorska-Markiewicz, B. (2012). Prevalence, Pathophysiology, Health Consequences and Treatment Options of Obesity in the Elderly: A Guideline. *Obesity Facts, 5*(3), 460-483. doi:10.1159/000341193

Matravadia, S., Herbst, E. A. F., Jain, S. S., Mutch, D. M., & Holloway, G. P. (2014). Both linoleic and α-linolenic acid prevent insulin resistance but have divergent impacts on skeletal muscle mitochondrial bioenergetics in obese Zucker rats. *American Journal of Physiology-Endocrinology and Metabolism, 307*(1), E102-E114. doi:10.1152/ajpendo.00032.2014

Matsubara, M., Maruoka, S., & Katayose, S. (2002). Inverse relationship between plasma adiponectin and leptin concentrations in normal-weight and obese women. *European Journal of Endocrinology of the European Federation of Endocrine Societies, 147*(2), 173-180. doi:10.1530/eje.0.1470173

Matthews, D. R., Hosker, J. P., Rudenski, A. S., Naylor, B. A., Treacher, D. F., & Turner, R. C. (1985). Homeostasis model assessment: insulin resistance and beta-cell function from fasting plasma glucose and insulin concentrations in

man. *Diabetologia, 28*(7), 412-419. Retrieved from https://www.ncbi.nlm.nih.gov/pubmed/3899825

Mauro, A. (1961). Satellite cell of skeletal muscle fibers. *J Biophys Biochem Cytol, 9*, 493-495.

McCoin, C. S., Knotts, T. A., & Adams, S. H. (2015). Acylcarnitines--old actors auditioning for new roles in metabolic physiology. *Nature Reviews: Endocrinology, 11*(10), 617-625. doi:10.1038/nrendo.2015.129

McCormick, R., & Vasilaki, A. (2018). Age-related changes in skeletal muscle: changes to life-style as a therapy. *Biogerontology, 19*(6), 519-536. doi:10.1007/s10522-018-9775-3

McCroskery, S., Thomas, M., Maxwell, L., Sharma, M., & Kambadur, R. (2003). Myostatin negatively regulates satellite cell activation and self-renewal. *The Journal of Cell Biology, 162*(6), 1135-1147. doi:10.1083/jcb.200207056

McFarlane, C., Hui, G. Z., Amanda, W. Z. W., Lau, H. Y., Lokireddy, S., Xiaojia, G., . . . Kambadur, R. (2011). Human myostatin negatively regulates human myoblast growth and differentiation. *American Journal of Physiology. Cell Physiology, 301*(1), C195-C203. doi:10.1152/ajpcell.00012.2011

McFarlane, C., Plummer, E., Thomas, M., Hennebry, A., Ashby, M., Ling, N., . . . Kambadur, R. (2006). Myostatin induces cachexia by activating the ubiquitin proteolytic system through an NF-kappaB-independent, FoxO1-dependent mechanism. *Journal of Cellular Physiology, 209*(2), 501-514. doi:10.1002/jcp.20757

McFarlane, C., Vajjala, A., Arigela, H., Lokireddy, S., Ge, X., Bonala, S., . . . Sharma, M. (2014). Negative Auto-Regulation of Myostatin Expression is Mediated by Smad3 and MicroRNA-27. *PloS One, 9*(1), e87687. doi:10.1371/journal.pone.0087687

McIntyre, E. A., Halse, R., Yeaman, S. J., & Walker, M. (2004). Cultured muscle cells from insulin-resistant type 2 diabetes patients have impaired insulin, but normal 5-amino-4-imidazolecarboxamide riboside-stimulated, glucose uptake. *Journal of Clinical Endocrinology and Metabolism, 89*(7), 3440-3448. doi:10.1210/jc.2003-031919

McKay, B. R., Ogborn, D. I., Bellamy, L. M., Tarnopolsky, M. A., & Parise, G. (2012). Myostatin is associated with age-related human muscle stem cell dysfunction. *FASEB Journal, 26*(6), 2509-2521. doi:10.1096/fj.11-198663

McLaughlin, T., Lamendola, C., Liu, A., & Abbasi, F. (2011). Preferential Fat Deposition in Subcutaneous Versus Visceral Depots Is Associated with Insulin Sensitivity. *The Journal of Clinical Endocrinology & Metabolism, 96*(11), E1756-E1760. doi:10.1210/jc.2011-0615

McMahon, C. D., Popovic, L., Jeanplong, F., Oldham, J. M., Kirk, S. P., Osepchook, C. C., . . . Bass, J. J. (2003). Sexual dimorphism is associated with decreased expression of processed myostatin in males. *American Journal of Physiology: Endocrinology and Metabolism, 284*(2), E377-381. doi:10.1152/ajpendo.00282.2002

McPherron, A. C., Lawler, A. M., & Lee, S. J. (1997). Regulation of skeletal muscle mass in mice by a new TGF-beta superfamily member. *Nature, 387*(6628), 83-90. doi:10.1038/387083a0

McPherron, A. C., & Lee, S. J. (2002). Suppression of body fat accumulation in myostatin-deficient mice. *Journal of Clinical Investigation, 109*(5), 595-601. doi:10.1172/jci13562

Meador, B. M., Mirza, K. A., Tian, M., Skelding, M. B., Reaves, L. A., Edens, N. K., . . . Pereira, S. L. (2015). The Green Tea Polyphenol Epigallocatechin-3-Gallate (EGCg) Attenuates Skeletal Muscle Atrophy in a Rat Model of Sarcopenia. *The Journal of frailty & aging, 4*(4), 209-215. doi:10.14283/jfa.2015.58

Meerbrey, K. L., Hu, G., Kessler, J. D., Roarty, K., Li, M. Z., Fang, J. E., . . . Elledge, S. J. (2011). The pINDUCER lentiviral toolkit for inducible RNA interference in vitro and in vivo. *Proceedings of the National Academy of Sciences of the United States of America, 108*(9), 3665-3670. doi:10.1073/pnas.1019736108

Meier, J. J., Veldhuis, J. D., & Butler, P. C. (2005). Pulsatile Insulin Secretion Dictates Systemic Insulin Delivery by Regulating Hepatic Insulin Extraction In Humans. *Diabetes, 54*(6), 1649-1656. doi:10.2337/diabetes.54.6.1649

Meigs, J. B., Cupples, L. A., & Wilson, P. W. (2000). Parental transmission of type 2 diabetes: the Framingham Offspring Study. *Diabetes, 49*(12), 2201-2207. doi:10.2337/diabetes.49.12.2201

Mena, P., & Del Rio, D. (2018). Gold Standards for Realistic (Poly)phenol Research. *Journal of Agricultural and Food Chemistry, 66*(31), 8221-8223. doi:10.1021/acs.jafc.8b03249

Merrill, A. H., Jr. (2002). De novo sphingolipid biosynthesis: a necessary, but dangerous, pathway. *Journal of Biological Chemistry, 277*(29), 25843-25846. doi:10.1074/jbc.R200009200

Merrill, A. H., Jr., & Jones, D. D. (1990). An update of the enzymology and regulation of sphingomyelin metabolism. *Biochimica et Biophysica Acta, 1044*(1), 1-12. doi:10.1016/0005-2760(90)90211-f

Michel, M. C., Murphy, T. J., & Motulsky, H. J. (2020). New Author Guidelines for Displaying Data and Reporting Data Analysis and Statistical Methods in Experimental Biology. *Molecular Pharmacology, 97*(1), 49-60. doi:10.1124/mol.119.118927

Middelbeek, R. J. W., Chambers, M. A., Tantiwong, P., Treebak, J. T., An, D., Hirshman, M. F., . . . Goodyear, L. J. (2013). Insulin stimulation regulates AS160 and TBC1D1 phosphorylation sites in human skeletal muscle. *Nutrition & Diabetes, 3*(6), e74-e74. doi:10.1038/nutd.2013.13

Mihalik, S. J., Goodpaster, B. H., Kelley, D. E., Chace, D. H., Vockley, J., Toledo, F. G., & DeLany, J. P. (2010). Increased levels of plasma acylcarnitines in obesity and type 2 diabetes and identification of a marker of glucolipotoxicity. *Obesity (Silver Spring), 18*(9), 1695-1700. doi:10.1038/oby.2009.510

Milan, G., Dalla Nora, E., Pilon, C., Pagano, C., Granzotto, M., Manco, M., . . . Vettor, R. (2004). Changes in muscle myostatin expression in obese subjects after weight loss. *Journal of Clinical Endocrinology and Metabolism, 89*(6), 2724-2727. doi:10.1210/jc.2003-032047

Milek, M., Moulla, Y., Kern, M., Stroh, C., Dietrich, A., Schön, M. R., . . . Guiu-Jurado, E. (2022). Adipsin Serum Concentrations and Adipose Tissue Expression in People with Obesity and Type 2 Diabetes. *International Journal of Molecular Sciences, 23*(4), 2222. Retrieved from https://www.mdpi.com/1422-0067/23/4/2222

Miller, M. E., Rejeski, W. J., Messier, S. P., & Loeser, R. F. (2001). Modifiers of change in physical functioning in older adults with knee pain: the Observational Arthritis Study in Seniors (OASIS). *Arthritis and Rheumatism,*

45(4), 331-339. doi:10.1002/1529-0131(200108)45:4<331::Aid-art345>3.0.Co;2-6

Miura, T., Kishioka, Y., Wakamatsu, J., Hattori, A., Hennebry, A., Berry, C. J., . . . Nishimura, T. (2006). Decorin binds myostatin and modulates its activity to muscle cells. *Biochemical and Biophysical Research Communications, 340*(2), 675-680. doi:10.1016/j.bbrc.2005.12.060

Mojsov, S., Weir, G. C., & Habener, J. F. (1987). Insulinotropin: glucagon-like peptide I (7-37) co-encoded in the glucagon gene is a potent stimulator of insulin release in the perfused rat pancreas. *Journal of Clinical Investigation, 79*(2), 616-619. doi:10.1172/jci112855

Montell, E., Turini, M., Marotta, M., Roberts, M., Noé, V., Ciudad, C. J., . . . Gómez-Foix, A. M. (2001). DAG accumulation from saturated fatty acids desensitizes insulin stimulation of glucose uptake in muscle cells. *American Journal of Physiology: Endocrinology and Metabolism, 280*(2), E229-237. doi:10.1152/ajpendo.2001.280.2.E229

Morais, J. A., Jacob, K. W., & Chevalier, S. (2018). Effects of aging and insulin resistant states on protein anabolic responses in older adults. *Experimental Gerontology, 108*, 262-268. doi:10.1016/j.exger.2018.04.025

Morissette, M. R., Cook, S. A., Buranasombati, C., Rosenberg, M. A., & Rosenzweig, A. (2009). Myostatin inhibits IGF-I-induced myotube hypertrophy through Akt. *American Journal of Physiology-Cell Physiology, 297*(5), 1124-1132. doi:10.1152/ajpcell.00043.2009

Morley, J. E. (2008). Sarcopenia: diagnosis and treatment. *The Journal of Nutrition, Health & Aging, 12*(7), 452-456.

Morley, J. E. (2016). Pharmacologic Options for the Treatment of Sarcopenia. *Calcified Tissue International, 98*(4), 319-333. doi:10.1007/s00223-015-0022-5

Morley, J. E., Baumgartner, R. N., Roubenoff, R., Mayer, J., & Nair, K. S. (2001). Sarcopenia. *Journal of Laboratory and Clinical Medicine, 137*(4), 231-243. doi:10.1067/mlc.2001.113504

Morrison, S., & McGee, S. L. (2015). 3T3-L1 adipocytes display phenotypic characteristics of multiple adipocyte lineages. *Adipocyte, 4*(4), 295-302. doi:10.1080/21623945.2015.1040612

Morton, R. W., Traylor, D. A., Weijs, P. J. M., & Phillips, S. M. (2018). Defining anabolic resistance: implications for delivery of clinical care nutrition. *Current Opinion in Critical Care, 24*(2), 124-130. doi:10.1097/mcc.0000000000000488

Mostad, I. L., Bjerve, K. S., Basu, S., Sutton, P., Frayn, K. N., & Grill, V. (2009). Addition of n-3 fatty acids to a 4-hour lipid infusion does not affect insulin sensitivity, insulin secretion, or markers of oxidative stress in subjects with type 2 diabetes mellitus. *Metabolism: Clinical and Experimental, 58*(12), 1753-1761. doi:10.1016/j.metabol.2009.06.003

Mthembu, S. X. H., Dludla, P. V., Nyambuya, T. M., Kappo, A. P., Madoroba, E., Ziqubu, K., . . . Mazibuko-Mbeje, S. E. (2021). Experimental models of lipid overload and their relevance in understanding skeletal muscle insulin resistance and pathological changes in mitochondrial oxidative capacity. *Biochimie*. doi:10.1016/j.biochi.2021.09.010

Mueckler, M., Caruso, C., Baldwin, S. A., Panico, M., Blench, I., Morris, H. R., . . . Lodish, H. F. (1985). Sequence and structure of a human glucose transporter. *Science, 229*(4717), 941-945.

Muoio, Deborah M., & Neufer, P. D. (2012). Lipid-Induced Mitochondrial Stress and Insulin Action in Muscle. *Cell Metabolism, 15*(5), 595-605. doi:10.1016/j.cmet.2012.04.010

Muramatsu, H., Kuramochi, T., Katada, H., Ueyama, A., Ruike, Y., Ohmine, K., . . . Nezu, J. (2021). Novel myostatin-specific antibody enhances muscle strength in muscle disease models. *Scientific Reports, 11*(1), 2160. doi:10.1038/s41598-021-81669-8

Murton, A. J., Marimuthu, K., Mallinson, J. E., Selby, A. L., Smith, K., Rennie, M. J., & Greenhaff, P. L. (2015). Obesity Appears to Be Associated With Altered Muscle Protein Synthetic and Breakdown Responses to Increased Nutrient Delivery in Older Men, but Not Reduced Muscle Mass or Contractile Function. *Diabetes, 64*(9), 3160-3171. doi:10.2337/db15-0021

Muscaritoli, M., Anker, S. D., Argilés, J., Aversa, Z., Bauer, J. M., Biolo, G., . . . Sieber, C. C. (2010). Consensus definition of sarcopenia, cachexia and pre-cachexia: Joint document elaborated by Special Interest Groups (SIG) "cachexia-anorexia in chronic wasting diseases" and "nutrition in geriatrics". *Clinical Nutrition, 29*(2), 154-159. doi:https://doi.org/10.1016/j.clnu.2009.12.004

Musialowska, D., Zbroch, E., Koc-Zorawska, E., Musialowski, P., & Malyszko, J. (2018). Endocan Concentration in Patients With Primary Hypertension. *Angiology, 69*(6), 483-489. doi:10.1177/0003319717736158

Myers, M. G., Backer, J. M., Sun, X. J., Shoelson, S., Hu, P., Schlessinger, J., . . . White, M. F. (1992). IRS-1 activates phosphatidylinositol 3'-kinase by associating with src homology 2 domains of p85. *Proceedings of the National Academy of Sciences, 89*(21), 10350-10354. doi:10.1073/pnas.89.21.10350

Nagai, H., Tanaka, T., Goto, T., Kusudo, T., Takahashi, N., & Kawada, T. (2014). Phenolic compounds from leaves of Casimiroa edulis showed adipogenesis activity. *Bioscience, Biotechnology, and Biochemistry, 78*(2), 296-300. doi:10.1080/09168451.2014.877821

Najjar, S. (2003). Insulin Action: Molecular Basis of Diabetes. In *eLS*.

Nam, S. Y., Lee, E. J., Kim, K. R., Cha, B. S., Song, Y. D., Lim, S. K., . . . Huh, K. B. (1997). Effect of obesity on total and free insulin-like growth factor (IGF)-1, and their relationship to IGF-binding protein (BP)-1, IGFBP-2, IGFBP-3, insulin, and growth hormone. *International Journal of Obesity and Related Metabolic Disorders, 21*(5), 355-359. doi:10.1038/sj.ijo.0800412

Napolitano, A., Lowell, B. B., Damm, D., Leibel, R. L., Ravussin, E., Jimerson, D. C., . . . et al. (1994). Concentrations of adipsin in blood and rates of adipsin secretion by adipose tissue in humans with normal, elevated and diminished adipose tissue mass. *International Journal of Obesity and Related Metabolic Disorders, 18*(4), 213-218.

Nardi, F., Lipina, C., Magill, D., Hage Hassan, R., Hajduch, E., Gray, A., & Hundal, H. S. (2014). Enhanced insulin sensitivity associated with provision of mono and polyunsaturated fatty acids in skeletal muscle cells involves counter modulation of PP2A. *PloS One, 9*(3), e92255-e92255. doi:10.1371/journal.pone.0092255

Nathans, D. (1964). PUROMYCIN INHIBITION OF PROTEIN SYNTHESIS: INCORPORATION OF PUROMYCIN INTO PEPTIDE CHAINS. *Proceedings of the National Academy of Sciences of the United States of America, 51*(4), 585-592. doi:10.1073/pnas.51.4.585

NCD, R. F. C. (2016). Trends in adult body-mass index in 200 countries from 1975 to 2014: a pooled analysis of 1698 population-based measurement studies with 19·2 million participants. *The Lancet, 387*(10026), 1377-1396. doi:https://doi.org/10.1016/S0140-6736(16)30054-X

Nehlin, J. O., Just, M., Rustan, A. C., & Gaster, M. (2011). Human myotubes from myoblast cultures undergoing senescence exhibit defects in glucose and lipid metabolism. *Biogerontology, 12*(4), 349-365. doi:10.1007/s10522-011-9336-5

NHS. (2019a). Obesity Overview. Retrieved from https://www.nhs.uk/conditions/obesity/

NHS. (2019b). *Statistics on Obesity, Physical Activity and Diet, England, 2019*.

NHS. (2022). *Finalised Patient Reported Outcome Measures (PROMs) in England for Hip & Knee Replacements*.

Nicholson, T., Church, C., Baker, D. J., & Jones, S. W. (2018). The role of adipokines in skeletal muscle inflammation and insulin sensitivity. *J Inflamm (Lond), 15*, 9. doi:10.1186/s12950-018-0185-8

Nickerson, J. G., Alkhateeb, H., Benton, C. R., Lally, J., Nickerson, J., Han, X.-X., . . . Bonen, A. (2009). Greater Transport Efficiencies of the Membrane Fatty Acid Transporters FAT/CD36 and FATP4 Compared with FABPpm and FATP1 and Differential Effects on Fatty Acid Esterification and Oxidation in Rat Skeletal Muscle*. *Journal of Biological Chemistry, 284*(24), 16522-16530. doi:https://doi.org/10.1074/jbc.M109.004788

Nikawa, T., Ulla, A., & Sakakibara, I. (2021). Polyphenols and Their Effects on Muscle Atrophy and Muscle Health. *Molecules (Basel, Switzerland), 26*(16), 4887. doi:10.3390/molecules26164887

Nipp, R. D., Fuchs, G., El-Jawahri, A., Mario, J., Troschel, F. M., Greer, J. A., . . . Fintelmann, F. J. (2018). Sarcopenia Is Associated with Quality of Life and Depression in Patients with Advanced Cancer. *Oncologist, 23*(1), 97-104. doi:10.1634/theoncologist.2017-0255

Nishi, M., Yasue, A., Nishimatu, S., Nohno, T., Yamaoka, T., Itakura, M., . . . Noji, S. (2002). A missense mutant myostatin causes hyperplasia without hypertrophy in the mouse muscle. *Biochemical and Biophysical Research Communications, 293*(1), 247-251. doi:10.1016/s0006-291x(02)00209-7

Nitert, M. D., Dayeh, T., Volkov, P., Elgzyri, T., Hall, E., Nilsson, E., . . . Ling, C. (2012). Impact of an exercise intervention on DNA methylation in skeletal muscle from first-degree relatives of patients with type 2 diabetes. *Diabetes, 61*(12), 3322-3332. doi:10.2337/db11-1653

Noshadi, B., Ercetin, T., Luise, C., Yuksel, M. Y., Sippl, W., Sahin, M. F., . . . Gulcan, H. O. (2020). Synthesis, Characterization, Molecular Docking, and Biological Activities of Some Natural and Synthetic Urolithin Analogs. *Chemistry & Biodiversity, 17*(8), e2000197. doi:10.1002/cbdv.202000197

Notman, R., Noro, M., O'Malley, B., & Anwar, J. (2006). Molecular basis for dimethylsulfoxide (DMSO) action on lipid membranes. *Journal of the American Chemical Society, 128*(43), 13982-13983. doi:10.1021/ja063363t

Nowotny, B., Zahiragic, L., Krog, D., Nowotny, P. J., Herder, C., Carstensen, M., . . . Roden, M. (2013). Mechanisms underlying the onset of oral lipid-induced skeletal muscle insulin resistance in humans. *Diabetes, 62*(7), 2240-2248. doi:10.2337/db12-1179

O'Leary, M. F., Wallace, G. R., Bennett, A. J., Tsintzas, K., & Jones, S. W. (2017). IL-15 promotes human myogenesis and mitigates the detrimental effects of

TNFα on myotube development. *Scientific Reports, 7*(1), 12997. doi:10.1038/s41598-017-13479-w

O'Leary, M. F., Wallace, G. R., Davis, E. T., Murphy, D. P., Nicholson, T., Bennett, A. J., . . . Jones, S. W. (2018). Obese subcutaneous adipose tissue impairs human myogenesis, particularly in old skeletal muscle, via resistin-mediated activation of NFκB. *Scientific Reports, 8*(1), 15360. doi:10.1038/s41598-018-33840-x

Ojima, K., Oe, M., Nakajima, I., Shibata, M., Chikuni, K., Muroya, S., & Nishimura, T. (2014). Proteomic analysis of secreted proteins from skeletal muscle cells during differentiation. *EuPA Open Proteomics, 5*, 1-9. doi:https://doi.org/10.1016/j.euprot.2014.08.001

Okla, M., Kang, I., Kim, D. M., Gourineni, V., Shay, N., Gu, L., & Chung, S. (2015). Ellagic acid modulates lipid accumulation in primary human adipocytes and human hepatoma Huh7 cells via discrete mechanisms. *The Journal of Nutritional Biochemistry, 26*(1), 82-90. doi:10.1016/j.jnutbio.2014.09.010

Olefsky, J. M., & Nolan, J. J. (1995). Insulin resistance and non-insulin-dependent diabetes mellitus: cellular and molecular mechanisms. *The American Journal of Clinical Nutrition, 61*(4), 980S-986S. doi:10.1093/ajcn/61.4.980S

Oliveira, A. F., Cunha, D. A., Ladriere, L., Igoillo-Esteve, M., Bugliani, M., Marchetti, P., & Cnop, M. (2015). In vitro use of free fatty acids bound to albumin: A comparison of protocols. *Biotechniques, 58*(5), 228-233. doi:10.2144/000114285

Opie, L. H., & Walfish, P. G. (1963). Plasma free fatty acid concentrations in obesity. *New England Journal of Medicine, 268*, 757-760. doi:10.1056/nejm196304042681404

Ormazabal, V., Nair, S., Elfeky, O., Aguayo, C., Salomon, C., & Zuñiga, F. A. (2018). Association between insulin resistance and the development of cardiovascular disease. *Cardiovascular Diabetology, 17*(1), 122. doi:10.1186/s12933-018-0762-4

Owei, I., Umekwe, N., Provo, C., Wan, J., & Dagogo-Jack, S. (2017). Insulin-sensitive and insulin-resistant obese and non-obese phenotypes: role in prediction of incident pre-diabetes in a longitudinal biracial cohort. *BMJ open diabetes research & care, 5*(1), e000415-e000415. doi:10.1136/bmjdrc-2017-000415

Pajak, B., Siwiak, E., Sołtyka, M., Priebe, A., Zieliński, R., Fokt, I., . . . Priebe, W. (2019). 2-Deoxy-d-Glucose and Its Analogs: From Diagnostic to Therapeutic Agents. *International Journal of Molecular Sciences, 21*(1). doi:10.3390/ijms21010234

Palsgaard, J., Brons, C., Friedrichsen, M., Dominguez, H., Jensen, M., Storgaard, H., . . . Vaag, A. (2009). Gene expression in skeletal muscle biopsies from people with type 2 diabetes and relatives: differential regulation of insulin signaling pathways. *PloS One, 4*(8), e6575. doi:10.1371/journal.pone.0006575

Pannala, R., Basu, A., Petersen, G. M., & Chari, S. T. (2009). New-onset diabetes: a potential clue to the early diagnosis of pancreatic cancer. *Lancet Oncology, 10*(1), 88-95. doi:10.1016/s1470-2045(08)70337-1

Paolisso, G., De Riu, S., Marrazzo, G., Verza, M., Varricchio, M., & D'Onofrio, F. (1991). Insulin resistance and hyperinsulinemia in patients with chronic congestive heart failure. *Metabolism: Clinical and Experimental, 40*(9), 972-977. doi:https://doi.org/10.1016/0026-0495(91)90075-8

Parikh, H. M., Elgzyri, T., Alibegovic, A., Hiscock, N., Ekström, O., Eriksson, K.-F., . . . Hansson, O. (2021). Relationship between insulin sensitivity and gene expression in human skeletal muscle. *BMC Endocrine Disorders, 21*(1), 32. doi:10.1186/s12902-021-00687-9

Paris, M. T., Bell, K. E., & Mourtzakis, M. (2020). Myokines and adipokines in sarcopenia: understanding cross-talk between skeletal muscle and adipose tissue and the role of exercise. *Current Opinion in Pharmacology, 52*, 61-66. doi:10.1016/j.coph.2020.06.003

Park, J.-J., Berggren, J. R., Hulver, M. W., Houmard, J. A., & Hoffman, E. P. (2006). GRB14, GPD1, and GDF8 as potential network collaborators in weight loss-induced improvements in insulin action in human skeletal muscle. *Physiological Genomics, 27*(2), 114-121. doi:10.1152/physiolgenomics.00045.2006

Park, S.-Y., Cho, Y.-R., Kim, H.-J., Higashimori, T., Danton, C., Lee, M.-K., . . . Kim, J. K. (2005). Unraveling the Temporal Pattern of Diet-Induced Insulin Resistance in Individual Organs and Cardiac Dysfunction in c57bl/6 Mice. *Diabetes, 54*(12), 3530-3540. doi:10.2337/diabetes.54.12.3530

Park, S. Y., Kim, M. H., Ahn, J. H., Lee, S. J., Lee, J. H., Eum, W. S., . . . Kwon, H. Y. (2014). The Stimulatory Effect of Essential Fatty Acids on Glucose Uptake Involves Both Akt and AMPK Activation in C2C12 Skeletal Muscle Cells. *The Korean journal of physiology & pharmacology : official journal of the Korean Physiological Society and the Korean Society of Pharmacology, 18*(3), 255-261. doi:10.4196/kjpp.2014.18.3.255

Patel, H. P., Al-Shanti, N., Davies, L. C., Barton, S. J., Grounds, M. D., Tellam, R. L., . . . Sayer, A. A. (2014). Lean mass, muscle strength and gene expression in community dwelling older men: findings from the Hertfordshire Sarcopenia Study (HSS). *Calcified Tissue International, 95*(4), 308-316. doi:10.1007/s00223-014-9894-z

Patková, J., Anděl, M., & Trnka, J. (2014). Palmitate-Induced Cell Death and Mitochondrial Respiratory Dysfunction in Myoblasts are Not Prevented by Mitochondria-Targeted Antioxidants. *Cellular Physiology and Biochemistry, 33*(5), 1439-1451. doi:10.1159/000358709

Peake, J., Gatta, P. D., & Cameron-Smith, D. (2010). Aging and its effects on inflammation in skeletal muscle at rest and following exercise-induced muscle injury. *American Journal of Physiology-Regulatory, Integrative and Comparative Physiology, 298*(6), R1485-R1495. doi:10.1152/ajpregu.00467.2009

Pearson, S. J., Young, A., Macaluso, A., Devito, G., Nimmo, M. A., Cobbold, M., & Harridge, S. D. (2002). Muscle function in elite master weightlifters. *Medicine and Science in Sports and Exercise, 34*(7), 1199-1206. doi:10.1097/00005768-200207000-00023

Pedersen, B. K. (2019). Physical activity and muscle–brain crosstalk. *Nature Reviews Endocrinology, 15*(7), 383-392. doi:10.1038/s41574-019-0174-x

Pedersen, B. K., Åkerström, T. C. A., Nielsen, A. R., & Fischer, C. P. (2007). Role of myokines in exercise and metabolism. *Journal of Applied Physiology, 103*(3), 1093-1098. doi:10.1152/japplphysiol.00080.2007

Pedersen, B. K., & Febbraio, M. A. (2008). Muscle as an Endocrine Organ: Focus on Muscle-Derived Interleukin-6. *Physiological Reviews, 88*(4), 1379-1406. doi:10.1152/physrev.90100.2007

Peiris, H. N., Ponnampalam, A. P., Mitchell, M. D., & Green, M. P. (2010). Brief Communication: Sexual dimorphic expression of myostatin and follistatin like-3 in a rat trans-generational under-nutrition model. *Nutrition & Metabolism, 7*(1), 44. doi:10.1186/1743-7075-7-44

Pelle, M. C., Provenzano, M., Zaffina, I., Pujia, R., Giofrè, F., Lucà, S., . . . Arturi, F. (2022). Role of a Dual Glucose-Dependent Insulinotropic Peptide (GIP)/Glucagon-like Peptide-1 Receptor Agonist (Twincretin) in Glycemic Control: From Pathophysiology to Treatment. *Life, 12*(1), 29. Retrieved from https://www.mdpi.com/2075-1729/12/1/29

Pellegrinelli, V., Rouault, C., Rodriguez-Cuenca, S., Albert, V., Edom-Vovard, F., Vidal-Puig, A., . . . Lacasa, D. (2015). Human Adipocytes Induce Inflammation and Atrophy in Muscle Cells During Obesity. *Diabetes, 64*(9), 3121-3134. doi:10.2337/db14-0796

Peng, G., Li, L., Liu, Y., Pu, J., Zhang, S., Yu, J., . . . Liu, P. (2011). Oleate Blocks Palmitate-Induced Abnormal Lipid Distribution, Endoplasmic Reticulum Expansion and Stress, and Insulin Resistance in Skeletal Muscle. *Endocrinology, 152*(6), 2206-2218. doi:10.1210/en.2010-1369

Perreault, L., Bergman, B. C., Hunerdosse, D. M., & Eckel, R. H. (2010). Altered intramuscular lipid metabolism relates to diminished insulin action in men, but not women, in progression to diabetes. *Obesity (Silver Spring), 18*(11), 2093-2100. doi:10.1038/oby.2010.76

Perreault, M., Roke, K., Badawi, A., Nielsen, D. E., Abdelmagid, S. A., El-Sohemy, A., . . . Mutch, D. M. (2014). Plasma levels of 14:0, 16:0, 16:1n-7, and 20:3n-6 are positively associated, but 18:0 and 18:2n-6 are inversely associated with markers of inflammation in young healthy adults. *Lipids, 49*(3), 255-263. doi:10.1007/s11745-013-3874-3

Perry, B. D., Rahnert, J. A., Xie, Y., Zheng, B., Woodworth-Hobbs, M. E., & Price, S. R. (2018). Palmitate-induced ER stress and inhibition of protein synthesis in cultured myotubes does not require Toll-like receptor 4. *PloS One, 13*(1), e0191313. doi:10.1371/journal.pone.0191313

Petersen, K. F., Dufour, S., Befroy, D., Garcia, R., & Shulman, G. I. (2004). Impaired mitochondrial activity in the insulin-resistant offspring of patients with type 2 diabetes. *The New England journal of medicine, 350*(7), 664-671. doi:10.1056/NEJMoa031314

Petersen, M. C., & Jurczak, M. J. (2016). CrossTalk opposing view: Intramyocellular ceramide accumulation does not modulate insulin resistance. *The Journal of Physiology, 594*(12), 3171-3174. doi:10.1113/JP271677

Philip, B., Lu, Z., & Gao, Y. (2005). Regulation of GDF-8 signaling by the p38 MAPK. *Cellular Signalling, 17*(3), 365-375. doi:10.1016/j.cellsig.2004.08.003

Piccirillo, R. (2019). Exercise-Induced Myokines With Therapeutic Potential for Muscle Wasting. *Frontiers in Physiology, 10*, 287. doi:10.3389/fphys.2019.00287

Pirruccello-Straub, M., Jackson, J., Wawersik, S., Webster, M. T., Salta, L., Long, K., . . . Donovan, A. (2018). Blocking extracellular activation of myostatin as a strategy for treating muscle wasting. *Scientific Reports, 8*(1), 2292. doi:10.1038/s41598-018-20524-9

Ploug, T., & Ralston, E. (1998). Anatomy of glucose transporters in skeletal muscle. Effects of insulin and contractions. *Advances in Experimental Medicine and Biology, 441*, 17-26.

Ploug, T., van Deurs, B., Ai, H., Cushman, S. W., & Ralston, E. (1998). Analysis of GLUT4 Distribution in Whole Skeletal Muscle Fibers: Identification of Distinct Storage Compartments That Are Recruited by Insulin and Muscle Contractions. *The Journal of Cell Biology, 142*(6), 1429-1446. doi:10.1083/jcb.142.6.1429

Pociot, F., & Lernmark, Å. (2016). Genetic risk factors for type 1 diabetes. *The Lancet, 387*(10035), 2331-2339. doi:10.1016/S0140-6736(16)30582-7

Podrez, E. A., Abu-Soud, H. M., & Hazen, S. L. (2000). Myeloperoxidase-generated oxidants and atherosclerosis. *Free Radical Biology and Medicine, 28*(12), 1717-1725. doi:10.1016/s0891-5849(00)00229-x

Pogodziński, D., Ostrowska, L., Smarkusz-Zarzecka, J., & Zyśk, B. (2022). Secretome of Adipose Tissue as the Key to Understanding the Endocrine Function of Adipose Tissue. *International Journal of Molecular Sciences, 23*(4), 2309. doi:10.3390/ijms23042309

Pollard, D. A., Pollard, T. D., & Pollard, K. S. (2019). Empowering statistical methods for cellular and molecular biologists. *Molecular Biology of the Cell, 30*(12), 1359-1368. doi:10.1091/mbc.E15-02-0076

Pomeroy, C., Mitchell, J., Eckert, E., Raymond, N., Crosby, R., & Dalmasso, A. P. (2003). Effect of body weight and caloric restriction on serum complement proteins, including Factor D/adipsin: studies in anorexia nervosa and obesity. *Clinical and Experimental Immunology, 108*(3), 507-515. doi:10.1046/j.1365-2249.1997.3921287.x

Poortmans, J. R., Carpentier, A., Pereira-Lancha, L. O., & Lancha, A. (2012). Protein turnover, amino acid requirements and recommendations for athletes and active populations. *Brazilian Journal of Medical and Biological Research, 45*(10), 875-890. doi:10.1590/S0100-879X2012007500096

Poulose, N., Prasad, C. N., Haridas, N., & Gopalakrishnapillai, A. (2011). Ellagic Acid Stimulates Glucose Transport in Adipocytes and Muscles through AMPK Mediated Pathway. *Journal of Diabetes & Metabolism, 02*. doi:10.4172/2155-6156.1000149

Powell, D. J., Hajduch, E., Kular, G., & Hundal, H. S. (2003). Ceramide Disables 3-Phosphoinositide Binding to the Pleckstrin Homology Domain of Protein Kinase B (PKB)/Akt by a PKCζ-Dependent Mechanism. *Molecular and Cellular Biology, 23*(21), 7794-7808. doi:doi:10.1128/MCB.23.21.7794-7808.2003

Präbst, K., Engelhardt, H., Ringgeler, S., & Hübner, H. (2017). Basic Colorimetric Proliferation Assays: MTT, WST, and Resazurin. *Methods in Molecular Biology, 1601*, 1-17. doi:10.1007/978-1-4939-6960-9_1

Pramono, A., Jocken, J. W. E., & Blaak, E. E. (2019). Vitamin D deficiency in the aetiology of obesity-related insulin resistance. *Diabetes/Metabolism Research and Reviews, 35*(5), e3146. doi:https://doi.org/10.1002/dmrr.3146

Prelich, G. (2012). Gene overexpression: uses, mechanisms, and interpretation. *Genetics, 190*(3), 841-854. doi:10.1534/genetics.111.136911

Przybyla, B., Gurley, C., Harvey, J. F., Bearden, E., Kortebein, P., Evans, W. J., . . . Dennis, R. A. (2006). Aging alters macrophage properties in human skeletal muscle both at rest and in response to acute resistance exercise. *Experimental Gerontology, 41*(3), 320-327. doi:10.1016/j.exger.2005.12.007

Ptashne, M. (1992). *A Genetic Switch: Phage (Lambda) and Highter Organisms*. Cambridge, MA: Cell Press.

Qaddoumi, M. G., Alanbaei, M., Hammad, M. M., Al Khairi, I., Cherian, P., Channanath, A., . . . Abubaker, J. (2020). Investigating the Role of Myeloperoxidase and Angiopoietin-like Protein 6 in Obesity and Diabetes. *Scientific Reports, 10*(1), 6170. doi:10.1038/s41598-020-63149-7

Qiu, J., Thapaliya, S., Runkana, A., Yang, Y., Tsien, C., Mohan, M. L., . . . Dasarathy, S. (2013). Hyperammonemia in cirrhosis induces transcriptional regulation of myostatin by an NF-κB-mediated mechanism. *Proceedings of the National Academy of Sciences of the United States of America, 110*(45), 18162-18167. doi:10.1073/pnas.1317049110

Rachek, L. I., Musiyenko, S. I., LeDoux, S. P., & Wilson, G. L. (2007). Palmitate Induced Mitochondrial Deoxyribonucleic Acid Damage and Apoptosis in L6 Rat Skeletal Muscle Cells. *Endocrinology, 148*(1), 293-299. doi:10.1210/en.2006-0998

Raimundo, A. F., Ferreira, S., Tomás-Barberán, F. A., Santos, C. N., & Menezes, R. (2021). Urolithins: Diet-Derived Bioavailable Metabolites to Tackle Diabetes. *Nutrients, 13*(12). doi:10.3390/nu13124285

Rainha, J., Gomes, D., Rodrigues, L. R., & Rodrigues, J. L. (2020). Synthetic Biology Approaches to Engineer Saccharomyces cerevisiae towards the Industrial Production of Valuable Polyphenolic Compounds. *Life, 10*(5), 56. Retrieved from https://www.mdpi.com/2075-1729/10/5/56

Randle, P. J., Garland, P. B., Hales, C. N., & Newsholme, E. A. (1963). The glucose fatty-acid cycle. Its role in insulin sensitivity and the metabolic disturbances of diabetes mellitus. *Lancet, 1*(7285), 785-789. doi:10.1016/s0140-6736(63)91500-9

Raposo, G., & Stoorvogel, W. (2013). Extracellular vesicles: exosomes, microvesicles, and friends. *The Journal of Cell Biology, 200*(4), 373-383. doi:10.1083/jcb.201211138

Ratkevicius, A., Joyson, A., Selmer, I., Dhanani, T., Grierson, C., Tommasi, A. M., . . . Wackerhage, H. (2011). Serum concentrations of myostatin and myostatin-interacting proteins do not differ between young and sarcopenic elderly men. *Journals of Gerontology. Series A: Biological Sciences and Medical Sciences, 66*(6), 620-626. doi:10.1093/gerona/glr025

Raue, U., Slivka, D., Jemiolo, B., Hollon, C., & Trappe, S. (2006). Myogenic gene expression at rest and after a bout of resistance exercise in young (18-30 yr) and old (80-89 yr) women. *J Appl Physiol (1985), 101*(1), 53-59. doi:10.1152/japplphysiol.01616.2005

Raue, U., Slivka, D., Jemiolo, B., Hollon, C., & Trappe, S. (2007). Proteolytic gene expression differs at rest and after resistance exercise between young and old women. *Journals of Gerontology. Series A: Biological Sciences and Medical Sciences, 62*(12), 1407-1412. doi:10.1093/gerona/62.12.1407

Raymond, F., Métairon, S., Kussmann, M., Colomer, J., Nascimento, A., Mormeneo, E., . . . Gómez-Foix, A. M. (2010). Comparative gene expression profiling between human cultured myotubes and skeletal muscle tissue. *BMC Genomics, 11*, 125-125. doi:10.1186/1471-2164-11-125

Razali, N. M., & Wah, Y. B. (2011). Power comparisons of shapiro-wilk, kolmogorov-smirnov, lilliefors and anderson-darling tests. *Journal of statistical modeling and analytics, 2*(1), 21-33.

Reaven, G. M. (2005). Compensatory hyperinsulinemia and the development of an atherogenic lipoprotein profile: the price paid to maintain glucose homeostasis in insulin-resistant individuals. *Endocrinology and Metabolism Clinics of North America, 34*(1), 49-62. doi:10.1016/j.ecl.2004.12.001

Rebalka, I. A., Monaco, C. M. F., Varah, N. E., Berger, T., D'Souza D, M., Zhou, S., . . . Hawke, T. J. (2018). Loss of the adipokine lipocalin-2 impairs satellite cell activation and skeletal muscle regeneration. *American Journal of Physiology: Cell Physiology, 315*(5), C714-c721. doi:10.1152/ajpcell.00195.2017

Reisz-Porszasz, S., Bhasin, S., Artaza, J. N., Shen, R., Sinha-Hikim, I., Hogue, A., . . . Gonzalez-Cadavid, N. F. (2003). Lower skeletal muscle mass in male transgenic mice with muscle-specific overexpression of myostatin. *American Journal of Physiology: Endocrinology and Metabolism, 285*(4), E876-888. doi:10.1152/ajpendo.00107.2003

Rennie, M. J., & Wilkes, E. A. (2005). Maintenance of the musculoskeletal mass by control of protein turnover: the concept of anabolic resistance and its relevance to the transplant recipient. *Annals of Transplantation, 10*(4), 31-34.

Retamales, A., Zuloaga, R., Valenzuela, C. A., Gallardo-Escarate, C., Molina, A., & Valdés, J. A. (2015). Insulin-like growth factor-1 suppresses the Myostatin signaling pathway during myogenic differentiation. *Biochemical and Biophysical Research Communications, 464*(2), 596-602. doi:10.1016/j.bbrc.2015.07.018

Reyna, S. M., Ghosh, S., Tantiwong, P., Meka, C. S. R., Eagan, P., Jenkinson, C. P., . . . Musi, N. (2008). Elevated toll-like receptor 4 expression and signaling in muscle from insulin-resistant subjects. *Diabetes, 57*(10), 2595-2602. doi:10.2337/db08-0038

Riccardi, G., Giacco, R., & Rivellese, A. A. (2004). Dietary fat, insulin sensitivity and the metabolic syndrome. *Clinical Nutrition, 23*(4), 447-456. doi:10.1016/j.clnu.2004.02.006

Richards, C. D. (2013). The enigmatic cytokine oncostatin m and roles in disease. *International Scholarly Research Notices, 2013*.

Richter, E. A., & Hargreaves, M. (2013). Exercise, GLUT4, and Skeletal Muscle Glucose Uptake. *Physiological Reviews, 93*(3), 993-1017. doi:10.1152/physrev.00038.2012

Ridker, P. M. (2001). High-Sensitivity C-Reactive Protein. *Circulation, 103*(13), 1813-1818. doi:doi:10.1161/01.CIR.103.13.1813

Ridker, P. M. (2003). Clinical Application of C-Reactive Protein for Cardiovascular Disease Detection and Prevention. *Circulation, 107*(3), 363-369. doi:doi:10.1161/01.CIR.0000053730.47739.3C

Ríos, R., Carneiro, I., Arce, V. M., & Devesa, J. (2001). Myostatin Regulates Cell Survival during C2C12 Myogenesis. *Biochemical and Biophysical Research Communications, 280*(2), 561-566. doi:https://doi.org/10.1006/bbrc.2000.4159

Ríos, R., Carneiro, I., Arce, V. M., & Devesa, J. (2002). Myostatin is an inhibitor of myogenic differentiation. *American Journal of Physiology: Cell Physiology, 282*(5), C993-999. doi:10.1152/ajpcell.00372.2001

Rivas, D. A., McDonald, D. J., Rice, N. P., Haran, P. H., Dolnikowski, G. G., & Fielding, R. A. (2016). Diminished anabolic signaling response to insulin induced by intramuscular lipid accumulation is associated with inflammation in aging but not obesity. *American journal of physiology. Regulatory, integrative and comparative physiology, 310*(7), R561-R569. doi:10.1152/ajpregu.00198.2015

Rivera, M. E., & Vaughan, R. A. (2021). Comparing the effects of palmitate, insulin, and palmitate-insulin co-treatment on myotube metabolism and insulin resistance. *Lipids, 56*(6), 563-578. doi:10.1002/lipd.12315

Rizzo, H. E., Escaname, E. N., Alana, N. B., Lavender, E., Gelfond, J., Fernandez, R., . . . Blanco, C. L. (2020). Maternal diabetes and obesity influence the fetal epigenome in a largely Hispanic population. *Clinical Epigenetics, 12*(1), 34. doi:10.1186/s13148-020-0824-9

Rizzoli, R., Reginster, J.-Y., Arnal, J.-F., Bautmans, I., Beaudart, C., Bischoff-Ferrari, H., . . . Bruyère, O. (2013). Quality of life in sarcopenia and frailty. *Calcified Tissue International, 93*(2), 101-120. doi:10.1007/s00223-013-9758-y

Robinson, W. R., Utz, R. L., Keyes, K. M., Martin, C. L., & Yang, Y. (2013). Birth cohort effects on abdominal obesity in the United States: the Silent Generation, Baby Boomers and Generation X. *International Journal of Obesity (2005), 37*(8), 1129-1134. doi:10.1038/ijo.2012.198

Roden, M., Price, T. B., Perseghin, G., Petersen, K. F., Rothman, D. L., Cline, G. W., & Shulman, G. I. (1996). Mechanism of free fatty acid-induced insulin resistance in humans. *Journal of Clinical Investigation, 97*(12), 2859-2865. Retrieved from https://www.ncbi.nlm.nih.gov/pmc/articles/PMC507380/

Rodgers, B. D., Wiedeback, B. D., Hoversten, K. E., Jackson, M. F., Walker, R. G., & Thompson, T. B. (2014). Myostatin stimulates, not inihibits, C2C12 myoblast proliferation. *Endocrinology, 155*(3), 670-675. doi:10.1210/en.2013-2107

Rodrigues, K. F., Pietrani, N. T., Bosco, A. A., Sousa, L. P., Ferreira, C. N., Sandrim, V. C., & Gomes, K. B. (2015). Endocan: a new biomarker associated with inflammation in type 2 diabetes mellitus? *Diabetes/Metabolism Research and Reviews, 31*(5), 479-480. doi:https://doi.org/10.1002/dmrr.2639

Rodriguez, J., Caille, O., Ferreira, D., & Francaux, M. (2017). Pomegranate extract prevents skeletal muscle of mice against wasting induced by acute TNF-α injection. *Molecular Nutrition & Food Research, 61*(4). doi:10.1002/mnfr.201600169

Rodriguez, J., Pierre, N., Naslain, D., Bontemps, F., Ferreira, D., Priem, F., . . . Francaux, M. (2017). Urolithin B, a newly identified regulator of skeletal muscle mass. *Journal of Cachexia, Sarcopenia and Muscle, 8*(4), 583-597. doi:https://doi.org/10.1002/jcsm.12190

Rodriguez, J., Vernus, B., Toubiana, M., Jublanc, E., Tintignac, L., Leibovitch, S., & Bonnieu, A. (2011). Myostatin inactivation increases myotube size through regulation of translational initiation machinery. *Journal of Cellular Biochemistry, 112*(12), 3531-3542. doi:10.1002/jcb.23280

Roh, Y. H., Hong, S. W., Chung, S. W., & Lee, Y. S. (2019). Altered gene and protein expressions of vitamin D receptor in skeletal muscle in sarcopenic patients who sustained distal radius fractures. *Journal of Bone and Mineral Metabolism, 37*(5), 920-927. doi:10.1007/s00774-019-00995-0

Rom, O., & Reznick, A. Z. (2016). The role of E3 ubiquitin-ligases MuRF-1 and MAFbx in loss of skeletal muscle mass. *Free Radical Biology and Medicine, 98*, 218-230. doi:https://doi.org/10.1016/j.freeradbiomed.2015.12.031

Rome, S., Forterre, A., Mizgier, M. L., & Bouzakri, K. (2019). Skeletal Muscle-Released Extracellular Vesicles: State of the Art. *Frontiers in Physiology, 10*(929). doi:10.3389/fphys.2019.00929

Rosen, B. S., Cook, K. S., Yaglom, J., Groves, D. L., Volanakis, J. E., Damm, D., . . . Spiegelman, B. M. (1989). Adipsin and Complement Factor D Activity: An Immune-Related Defect in Obesity. *Science, 244*(4911), 1483-1487. doi:doi:10.1126/science.2734615

Rosenberg, I. H. (1997). Sarcopenia: Origins and Clinical Relevance. *The Journal of Nutrition, 127*(5), 990S-991S. doi:10.1093/jn/127.5.990S

Rotar, O., Boyarinova, M., Orlov, A., Solntsev, V., Zhernakova, Y., Shalnova, S., . . . Shlyakhto, E. (2017). Metabolically healthy obese and metabolically unhealthy non-obese phenotypes in a Russian population. *European Journal of Epidemiology, 32*(3), 251-254. doi:10.1007/s10654-016-0221-z

Rotter, V., Nagaev, I., & Smith, U. (2003). Interleukin-6 (IL-6) induces insulin resistance in 3T3-L1 adipocytes and is, like IL-8 and tumor necrosis factor-alpha, overexpressed in human fat cells from insulin-resistant subjects. *Journal of Biological Chemistry, 278*(46), 45777-45784. doi:10.1074/jbc.M301977200

Rousseau, M., Guénard, F., Garneau, V., Allam-Ndoul, B., Lemieux, S., Pérusse, L., & Vohl, M.-C. (2019). Associations Between Dietary Protein Sources, Plasma BCAA and Short-Chain Acylcarnitine Levels in Adults. *Nutrients, 11*(1), 173. doi:10.3390/nu11010173

Rubenstein, A. B., Smith, G. R., Raue, U., Begue, G., Minchev, K., Ruf-Zamojski, F., . . . Sealfon, S. C. (2020). Single-cell transcriptional profiles in human skeletal muscle. *Scientific Reports, 10*(1), 229. doi:10.1038/s41598-019-57110-6

Russell, A. P. (2010). Molecular regulation of skeletal muscle mass. *Clinical and Experimental Pharmacology and Physiology, 37*(3), 378-384. doi:10.1111/j.1440-1681.2009.05265.x

Ruvolo, P. P. (2001). Ceramide regulates cellular homeostasis via diverse stress signaling pathways. *Leukemia, 15*(8), 1153-1160. doi:10.1038/sj.leu.2402197

Ryan, A. S., Berman, D. M., Nicklas, B. J., Sinha, M., Gingerich, R. L., Meneilly, G. S., . . . Elahi, D. (2003). Plasma Adiponectin and Leptin Levels, Body Composition, and Glucose Utilization in Adult Women With Wide Ranges of Age and Obesity. *Diabetes Care, 26*(8), 2383-2388. doi:10.2337/diacare.26.8.2383

Ryan, A. S., & Li, G. (2021). Skeletal muscle myostatin gene expression and sarcopenia in overweight and obese middle-aged and older adults. *JCSM Clinical Reports, 6*(4), 137-142. doi:https://doi.org/10.1002/crt2.43

Ryan, A. S., Li, G., Blumenthal, J. B., & Ortmeyer, H. K. (2013). Aerobic exercise + weight loss decreases skeletal muscle myostatin expression and improves insulin sensitivity in older adults. *Obesity (Silver Spring, Md.), 21*(7), 1350-1356. doi:10.1002/oby.20216

Ryan, A. S., Ortmeyer, H. K., & Sorkin, J. D. (2012). Exercise with calorie restriction improves insulin sensitivity and glycogen synthase activity in obese postmenopausal women with impaired glucose tolerance. *American Journal of Physiology. Endocrinology and Metabolism, 302*(1), E145-152. doi:10.1152/ajpendo.00618.2010

Ryu, D., Mouchiroud, L., Andreux, P. A., Katsyuba, E., Moullan, N., Nicolet-dit-Félix, A. A., . . . Auwerx, J. (2016). Urolithin A induces mitophagy and prolongs lifespan in C. elegans and increases muscle function in rodents. *Nature Medicine, 22*(8), 879-888. doi:10.1038/nm.4132

Sachs, S., Zarini, S., Kahn, D. E., Harrison, K. A., Perreault, L., Phang, T., . . . Bergman, B. C. (2019). Intermuscular adipose tissue directly modulates skeletal muscle insulin sensitivity in humans. *American journal of physiology. Endocrinology and metabolism, 316*(5), E866-E879. doi:10.1152/ajpendo.00243.2018

Saitoh, M., Ishida, J., Ebner, N., Anker, S. D., Springer, J., & von Haehling, S. (2017). Myostatin inhibitors as pharmacological treatment for muscle wasting and muscular dystrophy. *JCSM Clinical Reports, 2*(1), 1-10. doi:10.17987/jcsm-cr.v2i1.37

Salerno, M. S., Thomas, M., Forbes, D., Watson, T., Kambadur, R., & Sharma, M. (2004). Molecular analysis of fiber type-specific expression of murine myostatin promoter. *American Journal of Physiology: Cell Physiology, 287*(4), C1031-1040. doi:10.1152/ajpcell.00492.2003

Salucci, S., & Falcieri, E. (2020). Polyphenols and their potential role in preventing skeletal muscle atrophy. *Nutrition Research, 74*, 10-22. doi:10.1016/j.nutres.2019.11.004

Salvadó, L., Coll, T., Gómez-Foix, A. M., Salmerón, E., Barroso, E., Palomer, X., & Vázquez-Carrera, M. (2013). Oleate prevents saturated-fatty-acid-induced ER stress, inflammation and insulin resistance in skeletal muscle cells through an AMPK-dependent mechanism. *Diabetologia, 56*(6), 1372-1382. doi:10.1007/s00125-013-2867-3

Samuel, V. T., Petersen, K. F., & Shulman, G. I. (2010). Lipid-induced insulin resistance: unravelling the mechanism. *Lancet, 375*(9733), 2267-2277. doi:10.1016/s0140-6736(10)60408-4

San-Cristobal, R., Navas-Carretero, S., Martínez-González, M. Á., Ordovas, J. M., & Martínez, J. A. (2020). Contribution of macronutrients to obesity: implications for precision nutrition. *Nature Reviews Endocrinology, 16*(6), 305-320. doi:10.1038/s41574-020-0346-8

Sanada, K., Chen, R., Willcox, B., Ohara, T., Wen, A., Takenaka, C., & Masaki, K. (2018). Association of sarcopenic obesity predicted by anthropometric measurements and 24-y all-cause mortality in elderly men: The Kuakini Honolulu Heart Program. *Nutrition, 46*, 97-102. doi:10.1016/j.nut.2017.09.003

Sanchez-Infantes, D., White, U. A., Elks, C. M., Morrison, R. F., Gimble, J. M., Considine, R. V., . . . Stephens, J. M. (2014). Oncostatin M Is Produced in Adipose Tissue and Is Regulated in Conditions of Obesity and Type 2 Diabetes. *The Journal of Clinical Endocrinology & Metabolism, 99*(2), E217-E225. doi:10.1210/jc.2013-3555

Sandri, M., Barberi, L., Bijlsma, A. Y., Blaauw, B., Dyar, K. A., Milan, G., . . . Schiaffino, S. (2013). Signalling pathways regulating muscle mass in ageing skeletal muscle: the role of the IGF1-Akt-mTOR-FoxO pathway. *Biogerontology, 14*(3), 303-323. doi:10.1007/s10522-013-9432-9

Sarabhai, T., Koliaki, C., Mastrototaro, L., Kahl, S., Pesta, D., Apostolopoulou, M., . . . Roden, M. (2022). Dietary palmitate and oleate differently modulate insulin sensitivity in human skeletal muscle. *Diabetologia, 65*(2), 301-314. doi:10.1007/s00125-021-05596-z

Sarabia, V., Lam, L., Burdett, E., Leiter, L. A., & Klip, A. (1992). Glucose transport in human skeletal muscle cells in culture. Stimulation by insulin and metformin. *Journal of Clinical Investigation, 90*(4), 1386-1395. doi:10.1172/jci116005

Sarrazin, S., Adam, E., Lyon, M., Depontieu, F., Motte, V., Landolfi, C., . . . Delehedde, M. (2006). Endocan or endothelial cell specific molecule-1 (ESM-1): a potential novel endothelial cell marker and a new target for cancer therapy. *Biochimica et Biophysica Acta, 1765*(1), 25-37. doi:10.1016/j.bbcan.2005.08.004

Sartorelli, V., & Fulco, M. (2004). Molecular and cellular determinants of skeletal muscle atrophy and hypertrophy. *Science's STKE, 2004*(244), re11. doi:10.1126/stke.2442004re11

Sartori, R., Milan, G., Patron, M., Mammucari, C., Blaauw, B., Abraham, R., & Sandri, M. (2009). Smad2 and 3 transcription factors control muscle mass in adulthood. *American Journal of Physiology: Cell Physiology, 296*(6), C1248-1257. doi:10.1152/ajpcell.00104.2009

Sawada, K., Kawabata, K., Yamashita, T., Kawasaki, K., Yamamoto, N., & Ashida, H. (2012). Ameliorative effects of polyunsaturated fatty acids against palmitic acid-induced insulin resistance in L6 skeletal muscle cells. *Lipids in Health and Disease, 11*(1), 36. doi:10.1186/1476-511X-11-36

Scalbert, A., Morand, C., Manach, C., & Rémésy, C. (2002). Absorption and metabolism of polyphenols in the gut and impact on health. *Biomedicine and Pharmacotherapy, 56*(6), 276-282. doi:https://doi.org/10.1016/S0753-3322(02)00205-6

Schafer, M. J., Atkinson, E. J., Vanderboom, P. M., Kotajarvi, B., White, T. A., Moore, M. M., . . . LeBrasseur, N. K. (2016). Quantification of GDF11 and Myostatin in Human Aging and Cardiovascular Disease. *Cell Metabolism, 23*(6), 1207-1215. doi:https://doi.org/10.1016/j.cmet.2016.05.023

Schenk, S., & Horowitz, J. F. (2007). Acute exercise increases triglyceride synthesis in skeletal muscle and prevents fatty acid-induced insulin resistance. *Journal of Clinical Investigation, 117*(6), 1690-1698. doi:10.1172/jci30566

Schmidt, E. K., Clavarino, G., Ceppi, M., & Pierre, P. (2009). SUnSET, a nonradioactive method to monitor protein synthesis. *Nature methods, 6*(4), 275-277. doi:10.1038/nmeth.1314

Schmitz-Peiffer, C., Craig, D. L., & Biden, T. J. (1999). Ceramide generation is sufficient to account for the inhibition of the insulin-stimulated PKB pathway in C2C12 skeletal muscle cells pretreated with palmitate. *Journal of Biological Chemistry, 274*(34), 24202-24210. doi:10.1074/jbc.274.34.24202

Schmitz, O., Rungby, J., Edge, L., & Juhl, C. B. (2008). On high-frequency insulin oscillations. *Ageing Res Rev, 7*(4), 301-305. doi:10.1016/j.arr.2008.04.002

Schnyder, S., & Handschin, C. (2015). Skeletal muscle as an endocrine organ: PGC-1α, myokines and exercise. *Bone, 80*, 115-125. doi:10.1016/j.bone.2015.02.008

Schober, P., Boer, C., & Schwarte, L. A. (2018). Correlation Coefficients: Appropriate Use and Interpretation. *Anesthesia and Analgesia, 126*(5). Retrieved from https://journals.lww.com/anesthesia-analgesia/Fulltext/2018/05000/Correlation_Coefficients__Appropriate_Use_and.50.aspx

Schooneman, M. G., Vaz, F. M., Houten, S. M., & Soeters, M. R. (2012). Acylcarnitines: Reflecting or Inflicting Insulin Resistance? *Diabetes, 62*(1), 1-8. doi:10.2337/db12-0466

Schrager, M. A., Metter, E. J., Simonsick, E., Ble, A., Bandinelli, S., Lauretani, F., & Ferrucci, L. (2007). Sarcopenic obesity and inflammation in the InCHIANTI

study. *J Appl Physiol (1985), 102*(3), 919-925. doi:10.1152/japplphysiol.00627.2006

Schwartz, M. W., Seeley, R. J., Zeltser, L. M., Drewnowski, A., Ravussin, E., Redman, L. M., & Leibel, R. L. (2017). Obesity Pathogenesis: An Endocrine Society Scientific Statement. *Endocrine Reviews, 38*(4), 267-296. doi:10.1210/er.2017-00111

Seeram, N. P., Henning, S. M., Zhang, Y., Suchard, M., Li, Z., & Heber, D. (2006). Pomegranate juice ellagitannin metabolites are present in human plasma and some persist in urine for up to 48 hours. *Journal of Nutrition, 136*(10), 2481-2485. doi:10.1093/jn/136.10.2481

Sehl, M. E., & Yates, F. E. (2001). Kinetics of Human AgingI. Rates of Senescence Between Ages 30 and 70 Years in Healthy People. *The Journals of Gerontology: Series A, 56*(5), B198-B208. doi:10.1093/gerona/56.5.B198

Seidell, J. C., & Halberstadt, J. (2015). The Global Burden of Obesity and the Challenges of Prevention. *Annals of Nutrition and Metabolism, 66(suppl 2)*(Suppl. 2), 7-12. doi:10.1159/000375143

Sell, H., Eckardt, K., Taube, A., Tews, D., Gurgui, M., Echten-Deckert, G. V., & Eckel, J. (2008). Skeletal muscle insulin resistance induced by adipocyte-conditioned medium: underlying mechanisms and reversibility. *American Journal of Physiology-Endocrinology and Metabolism, 294*(6), E1070-E1077. doi:10.1152/ajpendo.00529.2007

Sengle, G., Ono, R. N., Sasaki, T., & Sakai, L. Y. (2011). Prodomains of transforming growth factor beta (TGFbeta) superfamily members specify different functions: extracellular matrix interactions and growth factor bioavailability. *Journal of Biological Chemistry, 286*(7), 5087-5099. doi:10.1074/jbc.M110.188615

Seo, K., Suzuki, T., Kobayashi, K., & Nishimura, T. (2019). Adipocytes suppress differentiation of muscle cells in a co-culture system. *Anim Sci J, 90*(3), 423-434. doi:10.1111/asj.13145

Sergi, D., Naumovski, N., Heilbronn, L. K., Abeywardena, M., O'Callaghan, N., Lionetti, L., & Luscombe-Marsh, N. (2019). Mitochondrial (Dys)function and Insulin Resistance: From Pathophysiological Molecular Mechanisms to the Impact of Diet. *Frontiers in Physiology, 10*. doi:10.3389/fphys.2019.00532

Seyoum, B., Fite, A., & Abou-Samra, A. B. (2011). Effects of 3T3 adipocytes on interleukin-6 expression and insulin signaling in L6 skeletal muscle cells. *Biochemical and Biophysical Research Communications, 410*(1), 13-18. doi:10.1016/j.bbrc.2011.05.073

Shahini, A., Vydiam, K., Choudhury, D., Rajabian, N., Nguyen, T., Lei, P., & Andreadis, S. T. (2018). Efficient and high yield isolation of myoblasts from skeletal muscle. *Stem Cell Research, 30*, 122-129. doi:https://doi.org/10.1016/j.scr.2018.05.017

Shan, T., Liang, X., Bi, P., & Kuang, S. (2013). Myostatin knockout drives browning of white adipose tissue through activating the AMPK-PGC1alpha-Fndc5 pathway in muscle. *FASEB Journal, 27*(5), 1981-1989. doi:10.1096/fj.12-225755

Shanely, R. A., Zwetsloot, K. A., Triplett, N. T., Meaney, M. P., Farris, G. E., & Nieman, D. C. (2014). Human skeletal muscle biopsy procedures using the modified Bergstrom technique. *J Vis Exp*(91), 51812. doi:10.3791/51812

Shankar, A., McMunn, A., Demakakos, P., Hamer, M., & Steptoe, A. (2017). Social isolation and loneliness: Prospective associations with functional status in older adults. *Health Psychology, 36*(2), 179-187. doi:10.1037/hea0000437

Sharma, M., Kambadur, R., Matthews, K. G., Somers, W. G., Devlin, G. P., Conaglen, J. V., . . . Bass, J. J. (1999). Myostatin, a transforming growth factor-beta superfamily member, is expressed in heart muscle and is upregulated in cardiomyocytes after infarct. *Journal of Cellular Physiology, 180*(1), 1-9. doi:10.1002/(sici)1097-4652(199907)180:1<1::Aid-jcp1>3.0.Co;2-v

Sharp, M., Lowery, R. P., Shields, K., Ormes, J., McCleary, S. A., Rauch, J., . . . Wilson, J. M. (2014). The effects of a myostatin inhibitor on lean body mass, strength, and power in resistance trained males. *Journal of the International Society of Sports Nutrition, 11*(Suppl 1), P42-P42. doi:10.1186/1550-2783-11-S1-P42

Shaw, L. M. (2011). The insulin receptor substrate (IRS) proteins. *Cell Cycle, 10*(11), 1750-1756. doi:10.4161/cc.10.11.15824

Shoelson, S. E., Lee, J., & Goldfine, A. B. (2006). Inflammation and insulin resistance. *The Journal of clinical investigation, 116*(7), 1793-1801. doi:10.1172/JCI29069

Shulman, G. I. (2000). Cellular mechanisms of insulin resistance. *Journal of Clinical Investigation, 106*(2), 171-176. doi:10.1172/jci10583

Siiteri, P. K. (1987). Adipose tissue as a source of hormones. *American Journal of Clinical Nutrition, 45*(1 Suppl), 277-282. doi:10.1093/ajcn/45.1.277

Silbernagle, S. D., Agamemnon. (2015). *Color Atlas of Physiology* (7th ed.). Stuttgart, DE: Theime.

Simoes, A. E., Pereira, D. M., Amaral, J. D., Nunes, A. F., Gomes, S. E., Rodrigues, P. M., . . . Rodrigues, C. M. (2013). Efficient recovery of proteins from multiple source samples after TRIzol((R)) or TRIzol((R))LS RNA extraction and long-term storage. *BMC Genomics, 14*, 181. doi:10.1186/1471-2164-14-181

Singh, A., D'Amico, D., Andreux, P. A., Dunngalvin, G., Kern, T., Blanco-Bose, W., . . . Rinsch, C. (2022). Direct supplementation with Urolithin A overcomes limitations of dietary exposure and gut microbiome variability in healthy adults to achieve consistent levels across the population. *European Journal of Clinical Nutrition, 76*(2), 297-308. doi:10.1038/s41430-021-00950-1

Singh, K., & Dilworth, F. J. (2013). Differential modulation of cell cycle progression distinguishes members of the myogenic regulatory factor family of transcription factors. *Febs j, 280*(17), 3991-4003. doi:10.1111/febs.12188

Sinha, S., Perdomo, G., Brown, N. F., & O'Doherty, R. M. (2004). Fatty acid-induced insulin resistance in L6 myotubes is prevented by inhibition of activation and nuclear localization of nuclear factor kappa B. *Journal of Biological Chemistry, 279*(40), 41294-41301. doi:10.1074/jbc.M406514200

Siriett, V., Salerno, M. S., Berry, C., Nicholas, G., Bower, R., Kambadur, R., & Sharma, M. (2007). Antagonism of Myostatin Enhances Muscle Regeneration During Sarcopenia. *Molecular Therapy, 15*(8), 1463-1470. doi:https://doi.org/10.1038/sj.mt.6300182

Smeuninx, B., McKendry, J., Wilson, D., Martin, U., & Breen, L. (2017). Age-Related Anabolic Resistance of Myofibrillar Protein Synthesis Is Exacerbated in Obese Inactive Individuals. *Journal of Clinical Endocrinology and Metabolism, 102*(9), 3535-3545. doi:10.1210/jc.2017-00869

Smiles, W. J., Churchward-Venne, T. A., van Loon, L. J. C., Hawley, J. A., & Camera, D. M. (2019). A single bout of strenuous exercise overcomes lipid-induced anabolic resistance to protein ingestion in overweight, middle-aged men. *FASEB journal: official publication of the Federation of American*

Societies for Experimental Biology, fj201801917R. doi:10.1096/fj.201801917R

Smith, R. C., & Lin, B. K. (2013). Myostatin inhibitors as therapies for muscle wasting associated with cancer and other disorders. *Current opinion in supportive and palliative care, 7*(4), 352-360. doi:10.1097/SPC.0000000000000013

Snijders, T., Nederveen, J. P., McKay, B. R., Joanisse, S., Verdijk, L. B., van Loon, L. J. C., & Parise, G. (2015). Satellite cells in human skeletal muscle plasticity. *Frontiers in Physiology, 6*. doi:10.3389/fphys.2015.00283

Sokolowska, E., & Blachnio-Zabielska, A. (2019). The Role of Ceramides in Insulin Resistance. *Frontiers in Endocrinology, 10*. doi:10.3389/fendo.2019.00577

Son, J. J., H., Lee, S., Kim, D., & Yoo, S. (2012). Sarcopenic phenotype in patients with newly diagnosed type 2 diabetes. *Endocrine Abstracts*(29), 544.

Song, N. J., Kim, S., Jang, B. H., Chang, S. H., Yun, U. J., Park, K. M., . . . Park, K. W. (2016). Small Molecule-Induced Complement Factor D (Adipsin) Promotes Lipid Accumulation and Adipocyte Differentiation. *PloS One, 11*(9), e0162228. doi:10.1371/journal.pone.0162228

Soverini, V., Moscatiello, S., Villanova, N., Ragni, E., Di Domizio, S., & Marchesini, G. (2010). Metabolic Syndrome and Insulin Resistance in Subjects with Morbid Obesity. *Obesity Surgery, 20*(3), 295-301. doi:10.1007/s11695-009-9999-z

Spiller, M. P., Kambadur, R., Jeanplong, F., Thomas, M., Martyn, J. K., Bass, J. J., & Sharma, M. (2002). The myostatin gene is a downstream target gene of basic helix-loop-helix transcription factor MyoD. *Molecular and Cellular Biology, 22*(20), 7066-7082. doi:10.1128/mcb.22.20.7066-7082.2002

St-Onge, M. P. (2005). Relationship between body composition changes and changes in physical function and metabolic risk factors in aging. *Current Opinion in Clinical Nutrition and Metabolic Care, 8*(5), 523-528.

Stanford, K. I., Middelbeek, R. J. W., Townsend, K. L., Lee, M.-Y., Takahashi, H., So, K., . . . Goodyear, L. J. (2015). A novel role for subcutaneous adipose tissue in exercise-induced improvements in glucose homeostasis. *Diabetes, 64*(6), 2002-2014. doi:10.2337/db14-0704

Steculorum, S. M., Ruud, J., Karakasilioti, I., Backes, H., Engström Ruud, L., Timper, K., . . . Brüning, J. C. (2016). AgRP Neurons Control Systemic Insulin Sensitivity via Myostatin Expression in Brown Adipose Tissue. *Cell, 165*(1), 125-138. doi:https://doi.org/10.1016/j.cell.2016.02.044

Stephen, W. C., & Janssen, I. (2009). Sarcopenic-obesity and cardiovascular disease risk in the elderly. *The Journal of Nutrition, Health & Aging, 13*(5), 460-466. doi:10.1007/s12603-009-0084-z

Stephens, F. B., Chee, C., Wall, B. T., Murton, A. J., Shannon, C. E., van Loon, L. J., & Tsintzas, K. (2015). Lipid-induced insulin resistance is associated with an impaired skeletal muscle protein synthetic response to amino acid ingestion in healthy young men. *Diabetes, 64*(5), 1615-1620. doi:10.2337/db14-0961

Stephens, F. B., Mendis, B., Shannon, C. E., Cooper, S., Ortori, C. A., Barrett, D. A., . . . Tsintzas, K. (2014). Fish oil omega-3 fatty acids partially prevent lipid-induced insulin resistance in human skeletal muscle without limiting acylcarnitine accumulation. *Clinical Science (London, England: 1979), 127*(5), 315-322. doi:10.1042/cs20140031

Stephens, J. M., Lee, J., & Pilch, P. F. (1997). Tumor necrosis factor-alpha-induced insulin resistance in 3T3-L1 adipocytes is accompanied by a loss of insulin receptor substrate-1 and GLUT4 expression without a loss of insulin receptor-mediated signal transduction. *Journal of Biological Chemistry, 272*(2), 971-976.

Storgaard, H., Jensen, C. B., Björnholm, M., Song, X. M., Madsbad, S., Zierath, J. R., & Vaag, A. A. (2004). Dissociation between fat-induced in vivo insulin resistance and proximal insulin signaling in skeletal muscle in men at risk for type 2 diabetes. *The Journal of Clinical Endocrinology and Metabolism, 89*(3), 1301-1311. doi:10.1210/jc.2003-031243

Straczkowski, M., Kowalska, I., Nikolajuk, A., Dzienis-Straczkowska, S., Kinalska, I., Baranowski, M., . . . Gorski, J. (2004). Relationship between insulin sensitivity and sphingomyelin signaling pathway in human skeletal muscle. *Diabetes, 53*(5), 1215-1221. doi:10.2337/diabetes.53.5.1215

Strasser, B. (2013). Physical activity in obesity and metabolic syndrome. *Annals of the New York Academy of Sciences, 1281*(1), 141-159. doi:https://doi.org/10.1111/j.1749-6632.2012.06785.x

Stratford, S., Hoehn, K. L., Liu, F., & Summers, S. A. (2004). Regulation of insulin action by ceramide: dual mechanisms linking ceramide accumulation to the inhibition of Akt/protein kinase B. *Journal of Biological Chemistry, 279*(35), 36608-36615. doi:10.1074/jbc.M406499200

Suckale, J., & Solimena, M. (2008). Pancreas islets in metabolic signaling--focus on the beta-cell. *Frontiers in Bioscience, 13*, 7156-7171.

Sugita, S., Kamei, Y., Oka, J., Suganami, T., & Ogawa, Y. (2007). Macrophage-colony stimulating factor in obese adipose tissue: studies with heterozygous op/+ mice. *Obesity (Silver Spring), 15*(8), 1988-1995. doi:10.1038/oby.2007.237

Summers, S. A. (2006). Ceramides in insulin resistance and lipotoxicity. *Progress in Lipid Research, 45*(1), 42-72. doi:10.1016/j.plipres.2005.11.002

Sundaram, V. K., Sampathkumar, N. K., Massaad, C., & Grenier, J. (2019). Optimal use of statistical methods to validate reference gene stability in longitudinal studies. *PloS One, 14*(7), e0219440. doi:10.1371/journal.pone.0219440

Szendroedi, J., Yoshimura, T., Phielix, E., Koliaki, C., Marcucci, M., Zhang, D., . . . Roden, M. (2014). Role of diacylglycerol activation of PKCθ in lipid-induced muscle insulin resistance in humans. *Proceedings of the National Academy of Sciences, 111*(26), 9597-9602. doi:doi:10.1073/pnas.1409229111

Takahashi, H., Kotani, K., Tanaka, K., Egucih, Y., & Anzai, K. (2018). Therapeutic Approaches to Nonalcoholic Fatty Liver Disease: Exercise Intervention and Related Mechanisms. *Frontiers in Endocrinology, 9*(588). doi:10.3389/fendo.2018.00588

Takao, N., Kurose, S., Miyauchi, T., Onishi, K., Tamanoi, A., Tsuyuguchi, R., . . . Kimura, Y. (2021). The relationship between changes in serum myostatin and adiponectin levels in patients with obesity undergoing a weight loss program. *BMC Endocrine Disorders, 21*(1), 147. doi:10.1186/s12902-021-00808-4

Tam, C. S., Xie, W., Johnson, W. D., Cefalu, W. T., Redman, L. M., & Ravussin, E. (2012). Defining Insulin Resistance From Hyperinsulinemic-Euglycemic Clamps. *Diabetes Care, 35*(7), 1605-1610. doi:10.2337/dc11-2339

Tardif, N., Salles, J., Guillet, C., Tordjman, J., Reggio, S., Landrier, J. F., . . . Walrand, S. (2014). Muscle ectopic fat deposition contributes to anabolic resistance in obese sarcopenic old rats through eIF2alpha activation. *Aging Cell, 13*(6), 1001-1011. doi:10.1111/acel.12263

Taylor, R. (1990). Interpretation of the correlation coefficient: a basic review. *Journal of diagnostic medical sonography, 6*(1), 35-39.

Taylor, R. (2008). Pathogenesis of type 2 diabetes: tracing the reverse route from cure to cause. *Diabetologia, 51*(10), 1781-1789. doi:10.1007/s00125-008-1116-7

Taylor, R. (2013). Banting Memorial lecture 2012: reversing the twin cycles of type 2 diabetes. *Diabetic Medicine: A Journal of the British Diabetic Association, 30*(3), 267-275. doi:10.1111/dme.12039

Taylor, W. E., Bhasin, S., Artaza, J., Byhower, F., Azam, M., Darril H. Willard, J., . . . Gonzalez-Cadavid, N. (2001). Myostatin inhibits cell proliferation and protein synthesis in C2C12 muscle cells. *American Journal of Physiology-Endocrinology and Metabolism, 280*(2), E221-E228. doi:10.1152/ajpendo.2001.280.2.E221

Thalacker-Mercer, A. E., Dell'Italia, L. J., Cui, X., Cross, J. M., & Bamman, M. M. (2010). Differential genomic responses in old vs. young humans despite similar levels of modest muscle damage after resistance loading. *Physiological Genomics, 40*(3), 141-149. doi:10.1152/physiolgenomics.00151.2009

Therakomen, V., Petchlorlian, A., & Lakananurak, N. (2020). Prevalence and risk factors of primary sarcopenia in community-dwelling outpatient elderly: a cross-sectional study. *Scientific Reports, 10*(1), 19551-19551. doi:10.1038/s41598-020-75250-y

Thiebaud, D., Jacot, E., Defronzo, R. A., Maeder, E., Jequier, E., & Felber, J.-P. (1982). The Effect of Graded Doses of Insulin on Total Glucose Uptake, Glucose Oxidation, and Glucose Storage in Man. *Diabetes, 31*(11), 957-963. doi:10.2337/diacare.31.11.957

Thijssen, E., van Caam, A., & van der Kraan, P. M. (2014). Obesity and osteoarthritis, more than just wear and tear: pivotal roles for inflamed adipose tissue and dyslipidaemia in obesity-induced osteoarthritis. *Rheumatology, 54*(4), 588-600. doi:10.1093/rheumatology/keu464

Thomas, M., Langley, B., Berry, C., Sharma, M., Kirk, S., Bass, J., & Kambadur, R. (2000). Myostatin, a Negative Regulator of Muscle Growth, Functions by Inhibiting Myoblast Proliferation. *Journal of Biological Chemistry, 275*(51), 40235-40243. doi:10.1074/jbc.M004356200

Thompson, D. B., Pratley, R., & Ossowski, V. (1996). Human primary myoblast cell cultures from non-diabetic insulin resistant subjects retain defects in insulin action. *The Journal of clinical investigation, 98*(10), 2346-2350. doi:10.1172/JCI119046

Timmers, S., Schrauwen, P., & de Vogel, J. (2008). Muscular diacylglycerol metabolism and insulin resistance. *Physiology and Behavior, 94*(2), 242-251. doi:10.1016/j.physbeh.2007.12.002

Tkach, M., & Théry, C. (2016). Communication by Extracellular Vesicles: Where We Are and Where We Need to Go. *Cell, 164*(6), 1226-1232. doi:10.1016/j.cell.2016.01.043

Tomás-Barberan, F. A., Espín, J. C., & García-Conesa, M. T. Bioavailability and Metabolism of Ellagic Acid and Ellagitannins. In *Chemistry and Biology of Ellagitannins* (pp. 273-297).

Tomás-Barberán, F. A., González-Sarrías, A., García-Villalba, R., Núñez-Sánchez, M. A., Selma, M. V., García-Conesa, M. T., & Espín, J. C. (2017). Urolithins, the rescue of "old" metabolites to understand a "new" concept: Metabotypes as a nexus among phenolic metabolism, microbiota dysbiosis, and host health status. *Molecular Nutrition & Food Research, 61*(1). doi:10.1002/mnfr.201500901

Tominaga, K., & Suzuki, H. I. (2019). TGF-beta Signaling in Cellular Senescence and Aging-Related Pathology. *International Journal of Molecular Sciences, 20*(20). doi:10.3390/ijms20205002

Toney, A. M., Fan, R., Xian, Y., Chaidez, V., Ramer-Tait, A. E., & Chung, S. (2019). Urolithin A, a Gut Metabolite, Improves Insulin Sensitivity Through Augmentation of Mitochondrial Function and Biogenesis. *Obesity, 27*(4), 612-620. doi:https://doi.org/10.1002/oby.22404

Torabi, S., & DiMarco, N. M. (2016). Original Research: Polyphenols extracted from grape powder induce lipogenesis and glucose uptake during differentiation of murine preadipocytes. *Experimental Biology and Medicine, 241*(16), 1776-1785. doi:10.1177/1535370216645213

Tornatore, L., Thotakura, A. K., Bennett, J., Moretti, M., & Franzoso, G. (2012). The nuclear factor kappa B signaling pathway: integrating metabolism with inflammation. *Trends in Cell Biology, 22*(11), 557-566. doi:https://doi.org/10.1016/j.tcb.2012.08.001

Touchberry, C. D., Wacker, M. J., Richmond, S. R., Whitman, S. A., & Godard, M. P. (2006). Age-related changes in relative expression of real-time PCR housekeeping genes in human skeletal muscle. *Journal of biomolecular techniques : JBT, 17*(2), 157-162.

Trendelenburg, A. U., Meyer, A., Rohner, D., Boyle, J., Hatakeyama, S., & Glass, D. J. (2009). Myostatin reduces Akt/TORC1/p70S6K signaling, inhibiting myoblast differentiation and myotube size. *American Journal of Physiology: Cell Physiology, 296*(6), C1258-1270. doi:10.1152/ajpcell.00105.2009

Trenerry, M. K., Carey, K. A., Ward, A. C., Farnfield, M. M., & Cameron-Smith, D. (2008). Exercise-induced activation of STAT3 signaling is increased with age. *Rejuvenation Res, 11*(4), 717-724. doi:10.1089/rej.2007.0643

Tsao, J., Vernet, D. A., Gelfand, R., Kovanecz, I., Nolazco, G., Bruhn, K. W., & Gonzalez-Cadavid, N. F. (2013). Myostatin genetic inactivation inhibits myogenesis by muscle-derived stem cells in vitro but not when implanted in the mdx mouse muscle. *Stem Cell Research & Therapy, 4*(1), 4. doi:10.1186/scrt152

Tsekoura, M., Kastrinis, A., Katsoulaki, M., Billis, E., & Gliatis, J. (2017). Sarcopenia and Its Impact on Quality of Life. *Advances in Experimental Medicine and Biology, 987*, 213-218. doi:10.1007/978-3-319-57379-3_19

Tsintzas, K., Chokkalingam, K., Jewell, K., Norton, L., Macdonald, I. A., & Constantin-Teodosiu, D. (2007). Elevated free fatty acids attenuate the insulin-induced suppression of PDK4 gene expression in human skeletal muscle: potential role of intramuscular long-chain acyl-coenzyme A. *Journal of Clinical Endocrinology and Metabolism, 92*(10), 3967-3972. doi:10.1210/jc.2007-1104

Tsintzas, K., Jones, R., Pabla, P., Mallinson, J., Barrett, D. A., Dong-Hyun, K., . . . Stephens, F. B. (2020). Effect of acute and short-term dietary fat ingestion on postprandial skeletal muscle protein synthesis rates in middle-aged, overweight, and obese men. *American Journal of Physiology-Endocrinology and Metabolism, 318*(3), E417-E429. doi:10.1152/ajpendo.00344.2019

Tsintzas, K., Norton, L., Chokkalingam, K., Nizamani, N., Cooper, S., Stephens, F., . . . Bennett, A. (2013). Independent and combined effects of acute physiological hyperglycaemia and hyperinsulinaemia on metabolic gene expression in human skeletal muscle. *Clinical Science, 124*(11), 675-686. doi:10.1042/cs20120481

Tsuchida, K., Nakatani, M., Hitachi, K., Uezumi, A., Sunada, Y., Ageta, H., & Inokuchi, K. (2009). Activin signaling as an emerging target for therapeutic interventions. *Cell Commun Signal, 7*, 15. doi:10.1186/1478-811x-7-15

Tsukuba, T., Okamoto, K., Yasuda, Y., Morikawa, W., Nakanishi, H., & Yamamoto, K. (2000). New Functional Aspects of Cathepsin D and Cathepsin E. *Molecules and Cells, 10*(6), 601-611. doi:10.1007/s10059-000-0601-8

Turcotte, L. P., Kiens, B., & Richter, E. A. (1991). Saturation kinetics of palmitate uptake in perfused skeletal muscle. *FEBS Letters, 279*(2), 327-329. doi:10.1016/0014-5793(91)80180-b

Turinsky, J., O'Sullivan, D. M., & Bayly, B. P. (1990). 1,2-Diacylglycerol and ceramide levels in insulin-resistant tissues of the rat in vivo. *The Journal of biological chemistry, 265*(28), 16880-16885. Retrieved from http://www.ncbi.nlm.nih.gov/pubmed/2211599

Turner, D. C., Gorski, P. P., Maasar, M. F., Seaborne, R. A., Baumert, P., Brown, A. D., . . . Sharples, A. P. (2020). DNA methylation across the genome in aged human skeletal muscle tissue and muscle-derived cells: the role of HOX genes and physical activity. *Scientific Reports, 10*(1), 15360. doi:10.1038/s41598-020-72730-z

Turner, N., Kowalski, G. M., Leslie, S. J., Risis, S., Yang, C., Lee-Young, R. S., . . . Bruce, C. R. (2013). Distinct patterns of tissue-specific lipid accumulation during the induction of insulin resistance in mice by high-fat feeding. *Diabetologia, 56*(7), 1638-1648. doi:10.1007/s00125-013-2913-1

van der Steeg, G. E., & Takken, T. (2021). Reference values for maximum oxygen uptake relative to body mass in Dutch/Flemish subjects aged 6-65 years: the LowLands Fitness Registry. *European Journal of Applied Physiology, 121*(4), 1189-1196. doi:10.1007/s00421-021-04596-6

van der Vusse, G. J. (2009). Albumin as fatty acid transporter. *Drug Metabolism and Pharmacokinetics, 24*(4), 300-307. doi:10.2133/dmpk.24.300

Van Harmelen, V., Reynisdottir, S., Cianflone, K., Degerman, E., Hoffstedt, J., Nilsell, K., . . . Arner, P. (1999). Mechanisms involved in the regulation of free fatty acid release from isolated human fat cells by acylation-stimulating protein and insulin. *Journal of Biological Chemistry, 274*(26), 18243-18251. doi:10.1074/jbc.274.26.18243

Vaux, D. L., Fidler, F., & Cumming, G. (2012). Replicates and repeats—what is the difference and is it significant? *EMBO Rep, 13*(4), 291-296. doi:https://doi.org/10.1038/embor.2012.36

Vessby, B., Uusitupa, M., Hermansen, K., Riccardi, G., Rivellese, A. A., Tapsell, L. C., . . . Storlien, L. H. (2001). Substituting dietary saturated for monounsaturated fat impairs insulin sensitivity in healthy men and women: The KANWU Study. *Diabetologia, 44*(3), 312-319. doi:10.1007/s001250051620

Visser, M., Bouter, L. M., McQuillan, G. M., Wener, M. H., & Harris, T. B. (1999). Elevated C-Reactive Protein Levels in Overweight and Obese Adults. *JAMA, 282*(22), 2131-2135. doi:10.1001/jama.282.22.2131

Vistisen, B., Hellgren, L. I., Vadset, T., Scheede-Bergdahl, C., Helge, J. W., Dela, F., & Stallknecht, B. (2008). Effect of gender on lipid-induced insulin

resistance in obese subjects. *European Journal of Endocrinology of the European Federation of Endocrine Societies, 158*(1), 61-68. doi:10.1530/eje-07-0493

Volanakis, J. E., & Narayana, S. V. L. (1996). Complement factor D, a novel serine protease. *Protein Science, 5*(4), 553-564. doi:https://doi.org/10.1002/pro.5560050401

Volpi, E., Mittendorfer, B., Rasmussen, B. B., & Wolfe, R. R. (2000). The response of muscle protein anabolism to combined hyperaminoacidemia and glucose-induced hyperinsulinemia is impaired in the elderly. *The Journal of Clinical Endocrinology and Metabolism, 85*(12), 4481-4490. doi:10.1210/jcem.85.12.7021

von Frankenberg, A. D., Marina, A., Song, X., Callahan, H. S., Kratz, M., & Utzschneider, K. M. (2017). A high-fat, high-saturated fat diet decreases insulin sensitivity without changing intra-abdominal fat in weight-stable overweight and obese adults. *European Journal of Nutrition, 56*(1), 431-443. doi:10.1007/s00394-015-1108-6

von Haehling, S., Morley, J. E., & Anker, S. D. (2010). An overview of sarcopenia: facts and numbers on prevalence and clinical impact. *Journal of Cachexia, Sarcopenia and Muscle, 1*(2), 129-133. doi:10.1007/s13539-010-0014-2

Vu, V., Dadson, K., Odisho, T., Kim, W., Zhou, X., Thong, F., & Sweeney, G. (2011). Temporal analysis of mechanisms leading to stimulation of glucose uptake in skeletal muscle cells by an adipokine mixture derived from primary rat adipocytes. *International Journal of Obesity, 35*(3), 355-363. doi:10.1038/ijo.2010.160

Wagner, K. R., Fleckenstein, J. L., Amato, A. A., Barohn, R. J., Bushby, K., Escolar, D. M., . . . Mendell, J. R. (2008). A phase I/IItrial of MYO-029 in adult subjects with muscular dystrophy. *Annals of Neurology, 63*(5), 561-571. doi:10.1002/ana.21338

Wagner, K. R., Liu, X., Chang, X., & Allen, R. E. (2005). Muscle regeneration in the prolonged absence of myostatin. *Proceedings of the National Academy of Sciences, 102*(7), 2519-2524. doi:doi:10.1073/pnas.0408729102

Walker, R. G., McCoy, J. C., Czepnik, M., Mills, M. J., Hagg, A., Walton, K. L., . . . Thompson, T. B. (2018). Molecular characterization of latent GDF8 reveals mechanisms of activation. *Proceedings of the National Academy of Sciences of the United States of America, 115*(5), E866-E875. doi:10.1073/pnas.1714622115

Wall, B. T., Gorissen, S. H., Pennings, B., Koopman, R., Groen, B. B., Verdijk, L. B., & van Loon, L. J. (2015). Aging Is Accompanied by a Blunted Muscle Protein Synthetic Response to Protein Ingestion. *PloS One, 10*(11), e0140903. doi:10.1371/journal.pone.0140903

Wang, D.-T., Yang, Y.-J., Huang, R.-H., Zhang, Z.-H., & Lin, X. (2015). Myostatin Activates the Ubiquitin-Proteasome and Autophagy-Lysosome Systems Contributing to Muscle Wasting in Chronic Kidney Disease. *Oxidative Medicine and Cellular Longevity, 2015*, 684965-684965. doi:10.1155/2015/684965

Wang, H., & Wang, B. (2016). Extracellular vesicle microRNAs mediate skeletal muscle myogenesis and disease. *Biomedical reports, 5*(3), 296-300. doi:10.3892/br.2016.725

Wang, H., & Ye, J. (2015). Regulation of energy balance by inflammation: common theme in physiology and pathology. *Reviews in Endocrine & Metabolic Disorders, 16*(1), 47-54. doi:10.1007/s11154-014-9306-8

Wang, M., Yu, H., Kim, Y. S., Bidwell, C. A., & Kuang, S. (2012). Myostatin facilitates slow and inhibits fast myosin heavy chain expression during myogenic differentiation. *Biochemical and Biophysical Research Communications, 426*(1), 83-88. doi:https://doi.org/10.1016/j.bbrc.2012.08.040

Wang, Y., Lam, K. S. L., Kraegen, E. W., Sweeney, G., Zhang, J., Tso, A. W., . . . Xu, A. (2007). Lipocalin-2 Is an Inflammatory Marker Closely Associated with Obesity, Insulin Resistance, and Hyperglycemia in Humans. *Clinical Chemistry, 53*(1), 34-41. doi:10.1373/clinchem.2006.075614

Wannamethee, S. G., & Atkins, J. L. (2015). Muscle loss and obesity: the health implications of sarcopenia and sarcopenic obesity. *Proceedings of the Nutrition Society, 74*(4), 405-412. doi:10.1017/S002966511500169X

Warram, J. H., Martin, B. C., Krolewski, A. S., Soeldner, J. S., & Kahn, C. R. (1990). Slow glucose removal rate and hyperinsulinemia precede the development of type II diabetes in the offspring of diabetic parents. *Annals of Internal Medicine, 113*(12), 909-915. doi:10.7326/0003-4819-113-12-909

Wasserman, D. H. (2009). Four grams of glucose. *American Journal of Physiology: Endocrinology and Metabolism, 296*(1), E11-21. doi:10.1152/ajpendo.90563.2008

Watts, R., McAinch, A. J., Dixon, J. B., O'Brien, P. E., & Cameron-Smith, D. (2013). Increased Smad signaling and reduced MRF expression in skeletal muscle from obese subjects. *Obesity, 21*(3), 525-528. doi:https://doi.org/10.1002/oby.20070

Weisberg, S. P., McCann, D., Desai, M., Rosenbaum, M., Leibel, R. L., & Ferrante, A. W., Jr. (2003). Obesity is associated with macrophage accumulation in adipose tissue. *Journal of Clinical Investigation, 112*(12), 1796-1808. doi:10.1172/jci19246

Weiss, M., Steiner, D. F., & Philipson, L. H. (2000). Insulin Biosynthesis, Secretion, Structure and Structure-Activity Relationships. In *Endotext*. South Dartmouth, MA.

Welle, S., Bhatt, K., Shah, B., & Thornton, C. (2002). Insulin-like growth factor-1 and myostatin mRNA expression in muscle: comparison between 62-77 and 21-31 yr old men. *Experimental Gerontology, 37*(6), 833-839. doi:10.1016/s0531-5565(02)00025-6

Welle, S. L. (2009). Myostatin and muscle fiber size. Focus on "Smad2 and 3 transcription factors control muscle mass in adulthood" and "Myostatin reduces Akt/TORC1/p70S6K signaling, inhibiting myoblast differentiation and myotube size". *American Journal of Physiology: Cell Physiology, 296*(6), C1245-1247. doi:10.1152/ajpcell.00154.2009

Welsh, G. I., Hers, I., Berwick, D. C., Dell, G., Wherlock, M., Birkin, R., . . . Tavare, J. M. (2005). Role of protein kinase B in insulin-regulated glucose uptake. *Biochemical Society Transactions, 33*(Pt 2), 346-349. doi:10.1042/bst0330346

White, R. T., Damm, D., Hancock, N., Rosen, B. S., Lowell, B. B., Usher, P., . . . Spiegelman, B. M. (1992). Human adipsin is identical to complement factor D and is expressed at high levels in adipose tissue. *Journal of Biological Chemistry, 267*(13), 9210-9213. doi:https://doi.org/10.1016/S0021-9258(19)50409-4

White, T. A., & LeBrasseur, N. K. (2014). Myostatin and sarcopenia: opportunities and challenges - a mini-review. *Gerontology, 60*(4), 289-293. doi:10.1159/000356740

Whitman, S. A., Wacker, M. J., Richmond, S. R., & Godard, M. P. (2005). Contributions of the ubiquitin–proteasome pathway and apoptosis to human skeletal muscle wasting with age. *Pflügers Archiv, 450*(6), 437-446. doi:10.1007/s00424-005-1473-8

Wildman, R. P., Muntner, P., Reynolds, K., & et al. (2008). The obese without cardiometabolic risk factor clustering and the normal weight with cardiometabolic risk factor clustering: Prevalence and correlates of 2 phenotypes among the us population (nhanes 1999-2004). *Archives of Internal Medicine, 168*(15), 1617-1624. doi:10.1001/archinte.168.15.1617

Wilhelmsen, A., Tsintzas, K., & Jones, S. W. (2021). Recent advances and future avenues in understanding the role of adipose tissue cross talk in mediating skeletal muscle mass and function with ageing. *GeroScience, 43*(1), 85-110. doi:10.1007/s11357-021-00322-4

Wilkinson, D. J., Piasecki, M., & Atherton, P. J. (2018). The age-related loss of skeletal muscle mass and function: Measurement and physiology of muscle fibre atrophy and muscle fibre loss in humans. *Ageing Res Rev, 47*, 123-132. doi:https://doi.org/10.1016/j.arr.2018.07.005

Willoughby, D. S. (2004). Effects of an alleged myostatin-binding supplement and heavy resistance training on serum myostatin, muscle strength and mass, and body composition. *International Journal of Sport Nutrition and Exercise Metabolism, 14*(4), 461-472. doi:10.1123/ijsnem.14.4.461

Wilt, F. H., & Hake, S. (2004). Principles of developmental biology.

Wolfman, N. M., McPherron, A. C., Pappano, W. N., Davies, M. V., Song, K., Tomkinson, K. N., . . . Lee, S.-J. (2003). Activation of latent myostatin by the BMP-1/tolloid family of metalloproteinases. *Proceedings of the National Academy of Sciences, 100*(26), 15842-15846. doi:10.1073/pnas.2534946100

Woodworth-Hobbs, M. E., Hudson, M. B., Rahnert, J. A., Zheng, B., Franch, H. A., & Price, S. R. (2014). Docosahexaenoic acid prevents palmitate-induced activation of proteolytic systems in C2C12 myotubes. *The Journal of Nutritional Biochemistry, 25*(8), 868-874. doi:10.1016/j.jnutbio.2014.03.017

Woodworth-Hobbs, M. E., Perry, B. D., Rahnert, J. A., Hudson, M. B., Zheng, B., & Price, S. R. (2017). Docosahexaenoic acid counteracts palmitate-induced endoplasmic reticulum stress in C2C12 myotubes: Impact on muscle atrophy. *Physiol Rep, 5*(23), e13530. doi:https://doi.org/10.14814/phy2.13530

Wroblewski, A. P., Amati, F., Smiley, M. A., Goodpaster, B., & Wright, V. (2011). Chronic exercise preserves lean muscle mass in masters athletes. *Physician and Sportsmedicine, 39*(3), 172-178. doi:10.3810/psm.2011.09.1933

Wu, H., & Ballantyne, C. M. (2017). Skeletal muscle inflammation and insulin resistance in obesity. *The Journal of clinical investigation, 127*(1), 43-54. doi:10.1172/JCI88880

Wu, H., Perrard, X. D., Wang, Q., Perrard, J. L., Polsani, V. R., Jones, P. H., . . . Ballantyne, C. M. (2010). CD11c expression in adipose tissue and blood and its role in diet-induced obesity. *Arteriosclerosis, Thrombosis, and Vascular Biology, 30*(2), 186-192. doi:10.1161/atvbaha.109.198044

Xia, B., Shi, X. C., Xie, B. C., Zhu, M. Q., Chen, Y., Chu, X. Y., . . . Wu, J. W. (2020). Urolithin A exerts antiobesity effects through enhancing adipose tissue thermogenesis in mice. *PLoS Biology, 18*(3), e3000688. doi:10.1371/journal.pbio.3000688

Xiao, C., Giacca, A., Carpentier, A., & Lewis, G. F. (2006). Differential effects of monounsaturated, polyunsaturated and saturated fat ingestion on glucose-stimulated insulin secretion, sensitivity and clearance in overweight and obese, non-diabetic humans. *Diabetologia, 49*(6), 1371-1379. doi:10.1007/s00125-006-0211-x

Xu, Q., Mariman, E. C. M., Goossens, G. H., Blaak, E. E., & Jocken, J. W. E. (2020). Cathepsin gene expression in abdominal subcutaneous adipose tissue of obese/overweight humans. *Adipocyte, 9*(1), 246-252. doi:10.1080/21623945.2020.1775035

Yaffe, D. (1968). Retention of differentiation potentialities during prolonged cultivation of myogenic cells. *Proceedings of the National Academy of Sciences of the United States of America, 61*(2), 477-483.

Yaffe, D., & Saxel, O. R. A. (1977). Serial passaging and differentiation of myogenic cells isolated from dystrophic mouse muscle. *Nature, 270*(5639), 725-727. doi:10.1038/270725a0

Yamakawa, H., Kusumoto, D., Hashimoto, H., & Yuasa, S. (2020). Stem Cell Aging in Skeletal Muscle Regeneration and Disease. *International Journal of Molecular Sciences, 21*(5), 1830. doi:10.3390/ijms21051830

Yamauchi, T., Kamon, J., Waki, H., Terauchi, Y., Kubota, N., Hara, K., . . . Kadowaki, T. (2001). The fat-derived hormone adiponectin reverses insulin resistance associated with both lipoatrophy and obesity. *Nature Medicine, 7*(8), 941-946. doi:10.1038/90984

Yan, Q. W., Yang, Q., Mody, N., Graham, T. E., Hsu, C. H., Xu, Z., . . . Rosen, E. D. (2007). The adipokine lipocalin 2 is regulated by obesity and promotes insulin resistance. *Diabetes, 56*(10), 2533-2540. doi:10.2337/db07-0007

Yang, J., Guo, Y., Henning, S. M., Chan, B., Long, J., Zhong, J., . . . Li, Z. (2020). Ellagic Acid and Its Microbial Metabolite Urolithin A Alleviate Diet-Induced Insulin Resistance in Mice. *Molecular Nutrition & Food Research, 64*(19), 2000091. doi:https://doi.org/10.1002/mnfr.202000091

Yang, M., Wei, D., Mo, C., Zhang, J., Wang, X., Han, X., . . . Xiao, H. (2013). Saturated fatty acid palmitate-induced insulin resistance is accompanied with myotube loss and the impaired expression of health benefit myokine genes in C2C12 myotubes. *Lipids in Health and Disease, 12*(1), 104. doi:10.1186/1476-511X-12-104

Yang, S.-N., & Berggren, P.-O. (2006). The Role of Voltage-Gated Calcium Channels in Pancreatic β-Cell Physiology and Pathophysiology. *Endocrine Reviews, 27*(6), 621-676. doi:10.1210/er.2005-0888

Yang, S. N., & Berggren, P. O. (2005). Beta-cell CaV channel regulation in physiology and pathophysiology. *American Journal of Physiology: Endocrinology and Metabolism, 288*(1), E16-28. doi:10.1152/ajpendo.00042.2004

Yang, W., Chen, Y., Zhang, Y., Wang, X., Yang, N., & Zhu, D. (2006). Extracellular signal-regulated kinase 1/2 mitogen-activated protein kinase pathway is involved in myostatin-regulated differentiation repression. *Cancer Research, 66*(3), 1320-1326. doi:10.1158/0008-5472.Can-05-3060

Yao, T., & Asayama, Y. (2017). Animal-cell culture media: History, characteristics, and current issues. *Reproductive Medicine and Biology, 16*(2), 99-117. doi:https://doi.org/10.1002/rmb2.12024

Yarasheski, K. E., Bhasin, S., Sinha-Hikim, I., Pak-Loduca, J., & Gonzalez-Cadavid, N. F. (2002). Serum myostatin-immunoreactive protein is increased in 60-92 year old women and men with muscle wasting. *The Journal of Nutrition, Health & Aging, 6*(5), 343-348. Retrieved from https://www.ncbi.nlm.nih.gov/pubmed/12474026

Yarmolinsky, M. B., & Haba, G. L. (1959). INHIBITION BY PUROMYCIN OF AMINO ACID INCORPORATION INTO PROTEIN. *Proceedings of the National Academy of Sciences of the United States of America, 45*(12), 1721-1729. doi:10.1073/pnas.45.12.1721

Yasar, E., Tek, N. A., Tekbudak, M. Y., Yurtdaş, G., Gülbahar, Ö., Uyar, G. Ö., . . . Erten, Y. (2022). The Relationship Between Myostatin, Inflammatory Markers, and Sarcopenia in Patients With Chronic Kidney Disease. *Journal of Renal Nutrition*. doi:https://doi.org/10.1053/j.jrn.2022.01.011

Yi, L., He, J., Liang, Y., Yuan, D., Gao, H., & Zhou, H. (2007). Simultaneously quantitative measurement of comprehensive profiles of esterified and non-esterified fatty acid in plasma of type 2 diabetic patients. *Chemistry and Physics of Lipids, 150*(2), 204-216. doi:10.1016/j.chemphyslip.2007.08.002

Yilmaz, M. I., Siriopol, D., Saglam, M., Kurt, Y. G., Unal, H. U., Eyileten, T., . . . Kanbay, M. (2014). Plasma endocan levels associate with inflammation, vascular abnormalities, cardiovascular events, and survival in chronic kidney disease. *Kidney International, 86*(6), 1213-1220. doi:https://doi.org/10.1038/ki.2014.227

Yki-Jarvinen, H., Puhakainen, I., & Koivisto, V. A. (1991). Effect of free fatty acids on glucose uptake and nonoxidative glycolysis across human forearm tissues in the basal state and during insulin stimulation. *Journal of Clinical Endocrinology and Metabolism, 72*(6), 1268-1277. doi:10.1210/jcem-72-6-1268

Yu, C., Chen, Y., Cline, G. W., Zhang, D., Zong, H., Wang, Y., . . . Shulman, G. I. (2002). Mechanism by which fatty acids inhibit insulin activation of insulin receptor substrate-1 (IRS-1)-associated phosphatidylinositol 3-kinase activity in muscle. *Journal of Biological Chemistry, 277*(52), 50230-50236. doi:10.1074/jbc.M200958200

Yuan, Y., Xu, Y., Xu, J., Liang, B., Cai, X., Zhu, C., . . . Shu, G. (2017). Succinate promotes skeletal muscle protein synthesis via Erk1/2 signaling pathway. *Molecular Medicine Reports, 16*(5), 7361-7366. doi:10.3892/mmr.2017.7554

Yuzefovych, L., Wilson, G., & Rachek, L. (2010). Different effects of oleate vs. palmitate on mitochondrial function, apoptosis, and insulin signaling in L6 skeletal muscle cells: role of oxidative stress. *American Journal of Physiology: Endocrinology and Metabolism, 299*(6), E1096-1105. doi:10.1152/ajpendo.00238.2010

Zaki, M., Basha, W., Reyad, H., Mohamed, R., Hassan, N., & Kholousi, S. (2018). Association between Myeloperoxidase Levels and Risk of Insulin Resistance in Egyptian Obese Women. *Open Access Maced J Med Sci, 6*(4), 629-633. doi:10.3889/oamjms.2018.164

Zammit, P. S. (2017). Function of the myogenic regulatory factors Myf5, MyoD, Myogenin and MRF4 in skeletal muscle, satellite cells and regenerative

myogenesis. *Seminars in Cell and Developmental Biology, 72*, 19-32. doi:https://doi.org/10.1016/j.semcdb.2017.11.011

Zammit, P. S., Golding, J. P., Nagata, Y., Hudon, V., Partridge, T. A., & Beauchamp, J. R. (2004). Muscle satellite cells adopt divergent fates: a mechanism for self-renewal? *Journal of Cell Biology, 166*(3), 347-357. doi:10.1083/jcb.200312007

Zammit, P. S., Relaix, F., Nagata, Y., Ruiz, A. P., Collins, C. A., Partridge, T. A., & Beauchamp, J. R. (2006). Pax7 and myogenic progression in skeletal muscle satellite cells. *Journal of Cell Science, 119*(Pt 9), 1824-1832. doi:10.1242/jcs.02908

Zhang, C., McFarlane, C., Lokireddy, S., Bonala, S., Ge, X., Masuda, S., . . . Kambadur, R. (2011). Myostatin-deficient mice exhibit reduced insulin resistance through activating the AMP-activated protein kinase signalling pathway. *Diabetologia, 54*(6), 1491-1501. doi:10.1007/s00125-011-2079-7

Zhang, C., McFarlane, C., Lokireddy, S., Masuda, S., Ge, X., Gluckman, P. D., . . . Kambadur, R. (2012). Inhibition of myostatin protects against diet-induced obesity by enhancing fatty acid oxidation and promoting a brown adipose phenotype in mice. *Diabetologia, 55*(1), 183-193. doi:10.1007/s00125-011-2304-4

Zhang, J., Wu, Y., Zhang, Y., LeRoith, D., Bernlohr, D. A., & Chen, X. (2008). The Role of Lipocalin 2 in the Regulation of Inflammation in Adipocytes and Macrophages. *Molecular Endocrinology, 22*(6), 1416-1426. doi:10.1210/me.2007-0420

Zhang, R., Brennan, M. L., Shen, Z., MacPherson, J. C., Schmitt, D., Molenda, C. E., & Hazen, S. L. (2002). Myeloperoxidase functions as a major enzymatic catalyst for initiation of lipid peroxidation at sites of inflammation. *Journal of Biological Chemistry, 277*(48), 46116-46122. doi:10.1074/jbc.M209124200

Zhang, S., Al-Maghout, T., Cao, H., Pelzl, L., Salker, M. S., Veldhoen, M., . . . Singh, Y. (2019). Gut Bacterial Metabolite Urolithin A (UA) Mitigates Ca2+ Entry in T Cells by Regulating miR-10a-5p. *Frontiers in Immunology, 10*. doi:10.3389/fimmu.2019.01737

Zhang, Y., Proenca, R., Maffei, M., Barone, M., Leopold, L., & Friedman, J. M. (1994). Positional cloning of the mouse obese gene and its human homologue. *Nature, 372*(6505), 425-432. doi:10.1038/372425a0

Zhao, Y., Wieman, H. L., Jacobs, S. R., & Rathmell, J. C. (2008). Mechanisms and methods in glucose metabolism and cell death. *Methods in Enzymology, 442*, 439-457. doi:10.1016/s0076-6879(08)01422-5

Zhou, X., Wang, J. L., Lu, J., Song, Y., Kwak, K. S., Jiao, Q., . . . Han, H. Q. (2010). Reversal of cancer cachexia and muscle wasting by ActRIIB antagonism leads to prolonged survival. *Cell, 142*(4), 531-543. doi:10.1016/j.cell.2010.07.011

Zhu, X., Hadhazy, M., Wehling, M., Tidball, J. G., & McNally, E. M. (2000). Dominant negative myostatin produces hypertrophy without hyperplasia in muscle. *FEBS Letters, 474*(1), 71-75. doi:https://doi.org/10.1016/S0014-5793(00)01570-2

Zhu, X., Topouzis, S., Liang, L. F., & Stotish, R. L. (2004). Myostatin signaling through Smad2, Smad3 and Smad4 is regulated by the inhibitory Smad7 by a negative feedback mechanism. *Cytokine, 26*(6), 262-272. doi:10.1016/j.cyto.2004.03.007

Zimmers, T. A., Davies, M. V., Koniaris, L. G., Haynes, P., Esquela, A. F., Tomkinson, K. N., . . . Lee, S.-J. (2002). Induction of Cachexia in Mice by Systemically Administered Myostatin. *Science, 296*(5572), 1486-1488. doi:10.1126/science.1069525

Zoso, A., Zambon, A., Gagliano, O., Giulitti, S., Prevedello, L., Fadini, G. P., . . . Elvassore, N. (2019). Cross-talk of healthy and impaired human tissues for dissection of disease pathogenesis. *Biotechnology Progress, 35*(2), e2766. doi:10.1002/btpr.2766

Zuriaga, M. A., Fuster, J. J., Gokce, N., & Walsh, K. (2017). Humans and Mice Display Opposing Patterns of "Browning" Gene Expression in Visceral and Subcutaneous White Adipose Tissue Depots. *Frontiers in Cardiovascular Medicine, 4*(27). doi:10.3389/fcvm.2017.00027

Zurlo, F., Larson, K., Bogardus, C., & Ravussin, E. (1990). Skeletal muscle metabolism is a major determinant of resting energy expenditure. *The Journal of clinical investigation, 86*(5), 1423-1427. doi:10.1172/JCI114857

Zuurveld, J. G., Oosterhof, A., Veerkamp, J. H., & van Moerkerk, H. T. (1985). Oxidative metabolism of cultured human skeletal muscle cells in comparison with biopsy material. *Biochimica et Biophysica Acta, 844*(1), 1-8. doi:10.1016/0167-4889(85)90226-5

Appendices

Appendix 1. Supplement to Chapter 5

A

	Younger	Older
n (M/F)	0/2	1/1
Age (years)	24 ± 6	73 ± 14
Height (m)	1.62 ± 0.11	1.69 ± 0.08
Weight (kg)	55.5 ± 2.1	68.0 ± 10.0
BMI (kg·m^{-2})	21.3 ± 2.1	23.7 ± 1.1
Waist (cm)	69 ± 4	87 ± 15
Hip (cm)	81 ± 2	101 ± 5

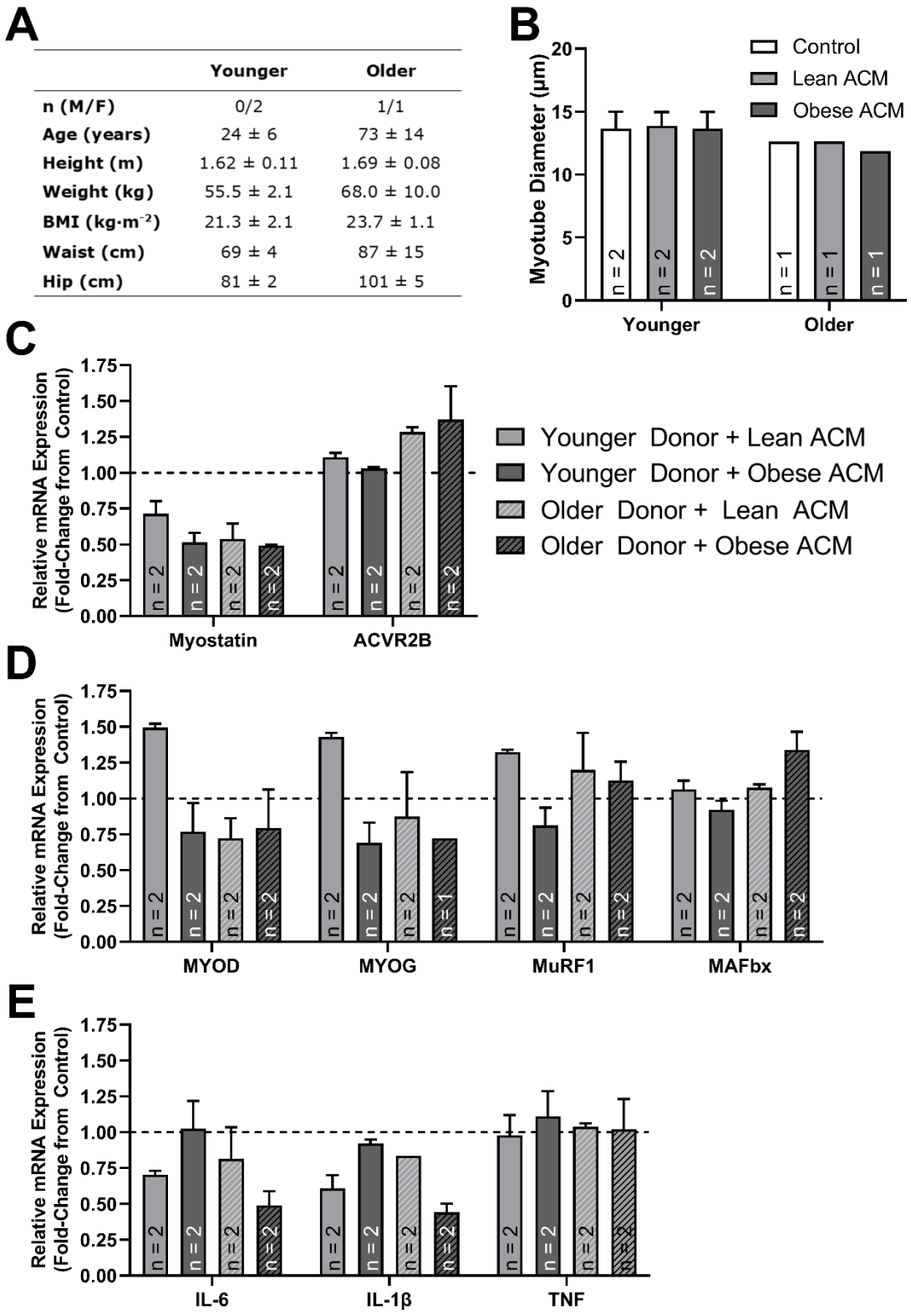

Supplementary Figure 1.1. Exploratory comparison of the effects of Lean and Obese subcutaneous adipose tissue secretome on primary human myotubes derived from younger and older donors.

Muscle tissue donors from whom myogenic cultures were established, and gene expression data was available, were stratified into Younger (n = 2) and Older (n = 2) groups (**A**). A comparison of the effects of Control (unconditioned medium) versus Lean and Obese subcutaneous adipose tissue secretome (ACM) on Mean (± SEM) diameter of myotubes derived from Younger (n = 2) and Older (n = 1) donors (**B**). The effects of Lean (light grey bars) and Obese (dark grey bars) secretome on gene expression was compared between myotubes derived from Younger (solid bars; n = 2) and Older donors (striped bars; n = 2). The relative mRNA expression of myostatin and its receptor (**C**); the myogenic regulatory factors MYOD and MYOG and muscle-specific E3 ligases MuRF1 and MAFbx (**D**); and the inflammatory markers IL-6, IL-1β and TNF (**E**). Gene expression data presented as Mean (± SEM) of fold-change from cells exposed to unconditioned Control medium (normalised to = 1). Thus, values above the dashed line reflect relative increases and values below the line reflect relative decreases from Control-treated cells.

Appendix 2. An Inducible Model of Myostatin Overexpression

Introduction

There has been great interest in the application of novel methods to suppress and restrain the expression and function of myostatin in skeletal muscle tissue and cells, with a view to improving anabolism and, perhaps, insulin sensitivity. Yet the multifactorial involvement of myostatin and its relative importance in insulin signalling and sensitivity remains poorly understood. To that effect, studies investigating myostatin gain-of-function, through overexpression of myostatin or its signalling components, offer a useful technique to elucidate its mechanisms; can identify complimentary interactivity with loss-of-function studies; and will help to establish the viability of myostatin suppression as a therapeutic target (Prelich, 2012).

Animal studies have shown effects of myostatin overexpression that consistently mirror the effects of *in vivo* knockout or knockdown studies, but offer limited insight into cell-type-specific mechanisms and may be impeded by off-target effects. Indeed, male, but not female, transgenic mice that selectively overexpress myostatin in skeletal muscle and have subsequently greater muscle myostatin protein content, have significantly reduced muscle weight, cross-sectional area and myonuclear number (Reisz-Porszasz et al., 2003). Similarly, localised ectopic expression of myostatin in the tibialis anterior muscle of adult male rats through gene electrotransfer reduced specific muscle mass and cross-sectional area by 20% and 30%, respectively after 14 days (Durieux et al., 2007). This was associated with a marked decrease in the expression of muscle structural genes and myogenic transcription factors. In a follow up study, Amirouche et al. (2009) reported that local overexpression did not alter the expression of key muscle atrogenes or proteasome components, but did suppress the Akt/mTOR signalling pathway, suggesting that myostatin predominantly perturbs muscle mass through suppression of protein translation, rather than up-regulation of proteasomal degradation.

Overexpression of Myostatin in Myogenic Culture Models

Early work employing transient transfection of C2C12 myoblasts with a myostatin expression vector was demonstrated to inhibit the rate of proliferation by ~50%, but enhanced the survival of differentiating cells (Ramón Ríos, Carneiro, Arce, & Devesa, 2001). Similarly, stable transfection of myostatin in C2C12 myoblasts inhibited cell proliferation and differentiation, which was likely mediated through

a reduction in MYOD and MYOG protein expression and altering the phosphorylation pattern of MYOD, although there were no changes in their mRNA expression (Joulia et al., 2003).

Adenoviral overexpression of myostatin was found to suppress hypertrophy and IGF-1-mediated Akt phosphorylation in C2C12 myotubes (Morissette, Cook, Buranasombati, Rosenberg, & Rosenzweig, 2009). Conversely, when only the NH_2-terminal portion of myostatin (the myostatin propeptide), which has been demonstrated to bind to and inhibit the mature myostatin homodimer (Hill et al., 2002), was overexpressed, hypertrophy and basal Akt phosphorylation were increased. This has been corroborated *in vivo* by injection of adeno-associated virus expressing the myostatin propeptide in rats, which increased muscle size, glucose uptake and tolerance and glycogen storage, however PI3K and AMPK signalling was mildly perturbed (Cleasby et al., 2014).

Not all *in vitro* overexpression studies support prior *in vivo* findings, however. Wang et al. (2015) transfected C2C12 myoblasts with a myostatin plasmid prior to differentiation into myotubes. Transfection increased myostatin protein expression by ~90%, but in contrast to the *in vivo* work of Amirouche et al. (2009) myotubes demonstrated greater formation of autophagosomes, which was accompanied by increased expression of the E3 ubiquitin ligases MAFbx and MuRF1, demonstrating that myostatin-associated activation of the ubiquitin-proteasome and autophagy-lysosome systems drives myotube atrophy. This was further supported through the use of small interfering RNA (siRNA) to disrupt and suppress myostatin expression, which decreased expression of genes associated with autophagy and ubiquitination in response to TNF-α treatment.

One main limitation of previous overexpression studies, as indeed is the case for *many in vitro* studies, is a dearth of investigations using primary human cells. As previously described, the relevance of C2C12 myotubes as a model of human skeletal muscle is limited compared to human primary myotubes and in the context of myostatin's function, is contested by reports of both direct stimulation and inhibition of myoblast proliferation by myostatin treatment (Joulia et al., 2003; Rodgers et al., 2014). The emergence of next generation tools to affect expression in primary cells, offers great promise for advancing our understanding, through models that are best poised to more accurately reflect functional human cascades.

The pINDUCER Toolkit

Advances in loss- and gain-of-function technologies have provided powerful means to investigate the molecular mechanisms responsible for biological processes. While techniques to elicit RNA interference (RNAi) have been revolutionary in mammalian biology, these advances have been hindered by the inability to modulate timing and level of gene activity. To that effect, Meerbrey et al. (2011) developed a third-generation inducible short hairpin RNA (shRNA) expression lentiviral tool kit, coined pINDUCER, to enable robust, inducible RNAi and cDNA expression in a multitude of cell types, that is both dose-dependent and reversible. This novel system bears several advantages of previous technologies. Namely, the authors propose that; as a single-vector system it avoids the need to use specialised cell lines or multiple vectors; there is minimal basal expression of the shRNAs yet high inducibility; there are incorporated reports for tracking transduced and shRNA-expressing cells; owing to a sortable marker, cells with greater inducibility can be sorted and isolated; and importantly, pINDUCER systems can function both *in vivo* and *in vitro*.

Gateway Cloning Technology

The Gateway® entry vector technology is dependent upon the bacteriophage lambda site-specific recombination system which enables the incorporation of lambda into the E. coli chromosome and the switch between lytic and lysogenic pathways (Ptashne, 1992). The lambda recombination occurs between well-characterised specific attachment (att) sites (attB and attP on the E. coli and lambda chromosomes, respectively) which provide the binding sites for recombination proteins. This recombination has no net loss or gain of nucleotides and does not require synthesis of DNA. Instead, the DNA segments bordering the recombination sites are switched such that the resultant recombination from lambda integration produces hybrid sequences (attL and attR, respectively) comprising att sequences from both parental vectors.

Aims

The primary aims of this work was to generate an inducible model of myostatin overexpression that could be applied to human primary myogenic cultures to study the direct effects of overexpressing myostatin on insulin signalling and sensitivity in a relevant model of human skeletal muscle.

Methods

Entry Clone Generation

A myostatin open reading frame expression clone with C-flag tag was purchased from Genecopoeia (Cat# EX-U1164-M35). To enable efficient Gateway cloning, attB primers were designed to amplify the sequence of interest and analysed using Oligo-analyser (Integrated DNA Technologies, IA, US) to avoid secondary structures and dimerization (Table 1). Briefly, forward and reverse primer structural criterion were: four guanine residues at the 5' end followed by the 25-bp *att*B1 (forward primer) or *att*B2 (reverse primer) site, followed by at least 18-25 bp of gene-specific sequence.

Supplemental Table 2.1 Primer sequences used to amplify myostatin sequence in expression clone.

attB Primer	Sequence (5'-3')
Forward	GGGG*ACAAGTTTGTACAAAAAAGCAGGCT*TC**ACCAATAGAAACTGGGCTTGTCG**
Reverse	GGGG*ACCACTTTGTACAAGAAAGCTGGGTT***CCTACTCAGACAATGCGATGCAA**

Note: *Italic* font indicates attB sequence, **Bold** font indicates MSTN primer sequence.

PCR was performed using Phusion reagents added to 100 ng of the MSTN plasmid DNA and 10 pmol·μL^{-1} of forward and reverse primers, in a total reaction volume of 50 μL. the following cycling conditions were applied: 30 s initial denaturation at 98 ^{0}C, followed by 35 cycles of 10 s denaturation at 98 ^{0}C, 30 s annealing at 66 ^{0}C and 1 min extension at 72 ^{0}C, before a final 7 min extension at 72 ^{0}C. Five microliters of the PCR product plus 1 μL of 6x Laemmli buffer was loaded into a 1% agarose gel, along with 10 μL of 1 kb DNA ladder mix, for electrophoretic separation of DNA at a constant voltage of 5 V·cm^{-1}. The gel was visualised under ultraviolet light using a trans-illuminator to confirm the presence and purity of the 1467 bp PCR product (Fig. 1). Approximate double-stranded DNA concentration of the PCR product was determined photospectrometrically to enable appropriate loading for subsequent application, however this method is not precisely quantitative due to the presence of primers within the product.

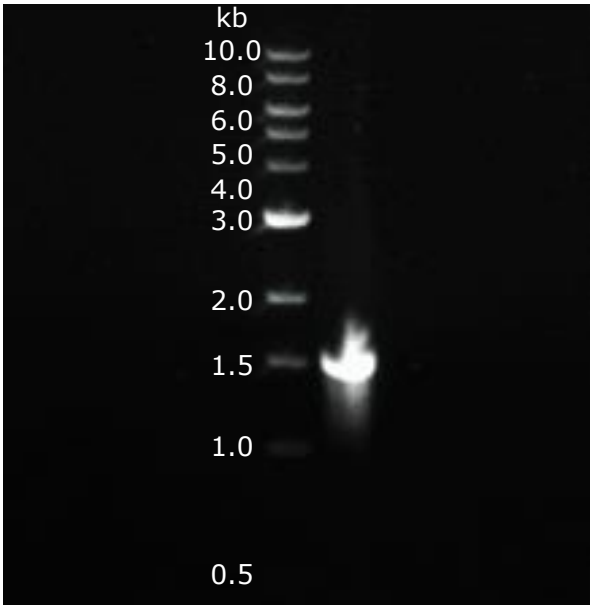

Supplemental Figure 2.1. Agarose gel electrophoresis of attB PCR product.

Band shows single product with migration that is consistent with the predicted size of 1467 bp.

Cloning into a Destination Vector

A one-tube protocol was employed to clone the attB-PCR product directly into a destination vector (Fig. 2). A 'BP' reaction was set up by loading ~100 ng of attB-PCR product, 200ng of pDONR vector, 3 µL of Gateway BP Clonase II enzyme mix, and Tris-EDTA buffer (pH 8.0) to produce a final volume of 15 µL, which was mixed and incubated overnight at 25 ^{0}C. To confirm BP reaction efficiency, 5 µL of the reaction mix was incubated for 10 min at 37 ^{0}C with the addition of 2 µL of proteinase K. Of the product of this reaction, 1 µL was transformed with 50 µL of One Shot TOP10 competent E. Coli (as otherwise described below) and streaked on LB agar plates containing 50 µg·mL^{-1} ampicillin and 30 µg·mL^{-1} chloramphenicol to facilitate selection of entry clones, the presence of which confirmed the success of the BP reaction. The remaining 10 µL BP reaction product underwent an LR reaction to facilitate recombination of the entry clone with the destination vector. The BP reaction product was incubated with 300 ng of the pINDUCER destination vector and 3 µL of Gateway LR Clonase II enzyme mix overnight for 20 h at 25 ^{0}C, after which 2 µL of proteinase K was added and incubated at 37^{0}C for 10min.

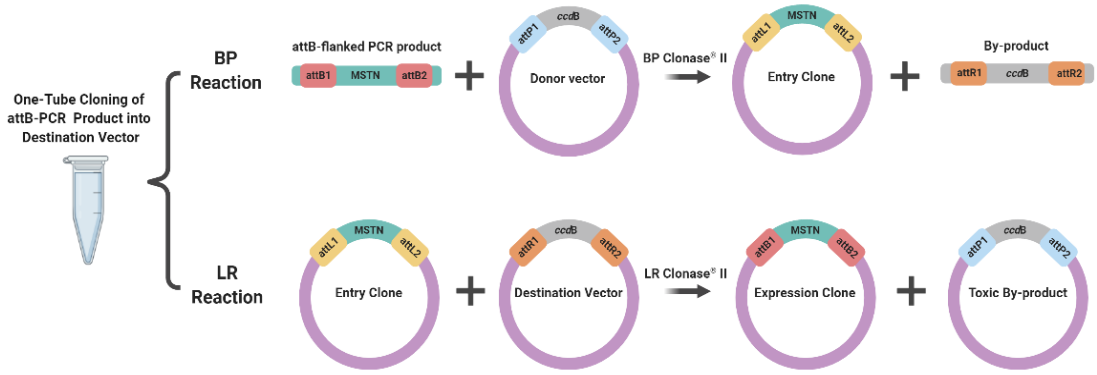

Supplemental Figure 2.2. An overview of the one-tube cloning principle in which the attB-PCR product is cloned directly into a destination vector via the BP and LR reactions.

Transformation

Chemically competent One Shot Stbl3 E. Coli were kept on ice for 30 min with 2 µL of LR reaction product. Following incubation, cells were heat-shocked at 42 ºC for 45 s to enable plasmid passage through the cell wall, then incubated on ice for 2 min, before 250 µL of Super Optimal Broth with catabolite repression outgrowth medium was added and incubated for 1 h at 37 ºC in a shaking incubator set to 225 RPM, to ensure generation of the antibiotic resistant proteins encoded within the plasmid backbone. Either 50 or 100 µL of transformed suspension was plated onto lysogeny broth agar plates with 100 µg·µL^{-1} ampicillin and incubated at 37 ºC overnight for the production of ampicillin-resistant colonies.

The following day, PCR was performed to identify positive colonies. Twenty distinct colonies were sampled by lightly brushing each colony with a pipette tip and suspending adherent bacteria in a 20 µL reaction with LNCX forward and pINDUCER20 reverse primers, using Bioline BioTaq (BIO-20140) reagents. The following cycling conditions were applied: 5 min initial denaturation at 96 ºC, followed by 30 cycles of 15 s denaturation at 96 ºC, 20 s annealing at 55ºC and 1 min extension at 72 ºC, before a final 5 min extension at 72 ºC. Five microliters of PCR product from those colonies, plus 1 µL 6x Laemmli buffer were run on a 1% agarose gel and visualised under UV light as described earlier. A previously successfully transformed plasmid was loaded as a positive control for PCR amplification. Positive colonies were identified by the presence of bands migrating to approximately 1.5 kb. Four of these colonies (gel lanes 1, 8, 13 and 15) were

then picked from the agar plate and transferred into 5 mL lysogeny broth for overnight culture (16 h) at 37 ºC in a shaking incubator.

Supplemental Figure 2.3. Agarose gel electrophoresis of PCR product from the selected transformed colonies.
Eighteen of the 20 selected colonies exhibited amplification of target sequence at approximately the correct size. A previously successfully generated plasmid was loaded in lane 1 as a positive control to confirm PCR success.

Mini and Midi Preps

After 16 h of culture, bacterial broths were centrifuged at 5000 x g for 10 min to pellet bacteria. Plasmid DNA was extracted and purified using a QIAprep Spin MiniPrep kit, according to manufacturer's instructions. Bacteria was re-suspended in 250 µL of resuspension buffer containing RNase, after which 250 µL of lysis buffer was added, gently mixed and incubated at room temperature for 5 min before 350 µL of neutralisation buffer was added. The solution was centrifuged for 10 min at 17,900 x g and the supernatant was applied to a spin column, which was centrifuged at max speed for 1 min before the flow-through was discarded and the column washed with 750 µL of wash buffer and centrifuged for 1 min again. Flow-through was discarded again and the column was centrifuged once more to remove any residual wash buffer. To elute the extracted plasmid DNA, 50 µL of elution buffer (10 mM Tris-Cl, pH 8.5) was added to the column, allowed to stand for 1 min at room temperature, and finally centrifuged at max speed for 1 min. Plasmid DNA concentration was determined photospectrometrically. Plasmid

DNA concentration was normalised to 100 ng·μL^{-1} and an aliquot of 10 μL of DNA was sent to Source BioScience for sequencing. Glycerol stocks of bacterial colonies were prepared and stored at -80ºC. To check for matching sequences, colony sequences were aligned with the target sequence which revealed that one colony (Fig. 1; lane 13) had total homology with the MSTN sequence.

A 5 mL starter culture was commenced by picking the colony with the correct sequence from the agar plate and incubating at 37 ºC, 225 RPM for 8 h, before centrifuging to pellet the bacteria. Based on previous optimisation, to ensure appropriate bacterial density, the bacterial pellet was transferred into a 200 mL culture and left overnight at 37 ºC. The following morning, the culture was spun down once more for 10 min at 5000 x g to pellet the bacteria, which was subsequently processed using Machery Nagel NucleoBond xtra Midi plasmid DNA purification kit according to manufacturer's instructions.

Briefly, cells were vigorously re-suspended in 8 mL of resuspension buffer containing RNase A, before the addition of 8 mL lysis buffer and gentle inversion to avoid shearing and releasing chromosomal DNA in the solution. NucleoBond Xtra column was equilibrated by the addition of 12 mL equilibration buffer around the rim of the filter. Following 5 min of lysis, 8 mL of neutralisation buffer was added and the suspension was applied to the equilibrated column filter and allowed to filter by gravity. The column was then first washed with 5 mL of equilibration buffer applied to the filter, before removing the filter and washing only the column with 8 mL of wash buffer. The transfer plasmid DNA (pINDUCER20-MSTN) was eluted in 5 mL of elution buffer and precipitated with 3.5 mL of room-temperature isopropanol. The DNA was vortexed and centrifuged at 15,000 x g for 30 min at 4 ºC and the supernatant was discarded. Pelleted plasmid DNA was washed in 2 mL room-temperature 70% ethanol and centrifuged at 15,000 x g for 5 min at room-temperature, before the ethanol was removed and the pellet allowed to air dry at room temperature for 10 min. Finally, based on prior optimisation, the pellet was re-suspended in 400 μL of Tris-EDTA buffer with gentle pipetting and the DNA concentration was determined.

Lentivirus Production

To produce lentivirus particles, ~1.4x10^6 HEK293FT cells, chosen for their high transfectability, rapid growth and ability to produce high viral titres, were plated on 10 cm culture dishes and grown overnight at 37 ºC, 5% CO_2 in Eagle's minimum essential medium (EMEM) containing 10% FBS and 1% L-Glutamine to achieve ~80% confluence. The transfection complex for each 10 cm dish comprised 2 μg of transfer plasmid; pINDUCER20-MSTN or pINDUCER20-GFP (to serve as a

positive control), 2 µg of pMD2.G packaging (addgene plasmid #12259) plasmid and 2 µg of psPAX2 envelope (addgene plasmid #12260) plasmid (6 µg total plasmid DNA), to which was added 600 µL serum-free Opti-MEM media (100 µL media per 1 µg plasmid DNA) with the addition of 18 µL of X-tremeGENE HP DNA transfection reagent (3 µL reagent per 1 µg plasmid DNA). The complete transfection complex was incubated at room temperature for 30 min. Culture medium was aspirated from the HEK293FT cells and replaced with 7 mL serum-free Opti-MEM, to which 600 µL of transfection complex was added in a dropwise manner and gently swirled to distribute and minimise toxicity. Following 6 h of incubation at 37 ^{0}C, 5% CO_2, medium was replaced with 12 mL of EMEM with 10% FBS and 1% L-Glutamine and returned to the incubator for 48 h. The lentivirus containing medium was then aspirated and filtered through a 0.45 µm filter and stored at 4 ^{0}C.

The lentiviral medium was gently layered on top of 1 mL of 10% sucrose in 10 mL thin-walled ultracentrifuge tubes to create a density gradient for separation. These were then centrifuged at 100,000 x g at 4 ^{0}C for 2 h (Optima LE-80K Ultra, Beckman Coulter, CA, US) and the supernatant subsequently delicately discarded. Ultracentrifuge tubes were inverted to drain any remaining supernatant, before 300 µL of PBS was added to the resultant pellet and left overnight at 4 ^{0}C to re-suspend. Viral stocks were made by adding 300 µL of 50% glycerol and these aliquots were stored at -80 ^{0}C.

Viral Titration

To determine the viral titre, a QuickTiter Lentivirus Titre Kit (Cell Biolabs Inc, CA, US) was used. This enzyme-linked immunoassay detects only lentivirus-associated HIV-1 p24 core protein and not free p24 generated by HEK293FT cells during transient transfection, by first employing a virus pulldown by forming complexes with ViraBind reagents. Briefly, lentiviral samples were dilute 1:500 in 1 mL fresh medium used for HEK293FT culture, before 10 µL ViraBind reagent A and was added and inverted, followed by 10 µL reagent B, which was subsequently incubated for 30 min at 37 ^{0}C. Fresh culture medium was also processed and assayed in the same fashion to serve as a blank. Diluted sample complexes were centrifuged for 5 min at 12,000 RPM; the supernatant was aspirated, and the pellet re-suspended in 250 µL sample diluent (0.5% Triton X-100) and incubated for a further 30 min to inactivate the viruses. Standards were prepared by making serial dilutions of recombinant HIV-1 p24 antigen in sample diluent, ranging from 1-100 ng·mL^{-1}. Samples and standards were assayed in duplicate by adding 100

µL of inactivated sample or standard to the wells of an anti-p24 antibody coated plate and incubated overnight at 4ºC.

The following day, the wells were emptied and washed three times with 250 µL wash buffer and blotted dry. One hundred microlitres of FITC-conjugated anti-p24 monoclonal antibody, diluted to 1:1000 in assay diluent (0.02% Thimerosal), was added to each well and incubated at room temperature on an orbital shaker for 1 h. Wells were washed again three times and 100 µL of HRP-conjugated anti-FITC monoclonal antibody, diluted to 1:1000, was added to each well and incubated again for 1 h. The plate was again washed three times before the addition of 100 µL substrate solution to each well, which was incubated at room temperature for 15 min. The enzymatic reaction was terminated with the addition of 100 µL stop solution (0.5N sulphuric acid) per well. Absorbance was read at 450 nm on a spectrophotometer and a standard curve was generated, from which viral titre was determined as follows:

$$p24\ Titer = p24\ (ng \cdot mL^{-1}) \times Dilution\ Factor \times 0.25mL/1mL$$

Given that there are approximately 2000 molecules of p24 per lentiviral particle (LP) and the molecular weight of p24 is 24 kDa, 1 LP contains approximately:

$$\frac{2000\ (24 \times 10^3)}{6 \times 10^{23}} = 8 \times 10^{-5} pg\ of\ p24$$

$$Therefore\colon\ 1\ ng\ p24 = \frac{1}{8 \times 10^{-8}} = 1.25 \times 10^7\ LP$$

For reasonably packaged lentiviral vectors, 1 transduction unit (TU) is between 100-1000 LP.

$$Therefore\colon\ 1 \times 10^6\ TU \cdot mL^{-1} = 1 \times 10^{8-9}\ LP \cdot mL^{-1} = 8\ to\ 80\ ng \cdot mL^{-1}$$

Viral Transduction

MDA-468 cells were seeded on uncoated 6- and 12-well plates at densities of $4x10^5$ and $1.5x10^5$ cells·well^{-1}, respectively, and incubated overnight. Based on prior optimisation, the multiplicity of infection (MOI) of these cells was determined to be 7 viral particles per cell. Thus, MDA-468 cells were infected in a dropwise manner with GFP virus at MOI 7 and 12, and with Myostatin virus at MOI 3.5, 7 and 12. To improve infection efficiency, 1 µg·mL^{-1} of Polybrene, a cationic polymer, was added to the medium to neutralise charge repulsion between viral particles and the cell surface. One well was treated with an empty plasmid to determine any effects of virus treatment alone and one further well received no virus, only doxycycline treatment upon induction. Cells were incubated with viral medium for

4 h, after which medium was removed and replaced with the addition of 1 μg·mL^{-1} Doxycycline to induce expression of the inserted gene and incubated for 48 h.

Cells infected with the GFP plasmid were imaged on a Zeiss 200 mm wide-field fluorescent microscope to confirm if the infection had worked by checking for fluorescence in the FITC channel. Fluorescent imaging confirmed the doxycycline-induced expression of GFP in the GFP infected cells. Culture media from the cells infected with the myostatin plasmid was collected and stored at -80 ^{0}C for subsequent precipitation of protein from the media to investigate whether myostatin was being secreted. Cells were then washed once in ice-cold PBS before being scraped in 1 mL ice-cold PBS, transferred to Eppendorf tubes and centrifuged for 5 min at 800 x g. The cell pellets were re-suspended in 100 μL ice-cold RIPA buffer with protease inhibitor and incubated at 4 ^{0}C for 30 min to allow complete cell dissociation and centrifuged for 15 min at 10,000 x g to pellet any remaining cellular debris. Supernatant was transferred to clean tubes and stored at -20^{0}C. Protein content of cell lysates was determined by BCA assay and 10 μg total protein was loaded onto 12% acrylamide gels and separated via SDS-PAGE. Separated proteins were transferred overnight onto PVDF membranes and probed with anti-myostatin antibody to confirm whether induction of myostatin was successful (Fig. 4).

It was revealed that the process had not been successful and myostatin protein content was not increased with any of the MOIs tested (Fig. 4; lanes 6, 7 and 8), relative to the negative control treated cells (Fig. 4; lanes 3, 4 and 5). Indeed, greater MOI appeared to have the opposite effect to that required, presumably demonstrating toxicity of the higher viral titre.

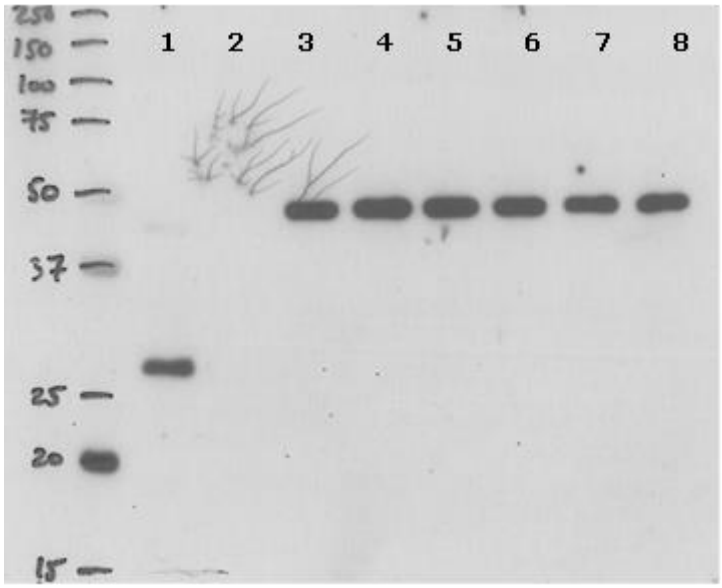

Supplemental Figure 2.4. Unsuccessful attempt to induce myostatin expression in MDA-468 cells infected with the generated MSTN viral medium at various MOIs.

MDA-468 cells were incubated with the generated myostatin viral medium for 4 h, which was then replaced with 1 $\mu g \cdot mL^{-1}$ Doxycycline for 48 h to induce expression of the inserted gene. Cells were lysed in RIPA buffer and 10 µg of protein was separated via SDS before probing with an anti-myostatin antibody. (1) Skeletal muscle (+ve), (2) No lysate, (3) - Virus - Dox, (4) – Virus + Dox, (5) Empty pINDUCER vector, (6) MSTN + Dox (MOI 3.5), (7) MSTN + Dox (MOI 7), (8) MSTN + Dox (MOI 12).

Troubleshooting and Termination

The entire process here described was repeated with fresh reagents and new aliquots of HEK293FT and MDA-468 cells with the same result (data not shown). At this point, the University was closed due to the COVID-19 pandemic. Upon resumption of laboratory activities (as detailed in Appendix 3. COVID-19 Impact Statement), a further repeat of these processes was performed with one modification such that the lentiviral production process instead used HEK293 cells as it was suspected that this could be the source of the problem, but this was also to no avail. After further efforts to troubleshoot, and in light of the limited time left for completion of my studies and the absence of the postdoctoral fellow who had been supporting this work, this project was halted at this point.

With additional time and support, further options could have been explored to resolve these challenges. One such logical troubleshooting step would be to repeat the process without using the one-tube cloning protocol, and to instead separate the BP and LR reactions, with PCR purification of the attB-PCR product after the BP reaction in order to remove attB primers and primer-dimers. If this did not resolve the issue, a significant alteration to the protocol is now viable. Indeed, in the interim since this project was commenced, a new commercially available lentiviral open reading frame cDNA clone of MSTN has since become available (EX-U1164-Lv105) which may potentially have negated the issue if indeed it was occurring at the point of cloning. Unfortunately, however, this was deemed too great a demand of my time and resources which were now highly limited.

Appendix 3. COVID-19 Impact Statement

University of Nottingham
UK | CHINA | MALAYSIA

COVID19 Impact Statement 2020
For use by PGRs with a funding end date **after 1st April 2021**

The University of Nottingham aims to support all our PGRs to complete their degrees within their period of funded study, by meeting our Doctoral Outcomes. We recognise, and aim to take into account, personal circumstances that may affect a PGR's ability to achieve this.

This Impact Statement should be used to provide details and evidence of impact for:

- applications for an additional funded period of registered study;
- applications for a funded extension to Thesis Pending;
- the thesis examination.

It will also be used to determine both the case and length of a COVID extension to study **up to a maximum of six months** (twelve for part time PGRs). **Please note that it is expected that most approved extensions will reflect the duration of enforced change in activity during lockdown, and that extensions of longer duration will be the exception rather than the rule.** You should show in this form how you have attempted to lessen the impact of the COVID pandemic on your research progress.

Please keep a completed copy of this form as you may want to refer to it as evidence of impact in your annual review process and/or thesis examination. You will also need to use it copy/paste your responses for submission in the online version of the form which will be the format used to make your extension request.

Please carefully consider your case for any extension with reference to the University's online Policy on Circumstances Affecting Students' Ability to Study and Complete Assessments (under Exceptional Guidance to Extenuating Circumstances Panels) and section 16 of the PhD Regulations (see Appendix 2, section 1), relating to existing regulations on circumstances that may or may not be usual grounds for an extension, and the Exceptional Regulations for UKRI funded PGR extensions (which can be found on the same site as this form).

We strongly encourage you to discuss the completion of this form with your supervisors. If you prefer, you can alternatively discuss the form with an appropriate member of PGR support staff such as your DTP/CDT Director or Manager, DTP/CDT Welfare Officer, School Postgraduate Student Advisor, School PGR Director or other member of the Welfare team, or the Researcher Academy Faculty Lead (formerly Associate Dean for the Graduate School).

To ensure that you cover the full impact of the COVID-19 pandemic on you and your research **since March 15th 2020**, please complete all relevant sections of the form. You can be very brief but please include all relevant information even in note or bullet form.

When applying for an extension to either your period of registered study (i.e. when active data collection is to be done) or to Thesis Pending, or both you should show, briefly how/whether your work to date already meets some of the University and QAA Doctoral Outcomes, and clarify which doctoral outcomes are not currently met and how your plan will enable you to meet these (Appendix 1).

Under the exceptional conditions of the COVID-19 pandemic, in addition to the usual circumstances that may be grounds for an extension, you can and should also consider, and evidence if asked to do so, the additional circumstances listed in Section 1. These include but are not limited to:

- your ability to work effectively now that you are not in your usual working environment;
- any change in access to research settings or facilities, such as archives, field-sites, laboratories, software, or databases;
- any changes in your personal circumstances or environment resulting from remote working, or national restrictions , including those related to:
    - caring responsibilities,
    - disability and/or being at higher risk from coronavirus
    - impacts on your supervisory team that have affected your research progress

v.1 05/20

- your mental health, and whether you have access to mental health support if needed,
- any financial impacts, either personal or on the research in progress or planned.
- any other considerations that should be taken into account, whether these do or do not relate to any protected characteristics.

This form should capture the impact of the pandemic on you and your research progress, not solely any impact of the University closure itself.

For further information including addressing future impacts; privacy and confidentiality of information submitted, and additional notes and guidance please see Appendix 2.

The information collected in this form will be used for the purposes of assessing your case for a funded extension to your doctoral studies, to provide information to your funder; to inform the University of the range of impacts that our PGRs have experienced, and to inform policy decisions on how to support our PGRs in future. The document will also aid discussion and decision making, to ensure consistency in evaluation of the impacts for different people.

All information used for other than the stated purposes will be anonymised, and all personal information through which anyone could be identified removed. The information on this form will not be shared with anyone, including supervisory teams, for other than the stated purposes, without your permission.

Background Information – your details			
Family Name:	Wilhelmsen	First Name(s)	Andrew John
ID:	4342419	School:	Life Sciences
Please identify your relevant funder(s)	AHRC/ BBSRC/ ESRC/EPSRC/**MRC**/NERC/ STFC/University of Nottingham/**Charity**/ Industry/ international scholarship/self funded	Dates of impact: (the date from which the impact has had an effect).	15/03/2020
Start date	01/10/2018	Funding end date	01/10/2021
Length of extension requested: (up to a maximum of twenty six (26) weeks)	Maximum available (26 weeks)	Programme length (3, 3.5, 4 years) and full time or part time	3 years Full time

The primary areas of impact:

Please tick all that are relevant for the ways in which you have been affected by the COVID pandemic and the resulting effect(s) on you and/or your research progression. You can give more details on these impacts, if you wish, on the next page.

Note: We will ask you to explain whether and how you have been able to manage or reduce any of these impacts in Section 2, on p.5.

The ways in which you have been affected (choose all that apply)

☒ additional/new caring responsibilities
☐ specific impact resulting from remote working as a result of a disability*
☐ being at higher risk of coronavirus;
☐ personal financial impact;
☐ new illness, accident or hospitalisation, including any mental health problems
☐ lack of access to mental health support (if needed);
☒ death or illness of a partner/close relative*
☐ illness of a relative for whom you are a carer
☐ impacts related to any protected characteristics*
☐ an impact on your supervisory team that has affected your supervision or progress
☐ military or other service (e.g. NHS) that has not already been accommodated
☐ parental leave that has not already been accommodated
☐ redeployment to work in another area (e.g. COVID) where this has not already been accommodated.
☐ other events not on this list that are specifically related to the COVID pandemic (please describe below)

The ways in which your research activity has been affected
(for each that applies, please also indicate whether you have tried to mitigate the effect in this area).

	Was any mitigation possible?
☒ Disruption of planned activities	Yes/**No**
☒ Access to facilities/archives/lab/equipment/field sites etc	Yes/**No**
☒ Postponement of critical activities where alternatives are not available	Yes/**No**
☐ Access to other research resources including financial impact	Yes/No
☒ Ability to achieve a planned outcome/ milestone/deliverable	Yes/**No**
☒ Access a research partner, including research-related placements	Yes/**No**
☒ Inability to devote your usual time to research activity	**Yes**/No
☐ *Lack of usual supervisory support for thesis progression/writing	Yes/No
☐ *Lack of usual supervisory support to help manage risk and mitigate plans	Yes/No
☐ Other (please describe below)	Yes/No

*We are collecting this information in order to fully understand how you have been affected. Any information that you give here will only be used as information to inform us and will not be shared with anyone other than the teams considering the cases for extension and collating information for submission to UKRI.

1. DESCRIBING THE IMPACT

(Please complete this section to provide us with more detailed information)

For example you could write a short clear description of the nature of the impacts or problems that you face/have faced, make making this description as brief, and specific as possible. You could also give more detail on the nature of the impacts on your research progress.

We understand that personal and research impacts will be related, so if it helps you could structure the content in line with the impacts you identified in the tick boxes above.

Section 1, additional guidance

v.1 05/20

The impact **on you**:

Spring 2020:

Due to COVID-19 restrictions, my sister who has ongoing severe mental health challenges went through childbirth with very limited professional or personal support, where normally she receives extensive help, which had a very negative effect on her wellbeing. I subsequently returned to my hometown and **spent a period of two weeks during lockdown providing care** for my disabled and high-risk father while my mother (his carer) was in and out of hospital with my sister for several weeks. I then swapped responsibilities to care for my sister and her new-born when my mother had to return to work, while my sister was still unable to cope. This impacted my ability to work almost entirely during this period.

Spring/Summer 2021:

In April 2021, my father (with Parkinson's Disease) suffered a fall and fractured his hip, leading to surgery and serious psychological disturbances in response to changes to his medication, however due to COVID family were allowed to see him while in hospital, which worsened his state considerably. The combination of physical disability and mental health impact that this subsequently had on him was too great of a burden for my mother to solely handle and as such I **returned home for two weeks to assist with looking after him**. In early August 2021 my father had another serious fall, fracturing his other hip, requiring further surgery. This time the physical disablement was more severe as the first hip had still not yet fully recovered. I therefore took **a further period of two weeks leave** as soon as he left hospital to again to assist my mother and father in their daily needs.

The impact **on your research**:

Summer 2020:

Prior to the March closure, I was about to commence recruitment for an *in vivo* human physiology study, involving overweight/obese older adults for which I had sought and gained ethical approval. This was obviously halted since then and unlikely to be able to resume any time soon due to the nature of the participants making them high-risk for infection severity and the unavoidable physical contact required to run such a study. I anticipate serious delays running this study and indeed it may ultimately become non-feasible within my period of registered study.

My additional ongoing study requiring regular human muscle biopsies to be taken for primary cell culture experiments suffers the same issue as the last. Furthermore, I was in the process of developing a lentiviral vector to model over-expression of gene of interest in primary cells, which was also being undertaken at the med school. During closure, the freezer that had many of my reagents and generated components in failed and defrosted, losing those elements and the time and money they cost.

My main concern at present is that collectively, my first year involved a lot of learning new techniques and trial and error, resulting in very little data being generated, whereas just recently things have finally started accelerating and coming together. A delay at this time is of course halting my ability to generate new data and I fear, in light of the current situation and my earlier lack of substantial results, I won't have sufficient data to write up, come the end of 3rd year.

Winter 2020/Spring 2021:

Following the protracted **closure of the whole university for ~5 months**, I have since returned – in principle – to work since the autumn. **Authorisation to recommence non-essential human volunteer activity at the University was only being given in April 2021**, preventing any human volunteer research with a required face-to-face (as is vital for this project). Therefore, this has **severely restricted my work for the first 4 months of the year**.

This project requires clinical support from clinical research fellows (CRFs) due to the bio-sampling (e.g., muscle biopsies) involved. For the early part of this year many of the CRF's who support research projects in our group needed to return to full-time clinical work to facilitate the NHS response to Covid-19, and even upon their return to research activity, their **availability to support my PhD project was limited** due to an increased need to cover clinical shifts (due to high levels of staff sickness/ enforced isolation) and a need to progress their own research. Exacerbating this challenge, our human physiology group resident Doctor (who had previously performed most of the necessary invasive work for my project**) finished his contract in August 2020** and we therefore require a new full time clinical fellow to replace them in order to perform the clinical procedures and provide the necessary clinical cover during screening and main experimental visits.

Immediately prior to the first lockdown, I was working with a post-doctoral research fellow to generate an inducible lentiviral vector to overexpress myostatin in primary myotubes. The post-doc who I was working and continuing to develop and troubleshoot these methods with **finished her contract over the winter of 2020/2021**, so I was no longer able to work with her on this project, and as such must carry on independently. One of the two technicians within that lab also took voluntary redundancy during this period and **the lab is now running at severely restricted capacity** due to loss of staff and covid safety measures. Given my relative inexperience in these particular molecular biology techniques, and having hit a repeatedly problematic point of vector development, in tandem with the loss of previously generated and purchased resources during the freezer thawing of the first lockdown, it has become too great a burden on my now highly limited time and resources to continue to pursue this particular branch of work, and I have subsequently deemed **the creation of a chapter of work based on these methods as untenable given the available time frame and the current absence of provision of an extension from the university**. I will write up what I have and what I have achieved thus far and include it as an appendix at the end of my thesis.

The planned **secondment within my PhD programme** to work at the laboratories of Nestle/Amazentis in Switzerland for up to 12 months **remains unfeasible due to travel restrictions**.

Spring 2021:

Delays in the School's approval of the post meant that we **were not able to appoint and subsequently begin working with a new clinician until May, 2021.** This meant I was not able to arrange participant clinical procedures until then, meaning I had limited primary cell culture lab work to do until May 2021 **(14 months since the University first closed due to lockdown)**. Even after we cautiously returned to the University, **my ability to recruit participants has been severely restricted** compared to pre-COVID times. Pertinently, some of my work **requires the recruitment of older adults with obesity,** who are therefore considered more clinically vulnerable. For many individuals, reticence to participate in research is due to concerns about Covid-19 transmission, seemingly amplified by our location on a hospital site. Other individuals have stated "a lack of time" for participation in research due to the need to fulfil activities and commitments that were delayed by the pandemic, with some potential

volunteers presumably being more hesitant to participate in non-essential research that involves face-to-face interaction. Furthermore, our new clinician required training and practice in clinical procedures that are essential for my work (principally muscle biopsies), meaning I could not so freely schedule in participant visits and have high confidence in obtaining the necessary biological samples. Indeed, **numerous participants that I recruited, screened, and arranged for biopsies did not yield successful samples** due to this, costing more time and losing the participants who were difficult to recruit.

Summer 2021:

While the direct impact of COVID is reducing, and I am slowly being able to recruit more participants, the combined impact of COVID and Brexit on the supply chain and procurement is getting worse. **Basic reagents and consumables are on back order**, and some have arrived defrosted after getting severely delayed. As a result I am currently not able to work at maximal capacity on all experimental work due to fundamental unavailability of essentials such as qPCR plates. In addition to these challenges, restrictive access to laboratory spaces within the Medical School and lab-specific COVID-19 risk management strategies **are in place until the start of the 2021 Autumn Semester** such as shift working and equipment booking, meant I had **less access than usual to standard laboratory space and facilities** that are essential to my daily work.

2. ACTIONS TAKEN TO MINIMISE THE IMPACT

a) How have you tried to mitigate the risk to your project?

Please **briefly** explain how you are trying to minimise the impact of the situation on your research activities and progress. **With reference to the time between the COVID pandemic, national lockdown and the end of your funded period, if you have not tried to alter your plans to lessen the impact of this on your research progress, it's particularly important to explain here why you have taken this decision.**

For example,

- have you discussed how to do this with your supervisors?
- have you considered different ways to get the research done, such as changing your research plans to alter the order in which you do different elements?
- have you altered your research design, for example to conduct research online, or using other digital resources?
  what constraints or barriers did you have to try to remove, modify or overcome?
- **If you have not tried to alter your plans at all, why not?**

Try to show how/whether your work to date already meets some of the University and QAA Doctoral Outcomes, clarify which doctoral outcomes are not currently met and how your plan will enable you to meet these.

Section 2 additional guidance

Actions you have taken to minimise the impact:

Summer 2020:

The decision was made to use the first lockdown period to focus on analysing past data and **writing up the literature review, methods thus far and preliminary results sections for my thesis**. We discussed potential ideas about alternative ways to avoid running human studies or to run them differently. These included sourcing primary myoblasts from partner institutions cryobanks or from commercial suppliers; relocating to another research institution to run the in vivo study if elsewhere should resume *in vivo* research activities before we are able to (ie. Birmingham, Exeter, or Nestle's facility in Lausanne). Unfortunately, some of these barriers are unavoidable, as physiology research fundamentally requires some hands-on involvement of patients/participants and in the context of my research, these include elderly and obese individuals, who present with particularly high risks for coronavirus, thus meaning it is unlikely we will be able to resume these activities, particularly the planned chronic interventional *in vivo* study for the foreseeable future. We will, however, shift my research focus to predominantly focus on *in vitro* work as much as possible, to compensate.

I also used the lockdown period to **author a review paper** that is pertinent to the topic of my thesis - discussing the involvement of adipose-muscle cross talk in the regulation of skeletal muscle mass with ageing. This was subsequently **published in *GeroScience***. Additionally, I worked with data generated from a previous PhD student within our group to **write up a paper based on an *in vivo* study** that they undertook investigating the effects of lipid overload on insulin and anabolic sensitivity in skeletal muscle, which I had a degree of involvement in. This was subsequently **submitted to *Clinical Nutrition***.

Winter/Spring 2020/2021:

I have gained access to a selection of skeletal muscle samples generated from a previous study involving well-characterised adults of varying age and adiposity, from whom I am **undertaking a cross-sectional analysis** of the gene and protein expression of factors related to myostatin, which will form a short Chapter of my thesis.

Furthermore, I have been **collaborating with researchers at the University of Bath**, who have generated a vast number of adipose tissue biopsy samples during an in vivo intermittent fasting study. They have sent us the samples and I have extracted RNA from ~120 adipose tissue samples; synthesised cDNA; ran gene arrays on these samples; quantified and visualised the data for them to contribute to their paper. I have also written the relevant methods for this manuscript and reviewed and contributed to the manuscript which was subsequently **published in *Science Translational Medicine*.**

Summer 2021:

During this time, I continued working on the publication review process of the aforementioned manuscripts and **undertook work using commercially available myoblasts and also sourced some cryopreserved cells from collaborators** at Birmingham in order to continue cell culture experiments. Now that human recruitment is just about viable once more, albeit severely restricted, I have been **screening and recruiting as many eligible participants as possible** to undertake more in vivo work using primary human muscle cells.

Autumn 2021:

It has not been possible to undertake the agreed secondment with Nestle/Amazentis in Switzerland. Instead, **I have proposed, designed, pitched and received approval for an in vitro study** to them that I can run here in our own labs on samples I can generate in house, using a nutraceutical compound that they are very excited about, and we collectively believe could have insulin-sensitising effect in skeletal muscle cells, but has not yet been explored. I must complete this project by early 2022, however, as my funding period is running out. Thus, this study will be more of a pilot, and we will send additionally generated samples to them for further analysis.

b) List the aspects of your research plan that you have managed to achieve or progress during the period of impact.

During period of closure:

- Updated and substantially extended thesis literature review
- Written general methods, as well as introductions and methods and compiled preliminary results to 3 experimental chapters
- Considered future cell-based experimental designs
- Undertaken several online training courses and seminars to fulfil training requirements
- Completed 2nd year annual review
- Authored, submitted and rebutted a review manuscript
- Undertook experimental work for collaborators at Bath Uni and supported the creation and submission of their manuscript
- Actively writing a manuscript based on prior unpublished work within our group

Upon phased reopening of facilities:

- Screening and recruiting as many participants as possible
- Undertaken cross-sectional analysis of previously generated samples
- Developed novel model of ex vivo/in vitro adipose-muscle cross talk
- Secured resources and collaborative agreement with Nestle/Amazentis for upcoming work